AVALIAÇÃO POR TOMOGRAFIA COMPUTADORIZADA DA AURÍCULA ESQUERDA E VEIAS PULMONARES — CONTEXTO ANÁTOMO-CLÍNICO

HUGO MIGUEL RODRIGUES MARQUES

Tese para obtenção do grau de Doutor em Medicina

na Especialidade em Cirurgia e Morfologia Humana (Medicina da Imagem)

na NOVA Medical School | Faculdade de Ciências Médicas

Setembro, 2017

AVALIAÇÃO POR TOMOGRAFIA COMPUTADORIZADA DA AURÍCULA ESQUERDA E VEIAS PULMONARES — CONTEXTO ANÁTOMO-CLÍNICO

Hugo Miguel Rodrigues Marques

Orientadores:

Professor Doutor João Martins Pisco

Professor Catedrático Jubilado da NMS|FCM, UNL

Professor Doutor João Erse de Goyri O'Neill

Professor Catedrático da NMS|FCM, UNL

Prof. Dr. Pedro Manuel Pulido Garcia Adragão

Professor Auxiliar Convidado da NMS|FCM, UNL

Tese para obtenção do grau de Doutor em Medicina

na Especialidade em Cirurgia e Morfologia Humana (Medicina da Imagem)

Setembro, 2017

HUGO MIGUEL RODRIGUES MARQUES

AVALIAÇÃO POR TOMOGRAFIA COMPUTADORIZADA DA AURÍCULA ESQUERDA E VEIAS PULMONARES — CONTEXTO ANÁTOMO-CLÍNICO

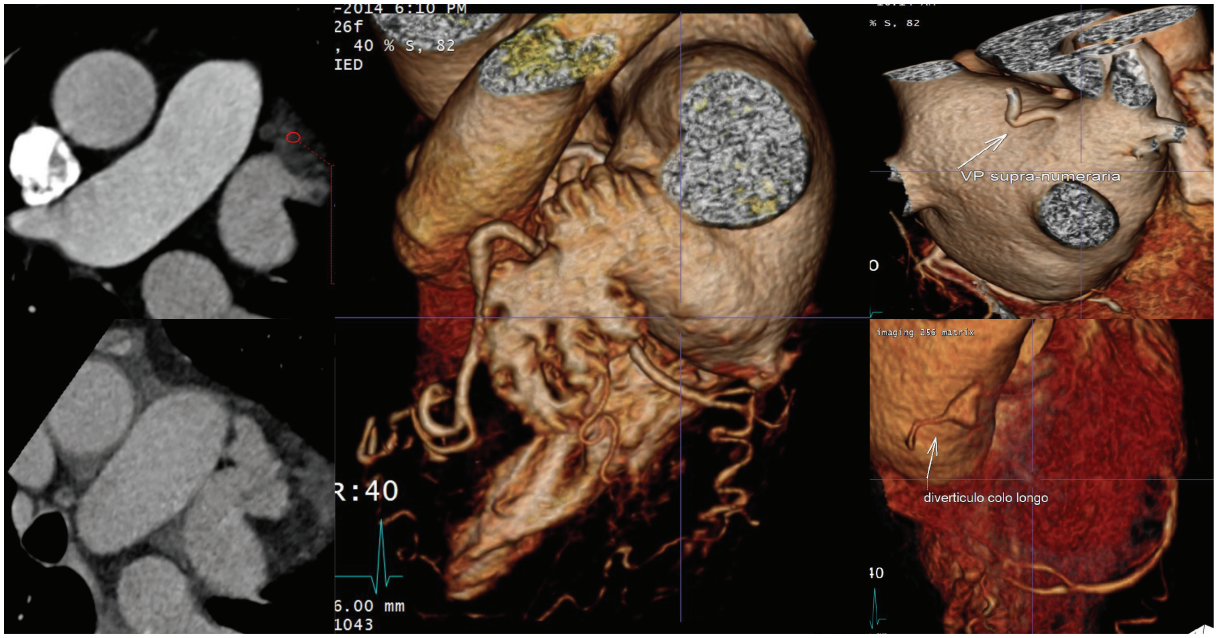

Setembro, 2017

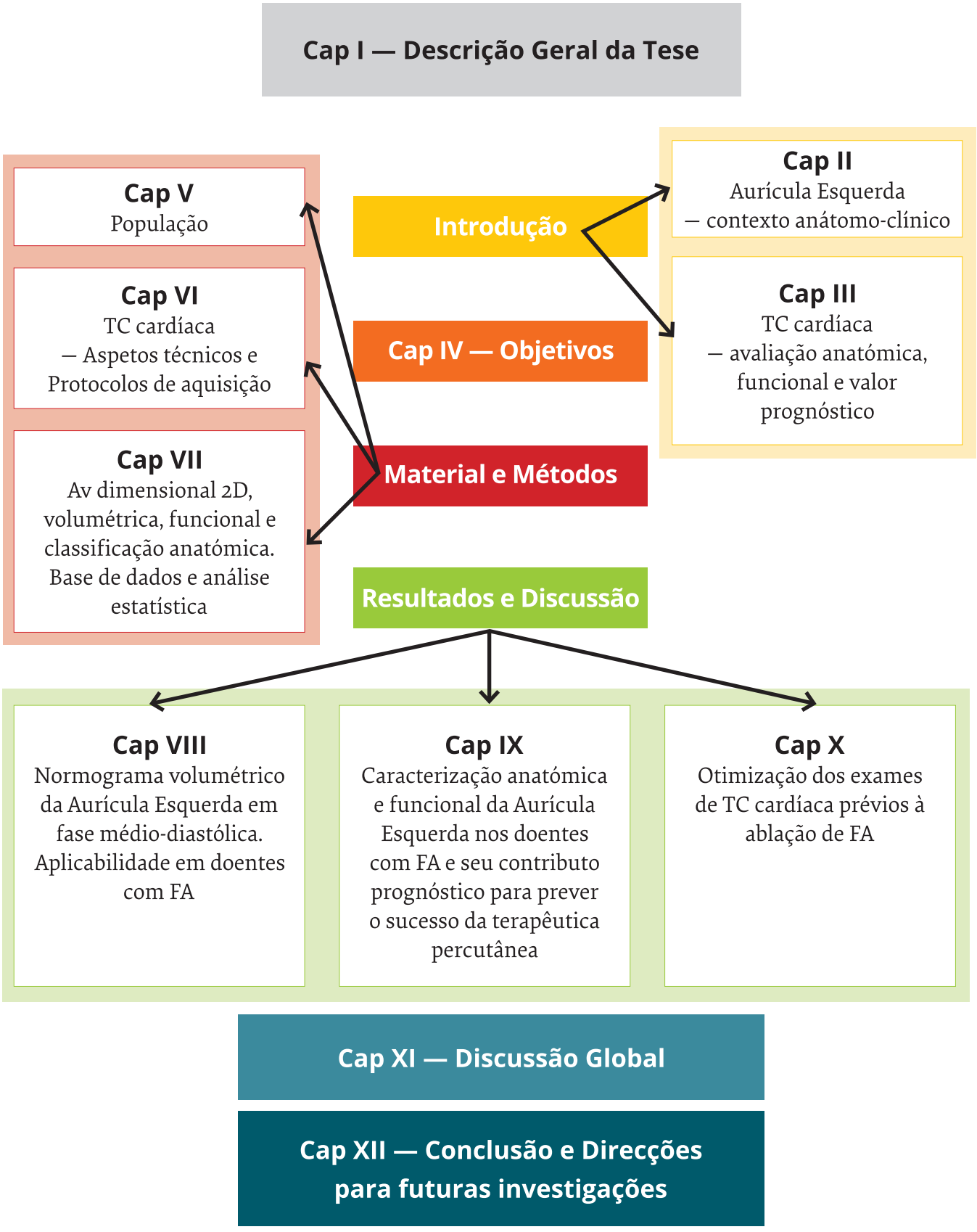
Cap I — Descrição Geral da Tese
Cap V
População
Cap VI
TC cardíaca
— Aspetos técnicos e
Protocolos de aquisição
Cap VII
Av dimensional 2D,
volumétrica, funcional e
classificação anatómica.
Base de dados e análise
estatística
Introdução
Cap IV — Objetivos
Material e Métodos
Resultados e Discussão
Cap II
Aurícula Esquerda
— contexto anátomo-clínico
Cap III
TC cardíaca
— avaliação anatómica,
funcional e valor
prognóstico
Cap VIII
Normograma volumétrico
da Aurícula Esquerda em
fase médio-diastólica.
Aplicabilidade em doentes
com FA
Cap IX
Caracterização anatómica
e funcional da Aurícula
Esquerda nos doentes
com FA e seu contributo
prognóstico para prever
o sucesso da terapêutica
percutânea
Cap X
Otimização dos exames
de TC cardíaca prévios à
ablação de FA
Cap XI — Discussão Global
Cap XII — Conclusão e Direcções
para futuras investigações

Às minhas meninas e menino...

"Almeja o todo para ires conseguindo as suas partes..."

"Conhecer não é demonstrar nem explicar, é aceder à visão..."

Saint-Exupéry

ÍNDICE

AGRADECIMENTOS

Agradeço aos orientadores desta tese, ao Professor Doutor Martins Pisco, ao Professor Doutor João Goyri O´Neill e ao Prof. Dr. Pedro Adragão o apoio e estímulo que demonstraram, a disponibilidade sempre presente e as perguntas desafiantes. Constituíram, na sua diversidade, uma mais valia inestimável.

À Dra Luísa Figueiredo, diretora do Serviço de Radiologia do Hospital de Santa Marta, onde me formei como Radiologista, o apoio incondicional, o estímulo na hora certa e os ensinamentos e carinho maternos que sempre me dispensou.

Ao Prof. Dr. Pedro Gonçalves, com quem iniciei a realização de exames de TC cardíaco e a UNICA (Unidade de imagem cardiovascular por TC e RM – Hospital da Luz), pela amizade e companheirismo. Pelo papel de enorme relevo que teve ao longo deste período, acreditando neste projeto. Pelo permitir ver por outros olhos, alargar horizontes, potenciando o complemento entre as nossas formações de base (Cardiologia e Radiologia).

Ao Dr. António Miguel Ferreira, membro da UNICA, com quem tive o privilégio de privar desde os tempos de estudante universitário, contribuindo decisivamente para o "estar sempre à procura".... que caracteriza a nossa amizade.

Ao Prof. Dr. Nuno Cardim, membro da UNICA pelos conselhos, ensinamentos e amizade.

Aos restantes constituintes da UNICA (técnicos e enfermeiros) pelo seu profissionalismo e competência, sem os quais o Serviço ao doente seria por certo inferior.

Aos colegas de serviço do Hospital da Luz e do Hospital de Santa Marta pelo apoio amigo sempre que necessário e o estímulo para perseverar.

Aos internos de Radiologia e Cardiologia que têm feito formação connosco, é da sua procura pelo conhecimento que alimento a minha.

Aos doentes, porque no final é por eles e para eles.

À família, frequentemente a mais sacrificada, mas cuja incondicionalidade, generosidade e afeto permitiu esta conquista.

RESUMO

A **Aurícula Esquerda** é uma câmara cardíaca com origem embriológica complexa que apresenta contributo prognóstico independente em diversas situações clínicas.

É nela que tem origem a arritmia cardíaca crónica mais prevalente, a **Fibrilhação Auricular**, que afeta 2,5% dos portugueses com mais de 40 anos.

A fibrilhação auricular apresenta relevante morbi-mortalidade *per se* e pela frequente associação a terapêutica anti-agregante ou anti-coagulante.

A Ablação Percutânea da fibrilhação auricular é um tratamento com crescente aplicabilidade, seguro, com bons resultados globais, mas com taxas de recidiva a longo prazo relativamente altas. É habitualmente precedido da realização de exame de **tomografia computorizada cardíaca** para avaliação anatómica e, por vezes, com intuito de excluir trombo intra-cavitário.

A informação contida no exame de TC quer anatómica quer funcional poderá ter **relevância prognóstica** e ajudar a uma escolha otimizada dos doentes que irão beneficiar mais do tratamento, potenciando o binómio custo-benefício.

A **TC cardíaca** para avaliação coronária tem assistido a um enorme aumento de utilização apropriada, sendo considerada por algumas sociedades o exame de primeira linha para avaliação do doente com dor torácica estável de possível etiologia cardíaca. Estima-se que a aplicação destas *guidelines* condicione um crescimento de cerca de 600% no número destes exames. A evolução tecnológica que acompanhou o desenvolvimento destas técnicas de TC cardíaca permite, hoje, a avaliação das coronárias na grande maioria dos casos com informação obtida **apenas em fase médio-diastólica** (cerca de 70% do intervalo entre onda R (RR)). A ausência de informação telesistólica e telediastólica não permite a avaliação funcional cardíaca. A avaliação

dimensional das câmaras cardíacas fica igualmente condicionada pela inexistência de normogramas para essa fase do ciclo cardíaco (70% do RR).

Neste contexto, foi possível desenvolver um normograma do volume da aurícula esquerda em fase médio-diastólica. Confirmámos uma boa correlação entre os volumes obtidos a 70% do intervalo RR e os volumes máximos, e criámos uma regressão para obter o volume máximo da aurícula esquerda com base no diâmetro axial máximo e altura máxima em plano sagital avaliado a 70% do intervalo RR. Esta regressão permite, de forma eficiente e sem necessidade de software dedicado, fazer a avaliação quantitativa da aurícula esquerda na maioria dos exames de coronariografia por TC, inclusive naqueles que, por utilizarem tecnologia mais recente, adquirem informação apenas na fase medio-diastólica.
A aplicabilidade deste normograma a doentes com FA foi testada, tendo permitido identificar todos os doentes com FA que tinham dilatação da AEsq.

Descobrimos um marcador anatómico (o padrão de drenagem das veias pulmonares à direita) com relevância significativa e independente na taxa de recidiva após ablação percutânea da fibrilhação auricular.

Identificámos fatores identificáveis na TC cardíaca, efetuada em contexto prévio à ablação de FA, que se correlacionam com o *score* de risco de eventos embólicos CHA_2DS_2VASc, lançando assim os fundamentos para um eventual *score* incluindo parâmetros clínicos e imagiológicos.

Por fim, analisámos a otimização do protocolo e a qualidade de imagem dos exames de TC cardíaca realizados num contexto pré-ablação e foi possível descrever um protocolo, com doses de radiação submilisivert e sem condicionar a qualidade de imagem.

ACRÓNIMOS

AEsqFej	Fração de ejeção da aurícula esquerda
AEsqFejACT	Fração de ejeção ativa da aurícula esquerda
ASC	Área de superfície corporal
AVC	Acidente vascular cerebral
AIT	Acidente isquémico transitório
bpm	batimentos por minuto
CSVE	Câmara de saída do ventrículo esquerdo
DM	diabetes mellitus
DPOC	Doença pulmonar obstrutiva crónica
DRC	Doença renal crónica
FBP	*Filtered Back Projection*
FC	Frequência cardíaca
Fej	Fração de ejeção
FFR	*Fractional flow reserve*
HTA	Hipertensão arterial
IMC	Índice de massa corporal
IVUS	*Intravascular ultrasound*
KeV	Kilo electrão volt
kV	kilo Volt
MD	médio-diastólico
OCT	*Optic Coerence Tomography*
RM	Ressonância magnética
ROI	*Region of interest*
RR	intervalo RR
SCA	Síndroma coronário agudo

TArt	Tensão arterial
TC	Tomografia cardíaca
VAAEsq	Volume apêndice auricular esquerdo
VAAEsqMax	Volume máximo do apêndice auricular esquerdo
VAAEsqMaxi	Volume máximo indexado do apêndice auricular esquerdo
VAAEsqMin	Volume minimo do apêndice auricular esquerdo
VAAEsqMini	Volume minimo indexado do apêndice auricular esquerdo
VAAEsqPS	Volume pré-sistólico do apêndice auricular esquerdo
VAEsq	Volume da aurícula esq
VAEsqMax	Volume máximo da aurícula esquerda
VAEsqMaxi	Volume máximo indexado da aurícula esquerda
VAEsqMin	Volume minimo da aurícula esquerda
VAEsqMini	Volume minimo indexado da aurícula esquerda
VAEsqPS	Volume pré-sistólico da aurícula esquerda
VPEsq	Veia pulmonar esquerda (tronco comum de drenagem)
VPIDrt	Veia pulmonar inferior direita
VPIEsq	Veia pulmonar inferior esquerda
VPM	Veia pulmonar média
VPSDrt	Veia pulmonar superior direita
VPSEsq	Veia pulmonar superior esquerda
vs	*versus*

CAPÍTULO I

Descrição geral da tese

SUMÁRIO

1.1. INTRODUÇÃO SUMÁRIA DA TESE

Foi num contexto de enorme desenvolvimento tecnológico e de aplicabilidade clínica apropriada da TC cardíaca que surgiu o tema desta tese, procurando conciliar o conhecimento anatómico com relevância clínica às mais valias que as novas técnicas de imagem poderiam dar.

Assim foi escolhida uma aplicação recente da TC cardíaca, como a avaliação única do doente no contexto pré-ablativo e procurou-se otimizar a técnica quer a nível do protocolo de aquisição, quer na utilização de toda a informação possível de ser obtida que pudesse ter relevância clínica e prognóstica.

A esta intensão, associou-se o projeto complementar da avaliação dimensional da AEsq, procurando antecipar necessidades futuras quando os aparelhos de TC no futuro permitissem a avaliação coronária apenas em fase medio-diastólica na grande maioria dos doentes. Aqui o futuro é hoje, enaltecendo a importância do normograma que apresentamos.

1.2. DESCRIÇÃO SUMÁRIA DA TESE

A tese está dividida em 12 capítulos, cuja organização é ilustrada pela **Figura 1**.

No presente capítulo (***capítulo I)*** faz-se uma introdução sumária ao tema e aos motivos da tese.

A **INTRODUÇÃO** subdivide-se em dois capítulos de contextualização.
No **Capítulo II** abordamos o contexto anatómico e clínico.
No **Capítulo III** centramos as atenções no método de imagem utilizado a tomografia computorizada.

O **Capítulo IV** é dedicado aos **OBJETIVOS** da tese.

O **MATERIAL E MÉTODOS** encontra-se dividido em 3 capítulos.
No **Capítulo V** descrevemos os diferentes grupos da população de estudo.
No **Capítulo VI** fazemos uma introdução complementar às questões técnicas relevantes da TC para posteriormente descrevermos os protocolos de aquisição das TC cardíacas em cada grupo de estudo.
No **Capítulo VII,** descrevemos em detalhe a forma de obtenção dos dados quantitativos de dimensões 2D, volumétricos e funcionais, para além das classificações utilizadas para caracterizar o AAEsq e o padrão de drenagem das veias pulmonares. Ainda neste capítulo fazemos uma breve revisão dos métodos estatísticos utilizados.

Os **RESULTADOS E DISCUSSÃO** são âmbito de 3 capítulos, um para cada objetivo da tese.
Assim, no **Capítulo VIII** apresentamos o normograma volumétrico da aurícula esquerda em fase médio-diastólica.
No **Capítulo IX** fazemos a caracterização anatómica e funcional da aurícula esquerda e exploramos o seu contributo prognóstico na determinação de sucesso da terapêutica ablativa percutânea.
No **Capítulo X** fazemos a avaliação da otimização do protocolo de TC cardíaca como exame único, prévio à ablação percutânea de FA.

O **Capítulo XI**, de discussão global, procura sumarizar e agregar, correlacionando os três capítulos anteriores

No **Capítulo XII** descrevem-se as **CONCLUSÕES e lançam-se desafios**.

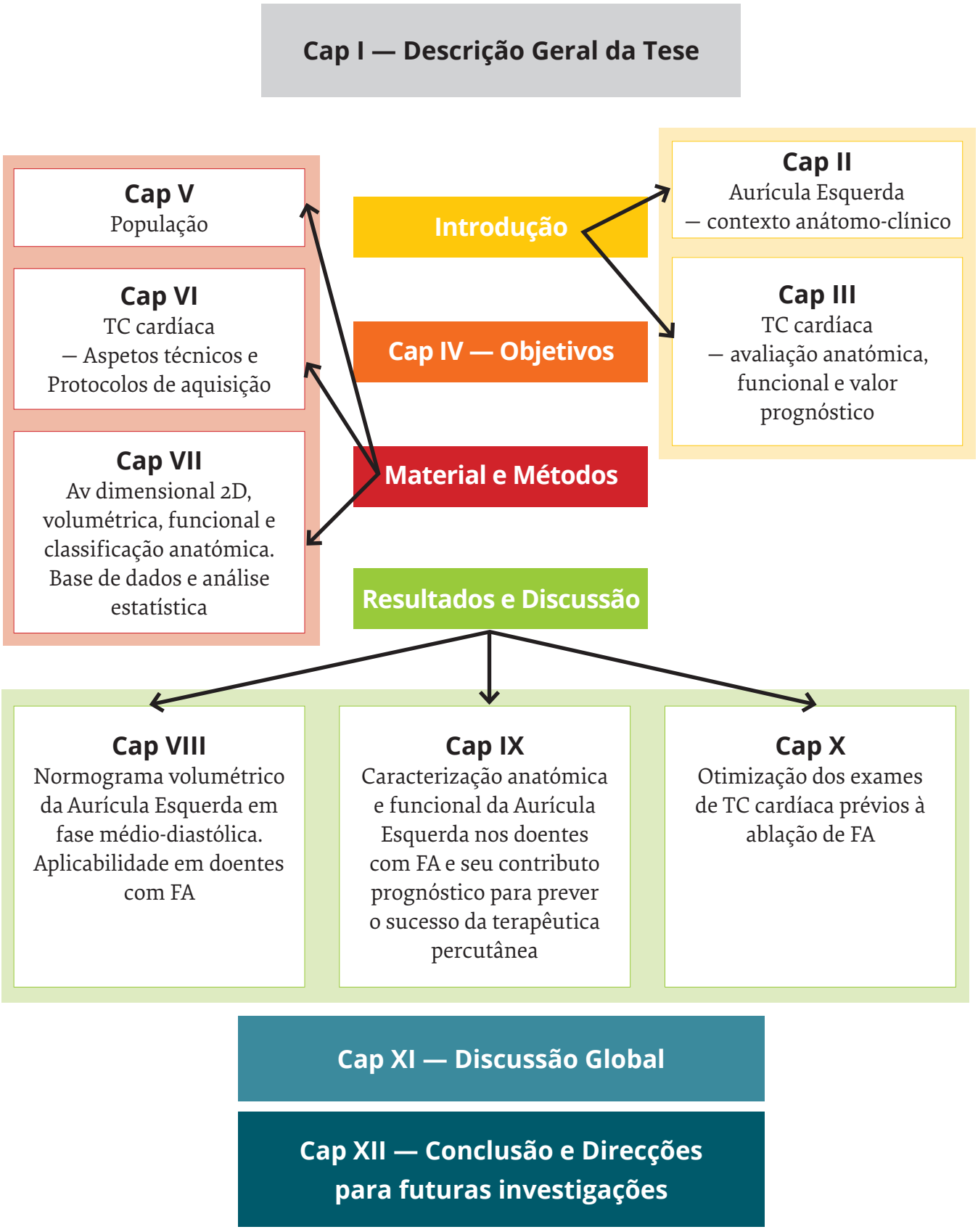

FIGURA 1
Organização dos diferentes capítulos da Tese

ANEXOS

HOSPITAL DA LUZ

COMISSÃO DE ÉTICA PARA A SAÚDE

Exmo. Sr.

Dr. Hugo Marques

Unidade de Imagiologia

Hospital da Luz

Assunto: *AVALIAÇÃO POR TOMOGRAFIA COMPUTORIZADA DA AURÍCULA ESQUERDA E VEIAS PULMONARES - CONTEXTO ANÁTOMO-CLÍNICO*

CC.: Director Clínico / Conselho de Administração

A **Comissão de Ética para a Saúde** do Hospital da Luz, reunida a 15 de Abril de 2009 aprovou por unanimidade a realização do estudo clínico *AVALIAÇÃO POR TOMOGRAFIA COMPUTORIZADA DA AURÍCULA ESQUERDA E VEIAS PULMONARES - CONTEXTO ANÁTOMO-CLÍNICO* de que V. Exa. é investigador principal .

Com os melhores cumprimentos

Lisboa, 15/04/2009

Pel'A Comissão de Ética para a Saúde

João Sá, Presidente

QUESTIONÁRIO ANGIOTCS CARDÍACAS

Foi-lhe solicitada pelo seu medico assistente a realização de uma angioTC cardíaca. O centro de Imagiologia do Hospital da Luz é uma referencia nesta área, fruto não só do elevado numero de exames mas sobretudo da investigação científica, apresentada regularmente em reuniões nacionais e internacionais de Cardiologia e de Imagiologia e estando em curso 2 teses de doutoramento nesta área.

Para este efeito, gostaríamos de pedir a sua colaboração no preenchimento deste questionário, cuja informação (bem como a do resultado do seu exame) será introduzida numa base de dados, para análise pelos médicos responsáveis pelos exames de angioTC cardíaca. Será sempre respeitada a sua confidencialidade, retirada a sua identificação de qualquer imagem que possa vir a ser apresentada e/ou publicada, estando estes dados abrangidos pelo obrigatório "segredo médico profissional".

Tem tensão arterial elevada ou toma medicação para a tensão arterial ?
☐ SIM ☐ NÃO

Tem o colesterol elevado ou toma medicação para o colesterol ?
☐ SIM ☐ NÃO

Tem diabetes?
☐ SIM ☐ NÃO

É fumador (ou ex-fumador há menos de 1 ano)?
☐ SIM ☐ NÃO

Tem história de doença cardiovascular na família (enfarte do miocárdio ou acidente vascular cerebral - AVC)?
☐ SIM ☐ NÃO

Se sim, esses antecedentes são num familiar direto (Pai, Mãe, Irmãos) e em idade prematura (num homem <55 anos; numa mulher <65 anos)?
☐ SIM ☐ NÃO

Sabe o nome dos medicamentos que toma regularmente?

_____

_____

Autorizo que os meus dados sejam incluídos em bases de dados para investigação científica e aceito ser eventualmente contactado telefonicamente de futuro para seguimento e atualização da minha situação clinica.

*Data*____/____/_____*Assinatura*_____

CAPÍTULO II

Aurícula esquerda

Contexto anátomo-clínico

RESUMO

A aurícula esquerda (AEsq) centra as atenções do trabalho investigacional produzido nesta tese.

É uma câmara cardíaca com origem embrionária complexa, que apesar da interdependência com o ventrículo esquerdo, apresenta contribuição prognóstica independente em diversas situações clínicas.

Este capítulo faz a contextualização anatómica e clínica da aurícula esquerda, com especial ênfase na principal doença com ela relacionável, a fibrilhação auricular (FA) e o método terapêutico ablativo percutâneo.

Fomos coautores de dois manuscritos, o primeiro que versa o desenvolvimento de um *score* preditor de recidiva de FA após terapêutica ablativa percutânea (**Manuscrito 1**) e o outro sobre a comparação de duas formas ablativas em relação à segurança e sucesso do procedimento (**Manuscrito 2**).

MANUSCRITOS

Manuscrito 1

Development and Validation of a Risk Score for Predicting Atrial Fibrillation Recurrence After a First Catheter Ablation Procedure — ATLAS score.

Mesquita, J.F., A.M.; Cavaco, D.; Costa, F.M.; Carmo, P.; **Marques**, **H**.; Morgado, F.; Mendes, Miguel; Adragão, P., Europace, 2017, https://doi.org/10.1093/europace/eux265

Manuscrito 2

Safety and Long-Term Outcomes of Catheter Ablation of Atrial Fibrillation Using Magnetic Navigation versus Manual Conventional Ablation: A Propensity-Score Analysis**.**

Adragão, P.P., Cavaco, D., Ferreira, A.M., Costa, F.M., Parreira, L., Carmo, P., Morgado, F.B., Santos, K.R., Santos, P.G., Carvalho, M.S., Durazzo, A., **Marques**, **H**., Goncalves, P.A., Raposo, L., and Mendes, M., J, Cardiovasc Electrophysiol, 2016, 27 Suppl 1: p. S11-6.

SUMÁRIO

2.1. INTRODUÇÃO

A aurícula esquerda (AEsq) centra as atenções do trabalho investigacional produzido nesta tese.
É uma câmara cardíaca com origem embrionária complexa, que apesar da interdependência com o ventrículo esquerdo, apresenta contribuição prognóstica independente em diversas situações clínicas.

A aurícula esquerda resulta da fusão do botão embrionário das veias pulmonares com a aurícula esquerda primitiva, sendo que a sua porção de parede lisa resulta do botão embrionário das veias pulmonares, enquanto que a AEsq primitiva, com a sua parede trabeculada dá origem ao apêndice auricular (1) .
Esta diferença embriológica condiciona as diferenças anatómica/morfológica conhecidas, no entanto a sua relevância clínica carece de avaliação, nomeadamente na tradução de diferenças etiopatogénicas e prognósticas destas duas zonas.

São poucas as medições em Cardiologia com um impacto tão amplo como o da dimensão da AEsq, que está, entre outros, independentemente associada ao risco de:

- FA e sua recorrência;
- eventos tromboembólicos;
- insuficiência cardíaca;
- enfarte do miocárdio;
- mortalidade cardiovascular

A ecocardiografia é o método imagiológico mais frequentemente utilizado para a avaliação da aurícula esquerda, no entanto subestima as dimensões da AEsq quando comparada com a ressonância magnética (RM).
O aumento crescente da utilização da TC coronária, com a sua ótima capacidade de avaliação morfológica, aliada a obtenção de informação volumétrica (tridimensional), cria uma oportunidade de avaliação das câmaras cardíacas, incluindo a aurícula esquerda.
No entanto, é ainda uma área com alguns deficits de conhecimento básico e portanto com grande campo investigacional.

A fibrilhação auricular é a arritmia crónica mais frequente, com morbilidade e mortalidade relevante, sendo a AEsq a peça central da sua génese, perpetuação e recidiva.

2.2. AURÍCULA ESQUERDA

A AEsq participa no ajuste da volémia e no equilíbrio hemodinâmico, nomeadamente através de influência na natriurese, na vasodilatação, na inibição do sistema simpático e do sistema renina-angiotensina-aldosterona.
É igualmente um sensor de volume e um barómetro da função diastólica do ventrículo esquerdo (2).

2.2.1. Morfologia

A avaliação morfológica da AEsq permite a exclusão de trombos e massas, assim como a deteção de variantes anatómicas, como divertículos e apêndices acessórios.
Os divertículos da AEsq são evaginações de parede lisa que podem ter um colo com diferente comprimento (ver **Figura 1**).
Já os apêndices acessórios são igualmente evaginações mas com parede crenada, com aparência semelhante à conferida pelos músculos pectíneos (ver **Figura 2**).
A frequência de divertículos tem sido descrita em cerca de 45% da população referenciada para a realização de TC cardíaca e a de apêndices acessórios em cerca de 5% (3).

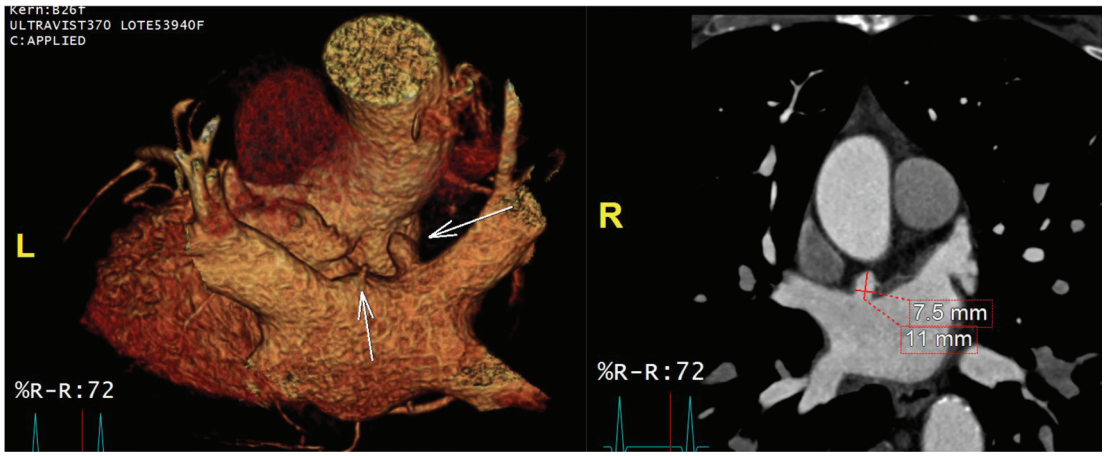

FIGURA 1

Visualizam-se dois divertículos da AEsq na imagem volumétrica 3D. Na imagem axial oblíqua observamos a dimensão do maior divertículo.

(Imagens Hugo Marques — UNICA — Hospital da Luz.)

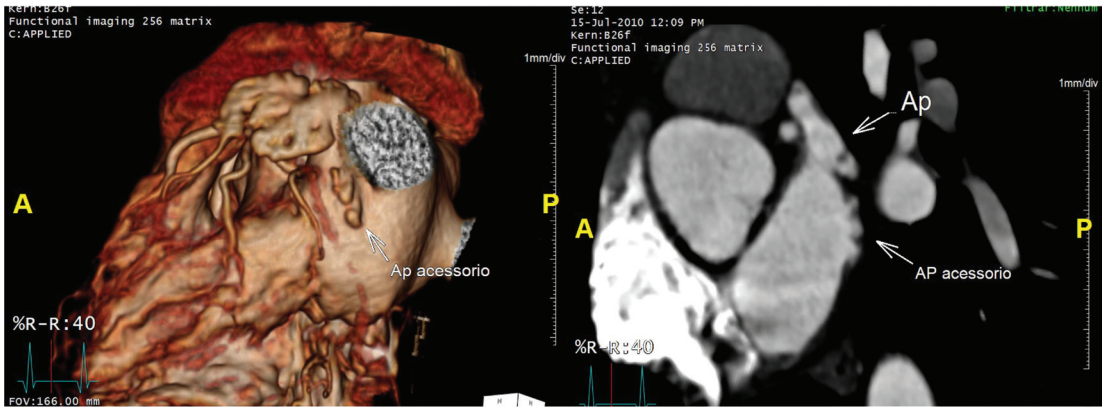

FIGURA 2

Apêndice acessório. Imagem de reconstrução 3 dimensional e numa imagem axial oblíqua mostrando a relação com o AAEsq principal.

(Imagens Hugo Marques — UNICA — Hospital da Luz.)

Estas estruturas poderão ter relevância na génese de doenças como a FA, mas podem também contribuir como locais de eventual maior probabilidade de formação de trombos (4). É ainda relevante o seu conhecimento prévio à terapêutica ablativa de FA ou de oclusão do AAEsq.

2.2.2. Dimensão

A avaliação da dimensão da aurícula esquerda pode ser realizada por avaliação de diâmetros, áreas ou volumes, sendo o volume a forma de avaliação dimensional com maior relevância prognóstica (5).

O volume depende tanto da pré-carga: função sobretudo da volémia; como da pós--carga: função sobretudo das propriedades elásticas e pressão do VESq.

São causas de dilatação da AEsq: a sobrecarga de pressão, (condicionada por exemplo por estenose mitral ou disfunção diastólica do VEsq) e/ou a sobrecarga de volume (condicionada por insuficiência mitral, situações clinicas de débito cardíaco aumentado, shunts e fístulas).

O volume da AEsq pode ser avaliado em diferentes fases do ciclo cardíaco. Assim podemos medir o volume máximo em fase tele-sistólica (a medida volumétrica mais frequentemente utilizada) (ver **Figura 3**), o volume mínimo em fase tele-diastólica e o volume pré-sístole auricular.

O volume máximo indexado à superfície corporal (VAEsqMaxi) é a medida da aurícula esquerda com maior correlação com doença cardiovascular, conferindo uma estratificação de risco adequada e uniforme (6).

Há, no entanto, outros estudos que referem a importância do volume mínimo indexado (VAEsqMini), como sendo o que apresenta maior correlação com a disfunção diastólica do VEsq, tendo sido o melhor preditor de eventos cardiovasculares major — *MACE (major adverse cardiac effects)* (7) e o melhor preditor de desenvolvimento de FA (8).

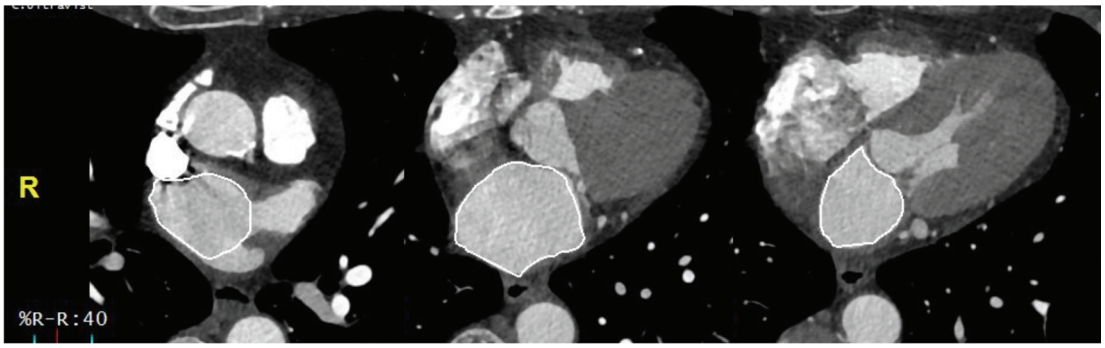

FIGURA 3

Avaliação volumétrica da AEsq: efetuada desenhando regiões de interesse (ROI) limitadas pela parede da AEsq, excluindo o AAEsq, as veias pulmonares e o VEsq, em cortes axiais consecutivos e posteriormente fazendo o sumatório dos volumes resultantes (áreas x espessura de corte).

(Imagens Hugo Marques — UNICA — Hospital da Luz.)

2.2.3. Função

Classicamente descrevem-se três fases funcionais da AEsq:

> Função Reservatório — entre o fecho e a abertura da válvula mitral, durante a sístole ventricular.
> Influenciada pela elasticidade da AEsq, pelo retorno venoso pulmonar e, de forma menos relevante, pela contractilidade e relaxamento da AEsq, pela descida da base do VEsq durante a sístole e pelo volume telesistólico do VEsq.

> Função Conduto — após a abertura da válvula mitral até à sístole auricular — durante parte da diástole ventricular.
> Interligada à função reservatório e dependente da elasticidade da AEsq e da elasticidade e da capacidade de relaxamento do VESq.
> Depende também da não obstrução provocada pela válvula mitral.

> Função Ativa/Bomba — durante a sístole da aurícula esquerda até ao encerramento da válvula mitral — fase final da diástole ventricular.
> Reflecte a magnitude e *timing* da contracção da AEsq influenciada pela pré-carga (volume pré-sistólico da AEsq) e pela pós-carga (volume telediastólico do VEsq) e pela reserva sistólica do VEsq.
> Contribui para cerca de 25% da fracção de ejeção do VEsq (9-12), tornando-se essencial na presença de disfunção diastólica do VEsq, em que é responsável por 50% do débito cardíaco.

Para a avaliação das fases funcionais da AEsq é necessário medir o volume auricular máximo (VAEsqMax), o volume auricular mínimo (VAEsqMin) e o volume auricular pré-sístole auricular (VAEsqPS) (ver **Figura 4**).
Assim, podemos determinar para além da função global da AEsq, o índice de expansibilidade — relacionável com a função reservatório; a função passiva — relacionável com a função conduto; a função ativa — relacionável com a função bomba.

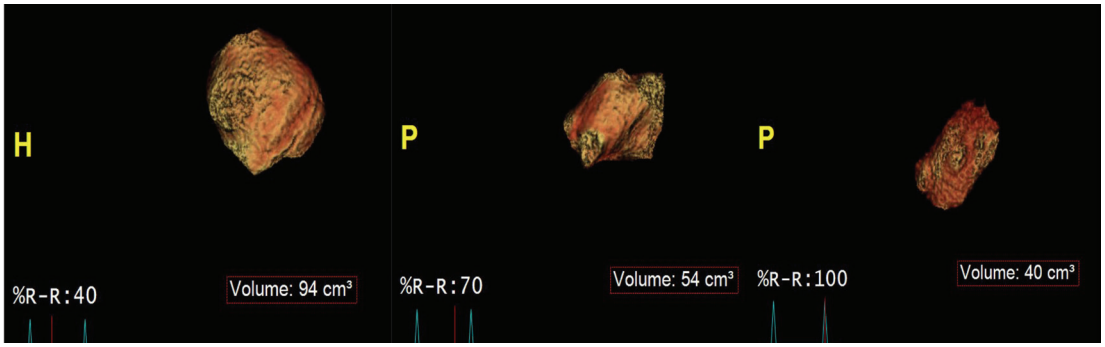

FIGURA 4

Avaliação volumétrica da AEsq na fase de volume máximo (neste caso aos 40% do intevalo RR), na fase pré-sistole auricular (neste caso a 70% do intervalo RR) e na fase de volume mínimo (neste caso a 100% do RR). *(Imagens Hugo Marques — UNICA — Hospital da Luz.)*

TABELA 1

Avaliação funcional da AEsq — definições e fórmula de cálculo.

Função reservatório	Índice de expansibilidade	(VAEsqMax –VAEsqMin) / VAEsqMin
Função conduto	Fração de Ejeção Passiva	**Volume sistólico passivo da AEsq** (VAEsqMax –VAEsqPS) / VAEsqMax
Função Ativa	Fração de Ejeção ativa (FejACT)	**Volume sistólico ativo da AEsq** (VAEsqPS –VAEsqMin) / VAEsqPS
Função AEsq	Fração de Ejeção (Fej)	(VAEsqMax –VAEsqMin) / VAEsqMax

Diferentes entidades influenciam estas fases de forma diversa:

- HTA — não modifica a função de conduto, mas aumenta a função ativa e a Fej da AEsq. (13).
- Exercício físico vigoroso — aumenta o VAEsqMax, a função ativa e passiva.
- Status pós ablação de FA — melhoria da função reservatório e da Fej da AEsq. (14, 15)
- Status pós tratamento da apneia do sono — por melhoria da função diastólica do VEsq e sem alterar o volume máximo da AEsq, provoca uma melhoria da função de conduto, com a compensatória diminuição da função ativa.

Nos últimos anos, as técnicas de deformação miocárdica, inicialmente utilizadas para avaliar a função VEsq foram também extendidas a outras cavidades,

nomeadamente à AEsq. Apesar da sua complexidade técnica (paredes de espessura finas, necessidade de exclusão do AAEsq e veias pulmonares), um grande número de trabalhos publicados têm mostrado a exequibilidade e reprodutibilidade das técnicas de deformação miocárdica (*Speckle-tracking-STE*) na avaliação do miocárdio da aurícula esquerda, permitindo estabelecer os seus valores de referência e tendo-se revelado um dos principais focos de investigação em ecocardiografia (16, 17).

GRÁFICO 1

Fases funcionais da AEsq e a sua relação com o "strain longitudinal" ao longo do ciclo cardíaco.

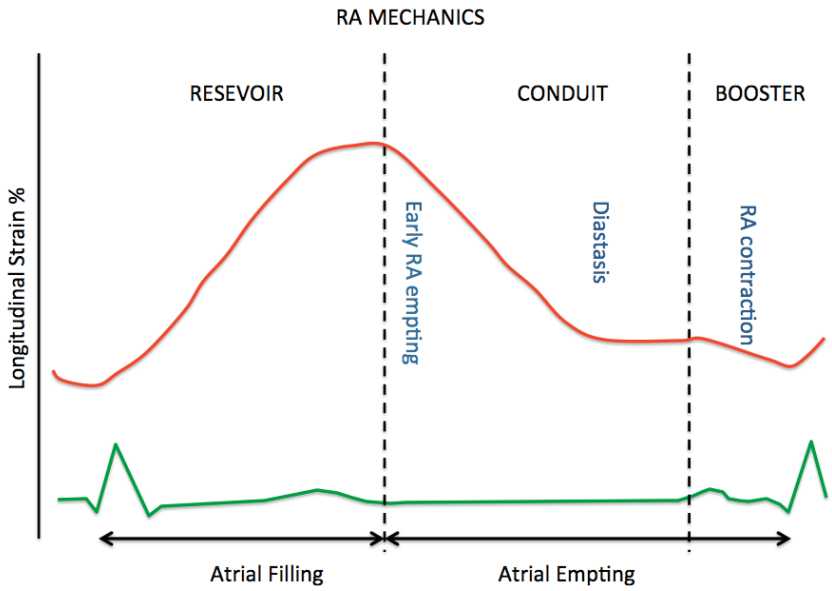

A disponibilidade, custo, inocuidade e resolução temporal (2D 10-20ms; 3D 50-75ms) fazem da ecocardiografia o estudo de escolha para a avaliação funcional da AEsq. No entanto, esta avaliação é também possível em exames de RM (resolução temporal 20-50ms), bem como em TC com sincronização eletrocardiográfica e aquisição retrospetiva (resolução temporal 75-250ms).

2.2.4. Estrutura

A avaliação estrutural não invasiva da AEsq poderá ajudar a entender a forma de relacionamento causa/efeito em diferentes contextos e doenças.

A espessura da parede e a presença de fibrose são as duas informações diretas que têm sido avaliadas.

A estrutura da AEsq condiciona a sua dimensão e a função.
Enquanto a espessura da parede pode ser avaliada por ecografia, TC ou RM, a avaliação de fibrose é mais difícil e tem sido efetuada por RM. A resolução espacial dos métodos tridimensionais de avaliação do realce tardio por RM tem sido apontada como uma limitação, no entanto, em centros especializados têm tido bons resultados, com boa correlação prognóstica em doentes com FA pré e após ablação térmica (18, 19).

2.2.5. Contributo prognóstico

Índices dimensionais e funcionais da AEsq são marcadores de risco cardiovascular na população geral (20-28).
O volume da AEsq e a disfunção sistólica são fatores de risco independentes para o desenvolvimento de FA, sendo que a disfunção sistólica é incremental ao VAEsqMaxi. Este aspeto sugere que a diminuição da função ativa da AEsq é um marcador de maior *remodeling* do que apenas a dilatação (29).

O contributo prognóstico depende da população em estudo, são exemplos:

- População geral jovem — VAEsqMaxi >24ml/m² foi preditor de *MACE* e mortalidade de todas as causas (30)
- Doentes idosos com doença cardiovascular — VAEsqMaxi preditor de mortalidade e eventos cardiovasculares (31, 32)
- População geral — o VAEsqMin foi superior e independente do VAEsqMax para desenvolvimento inicial de FA
- População geral — o VAEsqMin foi em analise multivariável o melhor preditor para *MACE*
- Em doentes com HTA crónica e sem doença cardiovascular, a disfunção sistólica da AEsq foi o preditor mais potente de *MACE* e mortalidade de todas as causas (24)
- Doentes com miocardiopatia (22, 26)
  - VAEsqMax foi preditor de insuficiência cardíaca (IC) independente da função VEsq
  - Na presença de IC, o VAEsq Max e a disfunção AEsq foram preditores de hospitalização, *MACE* e mortalidade

  - Na presença de doença coronária, na ausência de arritmias e de patologia valvular mitral — o VAEsqMaxi>50ml/m² foi tão relevante como a função sistolica do VEsq em predizer hospitalização e morte por insuficiencia cardíaca
- Doentes com FA
  - Tanto a dilatação como a disfunção da AEsq são preditores de eventos (33-37)
  - A fibrose da AEsq é preditor de risco de *MACE*, sobretudo de AVC e AIT (38)
  - O VAEsqMax é mais importante do que o tipo de FA para predizer sucesso de longo prazo após ablação térmica (39, 40)
  - A presença de fibrose previa à ablação torna a ablação menos eficaz (18, 41)
  - A fibrose correlaciona-se com maior probabilidade de AVC (42)
  - A fibrose "de novo" após ablação prediz sucesso da ablação (19)

2.3. APÊNDICE AURICULAR ESQUERDO

Sendo o apêndice auricular esquerdo (AAEsq), o principal local de formação de trombos e um possível *trigger* de FA, a importância do seu estudo pode revestir-se de maior relevância se pensarmos que a sua diferente génese embriológica e a diferente influência ventricular esquerda na sua função poderão fazer diferir a correlação com a restante aurícula esquerda nos diferentes contextos nosológicos (43, 44).

Anatomicamente, o AAEsq apresenta um *ostium*, um colo e um corpo que pode apresentar diferentes lobos.
Para cima e para trás encontramos o *ostium* da VPSesq e na face epicárdica correlaciona-se com o sulco aurículo-ventricular onde se encontra a artéria circunflexa e a grande veia cardíaca. Em cerca de 30% dos casos a artéria para o nódulo sino-auricular tem origem na artéria circunflexa e pode passar por baixo ou por fora e por cima do AAEsq (ver **Figura 5**).
O nervo frénico correlaciona-se com o AAEsq, na sua vertente póstero-lateral, mas em topografia extra-pericárdica.
O AAEsq é avaliado no decurso da avaliação da AEsq.

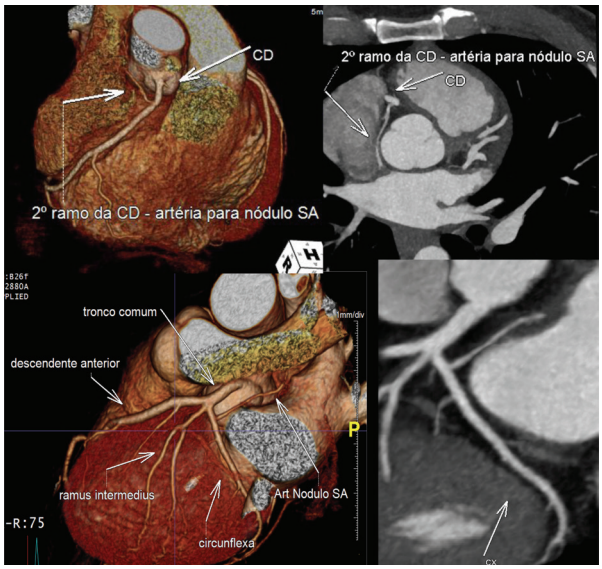

FIGURA 5
Artérias do nódulo sino-auricular. Esta artéria é frequentemente o 2.º ramo da artéria coronária direita (doente de cima). Mas pode ter origem na artéria circunflexa (imagens fila inferior). *(Imagens Hugo Marques – UNICA – Hospital da Luz.)*

A ecocardiografia transesofágica tem sido considerado o *gold standard* não invasivo para avaliação de trombos dentro do AAEsq, no entanto a RM apresenta boa acuidade e a TC, em metanálise recente, foi considerada alternativa ao ETE (45).

2.3.1. Morfologia

Existem diversas classificações do AAEsq por TC, com relevância prognóstica, umas relacionáveis com o número de lobos e trabeculação (46) e outras com a forma/tipo (47, 48) (ver **Figura 6a e 6b**).

No entanto, apesar das ótimas imagens conseguidas por TC, a reprodutibilidade da classificação de Wang e Di Biase pode não ser tão alta, como evidenciada pelo estudo de Taina et al (49).

2.3.2. Dimensão, Função e Estrutura

O AAEsq é mais distensível do que a AEsq, servindo de tampão para manter constantes o volume e a pressão da AEsq. A dimensão e função do AAEsq é provavelmente mais dependente do VEsq do que a AEsq, o que ajudaria a explicar a maior relação direta entre a probabilidade de trombo e evento cardiovascular com a função VESq do que com a dilatação da AEsq nos doentes em FA.

A dimensão do AAEsq não se correlaciona fortemente com a dimensão da AEsq (ver **Capítulo IX**).

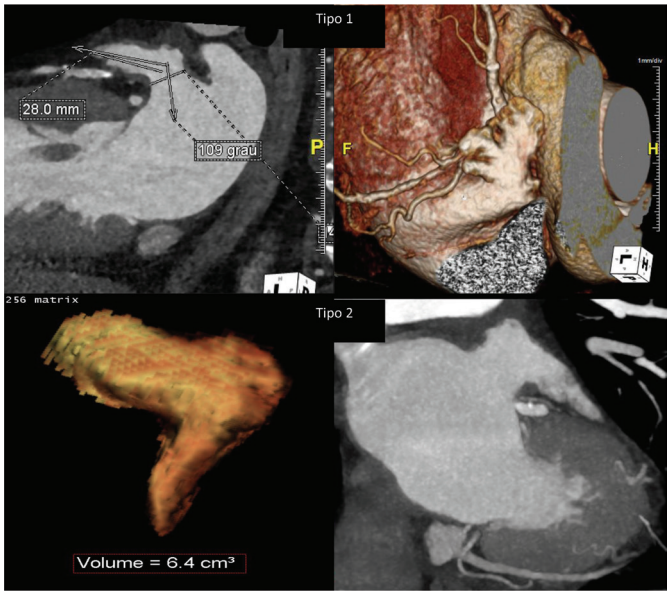

FIGURA 6a
Classificação morfológica dos AAEsq baseada em Wang e Di Biase, com correlação dimensional de Kimura.
(Imagens Hugo Marques — UNICA — Hospital da Luz.)

Tipo 1 Cactus
Tipo 2 Chicken Wing
Tipo 3 Windsock
Tipo 4 Cauliflower

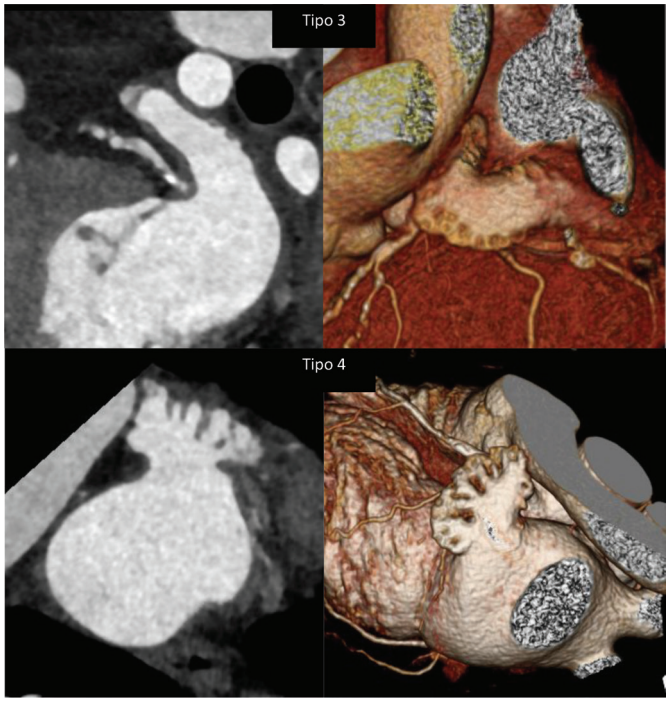

FIGURA 6b
Classificação morfológica dos AAEsq baseada em Wang e Di Biase, com correlação dimensional de Kimura.
(Imagens Hugo Marques — UNICA — Hospital da Luz.)

Tipo 1 Cactus
Tipo 2 Chicken Wing
Tipo 3 Windsock
Tipo 4 Cauliflower

A modificação estrutural que acontece em doentes com FA é semelhante à que ocorre na AEsq, com dilatação, inflamação, disfunção e fibrose (50, 51), o que favorece a presença de trombo dado a maior estase, a disfunção do endotélio e o estado pro-coagulante que daí resulta.

2.3.3. Contributo prognóstico

O aumento do comprimento, do número de lobos e volumétrico, a fibrose da parede, uma menor dimensão do *ostium* assim como uma morfologia não "*chicken wing*" estão associados a estase e a maior probabilidade de trombo (52-55).

2.4. VEIAS PULMONARES

Embriologicamente, o botão das veias pulmonares dá origem à aurícula esquerda. A presença de endotélio auricular nas veias pulmonares permite que estas sejam o local de origem e perpetuação da fibrilhação auricular (56, 57).

Existem diferentes padrões de veias pulmonares, sendo que a existência de 4 *ostiae* é o mais frequente, com duas veias pulmonares à direita (drenando a média na veia pulmonar superior direita) e duas à esquerda (ver **Figura 7**).
O padrão das veias pulmonares e a dimensão dos seus *ostiae* podem estar relacionados com a recorrência de FA após terapêutica ablativa (58, 59).

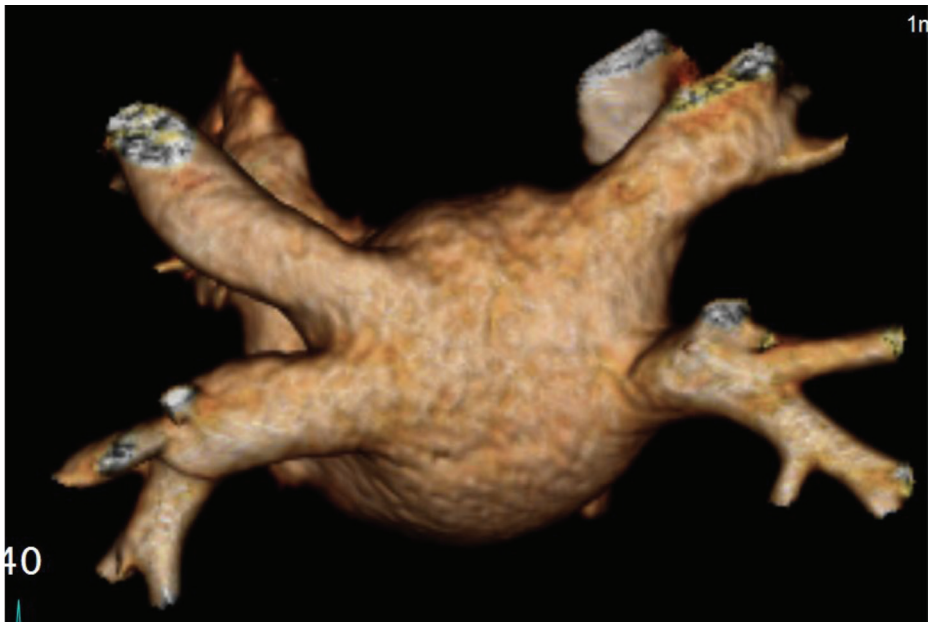

FIGURA 7
Imagem volumetrica 3D do padrão habitual das veias pulmonares, com 4 *ostiae*, 2 à direita e 2 à esquerda sem parede livre entre eles.
(Imagens Hugo Marques – UNICA – Hospital da Luz.)

2.5. FIBRILHAÇÃO AURICULAR

É a arritmia crónica mais frequente, com uma incidência e prevalência que aumenta com a idade , desde cerca de 3% dos adultos com mais de 20 anos até chegar a afetar quase 10% das pessoas com mais de 80 anos (60). Em Portugal afeta 2,5% da população com mais de 40 anos (61).

Pode aparecer em doentes sem causa aparente, no entanto são fatores de risco: a doença valvular (sobretudo mitral reumática), a insuficiência cardíaca, o exercício físico vigoroso, a apneia do sono, a DPCO, a DRC, a HTA, a diabetes, a doença coronária, a disfunção tiroideia, o consumo de álcool, a obesidade e a idade avançada. Há igualmente um substrato genético predisponente. Na ausência de patologia valvular como seu fator fisiopatológico, a FA designa-se como "não valvular".

Caracteriza-se por FC marcadamente irregulares e frequentemente altas, aspeto que se extremo pode condicionar morbilidade por diminuição do débito cardíaco e/ /ou desencadear de isquemia. No entanto, a principal fonte de morbilidade e mortalidade prende-se com a propensão para a formação de trombos.

Cerca de 10 a 40% dos doentes com FA são hospitalizados em cada ano.

A FA está independentemente associada a um risco 2 vezes maior de morte (de todas as causas) no homem e 1,5 vezes nas mulheres.

O risco de evento tromboembólico pode ser calculado com o *score* CHA_2DS_2VASc (62).

TABELA 2

Tabela com o score CHA_2DS_2VASc

	Condição	Pontos
C	Insuficiência Cardíaca	1
H	Hipertensão	1
A2	> ou = 75 anos	2
D	DM	1
S2	Sexo feminino	2
V	Doença vascular	1
A	(65-74) anos	1
Sc	História de AVC / AIT / Tromboembolismo	1

Pontuação:

2 — risco alto — anticoagulação plena

1 — risco intermédio — zona cinzenta, anticoagulação individualizada

0 — risco baixo — só antiagregação ou sem terapêutica

A FA pode ser classificada em:

- Paroxística — na maioria das vezes termina sozinha em 48h, mas pode durar até 7 dias
- Persistente — FA de duração superior a 7 dias
- Persistente de longa data — FA que dura há mais de um ano e quando se adaptam medidas de controlo de ritmo
- Permanente — quando é aceite e não se fazem mais medidas de controlo de ritmo

Idealmente o objetivo clínico é a conversão dos doentes a ritmo sinusal (o que pode ser conseguido com cardioversão farmacológica ou elétrica) e a sua preservação (ausência de recidivas de FA). A preservação do ritmo sinusal pode ser efetuada através de terapêutica médica (por exemplo fármacos antiarrítmicos classe III) ou de técnicas ablativas percutâneas e/ou cirúrgicas.
Na impossibilidade de conversão a ritmo sinusal, a terapêutica centra-se na prevenção de morbi-mortalidade, com controlo de resposta ventricular e prevenção da formação de trombos. Este último aspeto pode ser efetuado farmacologicamente ou por encerramento cirúrgico ou percutâneo do AAEsq.

2.6. TRATAMENTO PERCUTÂNEO DA FA

2.6.1. Ablação percutânea de FA

A ablação percutânea da FA é atualmente uma das terapêuticas com maior indicação nos casos de FA sintomática, sobretudo em doentes com FA paroxística e aurículas não muito dilatadas.
Esta terapêutica, que visa o retorno a ritmo sinusal e a cura da FA, teve origem nos bons resultados obtidos no Hospital de Santa Cruz em 1996, pela equipa liderada por Queiroz e Melo, nos doentes submetidos a uma cirurgia inovadora, que substituía a fragmentação da aurícula cirúrgica (no *Maze* clássico) por uma aplicação intra-operatória de radiofrequência a isolar as veias pulmonares. (63). Esta fragmentação intra-operatória, mas não cirúrgica permitia menor morbilidade e comprovava a eficácia do isolamento termoeléctrico por radiofrequência. Ainda em 1996, a equipa

liderada por Adragão verificou a exequibilidade da realização do procedimento de fragmentação termoeléctrica por radiofrequência apenas por via percutânea (ver **Figura 8**). A equipa de Adragão apresentou os cinco primeiros casos mundiais em 1997 no Congresso Português de Cardiologia e na sessão inaugural do North American Society of Pacing and Electrophysiology, (atualmente Heart Rhythm Society). (64, 65).

Em 1998 Haissaguerre confirmou a importância dos focos localizados nas veias pulmonares e a possibilidade da sua ablação após Jais ter descrito a origem focal da FA, neles (56, 57). No entanto, a aplicação de radiofrequência nas veias pulmonares resultou numa incidência inaceitável de estenoses, pelo que a técnica atual tem por base a técnica inicialmente descrita pelo grupo português de Adragão.
A ablação percutânea consiste na colocação de um cateter ablativo (por radiofrequência) ou balão de crioablação na AEsq junto dos *ostiae* das veias pulmonares e, por ablação e subsequente indução de fibrose conseguir o isolamento elétrico das mesmas. Consoante o tipo de FA poderão estar indicadas outras zonas de ablação. Outro dos avanços relevantes da técnica ocorreu com o desenvolvimento de mapeamento tridimensional (permitindo por exemplo fusão com as imagens de TC), com a localização precisa dos pontos de ablação, assim como a utilização de sistemas robotizados para facilitar o procedimento, sendo Pappone uma figura destacada neste contexto (66).

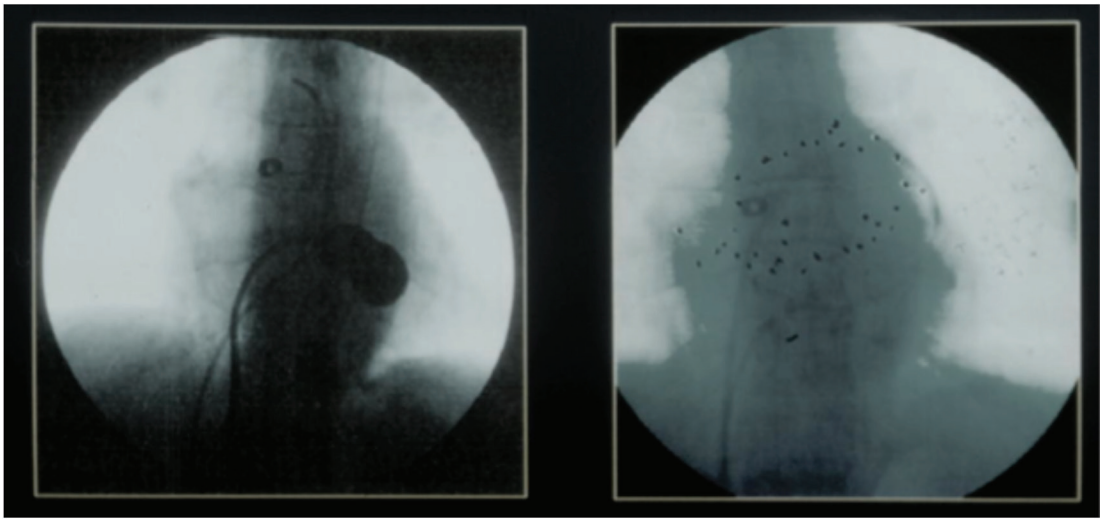

FIGURA 8
Valvuloplastia Mitral de balão e 1.º isolamento das veias pulmonares. Hospital de Santa Cruz, Lisboa 1996 *(imagem cedida pelo Prof. Dr. P. Adragão)*.

Apesar de poder curar a FA e ser um procedimento seguro com baixa morbilidade e mortalidade (67), esta terapêutica tem taxas de recidiva não desprezíveis (60), sendo que os resultados do nosso grupo foram publicados por Adragão et al. (68) com taxas de recidiva anuais na ordem dos 20% sendo que outros referem recidivas superiores a 50% aos 6 anos (69).

O sucesso da terapêutica ablativa é dependente de vários fatores: desde o tipo de FA, à fibrose pré-existente na aurícula, à fibrose que foi possível induzir, até a marcadores dimensionais auriculares como o volume máximo (18, 19, 40).

O nosso grupo publicou uma comparação prognóstica (segurança e avaliação de recidiva) entre doentes em que a ablação foi realizada com e sem navegação magnética (68).

A importância de identificar pré-procedimento quais os doentes que mais iriam beneficiar da sua realização, neste contexto de resposta heterogénea e percentagem de recidiva alta, é fundamental numa medicina de custo-benefício. Este aspeto foi alvo de investigação pelo nosso grupo, tendo sido desenvolvido o *score* ATLAS (70) (**Manuscrito 1**).

O ATLAS tem em linha de conta a idade, o tipo de FA, o volume auricular, o sexo e os hábitos tabágicos. O principal fator de ponderação é o volume da AEsq.

TABELA 3

ATLAS score

Variable	Number of points
Age > 60 years	1
Type of AF (non-paroxysmal)	2
Left **a**trial volume indexed to BSA	1 point per each 10 mL/m^2 (rounded to nearest integer)
Sex (female)	4
Smoking (current cigarette smoking)	7

Um *score* ATLAS é baixo até 5 pontos, intermédio de 6 e 10 e alto se maior que 10.

2.6.2. Oclusão do AAEsq

Esta terapêutica visa excluir a principal fonte embólica nos doentes com FA, podendo ser realizada percutâneamente ou através de cirurgia.

A imagem por TC tem utilidade quer para planeamento do procedimento, quer para avaliar o resultado e as complicações (ver **Figura 9** e **Capítulo III**).

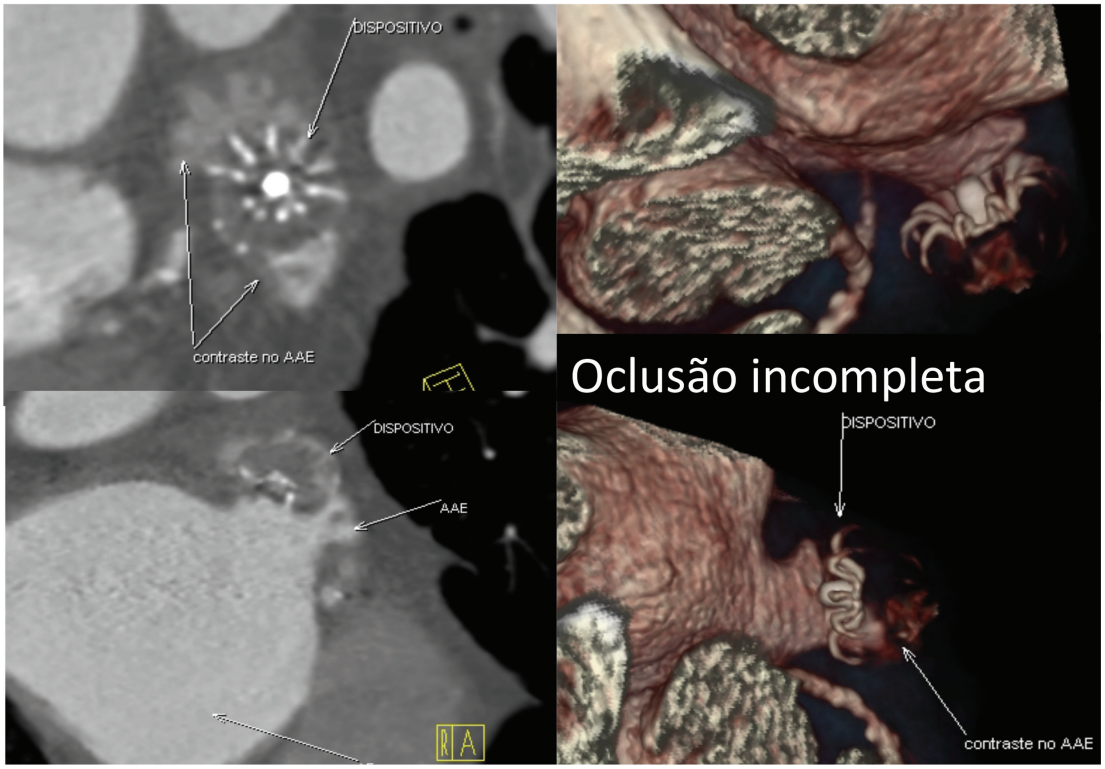

FIGURA 9

Dispositivo para oclusão do AAEsq muito introduzido, com trombo associado e permeabilidade parcial do apêndice — maior risco de evento tromboembólico. *Imagem da slide da apresentação da palestra do Arritmias 2017 — Congresso da Associação Portuguesa de Arritmologia, Pacing e Electrofisiologia. (Imagens Hugo Marques — UNICA — Hospital da Luz.)*

BIBLIOGRAFIA

1. Hara H, Virmani R, Holmes DR, Jr., et al. Is the left atrial appendage more than a simple appendage? Catheterization and cardiovascular interventions : official journal of the Society for Cardiac Angiography & Interventions. 2009;74(2):234-42.
2. To AC, Flamm SD, Marwick TH, et al. Clinical utility of multimodality LA imaging: assessment of size, function, and structure. JACC Cardiovasc Imaging. 2011;4(7):788-98.
3. Genc B, Solak A, Kantarci M, et al. Anatomical features and clinical importance of left atrial diverticula: MDCT findings. Clin Anat. 2014;27(5):738-47.
4. De Ponti R, Lumia D, Marazzi R, et al. Left atrial diverticula in patients undergoing atrial fibrillation ablation: morphologic analysis and clinical impact. J Cardiovasc Electrophysiol. 2013;24(11):1232-9.
5. Tsang TS, Abhayaratna WP, Barnes ME, et al. Prediction of cardiovascular outcomes with left atrial size: is volume superior to area or diameter? J Am Coll Cardiol. 2006;47(5):1018-23.
6. Hoit BD. Left atrial size and function: role in prognosis. J Am Coll Cardiol. 2014;63(6):493-505.
7. Caselli S, Canali E, Foschi ML, et al. Long-term prognostic significance of three-dimensional echocardiographic parameters of the left ventricle and left atrium. Eur J Echocardiogr. 2010;11(3):250-6.
8. Fatema K, Barnes ME, Bailey KR, et al. Minimum vs. maximum left atrial volume for prediction of first atrial fibrillation or flutter in an elderly cohort: a prospective study. Eur J Echocardiogr. 2009;10(2):282-6.
9. Pozzoli M, Capomolla S, Sanarico M, et al. Doppler evaluations of left ventricular diastolic filling and pulmonary wedge pressure provide similar prognostic information in patients with systolic dysfunction after myocardial infarction. Am Heart J. 1995;129(4):716-25.
10. Pagel PS, Kehl F, Gare M, et al. Mechanical function of the left atrium: new insights based on analysis of pressure-volume relations and Doppler echocardiography. Anesthesiology. 2003;98(4):975-94.
11. Mitchell JH, Shapiro W. Atrial function and the hemodynamic consequences of atrial fibrillation in man. Am J Cardiol. 1969;23(4):556-67.
12. Appleton CP, Hatle LK, Popp RL. Relation of transmitral flow velocity patterns to left ventricular diastolic function: new insights from a combined hemodynamic and Doppler echocardiographic study. J Am Coll Cardiol. 1988;12(2):426-40.

13. Eshoo S, Ross DL, Thomas L. Impact of mild hypertension on left atrial size and function. Circ Cardiovasc Imaging. 2009;2(2):93-9.
14. Delgado V, Vidal B, Sitges M, et al. Fate of left atrial function as determined by real--time three-dimensional echocardiography study after radiofrequency catheter ablation for the treatment of atrial fibrillation. Am J Cardiol. 2008;101(9):1285-90.
15. Marsan NA, Tops LF, Holman ER, et al. Comparison of left atrial volumes and function by real-time three-dimensional echocardiography in patients having catheter ablation for atrial fibrillation with persistence of sinus rhythm versus recurrent atrial fibrillation three months later. Am J Cardiol. 2008;102(7):847-53.
16. Saraiva RM, Demirkol S, Buakhamsri A, et al. Left atrial strain measured by two--dimensional speckle tracking represents a new tool to evaluate left atrial function. J Am Soc Echocardiogr. 2010;23(2):172-80.
17. Cameli M, Caputo M, Mondillo S, et al. Feasibility and reference values of left atrial longitudinal strain imaging by two-dimensional speckle tracking. Cardiovascular ultrasound. 2009;7:6.
18. Marrouche NF, Wilber D, Hindricks G, et al. Association of atrial tissue fibrosis identified by delayed enhancement MRI and atrial fibrillation catheter ablation: the DECAAF study. JAMA. 2014;311(5):498-506.
19. McGann CJ, Kholmovski EG, Oakes RS, et al. New magnetic resonance imaging-based method for defining the extent of left atrial wall injury after the ablation of atrial fibrillation. J Am Coll Cardiol. 2008;52(15):1263-71.
20. Benjamin EJ, D'Agostino RB, Belanger AJ, et al. Left atrial size and the risk of stroke and death. The Framingham Heart Study. Circulation. 1995;92(4):835-41.
21. Chinali M, de Simone G, Roman MJ, et al. Left atrial systolic force and cardiovascular outcome. The Strong Heart Study. Am J Hypertens. 2005;18(12 Pt 1):1570-6; discussion 7.
22. Gottdiener JS, Kitzman DW, Aurigemma GP, et al. Left atrial volume, geometry, and function in systolic and diastolic heart failure of persons > or =65 years of age (the cardiovascular health study). Am J Cardiol. 2006;97(1):83-9.
23. Gupta S, Matulevicius SA, Ayers CR, et al. Left atrial structure and function and clinical outcomes in the general population. Eur Heart J. 2013;34(4):278-85.
24. Kaminski M, Steel K, Jerosch-Herold M, et al. Strong cardiovascular prognostic implication of quantitative left atrial contractile function assessed by cardiac magnetic resonance imaging in patients with chronic hypertension. J Cardiovasc Magn Reson. 2011;13:42.
25. Pritchett AM, Mahoney DW, Jacobsen SJ, et al. Diastolic dysfunction and left atrial volume: a population-based study. J Am Coll Cardiol. 2005;45(1):87-92.
26. Takemoto Y, Barnes ME, Seward JB, et al. Usefulness of left atrial volume in predicting first congestive heart failure in patients > or = 65 years of age with well-preserved left ventricular systolic function. Am J Cardiol. 2005;96(6):832-6.
27. Vasan RS, Larson MG, Levy D, et al. Doppler transmitral flow indexes and risk of atrial fibrillation (the Framingham Heart Study). Am J Cardiol. 2003;91(9):1079-83.
28. Wang M, Yip GW, Wang AY, et al. Peak early diastolic mitral annulus velocity by tissue Doppler imaging adds independent and incremental prognostic value. J Am Coll Cardiol. 2003;41(5):820-6.

29. Abhayaratna WP, Fatema K, Barnes ME, et al. Left atrial reservoir function as a potent marker for first atrial fibrillation or flutter in persons > or = 65 years of age. Am J Cardiol. 2008;101(11):1626-9.
30. Leung DY, Boyd A, Ng AA, et al. Echocardiographic evaluation of left atrial size and function: current understanding, pathophysiologic correlates, and prognostic implications. Am Heart J. 2008;156(6):1056-64.
31. Tsang TS, Barnes ME, Gersh BJ, et al. Prediction of risk for first age-related cardiovascular events in an elderly population: the incremental value of echocardiography. J Am Coll Cardiol. 2003;42(7):1199-205.
32. Moller JE, Hillis GS, Oh JK, et al. Left atrial volume: a powerful predictor of survival after acute myocardial infarction. Circulation. 2003;107(17):2207-12.
33. Inaba Y, Yuda S, Kobayashi N, et al. Strain rate imaging for noninvasive functional quantification of the left atrium: comparative studies in controls and patients with atrial fibrillation. J Am Soc Echocardiogr. 2005;18(7):729-36.
34. Mochizuki A, Yuda S, Oi Y, et al. Assessment of left atrial deformation and synchrony by three-dimensional speckle-tracking echocardiography: comparative studies in healthy subjects and patients with atrial fibrillation. J Am Soc Echocardiogr. 2013;26(2):165-74.
35. Providencia R, Trigo J, Paiva L, et al. The role of echocardiography in thromboembolic risk assessment of patients with nonvalvular atrial fibrillation. J Am Soc Echocardiogr. 2013;26(8):801-12.
36. Schneider C, Malisius R, Krause K, et al. Strain rate imaging for functional quantification of the left atrium: atrial deformation predicts the maintenance of sinus rhythm after catheter ablation of atrial fibrillation. Eur Heart J. 2008;29(11):1397-409.
37. Di Salvo G, Caso P, Lo Piccolo R, et al. Atrial myocardial deformation properties predict maintenance of sinus rhythm after external cardioversion of recent-onset lone atrial fibrillation: a color Doppler myocardial imaging and transthoracic and transesophageal echocardiographic study. Circulation. 2005;112(3):387-95.
38. King JB, Azadani PN, Suksaranjit P, et al. Left Atrial Fibrosis and Risk of Cerebrovascular and Cardiovascular Events in Patients With Atrial Fibrillation. J Am Coll Cardiol. 2017;70(11):1311-21.
39. Abecasis J, Dourado R, Ferreira A, et al. Left atrial volume calculated by multi-detector computed tomography may predict successful pulmonary vein isolation in catheter ablation of atrial fibrillation. Europace. 2009;11(10):1289-94.
40. Costa FM, Ferreira AM, Oliveira S, et al. Left atrial volume is more important than the type of atrial fibrillation in predicting the long-term success of catheter ablation. Int J Cardiol. 2015;184:56-61.
41. Verma A, Wazni OM, Marrouche NF, et al. Pre-existent left atrial scarring in patients undergoing pulmonary vein antrum isolation: an independent predictor of procedural failure. J Am Coll Cardiol. 2005;45(2):285-92.
42. Daccarett M, Badger TJ, Akoum N, et al. Association of left atrial fibrosis detected by delayed-enhancement magnetic resonance imaging and the risk of stroke in patients with atrial fibrillation. J Am Coll Cardiol. 2011;57(7):831-8.

43. Blackshear JL, Odell JA. Appendage obliteration to reduce stroke in cardiac surgical patients with atrial fibrillation. Ann Thorac Surg. 1996;61(2):755-9.
44. Di Biase L, Burkhardt JD, Mohanty P, et al. Left atrial appendage: an underrecognized trigger site of atrial fibrillation. Circulation. 2010;122(2):109-18.
45. Romero J, Husain SA, Kelesidis I, et al. Detection of left atrial appendage thrombus by cardiac computed tomography in patients with atrial fibrillation: a meta-analysis. Circ Cardiovasc Imaging. 2013;6(2):185-94.
46. Erol B, Karcaaltincaba M, Aytemir K, et al. Analysis of left atrial appendix by dual-source CT coronary angiography: morphologic classification and imaging by volume rendered CT images. European journal of radiology. 2011;80(3):e346-50.
47. Wang Y, Di Biase L, Horton RP, et al. Left atrial appendage studied by computed tomography to help planning for appendage closure device placement. J Cardiovasc Electrophysiol. 2010;21(9):973-82.
48. Kimura T, Takatsuki S, Inagawa K, et al. Anatomical characteristics of the left atrial appendage in cardiogenic stroke with low CHADS2 scores. Heart Rhythm. 2013;10(6):921-5.
49. Taina M, Korhonen M, Haataja M, et al. Morphological and volumetric analysis of left atrial appendage and left atrium: cardiac computed tomography-based reproducibility assessment. PLoS One. 2014;9(7):e101580.
50. Frustaci A, Chimenti C, Bellocci F, et al. Histological substrate of atrial biopsies in patients with lone atrial fibrillation. Circulation. 1997;96(4):1180-4.
51. Shirani J, Alaeddini J. Structural remodeling of the left atrial appendage in patients with chronic non-valvular atrial fibrillation: Implications for thrombus formation, systemic embolism, and assessment by transesophageal echocardiography. Cardiovasc Pathol. 2000;9(2):95-101.
52. Akoum N, Fernandez G, Wilson B, et al. Association of atrial fibrosis quantified using LGE-MRI with atrial appendage thrombus and spontaneous contrast on transesophageal echocardiography in patients with atrial fibrillation. J Cardiovasc Electrophysiol. 2013;24(10):1104-9.
53. Beinart R, Heist EK, Newell JB, et al. Left atrial appendage dimensions predict the risk of stroke/TIA in patients with atrial fibrillation. J Cardiovasc Electrophysiol. 2011;22(1):10-5.
54. Di Biase L, Santangeli P, Anselmino M, et al. Does the left atrial appendage morphology correlate with the risk of stroke in patients with atrial fibrillation? Results from a multicenter study. J Am Coll Cardiol. 2012;60(6):531-8.
55. Yamamoto M, Seo Y, Kawamatsu N, et al. Complex left atrial appendage morphology and left atrial appendage thrombus formation in patients with atrial fibrillation. Circ Cardiovasc Imaging. 2014;7(2):337-43.
56. Haissaguerre M, Jais P, Shah DC, et al. Spontaneous initiation of atrial fibrillation by ectopic beats originating in the pulmonary veins. N Engl J Med. 1998;339(10):659-66.
57. Jais P, Haissaguerre M, Shah DC, et al. A focal source of atrial fibrillation treated by discrete radiofrequency ablation. Circulation. 1997;95(3):572-6.
58. Guler E, Guler GB, Demir GG, et al. Effect of Pulmonary Vein Anatomy and Pulmonary Vein Diameters on Outcome of Cryoballoon Catheter Ablation for Atrial Fibrillation. Pacing Clin Electrophysiol. 2015;38(8):989-96.

59. McLellan AJ, Ling LH, Ruggiero D, et al. Pulmonary vein isolation: the impact of pulmonary venous anatomy on long-term outcome of catheter ablation for paroxysmal atrial fibrillation. Heart Rhythm. 2014;11(4):549-56.
60. Kirchhof P, Benussi S, Kotecha D, et al. 2016 ESC Guidelines for the management of atrial fibrillation developed in collaboration with EACTS. Eur Heart J. 2016;37(38):2893-962.
61. Bonhorst D, Mendes M, Adragao P, et al. Prevalence of atrial fibrillation in the Portuguese population aged 40 and over: the FAMA study. Rev Port Cardiol. 2010;29(3):331-50.
62. Naccarelli GV, Panaccio MP, Cummins G, et al. CHADS2 and CHA2DS2-VASc risk factors to predict first cardiovascular hospitalization among atrial fibrillation/atrial flutter patients. Am J Cardiol. 2012;109(10):1526-33.
63. Melo JQ, Neves J, Adragao P, et al. When and how to report results of surgery on atrial fibrillation. European journal of cardio-thoracic surgery : official journal of the European Association for Cardio-thoracic Surgery. 1997;12(5):739-44; discussion 44-5.
64. Adragao PP, Cavaco D, Ferreira AM, et al. Safety and Long-Term Outcomes of Catheter Ablation of Atrial Fibrillation Using Magnetic Navigation versus Manual Conventional Ablation: A Propensity-Score Analysis. J Cardiovasc Electrophysiol. 2016;27 Suppl 1:S11-6.
65. Adragão P MF, Parreira L, Morgado F, Almeida M, Ribeiras R, Bonhorst D, Seabra Gomes R. . Radiofrequency ablation of atrial fibrillation and simultaneous mitral valvuloplasty by percutaneus approach: a new method - first experience. Rev Port Cardiol. 1997;16(Supl I):I-1.
66. Pappone C, Rosanio S, Oreto G, et al. Circumferential radiofrequency ablation of pulmonary vein ostia: A new anatomic approach for curing atrial fibrillation. Circulation. 2000;102(21):2619-28.
67. Cappato R, Calkins H, Chen SA, et al. Updated worldwide survey on the methods, efficacy, and safety of catheter ablation for human atrial fibrillation. Circulation Arrhythmia and electrophysiology. 2010;3(1):32-8.
68. Adragao PP, Cavaco D, Ferreira AM, et al. Safety and Long-Term Outcomes of Catheter Ablation of Atrial Fibrillation Using Magnetic Navigation versus Manual Conventional Ablation: A Propensity-Score Analysis. J Cardiovasc Electrophysiol. 2016;27 Suppl 1:S11-6.
69. Bertaglia E, Tondo C, De Simone A, et al. Does catheter ablation cure atrial fibrillation? Single-procedure outcome of drug-refractory atrial fibrillation ablation: a 6-year multicentre experience. Europace. 2010;12(2):181-7.
70. Mesquita JF, A.M.; Cavaco, D.; Costa, F.M.; Carmo, P.; Marques, H.; Morgado, F.; Mendes, Miguel; Adragão, P. Development and validation of a risk score for predicting atrial fibrillation recurrence after a first catheter ablation procedure — ATLAS score. Europace. 2017.

ANEXOS

MANUSCRITO 1

Development and validation of a risk score for predicting atrial fibrillation recurrence after a first catheter ablation procedure — ATLAS score.

Mesquita, J.F., A.M.; Cavaco, D.; Costa, F.M.; Carmo, P.;
Marques, **H**.; Morgado, F.; Mendes, Miguel; Adragão, P.,

Europace, 2017
https://doi.org/10.1093/europace/eux265

Manuscrito 1

Europace (2017) **0**, 1–8
doi:10.1093/europace/eux265

CLINICAL RESEARCH

Development and validation of a risk score for predicting atrial fibrillation recurrence after a first catheter ablation procedure – ATLAS score

João Mesquita[1†*], António Miguel Ferreira[1,2†], Diogo Cavaco[1,2], Francisco Moscoso Costa[1,2], Pedro Carmo[1,2], Hugo Marques[3], Francisco Morgado[1], Miguel Mendes[1], and Pedro Adragão[1,2]

[1]Cardiology Department, Hospital de Santa Cruz, Av. Prof. Reinaldo dos Santos, 2790-134 Carnaxide, Lisbon, Portugal; [2]Cardiology Department, Hospital da Luz, Lisbon, Portugal; and [3]Radiology Department, Hospital da Luz, Lisbon, Portugal

Received 5 April 2017; editorial decision 11 July 2017; accepted 12 July 2017

Aims Several predictors of relapse after catheter ablation of atrial fibrillation (AF) have been established, but assessing each patient's individual risk remains challenging. Our aim was to develop and validate a score to estimate the risk of AF recurrence after the first radiofrequency pulmonary vein isolation (PVI) procedure.

Methods and results Independent predictors of AF relapse were identified retrospectively in a two-centre registry of 1934 patients who underwent a first PVI procedure. Using the Cox regression hazard ratios of designated variables, a risk score was developed in a random sample of 50% of the patients (development cohort) and validated in the remaining (validation cohort) half. The accuracy and discriminative power of the predictive model were assessed in both subgroups. During a follow-up of 4.2 ± 2.7 years, 522 patients (27%) relapsed. Five independent predictors of AF recurrence were identified and included in the score: age >60 years (1 point), female sex (4 points), non-paroxysmal AF (2 points), current smoking (7 points) and indexed left atrial volume (1 point for each 10 mL/m^2). The score showed good discriminative power (censored c-statistic of 0.75 in both cohorts). In the development group, AF relapse rates were 8, 11, and 17%/year for low (<6 points), intermediate (6–10 points), and high-risk patients (>10 points), respectively ($P < 0.001$). In the validation group, AF recurrence rates were 8, 11, and 18%/year, respectively ($P < 0.001$).

Conclusion A simple risk score to estimate the rate of AF recurrence after ablation was developed and validated. An external assessment of its usefulness as a patient selection tool seems warranted.

Keywords Atrial fibrillation • Atrial fibrillation recurrence • Pulmonary vein isolation • Radiofrequency catheter ablation • Prognosis • Risk score

Introduction

Pulmonary vein isolation (PVI) is now a well-established treatment for selected patients with atrial fibrillation (AF).[1] However, despite high early success rates, AF recurrence is common during follow-up, offsetting the potential benefits of the procedure.[2–4] Identifying the patients who are unlikely to remain in sinus rhythm seems a logical way to improve success rates and avoid the unnecessary risks and costs of ineffective ablations. While several predictors of AF relapse have been identified,[2,3] assessing each patient's individual risk of recurrence remains challenging, in part due to the absence of a risk stratification tool that would condense the prognostic information conveyed by several different variables. The purpose of this study was to develop and validate a score to assess the risk of AF recurrence after a first radiofrequency PVI procedure.

* Corresponding author. *E-mail address:* jpmesquita@chlo.min-saude.pt

† The first two authors contributed equally to the study.

cont.

Manuscrito 1

What's new?

- Development and validation of a clinical risk score to estimate the risk of atrial fibrillation (AF) recurrence after a first catheter ablation procedure.
- Identification of long-term independent predictors of AF recurrence in a large dataset of patients.
- Recognition of left atrial volume as the main determinant of AF recurrence after catheter ablation.

Methods

Patient population and study design

All consecutive patients with symptomatic drug-refractory AF undergoing percutaneous PVI in two Portuguese centres (Hospital Santa Cruz, Carnaxide, Portugal; and Hospital da Luz, Lisbon, Portugal) were included in an observational registry, which we used for this retrospective study. The first centre enrolled patients between May 2005 and November 2015, and the second centre between June 2007 and September 2015. From a pool of 2836 procedures, we excluded patients with previous AF ablations ($n = 428$), and those without 3D quantification of LA volume neither by computed tomography (CT) nor electroanatomical mapping ($n = 352$). The latter was used as an exclusion criterion, since left atrial (LA) volume has been shown to be a powerful prognostic marker in this setting.[5,6] Patients who were lost to follow-up less than 6 months after the procedure were also excluded ($n = 122$). The final study population ($n = 1934$) was randomized on a 1:1 ratio into development and validation cohorts. In the development cohort, Cox regression analysis was used to identify independent predictors of clinical and/or electrocardiographic AF recurrence. The β regression coefficients of the selected variables were then used to develop a risk score whose accuracy and discriminative power were evaluated in the validation cohort.

Atrial fibrillation was categorized as paroxysmal if self-terminated in <7 days, persistent if episodes lasted ≥7 days or required cardioversion, or long-standing persistent if AF was maintained for more than 12 months.[1] The majority of patients ($n = 1332$, 69%) underwent a 64-slice cardiac CT scan less than 48 h before the ablation procedure for the assessment of pulmonary vein anatomy, measurement of LA volume, exclusion of thrombi, and integration with electroanatomical mapping.[6] Left atrial volume was calculated by tracing the LA borders on CT images, excluding the pulmonary veins and the left atrial appendage. In patients where cardiac CT could not be performed (mainly for logistical reasons), LA volume was estimated from CARTO® (Biosense Webster Inc., Diamond Bar, CA, USA) electroanatomical mapping at the time of ablation. Left atrial volumes were indexed to body surface area (BSA). In patients who had LA volume estimated by different methods (2D echocardiogram, cardiac CT and/or electroanatomical mapping), a correlation analysis was performed to assess comparison between all methods.

Pulmonary vein isolation protocol

Pulmonary vein isolation was guided by electroanatomical mapping, using either NavX® (St Jude Medical® Inc, St Paul, MN, USA) or CARTO® systems. The right femoral vein was used as the preferred vascular access, through which three catheter electrodes were introduced: (i) a decapolar catheter, advanced through the coronary sinus; (ii) a variable circular mapping catheter, placed in the pulmonary veins; and (iii) an irrigated-tip ablation catheter. Left atrial access was established by trans-septal puncture. Radiofrequency ablation was performed more than 5 mm from the PV ostia, with continuous lesions enclosing the left and right pairs of PV. At Hospital Santa Cruz, all patients underwent conventional manually guided ablation, while at Hospital da Luz a Niobe II magnetic navigation system (Stereotaxis® Inc., St. Louis, MO, USA) was used. If typical atrial flutter was previously documented or observed at the time of the procedure, an additional cavotricuspid isthmus (CTI) ablation was performed ($n = 164$ patients). The treatment was considered successful if complete electrophysiological PVI was achieved. When required, an electrical cardioversion was performed at the end of the procedure. Oral anticoagulation was resumed 6 h after the ablation, maintained for 6 months and then withdrawn or continued according to CHA_2DS_2-VASc criteria ($CHADS_2$ before 2009). Patients on vitamin K antagonists with subtherapeutic international normalized ratio (INR) were kept on subcutaneous enoxaparin 1 mg/kg every 12 h until an adequate INR was achieved. As a general rule, class I/III antiarrhythmic drugs were maintained in all patients for the first 3 months after the procedure and then withdrawn if there was no AF recurrence. A proton pump inhibitor was also prescribed for the first month after the ablation.

Study endpoint and patient follow-up

The study endpoint was AF recurrence, defined as symptomatic or documented AF and/or other atrial arrhythmias, after a 3-month blanking period. Symptomatic AF was defined as the presence of symptoms considered to be likely due to AF episodes. Documented AF was defined by the presence of at least one episode of AF lasting more than 30 s in any electrocardiogram (ECG), 24 h Holter monitoring or event-loop recording. The follow-up protocol comprised outpatient visits with 12-lead ECG and 24 h Holter monitoring on the 1st, 3rd, 6th, and 12th months post-ablation, followed by yearly assessments. Patients were encouraged to contact the department if they experienced symptoms of AF recurrence. Whenever clinical records were insufficient, a structured telephonic interview was conducted. Patients who were kept on antiarrhythmic drugs after the 3rd month of follow-up were not considered as failed ablation.

Statistical analysis

Normally and non-normally distributed variables were expressed as mean ± standard deviation and median, respectively. Differences between groups were assessed using independent samples *t*-test and Fisher's exact test for continuous and categorical variables, respectively. The study population was split into development and validation cohorts by generating a random number for each patient and assigning odd and even numbers to each of these groups.

Univariate proportional-hazards Cox regression was used to identify predictors of time to AF recurrence in the development cohort. The following variables were assessed: age, sex, type of AF (paroxysmal vs. non-paroxysmal), indexed LA volume, body mass index, hypertension, diabetes, cigarette smoking, hypercholesterolaemia, known obstructive coronary artery disease, and left ventricular systolic dysfunction (ejection fraction <50%). Smoking was defined as any cigarette consumption during the previous 6 months. In order to simplify clinical score calculations, age was dichotomized using a threshold (60 years) identified with receiver-operating characteristics (ROC) curve analysis.

Pearson's correlation with a two-tailed test of significance was used to evaluate LA volume estimation by different methods.

Variables with a *P*-value ≤0.10 in univariate analysis were entered simultaneously in a multivariate Cox regression model and considered to be statistically significant if $P < 0.05$. Multicollinearity was excluded by assessing Pearson's correlation coefficient between pairs of continuous variables (all <0.60). In order to create a practical risk score, each of the independent predictors was assigned a number of weighted points proportional to its β regression coefficient value (rounded to the nearest

cont.

Manuscrito 1

Table 1 Baseline patient characteristics

	All patients (*n*=1934)	Development group (*n*=960)	Validation group (*n*=974)	*P*-value
Age (years)	59±11	58±12	59±11	0.04
Male sex—no. (%)	1330 (69)	664 (69)	666 (68)	0.40
Body mass index—kg/m^2 (IQR)	27 (5)	26 (5)	27 (5)	0.53
Type of AF				0.41
Paroxysmal—no. (%)	1488 (77)	734 (76)	754 (77)	–
Persistent—no. (%)	284 (15)	147 (15)	137 (14)	–
Long-standing—no. (%)	162 (8)	74 (8)	88 (9)	–
Indexed LA volume mL/m^2 (IQR)	54 (44-65)	55 (44-65)	54 (44-66)	0.49
Hypertension—no. (%)	770 (40)	380 (40)	390 (40)	0.89
Diabetes mellitus—no. (%)	136 (7)	62 (7)	74 (8)	0.38
Hypercholesterolemia—no. (%)	408 (21)	204 (21)	204 (21)	0.78
Current smoking—no. (%)	188 (10)	94 (10)	94 (10)	0.88
Known coronary heart disease—no. (%)	82 (4)	44 (5)	38 (4)	0.43
LV systolic dysfunction—no. (%)	153 (8)	81 (8)	72 (7)	0.31
Previous stroke—no. (%)	46 (2)	21 (2)	25 (3)	0.66
CHA_2DS_2-VASc—no. (IQR)	2 (2)	2 (2)	2 (2)	0.43
Patients with at least 1 antiarrhythmic drug—no. (%)	1840 (95)	918 (96)	922 (95)	0.46

AF, atrial fibrillation; LA, left atrium; IQR, interquartile range; LV, left ventricle.

integer)—the smallest beta-coefficient was identified and regarded as the least common denominator, by which all others where then divided, yielding the multiplying coefficient for each variable in the score. The resulting score, defined as the sum of the points assigned to the risk factors of each individual, was calculated in both the development and validation cohorts. Score thresholds for defining low, intermediate, and high-risk of relapse were chosen in the development cohort through analysis of (i) log-rank and (ii) χ^2 tests, (iii) statistically significant differences between ATLAS score values, (iv) visual inspection of Kaplan–Meier curves of AF-free survival, (v) pairwise comparison between all risk strata, and (vi) patients representation in each stratum. These thresholds were then applied to the validation cohort.

Differences in actuarial curves were assessed with the log-rank test. The score's discriminative power (i.e. the extent to which the model can differentiate those who will or will not relapse) was evaluated by the censored C-index.[7] Model calibration (reflecting how close predicted recurrence rates are to the actual observed rates) was assessed by the calibration-in-the-large statistic and calibration slope.[8] Statistical analysis was performed using Statistical Package for Social Sciences (SPSS) version 22.0 (SPSS Inc., Chicago, IL, USA) for Mac OS. Statistical significance was set at P <0.05 (two-sided).

Ethical standards

All human and animal studies have been approved by the appropriate ethics committee and have therefore been performed in accordance with the ethical standards laid down in the 1964 Declaration of Helsinki and its later amendments. The patients signed an informed consent both for the procedure and publication of any relevant data.

Results

The baseline clinical characteristics of the 1934 patients included in this study are summarized in *Table 1*. Overall, the development and validation cohorts were well balanced, except for a small but statistically significant difference in mean age. Regarding LA size assessment, 2D echocardiogram correlated poorly with cardiac CT (n = 227, r = 0.43, P < 0.001) and electroanatomical mapping (n = 416, r = 0.47, P < 0.001). A good correlation between CT and CARTO® volume estimation methods was observed (n = 748, r = 0.77, P < 0.001) (Supplementary material online, *Figure S1*).

During a mean follow-up of 4.2 ± 2.7 years, 522 patients (27%) experienced AF recurrence (259 and 263 in the development and validation groups, respectively, P = 0.88). Less than 5% of these recurrences in both groups were due to atrial arrhythmias other than AF (P = 0.58). The majority of AF relapses were established by both symptoms and electrocardiographic documentation (n = 282; 54%), whereas clinical relapse (n = 177; 34%) and documented silent AF (n = 63; 12%) accounted for the remainder adjudicated recurrences.

Although atrial flutter was previously documented or induced in 164 patients, an additional CTI ablation was performed in 480 patients—criteria based on operator's decision. CTI ablation had no impact in AF-free survival (HR 1.09, 95% CI 0.84–1.41, P = 0.54) and AF annual relapse rates.[9] Maintaining antiarrhythmic drug therapy after the 3-month blanking period had no impact in AF relapse in the subgroup of patients who received CTI ablation.

At the end of the procedure, 433 patients underwent electrical cardioversion.

After the 3rd month of follow-up, 217 patients (11%) were kept on antiarrhythmic drug therapy (109 in the derivation group and 108 in the validation group, P = 0.71), with 52% relapsing in each group (P = 0.76). The vast majority was prescribed class III antiarrhythmic agents—amiodarone [153 (71%) patients], sotalol [33 (15%) patients]—but also a selection of class I C drugs—flecainide [16 (7%) patients], and propafenone [15 (7%) patients]—again without significant differences between both development

cont.

Manuscrito 1

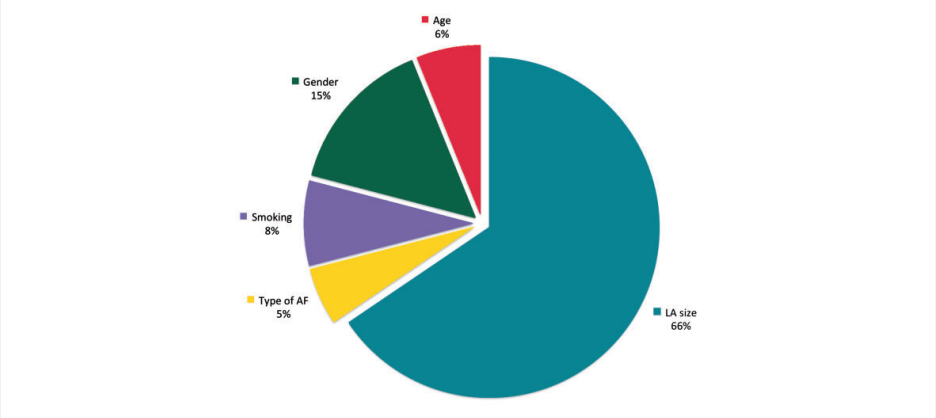

Figure 1 Relative contribution of the five components of the ATLAS score to each individual's final score value.

Table 2 Predictors of time to AF recurrence in univariate and multivariate Cox regression analysis

	Univariate analysis			Multivariate analysis			
	HR *(NA)*	95% CI	*P*-value	(B)	aHR	95% CI	*P*-value
Age >60 years	1.32	1.11–1.57	0.002	0.12	1.25	1.04-1.49	0.017
Female sex	1.19	0.99–1.43	0.06	0.39	1.25	1.03–1.52	0.023
Smoking	1.75	1.31–2.33	<0.001	0.65	1.88	1.40–2.51	<0.001
Non-paroxysmal AF	1.28	1.06–1.55	0.01	0.22	1.24	1.02–1.50	0.032
LA volume (each 10 mL/m^2)	1.01	1.01–1.02	<0.001	0.11	1.12	1.04–1.17	<0.001
Hypercholesterolaemia	1.36	1.1–1.68	0.005	0.19	1.21	0.96–1.51	0.110
Diabetes mellitus	1.46	1.06-2.01	0.02	0.29	1.33	0.96-1.84	0.090
Hypertension	1.05	0.81-1.36	0.696			Not included	
BMI (kg/m^2)	0.75	0.51-1.08	0.12			Not included	
LV systolic dysfunction	0.95	0.45-2.01	0.78			Not included	
Known CAD	1.03	0.55–1.93	0.94			Not included	
CHA_2DS_2–VASc	1.04	0.97–1.11	0.30			Not included	

HR, non-adjusted hazard ratio; aHR, adjusted hazard ratio; CI, confidence interval; (B), β coefficient; AF, atrial fibrillation; LA, left atria; LVSD, left ventricular systolic dysfunction; BMI, body mass index; LV, left ventricle; CAD, coronary artery disease.

Table 3 Calculation of the ATLAS score

Variable	Number of points
Age > 60 years	1
Type of AF (non-paroxysmal)	2
Left **a**trial volume indexed to BSA	1 point per each 10 mL/m^2 (rounded to nearest integer)
Sex (female)	4
Smoking (current cigarette smoking)	7

Example: A 64 years-old non-smoker woman with paroxysmal AF and an LA volume of 57 mL/m^2 would have an ATLAS score of 11 (=1 + 0 + 6 + 4 + 0).

and validation groups. A secondary analysis excluding these patients yielded the same independent predictors of recurrence and similar regression coefficients (Supplementary material online, *Table S1* and *Figure* S2).

The results of Cox regression analysis are presented in *Table 2*. Seven variables associated with AF recurrence were identified in univariate analysis and entered into the multivariate model, yielding five independent predictors of relapse. Each of these variables was assigned a number of points proportional to its β coefficient (*Table 3*). In order to aid memorization, the acronym ATLAS (A, Age; T, Type of AF; LA, LA volume; S, Sex and Smoking) was created. The relative contribution of the five variables to each individual's ATLAS score is

cont.

Manuscrito 1

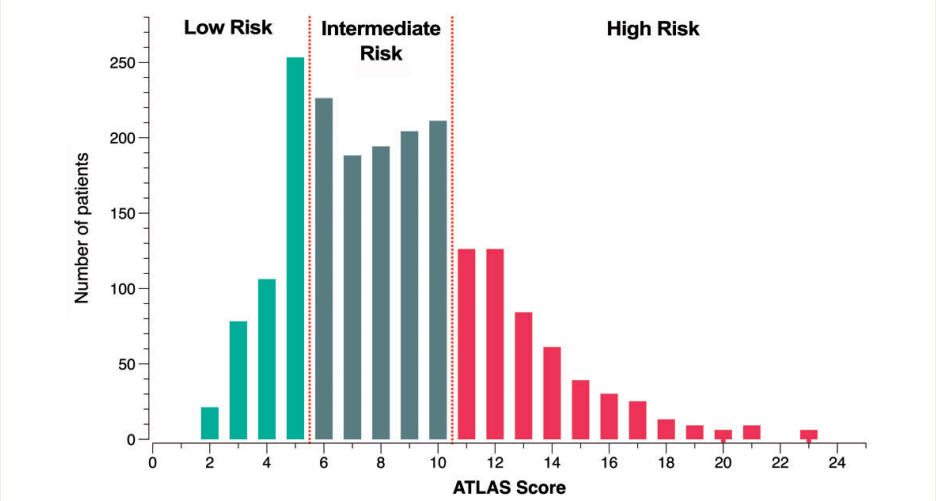

Figure 2 Histogram of ATLAS score values. The vertical dashed lines represent the boundaries between low (<6 points), intermediate (6–10 points), and high-risk categories (>10 points).

presented in *Figure 1*, showing that, on average, indexed LA volume accounts for two thirds of the total value.

The distribution of the ATLAS score in the overall population is depicted in *Figure 2*. The median score was 8 (IQR 6–11), with no significant difference between the development and validation groups (both with median scores of 8, $P = 0.890$).

The score displayed good discriminatory power for earlier AF recurrence, with a censored C-index of 0.75. Three risk categories were defined: low-risk (<6 points), intermediate-risk (6–10 points), and high-risk (>10 points). These categories corresponded to 23.5, 52.5, and 24.0% of the total population, respectively. The AF-free survival curves of low-, intermediate-, and high-risk patients are presented in *Figure 3*. There was a statistically significant difference in AF-free survival between the three risk score categories (log-rank $P < 0.001$ in both the development and validation cohorts). The hazard ratio for intermediate-risk was 1.10 [95% CI 0.90–1.35 (*P*-value 0.35)] and for high-risk 1.60 [95% CI 1.28–2.00 (*P*-value <0.001)].

Within each risk category, there were no statistically significant differences in yearly relapse rates between the development and validation cohorts: 8, 11, and 17%/year for low-, intermediate- and high-risk patients in the development cohort, vs. 8, 11, and 18%/year in the validation cohort.

Analysis of yearly relapse rates showed a significant gradient of risk of AF recurrence across the spectrum of ATLAS score values (*Figure 4*). The calibration-in-the-large statistic (0.077, $P = 0.272$) and a calibration slope of 0.93 showed an overall good calibration, supporting the validity of the prediction model.

The ATLAS score was developed in a population mostly composed of paroxysmal AF patients (77%). Since there is an underrepresentation of non-paroxysmal AF, a subgroup analysis was performed to assess applicability to these patients. The ATLAS score retained its predictive power and ability to identify high-risk patients for AF relapse after a first PVI, regardless of the type of AF (paroxysmal vs. non-paroxysmal) (Supplementary material online, *Figure S3*). The annual relapse rates were similar in the low/intermediate-risk categories (10%/year in both groups) but higher in the high-risk group of patients with non-paroxysmal AF (19%/year vs. 15%/year).

Discussion

Prognosis after pulmonary vein isolation is remarkably heterogeneous, with some patients experiencing early relapse while others remain free of AF for years.[2,10] In this study, we developed and validated a score that estimates the risk of recurrence after a first PVI procedure. Two important aspects of a risk prediction model were assessed: discrimination (the ability to identify those who will relapse) and calibration (reflecting how close predicted recurrence rates are to the actual observed rates). The ATLAS score showed good discriminative power, substantiated in a censored C-statistic of 0.75 and a more than three-fold difference in the yearly rate of AF relapse across the spectrum of score values. Model calibration was similarly good, with a calibration slope of 0.93 supporting the accuracy of the score.

In our cohort, patients who were kept on antiarrhythmic drugs after the 3-month blanking period were not considered failed ablation. Although this remains controversial, the current body of evidence supports that antiarrhythmic drugs are not superior to other agents (e.g. beta-blocker) in maintaining sinus rhythm after PVI.[11,12] Nevertheless,

cont.

Manuscrito 1

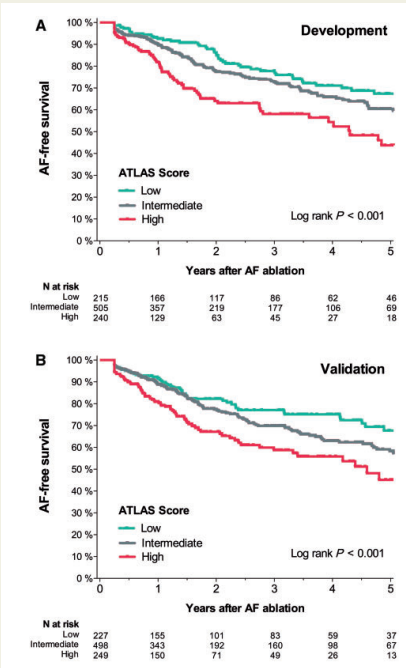

Figure 3 Kaplan–Meier curves of AF-free survival of patients with low, intermediate, and high-risk ATLAS scores in the development cohort (*A*) and validation cohort (*B*).

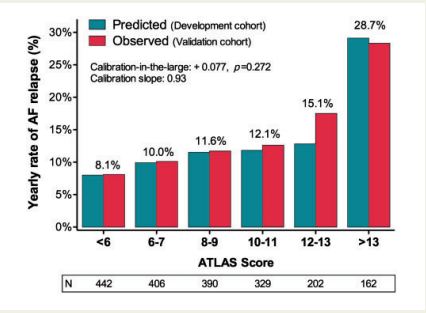

Figure 4 Predicted vs. observed rates of AF relapse across categories of ATLAS scores. The numbers on top of the columns refer to the recurrence rates of the development and validation cohorts combined.

our sensitivity and subgroup analysis demonstrated that this had no impact in the ATLAS score predictive/discriminative power.

Studies assessing AF recurrence after PVI have shown some discordance regarding the predictors of relapse.[2–4] Our analysis yielded five independent predictors of recurrence: LA volume, female sex, cigarette smoking, age, and type of AF (paroxysmal vs. non-paroxysmal). Left atrial volume showed the strongest association with AF-free survival, outweighing all other factors. Although LA size has long been recognized as a prognostic marker, only 4 of the 20 studies included in a recent review found an independent association with relapse rates.[3] However, in those studies LA size was assessed using echocardiographic diameters, which tend to underestimate LA enlargement and correlate poorly with more accurate techniques, such as cardiac CT and magnetic resonance.[13–16] Additionally, a higher inter-observer variability has also been reported with 2D echocardiographic assessment of LA size.[17] It is well recognized that clinical scores demand a trade-off between simplicity and accuracy, but our findings suggest that any prediction tool that does not include LA volume (or an adequate surrogate) assessed by a more precise technique will compromise accuracy in a significant manner. Therefore, we believe that the increase in score complexity associated with adding a reproducible LA volume CT-scan estimation is justified. In studies where LA volume was used, a robust independent association between LA dilatation and AF relapse was found.[5,6] Larger LA volumes probably reflect more extensive remodelling and also larger surface area and greater wall stress and thickness, possibly rendering the tissue more resistant to the creation of transmural lesions. Left atrial dilatation may also increase the likelihood that, once PV reconnection occurs, AF is induced and sustained.

With some surprise, cigarette smoking emerged as an independent predictor of AF recurrence. Although smoking has been previously associated with an increased risk of AF in the general population,[18,19] thus far only one small study showed an association between smoking and AF recurrence after PVI.[20] This relationship is not necessarily causal, but nicotine has been shown to increase atrial vulnerability to fibrillation[21] and induce atrial fibrosis,[22] itself a strong predictor of AF recurrence after ablation.[23] Further studies are warranted to confirm and assess the possible mechanisms of this link.

Gender was also independently associated with AF-free survival in our cohort. Other studies have shown higher recurrence rates in women,[5,24,25] although this was not a universal finding. Later referral, higher incidence of non-PV triggers, and gender-related anatomical differences are some of the possible explanations.[26–28]

To the best of our knowledge, two other scores have been linked to AF recurrence after PVI. The DR-FLASH score was developed to identify patients with low voltage areas on LA electrograms that could require extensive substrate modification instead of PVI alone.[24] Even though it was not the purpose of the score, its association with long-term recurrence of AF was tested in a retrospective cohort of 484 patients, where those with scores >3 were almost twice as likely to experience an AF recurrence within 1 year after ablation. The recently published CAAP-AF score was developed specifically for predicting long-term freedom from AF after ablation. It includes age, type of AF, LA diameter, sex, number of failed antiarrhythmic drugs, and coronary artery disease.[29] Unfortunately, we could not perform a direct comparison between ATLAS and these two scores, since our registry database lacks some of the variables required for its calculation.

cont.

Manuscrito 1

Even though the ATLAS score was devised to estimate the rate of AF relapse and aid decision-making, it is no substitute for sound clinical judgment. There is currently no consensus on what constitutes an acceptable rate of recurrence, and this will probably depend on the clinical setting, procedural risk, and patient preference, among other factors. Consequently, thresholds for classifying patients as low, intermediate or high-risk are largely arbitrary. Users of the ATLAS score might choose to employ other clinically meaningful risk thresholds.

Limitations

Various limitations of this study should be recognized. Atrial fibrillation relapse is most likely underestimated in this population, since recurrences are frequently asymptomatic and our follow-up protocol did not include continuous ECG monitoring. However, since the main goal of AF ablation is to improve symptoms, we believe our pragmatic follow-up protocol captures the essential benefit of the procedure.

Several variables with established prognostic value (e.g. AF burden, left atrial fibrosis, obstructive sleep apnea, etc.) were not systematically evaluated, preventing their inclusion in the model.

Smoking was assessed as a dichotomous variable (and not in pack-year units). Notwithstanding the possible loss of information, this approach replicates the assessment of smoking status in commonly used cardiovascular risk calculators such as the heart SCORE[30] and the ASCVD algorithm.[31]

Different methods were used to measure LA volume, and several patients were lost to follow-up. Assessment of LA volume by cardiac CT may also be regarded as a limitation, since this information is usually unavailable when a patient is being considered for AF ablation. However, in our cohort, this was the single most important prognostic factor.

Although the subgroup analysis showed no significant differences in AF relapse regarding the type of AF, an underrepresentation of non-paroxysmal AF patients in our cohort warrants additional validation in external populations.

Further studies will be required to ascertain whether it can be replaced by a more easily obtainable measure of LA dilatation without significant loss of prognostic information. Finally, although the ATLAS score showed good discriminative power and calibration, its portability to other populations remains to be established.

Despite these limitations, our findings could have important implications for clinical practice. After external validation, the ATLAS score may become a useful tool for clinicians to refine patient selection and inform patient–physician discussions, for researchers to design clinical trials, and for policymakers to improve the allocation of healthcare resources.

Conclusion

We developed and internally validated a risk model to estimate the rate of AF recurrence after a first PVI procedure. The resulting 5-variable score (ATLAS: Age > 60 years, Type of AF, indexed Left Atrial volume, Sex and Smoking) showed good discriminative power and good calibration. If validated in independent datasets, this score might prove a useful tool for selecting patients who will benefit the most from AF ablation, avoiding the unnecessary risks and costs of ineffective procedures.

Supplementary material

Supplementary material is available at *Europace* online.

Conflict of interest: none declared.

References

1. Kirchhof P, Benussi S, Kotecha D, Ahlsson A, Atar D, Casadei B *et al.* 2016 ESC Guidelines for the management of atrial fibrillation developed in collaboration with EACTS. *Europace* 2016;**18**:1609–78.
2. Ganesan AN, Shipp NJ, Brooks AG, Kuklik P, Lau DH, Lim HS *et al.* Long-term outcomes of catheter ablation of atrial fibrillation: a systematic review and meta-analysis. *J Am Heart Assoc* 2013;**2**:e004549.
3. Balk EM, Garlitski AC, Alsheikh-Ali AA, Terasawa T, Chung M, Ip S. Predictors of atrial fibrillation recurrence after radiofrequency catheter ablation: a systematic review. *J Cardiovasc Electrophysiol* 2010;**21**:1208–16.
4. Brooks AG, Stiles MK, Laborderie J, Lau DH, Kuklik P, Shipp NJ *et al.* Outcomes of long-standing persistent atrial fibrillation ablation: a systematic review. *Heart Rhythm* 2010;**7**:835–46.
5. Costa FM, Ferreira AM, Oliveira S, Santos PG, Durazzo A, Carmo P *et al.* Left atrial volume is more important than the type of atrial fibrillation in predicting the long-term success of catheter ablation. *Int J Cardiol* 2015;**184**:56–61.
6. Abecasis J, Dourado R, Ferreira A, Saraiva C, Cavaco D, Santos KR *et al.* Left atrial volume calculated by multi-detector computed tomography may predict successful pulmonary vein isolation in catheter ablation of atrial fibrillation. *Europace* 2009;**11**:1289–94.
7. Kim Y, Kong L. Estimation of C-index for cox proportional hazards model with censored biomarker covariate subject to limits of detection. *J Biopharm Stat* 2015;**25**:459–73.
8. Steyerberg EW, Vergouwe Y. Towards better clinical prediction models: seven steps for development and an ABCD for validation. *Eur Heart J* 2014;**35**:1925–31.
9. Mesquita J, Ferreira A, Cavaco D, Madeira M, Costa F, Freitas P *et al.* Impact of cavotricuspid isthmus ablation in atrial fibrillation recurrence after a first pulmonary vein isolation procedure: a propensity score analysis. *Heart Rhythm* 2017;**14**:112.
10. Shah AN, Mittal S, Sichrovsky TC, Cotiga D, Arshad A, Maleki K *et al.* Long-term outcome following successful pulmonary vein isolation: pattern and prediction of very late recurrence. *J Cardiovasc Electrophysiol* 2008;**19**:661–7.
11. Sohns C, Gruben V, von, Sossalla S, Bergau L, Seegers J, Vollmann D *et al.* Antiarrhythmic drug therapy for maintaining sinus rhythm early after pulmonary vein ablation in patients with symptomatic atrial fibrillation. *Cardiovasc Ther* 2014;**32**:7–12.
12. Stabile G, Iuliano A, Agresta A, Rocca VL, D'Ascia S, Simone AD. Antiarrhythmic therapy following ablation of atrial fibrillation. *Expert Rev Cardiovasc Ther* 2013;**11**:837–42.
13. Avelar E, Durst R, Rosito G. A, Thangaroopan M, Kumar S, Tournoux F *et al.* Comparison of the accuracy of multidetector computed tomography versus two-dimensional echocardiography to measure left atrial volume. *Am J Cardiol* 2010;**106**:104–9.
14. Hof I, Arbab-Zadeh A, Scherr D, Chilukuri K, Dalal D, Abraham T *et al.* Correlation of left atrial diameter by echocardiography and left atrial volume by computed tomography. *J Cardiovasc Electrophysiol* 2009;**20**:159–63.
15. Rabbat MG, Wilber D, Thomas K, Malick O, Bashir A, Agrawal A *et al.* Left atrial volume assessment in atrial fibrillation using multimodality imaging: a comparison of echocardiography, invasive three-dimensional CARTO and cardiac magnetic resonance imaging. *Int J Cardiovasc Imaging* 2015;**31**:1011–8.
16. Mahabadi AA, Samy B, Seneviratne SK, Toepker MH, Bamberg F, Hoffmann U *et al.* Quantitative assessment of left atrial volume by electrocardiographic-gated contrast-enhanced multidetector computed tomography. *J Cardiovasc Comput Tomogr* 2009;**3**:80–7.
17. Jiamsripong P, Honda T, Reuss CS, Hurst RT, Chaliki HP, Grill DE *et al.* Three methods for evaluation of left atrial volume. *Eur J Echocardiogr* 2008;**9**:351–5.
18. Heeringa J, Kors JA, Hofman A, Rooij FJA. V, Witteman JCM. Cigarette smoking and risk of atrial fibrillation: the Rotterdam Study. *Am Heart J* 2008;**156**:1163–9.
19. Dixit S, Pletcher MJ, Vittinghoff E, Imburgia K, Maguire C, Whitman IR *et al.* Secondhand smoke and atrial fibrillation: data from the health eHeart study. *Heart Rhythm* 2016;**13**:3–9.
20. Fukamizu S, Sakurada H, Takano M, Hojo R, Nakai M, Yuba T *et al.* Effect of cigarette smoking on the risk of atrial fibrillation recurrence after pulmonary vein isolation. *J Arrhythmia* 2010;**26**:21–9.
21. Hayashi H, Omichi C, Miyauchi Y, Mandel WJ, Lin S-F, Chen P-S *et al.* Age-related sensitivity to nicotine for inducible atrial tachycardia and atrial fibrillation. *Am J Physiol Heart Circ Physiol* 2003;**285**:H2091–8.

cont.

Manuscrito 1

22. Goette A, Lendeckel U, Kuchenbecker A, Bukowska A, Peters B, Klein HU *et al.* Cigarette smoking induces atrial fibrosis in humans via nicotine. *Heart* 2007;**93**: 1056–63.
23. Marrouche NF, Wilber D, Hindricks G, Jais P, Akoum N, Marchlinski F *et al.* Association of atrial tissue fibrosis identified by delayed enhancement MRI and atrial fibrillation catheter ablation: the DECAAF study. *JAMA* 2014;**311**: 498–506.
24. Kosiuk J, Dinov B, Kornej J, Acou WJ, SchNbauer R, Fiedler L *et al.* Prospective, multicenter validation of a clinical risk score for left atrial arrhythmogenic substrate based on voltage analysis: DR-FLASH score. *Heart Rhythm* 2015;**12**: 2207–12.
25. Winkle RA, Mead RH, Engel G, Patrawala RA. Long-term results of atrial fibrillation ablation: the importance of all initial ablation failures undergoing a repeat ablation. *Am Heart J* 2011;**162**:193–200.
26. Forleo GB, Tondo C, De L, Russo AD, Casella M, De V *et al.* Gender-related differences in catheter ablation of atrial fibrillation. *Europace* 2007;**9**:613–20.
27. Roten L, Rimoldi SF, Schwick N, Sakata T, Heimgartner C, Fuhrer J *et al.* Gender differences in patients referred for atrial fibrillation management to a tertiary center. *Pacing Clin Electrophysiol* 2009;**32**:622–6.
28. Patel D, Mohanty P, Biase LD, Sanchez JE, Shaheen MH, Burkhardt JD *et al.* Outcomes and complications of catheter ablation for atrial fibrillation in females. *Heart Rhythm* 2010;**7**:167–72.
29. Winkle RA, Jarman JWE, Mead RH, Engel G, Kong MH, Fleming W *et al.* Predicting atrial fibrillation ablation outcome: the CAAP-AF score. *Heart Rhythm* 2016;**13**:2119–25.
30. Piepoli MF, Hoes AW, Agewall S, Albus C, Brotons C, Catapano AL *et al.* 2016 European Guidelines on cardiovascular disease prevention in clinical practice. *Eur Heart J* 2016;**37**:2315–81.
31. Goff DC, Lloyd-Jones DM, Bennett G, Coady S, D'agostino RB, Gibbons R *et al.* 2013 ACC/AHA guideline on the assessment of cardiovascular risk: a report of the American college of cardiology/American heart association task force on practice guidelines. *J Am Coll Cardiol* 2014;**63**:2935–59.

MANUSCRITO 2

Safety and Long-Term Outcomes of Catheter Ablation of Atrial Fibrillation Using Magnetic Navigation versus Manual Conventional Ablation: A Propensity-Score Analysis.

Adragão, P.P., Cavaco, D., Ferreira, A. M., Costa, F.M., Parreira, L., Carmo, P., Morgado, F.B., Santos, K.R., Santos, P.G., Carvalho, M.S., Durazzo, A., **Marques**, **H**., Goncalves, P.A., Raposo, L., and Mendes, M.

J Cardiovasc Electrophysiol, 2016
27 Suppl 1: p. S11-6

Manuscrito 2

cont.

Manuscrito 2

Safety and Long-Term Outcomes of Catheter Ablation of Atrial Fibrillation Using Magnetic Navigation versus Manual Conventional Ablation: A Propensity-Score Analysis

PEDRO PULIDO ADRAGÃO, M.D., PH.D.,*,† DIOGO CAVACO, M.D.,*,† ANTÓNIO MIGUEL FERREIRA, M.D.,*,‡ FRANCISCO MOSCOSO COSTA, M.D.,*,† LEONOR PARREIRA, M.D.,† PEDRO CARMO, M.D.,*,† FRANCISCO BELLO MORGADO, M.D.,*,† KATYA REIS SANTOS, M.D.,† PEDRO GALVÃO SANTOS, M.D.,*,† MARIA SALOMÉ CARVALHO, M.D.,*,† ANAI DURAZZO, M.D.,* HUGO MARQUES, M.D.,‡ PEDRO ARAÚJO GONÇALVES, M.D., PH.D.,*,† LUÍS RAPOSO, M.D.,*,† and MIGUEL MENDES, M.D.*

From the *Cardiology Department, Hospital Santa Cruz, Western Lisbon Hospital Center, Lisbon, Portugal; †Cardiology Department, Hospital da Luz, Lisbon, Portugal; and ‡Cardiovascular Imaging Department, Hospital da Luz, Lisbon, Portugal

Magnetic versus Manual Ablation of Atrial Fibrillation. ***Introduction:*** **Whether or not the potential advantages of using a magnetic navigation system (MNS) translate into improved outcomes in patients undergoing atrial fibrillation (AF) ablation is a question that remains unanswered.**

Methods and Results: **In this observational registry study, we used propensity-score matching to compare the outcomes of patients with symptomatic drug-refractory AF who underwent catheter ablation using MNS with the outcomes of those who underwent catheter ablation using conventional manual navigation. Among 1,035 eligible patients, 287 patients in each group had similar propensity scores and were included in the analysis. The primary efficacy outcome was the rate of AF relapse after a 3-month blanking period. At a mean follow-up of 2.6 ± 1.5 years, AF ablation with MNS was associated with a similar risk of AF relapse as compared with manual navigation (18.4% per year and 22.3% per year, respectively; hazard ratio 0.81, 95% CI 0.63–1.05; P = 0.108). Major complications occurred in two patients (0.7%) using MNS, and in six patients (2.1%) undergoing manually navigated ablation (P = 0.286). Fluoroscopy times were 21 ± 10 minutes in the manual navigation group, and 12 ± 9 minutes in the MNS group (P < 0.001), whereas total procedure times were 152 ± 52 minutes and 213 ± 58 minutes, respectively (P < 0.001).**

Conclusions: **In this propensity-score matched comparison, magnetic navigation and conventional manual AF ablations seem to have similar relapse rates and a similar risk of complications. AF ablations with magnetic navigation take longer to perform but expose patients to significantly shorter fluoroscopy times.**
(J Cardiovasc Electrophysiol, Vol. 27, pp. S11-S16, March 2016)

atrial fibrillation, catheter ablation, efficacy, magnetic navigation system, manual ablation, propensity score, safety

Introduction

Catheter ablation has now become a well-established treatment for selected patients with atrial fibrillation (AF).[1-3] Enduring success of pulmonary vein isolation (PVI) depends on the creation of permanent and uninterrupted transmural scar in order to block electrical conduction between the left atrium (LA) and the pulmonary veins. The creation of this scar can be challenging even for experienced electrophysiologists and recurrences are common, usually due to pulmonary vein reconduction.[4,5] Procedures are also associated with a relatively high level of radiation exposure and a non-negligible risk of complications.[6]

Recently, a magnetic navigation system (MNS) was introduced as a way to ensure stable and reproducible catheter positioning, provide adequate tissue contact, and reduce radiation exposure to both patient and physician.[7,8]

Whether or not these potential advantages translate into improved clinical outcomes is an important question that remains essentially unanswered.

The purpose of this study was to assess the safety and long-term efficacy of a single AF ablation procedure using MNS as compared to conventional manual navigation.

This manuscript was processed by a guest editor.

Disclosures: None.

Address for correspondence: Francisco Moscoso Costa, M.D., Hospital Santa Cruz—Cardiology Department, Av. Professor Reinaldo dos Santos, 2799-523 Carnaxide, Portugal. Fax: 351-214-188-095; Email: fmoscosocosta@gmail.com

Manuscript received 4 November 2015; Revised manuscript received 23 December 2015; Accepted for publication 28 December 2015.

doi: 10.1111/jce.12900

Methods

Patient Characteristics and Study Design

We conducted a registry-based analysis of all consecutive patients with symptomatic drug-refractory AF undergoing percutaneous PVI in 2 centers (Hospital Santa Cruz,

cont.

Manuscrito 2

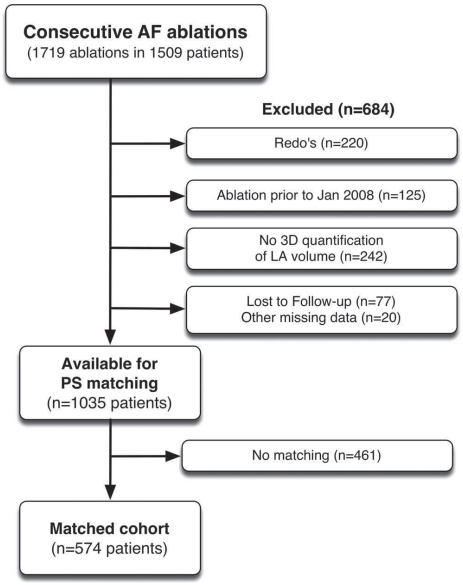

Figure 1. *Patient selection and study design.*

Carnaxide, Portugal; and Hospital da Luz, Lisbon, Portugal). In order to account for the learning curve with new technology, AF ablations performed during the first 6 months after the introduction of magnetic navigation (i.e., July through December 2007) were excluded. The analyzed procedures were performed between January 2008 and April 2014, when both techniques were in use. Exclusion criteria also comprised any previous AF ablation procedure, no 3-dimensional quantification of LA volume, and loss to follow-up (Fig. 1).

Data on patient demographics, symptoms, and previous medical history were obtained from a pre-procedure interview, supplemented with information provided by the referring physician and electronic medical records. AF was categorized as paroxysmal if self-terminated in <7 days, persistent if episodes lasted ≥7 days or required pharmacological or electrical cardioversion, or longstanding persistent if AF was maintained for more than 12 months.[3] The presence of structural heart disease (known cardiomyopathy, moderate or severe valvular heart disease, congenital heart disease, or left ventricular systolic dysfunction from any cause) was assessed by clinical history, physical examination, and transthoracic echocardiography. Sixty-four slice cardiac computed tomography performed less than 48 hours before the ablation procedure was used to assess LA volume, an important predictor of AF recurrence.[9] When cardiac CT could not be performed for logistical reasons (n = 162, 28.2%), electroanatomical mapping at the time of ablation was used to calculate LA volume, as previously described.[10-12]

This study was approved by both of the institutional review boards and all patients gave written informed consent.

Ablation Protocol

Ablation procedures were guided by CARTO™ (Biosense Webster® Inc., Diamond Bar, CA, USA) or NavX™ (St. Jude Medical® Inc., St. Paul, MN, USA) electroanatomical mapping. Three catheters were introduced via right femoral venous access under local anesthesia. A multipolar diagnostic catheter was placed in the coronary sinus. An irrigated-tip ablation catheter and a duodecapolar circular mapping catheter were placed at the pulmonary veins (PV) ostia via transeptal access. In Hospital Santa Cruz all patients underwent conventional manually guided ablation, whereas in Hospital da Luz a Niobe II magnetic navigation system (Stereotaxis® Inc., St. Louis, MO, USA) was used. Irrigated radiofrequency ablation was performed with continuous lesions encircling both pairs of pulmonary veins and deployed more than 5 mm from the PV ostia in order to achieve pulmonary vein isolation. In patients with previously documented typical atrial flutter or when typical sustained atrial flutter occurred during the procedure, a cavotricuspid isthmus ablation line was also performed. Whenever necessary, patients were cardioverted to sinus rhythm at the end of the procedure. Anticoagulation was restarted within 24 hours, maintained for 6 months, and then suspended according to $CHADS_2$ criteria (CHA_2DS_2-VASc from 2013 onward). As a general rule, patients were maintained on class I or III antiarrhythmic drugs for the first 3 months and then withdrawn if there was no AF recurrence. Despite this department guidance, the decision to withhold drug therapy was ultimately left to the treating electrophysiologist. Proton pump inhibition was used by protocol during the first month. Throughout the study period, the ablation procedures were performed by the same team of experienced electrophysiologists, who worked in both institutions.

Study Endpoints and Patient Follow-Up

The efficacy endpoint was AF recurrence, defined as the presence of symptomatic or documented AF after a 3-month blanking period. Symptomatic AF was defined as the presence of symptoms possibly related to AF episodes. Documented AF was defined by the presence of at least one episode of AF lasting more than 30 seconds in any electrocardiogram (ECG), 24-hour Holter monitoring or event-loop recording. AF recurrence was assessed independently of the use of antiarrhythmic drugs at the time of relapse. The follow-up protocol consisted of outpatient visits with 12-lead ECGs and 24-hour Holter monitoring at 1, 3, 6, and 12 months in the first year, and yearly thereafter. Patients were encouraged to contact the department whenever they experienced symptoms of AF recurrence or signs of complications. Additional ECGs, 24-hour Holter monitoring, and event-loop recordings were performed whenever necessary to assess symptoms of possible recurrence. When clinical records were insufficient, a structured telephonic interview was conducted. Seventy-seven patients (5.1%) were lost to follow-up and excluded from this analysis.

The primary safety endpoint was the occurrence of any major complication, defined as a complication that results in permanent injury or death, requires intervention for treatment, or prolongs or requires hospitalization for more than 48 hours.[3] Our secondary safety endpoint was fluoroscopic time.

cont.

Manuscrito 2

Statistical Analysis

Given the differences in the baseline characteristics between patients undergoing PVI with MNS versus conventional manual navigation, propensity-score matching was used to identify a cohort of individuals with similar baseline characteristics. The propensity score (PS) is a conditional probability of receiving a particular treatment given a set of baseline-measured covariates.[13] The PS was estimated by a multivariable logistic regression model with 'AF ablation using MNS' as the dependent variable, and the following baseline characteristics as covariates: age, gender, body mass index, type of AF, hypertension, structural heart disease, and indexed left atrial volume. For every MNS ablation, matching patients with the closest propensity score were identified from the pool of manual navigation ablations. The maximal allowable difference in propensity score for matching was 0.2 (caliper width equal to 0.2 of the standard deviation of the logit of the propensity score). When 2 or more manual navigation patients had the same propensity-score match, the match for the analysis was chosen randomly. Matched subjects were removed from the pool and the next MNS ablation and its matched manual navigation patient were selected until no further matches could be identified.

Comparisons between groups were performed using independent samples *t*-test and Fisher's exact test for continuous and categorical variables, respectively. Kaplan–Meier curves were used to describe the occurrence of AF relapse over time, and any differences in AF-free survival were assessed with the log-rank test. Annualized event rates for AF relapse were also calculated by dividing total numbers of first events by total number of person-years of follow-up for each group. Finally, the comparative risk of AF relapse was further adjusted for in the matched cohort with the use of a Cox proportional-hazards model. This model included the treatment modality (MNS vs. conventional manual navigation), the propensity score, and potentially confounding variables whose standardized difference between groups remained above 10% after matching.[14] Statistical analyses were performed with SPSS version 19.0 (SPSS® Inc., Chicago, IL, USA). Two-tailed P values <0.05 were considered statistically significant.

Results

Among the 1,509 registry patients, 1,035 were available for matching, of whom 633 (61.2%) underwent PVI with MNS and 402 (38.8%) with conventional manual navigation. Before propensity-score matching, there were significant differences between the 2 groups in several of the baseline characteristics (Table 1). Using the propensity score, 287 patients who underwent AF ablation using MNS were matched with 287 who underwent ablation with conventional manual navigation. The C-statistic for the model was 0.82. After matching, the 2 cohorts were well balanced with respect to baseline variables except for indexed LA volume, where a trend toward smaller left atriums in the MNS group was still observed (standardized difference of 12%, $P = 0.088$). PVI was achieved in all patients. Overall, 63 patients (11.0%) remained on antiarrhythmic drugs for longer than 3 months after ablation, despite the absence of AF recurrence. The proportion of antiarrhythmic drug persistence was similar between patients who underwent PVI with manual navigation versus MNS (13.1% vs. 9.9%, respectively, $P = 0.284$).

At a mean follow-up of 2.6 ± 1.5 years, 251 patients (43.7%) experienced AF relapse (131 in the manual navigation group and 120 in the MNS group). Recurrences occurred a median of 1.2 years after the ablation procedure (interquartile range 0.5–2.5), and were established by symptoms in 69 cases, by electrocardiographic documentation of AF in 27 patients, and by both in the remainder 155 subjects. Kaplan–Meier AF-free survival curves for the matched MNS and manual navigation patients are presented in Figure 2. AF ablation with MNS was associated with a similar risk of AF relapse as compared with conventional manual navigation (18.4% per year and 22.3% per year, respectively; hazard ratio 0.81, 95% CI 0.63–1.05; $P = 0.108$). Further Cox regression adjustment for propensity-score value and indexed LA volume confirmed that treatment modality (MNS vs. manual navigation) was not an independent predictor of AF relapse in this cohort (Table 2).

Safety Outcomes

Observed complications and procedure characteristics are detailed in Table 3. Major complications occurred in 2 patients (0.7%) using the MNS, and 6 patients (2.1%) undergoing conventional manually navigated ablation ($P = 0.286$). Fluoroscopy times were significantly shorter with MNS, with an average 9-minute reduction in exposure as compared to manual navigation. On average, procedures using MNS took 61 minutes longer to perform and applied radiofrequency for 23 minutes longer than manual conventional navigation.

Discussion

Ever since its introduction in 2003, magnetic navigation for AF ablation has been proposed as a way to overcome some of the limitations of this demanding procedure. The potential advantages of magnetic navigation include finer control of small catheter movements, greater stability, and the possibility of standardizing catheter positions, which could theoretically produce better electrical isolation of the pulmonary veins.[15] Magnetic guidance, and the need of lower forces to maintain stable tissue contact, might also mean less fluoroscopy time and fewer complications. Notwithstanding these potential benefits, and despite being used for several years, magnetic navigation for PVI has never been compared to conventional manual ablation in a large randomized controlled trial with long-term follow-up. Applying a pseudo-randomization procedure to a large dataset of patients, we sought to compare the safety and long-term efficacy of a single AF ablation procedure performed with each of these techniques. Our results suggest that the 2 methods have similar relapse rates and a similar risk of complications. According to our findings, AF ablations with magnetic navigation take longer to perform, but expose patients to significantly shorter fluoroscopy times.

To the best of our knowledge, this is the largest and longest follow-up comparison between MNS and manually navigated AF ablation. Several studies have addressed this subject, but these have generally been limited by non-randomized design, small sample sizes, and relatively short follow-up periods.[8,16-22] The available evidence gathered in 2 recent systematic reviews and meta-analyses suggests that both techniques have similar relapse rates, a notion that is strengthened by our study.[15,23]

cont.

Manuscrito 2

TABLE 1
Baseline Characteristics Before and After Propensity-Score Matching

	Before Matching				After Matching			
Characteristic	**Manual Navigation (n = 402)**	**Magnetic Navigation (n = 633)**	**Standardized Difference**	**P Value**	**Manual Navigation (n = 287)**	**Magnetic Navigation (n = 287)**	**Standardized Difference**	**P Value**
Age (years)	57.7 ± 11.0	59.2 ± 11.1	13.6%	0.036	57.9 ± 11.2	58.3 ± 10.7	3.7%	0.640
Male sex	274 (68.2%)	437 (69.0%)	1.7%	0.783	194 (67.6%)	201 (70.0%)	5.2%	0.589
Body mass index (kg/m^2)	27.7 ± 3.8	27.0 ± 3.8	18.4%	<0.001	27.6 ± 3.8	27.7 ± 4.0	2.6%	0.724
Body surface area (m^2)	1.96 ± 0.22	1.93 ± 0.21	14.0%	<0.001	1.96 ± 0.22	1.96 ± 0.22	0.1%	0.990
Paroxysmal AF	291 (72.4%)	493 (77.9%)	12.3%	0.053	207 (72.1%)	213 (74.2%)	4.7%	0.638
Hypertension	160 (39.8%)	233 (36.8%)	6.2%	0.358	112 (39.0%)	109 (38.0%)	2.1%	0.864
Structural heart disease	36 (9.0%)	35 (5.5%)	15.7%	0.043	21 (7.3%)	22 (7.7%)	1.5%	1.000
Indexed LA volume (mL/m^2)	63 ± 18	46 ± 16	99.8%	<0.001	57 ± 16	55 ± 18	11.7%	0.088

Standardized differences of less than 10.0% indicate a relatively small imbalance between groups.

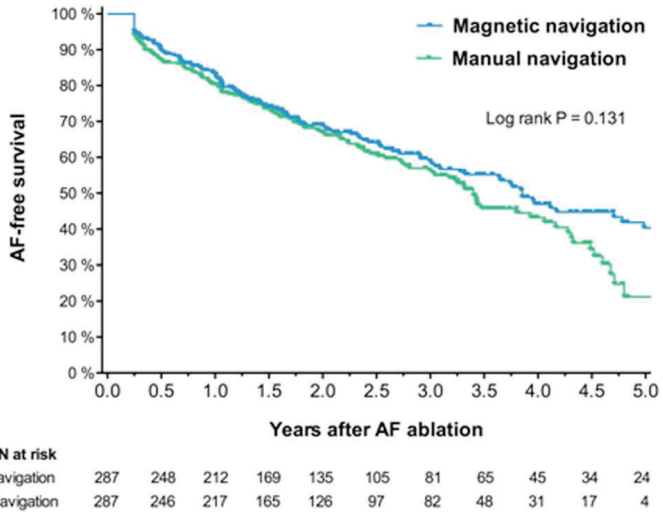

Figure 2. *Kaplan–Meier AF-free survival curves after single ablation procedure.*

TABLE 2
Cox Regression Adjustment for Propensity Score and Indexed Left Atrium Volume in the Matched Cohort

Variable	**Adjusted HR**	**95% CI**	**P Value**
Propensity score	0.78	0.23–2.70	0.694
Indexed LA volume*	1.08	0.94–1.26	0.284
Magnetic navigation	0.81	0.63–1.04	0.104

HR = hazard ratio; CI = confidence interval.
*Hazard ratio for each 10 mL/m^2 increment.

The reasons for the apparent similar results of MNS in terms of long-term efficacy are beyond the scope of this study, but it can be speculated that the potential advantages of MNS including catheter stability are balanced by the higher contact forces of conventional manual ablation.[24,25]

Our results are also in general agreement with the published evidence regarding the safety of AF ablation with each of the 2 navigation methods. One of the systematic reviews and meta-analyses comparing MNS to conventional manual navigation reported less peri-procedural complications, while the other found similar complication rates except for pericardial tamponade or effusion requiring intervention/hospitalization, which were significantly less numerous when MNS was used.[15,23] In our study, major complications were relatively rare and, although numerically more frequent in the manual navigation group, this difference did not reach statistical significance. However, it should be recognized that our analysis is underpowered to detect differences in major

cont.

Manuscrito 2

TABLE 3
Observed Complications and Procedure Characteristics in the Matched Cohort of Patients Undergoing Ablation with Manual versus Magnetic Navigation

	Manual Navigation (n = 287)	Magnetic Navigation (n = 287)	P Value
Complications			
Death	0	0	NA
Atrioesophageal fistula	0	0	NA
Stroke or TIA	0	1 (0.35%)	1.000
Cardiac tamponade/perforation	2 (0.70%)	1 (0.35%)	1.000
Pulmonary vein stenosis	0	0	NA
Major bleeding	1 (0.35%)	0	1.000
Vascular access complication	5 (1.74%)	1 (0.35%)	0.216
Any major complication	6 (2.09%)	2 (0.70%)	0.286
Fluoroscopy time	21 ± 10 minutes	12 ± 9 minutes	<0.001
Radiofrequency application duration	31 ± 18 minutes	54 ± 22 minutes	<0.001
Procedure duration	152 ± 52 minutes	213 ± 58 minutes	<0.001

NA = non-applicable.

complications, since these are relatively infrequent events, best assessed in large randomized controlled trials or multicenter registries.

Finally, our findings corroborate other studies showing that MNS ablations take longer to perform but expose patients to less fluoroscopy time.[8,17-22,26] Since the radiofrequency power was similar by protocol in both groups, the lower contact force in the MNS might be responsible for a longer time to achieve pulmonary vein isolation. Regarding fluoroscopy time, given that a significant proportion of patients need repeat procedures in order to remain free of AF, the reduction in fluoroscopy time seems an important goal. This may be particularly relevant for younger patients (especially women) since they are more susceptible to the biological effects of ionizing radiation.[27] On the other hand, longer procedure times may pose additional challenges to already overloaded electrophysiology departments struggling to treat an ever increasing number of patients with AF.

Limitations

Some limitations of this study should be taken into account. First, the observational design of the study: even though propensity scoring can provide excellent matching of baseline characteristics, it does not guarantee the absence of significant differences in covariables that were not systematically collected and entered into the model, such as AF burden, sleep apnea, and LA fibrosis. Some of our patients were lost to follow-up, and AF relapse may be underreported, since recurrences are frequently asymptomatic and the follow-up protocol did not include continuous ECG monitoring. Finally, sample size limitations preclude subgroup analyses based on type of AF or other baseline characteristics.

Conclusion

In this propensity-score matched comparison, magnetic navigation and conventional manual AF ablations seem to have similar relapse rates and a similar risk of complications. AF ablations with magnetic navigation take longer to perform but expose patients to significantly shorter fluoroscopy times. Large truly randomized controlled trials are warranted to confirm these findings.

Acknowledgments: We would like to thank cardiology technologists Elisabete Vaz, Rita Canuto, Rita Quaresma, Ana Sofia Soares, and Lia Marques for their valuable support in database management.

References

1. Camm AJ, Lip GY, De Caterina R, Savelieva I, Atar D, Hohnloser SH, Hindricks G, Kirchhof P: Guidelines-CPG ESCCfP, Document R: 2012 focused update of the ESC Guidelines for the management of atrial fibrillation: An update of the 2010 ESC guidelines for the management of atrial fibrillation—developed with the special contribution of the European Heart Rhythm Association. Europace 2012;14:1385-1413.
2. January CT, Wann LS, Alpert JS, Calkins H, Cleveland JC Jr, Cigarroa JE, Conti JB, Ellinor PT, Ezekowitz MD, Field ME, Murray KT, Sacco RL, Stevenson WG, Tchou PJ, Tracy CM, Yancy CW: 2014 AHA/ACC/HRS Guideline for the Management of Patients With Atrial Fibrillation: A Report of the American College of Cardiology/American Heart Association Task Force on Practice Guidelines and the Heart Rhythm Society. J Am Coll Cardiol 2014;64:2246-2280.
3. Calkins H, Kuck KH, Cappato R, Brugada J, Camm AJ, Chen SA, Crijns HJ, Damiano RJ Jr, Davies DW, DiMarco J, Edgerton J, Ellenbogen K, Ezekowitz MD, Haines DE, Haissaguerre M, Hindricks G, Iesaka Y, Jackman W, Jalife J, Jais P, Kalman J, Keane D, Kim YH, Kirchhof P, Klein G, Kottkamp H, Kumagai K, Lindsay BD, Mansour M, Marchlinski FE, McCarthy PM, Mont JL, Morady F, Nademanee K, Nakagawa H, Natale A, Nattel S, Packer DL, Pappone C, Prystowsky E, Raviele A, Reddy V, Ruskin JN, Shemin RJ, Tsao HM, Wilber D: 2012 HRS/EHRA/ECAS Expert Consensus Statement on Catheter and Surgical Ablation of Atrial Fibrillation: Recommendations for patient selection, procedural techniques, patient management and follow-up, definitions, endpoints, and research trial design. Europace 2012;14:528-606.
4. Ganesan AN, Shipp NJ, Brooks AG, Kuklik P, Lau DH, Lim HS, Sullivan T, Roberts-Thomson KC, Sanders P: Long-term outcomes of catheter ablation of atrial fibrillation: A systematic review and meta-analysis. J Am Heart Assoc 2013;2:e004549.
5. Ouyang F, Antz M, Ernst S, Hachiya H, Mavrakis H, Deger FT, Schaumann A, Chun J, Falk P, Hennig D, Liu X, Bansch D, Kuck KH: Recovered pulmonary vein conduction as a dominant factor for recurrent atrial tachyarrhythmias after complete circular isolation of the pulmonary veins: Lessons from double Lasso technique. Circulation 2005;111:127-135.
6. Gupta A, Perera T, Ganesan A, Sullivan T, Lau DH, Roberts-Thomson KC, Brooks AG, Sanders P: Complications of catheter ablation of atrial fibrillation: A systematic review. Circ Arrhythm Electrophysiol 2013;6:1082-1088.
7. Ernst S, Ouyang F, Linder C, Hertting K, Stahl F, Chun J, Hachiya H, Bansch D, Antz M, Kuck KH: Initial experience with remote catheter ablation using a novel magnetic navigation system: Magnetic remote catheter ablation. Circulation 2004;109:1472-1475.
8. Pappone C, Vicedomini G, Manguso F, Gugliotta F, Mazzone P, Gulletta S, Sora N, Sala S, Marzi A, Augello G, Livolsi L, Santagostino

cont.

Manuscrito 2

A, Santinelli V: Robotic magnetic navigation for atrial fibrillation ablation. J Am Coll Cardiol 2006;47:1390-1400.
9. Abecasis J, Dourado R, Ferreira A, Saraiva C, Cavaco D, Santos KR, Morgado FB, Adragao P, Silva A: Left atrial volume calculated by multi-detector computed tomography may predict successful pulmonary vein isolation in catheter ablation of atrial fibrillation. Europace 2009;11:1289-1294.
10. Tops LF, Bax JJ, Zeppenfeld K, Jongbloed MR, Lamb HJ, van der Wall EE, Schalij MJ: Fusion of multislice computed tomography imaging with three-dimensional electroanatomic mapping to guide radiofrequency catheter ablation procedures. Heart Rhythm 2005;2:1076-1081.
11. Heist EK, Chevalier J, Holmvang G, Singh JP, Ellinor PT, Milan DJ, D'Avila A, Mela T, Ruskin JN, Mansour M: Factors affecting error in integration of electroanatomic mapping with CT and MR imaging during catheter ablation of atrial fibrillation. J Interv Card Electrophysiol 2006;17:21-27.
12. Costa FM, Ferreira AM, Oliveira S, Santos PG, Durazzo A, Carmo P, Santos KR, Cavaco D, Parreira L, Morgado F, Adragao P: Left atrial volume is more important than the type of atrial fibrillation in predicting the long-term success of catheter ablation. Int J Cardiol 2015;184:56-61.
13. D'Agostino RB Jr: Propensity score methods for bias reduction in the comparison of a treatment to a non-randomized control group. Stat Med 1998;17:2265-2281.
14. Normand ST, Landrum MB, Guadagnoli E, Ayanian JZ, Ryan TJ, Cleary PD, McNeil BJ: Validating recommendations for coronary angiography following acute myocardial infarction in the elderly: A matched analysis using propensity scores. J Clin Epidemiol 2001;54:387-398.
15. Proietti R, Pecoraro V, Di Biase L, Natale A, Santangeli P, Viecca M, Sagone A, Galli A, Moja L, Tagliabue L: Remote magnetic with open-irrigated catheter vs. manual navigation for ablation of atrial fibrillation: A systematic review and meta-analysis. Europace 2013;15:1241-1248.
16. Sorgente A, Chierchia GB, Capulzini L, Yazaki Y, Muller-Burri A, Bayrak F, Sarkozy A, de Asmundis C, Paparella G, Brugada B: Atrial fibrillation ablation: A single center comparison between remote magnetic navigation, cryoballoon and conventional manual pulmonary vein isolation. Indian Pacing Electrophysiol J 2010;10:486-495.
17. Miyazaki S, Shah AJ, Xhaet O, Derval N, Matsuo S, Wright M, Nault I, Forclaz A, Jadidi AS, Knecht S, Rivard L, Liu X, Linton N, Sacher F, Hocini M, Jais P, Haissaguerre M: Remote magnetic navigation with irrigated tip catheter for ablation of paroxysmal atrial fibrillation. Circ Arrhythm Electrophysiol 2010;3:585-589.
18. Arya A, Zaker-Shahrak R, Sommer P, Bollmann A, Wetzel U, Gaspar T, Richter S, Husser D, Piorkowski C, Hindricks G: Catheter ablation of atrial fibrillation using remote magnetic catheter navigation: A case-control study. Europace 2011;13:45-50.
19. Bauernfeind T, Akca F, Schwagten B, de Groot N, Van Belle Y, Valk S, Ujvari B, Jordaens L, Szili-Torok T: The magnetic navigation system allows safety and high efficacy for ablation of arrhythmias. Europace 2011;13:1015-1021.
20. Choi MS, Oh YS, Jang SW, Kim JH, Shin WS, Youn HJ, Jung WS, Lee MY, Seong KB: Comparison of magnetic navigation system and conventional method in catheter ablation of atrial fibrillation: Is magnetic navigation system is more effective and safer than conventional method? Korean Circ J 2011;41:248-252.
21. Luthje L, Vollmann D, Seegers J, Dorenkamp M, Sohns C, Hasenfuss G, Zabel M: Remote magnetic versus manual catheter navigation for circumferential pulmonary vein ablation in patients with atrial fibrillation. Clin Res Cardiol 2011;100:1003-1011.
22. Solheim E, Off MK, Hoff PI, De Bortoli A, Schuster P, Ohm OJ, Chen J: Remote magnetic versus manual catheters: Evaluation of ablation effect in atrial fibrillation by myocardial marker levels. J Interv Card Electrophysiol 2011;32:37-43.
23. Shurrab M, Danon A, Lashevsky I, Kiss A, Newman D, Szili-Torok T, Crystal E: Robotically assisted ablation of atrial fibrillation: A systematic review and meta-analysis. Int J Cardiol 2013;169:157-165.
24. Adragao P MCF, Cavaco D, Parreira L, Santos P, Carmo P, Carvalho S, Teixeira T, Soares A, Abecasis M: Pulmonary vein reconnection: Is contact force more important than stability? European Heart J 2015;36:731.
25. Kumar S, Chan M, Lee J, Wong MC, Yudi M, Morton JB, Spence SJ, Halloran K, Kistler PM, Kalman JM: Catheter-tissue contact force determines atrial electrogram characteristics before and lesion efficacy after antral pulmonary vein isolation in humans. J Cardiovasc Electrophysiol 2014;25:122-129.
26. Kim AM, Turakhia M, Lu J, Badhwar N, Lee BK, Lee RJ, Marcus GM, Tseng ZH, Scheinman M, Olgin JE: Impact of remote magnetic catheter navigation on ablation fluoroscopy and procedure time. Pacing Clin Electrophysiol 2008;31:1399-1404.
27. Picano E, Vano E, Rehani MM, Cuocolo A, Mont L, Bodi V, Bar O, Maccia C, Pierard L, Sicari R, Plein S, Mahrholdt H, Lancellotti P, Knuuti J, Heidbuchel H, Di Mario C, Badano LP: The appropriate and justified use of medical radiation in cardiovascular imaging: A position document of the ESC Associations of Cardiovascular Imaging, Percutaneous Cardiovascular Interventions and Electrophysiology. Eur Heart J 2014;35:665-672.

CAPÍTULO III

TC Cardíaca

Avaliação anatómica, funcional e valor prognóstico

RESUMO

Neste capítulo é feita uma revisão da utilização da TC cardíaca nos diferentes contextos clínicos e do seu contributo prognóstico na doença cardiovascular.
O capítulo é acompanhado de vários manuscritos da nossa coautoria.
Apresentamos um artigo de revisão (**Manuscrito 3**) sobre TC cardíaca (1) e um artigo sobre a contextualização do estudo multicêntrico PARADIGM que avalia a progressão da doença coronária detetada por TC (**Manuscrito 4**)(2) e as suas implicações prognósticas.
Ainda dentro do âmbito da utilização da TC cardíaca no contexto da doença coronária estável anexamos o artigo sobre custo-eficácia (**Manuscrito 5**)(3).
Referente à avaliação morfo-funcional e na comparação com outras técnicas anexamos dois artigos (**Manuscritos 6** e **7**) (4, 5).
No contexto do valor prognóstico e da sua implicação em populações específicas ou com fatores de risco determinados anexamos os **Manuscritos 8 — 14** (6-12).
Na integração de diversos parâmetros com valor prognóstico, utilizando técnicas de inteligência artificial, incluímos o **Manuscrito 15** (13).
Por fim descrevemos, em maior pormenor, a utilização da TC cardíaca nos doentes com FA.

MANUSCRITOS

Manuscrito 3

Cardiac CT: the end of invasive coronary angiography as a diagnostic procedure?

Goncalves Pde, A. and **Marques**, **H**., Rev Port Cardiol, 2009. **28**(7-8): p. 825-42.

Manuscrito 4

Rationale and design of the Progression of AtheRosclerotic PlAque DetermIned by Computed TomoGraphic Angiography IMaging (PARADIGM) registry: A comprehensive exploration of plaque progression and its impact on clinical outcomes from a multicenter serial coronary computed tomographic angiography study.

Lee, S.E., H.J. Chang, A. Rizvi, M. Hadamitzky, Y.J. Kim, E. Conte, D. Andreini, G. Pontone, V. Volpato, M.J. Budoff, I. Gottlieb, B.K. Lee, E.J. Chun, F. Cademartiri, E. Maffei, **H. Marques**, J.A. Leipsic, S. Shin, J.H. Choi, N. Chung, and J.K. Min, Am Heart J, 2016. **182**: p. 72-79.

Manuscrito 5

Cost-effectiveness of different diagnostic strategies in suspected stable coronary artery disease in Portugal.

Ferreira, A.M., **Marques**, **H**., Goncalves, P.A., and Cardim, N., Arq Bras Cardiol, 2014. **102**(4): p. 391-402.

Manuscrito 6

Modified continuity equation using left ventricular outflow tract three-dimensional imaging for aortic valve area estimation.

Pinto Teixeira, P., Ramos, R., Rio, P., Moura Branco, L., Portugal, G., Abreu, A., Galrinho, A., **Marques**, **H**., Figueiredo, L., and Cruz Ferreira, R., Echocardiography, 2017. **34**(7): p. 978-985.

Manuscrito 7

Left ventricular diverticulum: a finding by cardiac CT angiography

Dourado, R., Goncalves, P.A., **Marques**, **H**., Gaspar, A., Machado, F.P., and Roquette, J.,. Rev Port Cardiol, 2009. **28**(3): p. 341-4.

Manuscrito 8

White-coat hypertension during coronary computed tomography angiography is associated with higher coronary atherosclerotic burden.

Costa, C., de Araujo Goncalves, P., Ferreira, A., Pitta, M.L., Dores, H., Cardim, N., and **Marques**, **H**., Coron Artery Dis, 2017. **28**(1): p. 57-62.

Manuscrito 9

Diabetes as an independent predictor of high atherosclerotic burden assessed by coronary computed tomography angiography: the coronary artery disease equivalent revisited.

de Araujo Goncalves, P., Garcia-Garcia, H. M., Carvalho, M.S., Dores, H., Sousa, P. J., **Marques**, **H**., Ferreira, A., Cardim, N., Teles, R.C., Raposo, L., Gabriel, H.M., Almeida, M., Aleixo, A., Carmo, M.M., Machado, F. P., and Mendes, M., Int J Cardiovasc Imaging, 2013. **29**(5): p. 1105-14.

Manuscrito 10

Prevalence and predictors of coronary artery disease in patients with a calcium score of zero.

de Carvalho, M.S., de Araujo Goncalves, P., Garcia-Garcia, H.M., de Sousa, P.J., Dores, H., Ferreira, A., Cardim, N., Carmo, M.M., Aleixo, A., Mendes, M., Machado, F.P., Roquette, J., and **Marques**, **H**., Int J Cardiovasc Imaging, 2013. **29**(8): p. 1839-46.

Manuscrito 11

Relationship of Hypertension to Coronary Atherosclerosis and Cardiac Events in Patients With Coronary Computed Tomographic Angiography.

Nakanishi, R., Baskaran, L., Gransar, H., Budoff, M.J., Achenbach, S., Al-Mallah, M., Cademartiri, F., Callister, T.Q., Chang, H.J., Chinnaiyan, K., Chow, B.J.W., DeLago, A., Hadamitzky, M., Hausleiter, J., Cury, R., Feuchtner, G., Kim, Y.J., Leipsic, J., Kaufmann, P.A., Maffei, E., Raff, G., Shaw, L.J., Villines, T.C., Dunning, A., **Marques**, **H**., Pontone, G., Andreini, D., Rubinshtein, R., Bax, J., Jones, E., Hindoyan, N., Gomez, M., Lin, F.Y., Min, J.K., and Berman, D.S., Hypertension, 2017. **70**(2): p. 293-299.

Manuscrito 12

Sex-Specific Associations Between Coronary Artery Plaque Extent and Risk of Major Adverse Cardiovascular Events: The CONFIRM Long-Term Registry.

Schulman-Marcus, J., Hartaigh, B.O., Gransar, H., Lin, F., Valenti, V., Cho, I., Berman, D., Callister, T., DeLago, A., Hadamitzky, M., Hausleiter, J., Al-Mallah, M., Budoff, M., Kaufmann, P., Achenbach, S., Raff, G., Chinnaiyan, K., Cademartiri, F., Maffei, E., Villines, T., Kim, Y.J., Leipsic, J., Feuchtner, G., Rubinshtein, R., Pontone, G., Andreini, D., **Marques**, **H**., Shaw, L., and Min, J.K., JACC Cardiovasc Imaging, 2016. **9**(4): p. 364-372.

Manuscrito 13

Long-term prognostic impact of CT-Leaman score in patients with non--obstructive CAD: Results from the COronary CT Angiography EvaluatioN For Clinical Outcomes InteRnational Multicenter (CONFIRM) study.

Andreini, D., Pontone, G., Mushtaq, S., Gransar, H., Conte, E., Bartorelli, A.L., Pepi, M., Opolski, M.P., B, O.H., Berman, D.S., Budoff, M.J., Achenbach, S., Al-Mallah, M., Cademartiri, F., Callister, T.Q., Chang, H.J., Chinnaiyan, K., Chow, B.J., Cury, R., Delago, A., Hadamitzky, M., Hausleiter, J., Feuchtner, G., Kim, Y.J., Kaufmann, P.A., Leipsic, J., Lin, F.Y., Maffei, E., Raff, G., Shaw, L.J., Villines, T.C., Dunning, A., **Marques**, **H**., Rubinshtein, R., Hindoyan, N., Gomez, M., and Min, J.K., Int J Cardiol, 2017. **231**: p. 18-25.

Manuscrito 14

Coronary computed tomography angiography-adapted Leaman score as a tool to noninvasively quantify total coronary atherosclerotic burden.

de Araujo Goncalves, P., Garcia-Garcia, H.M., Dores, H., Carvalho, M.S., Jeronimo Sousa, P., **Marques**, **H**., Ferreira, A., Cardim, N., Campante Teles, R., Raposo, L., Mesquita Gabriel, H., Sousa Almeida, M., Aleixo, A., Mota Carmo, M., Pereira Machado, F., and Mendes, M., Int J Cardiovasc Imaging, 2013. **29**(7): p. 1575-84.

Manuscrito 15

Machine learning for prediction of all-cause mortality in patients with suspected coronary artery disease: a 5-year multicentre prospective registry analysis.

Motwani, M., Dey, D., Berman, D.S., Germano, G., Achenbach, S., Al-Mallah, M.H., Andreini, D., Budoff, M.J., Cademartiri, F., Callister, T.Q., Chang, H.J., Chinnaiyan, K., Chow, B.J., Cury, R.C., Delago, A., Gomez, M., Gransar, H., Hadamitzky, M., Hausleiter, J., Hindoyan, N., Feuchtner, G., Kaufmann, P.A., Kim, Y.J., Leipsic, J., Lin, F.Y., Maffei, E., **Marques**, **H**., Pontone, G., Raff, G., Rubinshtein, R., Shaw, L.J., Stehli, J., Villines, T.C., Dunning, A., Min, J.K., and Slomka, P.J., Eur Heart J, 2017. **38**(7): p. 500-507.

SUMÁRIO

3.1. INTRODUÇÃO

A TC cardíaca tem sido um exame com crescente importância no arsenal diagnóstico. Este aspeto tem vindo a ser comprovado pelas sucessivas *guidelines* do seu uso apropriado, com a triplicação de indicações consideradas adequadas entre as duas últimas publicações (2006 e 2010) (14, 15).

A TC cardíaca evoluiu de um exame sem contraste para avaliação do risco cardiovascular (*score* de cálcio), para um exame de exclusão de doença coronária obstrutiva: posteriormente, para deteção de doença coronária e atualmente poderá funcionar como exame único na avaliação do doente com suspeita de doença coronária, dadas as suas capacidades pluripotenciais.

Para elas contribuiu uma evolução tecnológica impar no campo da imagem médica, aliando uma resolução de contraste muito elevada com a utilização de contraste iodado, às resoluções temporais nativas a chegarem aos 66ms, às resoluções espaciais de 0,23mm e a capacidade de obter informação volumétrica de todo o coração apenas num batimento cardíaco (quer por técnicas de movimento de mesa muito elevado e/ /ou por aumento do número de detetores). As técnicas de energia espetral contribuem por um lado, para a redução da dose de contraste iodado necessária; e por outro, permitem a quantificação de iodo por *voxel*, o que permite fazer a avaliação quantitativa.
O desenvolvimento de reconstrução iterativa contribuiu para o aumento da qualidade de imagem, ao otimizar os rácios sinal/ruído, que por sua vez permitem uma redução da dose de radiação e de contraste.
O desenvolvimento e as diferentes utilizações do *gating* prospetivo, assim como a capacidade da ampola produzir maior miliamperagem a kV mais baixos contribuem para a marcada redução de dose de radiação.

Todos estes fatores permitem avaliar mais doentes (mesmo com menor capacidade de modulação de frequência cardíaca ou inclusivamente doentes arrítmicos), com menor contraste, menor radiação e maior acuidade.

3.2. TC CARDÍACA

3.2.1. Avaliação de doença coronária

A TC cardíaca permite a deteção de placas, inclusive as não calcificadas e as não obstrutivas, de forma não invasiva. Consegue determinar características associadas a placas com menor grau de estabilidade, consideradas "vulneráveis", responsáveis por mais de 50% dos eventos coronários agudos(16).

Consegue ainda detetar doentes em risco de progressão rápida da doença aterosclerótica coronária.

Permite igualmente a extrapolação do significado funcional de uma estenose anatómica, através de diferentes técnicas como o gradiente intraluminal, o *fractional flow reserve* (FFR) virtual, de técnicas de perfusão quantitativa de primeira passagem ou de técnicas de energia espetral. A avaliação do FFR virtual permite ainda simular efeito terapêutico de eventual revascularização (17).

Permite também a avaliação de viabilidade, através da avaliação do realce tardio por TC ou ainda por técnicas de energia espetral (18).

Por todas estas capacidades clínicas, associadas à sua grande disponibilidade, à marcada e continua redução de dose de radiação e sobretudo ao facto de ser não invasivo, tornam a TC cardíaca um verdadeiro *game changer* na avaliação do doente com suspeita de doença coronária. Tudo isto é espelhado nas recentes *guidelines* da NICE (National Institute for Health and Care Excellences (NICE) *Clinical Guideline* 95) que, tendo especial ponderação do binómio custo-eficácia, considerou a TC cardíaca (coronária) como exame de primeira linha em doentes com dor torácica de possível causa coronária, ultrapassando na hierarquia diagnóstica exames tão frequentes como

o ECG com prova de esforço. Calcula-se que a aderência a estas *guidelines* provoque um crescimento dos exames de TC cardíaca na ordem dos 600% no Reino Unido.
Em 2014 publicámos um artigo sobre a avaliação de custo-eficácia de diferentes estratégias diagnósticas em doentes com doença coronária estável em Portugal (**Manuscrito 5**) (3).

3.2.2. Avaliação morfo-funcional

A capacidade de avaliação funcional da TC cardíaca apresenta boa acuidade, com boa correlação com a RM (considerada o *gold standard*).
A capacidade de medir dimensões e volumes é inclusive superior às da ecocardiografia, sendo por exemplo: superior na avaliação da real dimensão do anel aórtico para adequada escolha de prótese a ser colocada por via endovascular, bem como para a avaliação dimensional da câmara de saída do ventrículo esquerdo (CSVE), mesmo em relação à ecografia transesofágica 3D (**Manuscrito 6**) (4).
A avaliação da morfologia miocárdica é igualmente efetuada com grande qualidade, permitindo a deteção de pequenas variantes como criptas miocárdicas e divertículos (**Manuscrito 7**) (5).
São portanto indicações apropriadas *per se* ou quando métodos mais baratos e sem radiação têm resultados insuficientes (por exemplo em casos de má janela acústica ecocardiográfica).

3.2.3. Valor prognóstico

São múltiplos e diversos os parâmetros de TC cardíaca com valor prognóstico, com grande evidência clínica.
Para além dos parâmetros que podem ser avaliados por outras técnicas, como por exemplo a disfunção sistólica em caso de doença coronária obstrutiva, existem alguns parâmetros que, de forma não invasiva, apenas podem ser obtidos pelo exame de TC. Dentro destes salientamos os seguintes:

- Presença e quantificação do cálcio coronário (19)
- Presença de placas coronárias não obstrutivas (20-22)
- Localização e grau de estenose de placas coronárias (**Manuscritos 13** e **14**) (11, 12)

> Presença de características de vulnerabilidade nas placas coronárias (23)
> Critérios de maior probabilidade de progressão rápida da doença coronária

Estes e/ou outros parâmetros foram ainda testados em diferentes grupos mantendo valor prognóstico, como por exemplo homens *versus* mulheres (**Manuscrito 8**) (10), em doentes com suspeita de SCA em contexto de urgência, em mulheres jovens (com história familiar de doença coronária precoce — *score* de cálcio) ou em doentes diabéticos, para citar apenas alguns (**Manuscrito 9**, **10** e **11**) (6, 7, 9).
Não há outra medida em Cardiologia que comprovadamente confira um tão bom prognóstico a médio prazo para eventos coronários do que um *score* de cálcio igual a zero (doentes fora de um contexto agudo). No entanto podem ser definidos preditores de doença nestes doentes como publicado pelo nosso grupo (**Manuscrito 12**) (8).
A integração dos diversos fatores com técnicas de inteligência artificial permite aumentar ainda mais o valor prognóstico da TC cardíaca (**Manuscrito 15**) (13).

3.3. TC CARDÍACA EM DOENTES COM FIBRILHAÇÃO AURICULAR

A avaliação de doentes arrítmicos durante a aquisição sempre colocou dificuldades acrescidas na avaliação cardíaca por TC, sendo fonte de artefactos e portanto condicionando a acuidade do método.

Com o desenvolvimento tecnológico, associado a centros de grande volume e treino, foi possível começar a avaliar estes doentes, inclusive as coronárias. Este aspeto deveu-se sobretudo à melhoria da resolução temporal (permite avaliação de coronárias mesmo em intervalos RR menores) e à capacidade de obter a informação volumétrica cardíaca em menos rotações (idealmente todo o volume num só batimento cardíaco) (24).
Há, no entanto, diversas outras formas de permitir melhores imagens (mesmo em aparelhos menos recentes), com menos artefactos ao adquirir e reconstruir imagens de forma específica para cada doente e cada tipo de arritmia. São exemplo disso a menor modulação da dose ao longo do RR, a utilização de *pitch* menores ou até aquisições axiais *step and shoot* com rejeição de extrassístoles se estas forem em número

reduzido. Mas, num contexto de FA, talvez a mais importante seja a reconstrução em tempo absoluto após a onda T, local isovolumétrico do ciclo cardíaco e temporalmente constante em doentes em FA

Esta capacidade de "retirar" a arritmia (os artefactos condicionados pela arritmia) das imagens permite manter níveis de acuidade dos exames de TC, mesmo para avaliação de pequenas estruturas com grande movimento como são as coronárias (ver **Figura 1**).

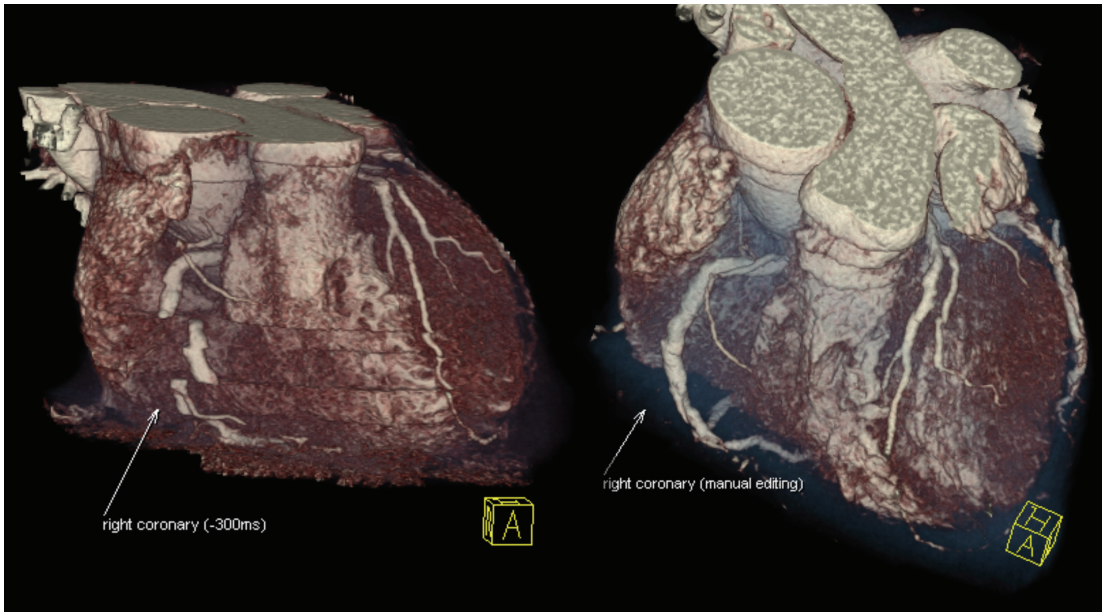

FIGURA 1

Importância da reconstrução após edição manual do ECG para aumentar a acuidade da coronariografia por TC nos doentes em FA durante a aquisição. Imagem da apresentação oral "Coronary CT Angiography in Patients in Atrial Fibrillation Initial Experience with Dual-Source Technology" efetuada no 2nd World Congress of Thoracic Imaging, Valencia 2009.

H. Marques, P. Gonçalves, N. Costa, P. Sousa, F. Machado, A. Gaspar, J. Roquette

(Imagens Hugo Marques — UNICA — Hospital da Luz.)

Para além da avaliação da doença coronária, a TC cardíaca tem outras utilidades nos doentes com FA, nomeadamente:

- antes da realização de tratamento ablativo percutâneo para fornecer mapa anatómico da aurícula e veias pulmonares
- para avaliar a presença de trombo antes de terapêutica ablativa ou de conversão a ritmo sinusal (ver **Figura 2**)

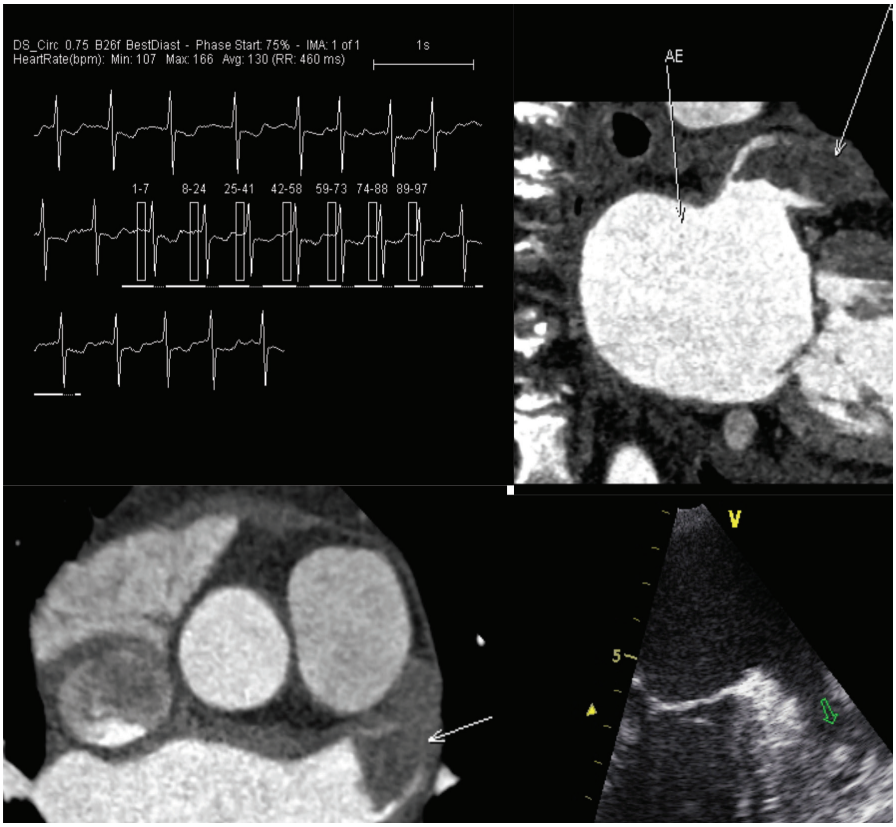

FIGURA 2

Presença de trombo dentro do AAEsq, facilmente diagnosticado, mesmo num doente com FC média próxima dos 100bpm. O trombo foi posteriormente confirmado por ETE.
Imagem do slide da apresentação da palestra do Congresso Nacional de Cardiologia 2017 – Simpósio Luso-Brasileiro – Importância da imagem em Intervenção Cardiovascular – Fibrilhação Auricular.
(Imagens Hugo Marques — UNICA — Hospital da Luz.)

- para avaliação morfológica do AAEsq sobretudo em doentes que irão realizar a sua oclusão de forma percutânea, bem como para avaliar o resultado dessa intervenção
- avaliação de complicações das terapêuticas referidas

Para além do impacto prognóstico que advém da exclusão de trombo antes da conversão a ritmo sinusal ou da intervenção terapêutica (ablativa ou encerramento do AAESQ), a TC fornece outras informações com valor prognóstico nestes doentes. Por exemplo o volume auricular é o principal fator que contribui para o sucesso da terapêutica ablativa, inclusive mais importante do que o tipo de FA (25), sendo ainda o principal contribuidor para o *score* ATLAS — *score* preditor de recidiva após tratamento ablativo percutâneo (26) (**Manuscrito 1 — Capítulo II**).

Embora não seja utilizada em todos os centros num contexto pré-encerramento percutâneo (ou cirúrgico) do AAEsq, a TC cardíaca pode ter um papel relevante.
Permite avaliar o retorno venoso, o septo inter-auricular, a dimensão da aurícula esquerda e a presença de trombo intracardíaco.
Para além desta informação, é o método mais fiável para avaliar a relação do AAEsq com estruturas adjacentes nomeadamente o *ostium* da VPSEsq e a artéria circunflexa, permitindo ainda determinar a dimensão e morfologia do *ostium* do AAEsq e do AAESQ (ver **Figura 3**). Estes aspetos têm relevância prognóstica (27-32).

A TC é ainda um método com grande acuidade para identificar apêndices acessórios e divertículos da AEsq, que são fonte embolígena (33), relativamente frequente não abordada pelo encerramento.
Assim a TC tem utilidade quer no planeamento, quer na avaliação do resultado e na prevenção e diagnóstico de complicações.

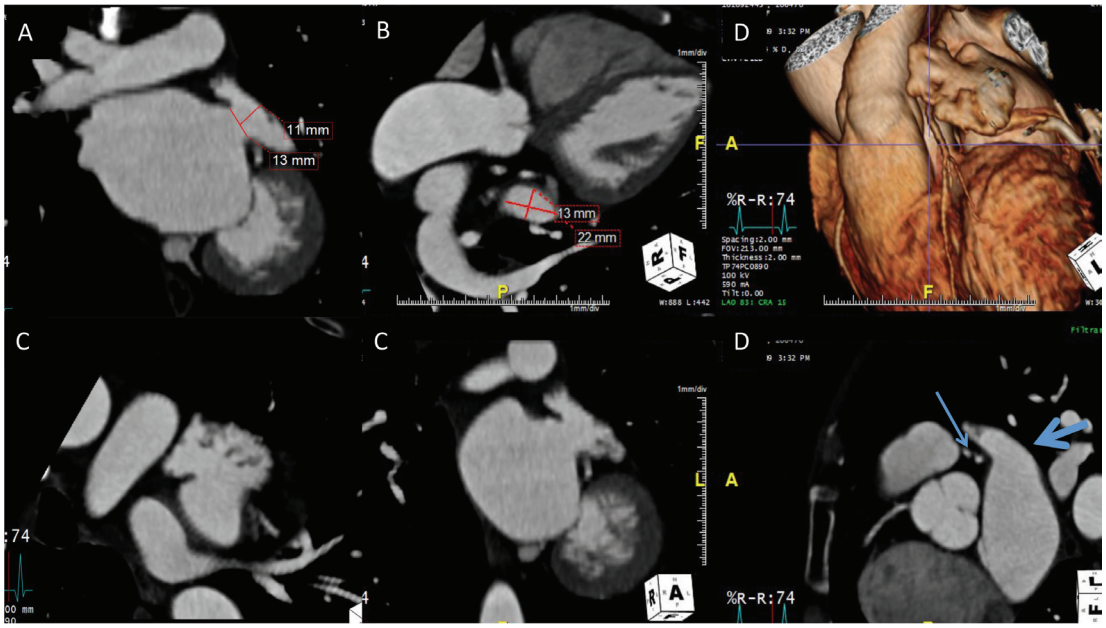

FIGURA 3

Diferente informação fornecida pela TC num contexto prévio a encerramento percutâneo do AAEsq. A) comprimento da câmara de entrada do AAEsq. B) diâmetro do *ostium* do AAEsq. C) exclusão de trombo. D)correlação entre o *ostium* do AAEsq (seta espessa) e a artéria circunflexa (seta fina). Imagem do slide da apresentação da palestra do 1st Edition – New frontiers in Cardiology – Focus on LAA Closure – Hugo Marques – 2015.

(Imagens Hugo Marques — UNICA — Hospital da Luz.)

BIBLIOGRAFIA

1. Goncalves Pde A, Marques H. Cardiac CT: the end of invasive coronary angiography as a diagnostic procedure? Rev Port Cardiol. 2009;28(7-8):825-42.
2. Lee SE, Chang HJ, Rizvi A, et al. Rationale and design of the Progression of AtheRosclerotic PlAque DetermIned by Computed TomoGraphic Angiography IMaging (PARADIGM) registry: A comprehensive exploration of plaque progression and its impact on clinical outcomes from a multicenter serial coronary computed tomographic angiography study. Am Heart J. 2016;182:72-9.
3. Ferreira AM, Marques H, Goncalves PA, et al. Cost-effectiveness of different diagnostic strategies in suspected stable coronary artery disease in Portugal. Arq Bras Cardiol. 2014;102(4):391-402.
4. Pinto Teixeira P, Ramos R, Rio P, et al. Modified continuity equation using left ventricular outflow tract three-dimensional imaging for aortic valve area estimation. Echocardiography (Mount Kisco, NY). 2017;34(7):978-85.
5. Dourado R, Goncalves PA, Marques H, et al. Left ventricular diverticulum: a finding by cardiac CT angiography. Rev Port Cardiol. 2009;28(3):341-4.
6. Costa C, de Araujo Goncalves P, Ferreira A, et al. White-coat hypertension during coronary computed tomography angiography is associated with higher coronary atherosclerotic burden. Coron Artery Dis. 2017;28(1):57-62.
7. de Araujo Goncalves P, Garcia-Garcia HM, Carvalho MS, et al. Diabetes as an independent predictor of high atherosclerotic burden assessed by coronary computed tomography angiography: the coronary artery disease equivalent revisited. Int J Cardiovasc Imaging. 2013;29(5):1105-14.
8. de Carvalho MS, de Araujo Goncalves P, Garcia-Garcia HM, et al. Prevalence and predictors of coronary artery disease in patients with a calcium score of zero. Int J Cardiovasc Imaging. 2013;29(8):1839-46.
9. Nakanishi R, Baskaran L, Gransar H, et al. Relationship of Hypertension to Coronary Atherosclerosis and Cardiac Events in Patients With Coronary Computed Tomographic Angiography. Hypertension. 2017;70(2):293-9.
10. Schulman-Marcus J, Hartaigh BO, Gransar H, et al. Sex-Specific Associations Between Coronary Artery Plaque Extent and Risk of Major Adverse Cardiovascular Events: The CONFIRM Long-Term Registry. JACC Cardiovasc Imaging. 2016;9(4):364-72.

11. Andreini D, Pontone G, Mushtaq S, et al. Long-term prognostic impact of CT-Leaman score in patients with non-obstructive CAD: Results from the COronary CT Angiography EvaluatioN For Clinical Outcomes InteRnational Multicenter (CONFIRM) study. Int J Cardiol. 2017;231:18-25.
12. de Araujo Goncalves P, Garcia-Garcia HM, Dores H, et al. Coronary computed tomography angiography-adapted Leaman score as a tool to noninvasively quantify total coronary atherosclerotic burden. Int J Cardiovasc Imaging. 2013;29(7):1575-84.
13. Motwani M, Dey D, Berman DS, et al. Machine learning for prediction of all-cause mortality in patients with suspected coronary artery disease: a 5-year multicentre prospective registry analysis. Eur Heart J. 2017;38(7):500-7.
14. ACCF/ACR/SCCT/SCMR/ASNC/NASCI/SCAI/SIR 2006 appropriateness criteria for cardiac computed tomography and cardiac magnetic resonance imaging. A report of the American College of Cardiology Foundation Quality Strategic Directions Committee Appropriateness Criteria Working Group. Journal of the American College of Radiology : JACR. 2006;3(10):751-71.
15. Taylor AJ, Cerqueira M, Hodgson JM, et al. ACCF/SCCT/ACR/AHA/ASE/ASNC/NASCI/SCAI/SCMR 2010 Appropriate Use Criteria for Cardiac Computed Tomography. A Report of the American College of Cardiology Foundation Appropriate Use Criteria Task Force, the Society of Cardiovascular Computed Tomography, the American College of Radiology, the American Heart Association, the American Society of Echocardiography, the American Society of Nuclear Cardiology, the North American Society for Cardiovascular Imaging, the Society for Cardiovascular Angiography and Interventions, and the Society for Cardiovascular Magnetic Resonance. Journal of cardiovascular computed tomography. 2010;4(6):407.e1-33.
16. Virmani R, Burke AP, Farb A, et al. Pathology of the vulnerable plaque. J Am Coll Cardiol. 2006;47(8 Suppl):C13-8.
17. Benton SM, Jr., Tesche C, De Cecco CN, et al. Noninvasive Derivation of Fractional Flow Reserve From Coronary Computed Tomographic Angiography: A Review. Journal of thoracic imaging. 2017.
18. Rodriguez-Granillo GA. Delayed enhancement cardiac computed tomography for the assessment of myocardial infarction: from bench to bedside. Cardiovascular diagnosis and therapy. 2017;7(2):159-70.
19. Qazi AH, Zallaghi F, Torres-Acosta N, et al. Computed Tomography for Coronary Artery Calcification Scoring: Mammogram for the Heart. Progress in cardiovascular diseases. 2016;58(5):529-36.
20. Chow BJ, Small G, Yam Y, et al. Incremental prognostic value of cardiac computed tomography in coronary artery disease using CONFIRM: COroNary computed tomography angiography evaluation for clinical outcomes: an InteRnational Multicenter registry. Circ Cardiovasc Imaging. 2011;4(5):463-72.
21. Leipsic J, Taylor CM, Gransar H, et al. Sex-based prognostic implications of nonobstructive coronary artery disease: results from the international multicenter CONFIRM study. Radiology. 2014;273(2):393-400.
22. Xie JX, Eshtehardi P, Varghese T, et al. Prognostic Significance of Nonobstructive Left Main Coronary Artery Disease in Women Versus Men: Long-Term Outcomes From the CONFIRM

(Coronary CT Angiography Evaluation For Clinical Outcomes: An International Multicenter) Registry. Circ Cardiovasc Imaging. 2017;10(8).

23. Motoyama S, Sarai M, Harigaya H, et al. Computed tomographic angiography characteristics of atherosclerotic plaques subsequently resulting in acute coronary syndrome. J Am Coll Cardiol. 2009;54(1):49-57.
24. Andreini D, Pontone G, Mushtaq S, et al. Atrial Fibrillation: Diagnostic Accuracy of Coronary CT Angiography Performed with a Whole-Heart 230-microm Spatial Resolution CT Scanner. Radiology. 2017;284(3):676-84.
25. Costa FM, Ferreira AM, Oliveira S, et al. Left atrial volume is more important than the type of atrial fibrillation in predicting the long-term success of catheter ablation. Int J Cardiol. 2015;184:56-61.
26. Mesquita JF, A.M.; Cavaco, D.; Costa, F.M.; Carmo, P.; Marques, H.; Morgado, F.; Mendes, Miguel; Adragão, P. Development and validation of a risk score for predicting atrial fibrillation recurrence after a first catheter ablation procedure — ATLAS score. Europace. 2017.
27. Kwong Y, Troupis J. Cardiac CT imaging in the context of left atrial appendage occlusion. Journal of cardiovascular computed tomography. 2015;9(1):13-8.
28. Lopez-Minguez JR, Gonzalez-Fernandez R, Fernandez-Vegas C, et al. Comparison of imaging techniques to assess appendage anatomy and measurements for left atrial appendage closure device selection. The Journal of invasive cardiology. 2014;26(9):462-7.
29. O'Brien J, Al-Hassan D, Ng J, et al. Three-dimensional assessment of left atrial appendage orifice geometry and potential implications for device closure. Int J Cardiovasc Imaging. 2014;30(4):819-23.
30. Price MJ, Gibson DN, Yakubov SJ, et al. Early safety and efficacy of percutaneous left atrial appendage suture ligation: results from the U.S. transcatheter LAA ligation consortium. J Am Coll Cardiol. 2014;64(6):565-72.
31. Schulman-Marcus J, Lin FY, Gransar H, et al. Coronary revascularization vs. medical therapy following coronary-computed tomographic angiography in patients with low-, intermediate- and high-risk coronary artery disease: results from the CONFIRM long--term registry. Eur Heart J Cardiovasc Imaging. 2017;18(8):841-8.
32. Viles-Gonzalez JF, Kar S, Douglas P, et al. The clinical impact of incomplete left atrial appendage closure with the Watchman Device in patients with atrial fibrillation: a PROTECT AF (Percutaneous Closure of the Left Atrial Appendage Versus Warfarin Therapy for Prevention of Stroke in Patients With Atrial Fibrillation) substudy. J Am Coll Cardiol. 2012;59(10):923-9.
33. Nagai T, Fujii A, Nishimura K, et al. Large thrombus originating from left atrial diverticulum: a new concern for catheter ablation of atrial fibrillation. Circulation. 2011;124(9):1086-8.

ANEXOS

MANUSCRITO 3

Cardiac CT:
the end of invasive coronary angiography as a diagnostic procedure?

Goncalves Pde, A. and **Marques**, **H**.

Rev Port Cardiol, 2009
28(7-8): p. 825-42

Manuscrito 3

ARTIGOS DE REVISÃO

Angio TC cardíaca: o fim da coronariografia invasiva como modalidade diagnóstica? [67]

PEDRO DE ARAÚJO GONÇALVES, HUGO MARQUES

Hospital da Luz, Lisboa, Portugal

Rev Port Cardiol 2009; 28 (7-8): 825-842

RESUMO

Nos últimos anos temos assistido a uma rápida evolução na tecnologia de Tomografia computorizada (TC) multicortes, com uma melhoria crescente da resolução temporal e espacial, fazendo desta uma robusta modalidade na avaliação das artérias coronárias. Apesar da coronariografia invasiva ser ainda considerada o exame de referência para diagnostico de doença coronária, existem várias indicações para as quais a coronariografia por AngioTC cardíaca poderá vir a ser considerada o exame de primeira linha em detrimento da coronariografia por cateterismo cardíaco. Dado o seu elevado valor preditor negativo, esta técnica revela-se particularmente útil para excluir a presença de estenoses coronárias significativas, evitando assim procedimentos diagnósticos invasivos desnecessários, nomeadamente em doentes com probabilidade intermédia e exames de isquémia e/ou queixas inconclusivas ou na avaliação coronária que antecede a cirurgia valvular ou da aorta.

A angioTC cardíaca não se esgota na coronariografia não invasiva, e a avaliação cardíaca extra-coronária, nomeadamente da função ventricular esquerda, bem como a avaliação de achados extra-cardíacos contribuem para a rentabilidade deste exame.

Palavras-Chave

Angio TC cardíaca; Cateterismo cardíaco; Doença coronária; Diagnóstico.

ABSTRACT

Cardiac CT: the end of invasive coronary angiography as a diagnostic procedure?

In recent years, multislice computed tomographic (CT) technology has progressed rapidly, with significant improvements in spatial and temporal resolution, and has become a powerful technique for coronary artery evaluation. Although invasive angiography is still considered the gold standard for the diagnosis of coronary artery disease, there are several indications for which coronary CT angiography (CTA) may become the first-line exam, instead of invasive catheter-based coronary angiography. Because of its high negative predictive value, CTA is very useful to rule out significant coronary stenosis, thus avoiding unnecessary invasive diagnostic procedures, particularly in patients with intermediate probability and inconclusive stress tests and/or symptoms, or in routine coronary evaluation of patients scheduled for valvular or aortic surgery.

CTA is not limited to non-invasive coronary angiography; it can make important additional diagnostic contributions in both extra-coronary cardiac evaluation, such as left ventricular function, and assessment of extracardiac findings.

Key words

Cardiac CT; Cardiac catheterization; Coronary artery disease; Diagnosis.

Recebido para publicação: Janeiro de 2009 • Aceite para publicação: Março de 2009
Received for publication: January 2009 • Accepted for publication: March 2009

cont.

Manuscrito 3

Rev Port Cardiol
Vol. 28 Julho/Agosto 09 / July/August 09

INTRODUÇÃO

A coronariografia invasiva por cateterismo cardíaco tem sido considerada a modalidade de eleição para identificar a presença de doença coronária. Para além de confirmar a sua presença e caracterizar a anatomia coronária e a gravidade e distribuição das lesões, a sua maior vantagem reside na possibilidade de se realizar, quando indicada, revascularização miocárdica por angioplastia. No entanto, numa elevada percentagem dos casos, apenas é realizada a coronariografia diagnóstica, não sendo o doente subsequentemente submetido a angioplastia. Existem várias justificações para esta discrepância entre o número de coronariografias diagnósticas e o número de angioplastias: em primeiro lugar, em alguns casos não se confirmam as suspeitas dos exames não invasivos e na coronariografia não se documenta a presença de estenoses significativas; em segundo lugar, uma percentagem significativa é constituída por doentes com patologia valvular ou da aorta torácica com indicação cirúrgica, nos quais está indicada a realização de uma coronariografia na avaliação de rotina pré-operatória; em terceiro lugar, em alguns casos, após a coronariografia opta-se por outra modalidade terapêutica, nomeadamente optimização da terapêutica médica ou cirurgia de revascularização. Nas estatísticas mais recentemente publicadas da Sociedade Europeia de Cardiologia, a proporção média de procedimentos de intervenção para coronariografias foi de 33% ou seja, cerca de 2 em cada 3 das coronariografias invasivas não motivaram um procedimento de intervenção[1]. Apesar de se tratar actualmente de um procedimento bastante seguro, trata-se de um exame invasivo e assim tem um risco de complicações que, apesar de pouco frequentes, ocorrem por vezes em procedimentos puramente diagnósticos.

Com a evolução recente na tecnologia de tomografia computorizada multicortes, tornou-se possível a realização de uma coronariografia de uma forma não invasiva. A elevada acuidade diagnóstica demonstrada nos estudos comparativos com coronariografia invasiva, justificam que, para algumas indicações, a angiografia por tomografia computorizada (AngioTC) cardíaca seja considerada uma modalidade diagnóstica alternativa à coronariografia por cateterismo

INTRODUCTION

Invasive catheter-based coronary angiography is considered the first-line technique for detection of coronary artery disease (CAD). Besides confirming the presence of CAD and characterizing coronary anatomy and the severity and distribution of lesions, its main advantage is that it affords the possibility, when indicated, of performing myocardial revascularization by angioplasty. However, in a large percentage of cases, the procedure is merely diagnostic and the patient does not undergo angioplasty. There are various reasons for the discrepancy between the number of diagnostic exams and the number of angioplasties. Firstly, in some cases the suspicions aroused by non-invasive exams are not confirmed and coronary angiography does not detect significant stenosis; secondly, a significant proportion of patients have valvular or thoracic aortic disease with indication for surgery, coronary angiography being used in these patients for routine pre-operative evaluation; and thirdly, a different therapeutic approach may be chosen following coronary angiography, for example optimization of medical therapy or revascularization surgery. According to the latest statistics published by the European Society of Cardiology (ESC), the mean percentage of interventions during coronary angiography was 33%; in other words two out of three invasive angiograms do not result in an intervention[1]. Although the procedure is now very safe, it is an invasive exam and as such carries a risk of complications that, while uncommon, do sometimes occur during purely diagnostic procedures.

With the recent development of multislice computed tomographic technology, non-invasive coronary angiography is now feasible. Its high diagnostic accuracy demonstrated in comparative studies with invasive coronary angiography means that for certain indications cardiac CT angiography (CTA) is considered an alternative diagnostic modality to catheter-based coronary angiography[2-4].

The various indications for which cardiac CTA may replace catheter-based coronary angiography as the first-line exam are reviewed below.

cont.

Manuscrito 3

cardíaco[2-4].

De seguida, revêem-se varias indicações para as quais a coronariografia por AngioTC cardíaca poderá vir a ser considerada o exame de primeira linha em detrimento da coronariografia por cateterismo cardíaco.

EXCLUIR A PRESENÇA DE ESTENOSES CORONÁRIAS SIGNIFICATIVAS EM DOENTES COM PROBABILIDADE INTERMÉDIA DE DOENÇA CORONÁRIA

Vários trabalhos publicados na literatura documentam o elevado valor preditor negativo da angioTC cardíaca, que apresenta uma consistente baixa taxa de falsos negativos quando comparada com a técnica de referência - a coronariografia por cateterismo cardíaco. Num trabalho de revisão recentemente publicado pelo grupo de estudos da Sociedade Europeia de Cardiologia, reunindo os trabalhos publicados com os aparelhos de última geração (64 cortes e 64 cortes de dupla ampola), envolvendo mais de 800 doentes, com comparação sistemática com a angiografia convencional, a sensibilidade foi de 89%, a especificidade com 96% e o valor preditor negativo foi de 98%[2]. Assim, a consistente baixa taxa de falsos negativos torna este exame muito atractivo para a exclusão da presença de doença coronária em doentes com probabilidade intermédia de doença coronária e esta é de facto a indicação mais importante e mais frequente para a realização de uma angioTC cardíaca. Num trabalho recentemente publicado por Meijboom et al[5], a acuidade diagnóstica da angioTC cardíaca foi avaliada de acordo com a probabilidade pré-teste de doença coronária, tendo os autores concluído que esta é mais útil nos doentes com probabilidade baixa/intermédia, onde se pode excluir com elevado grau de certeza a presença de doença coronária significativa e evitar assim a coronariografia invasiva. Os doentes que mais se enquadram dentro desta indicação são os que tem exames de documentação de isquémia inconclusivos ou quando apesar de positivos, a probabilidade de acordo com a avaliação clínica (idade, sexo, queixas, perfil de risco) apontam para provavelmente se tratar de um falso positivo. A exclusão de estenoses coronárias com um exame com elevado valor preditor negativo como é o caso da angioTC cardíaca permite assim

EXCLUSION OF SIGNIFICANT CORONARY STENOSIS IN PATIENTS WITH INTERMEDIATE PROBABILITY OF CORONARY ARTERY DISEASE

Various studies have demonstrated the high negative predictive value of cardiac CTA, which has a consistently lower rate of false negatives than the gold standard technique of invasive catheter-based coronary angiography. A review published by the ESC working group involving over 800 patients and systematically comparing state-of-the-art equipment (64-slice and 64-slice dual source systems) with conventional angiography reported 89% sensitivity, 96% specificity and 98% negative predictive value for the former[2]. The consistently low false-negative rate makes this exam particularly attractive for excluding the presence of coronary artery disease in patients with intermediate probability for CAD and this is in fact the most common indication for performing cardiac CTA. In a recent study by Meijboom et al.[5], the diagnostic accuracy of cardiac CTA was assessed according to the pretest probability of CAD, the authors concluding that it was most useful in patients with low or intermediate probability, in whom it can exclude the presence of significant CAD with a high level of certainty and thus avoid invasive coronary angiography. The patients most likely to benefit from this indication are those with inconclusive ischemia testing or those with a positive test but in whom the probability based on clinical assessment (age, gender, symptoms and risk profile) suggests that it is probably a false positive. Using an exam with a high negative predictive value such as cardiac CTA to exclude coronary stenosis avoids unnecessary cardiac catheterization in such patients (*Figs. 1* and *2*).

CORONARY EVALUATION PRIOR TO CARDIAC SURGERY

Coronary angiography prior to surgery is indicated in a wide range of patients with valvular disease, to detect the presence of significant concomitant CAD. According to the latest ESC guidelines on the management of valvular heart disease, besides being indicated in patients with a history of CAD, suspected myocardial ischemia or left ventricular systolic dysfunction, coronary

cont.

Manuscrito 3

Rev Port Cardiol
Vol. 28 Julho/Agosto 09 / July/August 09

evitar nestes doentes a realização desnecessária de cateterismo cardíaco (*Fig. 1* e *2*)

angiography is also recommended in those with only a single risk factor, or even none in the case of men aged over 40 or postmenopausal women[6].

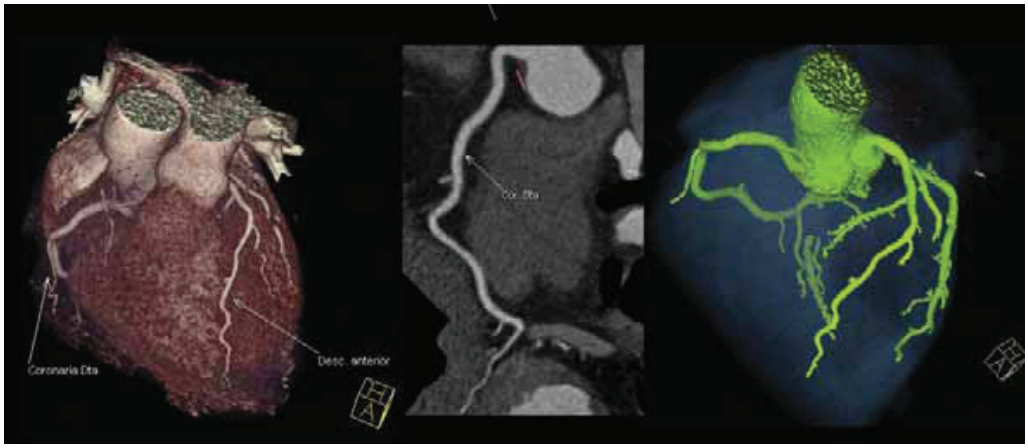

Figura 1. **Reconstruções de volume (VRT), multiplanar (MPR) e coronariografia virtual, em exame com boa qualidade de imagem documentando artéria coronária direita sem placas significativas.**

Figure 1. **Volume-rendered reconstruction (VRT), multi-planar reconstruction (MPR) and virtual coronary angiography: good quality images showing right coronary artery without significant plaques.**

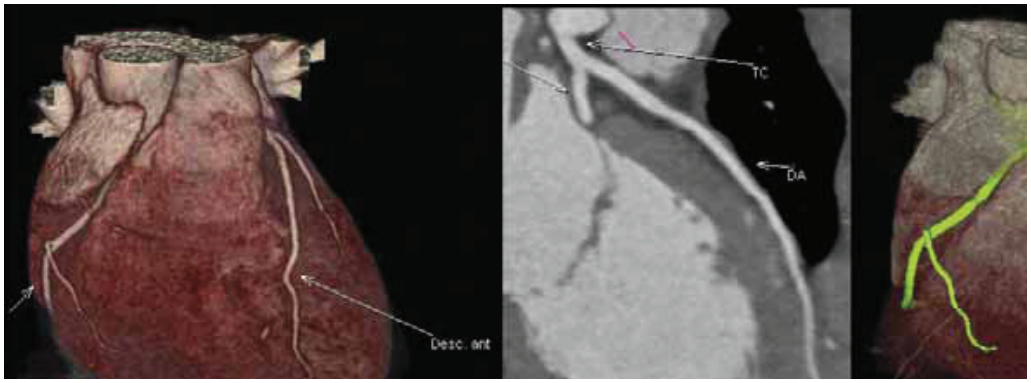

Figura 2. **Reconstruções de volume (VRT), multiplanar (MPR) e coronariografia virtual, em exame com boa qualidade de imagem documentando artéria descendente anterior sem placas significativas.**

Figure 2. **Volume-rendered reconstruction (VRT), multi-planar reconstruction (MPR) and virtual coronary angiography: good quality images showing left anterior descending artery without significant plaques.**

AVALIAÇÃO CORONÁRIA PRÉ-CIRURGIA CARDÍACA

Na presença de doença valvular com indicação cirúrgica, está indicada a realização de coronariografia, para avaliar a presença concomitante de doença coronária significativa, sendo esta indicação bastante abrangente. De acordo com as últimas recomendações de manejo

It is common in such patients to find no significant CAD, and even when it is present, coronary angiography is merely diagnostic, surgical revascularization being performed at the same time as valve surgery. This means that patients are exposed to the risks inherent in an invasive exam for purely diagnostic purposes. While the risks are low, they are not negligible, particularly in patients under anticoagulant

cont.

Manuscrito 3

das doenças valvulares da Sociedade Europeia de Cardiologia, para além de estar indicada em doentes com antecedentes de doença coronária, com suspeita de isquémia miocárdica ou com disfunção sistólica ventricular esquerda, a coronariografia está ainda indicada na presença de apenas um factor de risco e mesmo na ausência destes, caso se trate de um doente do sexo masculino com mais de 40 anos, ou de uma mulher pós menopausica[6].

Nestes doentes, é frequente não se encontrar doença coronária significativa e mesmo nos casos em que existe doença coronária associada à doença valvular, apenas é realizada a coronariografia diagnóstica, sendo a revascularização feita cirurgicamente aquando da cirurgia valvular. Deste modo, os doentes são expostos aos riscos inerentes a um exame invasivo, para fins puramente diagnósticos. Estes riscos, apesar de baixos, não são desprezíveis, nomeadamente em doentes anticoagulados ou na presença de insuficiência aórtica, reconhecidos preditores de complicações hemorrágicas.

Num estudo que incluiu 70 doentes com indicação para cirurgia valvular[7], foi avaliada a acuidade diagnóstica da angioTC cardíaca, em comparação com a coronariografia convencional. Neste trabalho, realizado com um aparelho de 64 cortes foram excluídos doentes com fibrilhação auricular e insuficiência renal e englobou vários tipos de valvulopatia, inclusive doentes com estenose aórtica. O desempenho diagnóstico da angioTC cardíaca foi excelente, com uma sensibilidade de 100%, especificidade de 92%, valor preditor positivo de 82% e valor preditor negativo de 100%. Dos 4 falsos positivos verificados, 3 foram em doentes cuja valvulopatia era estenose aórtica. Este constitui um subgrupo de doentes valvulares onde provavelmente esta técnica se depara ainda com algumas limitações, uma vez que se tratam habitualmente de doentes mais idosos, com maior probabilidade de doença coronária concomitante e com elevada prevalência de lesões coronárias calcificadas, cujo grau de estenose é habitualmente sobrevalorizado na angioTC. Num outro trabalho que incluiu apenas doentes com estenose aórtica, o valor médio de score de cálcio foi de 609±860 e foi identificado o limiar de 1000, valor a partir do qual a frequência de segmentos não interpretáveis era bastante elevada[8].

Os doentes com fibrilhação auricular, frequen-

therapy and those with aortic regurgitation, which are recognized predictors of bleeding complications.

A study of 70 patients referred for cardiac valve surgery[7] assessed the diagnostic accuracy of cardiac CTA compared to conventional coronary angiography. The study excluded patients with atrial fibrillation (AF) and renal failure, and covered various types of valve disease, including aortic stenosis. The diagnostic performance of cardiac CTA, using a 64-slice system, was excellent, with 100% sensitivity, 92% specificity, 82% positive predictive value and 100% negative predictive value. Three of the four false positives were in patients with aortic stenosis, and the technique probably still has certain limitations in this patient subgroup, since they are usually older and thus more likely to have concomitant CAD with a high prevalence of calcified lesions, in which the degree of stenosis is generally overestimated by CTA. In another study that included only patients with aortic stenosis, the mean calcium score was 609±860; a threshold of 1000 was identified, beyond which the proportion of non-interpretable segments was too high[8].

Patients with AF, which is common in the context of mitral disease, are another subgroup in whom coronary CTA has lower diagnostic accuracy. This arises from the need to synchronize the images acquired with the ECG, which is particularly difficult in the presence of considerable RR variability. The better temporal resolution of the latest 64-slice dual source CT systems may overcome this limitation and initial studies have been promising[9,10] (*Fig. 3*). Moreover, new 320-slice systems that provide sufficient craniocaudal coverage to acquire the entire heart in a single rotation, thus eliminating stair-step artifacts, also have great potential in these patients. For now, AF remains a significant obstacle to obtaining a good diagnostic quality CT coronary angiogram in most AF patients using standard 64-slice equipment.

Non-invasive coronary angiography is thus a good alternative for pre-operative evaluation of CAD in the context of valve disease. In fact, while not as yet a recommendation, the use of cardiac CTA by experienced centers is mentioned in the latest ESC guidelines on valvular heart disease as a way to exclude CAD in patients with low probability[6].

cont.

Manuscrito 3

Rev Port Cardiol
Vol. 28 Julho/Agosto 09 / July/August 09

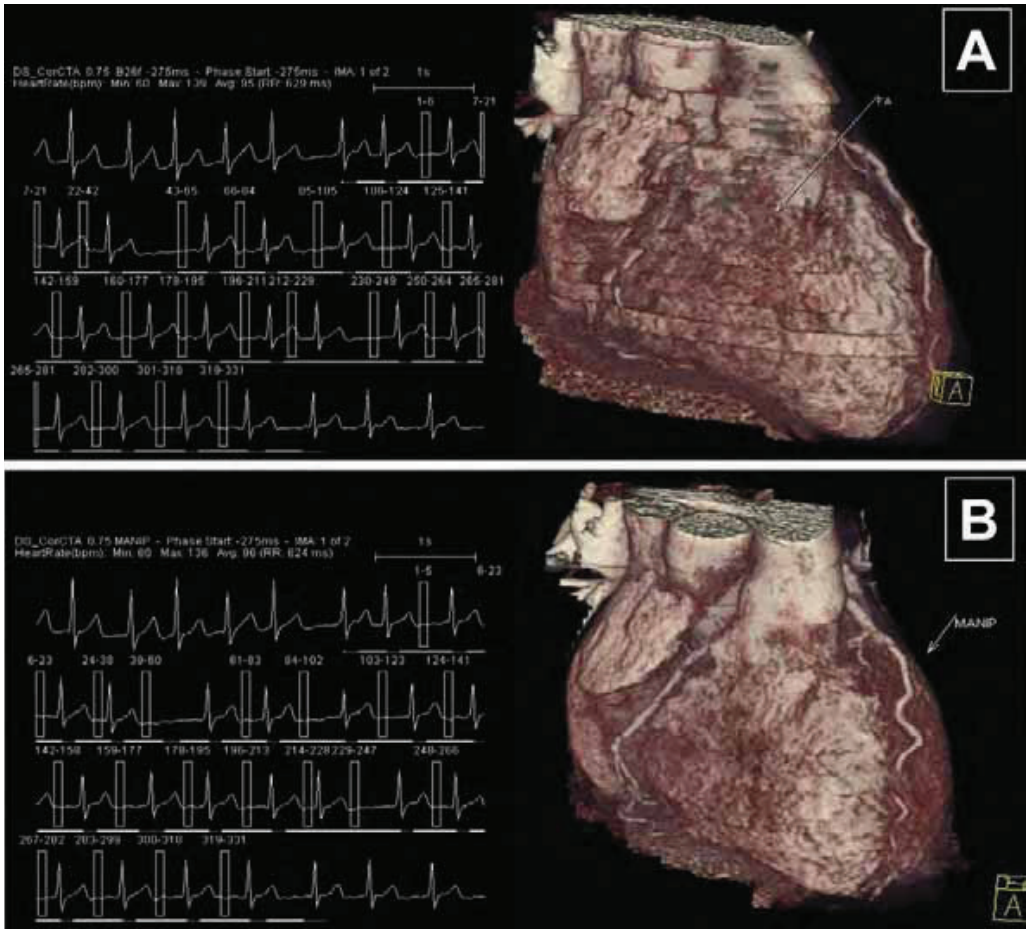

Figura 3 **Reconstruções de volume (VRT) do mesmo doente em fibrilhação auricular com resposta ventricular média de 95/min durante a aquisição, com grande variabilidade RR (60-139). A – reconstrução automática em -275 ms; B- reconstrução após edição manual do ECG.**

Figure 3 **Volume-rendered reconstruction (VRT) of the same patient in atrial fibrillation with mean ventricular rate of 95 bpm and considerable RR variability (60-139). A: automatic reconstruction at -275 ms; B: reconstruction after manual editing of the ECG.**

te no contexto de doença mitral, constituem um outro subgrupo em que a coronariografia por TC tem uma menor acuidade diagnóstica. Este facto resulta da necessidade de sincronizar com o ECG as imagens adquiridas, o que se torna particularmente difícil quando existe grande variabilidade RR. A elevada resolução temporal dos aparelhos de angioTC de última geração de 64 cortes de dupla ampola, poderá vir a ultrapassar esta limitação, sendo a experiência inicial bastante promissora[9,10] (*Fig. 3*). Por outro lado, os novos aparelhos de 320 cortes, ao permitir uma cobertura crâneo-caudal suficiente para a aquisição cardíaca total numa só rotação,

ASSESSMENT OF PATIENTS WITH PREVIOUS MYOCARDIAL REVASCULARIZATION

Monitoring of patients with previous surgical or percutaneous myocardial revascularization is by clinical assessment and ischemia testing, and control coronary angiography is not routinely indicated. However, it can be scheduled during follow-up in certain cases, generally following complex interventions, such as angioplasty of the left main coronary artery, or in patients enrolled in clinical trials evaluating new stents. Assessment of stent patency is hindered by

cont.

Manuscrito 3

eliminando assim os artefactos de escada, terão um elevado potencial de aplicação nestes doentes. De qualquer modo, a fibrilhação auricular é ainda uma importante limitação à realização de uma coronariografia por TC de boa qualidade diagnóstica, na grande maioria dos doentes, com os aparelhos *standard* de 64 cortes.

A realização da coronariografia não invasiva poderá ser assim uma boa alternativa para estudo pré-operatório de doença coronária no contexto de doença valvular. De facto, apesar de não constituir ainda uma recomendação, nas mais recentes *guidelines* de doenças valvulares da ESC, vem já referida a hipótese de, em doentes com baixa probabilidade, ser realizada a exclusão de doença coronária por angioTC cardíaca, em centros com experiência nesta técnica[6].

artifacts arising from the alloys used in stents, as well as by stent diameter, because of CTA's limited spatial resolution compared to conventional angiography. However, most modern stents of a reasonable caliber (>3 mm) can be assessed. In a recent review by the ESC Working Group of the results of various studies comparing 64-slice and 64-slice dual source systems with conventional angiography, 88% of the 684 stents included in these studies were correctly assessed[3]. Thus, for cases in which control angiography is indicated during follow-up and particularly when there is a low likelihood of need for further percutaneous intervention, CTA may be a good alternative (*Fig. 4*).

In patients with previous coronary bypass surgery, the usefulness of cardiac CTA depends mainly on the clinical reason for the exam. If the objective is to assess bypass graft patency, CTA is highly accurate, not only because of its sensitivity but also due to its high specificity in

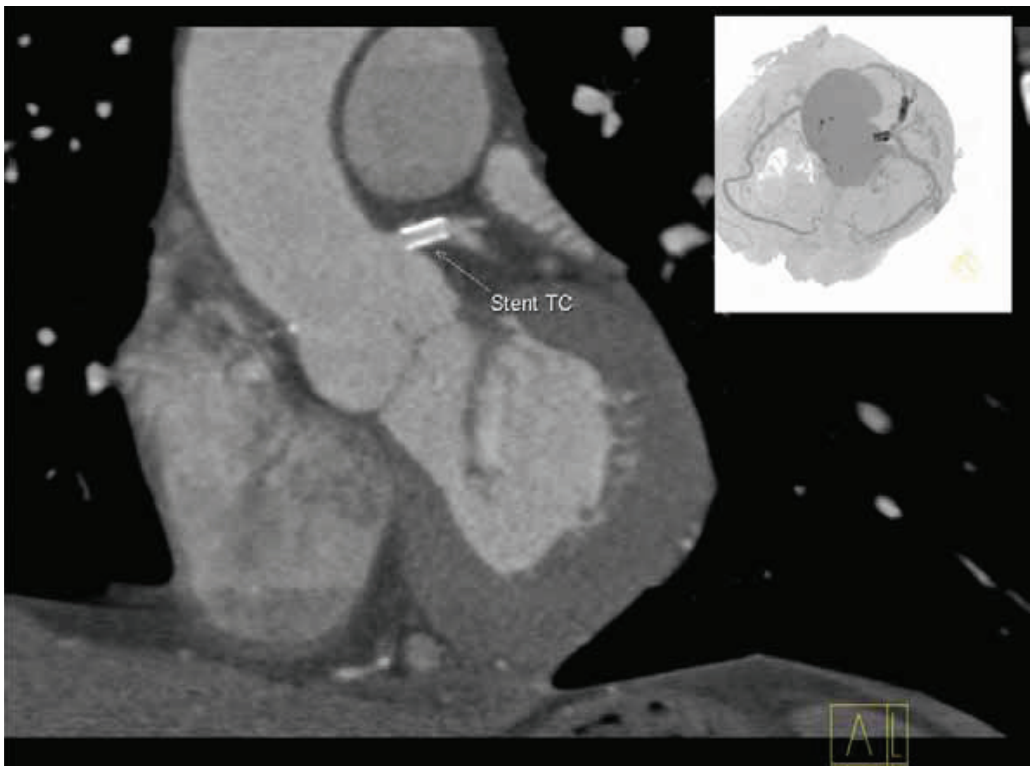

Figura 4. **Reconstrução multiplanar (MPR) e coronariografia virtual, documentando ausência de restenose de um *stent* Xience 3,5/8mm no tronco comum.**

Figure 4. **Multi-planar reconstruction (MPR) and virtual coronary angiography showing absence of restenosis in a 3.5x8.0mm Xience stent in the left main coronary artery.**

cont.

Manuscrito 3

Rev Port Cardiol
Vol. 28 Julho/Agosto 09 / July/August 09

AVALIAÇÃO DE DOENTES COM ANTECEDENTES DE REVASCULARIZAÇÃO MIOCÁRDICA

O seguimento dos doentes com antecedentes de revascularização miocárdica cirúrgica ou percutânea é feito clinicamente e com exames de documentação de isquémia, não estanto indicada a realização, por rotina, de uma nova coronariografia de controlo. No entanto, em determinados casos, fica planeada a realização de nova coronariografia no seguimento. Habitualmente tratam-se de casos de intervenções complexas, como é o caso da angioplastia do tronco comum ou então de doentes incluídos em ensaios clínicos para avaliação de novos *stents*. A avaliação da patência dos *stents* é prejudicada pelos artefactos resultantes das ligas metálicas dos *stents*. Esta depende não só do tipo de liga metálica, mas sobretudo do diâmetro do *stent*, dadas as limitações de resolução espacial desta técnica, em comparação com a angiografia convencional. De qualquer modo, a grande maioria dos *stents* de nova geração, desde que tenham um calibre razoável (>3mm), são passíveis de avaliação. Numa revisão recente do grupo de estudos da Sociedade Europeia de Cardiologia, englobando os resultados de vários trabalhos publicados com aparelhos de 64 cortes e 64 cortes de dupla ampola, com comparação sistemática com angiografia convencional, 88% dos 684 *stents* incluídos nestes estudos, foram correctamente avaliados[4]. Assim, para os casos em que esteja indicada uma nova coronariografia no seguimento e sobretudo quando se antecipa uma baixa probabilidade de nova intervenção percutânea, a coronariografia por TC poderá constituir uma boa alternativa. (*Fig. 4*)

No caso dos doentes com antecedentes de cirurgia coronária, a utilidade da angioTC cardíaca depende sobretudo da questão clínica. Se o objectivo for documentar a patência das pontagens, a acuidade da angioTC é elevada, não só pela habitual sensibilidade, mas também por uma elevada especificidade, dado tratar-se de vasos de maior calibre, com menor movimento e cujas lesões habitualmente não são calcificadas (*Fig. 5*). No caso das pontagens arteriais, apesar da presença de artefactos resultantes dos *clips* metálicos (*Fig. 6*), a sua avaliação é igualmente possível na grande maioria dos casos e é ainda possível avaliar a sua relação com a parede

assessing large caliber vessels that are liable to move less and in which the lesions are generally not calcified (*Fig. 5*). Arterial grafts can also be assessed in most cases, despite the presence of surgical clip artifacts (*Fig. 6*), as can their relationship to the thoracic wall, which is useful information when repeat sternotomy is necessary. A recent study assessing 418 bypass grafts in 138 patients with a standard 64-slice system reported 97% specificity, with no significant differences between venous and arterial grafts[11].

However, assessment of native circulation in such patients is more difficult due to the presence of advanced coronary atherosclerosis, frequently with widespread disease, multiple calcified plaques and small caliber arteries, all significant limitations given the current spatial resolution of CTA, even using the latest systems[12].

INDICATIONS IN THE EMERGENCY DEPARTMENT

Exclusion of acute coronary syndrome (ACS) in patients in the emergency department is sometimes difficult, particularly when initial assessment detects no significant ECG abnormalities and biomarkers of myocardial damage are negative. Patients often remain under observation, serial assessments being performed until the likelihood of ACS is considered low. In cases of an apparently normal ECG and negative biomarkers, using CTA to exclude significant coronary disease would enable rapid risk stratification and earlier discharge. Conversely, it could also identify patients who do in fact have significant coronary disease despite being considered at low risk on the basis of conventional assessment by ECG and biomarkers. Initial studies have demonstrated the high diagnostic accuracy of CTA in this context[13,14], as well as its cost-effectiveness, compared to stratification using standard algorithms[15]. A study following patients discharged early after exclusion of significant CAD by CTA reported no significant coronary events[16]. Further studies will help to validate the prognostic impact of this strategy.

Besides ACS, differential diagnosis of patients admitted to the emergency department with acute chest pain includes aortic dissection and pulmonary embolism. Protocols have been developed that enable assessment of these three

cont.

Figura 5. **Reconstruções de volume (VRT) e multiplanar (MPR) documentando lesão significativa do segmento médio de uma safena para obtusa marginal; imagem correspondente da coronariografia invasiva.**

Figure 5. **Volume-rendered reconstruction (VRT) and multi-planar reconstruction (MPR) showing significant lesion of the mid segment of a saphenous vein to obtuse marginal graft. Corresponding image from invasive coronary angiography.**

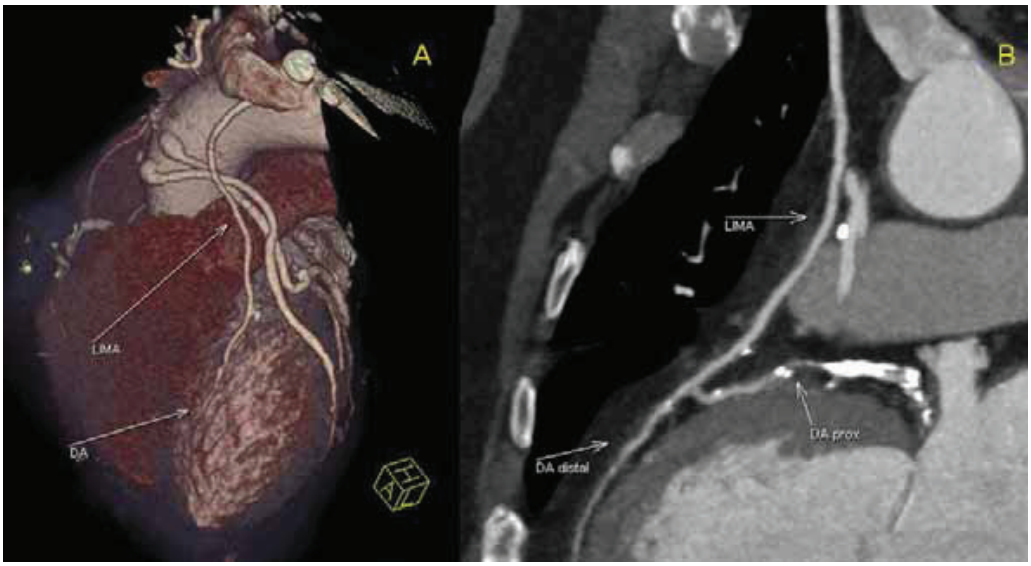

Figura 6. **Reconstruções de volume (VRT) e multiplanar (MPR) documentando patência da pontagem de mamária interna esquerda para a descendente anterior, bem como doença significativa calcificada suboclusiva na descendente anterior a montante da anastomose.**

Figure 6. **Volume-rendered reconstruction (VRT) and multi-planar reconstruction (MPR) showing patent internal mammary to left anterior descending graft (LAD), as well as significant calcified subocclusive disease in the LAD upstream of the anastomosis.**

torácica, informação útil nos casos em que é necessário nova esternotomia. De facto, num trabalho recentemente publicado que envolveu a avaliação de 418 pontagens em 138 doentes com um aparelho de 64 cortes convencional, a especificidade chegou aos 97% e não houve diferenças significativas entre pontagens venosas ou arteriais[11].

important pathologies in a single CT scan, known as "triple rule-out"[17,18].

Finally, for some patients admitted to the emergency department with chest pain, the diagnosis is myocarditis or myopericarditis. Such cases often present repolarization abnormalities on the ECG and positive biomarkers of myocardial damage, so differential diagnosis must be made

cont.

Manuscrito 3

Rev Port Cardiol
Vol. 28 Julho/Agosto 09 / July/August 09

No entanto, nestes doentes, a avaliação da circulação nativa torna-se mais difícil, dada a presença de aterosclerose coronária avançada, sendo frequente a presença de doença difusa, múltiplas placas calcificadas e artérias de pequeno calibre, limitações importantes perante a actual resolução espacial destes exames, mesmo com os aparelhos de última geração[12].

INDICAÇÕES NO SERVIÇO DE URGÊNCIA

A avaliação de doentes no serviço de urgência para exclusão da hipótese de síndrome coronário agudo (SCA) é por vezes difícil, sobretudo nos casos em que na avaliação inicial não se detectam alterações significativas no ECG e os biomarcadores de lesão miocárdica são negativos. Estes doentes ficam por vezes em observação, fazendo avaliações seriadas até ser considerada baixa a probabilidade de se tratar de um SCA. Nestes casos em que o ECG é "inocente" e os biomarcadores negativos, a exclusão de doença coronária significativa por angio TC poderá permitir uma rápida estratificação de risco, conduzindo a uma alta precoce. Por outro lado poderá também identificar alguns doentes que com base na avaliação convencional com ECG e biomarcadores seriam considerados de baixo risco e que apresentam de facto doença coronária significativa. Alguns estudos iniciais documentaram a elevada acuidade diagnóstica da angioTC neste contexto[13,14], bem como o custo-eficácia desta estratégia, quando comparada com a estratificação pelos algoritmos convencionais[15]. Num estudo em que foi feito o seguimento dos doentes a quem foi dada alta precoce, após exclusão de doença coronária significativa pela angio TC, foi documentada a ausência de eventos coronários significativos nesta população[16]. Mais trabalhos contribuirão certamente para validar o impacto prognóstico desta estratégia.

No diagnóstico diferencial do doente admitido no serviço de urgência com dor torácica aguda, para além dos síndromes coronários agudos fazem igualmente parte a dissecção da aorta e a embolia pulmonar. Foram já desenvolvidos protocolos que permitem avaliar estas 3 patologias importantes na mesma aquisição – protocolo *triple rule out*[17,18].

Finalmente, alguns doentes admitidos no

with ACS, for which they are generally referred for invasive coronary angiography to exclude CAD. Since many of these patients – usually young individuals with no history of cardiovascular disease and a low risk profile – have a low probability of CAD, this situation would be a good indication for non-invasive angiography using CTA. Studies have yet to be performed to validate this strategy.

CARDIAC CT ANGIOGRAPHY BEYOND NON-INVASIVE CORONARY ANGIOGRAPHY: EXTRA-CORONARY CARDIAC EVALUATION AND ASSESSMENT OF EXTRACARDIAC FINDINGS

Another advantage of CTA compared to conventional coronary angiography is that it can provide extra-coronary cardiac information and assess extracardiac findings in the same exam, without the need to increase radiation or contrast doses. Although extra-coronary cardiac evaluation is not usually the reason for the exam and most patients will already have undergone echocardiography, findings may be identified that went undetected in previous exams, particularly in patients with poor acoustic windows[19-21] (*Fig.* 7).

The technique also scans the thoracic segments included in cardiac acquisition, and extracardiac findings are common in the lung and mediastinal fields[22].

CARDIAC CT ANGIOGRAPHY BEYOND DOCUMENTING SIGNIFICANT STENOSIS: PLANNING REVASCULARIZATION STRATEGIES

Although exclusion of CAD is the main indication for cardiac CTA, when significant coronary stenosis is detected the information provided by this exam can be useful in planning revascularization strategies.

Recent studies have demonstrated the value of cardiac CTA to predict the outcome of recanalization of chronic occlusions[23,24] and to assess distribution patterns of coronary bifurcation lesions[25,26], which is useful in decisions regarding revascularization (*Fig. 8*).

Cardiac CTA can also characterize plaques,

cont.

Manuscrito 3

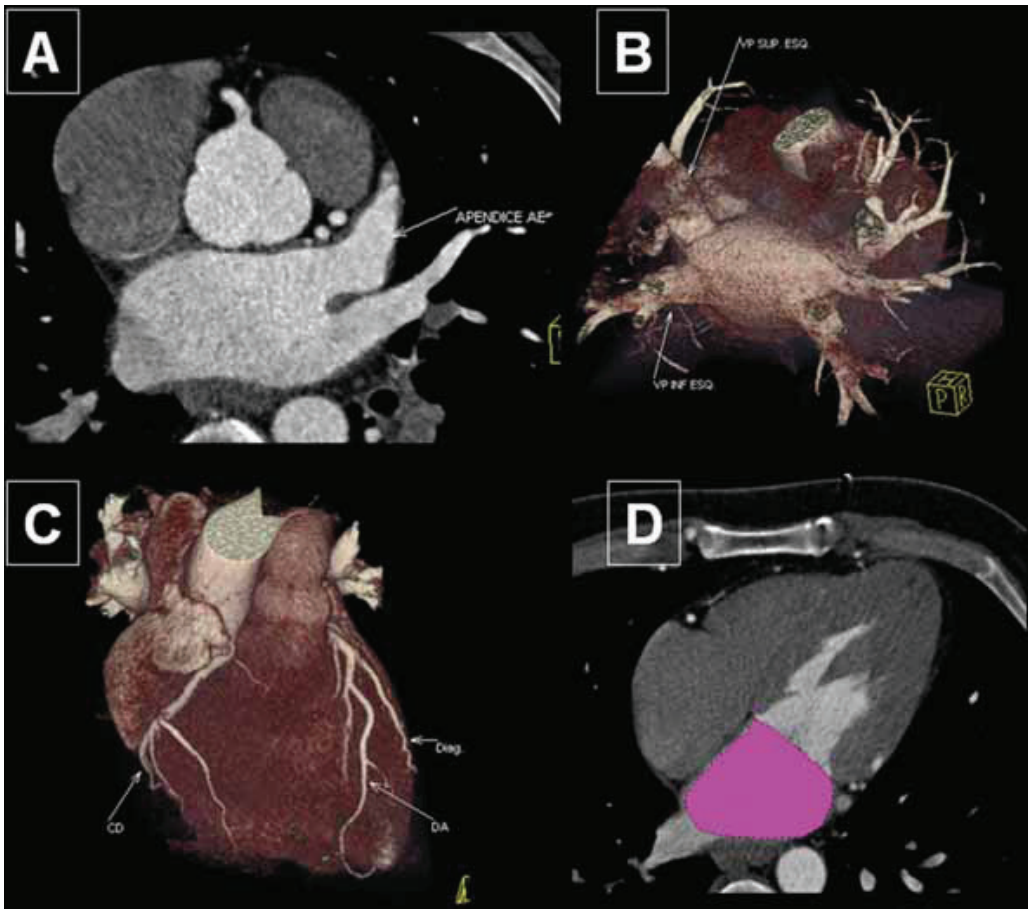

Figura 7. **Reconstruções de volume (VRT) e multiplanares (MPR) num doente que realizou angioTC cardíaca para avaliação pré-ablação de fibrilhação auricular. Para além da exclusão de trombo no apêndice auricular esquerdo (A), avaliação do padrão de distribuição das veias pulmonares (B), avaliação coronária (C) e medição do volume da aurícula esquerda (D), foi ainda diagnosticada uma miocardiopatia hipertrófica apical.**

Figure 7. **Volume-rendered reconstruction (VRT) and multi-planar reconstruction (MPR) of a patient undergoing cardiac CT angiography for pre-ablation assessment of atrial fibrillation. As well as excluding thrombus in the atrial appendage (A), assessing the distribution of the pulmonary veins (B), coronary evaluation (C), and measurement of left atrial volume (D), apical hypertrophic cardiomyopathy was also diagnosed.**

serviço de urgência por precordialgia, o diagnóstico é de miocardite ou miopericardite. Como é frequente estes casos se acompanharem de alterações da repolarização no ECG e de positividade dos biomarcadores de lesão miocárdica, torna-se necessário fazer o diagnóstico diferencial com síndrome coronário agudo, pelo que geralmente são propostos para a realização de coronariografia invasiva para exclusão de doença coronária. Como em muitos destes casos a probabilidade de doença coronária é baixa – tratam-se geralmente de indivíduos jovens, sem antecedentes cardiovasculares e com baixo perfil de risco - esta seria uma boa

particularly the presence of calcification, which is also important for coronary interventions, since angioplasty of calcified coronary lesions is generally more difficult and sometimes requires special devices.

OTHER INDICATIONS

There are other clinical situations for which cardiac CT could be considered the first-line exam instead of conventional coronary angiography, one of which is suspected anomalous origin of the coronary arteries, a known cause of sudden

cont.

Manuscrito 3

Rev Port Cardiol
Vol. 28 Julho/Agosto 09 / July/August 09

indicação para coronariografia não invasiva por angioTC. Aguardam-se ainda estudos que validem esta estratégia.

A ANGIO TC CARDÍACA PARA ALÉM DA CORONARIOGRAFIA NÃO INVASIVA: AVALIAÇÃO CARDÍACA EXTRA-CORONÁRIA E ACHADOS EXTRA-CARDÍACOS

Outra vantagem da angioTC em relação à coronariografia convencional reside na possibilidade de se obter no mesmo exame, informação cardíaca extra-coronária e avaliar achados extra-cardíacos, sem que para isso seja necessário aumentar a dose de radiação ou de contraste. No que diz respeito à avaliação cardíaca extra-coronária, embora este não seja habitualmente o motivo do exame e geralmente os doentes já tenham feito anteriormente um ecocardiograma, por vezes são documentados achados que passaram despercebidos nos exames anteriores, nomeadamente em doentes com deficiente janela acústica[19-21]. (*Fig. 7*)

Nestes exames é ainda feita uma leitura dos segmentos torácicos incluídos na aquisição cardíaca, sendo igualmente frequentes os achados extracardíacos nos campos pulmonares ou mediastínicos[22].

A ANGIO TC CARDÍACA PARA ALÉM DA DOCUMENTAÇÃO DE ESTENOSES SIGNIFICATIVAS: PLANEAMENTO DA ESTRATÉGIA DE REVASCULARIZAÇÃO

Embora a exclusão da presença de CAD seja a principal indicação para a realização de uma angioTC cardíaca, nos casos em que se identificam estenoses coronárias significativas a informação recolhida neste exame poderá ser útil no planeamento da estratégia de revascularização.

Trabalhos publicados recentemente demonstram a utilidade da angio-TC cardíaca para identificar preditores de sucesso de recanalização de oclusões crónicas[23,24] e para avaliar padrões de distribuição das lesões coronárias em bifurcação[25,26], informação útil para o planeamento da estratégia de revascularização (*Fig. 8*).

death in young athletes[27]. Cardiac CTA can determine not only the origin but the trajectory of anatomical variants, identifying malignant forms that course between the aorta and the pulmonary artery, which are difficult to characterize with conventional coronary angiography (*Fig. 9*).

Another indication is in patients with dilated cardiomyopathy (DCM), in whom a coronary etiology must generally be excluded. In a study involving 61 patients with DCM of undetermined cause that compared the performance of cardiac CTA with invasive angiography for detection of CAD[28], sensitivity and specificity of CTA were 99% and 96.2% respectively, even with a 16-slice system. The study also assessed the safety of the two diagnostic modalities; no complications were observed with cardiac CTA, while the rate of complications in patients undergoing invasive angiography was 16%, 9.8% due to acute heart failure and 6.5% related to vascular access.

Besides excluding the presence of significant coronary disease in patients with DCM, cardiac CTA also accurately measures volumes and ejection fraction in the same scan, thus avoiding the need to increase contrast or radiation doses. Since acquisition is synchronized with the ECG, reconstructions at different phases of the cardiac cycle can be compared in order to select the best systolic and diastolic phases. This, together with the technique's excellent endocardial definition and the fact that the 17 segments can be represented in multiplane reconstructions, leads to highly accurate and reproducible determination of volumes and ejection fraction. Given the prognostic and therapeutic implications of ejection fraction in patients with left ventricular dysfunction[29], this capability is an important additional advantage of non-invasive angiography, and further enhances the value of cardiac CTA in such patients (*Fig. 10*).

LIMITATIONS OF CARDIAC CT ANGIOGRAPHY

The limitations of cardiac CTA are related to spatial and temporal resolution, the lack of functional information and radiation doses.

The spatial resolution of CTA is inferior to that of invasive coronary angiography, making assessment of small caliber distal segments more

cont.

Manuscrito 3

Pedro de Araújo Gonçalves et al.
Rev Port Cardiol 2009; 28:825-42

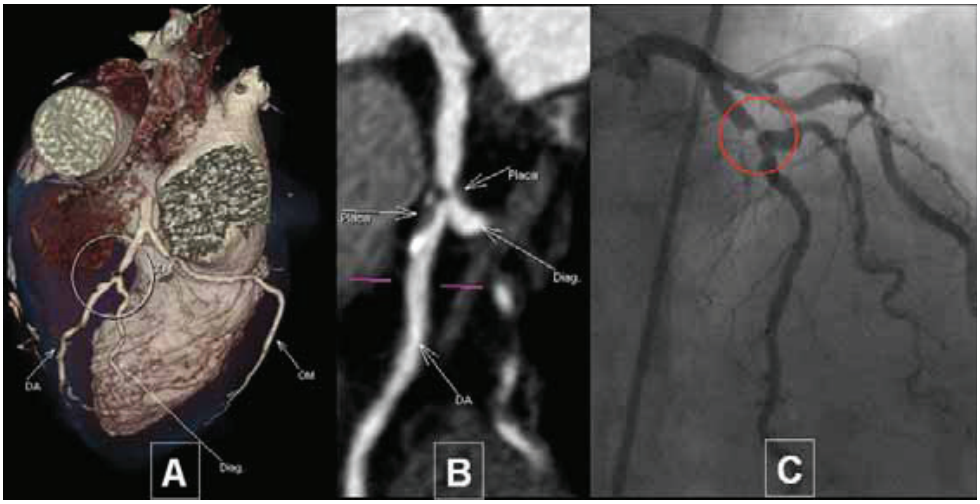

Figura 8 **Reconstruções de volume (VRT) documentando estenose significativa na descendente anterior, em bifurcação com a 1ª diagonal (A). Na reconstrução multiplanar (MPR) é possivel avaliar que se trata de placa predominantemente não calcificada e permite ainda apreciar o envolvimento do colateral pela placa (B), que não é perceptível na angiografia convencional (C).**

Figure 8 **Volume-rendered reconstruction (VRT) showing significant stenosis of the left anterior descending artery at the bifurcation with the first diagonal (A). In multi-planar reconstruction (MPR) it can be seen that this is a mainly non-calcified plaque, which also involves the collateral (B); this is not visible on conventional angiography (C).**

A angio TC cardíaca permite ainda avaliar o tipo de placa, nomeadamente a presença de calcificação, informação igualmente importante para a intervenção coronária, uma vez que a angioplastia de estenoses coronárias calcificadas é habitualmente mais difícil, exigindo por vezes a utilização de dispositivos específicos.

OUTRAS INDICAÇÕES

Existem ainda outras indicações clínicas, para as quais a angioTC cardíaca poderá ser considerada o exame de primeira linha, em vez da coronariografia invasiva convencional. Um destes exemplos é a suspeita de origem anómala das artérias, reconhecida causa de morte súbita em jovens[27]. A angioTC cardíaca permite delinear não só a origem mas sobretudo o trajecto das variantes anatómicas, permitindo assim identificar as variantes malignas, nas quais o trajecto se faz entre a aorta e a artéria pulmonar, aspectos difíceis de caracterizar na coronariografia convencional.

Outro exemplo é o dos doentes com Miocardiopatia Dilatada nos quais se tem habitualmen-

difficult, which is why most studies limit their analysis to segments of ≥1.5 mm. Evaluation of calcified lesions is also difficult, the degree of stenosis generally being overestimated by CTA. Special filters are usually employed in reconstructions aimed at assessing stent patency, and these should also be used in patients with calcified lesions to minimize the effect of blooming artifacts[8].

Temporal resolution is also inferior to conventional angiography, which hinders assessment of patients with high heart rates or arrhythmias. However, this limitation has been overcome by the latest 64-slice dual source systems, which can assess patients with high heart rates and even those in atrial fibrillation[9,10].

The lack of functional information is another limitation of the technique. The ability to provide data on the functional impact of plaques or stenosis as well as anatomical information would make cardiac CTA the most complete non-invasive method of assessing CAD. There are two lines of research in this area: one seeks to assess perfusion on the basis of myocardial density, which is linearly correlated with perfusion following administration of iodinated contrast; the

cont.

Manuscrito 3

Rev Port Cardiol
Vol. 28 Julho/Agosto 09 / July/August 09

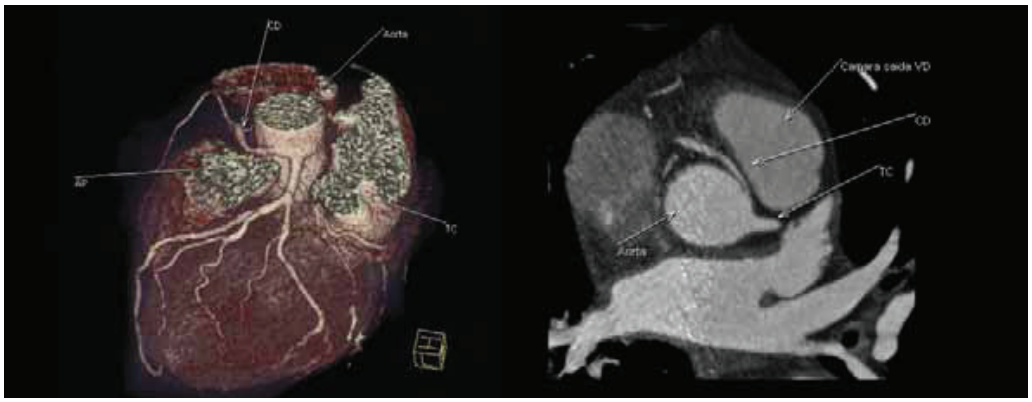

Figura 9. **Reconstruções de volume (VRT) e multiplanar (MPR) documentando origem anómala da coronária direita no seio de valsalva esquerdo, com trajecto interarterial, tratando-se por isso de uma variante maligna.**

Figure 9. **Volume-rendered reconstruction (VRT) and multi-planar reconstruction (MPR) showing anomalous origin of the right coronary artery in the left sinus of Valsalva, which has an interarterial course, and is therefore a malignant variant.**

te que excluir etiologia coronária. Num estudo que envolveu 61 doentes com miocardiopatia dilatada de etiologia indeterminada, foi avaliado o desempenho da angioTC cardíaca por comparação com a angiografia invasiva na detecção de doença coronária[28]. Nesta série, a sensibilidade e a especificidade foram de 99% e 96,2%, respectivamente, e tendo os exames sido realizados com um aparelho de apenas 16 cortes. Neste trabalho foi ainda avaliada a segurança das duas modalidades diagnósticas, não se tendo verificado complicações relacionadas com a angioTC cardíaca. Nos doentes submetidos a angiografia invasiva a taxa de complicações chegou aos 16%, sendo 9,8% por insuficiência cardíaca aguda e 6,5% por complicações relacionadas com o acesso vascular.

Nos doentes com miocardiopatia dilatada, para além de ser possível excluir a presença de doença coronária significativa, a angioTC cardíaca permite ainda calcular correctamente os volumes e a fracção de ejecção, na mesma aquisição, não sendo assim necessário aumentar a dose de contraste ou de radiação. Como a aquisição é sincronizada com o ECG, é possível comparar as reconstruções nas várias fases do ciclo cardíaco, para selecção da melhor fase sistólica e diastólica. Este facto, associado a uma óptima definição endocárdica e à possibilidade de se ter a representação dos 17 segmentos nas reconstruções multiplanares, torna assim possível uma avaliação bastante correcta e reprodutível dos volumes e fracção de ejecção.

other exploits the ability of dual energy methods to quantify iodine concentration in tissue. Both methods are still at the initial development stage in a few centers and there are various obstacles to be overcome, particularly the need to avoid a significant increase in radiation dose and the ability to perform exams under pharmacological stress.

Finally, the radiation dose in cardiac CTA, around 11 mSv even in studies with ECG-dependent dose modulation, is higher than in conventional coronary angiography, which is estimated at 7 mSv[30]. As well as ECG-dependent dose modulation, which is now routine in such exams, new protocols have recently been developed aimed at reducing the dose even further. One consists of reducing the voltage from 120 kV to 100 kV, which is feasible in most patients except the obese. In a study comparing the radiation doses of different protocols in 1035 patients, a mean dose of 5.4 mSv was obtained with 64-slice systems using a combination of ECG-dependent dose modulation and the 100 kV protocol, which corresponds to a 64% reduction compared to standard protocols[31]. Another recently developed protocol that has considerable potential to reduce the radiation dose even further consists of acquisition with prospective, rather than the usual retrospective, ECG triggering, known as step-and-shoot mode. Initial studies using this protocol have reported doses of 1.2 to 2.6 mSv[32].

The recently introduced 320-slice systems,

cont.

Dadas as reconhecidas implicações prognósticas e terapêuticas da fracção de ejecção nos doentes com disfunção ventricular esquerda[29], esta avaliação torna-se assim um complemento importante à coronariografia não invasiva, e contribui para a rentabilidade da angioTC cardíaca nestes doentes (*Fig. 10*).

which enable acquisition of the entire heart volume in a single RR interval, should also lead to significant reductions in radiation and contrast doses.

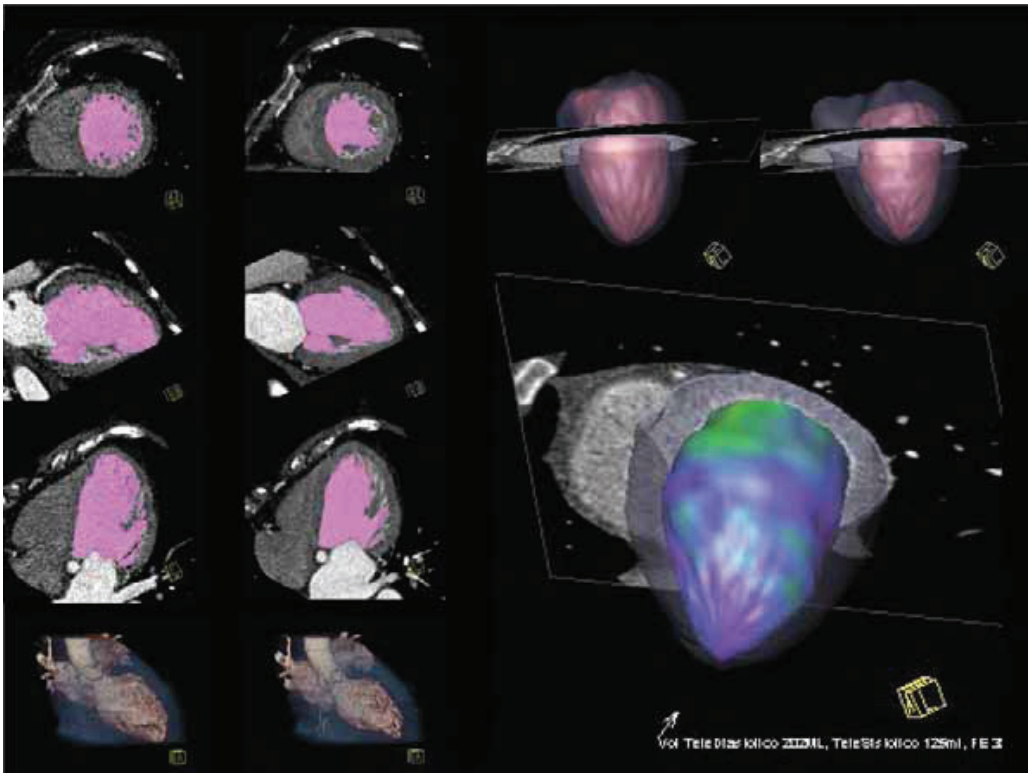

Figura 10. **Cálculo de volumes e fracção de ejecção em doente com miocardiopatia dilatada, a partir da delimitação do contorno endocárdico nas várias reconstruções multiplanares, com representação dos 17 segmentos miocárdicos.**

Figure 10. **Determination of volumes and ejection fraction in a patient with dilated cardiomyopathy by delimiting the endocardial outline in various multiplanar reconstructions, representing the 17 myocardial segments.**

LIMITAÇÕES DA ANGIOTC CARDÍACA

As limitações da AngioTC cardíaca estão relacionadas com resolução espacial, resolução temporal, ausência de informação funcional e dose de radiação.

A resolução espacial da angioTC cardíaca é inferior à da coronariografia invasiva o que dificulta a avaliação de segmentos distais de pequeno calibre, razão pela qual na maior parte dos estudos, a análise foi limitada aos segmentos com ≥ 1,5mm. A avaliação de lesões

CONCLUSION

Ongoing research and technological advances in the area of multislice computed tomography have progressively improved the spatial and temporal resolution of cardiac CTA exams. In addition to the current indications for use of the technique, notably exclusion of coronary artery disease in patients with intermediate probability, this diagnostic modality is also proving useful in other areas, and may become a first-line technique.

cont.

Manuscrito 3

Rev Port Cardiol
Vol. 28 Julho/Agosto 09 / July/August 09

calcificadas é igualmente difícil, sendo o grau de estenose habitualmente sobrevalorizado na angioTC. Existem filtros dedicados, que são habitualmente empregues na reconstrução de exames para avaliação da patência de *stents*, que devem igualmente ser empregues na presença de lesões calcificadas, para minimizar o efeito de *blooming*.

A resolução temporal é igualmente inferior à da coronariografia convencional, o que torna difícil a avaliação de doentes com frequências cardíacas altas e arritmias. Esta limitação tem vindo a ser ultrapassada com os aparelhos de angioTC cardíaca de última geração com 64 cortes e dupla ampola, sendo possível com estes aparelhos realizar exames em doentes com frequências cardíacas altas e mesmo em fibrilhação auricular[9,10].

A ausência de informação funcional tem sido apontada como uma das limitações desta técnica. A possibilidade de se adicionar à informação anatómica a informação do impacto funcional das placas/estenoses, tornaria a angioTC cardíaca o método não invasivo mais completo na avaliação da doença coronária. Existem nesta área duas linhas de investigação divergentes: uma que procura avaliar a perfusão através da densidade do miocárdio (uma vez que existe uma correlação linear entre a densidade do miocárdio e a sua perfusão após injecção de contraste iodado); a outra explorando as capacidades da codificação do iodo nos tecidos pelo método da dupla energia. Actualmente ainda em fase de desenvolvimento inicial em poucos centros, estes métodos têm várias barreiras a superar, nomeadamente a necessidade de não haver um aumento relevante de dose de radiação e a capacidade de ser realizado em condições de *stress* farmacológico.

Por fim, a dose de radiação atribuída à angio TC cardíaca, de cerca de 11 mSv em trabalhos com modulação da dose de acordo com o ECG, é mesmo assim superior à dose da coronariografia convencional, que está estimada em 7 mSv[30]. Para além da modulação da dose de radiação pelo ECG, utilizado actualmente por rotina nestes exames, foram recentemente desenvolvidos novos protocolos que visam reduzir ainda mais a dose de radiação destes exames. Um destes protocolos consiste na redução da kilovoltagem da ampola de 120 para 100Kv, possível na grande maioria dos doentes, à excepção dos obesos. Num trabalho em que foram comparadas

When significant coronary stenosis is detected, the information provided by cardiac CTA can be useful in planning revascularization strategies. However, the exam is not limited to assessment of the coronary tree, and the same acquisition protocol can be used for extracoronary cardiac evaluation, particularly multiplane reconstructions to determine ejection fraction and for assessment of extracardiac findings in the thoracic segments included in the scan.

It is hoped that some of the technique's current limitations will be overcome in the future, particularly with regard to radiation doses and assessment of calcified lesions, and that cardiac CT angiography will be able to combine both anatomical and functional information in the same non-invasive exam. Initial results have been extremely promising and we shall see what the future will bring.

cont.

as doses de radiação com diferentes protocolos em 1035 doentes, foi possível obter uma dose média de 5,4mSv em aparelhos de 64 cortes, com o uso combinado de modulação da dose de acordo com o ECG e utilização de protocolo de 100Kv, o que corresponde a uma redução de 64% em relação aos protocolos convencionais[31]. Um outro protocolo recentemente desenvolvido e com elevado potencial para reduzir ainda mais a dose de radiação consiste na aquisição sincronizada com o ECG de forma prospectiva em vez da habitual retrospectiva, o chamado protocolo *step and shot*. Estão descritas doses de 1,2 a 2,6 mSv nos trabalhos iniciais com este protocolo[32].

Finalmente, os aparelhos de 320 cortes recentemente introduzidos, que permitem realizar a aquisição de todo o volume cardíaco em apenas um intervalo RR, deverão igualmente conduzir a uma redução significativa da dose de radiação e de contraste.

CONCLUSÃO

A constante investigação e evolução tecnológica na área da TC multicortes tem vindo a permitir uma melhoria progressiva na resolução espacial e temporal dos exames de angioTC cardíaca. Para além das indicações actualmente aceites para esta técnica, nomeadamente a exclusão da presença de doença coronária em doentes com probabilidade intermédia, esta modalidade diagnóstica tem-se revelado útil também noutras área, podendo de futuro constituir-se como uma modalidade de primeira escolha.

Nos casos em que se documentam estenoses coronárias significativas, a informação recolhida pela angioTC cardíaca poderá ser útil no planeamento da estratégia de revascularização. Por outro lado, um exame de angioTC cardíaca não se limita à avaliação da árvore coronária, sendo possível com o mesmo protocolo de aquisição fazer ainda uma avaliação cardíaca extracoronária, nomeadamente com cálculo multiplanar da fracção de ejecção e fazer ainda uma apreciação de eventuais achados extracardíacos nos segmentos torácicos incluídos na aquisição.

De futuro, espera-se que seja possível ultrapassar algumas das presentes limitações desta técnica, nomeadamente no que diz respeito à dose de radiação, à avaliação de lesões calcificadas e à possibilidade da angioTC cardíaca poder vir a conciliar no mesmo método não invasivo a informação anatómica e funcional – os resultados iniciais têm sido muito promissores, veremos o que o futuro nos reserva.

Pedido de separatas para:
Adress for reprints:

Pedro de Araújo Gonçalves
Hospital da Luz
Av. dos Lusíadas, 100
1500-650 LISBOA
Tel.: +351966866455
e-mail: paraujogoncalves@yahoo.co.uk

BIBLIOGRAFIA / REFERENCES

1. Togni M, Balmer F, Pfiffner D, Maier W, Zeiher AM, Meier B, on behalf of the Working Group Interventional Cardiology and Coronary Pathophysiology of the European Society of Cardiology. Percutaneous coronary interventions in Europe 1992–2001. European Heart Journal 2004; 25(14):1208-1213.

2. Hamon M, Biondi-Zoccai GG, Malagutti P, et al. Diagnostic performance of multislice spiral computed tomography of coronary arteries as compared with conventional invasive coronary angiography: A meta-analysis. J Am Coll Cardiol. 2006;48:1896-1910.

3. Vanhoenacker PK, Heijenbrok-Kal MH, Van Heste R, et al. Diagnostic performance of multidetector CT angiography for assessment of coronary artery disease: Meta-analysis. Radiology. 2007;44:419-428.

4. Schroeder S, Achenbach S, Bengel F, et al. Cardiac computed tomography: indications, applications, limitations, and training requirements. Report of a Writing Group deployed by the Working Group Nuclear Cardiology and Cardiac CT of the European Society of Cardiology and the European Council of Nuclear Cardiology. Eur Heart J 2008;29:531-56.

5. Meijboom WB, van Mieghem CA, Mollet NR, et al. 64-slice computed tomography coronary angiography in patients with high, intermediate, or low pretest probability of significant coronary artery disease. J Am Coll Cardiol. 2007;50:1469-1475.

cont.

Manuscrito 3

Rev Port Cardiol
Vol. 28 Julho/Agosto 09 / July/August 09

6. Vahanian A, Baumgartner H, Bax J, et al., on behalf of the Task Force on the Management of Valvular Heart Disease of the European Society of Cardiology. Guidelines on the management of valvular heart disease. European Heart Journal 2007; 28:230-268.

7. Meijboom WB, Mollet NR, Van Mieghem CA, et al. Pre-operative computed tomography coronary angiography to detect significant coronary artery disease in patients referred for cardiac valve surgery. J Am Coll Cardiol. 2006;48:1658-1665.

8. Gilard M, Cornily JC, Pennec PY, et al. Accuracy of multislice computed tomography in the preoperative assessment of coronary disease in patients with aortic valve stenosis. J Am Coll Cardiol 2006;47:2020-4.

9. Marques H, Araújo Gonçalves P, Dourado R, et al. Dual source coronary CT angiography in patients in atrial fibrillation. European Radiology 2008; vol 18, suppl 3: C35.

10. Oncel D, Oncel G, Tastan A. Effectiveness of dual source CT coronary angiography for the evaluation of coronary artery disease in patients with atrial fibrillation: initial experience. Radiology 2007; 245(3): 703-11.

11. Meyer TS, Martinoff S, Hadamitzky M, et al. Improved noninvasive assessment of coronary artery bypass grafts with 64-slice computed tomographic angiography in an unselected patient population. J Am Coll Cardiol, 2007; 49(9): 946-50.

12. Dourado R, Araújo Gonçalves P, Marques H, et al. Avaliação de Pontagens Coronárias por Angio TC de 64 Cortes de Dupla Ampola. Rev Port Cardiol 2008; 27 (7-8): 995-998.

13. Hoffmann U, Nagurney JT, Moselewski F, et al. Coronary multidetector computed tomography in the assessment of patients with acute chest pain. Circulation. 2006;114:2251-2260.

14. Meijboom WB, Mollet NR, Van Mieghem CA, et al. 64-slice computed tomography coronary angiography in patients with non-ST elevation acute coronary syndrome. Heart. 2007;93:1386-1392.

15. Goldstein JA, Gallagher MJ, O'Neill WW, et al. A randomized controlled trial of multi-slice coronary computed tomography for evaluation of acute chest pain. J Am Coll Cardiol. 2007;49:863-871.

16. Rubinshtein R, Halon DA, Gaspar T, et al. Usefulness of 64-slice cardiac computed tomographic angiography for diagnosing acute coronary syndromes and predicting clinical outcome in emergency department patients with chest pain of uncertain origin. Circulation. 2007;115:1762-1768.

17. Takakuwa K, Halpern EJ. Evaluation of a "Triple Rule-Out" Coronary CT Angiography Protocol: Use of 64-Section CT in Low-to-Moderate Risk Emergency Department Patients Suspected of Having Acute Coronary Syndrome. Radiology 2008;248:438-446.

18. Gallagher MJ, Raff GL. Use of multislice CT for the evaluation of emergency room patients with chest pain: The so-called "Triple Rule-Out". Cathet Cardiov Interv 2008; 71:92-99.

19. Kirsch J, Williamson E, Araoz P. Non-compaction visualization using ECG-gated dual-source CT. International Journal of Cardiology 2007; 118: e46-e47.

20. Dourado R, Araújo Gonçalves P, Marques H, et al. Divertículo do ventrículo esquerdo: um achado por Angio TC cardíaca. Rev Port Cardiol 2009, in press.

21. Ghersin E, Lessick J, Litmanovich D, et al. Comprehensive multidetector CT assessment of apical hypertrophic cardiomyopathy. Brit J Radiol 2006; 79: e200-e204.

22. Wissner E, Wellnitz CV, Srivathsan K, et al. Value of multislice computed tomography angiography of the thorax in preparation for catheter ablation for the treatment of atrial fibrillation: The impact of unexpected cardiac and extracardiac findings on patient care. Eur J Radiol (2008), in press.

23. Mollet NR, Hoye A, Lemos PA, et al. Value of preprocedure multislice computed tomographic coronary angiography to predict the outcome of percutaneous recanalization of chronic total occlusions. Am J Cardiol 2005;95:240-243.

24. Maintz D, Kaneda H, Saito S, Shiono T, Miyashita Y, Takahashi S, Domae H. Sixty-four-slice computed tomography-facilitated percutaneous coronary intervention for chronic total occlusion. Int J Cardiol 2007;115:130-2.

25. Pflederer T, Ludwig J, Ropers D, et al. Measurement of coronary artery bifurcation angles by multidetector computed tomography. Invest Radiol 2006; 41:793-798.

26. Van Mieghem CA, Thury A, Meijboom WB, et al. Detection and characterization of coronary bifurcation lesions with 64-slice computed tomography coronary angiography. Eur Heart J 2007;28:1968-76.

27. Maron BJ. Sudden death in young athletes. N Engl J Med 2003;349: 1064-75.

28. Andreini D, Pontone G, Pepi M, et al. Diagnostic accuracy of multidetector computed coronary tomography angiography in patients with dilated cardiomyopathy. J Am Coll Cardiol 2007;49:2044-2050.

29. Dickstein K, Cohen-Solal A, Filippatos G, et al., on behalf of the Task Force for the Diagnosis and Treatment of Acute and Chronic Heart Failure 2008 of the European Society of Cardiology. ESC Guidelines for the diagnosis and treatment of acute and chronic heart failure 2008. Eur Heart J 2008: 29;2388-2442.

30. Einstein AJ, Moser KW, Thompson RC, et al. Radiation Dose to Patients From Cardiac Diagnostic Imaging. Circulation 2007;116;1290-1305.

31. Hausleiter J, Meyer T, Hadamitzky M, et al. Radiation dose estimates from cardiac multislice computed tomography in daily practice: impact of different scanning protocols on effective dose estimates. Circulation 2006;113:1305–1310.

32. Stolzmann P, Leschka S, Scheffel H, et al. Dual-Source CT in Step-and-Shoot Mode: Noninvasive Coronary Angiography with Low Radiation Dose. Radiology 2008; 249: 71-80.

MANUSCRITO 4

Rationale and design of the Progression of AtheRosclerotic PlAque DetermIned by Computed TomoGraphic Angiography IMaging (PARADIGM) registry: A comprehensive exploration of plaque progression and its impact on clinical outcomes from a multicenter serial coronary computed tomographic angiography study.

Lee, S.E., H.J. Chang, A. Rizvi, M. Hadamitzky, Y.J. Kim, E. Conte, D. Andreini, G. Pontone, V. Volpato, M.J. Budoff, I. Gottlieb, B.K. Lee, E.J. Chun, F. Cademartiri, E. Maffei, **H**. **Marques**, J.A. Leipsic, S. Shin, J.H. Choi, N. Chung, and J.K. Min,

Am Heart J, 2016
182: p. 72-79

Manuscrito 4

Trial Design

Rationale and design of the *P*rogression of *Athe**R**o*sclerotic Pl*A*que *D*eterm*I*ned by Computed Tomo*G*raphic Angiography I*M*aging (PARADIGM) registry: A comprehensive exploration of plaque progression and its impact on clinical outcomes from a multicenter serial coronary computed tomographic angiography study

Sang-Eun Lee, MD, [a] Hyuk-Jae Chang, MD, PhD, [a] Asim Rizvi, MD, [b] Martin Hadamitzky, MD, [c] Yong-Jin Kim, MD, PhD, [d] Edoardo Conte, MD, [e] Daniele Andreini, MD, [e] Gianluca Pontone, MD, [e] Valentina Volpato, MD, [e] Matthew J. Budoff, MD, [f] Ilan Gottlieb, MD, [g] Byoung Kwon Lee, MD, PhD, [h] Eun Ju Chun, MD, PhD, [i] Filippo Cademartiri, MD, PhD, [j] Erica Maffei, MD, [j] Hugo Marques, MD, [k] Jonathon A. Leipsic, MD, [l] Sanghoon Shin, MD, [m] Jung Hyun Choi, MD, PhD, [n] Namsik Chung, MD, PhD, [a] and James K. Min, MD [b] ***Seoul, South Korea; New York, NY; Munich, Germany; Milan, Italy; Los Angeles, CA; Rio de Janeiro, Brazil; Quebec, Vancouver, Canada; and Lisbon, Portugal***

Background The natural history of coronary artery disease (CAD) in patients with low-to-intermediate risk is not well characterized. Although earlier invasive serial studies have documented the progression of atherosclerotic burden, most were focused on high-risk patients only. The PARADIGM registry is a large, prospective, multinational dynamic observational registry of patients undergoing serial coronary computed tomographic angiography (CCTA). The primary aim of PARADIGM is to characterize the natural history of CAD in relation to clinical and laboratory data.

Design The PARADIGM registry (ClinicalTrials.gov NCT02803411) comprises ≥2,000 consecutive patients across 9 cluster sites in 7 countries. PARADIGM sites were chosen on the basis of adequate CCTA volume, site CCTA proficiency, local demographic characteristics, and medical facilities to ensure a broad-based sample of patients. Patients referred for clinically indicated CCTA will be followed up and enrolled if they had a second CCTA scan. Patients will also be followed up beyond serial CCTA performance to identify adverse CAD events that include cardiac and noncardiac death, myocardial infarction, unstable angina, target vessel revascularization, and CAD-related hospitalization.

Summary The results derived from the PARADIGM registry are anticipated to add incremental insight into the changes in CCTA findings in accordance with the progression or regression of CAD that confer prognostic value beyond demographic and clinical characteristics. (Am Heart J 2016;182:72-9.)

From the [a]Division of Cardiology, Severance Cardiovascular Hospital, Integrative Cardiovascular Imaging Center, Yonsei University Health System, Seoul, South Korea, [b]Dalio Institute of Cardiovascular Imaging, New York-Presbyterian Hospital and Weill Cornell Medical College, New York, NY, USA, [c]Division of Cardiology, University of Munich, Munich, Germany, [d]Seoul National University Hospital, South Korea, [e]Centro Cardiologico Monzino, IRCCS, Milan, Italy, [f]Department of Medicine, Harbor UCLA Medical Center, Los Angeles, CA, USA, [g]Department of Radiology, Casa de Saude São Jose, Rio de Janeiro, Brazil, [h]Gangnam Severance Hospital, South Korea, [i]Seoul National University Bundang Hospital, South Korea, [j]Department of Radiology, Montréal Heart Institute/Université de Montréal, Montréal, Quebec, Canada, [k]Hospital da Luz, Lisbon, Portugal, [l]Department of Radiology, St Paul's Hospital, University of British Columbia, Vancouver, Canada, [m]National Health Insurance Service Ilsan Hospital, South Korea, and [n]Busan University Hospital, South Korea.

Funding: This research was supported by Leading Foreign Research Institute Recruitment Program through the National Research Foundation of Korea funded by the Ministry of Science, ICT & Future Planning (Grant No. 2012027176) and GE Healthcare.
Submitted June 5, 2016; accepted September 17, 2016.
Reprint requests: Hyuk-Jae Chang, MD, PhD, Division of Cardiology Severance Cardiovascular Hospital, Integrative Cardiovascular Imaging Center, Yonsei University Health System, 50-1 Yonsei-ro, Seodaemun-gu, Seoul, 120-752 South Korea, or James K. Min, MD, Dalio Institute of Cardiovascular Imaging, New York-Presbyterian Hospital and Weill Cornell Medical College, 413 E. 69th Street, Suite 108, New York, NY 10021.
E-mails: hjchang@yuhs.ac, jkm2001@med.cornell.edu
0002-8703

http://dx.doi.org/10.1016/j.ahj.2016.09.003

cont.

Manuscrito 4

American Heart Journal
Volume 182

Ischemic heart disease remains the most important cause of morbidity and mortality worldwide.[1] At present, the development of the atherosclerotic lesion in the vessel wall is conceptualized as a sequential event,[2] wherein progression of atherosclerosis in coronary arteries leads to stenosis or plaque rupture with resultant atherothrombosis and eventual myocardial damage. To date, the temporal evolution of atherosclerotic progression has rarely been serially monitored or visualized, and assessment of treatment response toward coronary artery disease (CAD) has been inferred by cholesterol monitoring, rather than individualized direct imaging of the plaque due to limitations in noninvasive monitoring of the diseased vessel wall.

Further still, although previous clinical trials have demonstrated an effect of statin therapy in reducing cardiovascular disease events, these studies were most often conducted on a population level.[3] Hence, direct visualization of the serial changes in plaque and vessel wall may further our understanding in the natural history of disease progression and response to therapy, which might eventually facilitate in managing patients more efficiently.

To date, the progression or change in response to medical therapy of coronary plaque has been demonstrated mainly by invasive techniques including quantitative coronary angiography[4,5] or intravascular ultrasound (IVUS).[6-8] However, the invasiveness of these methods limits their use to patients who are undergoing invasive coronary angiography (ICA). As a consequence, most studies thus far have predominantly focused on patients with an acute coronary syndrome (ACS) or high risk of CAD, which comprise only a small portion of the patient population. To this end, of most patients with suspected CAD who have low-to-moderate risk and are therefore not eligible for ICA according to current guidelines,[9,10] the natural history, including sequential changes in plaque morphology or composition, is not well characterized.

Prior studies examining plaque progression have been primarily restricted to measures of obstructive CAD on a per-lesion basis,[4-8,11] and non–ischemic lesions or newly developed lesions on a follow-up basis are largely overlooked. The latter approach also limits our understanding of the progression of mild lesion or development of atherosclerotic plaques, despite the notion that non–ischemic lesions have been found to be associated with the development of future ACS in recent studies.[12-14] To wholly understand the progression of atherosclerosis in the coronary arteries, assessment of CAD should cover the entire coronary tree, which currently represents a challenge when relying on the use of invasive techniques only.

Moreover, most available studies that have assessed the progression of plaque by invasive procedures have included fewer numbers of patients or used a relatively shorter-term follow-up.[4-8,15] Although a sufficient number of patients were enrolled in some studies that used quantitative coronary analysis, the traditional reference method for assessing the severity of CAD was used.[16,17] Potential drawbacks of this technique include the underestimation of disease severity and the inability to assess changes in the vessel wall, as documented elsewhere.[18,19]

Recent developments in coronary computed tomographic angiography (CCTA) enable not only detection of luminal narrowing but also characterization of high-risk plaque morphology[20] and quantification of plaque volumes.[21-24] The relationship of CCTA-defined increasing burden of CAD and cardiovascular risk has been reported in the CONFIRM registry.[25] Furthermore, more recent studies have used fully or semiautomated plaque assessment methods, thereby permitting a higher accuracy and enhanced reproducibility as compared with a manual technique.[21,26,27] In addition, the relatively high radiation dose, which was a prior limiting factor of serial CCTA examinations, has substantially been reduced from 15 to 20 mSv to less than 1 mSv in selected patients.[28] Hence, CCTA has emerged as a potential alternative to invasive imaging modalities for serial interrogation of CAD, which assess interval changes on morphological plaque characteristics and evaluate the efficacy of treatments.

The PARADIGM registry (ClinicalTrials.gov NCT02803411) has been designed to directly address the natural history of coronary atherosclerosis, characteristics, and determinants of coronary plaque progression, as well as to define the impact of plaque progression in terms of adverse clinical outcomes in patients presenting with CAD. This report describes the rationale and design features of the PARADIGM registry.

Methods

Overall study design

The PARADIGM registry is a prospective, open-label, international, multicenter dynamic observational registry designed to evaluate associations between changes in serial CCTA imaging findings and clinical presentation and their ability to predict mortality and major adverse cardiac events (MACEs) in patients with CAD. The registry uses a collaborative design using contribution and merger of similar prospectively enrolled cohorts from 16 sites around the world. Patients who underwent CCTA will be prospectively followed up, and among them, patients with a second CCTA scan will be enrolled. The change in plaque composition, size, lumen dimensions, and arterial remodeling will be assessed along with their association with adverse clinical outcomes. Qualifying sites participated in data collection and common data analysis if the site collected data including clinical presentation, risk factors, CCTA data recordings, and follow-up data including all-cause mortality and MACE.

Study objectives

Primary objective. The primary objective of PARADIGM is to describe the natural course of coronary

cont.

Manuscrito 4

atherosclerotic plaque development and progression in CAD over time by CCTA in relation to demographic and laboratory data for refinement of risk stratification among patients with repeated CCTA. Specifically, we will explore the temporal changes in plaque composition and quantitative measures such as plaque volume by serial CCTA.

Secondary objectives. Secondary objectives will be as follows: (1) determine the most optimal and effective way to define the progression of plaque quantitatively assessed by serial CCTA; (2) identify the determinants of plaque progression; (3) evaluate the prognostic power of changes in CCTA findings in specific subgroups, including (but not limited to) gender, type 2 diabetes mellitus, dyslipidemia, and various ethnic backgrounds; (4) ascertain imaging parameters derived from serial CCTA that can be used in monitoring patients with CAD; (5) assess changes in serial CCTA findings and their possible association with clinical risk factors and symptoms for the purpose of developing a CCTA global risk score for patients with suspected CAD; and (6) test the efficacy and rationale of using CCTA imaging indicators as surrogate markers of atherosclerotic progression.

Study end points

The primary end point of the PARADIGM registry is to explore the temporal changes in plaque characteristics (volume and composition). Secondary end point is a composite of MACE in relation with primary end point, which comprise cardiac and noncardiac mortality, myocardial infarction, unstable angina requiring hospitalization, and revascularization.

Study eligibility criteria

Patient eligibility. All consecutive patients undergoing CCTA of 64-detector rows or greater at cluster sites are included within the PARADIGM registry if all inclusion criteria were met. Patient selection criteria included the following: (1) patients who underwent 2 or more clinically indicated CCTA with 64-detector rows or greater for CAD evaluation, (2) at least a 2-year interval between the baseline and follow-up CCTAs, and (3) prospective data collection for CAD risk factors.

Exclusion criteria included the following: (1) unavailable clinical or laboratory data within 1 month from baseline CCTA or follow-up CCTA and (2) uninterpretable CCTA.

Site eligibility. The site requirements for participating sites of the PARADIGM registry are as follows: (1) >200 patients per annum undergoing CCTA by 64-detector rows or greater, (2) incorporation of CCTA into daily clinical practice by members of the medical center other than those involved with the CCTA performance and interpretation, and (3) director of laboratory possessing level III–equivalent expertise in CCTA.

Study sites and participating centers

During the initial phase of the PARADIGM registry, 9 cluster sites contributed data from patients undergoing CCTA of 64-detector rows or greater. Seven countries in North America, Europe, South America, and Asia are presently represented in this multinational effort, including the United States, Canada, Italy, Germany, Brazil, Portugal, and South Korea. Data collection activities began in 2013 with a target of collecting data on approximately more than 2,000 patients.

The geographic clusters were selected to represent medical centers of different sizes and with different diagnostic capabilities, as well as patient populations with diverse clinical and demographic characteristics. Medical centers where CCTA has been incorporated into daily clinical cardiac practice were chosen. Each sites' principal investigator was required to obtain approval from the appropriate ethics committee or institutional review board.

Sites were eligible for merger into the PARADIGM registry if they performed prospective cohort collection of CCTA findings with >80% overlap with the predefined data dictionary. Databases had to include uniform collection of major categories of patient data, including demographics, history of CAD, Framingham risk factors, symptom indication for CCTA, raw image dataset of CCTA, and obtained follow-up data for all-cause mortality for ≥2 years with <30% loss to follow-up. Sites were allowed to provide both previously published and unpublished data.

Patient evaluation and follow-up

All PARADIGM study patients underwent initial and follow-up CCTA based on order from their primary physician. Demographic data, targeted medical history, cardiovascular risk factors, laboratory data, and development of clinical events were prospectively collected using electronic case report forms at the time of initial CCTA and at the time of follow-up CCTA (Table I).

Standardized definitions for cardiovascular risk factors were used. Medical history including previous stroke, transient ischemic accident, and peripheral artery disease were documented. If patients had chest pain, it was recorded based on one of the following terms: atypical chest pain, noncardiac chest pain, or typical chest pain.

Patient follow-up was performed by each local center by a dedicated physician or research nurse, or both. Patients were followed up for a development of MACE. Ascertainment of all-cause death was determined by direct interview, telephone contact, or review of medical records. The PARADIGM database will be locked in June 2016, and will be reopened every 3 months to update additional investigative sites' data and to update preexisting sites for longer follow-up evaluation.

Acquisition and interpretation of CCTA

All testing, image acquisition, and image postprocessing for CCTAs in the PARADIGM cohort are in direct accordance with Society of Cardiovascular Computed Tomography guidelines.[29,30] No restrictions were placed

cont.

Manuscrito 4

American Heart Journal
Volume 182

Table I. Collected clinical variables and clinical events

Age (y), mean ± SD	Medications, n (%)
Body mass index (kg/m^2)	Antiplatelets
Male gender, n (%)	Anticoagulations
Referral reasons for baseline and follow-up CCTA	β-Blockers
Interval between baseline and follow-up CCTA (y),mean ± SD	Calcium-channel blockers
Clinical follow-up time (y), mean ± SD	Diuretics
Family history of CAD, n (%)	ACEi/ARB
Hypertension, n (%)	Statins
Diabetes mellitus, n (%)	Oral hypoglycemic agents/Insulin
Dyslipidemia, n (%)	Insulin
Current smoker, n (%)	Clinical events, n (%)
Cardiac symptoms, n (%)	Revascularization
Typical chest pain	Hospitalization due to CAD
Atypical chest pain	Non-fatal myocardial infarction
Noncardiac chest pain	Cardiac death
Dyspnea on exertion	Noncardiac death

Abbreviations: *ACEi*, Angiotensin-converting enzyme inhibitor; *ARB*, angiotensin receptor blocker.

regarding the type of computed tomographic scanner or type of iodinated contrast, except where the performance of CCTA should be conducted using a scanner with ≥64-detector rows. As a consequence, the scanner type differed by center. Data regarding the method of electrocardiographic gating, defined as either retrospective helical gating or prospective axial triggering, CCTA scan parameters including tube current (mA), tube voltage (kV), dose-length products, and overall study quality (denoted as excellent, satisfactory, or poor), were recorded.

Datasets (baseline and follow-up) from each contributing centers will be transferred to an offline workstation for analysis using semiautomated plaque analysis software (QAngioCT Research Edition v2.1.9.1; Medis Medical Imaging Systems, Leiden, the Netherlands). Independent level III–experienced readers masked to clinical and test results will analyze all CCTAs. Both qualified and quantified analyses will be carried out on a per-patient, per-vessel, per-segment, and per-lesion level. All analyses will be performed in a single core laboratory.

The major vessels (left anterior descending artery, left circumflex artery, and right coronary artery) were considered for analysis using the modified 17-segment American Heart Association model for coronary segment classification.[31] Lesions were matched between baseline and follow-up CCTAs using branch points as landmarks.

The presence of coronary atherosclerosis is defined as any tissue structures >1 mm^2 that existed either within the coronary artery lumen or adjacent to the coronary artery lumen that could be discriminated from surrounding pericardial tissue, epicardial fat, or the vessel lumen itself.[32]

For qualitative analysis, the presence of positive remodeling, low attenuated plaque, and spotty calcification will be identified, and plaque type will be recorded as one of the following: noncalcified, calcified, or mixed calcified plaque. A remodeling index is defined as a maximal lesion vessel area divided by proximal reference vessel area, with positive remodeling defined as a remodeling index ≥1.1. Low attenuated plaque is defined as any voxel <30 Hounsfield units (HU) within a region of interest, and spotty calcification is defined by an intralesion calcific plaque <3 mm in length that comprised <90° of the lesion circumference.[20] Percentage of obstruction of the coronary artery lumen is based on a comparison of the luminal diameter of the segment exhibiting obstruction to the luminal diameter of the most normal-appearing site immediately proximal to the plaque. Diameter stenosis severity was graded as none (0%), very mild (1%-24%), mild (25%-49%), and moderate (50%-70%).[33]

For quantitative atherosclerotic plaque analysis, a semiautomated method will be used, which has been validated against IVUS in previous studies.[26] First, a centerline originating from the ostium defined by the observer will be automatically drawn. Then stretched multiplanar reformatted images will be generated, and the lumen and vessel borders will be detected longitudinally in 4 different cut planes by the software and will be corrected by the observer, as necessary. Based on these longitudinal contours, cross-sectional images at 0.5-mm intervals will be calculated to create transversal lumen and vessel wall contours. The settings for window level and width will be fixed at 740 HU and 220 HU, respectively.

To detect the progression or development of a plaque over time more efficiently, a no-gap method[34,35] will be used, assuming that there is no gap between the vessel wall and the lumen except where a plaque exists, instead of drawing each line separately throughout the entire vessel.

Plaque volume is defined as the difference between the vessel volume and lumen volume, and the mean plaque burden is calculated as the plaque volume divided by the vessel volume, multiplied by 100 to obtain the percentage value.

Imaging repository

All CCTA images will be sent to a core laboratory for image analysis. The core laboratory will perform qualitative and semiquantitative analyses for accuracy of CCTA. CCTA core laboratory interpretation will be used for post hoc analysis. Images will be stored either by Web-based server or locally by a single informatics core laboratory site.

Data management

Completed electronic case report forms will be entered by each site and checked locally for possible errors or omissions. Then, each sites' raw data file will be electronically transmitted to a central data repository at the Clinical and Data Coordinating Center, where they will undergo extensive cleaning and subsequent merging

cont.

Manuscrito 4

to generate the master PARADIGM dataset. On receipt, the CDCC will perform an additional check for possible errors, omissions, or erroneous values.

The CDCC will qualify all investigators by determining the following: knowledge and experience level with standard-of-care CCTA scanning and ICA procedures, adequate patient population to enroll within the scheduled timeline, and the presence of an established clinical research department. Completion of these requirements will be documented via a site qualification questionnaire or equivalent, along with documentation of investigator experience and background.

Sample size calculation

In previous studies that quantitatively measured total plaque volume changes using serial CCTA, total plaque volume increased by 2% to 4% per year, although each study enrolled different patient populations.[35-37] When assuming that total plaque volume increases 2.0% per year,[35] enrollment of 1,766 patients achieve 80% power at an α level of .05. An overall sample size of approximately 2,000 subjects were deemed necessary for study enrollment when permitting a 20% drop-out rate.

Statistical methods

Descriptive, univariate, and multivariate analyses will be conducted. In per-lesion and per-vessel analyses, continuous variables between groups will be analyzed using an independent t test, whereas those between categorical variables will be analyzed using a χ^2 test. Changes in lesion characteristics will be analyzed using mixed linear models. For the primary and secondary objectives, variables displaying significant relationships based on prior relevant literature as well as those with a P value <.1 in univariate Cox proportional hazard regression models will be defined as potential covariates and will be subsequently included in the multivariate analyses to evaluate the association of changes in CCTA parameters and clinical variables. Cutoff values for defining the plaque progression will be determined based on receiver operating characteristic curves.

Study limitations

Although this study will address many of the shortcomings of prior studies examining the natural history of CAD, it is not without limitations. For the present registry, only patients who had 2 or more CCTA scans will be enrolled. However, under current guidelines,[9,10] most patients diagnosed as having severe CAD according to their baseline CCTA would likely have been referred to ICA and may subsequent have undergone revascularization. In any case of patients with normal coronary anatomy at baseline CCTA, follow-up CCTA is typically not recommended during the warranty period.[38,39] Consequently, it would be anticipated that a large bulk of patients with either severe disease or normal coronaries at baseline CCTA would have been omitted from the current registry. Indeed, such a selection bias is often inherent with this type of study design, and given no current recommendations exist regarding serial CCTA in patients with suspected or known CAD, an observational study such as PARADIGM provides a unique opportunity to noninvasively demonstrate the natural course of CAD.

Funding and authorship

The PARADIGM registry is funded by the National Research Foundation of Korea and GE Healthcare. The authors are solely responsible for the design and conduct of this study, all study analyses, the drafting and editing of the manuscript, and its final contents.

Discussion

The PARADIGM registry is a prospective international multicenter dynamic observational cohort registry, which aims to describe and characterize the natural history of coronary atherosclerosis in patients with low-to-intermediate risk and, further, to find the determinants of atherosclerotic disease progression.

The results of this registry will inform clinicians about the clinical and pathological course of CAD by (1) underlining the clinical and CCTA characteristics of vulnerable patients who are most likely exposed to the occurrence of MACE and who might warrant follow-up, (2) determine the frequency and appropriate length of duration wherein vulnerable patients should be followed up using CCTA, (3) assess the clinical and CCTA characteristics which indicate the need for revascularization, and (4) highlight the treatment strategies which regress or delay the progression of CAD. Foremost, the anticipated results from PARADIGM are expected to help guide clinical decision making regarding the appropriate management of patients, by focusing on changes in CCTA as a surrogate marker of disease progression.

Previous studies using invasive techniques[40-43] have identified high-risk features such as thin-cap, low residual lumen area, and spotty calcification as the hallmark of high-risk plaques. These high-risk plaques identified by either IVUS or OCT were also associated with adverse clinical outcomes. However, given these invasive procedure–based studies were naturally performed on patients considered to be high risk, or those with previous ACS, there is a limitation as to how one should directly apply their results to patients with mild-to-intermediate risk. In patients with subclinical CAD, the probability of finding these high-risk plaques is low, and therefore, these techniques are not suitable to be used as an indicator of disease progression. Moreover, it has been conceived that atherosclerotic CAD is a generalized disorder with a dynamic nature of plaque morphology, and that

cont.

Manuscrito 4

American Heart Journal
Volume 182

Table II. Summary of published previous studies using serial CCTA

Reference	Patients		Interval between scans (y)	Design	Analysis method/findings
	n	Inclusion criteria			
Burgstahler et al[53]	46	Elevated CAD risk	1.3	Prospective	Semiquantitative assessment/ NCPV regressed by 24% in the statin therapy group
Hoffmann et al[51]	63	Clinically indicated	2.1	Retrospective	Quantitative assessment/ progression of NCPV slowed by 38% in the statin therapy group
Inoue et al[36]	32	Clinically indicated	1.0	Prospective observational	Quantitative assessment/ PV and LAP regressed in the statin therapy group
Papadopoulou et al[35]	32	ACS	3.3	Prospective observational	Quantitative assessment/ total atheroma volume increased by 47 mm^3 (6.7%)
Zeb et al[37]	100	No Hx of CAD	1.1	Retrospective	Quantitative assessment/ 28% decrease in NCPV in the statin therapy group
Lo et al[52]	40	HIV patient with subclinical CAD	1.0	Prospective randomized	Quantitative assessment/ 4.7% plaque volume regression in the statin therapy group
Lehman et al[54]	69	Acute chest pain in ED	2.0	Prospective observational cohort	Semi-quantitative assessment/ 12.7% increase in coronary plaque burden during a 2-y follow-up
Motoyama et al[55]	449 (subanalysis)	Clinically indicated	1.0	Retrospective observational cohort	Qualitative assessment/ CTA-verified HRP predicted ACS

Abbreviations: *NCPV*, Noncalcified plaque volume; *PV*, plaque volume; *LAP*, low attenuated plaque; *Hx*, history; *HIV*, human immunodeficiency virus; *ED*, emergency department; *HRP*, high-risk plaque.

therapeutic interventions for atherosclerosis are most effective when started at an early stage of the disease.[44] Therefore, rather than simply characterize and identify the presence of such coronary atherosclerotic plaques as high risk, quantitative assessment of disease burden and progression has remained a subject of intense interest.

The ability of CCTA to noninvasively image plaque composition as well as to assess the entire coronary tree wall thickening enables detection and monitoring of earlier stages of CAD.[45,46] It has been hypothesized that noninvasive imaging modalities such as CCTA further stratify intermediate-risk patients to a very high-risk group.[47,48] Moreover, in IVUS and CCTA comparative studies,[24,49,50] CCTA was been shown to accurately evaluate atherosclerotic plaque size, remodeling, eccentricity, and plaque composition. Based on the small mean differences between CCTA and IVUS with virtual histology measurements, it was suggested that quantitative CCTA analysis could be tolerated on a population level.[50] More recently, studies using QCA or IVUS-like parameters have also validated the reliability and reproducibility of CCTA in quantitatively assessing coronary atherosclerotic plaque.[26,27,35,37]

However, still there are limited data regarding plaque progression using CCTA. Although some have used serial CCTA findings to describe the progression or change in coronary plaques,[35-37,51-55] research to date has been limited by small study samples, relatively short durations of intervals between scans, and a focus on more particularistic subsets of patients or lesions. Also, these studies have primarily focused on high-risk populations (Table II). Moreover, there has been no consensus on optimized methodology with regard to quantifying plaque volume by CCTA in an effort to provide reproducible and standardized results.

To thoroughly understand the natural history of atherosclerotic CAD, and to optimize the CCTA methodology and clarify the role of CCTA in quantitative assessment of CAD, prospective studies of low- to moderate-risk populations are clearly needed. Noninvasive imaging methods such as CCTA that possess the ability to accurately estimate change in disease burden over time are critical to assess the response to medical treatments and to monitor the disease process. The PARADIGM registry is designed specifically to address these questions.

The PARADIGM registry will be the first to evaluate the quantitative assessment of disease burden using serial CCTA in populations with low-to-moderate risk, while using its large database collected from geographically diverse regions, which are representative of persons who are presently undergoing clinically indicated CCTA.

Furthermore, the results of this registry may allow for the contemporary revision of indications of CCTA and its role in monitoring patients with suspected CAD. Current guidelines worldwide do not recommend serial CCTA; however, results derived from PARADIGM may prove

cont.

Manuscrito 4

that direct visualization of the lesion may be adequate in monitoring patients who present with CAD.

New knowledge gained

Direct visualization of the natural course of atherosclerosis, as well as identification of the clinical determinants of plaque progression or regression, holds the potential to shift the paradigm of CAD monitoring among low- to moderate-risk patients with suspected CAD, with aims of offering earlier therapeutic strategies, which may facilitate in attenuating disease progression or even improve clinical outcomes. We firmly believe that the PARADIGM registry is appropriately designed to address these important questions in the most suitable manner.

References

1. Naghavi M, Wang H, Lozano R, et al. Global, regional, and national age-sex specific all-cause and cause-specific mortality for 240 causes of death, 1990-2013: a systematic analysis for the Global Burden of Disease Study 2013. Lancet 2015;385:117-71.
2. Sakakura K, Nakano M, Otsuka F, et al. Pathophysiology of atherosclerosis plaque progression. Heart Lung Circ 2013;22: 399-411.
3. Smith Jr SC, Grundy SM. 2013 ACC/AHA guideline recommends fixed-dose strategies instead of targeted goals to lower blood cholesterol. J Am Coll Cardiol 2014;64:601-12.
4. Vos J, De Feyter P, Kingma J, et al. Evolution of coronary atherosclerosis in patients with mild coronary artery disease studied by serial quantitative coronary angiography at 2 and 4 years follow-up. Eur Heart J 1997;18:1081-9.
5. Jukema JW, Bruschke AV, van Boven AJ, et al. Effects of lipid lowering by pravastatin on progression and regression of coronary artery disease in symptomatic men with normal to moderately elevated serum cholesterol levels: the Regression Growth Evaluation Statin Study (REGRESS). Circulation 1995;91:2528-40.
6. Nicholls SJ, Tuzcu EM, Wolski K, et al. Lowering the triglyceride/high-density lipoprotein cholesterol ratio is associated with the beneficial impact of pioglitazone on progression of coronary atherosclerosis in diabetic patients: insights from the PERISCOPE (Pioglitazone Effect on Regression of Intravascular Sonographic Coronary Obstruction Prospective Evaluation) study. J Am Coll Cardiol 2011;57:153-9.
7. Nicholls SJ, Tuzcu EM, Brennan DM, et al. Cholesteryl ester transfer protein inhibition, high-density lipoprotein raising, and progression of coronary atherosclerosis insights from ILLUSTRATE (Investigation of Lipid Level Management Using Coronary Ultrasound to Assess Reduction of Atherosclerosis by CETP Inhibition and HDL Elevation). Circulation 2008;118:2506-14.
8. Nissen SE, Tuzcu EM, Brewer HB, et al. Effect of ACAT inhibition on the progression of coronary atherosclerosis. N Engl J Med 2006;354: 1253-63.
9. Fihn SD, Gardin JM, Abrams J, et al. 2012 ACCF/AHA/ACP/AATS/PCNA/SCAI/STS guideline for the diagnosis and management of patients with stable ischemic heart disease: a report of the American College of Cardiology Foundation/American Heart Association task force on practice guidelines, and the American College of Physicians, American Association for Thoracic Surgery, Preventive Cardiovascular Nurses Association, Society for Cardiovascular Angiography and Interventions, and Society of Thoracic Surgeons. J Am Coll Cardiol 2012;60:e44-164.
10. Task Force M, Montalescot G, Sechtem U, et al. 2013 ESC guidelines on the management of stable coronary artery disease: the task force on the management of stable coronary artery disease of the European Society of Cardiology. Eur Heart J 2013;34:2949-3003.
11. Nicholls SJ, Tuzcu EM, Sipahi I, et al. Statins, high-density lipoprotein cholesterol, and regression of coronary atherosclerosis. JAMA 2007;297:499-508.
12. Dedic A, Kurata A, Lubbers M, et al. Prognostic implications of non-culprit plaques in acute coronary syndrome: non-invasive assessment with coronary CT angiography. Eur Heart J Cardiovasc Imaging 2014;15:1231-7.
13. McPherson JA, Maehara A, Weisz G, et al. Residual plaque burden in patients with acute coronary syndromes after successful percutaneous coronary intervention. J Am Coll Cardiol Img 2012;5:S76-85.
14. Stone GW, Maehara A, Lansky AJ, et al. A prospective natural-history study of coronary atherosclerosis. N Engl J Med 2011;364:226-35.
15. Berry C, L'Allier PL, Grégoire J, et al. Comparison of intravascular ultrasound and quantitative coronary angiography for the assessment of coronary artery disease progression. Circulation 2007;115: 1851-7.
16. Ornish D, Scherwitz LW, Billings JH, et al. Intensive lifestyle changes for reversal of coronary heart disease. JAMA 1998;280: 2001-7.
17. Brown BG, Zhao X-Q, Chait A, et al. Simvastatin and niacin, antioxidant vitamins, or the combination for the prevention of coronary disease. N Engl J Med 2001;345:1583-92.
18. White CW, Wright CB, Doty DB, et al. Does visual interpretation of the coronary arteriogram predict the physiologic importance of a coronary stenosis? N Engl J Med 1984;310:819-24.
19. Grondin CM, Dyrda I, Pasternac A, et al. Discrepancies between cineangiographic and postmortem findings in patients with coronary artery disease and recent myocardial revascularization. Circulation 1974;49:703-8.
20. Motoyama S, Sarai M, Harigaya H, et al. Computed tomographic angiography characteristics of atherosclerotic plaques subsequently resulting in acute coronary syndrome. J Am Coll Cardiol 2009;54: 49-57.
21. Boogers MJ, Broersen A, van Velzen JE, et al. Automated quantification of coronary plaque with computed tomography: comparison with intravascular ultrasound using a dedicated registration algorithm for fusion-based quantification. Eur Heart J 2012;33:1007-16.
22. de Graaf MA, Broersen A, Kitslaar PH, et al. Automatic quantification and characterization of coronary atherosclerosis with computed tomography coronary angiography: cross-correlation with intravascular ultrasound virtual histology. Int J Cardiovasc Imaging 2013;29: 1177-90.
23. Fischer C, Hulten E, Belur P, et al. Coronary CT angiography versus intravascular ultrasound for estimation of coronary stenosis and atherosclerotic plaque burden: a meta-analysis. J Cardiovasc Comput Tomogr 2013;7:256-66.
24. Hoffmann U, Moselewski F, Nieman K, et al. Noninvasive assessment of plaque morphology and composition in culprit and stable lesions in acute coronary syndrome and stable lesions in stable angina by multidetector computed tomography. J Am Coll Cardiol 2006;47: 1655-62.
25. Leipsic J, Taylor CM, Grunau G, et al. Cardiovascular risk among stable individuals suspected of having coronary artery disease with no

cont.

Manuscrito 4

American Heart Journal
Volume 182

modifiable risk factors: results from an international multicenter study of 5262 patients. Radiology 2013;267:718-26.
26. Park H-B, Lee BK, Shin S, et al. Clinical feasibility of 3D automated coronary atherosclerotic plaque quantification algorithm on coronary computed tomography angiography: comparison with intravascular ultrasound. Eur Radiol 2015;1-11.
27. Papadopoulou S-L, Garcia-Garcia HM, Rossi A, et al. Reproducibility of computed tomography angiography data analysis using semi-automated plaque quantification software: implications for the design of longitudinal studies. Int J Cardiovasc Imaging 2013;29:1095-104.
28. Meyer M, Haubenreisser H, Schoepf UJ, et al. Closing in on the K Edge: coronary CT angiography at 100, 80, and 70 kv—initial comparison of a second-versus a third-generation dual-source CT system. Radiology 2014;273:373-82.
29. Abbara S, Arbab-Zadeh A, Callister TQ, et al. SCCT guidelines for performance of coronary computed tomographic angiography: a report of the Society of Cardiovascular Computed Tomography Guidelines Committee. J Cardiovasc Comput Tomogr 2009;3: 190-204.
30. Raff GL, Abidov A, Achenbach S, et al. SCCT guidelines for the interpretation and reporting of coronary computed tomographic angiography. J Cardiovasc Comput Tomogr 2009;3:122-36.
31. Austen WG, Edwards J, Frye R, et al. A reporting system on patients evaluated for coronary artery disease. Report of the Ad Hoc Committee for Grading of Coronary Artery Disease, Council on Cardiovascular Surgery, American Heart Association. Circulation 1975:5-40.
32. Pontone G, Andreini D, Bertella E, et al. Impact of an intra-cycle motion correction algorithm on overall evaluability and diagnostic accuracy of computed tomography coronary angiography. Eur Radiol 2016;26:147-56.
33. Leipsic J, Abbara S, Achenbach S, et al. SCCT guidelines for the interpretation and reporting of coronary CT angiography: a report of the Society of Cardiovascular Computed Tomography Guidelines Committee. J Cardiovasc Comput Tomogr 2014;8:342-58.
34. Nakazato R, Shalev A, Doh J-H, et al. Aggregate plaque volume by coronary computed tomography angiography is superior and incremental to luminal narrowing for diagnosis of ischemic lesions of intermediate stenosis severity. J Am Coll Cardiol 2013;62:460-7.
35. Papadopoulou S-L, Neefjes LA, Garcia-Garcia HM, et al. Natural history of coronary atherosclerosis by multislice computed tomography. J Am Coll Cardiol Img 2012;5:S28-37.
36. Inoue K, Motoyama S, Sarai M, et al. Serial coronary CT angiography–verified changes in plaque characteristics as an end point: evaluation of effect of statin intervention. J Am Coll Cardiol Img 2010;3:691-8.
37. Zeb I, Li D, Nasir K, et al. Effect of statin treatment on coronary plaque progression—a serial coronary CT angiography study. Atherosclerosis 2013;231:198-204.
38. Min JK, Dunning A, Lin FY, et al. Age-and sex-related differences in all-cause mortality risk based on coronary computed tomography angiography findings: results from the International Multicenter CONFIRM (Coronary CT Angiography Evaluation for Clinical Outcomes: An International Multicenter Registry) of 23,854 patients without known coronary artery disease. J Am Coll Cardiol 2011;58:849-60.
39. Ostrom MP, Gopal A, Ahmadi N, et al. Mortality incidence and the severity of coronary atherosclerosis assessed by computed tomography angiography. J Am Coll Cardiol 2008;52:1335-43.
40. Calvert PA, Obaid DR, O'Sullivan M, et al. Association between IVUS findings and adverse outcomes in patients with coronary artery disease: the VIVA (VH-IVUS in Vulnerable Atherosclerosis) study. J Am Coll Cardiol Img 2011;4:894-901.
41. Cheng JM, Garcia-Garcia HM, de Boer SP, et al. In vivo detection of high-risk coronary plaques by radiofrequency intravascular ultrasound and cardiovascular outcome: results of the ATHEROREMO-IVUS study. Eur Heart J 2014;35:639-47.
42. Kataoka Y, Wolski K, Uno K, et al. Spotty calcification as a marker of accelerated progression of coronary atherosclerosis: insights from serial intravascular ultrasound. J Am Coll Cardiol 2012;59:1592-7.
43. Uemura S, K-i I, Soeda T, et al. Thin-cap fibroatheroma and microchannel findings in optical coherence tomography correlate with subsequent progression of coronary atheromatous plaques. Eur Heart J 2012;33:78-85.
44. Stone N, Robinson J, Lichtenstein A, et al. American College of Cardiology/American Heart Association Task Force on Practice Guidelines. 2013 ACC/AHA guideline on the treatment of blood cholesterol to reduce atherosclerotic cardiovascular risk in adults: a report of the American College of Cardiology/American Heart Association Task Force on Practice Guidelines. J Am Coll Cardiol 2014;63:2889-934.
45. Yamada M, Jinzaki M, Tanami Y, et al. Detection of a coronary artery vessel wall: performance of 0.3 mm fine-cell detector computed tomography—a phantom study. Phys Med Biol 2011;56:5235.
46. Abd-Elmoniem KZ, Unsal AB, Eshera S, et al. Increased coronary vessel wall thickness in HIV-infected young adults. Clin Infect Dis 2014;59:1779-86.
47. Braunwald E. Epilogue: what do clinicians expect from imagers? J Am Coll Cardiol 2006;47:C101.
48. Braunwald E. Noninvasive detection of vulnerable coronary plaques locking the barn door before the horse is stolen. J Am Coll Cardiol 2009;54:58-9.
49. Papadopoulou S-L, Neefjes LA, Schaap M, et al. Detection and quantification of coronary atherosclerotic plaque by 64-slice multidetector CT: a systematic head-to-head comparison with intravascular ultrasound. Atherosclerosis 2011;219:163-70.
50. Voros S, Rinehart S, Qian Z, et al. Prospective validation of standardized, 3-dimensional, quantitative coronary computed tomographic plaque measurements using radiofrequency backscatter intravascular ultrasound as reference standard in intermediate coronary arterial lesions: results from the ATLANTA (assessment of tissue characteristics, lesion morphology, and hemodynamics by angiography with fractional flow reserve, intravascular ultrasound and virtual histology, and noninvasive computed tomography in atherosclerotic plaques) I study. JACC: Cardiovascular Interventions 2011;4:198-208.
51. Hoffmann H, Frieler K, Schlattmann P, et al. Influence of statin treatment on coronary atherosclerosis visualised using multidetector computed tomography. Eur Radiol 2010;20:2824-33.
52. Lo J, Lu MT, Ihenachor EJ, et al. Effects of statin therapy on coronary artery plaque volume and high-risk plaque morphology in HIV-infected patients with subclinical atherosclerosis: a randomised, double-blind, placebo-controlled trial. Lancet HIV 2015;2:e52-63.
53. Burgstahler C, Reimann A, Beck T, et al. Influence of a lipid-lowering therapy on calcified and noncalcified coronary plaques monitored by multislice detector computed tomography: results of the New Age II Pilot Study. Invest Radiol 2007;42:189-95.
54. Lehman SJ, Schlett CL, Bamberg F, et al. Assessment of coronary plaque progression in coronary computed tomography angiography using a semiquantitative score. J Am Coll Cardiol Img 2009;2: 1262-70.
55. Motoyama S, Ito H, Sarai M, et al. Plaque characterization by coronary computed tomography angiography and the likelihood of acute coronary events in mid-term follow-up. J Am Coll Cardiol 2015;66:337-46.

MANUSCRITO 5

Cost-effectiveness of different diagnostic strategies in suspected stable coronary artery disease in Portugal.

Ferreira, A.M., **Marques**, **H**., Goncalves, P.A., and Cardim, N.,

Arq Bras Cardiol, 2014
102(4): p. 391-402

Manuscrito 5

Original Article

Cost-Effectiveness of Different Diagnostic Strategies in Suspected Stable Coronary Artery Disease in Portugal

António Miguel Ferreira[1,2], Hugo Marques[1,3,4], Pedro Araújo Gonçalves[1,2,4], Nuno Cardim[1,4]

Hospital da Luz[1], Lisboa; Hospital Santa Cruz - Centro Hospitalar de Lisboa Ocidental[2], Lisboa; Hospital Santa Marta - Centro Hospitalar de Lisboa Central[3], Lisboa; Faculdade de Ciências Médicas da Universidade Nova de Lisboa[4], Lisboa – Portugal

Abstract

Background: **Cost-effectiveness is an increasingly important factor in the choice of a test or therapy.**

Objective: **To assess the cost-effectiveness of various methods routinely used for the diagnosis of stable coronary disease in Portugal.**

Methods: **Seven diagnostic strategies were assessed. The cost-effectiveness of each strategy was defined as the cost per correct diagnosis (inclusion or exclusion of obstructive coronary artery disease) in a symptomatic patient. The cost and effectiveness of each method were assessed using Bayesian inference and decision-making tree analyses, with the pretest likelihood of disease ranging from 10% to 90%.**

Results: **The cost-effectiveness of diagnostic strategies was strongly dependent on the pretest likelihood of disease. In patients with a pretest likelihood of disease of ≤50%, the diagnostic algorithms, which include cardiac computed tomography angiography, were the most cost-effective. In these patients, depending on the pretest likelihood of disease and the willingness to pay for an additional correct diagnosis, computed tomography angiography may be used as a frontline test or reserved for patients with positive/inconclusive ergometric test results or a calcium score of >0. In patients with a pretest likelihood of disease of ≥ 60%, up-front invasive coronary angiography appears to be the most cost-effective strategy.**

Conclusions: **Diagnostic algorithms that include cardiac computed tomography angiography are the most cost-effective in symptomatic patients with suspected stable coronary artery disease and a pretest likelihood of disease of ≤50%. In high-risk patients (pretest likelihood of disease ≥ 60%), up-front invasive coronary angiography appears to be the most cost-effective strategy. In all pretest likelihoods of disease, strategies based on ischemia appear to be more expensive and less effective compared with those based on anatomical tests. (Arq Bras Cardiol. 2014; 102(4):391-402)**

Keywords: **Coronary disease / economics; Coronary disease / diagnosis; Cost-Benefit analysis.**

Introduction

Clinical assessment of an individual with suspected stable coronary artery disease (CAD) is usually complemented by noninvasive tests such as the ergometric test (ET), myocardial perfusion scintigraphy (MPS), or stress echocardiography (StressEcho). Cardiac computed tomography angiography (CCTA) has broadened the options for the assessment of CAD patients and is a potentially beneficial alternative for individuals with an intermediate or a low pretest likelihood of disease (PLD)[1]. However, the generalized adoption of new techniques that, although appealing, may entail additional costs and no added value, should be considered carefully with regard to the increasing economic pressure to which healthcare systems are exposed. Therefore, it is important to determine the cost-effectiveness of diagnostic strategies routinely used for the diagnosis of stable CAD and identify patients for whom CCTA is a cost-effective alternative.

Methods

The cost-effectiveness of seven diagnostic strategies was assessed: (1) ET followed by MPS in positive or inconclusive cases, (2) ET followed by 64-detector CCTA in positive or inconclusive cases, (3) MPS (as first option), (4) StressEcho with dobutamine (as first option), (5) CCTA (as first option), (6) calcium scoring (CaSc) followed by CCTA (CACS-CCTA) when CaSc > 0, and (7) invasive coronary angiography (CATH) as the first and only test. All considered strategies presuppose the end of the diagnostic procedures when a test is negative and a confirmation CATH when the last test of the noninvasive strategy is positive or inconclusive. In addition, an eight alternative was assessed in individuals with a PLD of 10%, which involved not performing any complementary diagnostic tests and assuming the absence of obstructive CAD.

Mailing Address: António Miguel Ferreira •
Hospital da Luz, Avenida Lusíada, 100. Postal Code 1500-650, Lisboa – Portugal
E-mail: miguelferreira.md@sapo.pt, amferreira.md@gmail.com
Manuscript received May 13, 2013; revised manuscript November 10, 2013; accepted December 10,2 013.

DOI: 10.5935/abc.20140042

cont.

Manuscrito 5

A decision-making tree analysis was performed according to the method described by Patterson et al[2,3] to assess the cost-effectiveness of each strategy according to PLD. In this method, hypothetical cohorts of patients with a certain PLD are subjected to each of the diagnostic strategies. Then, Bayesian inference is used to estimate the cost and effectiveness of each strategy according to the test characteristics. Sensitivity, specificity, and the rate of nondiagnostic tests were gathered from meta-analysis, clinical recommendations, and published series (Table 1). The rate of nondiagnostic ET and StressEcho tests was calculated as the mean percentage of patients who fail to reach the target heart rate. MPS was always considered to be diagnostic, and its accuracy was considered independent of the stress method used. In addition, CCTA tests were always considered diagnostic since the meta-analysis on its accuracy was performed on an intention-to-diagnose basis, assuming that all nondiagnostic tests would be false-positive, thereby decreasing the specificity of the test[4]. The sensitivity and specificity of CaSc > 0 for the diagnosis of obstructive CAD were obtained through combined analysis of the results of two international multicenter clinical trials[5,6]. We assumed that CATH tests would always be diagnostic, with a sensitivity and specificity of 100%.

Comparison of cost-effectiveness

The cost-effectiveness of each strategy was defined as the cost per correct diagnosis (inclusion or exclusion of obstructive CAD) in a symptomatic patient. According to this definition, a lower cost value per correct diagnosis translates into better cost-effectiveness. Comparison between the diagnostic strategies was made from the society's perspective (i.e., including all costs, regardless of the payer)[14]. To compare the incremental cost-effectiveness of each option with that of all the other alternatives, the diagnostic strategies were ranked in increasing order of cost and those outperformed by complete dominance (simultaneously more expensive and less effective) and incomplete dominance (less effective with a higher incremental cost-effectiveness ratio; ICER) were excluded. ICERs (added cost per additional correct diagnosis) were calculated for each strategy relative to the previous less expensive strategy.

Definition of cost

The cost of a diagnostic strategy includes direct and indirect costs. Direct cost was considered as the cost of the examinations performed for patients in each cohort, using the current *Tabela de Preços do Serviço Nacional de Saúde* (price list of the National Health Service), which was defined by the Ordinance 839-A/2009 of July 31, 2009, as a reference[15]. The price of cardiac CCTA was defined as the sum of the values of CCTA, intravenous contrast supplement, and post-processing (Table 2). In the CaSc-CCTA strategy, a cost of € 80.00 was assumed (identical to that of noncontrast chest CT)[15] for patients who only underwent CaSc, while a cost of € 207.10 was assumed for those who also underwent CCTA.

Table 1 – Sensitivity, specificity, and rate of nondiagnostic tests for each method as assumed in the economic model

	ET (%)	MPS (%)	StressEcho (%)	CCTA (%)	CACS > 0 (%)
Sensitivity	68[7]	87[8,9]	86[10]	98[4]	93[5,6]
Specificity	77[7]	81[11]	84[10]	85[4]	43[5,6]
Rate of nondiagnostic tests	17[12]	0	18[13]	0[4]	0

ET: ergometric test; MPS: myocardial perfusion scintigraphy; StresEco: stress echocardiogram with dobutamine; CCTA: computed tomography angiography of the coronary arteries; CaSc: calcium scoring

Table 2 – Price of tests included in the different diagnostic strategies (values for Portugal)

Code[15]	Designation	Price (€)
40315	Stress test in ergometric bicycle or treadmill with continuous ECG monitoring and recording at each stage	36.80
58015	Myocardial perfusion scintigraphy under pharmacological stress	424.40
40660	Transthoracic echocardiography under pharmacological stress (includes the cost of the drug)	121.80
16350	CCTA	(129.40)
16325	CT, intravenous contrast supplement	(62.60)
16345	Post-processing	(15.10)
-	Total cardiac CCTA (three codes)	207.10
-	Calcium scoring	80.00
40820	Left catheterization with selective coronary angiography	585.50

ECG: electrocardiogram, CCTA: computed tomography angiography of the coronary arteries, CT: computed tomography.

cont.

Manuscrito 5

The following indirect costs were included.

1. Cost associated with incidental findings during CaSc and cardiac CCTA. We assumed that 7% of these tests would exhibit incidental extracardiac findings of uncertain clinical significance, which would require direct investigation[16], usually to assess lung nodules. We assumed that these cases would require noncontrast chest CT a few months later[17] at an additional cost of € 80.00[15].

2. Cost associated with complications caused by diagnostic CATH. We assumed that the rate of major iatrogenic adverse cardiovascular events (death, myocardial infarction, or stroke) was 0.05%[18], while that of vascular access-related complications that required transfusion or surgery was 0.4% (for a rate of 80% for radial access use)[19]. With regard to major cardiovascular events, we considered acute myocardial infarction to be a typical complication[3,20] and estimated its cost by adding the cost for a homogeneous diagnostic group (HDG) of patients with nonfatal myocardial infarction without major complications (€3,671.53)[15] to the cost of 1 month of temporary incapacity to work, for a gross domestic product (GDP) *per capita* of €16,100, assuming that half of the population assessed for suspected CAD was active. The mean cost of an iatrogenic major cardiovascular event thus estimated was € 4,342. The mean cost of a vascular access complication requiring transfusion or surgery was estimated to be €1,500 (expert opinion).

3. Cost of false-negative tests. The potential cost of false-negative tests includes the cost of repeat tests for CAD diagnosis, other examinations for the differential diagnosis of chest pain, worse quality of life, and added risk for cardiovascular events due to the non-prescription of adequate medical therapy. These costs are particularly difficult to evaluate. Previous studies have used various methods to estimate that the cost of a false-negative test is 1.4–6.7 times higher than that of a false-positive test[3,20,21]. Therefore, false-negative tests were allocated a cost that was three times higher than that of a false-positive test (€1.818 for each false-negative test). In the scenario where no further testing is performed assuming the absence of CAD (a hypothesis considered for patients with PLD of 10%), the costs of false-negatives were the only ones taken into account.

We did not include the cost of complications caused by noninvasive tests in the model because serious complications resulting from these tests are very rare and would only marginally increase costs. In addition, the cost associated with potential exposure to ionizing radiation was not included because this was a short-term cost-effectiveness model; furthermore, there is great uncertainty about the effects of radiation doses used in these tests[22].

Sensitivity analysis

To assess the extent to which the results obtained depended on some of the variables under study, several sensitivity analyses were performed. Calculations were repeated using new assumptions such as decreasing the sensitivity and specificity values for cardiac CCTA to 96% and 81%, respectively (lower limits of 95% confidence intervals in the meta-analysis of 53 studies)[4], decreasing the cost of MPS to €207.10 (equating the cost of MPS with that of CCTA), decreasing the rate of inconclusive StressEcho tests to 5%, and assuming zero cost for false-negative tests.

Results

Figure 1 shows the cost-effectiveness plans for the diagnostic strategies for each scenario of PLD. In general, costs increase and the percentage of correct diagnosis decreases with increasing PLD (due to the increase in the number of false-negative tests).

The composition of direct and indirect costs is shown in Table 3 (simulation of the expected results when a cohort of 100 patients with a PPT of 30% is assessed).

Table 4 summarizes the results of incremental cost-effectiveness of the diagnostic strategies applied to hypothetical cohorts of 100 patients with a PLD of 10%–90%. Diagnostic strategies were presented in increasing order of cost and respective ICER for each assessed PLD. In all scenarios of PLD, the diagnostic strategies for ET-MPS, MPS, and StressEcho are dominated by alternative strategies that are less expensive and more effective. According to the cost-effectiveness criterion, choosing the best diagnostic strategy depends on the percentage of false-negative tests that one is willing to accept and on the willingness to pay for an additional correct diagnosis (Figure 2). For example, for a limit of €5,000 per additional correct diagnosis, the preferred strategy would be CACS-CCTA for patients with a PLD of 10%, CCTA for those with a PLD of 20%–40%, and CATH for those with a PLD of ≥50%.

Results of sensitivity analysis

To assess the robustness of the results and the influence of several assumptions, we reformulated the model by altering some parameters such as diagnostic accuracy of CCTA, price of MPS, rate of inconclusive StressEcho tests, and cost of false-negative tests.

The decrease in sensitivity and specificity of CCTA to 96% and 81%, respectively, resulted in the increase in total cost and ICER of the strategies that include CCTA. Nevertheless, the ET-MPS, MPS, and StressEcho diagnostic strategies remained dominated, with the increasing order of cost-effectiveness shown in Table 4 being maintained for every assessed PLD.

When the cost of MPS is equated to the cost of CCTA (€ 207.10), the cost-effectiveness of the ET-MPS and MPS diagnostic strategies improves. However, these strategies remained dominated by other diagnostic methods (less expensive and more effective) for all assessed PLDs (Table 5).

The decrease in the rate of inconclusive StressEcho tests from 18% to 5% resulted in the improvement of its cost-effectiveness; however, this method remained dominated by other diagnostic strategies for all the assessed PLDs. When the StressEcho strategy was compared with the dominant noninvasive strategies (more cost-effective), at each level of PLD, the StressEcho strategy entailed an additional cost of €303 to €2,700 per 100 patients, along with an increase in false-negative tests from 1.1% to 5.7%.

In the model where the absence of indirect costs is assumed in patients with false-negative tests, the ET-CCTA strategy is the least expensive for all levels of PLD. However, this diagnostic procedure resulted in a significant number of false-negative tests, particularly for intermediate or high PLDs. The transition to more effective strategies becomes less expensive with the increasing prevalence of obstructive CAD (Table 6).

cont.

Manuscrito 5

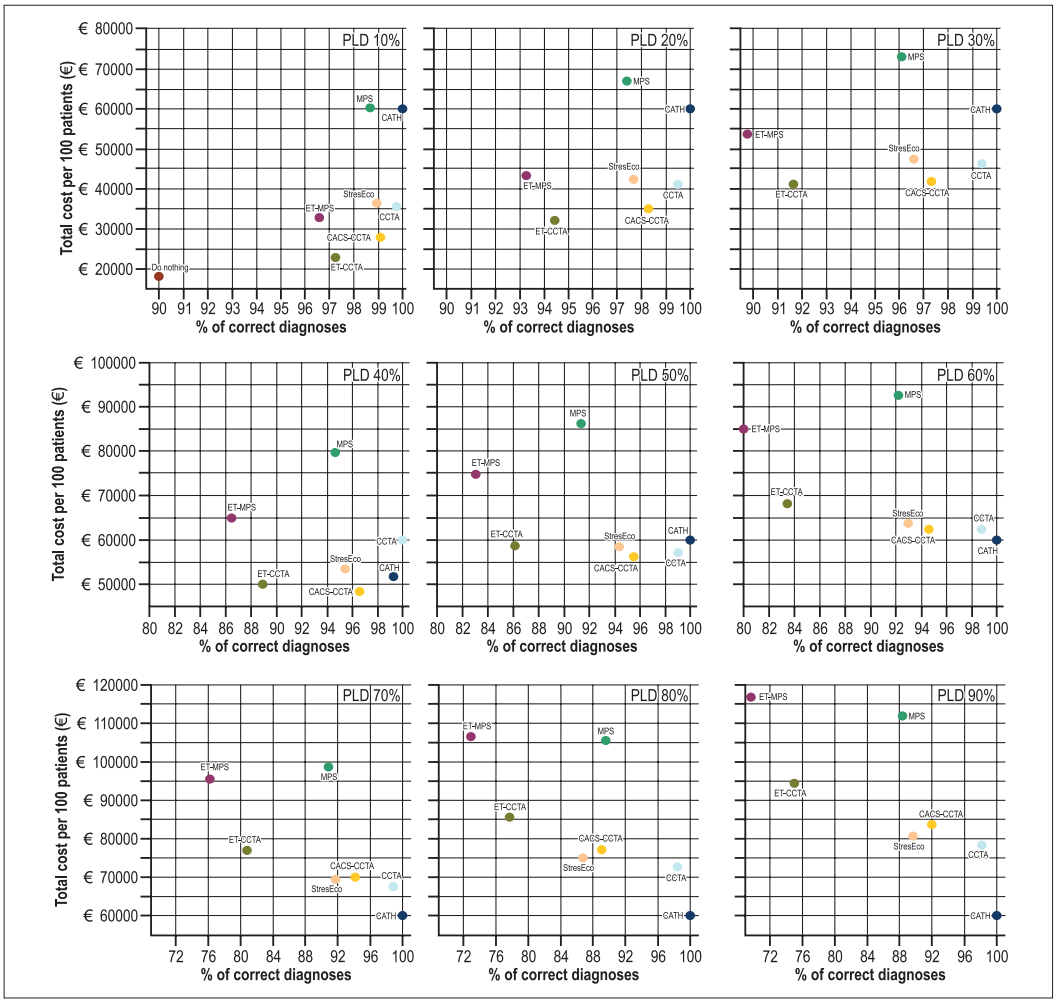

Figure 1 – *Cost-effectiveness plans for the diagnostic strategies according to the pretest likelihood of disease.*

Discussion

In recent years, the need to consider the cost of clinical decisions is becoming increasingly important. Cost-effectiveness analyses allow for more efficient use of health resources and rationalize the use of new technologies, often more expensive than their alternatives. To our knowledge, this is the first assessment of the cost-effectiveness of several strategies used for the diagnosis of stable CAD in Portugal. The results of this analysis indicate that, in this country, diagnostic algorithms that include cardiac CCTA are the most cost-effective methods in symptomatic patients with suspected obstructive CAD and a PLD of ≤50%. In high-risk patients (PLD > 50%), immediate CATH appears to be the most cost-effective strategy. The model suggests that ischemia imaging techniques (MPS and StressEcho) are more expensive and less effective compared with other diagnostic strategies for all assessed PLDs. With regard to patients with a PLD of ≤50% and the conservative scenario wherein the willingness to pay for an additional correct diagnosis is €1.000, the results of incremental cost-effectiveness indicate that it is advantageous to perform an ergometric test before CCTA in patients with a lower PLD (10%), do a "rule-out" CaSc before CCTA in patients with a PLD of 20-30%, and perform up-front CCTA in patients with a PLD of 40-50%. In the more liberal scenario (willingness to pay €5.000 for an additional correct diagnosis), the preferred strategy would be SCa-CCTA for patients with a PLD of 10%, CCTA for patients with a PLD of 20%–40%, and CATH for patients with a PLD of ≥ 50%.

cont.

Manuscrito 5

Table 3 – Results of cost-effectiveness of the diagnostic strategies for 100 patients with a pretest likelihood of disease of 30%

	ET-MPS	ET-CCTA	MPS	StressEcho	CCTA	CACS-CCTA	CATH
After non-invasive testing							
True positive	19.2	21.6	26.1	21.2	29.4	27.4	-
False positive	4.8	3.8	13.3	9.2	10.5	6.0	-
True negative	65.2	66.2	56.7	48.2	59.5	64.0	-
False negative	10.8	8.4	3.9	3.4	0.6	2.6	-
Inconclusive	0	0	0	18	0	0	-
Invasive Angiographies	24	25.4	39.4	48.4	39.9	33.4	100
Normal invasive Angiographies	4.8 (20%)	3.8 (15%)	13.3 (34%)	21.8 (45%)	10.5 (26%)	6 (18%)	70 (70%)
Correct diagnoses (after CATH when applicable)	89.2	91.6	96.1	96.6	99.4	97.4	100
Costs							
Noninvasive tests	€ 23.752	€ 13.475	€ 42.440	€ 12.180	€ 20.710	€ 16.642	-
CATH	€ 14.033	€ 14.860	€ 23.069	€ 28.303	€ 23.362	€ 19.543	€ 58.550
CATH complications de CATH	€ 318	€ 337	€ 523	€ 643	€ 530	€ 443	€ 1.327
Incidental findings	-	€ 265	-	-	€ 560	€ 560	-
False-negative tests	€ 19.693	€ 15.287	€ 7.090	€ 6.261	€ 1.091	€ 4.785	-
Total cost	€ 57.796	€ 44.224	€ 73.122	€ 47.386	€ 46.252	€ 41.973	€ 59.877
Cost per correct diagnosis	€ 648	€ 483	€ 761	€ 491	€ 465	€ 431	€ 599

ET: ergometric test, MPS: myocardial perfusion scintigraphy, CCTA: computed tomography angiography of the coronary arteries, StressEcho: stress echocardiography with dobutamine, CACS: calcium score, CATH: invasive coronary angiography

Ultimately, the selection of a diagnostic method on the basis of cost-effectiveness criteria depends on PLD and the willingness to pay for an additional correct diagnosis. Contrary to long-term cost-effectiveness studies, in this context, there is no commonly accepted cost-effectiveness limit [for example: € 30,000/quality-adjusted life-years (QALY)] to serve as a reference for the adoption or rejection of a diagnostic strategy. However, a recent study suggested that, for a CAD prevalence of ≥30%, values of incremental cost per correct diagnosis in the short-term model are similar to those of incremental cost per QALY estimated in long-term models[23]. In a more conservative scenario, the willingness of the Portuguese society to pay for an additional correct diagnosis will be at least ≥ €1.010, which corresponds to the sum of the direct costs of MPS followed by CATH, a diagnostic strategy that is well accepted and frequently used in Portugal.

Of the scenarios assessed in the sensitivity analysis, the one in which CCTA and MPS have the same price is particularly important because this is the case in some countries. Even in this scenario, MPS remains a dominated strategy (i.e., more expensive and less effective) because it is less accurate than CCTA, particularly in terms of sensitivity. The results would only be different in a scenario (not tested) where the price of scintigraphy was identical and where scintigraphy was more accurate.

In general, these results are in line with those obtained in other countries[17,20,24-29] that consider cardiac CCTA as a cost-effective method for the diagnosis or exclusion of obstructive CAD in patients with an intermediate PLD. This is probably because of a favorable combination of cost (relatively affordable) and accuracy. Better diagnostic accuracy simultaneously increases the denominator of the cost-effectiveness equation (number of correct diagnoses) and decreases the numerator, with lower indirect costs from false-negative and false-positive tests.

The interpretation of these results and analysis of their potential implications should consider several factors. First, it should be noted that the cost-effectiveness of diagnostic strategies is critically dependent on the adequate selection of patients. The calculation of PLD is a key step in selecting a cost-effective diagnostic strategy. This assessment can be easily and quickly made using validated clinical scores that were recently calibrated in European contemporary populations[30]. Second, the results of this analysis only apply to patients without known CAD. Therefore, these findings do not mean that functional tests are not useful or cost-effective in distinct contexts, namely in patients with established CAD. In the latter case, the performance of CCTA is suboptimal, and the key issues are the presence or absence of ischemia and the localization, extension, and severity of ischemia. Rather than seeing these results in terms of winners and losers, it is important to know the advantages and disadvantages of

cont.

Manuscrito 5

Table 4 – Incremental cost-effectiveness of the diagnostic strategies applied to hypothetical cohorts of 100 patients with a PLD of 10%–60%. For a PLD of >=60%, all strategies are dominated by the CATH strategy.

Pretest likelihood	Diagnostic strategy	Total cost (€)	Number of correct diagnoses*	False-negative tests*	ICER**
10%	No test	18.180	90.0	10.0	-
	ET-CCTA	24.473	97.2	2.8	€ 874
	CACS-CCTA	27.975	99.1	0.9	€ 1.819
	ET-MPS	34.667	96.4	3.6	Dominated
	CCTA	35.585	99.8	0.2	€ 11.234
	StressEcho	36.338	98.9	1.1	Dominated
	CATH	59.877	100	0	€ 121.461
	MPS	60.252	98.7	1.3	Dominated
20%	ET-CCTA	34.349	94.4	5.6	-
	CACS-CCTA	34.974	98.2	1.8	€ 162
	CCTA	40.918	99.6	0.4	€ 4.388
	StressEcho	41.862	97.7	2.3	Dominated
	ET-MPS	46.232	92.8	7.2	Dominated
	CATH	59.877	100	0	€ 47.397
	MPS	66.687	97.4	2.6	Dominated
30%	CACS-CCTA	41.973	97.4	2.6	-
	ET-CCTA	44.224	91.6	8.4	Dominated
	CCTA	46.252	99.4	0.6	€ 2.106
	StressEcho	47.386	96.6	3.4	Dominated
	ET-MPS	57.796	89.2	10.8	Dominated
	CATH	59.877	100	0	€ 22.709
	MPS	73.122	96.1	3.9	Dominated
40%	CACS-CCTA	48.972	96.5	3.5	-
	CCTA	51.585	99.2	0.8	€ 964
	StressEcho	52.910	95.4	4.6	Dominated
	ET-CCTA	54.099	88.8	11.2	Dominated
	CATH	59.877	100	0	€ 10.365
	ET-MPS	69.361	85.6	14.4	Dominated
	MPS	79.557	94.8	5.2	Dominated
50%	CACS-CCTA	55.971	95.6	4.4	-
	CCTA	56.919	99.0	1.0	€ 280
	StressEcho	58.434	94.3	6.7	Dominated
	CATH	59.877	100	0	€ 2.959
	ET-CCTA	63.975	86.0	14.0	Dominated
	ET-MPS	80.925	82.0	18.0	Dominated
	MPS	85.992	93.5	6.5	Dominated
60%	CATH	59.877	100	0	-
	CCTA	62.252	98.8	1.9	Dominated
	CACS-CCTA	62.970	94.7	5.3	Dominated
	StressEcho	63.958	93.1	6.9	Dominated
	ET-CCTA	73.850	83.2	16.8	Dominated
	MPS	92.427	92.2	7.8	Dominated
	ET-MPS	92.490	78.3	21.7	Dominated

** At the end of the diagnostic strategy, i.e., including the results of CATH when the noninvasive tests are positive or inconclusive ** Incremental cost per additional correct diagnosis. ICER: incremental cost-effectiveness ratio (Δ cost/Δ correct diagnosis), ET: ergometric test, CCTA: computed tomography angiography of the coronary arteries, CaSc: calcium scoring, MPS: myocardial perfusion scintigraphy, StressEcho: stress echocardiography*

cont.

Manuscrito 5

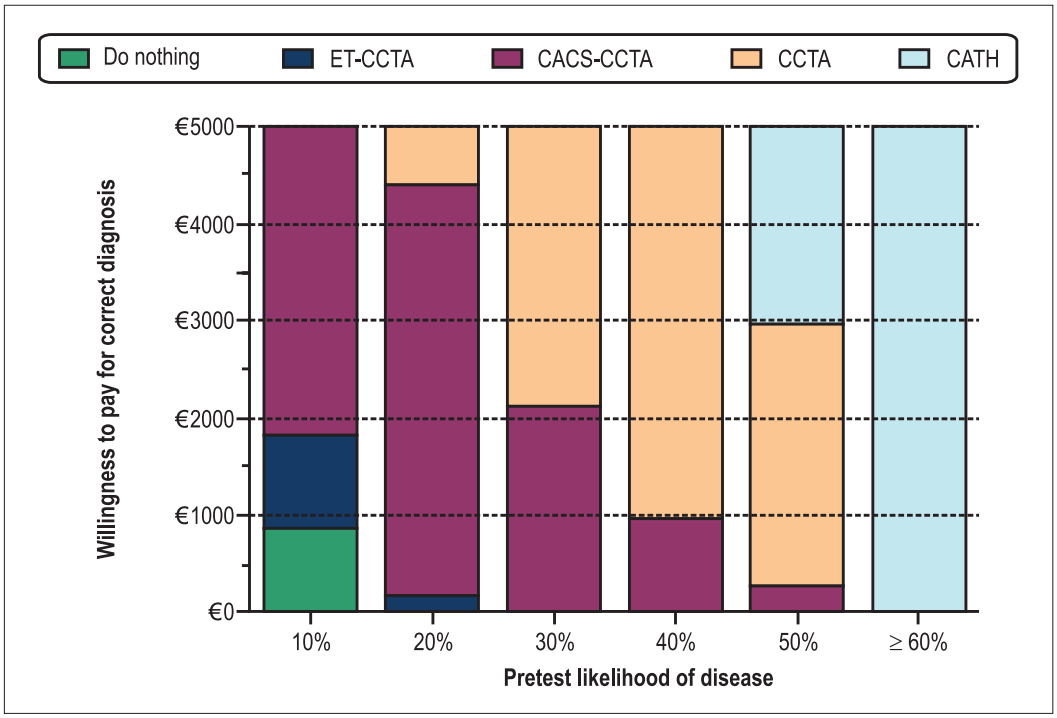

Figure 2 – *Choice of the most cost-effective diagnostic strategy according to the PLD and willingness to pay for a correct diagnosis. Once the maximum value that society is willing to pay for an additional correct diagnosis is established, the strategy that represents the best use of these resources is the one that intercepts the line of the value that society is willing to pay. For example, for a willingness to pay €1,500 per additional correct diagnosis, the best method would be ET-CCTA when the pretest likelihood of disease is 10%, CACS-CCTA when the pretest likelihood is 20%–30%, CCTA when the pretest likelihood is 40%–50%, and CATH when the pretest likelihood is ≥60%.*

the anatomical and functional methods in different contexts. Third, it should be acknowledged that the exclusive use of anatomical methods for the diagnosis of obstructive CAD carries some risks, namely the hazard of prompting unnecessary revascularizations. However, CATH, in the assessed strategies, had a diagnostic and not necessarily therapeutic objective (as in the COURAGE study)[31], and although both coronary angiographies (invasive or CT) essentially provide anatomical information, there is a possibility of complementing this assessment with functional information provided by coronary fraction flow reserve (FFR) measurement, which is emerging as the gold-standard and has been demonstrated to be cost-effective[32]. It is probable that, in the near future, CCTA will allow the assessment of ischemia using perfusion techniques[33] or virtual CFR measurements[34,35]; however, this is not yet an established procedure.

Limitations

This study has some limitations. First, it described a theoretical model, the results of which are dependent on factors such as sensitivity and specificity of various techniques that, in the real world, can be different from those reported in international studies of reference. With regard to CCTA, it should be noted that its specificity depends on PLD because of the varying prevalence of coronary calcifications. The use of intermediate values may have led to the underestimation of the cost-effectiveness of CCTA in patients with a lower PLD and overestimation in patients with a higher PLD[36]. Similarly, like in all analyses of this type, the results are only applicable to patients who are capable of undergoing any of the tests under study (i.e., able to exercise, without complete block of the left bundle branch, without severe renal impairment, and not allergic to iodinated contrast medium). We chose to exclude the costs and benefits related to periods after the diagnosis phase (such as costs of medication, revascularization, hospitalization, and possible gains in QALY) in the model because they entail greater complexity and uncertainty. However, there is evidence that the diagnosis of obstructive CAD (vs. false-negative tests) is associated with an increase of three QALYs over a period of 10 years[3]. Depending on the assumptions made, it is possible that long-term analysis produces results that are significantly different from those obtained in this analysis. In addition, to avoid a more complex analysis, not all possible diagnostic strategies were considered; we chose accessible and frequently utilized modalities and diagnostic procedures. Moreover, conclusive tests were classified as positive or negative, in a reductionist dichotomization which is inevitable in this type of analysis. Finally, cost-effectiveness should be one of the criteria considered in clinical decision-making. Other patient-related or context-

cont.

Manuscrito 5

Table 5 – Incremental cost-effectiveness of diagnostic strategies in hypothetical cohorts of 100 patients with a PLD of 10%–60%, considering identical prices for MPS and CCTA of the coronary arteries. For a PLD of ≥60%, all strategies were dominated by CATH

Pretest likelihood	Diagnostic strategy	Total cost (€)	Number of correct diagnoses*	False-negative tests*	ICER**
10%	No test	18.180	90.0	10.0	-
	ET-CCTA	24.473	97.2	2.8	€874
	ET-MPS	26.013	96.4	3.6	Dominated
	CACS-CCTA	27.975	99.1	0.9	€1.819
	CCTA	35.585	99.8	0.2	€11.234
	StressEcho	36.338	98.9	1.1	Dominated
	MPS	38.522	98.7	1.3	Dominated
	CATH	59.877	100	0	€121.461
20%	ET-CCTA	34.349	94.4	5.6	-
	CACS-CCTA	34.974	98.2	1.8	€162
	TET-MPS	36.766	92.8	7.2	Dominated
	CCTA	40.918	99.6	0.4	€4.388
	StressEcho	41.862	97.7	2.3	Dominated
	MPS	44.957	97.4	2.6	Dominated
	CATH	59.877	100	0	€47.397
30%	CACS-CCTA	41.973	97.4	2.6	-
	ET-CCTA	44.224	91.6	8.4	Dominated
	CCTA	46.252	99.4	0.6	€2.106
	StressEcho	47.386	96.6	3.4	Dominated
	ET-MPS	47.519	89.2	10.8	Dominated
	MPS	51.392	96.1	3.9	Dominated
	CATH	59.877	100	0	€22.709
40%	CACS-CCTA	48.972	96.5	3.5	-
	CCTA	51.585	99.2	0.8	€964
	StressEcho	52.910	95.4	4.6	Dominated
	ET-CCTA	54.099	88.8	11.2	Dominated
	MPS	57.827	94.8	5.2	Dominated
	ET-MPS	58.272	85.6	14.4	Dominated
	CATH	59.877	100	0	€10.365
50%	CACS-CCTA	55.971	95.6	4.4	-
	CCTA	56.919	99.0	1.0	€280
	StressEcho	58.434	94.3	6.7	Dominated
	CATH	59.877	100	0	€2.959
	ET-CCTA	63.975	86.0	14.0	Dominated
	MPS	64.262	93.5	6.5	Dominated
	ET-MPS	69.025	82.0	18.0	Dominated
60%	CATH	59.877	100	0	-
	CCTA	62.252	98.8	1.9	Dominated
	CACS-CCTA	62.970	94.7	5.3	Dominated
	StressEcho	63.958	93.1	6.9	Dominated
	MPS	70.697	92.2	7.8	Dominated
	ET-CCTA	73.850	83.2	16.8	Dominated
	ET-MPS	79.778	78.3	21.7	Dominated

** At the end of the diagnostic strategy, i.e., including the results of CATH when the noninvasive tests are positive or inconclusive. ** Incremental cost per additional correct diagnosis. ICER: incremental cost-effectiveness ratio (Δ cost/Δ correct diagnosis), ET: ergometric test, CCTA: computed tomography angiography of the coronary arteries, CaSc: calcium scoring, MPS: myocardial perfusion scintigraphy, StressEcho: stress echocardiography*

cont.

Manuscrito 5

Original Article

Table 6 – Incremental cost-effectiveness of diagnostic strategies in hypothetical cohorts of 100 patients with a PLD of 10%–90%. considering zero cost for false-negative tests. The dominated strategies are not shown

Pretest likelihood	Diagnostic strategy	Total cost (€)	Number of correct diagnoses*	False-negative tests*	ICER** (€)
10%	ET-CCTA	19.378	97.2	2.8	-
	CACS-CCTA	26.379	99.1	0.9	3.637
	CCTA	35.221	99.8	0.2	13.052
	CATH	59.877	100	0	123.279
20%	ET-CCTA	24.157	94.4	5.6	-
	CACS-CCTA	31.783	98.2	1.8	1.980
	CCTA	40.191	99.6	0.4	6.206
	CATH	59.877	100	0	49.215
30%	ET-CCTA	28.937	91.6	8.4	-
	CACS-CCTA	37.187	97.4	2.6	1.428
	CCTA	45.161	99.4	0.6	3.924
	CATH	€59.877	100	0	24.527
40%	ET-CCTA	33.717	88.8	11.2	-
	CACS-CCTA	42.591	96.5	3.5	1.152
	CCTA	50.131	99.2	0.8	2.782
	CATH	59.877	100	0	12.183
50%	ET-CCTA	38.496	86.0	14.0	-
	CACS-CCTA	47.995	95.6	4.4	987
	CCTA	55.101	99.0	1.0	2.098
	CATH	59.877	100	0	4.777
60%	ET-CCTA	37.581	83.4	16.6	-
	StressEcho	51.435	93.1	6.9	822
	CACS-CCTA	53.399	94.7	5.3	1.210
	CATH	59.877	100	0	1.231
70%	ET-CCTA	48.059	80.4	19.6	-
	StressEcho	54.872	92.0	8.0	588
	CATH	59.877	100	0	623
80%	ET-CCTA	52.836	77.6	22.4	-
	CATH	59.877	100	0	314
90%	ET-CCTA	57.615	74.8	25.2	-
	CATH	59.877	100	0	90

** At the end of the diagnostic strategy. i.e.. including the results of CATH when the noninvasive tests are positive or inconclusive. ** Incremental cost per additional correct diagnosis. ICER: incremental cost-effectiveness ratio (Δ cost/Δ correct diagnosis). ET: ergometric test. CCTA: computed tomography angiography of the coronary arteries. CaSc: calcium scoring. MPS: myocardial perfusion scintigraphy. StresEco: stress echocardiogram with dobutamine*

related factors (availability, experience, etc.) should be considered during the selection of a complementary diagnosis method.

Conclusions

The diagnostic algorithms that include cardiac CCTA are the most cost-effective in symptomatic patients with suspected stable coronary disease and a PLD of ≤50%. In these patients, depending on the PLD and the willingness to pay per correct diagnosis, CCTA may be used as a first-line test or reserved for patients with positive/inconclusive ergometric test results or CaSC > 0. In high-risk patients (PLD ≥ 60%), immediate CATH appears to be the most cost-effective strategy. For all PLDs, strategies based on ischemia tests appear to be more expensive and less effective compared with strategies based on anatomical tests.

cont.

Manuscrito 5

Author contributions

Conception and design of the research; Writing of the manuscript; Analysis and interpretation of the data and Critical revision of the manuscript for intellectual content: Gonçalves PA, Cardim N, Marques H, Ferreira AM. Acquisition of data and Statistical analysis: Ferreira AM.

Potential Conflict of Interest

No potential conflict of interest relevant to this article was reported.

Sources of Funding

There were no external funding sources for this study.

Study Association

This study is not associated with any thesis or dissertation work.

References

1. Taylor AJ, Cerqueira M, Hodgson JM, Mark D, Min J, O'Gara P, et al. ACCF/SCCT/ACR/AHA/ASE/ASNC/NASCI/SCAI/SCMR 2010 Appropriate Use Criteria for Cardiac Computed Tomography. A Report of the American College of Cardiology Foundation Appropriate Use Criteria Task Force, the Society of Cardiovascular Computed Tomography, the American College of Radiology, the American Heart Association, the American Society of Echocardiography, the American Society of Nuclear Cardiology, the North American Society for Cardiovascular Imaging, the Society for Cardiovascular Angiography and Interventions, and the Society for Cardiovascular Magnetic Resonance. J Cardiovasc Comput Tomogr. 2010;4(6):407. e1-33.
2. Patterson RE, Eng C, Horowitz SF, Gorlin R, Goldstein SR. Bayesian comparison of cost-effectiveness of different clinical approaches to diagnose coronary artery disease. J Am Coll Cardiol. 1984;4(2):278-89.
3. Patterson RE, Eisner RL, Horowitz SF. Comparison of cost-effectiveness and utility of exercise ECG, single photon emission computed tomography, positron emission tomography, and coronary angiography for diagnosis of coronary artery disease. Circulation. 1995;91(1):54-65.
4. Ollendorf DA, Kuba M, Pearson SD. The diagnostic performance of multi-slice coronary computed tomographic angiography: a systematic review. J Gen Intern Med. 2011;26(3):307-16.
5. Gottlieb I, Miller JM, Arbab-Zadeh A, Dewey M, Clouse ME, Sara L, et al. The absence of coronary calcification does not exclude obstructive coronary artery disease or the need for revascularization in patients referred for conventional coronary angiography. J Am Coll Cardiol. 2010;55(7):627-34.
6. Budoff MJ, Jollis JG, Dowe D, Min J, Group VCTS. Diagnostic accuracy of coronary artery calcium for obstructive disease: results from the ACCURACY trial. Int J Cardiol. 2013;166(2):505-8.
7. Gibbons RJ, Balady GJ, Bricker JT, Chaitman BR, Fletcher GF, Froelicher VF, et al. ACC/AHA 2002 guideline update for exercise testing: summary article: a report of the American College of Cardiology/American Heart Association Task Force on Practice Guidelines (Committee to Update the 1997 Exercise Testing Guidelines). Circulation. 2002;106(14):1883-92.
8. Klocke FJ, Baird MG, Lorell BH, Bateman TM, Messer JV, Berman DS, et al. ACC/AHA/ASNC guidelines for the clinical use of cardiac radionuclide imaging - executive summary: a report of the American College of Cardiology/American Heart Association Task Force on Practice Guidelines (ACC/AHA/ASNC Committee to Revise the 1995 Guidelines for the Clinical Use of Cardiac Radionuclide Imaging). J Am Coll Cardiol. 2003;42(7):1318-33.
9. Heijenbrok-Kal MH, Fleischmann KE, Hunink MG. Stress echocardiography, stress single-photon-emission computed tomography and electron beam computed tomography for the assessment of coronary artery disease: a meta-analysis of diagnostic performance. Am Heart J. 2007;154(3):415-23.
10. Sicari R, Nihoyannopoulos P, Evangelista A, Kasprzak J, Lancellotti P, Poldermans D, et al. Stress Echocardiography Expert Consensus Statement - Executive Summary: European Association of Echocardiography (EAE) (a registered branch of the ESC). Eur Heart J. 2009;30(3):278-89.
11. Hendel RC, Corbett JR, Cullom SJ, DePuey EG, Garcia EV, Bateman TM. The value and practice of attenuation correction for myocardial perfusion SPECT imaging: a joint position statement from the American Society of Nuclear Cardiology and the Society of Nuclear Medicine. J Nucl Cardiol. 2002;9(1):135-43.
12. Myers J, Prakash M, Froelicher V, Do D, Partington S, Atwood JE. Exercise capacity and mortality among men referred for exercise testing. N Engl J Med. 2002;346(11):793-801.
13. Hawthorne KM, Johri AM, Malhotra R, Hung J, Baggish A, Picard MH. Quality assessment in dobutamine stress echocardiography: what are the clinical predictors associated with a non-diagnostic test? Cardiol Res. 2012;3(2):73-9.
14. World Health Organization. (WHO). Making choices in health: WHO guide to cost-effectiveness analysis. [Accessed in 2012 Jan 10]. Available from: http://www.who.int/choice/book/en
15. Serviço Nacional de Saúde. Portaria 839-A/2009 de 31 de julho de 2009. [Acesso em 2013 jul 15]. Disponível em http://www.dre.pt/cgi/dr/s.exe
16. Machaalany J, Yam Y, Ruddy TD, Abraham A, Chen L, Beanlands RS, et al. Potential clinical and economic consequences of noncardiac incidental findings on cardiac computed tomography. J Am Coll Cardiol. 2009;54(16):1533-41.
17. Min JK, Gilmore A, Budoff MJ, Berman DS, O'Day K. Cost-effectiveness of coronary CT angiography versus myocardial perfusion SPECT for evaluation of patients with chest pain and no known coronary artery disease. Radiology. 2010;254(3):801-8.
18. Hamm CW, Albrecht A, Bonzel T, Kelm M, Lange H, Schachinger V, et al. [Diagnostic heart catheterization]. Clin Res Cardiol. 2008;97(8):475-512. Erratum in Clin Res Cardiol. 2008;97(12):925.
19. Jolly SS, Amlani S, Hamon M, Yusuf S, Mehta SR. Radial versus femoral access for coronary angiography or intervention and the impact on major bleeding and ischemic events: a systematic review and meta-analysis of randomized trials. Am Heart J. 2009;157(1):132-40.
20. Dewey M, Hamm B. Cost effectiveness of coronary angiography and calcium scoring using CT and stress MRI for diagnosis of coronary artery disease. Eur Radiol. 2007;17(5):1301-9.
21. Dorenkamp M, Bonaventura K, Sohns C, Becker CR, Leber AW. Direct costs and cost-effectiveness of dual-source computed tomography and invasive coronary angiography in patients with an intermediate pretest likelihood for coronary artery disease. Heart. 2012;98(6):460-7.
22. Kaufmann PA, Knuuti J. Ionizing radiation risks of cardiac imaging: estimates of the immeasurable. Eur Heart J. 2011;32(3):269-71.
23. Mowatt G, Vale L, Brazzelli M, Hernandez R, Murray A, Scott N, et al. Systematic review of the effectiveness and cost-effectiveness, and economic evaluation, of myocardial perfusion scintigraphy for the diagnosis and management of angina and myocardial infarction. Health Technol Assess. 2004;8(30):iii-iv, 1-207.

cont.

Manuscrito 5

24. Ladapo JA, Jaffer FA, Hoffmann U, Thomson CC, Bamberg F, Dec W, et al. Clinical outcomes and cost-effectiveness of coronary computed tomography angiography in the evaluation of patients with chest pain. J Am Coll Cardiol. 2009;54(25):2409-22.

25. Kreisz FP, Merlin T, Moss J, Atherton J, Hiller JE, Gericke CA. The pre-test risk stratified cost-effectiveness of 64-slice computed tomography coronary angiography in the detection of significant obstructive coronary artery disease in patients otherwise referred to invasive coronary angiography. Heart Lung Circ. 2009;18(3):200-7.

26. Amemiya S, Takao H. Computed tomographic coronary angiography for diagnosing stable coronary artery disease: a cost-utility and cost-effectiveness analysis. Circ J. 2009;73(7):1263-70.

27. Mowatt G, Cummins E, Waugh N, Walker S, Cook J, Jia X, et al. Systematic review of the clinical effectiveness and cost-effectiveness of 64-slice or higher computed tomography angiography as an alternative to invasive coronary angiography in the investigation of coronary artery disease. Health Technol Assess. 2008;12(17):iii-iv, ix-143.

28. National Institute for Health and Clinical Excellence 2010 (NICE). Chest pain of recent onset - assessment and diagnosis of recent onset chest pain or discomfort of suspected cardiac origin. NICE clinical guidelines, March 2010. [Acessed in 2013 Nov 7]. Available from http://publications.nice.org.uk/chest-pain-of-recent-onset-cg95

29. Genders TS, Ferket BS, Dedic A, Galema TW, Mollet NR, de Feyter PJ, et al. Coronary computed tomography versus exercise testing in patients with stable chest pain: comparative effectiveness and costs. Int J Cardiol. 2013;167(4):1268-75.

30. Genders TS, Steyerberg EW, Alkadhi H, Leschka S, Desbiolles L, Nieman K, et al. A clinical prediction rule for the diagnosis of coronary artery disease: validation, updating, and extension. Eur Heart J. 2011;32(11):1316-30.

31. Boden WE, O'Rourke RA, Teo KK, Hartigan PM, Maron DJ, Kostuk WJ, et al. Optimal medical therapy with or without PCI for stable coronary disease. N Engl J Med. 2007;356(15):1503-16.

32. Fearon WF, Yeung AC, Lee DP, Yock PG, Heidenreich PA. Cost-effectiveness of measuring fractional flow reserve to guide coronary interventions. Am Heart J. 2003;145(5):882-7.

33. Ko BS, Cameron JD, Defrance T, Seneviratne SK. CT stress myocardial perfusion imaging using multidetector CT: a review. J Cardiovasc Comput Tomogr. 2011;5(6):345-56.

34. Koo BK, Erglis A, Doh JH, Daniels DV, Jegere S, Kim HS, et al. Diagnosis of ischemia-causing coronary stenoses by noninvasive fractional flow reserve computed from coronary computed tomographic angiograms. Results from the prospective multicenter DISCOVER-FLOW (Diagnosis of Ischemia-Causing Stenoses Obtained Via Noninvasive Fractional Flow Reserve) study. J Am Coll Cardiol. 2011;58(19):1989-97.

35. Min JK, Leipsic J, Pencina MJ, Berman DS, Koo BK, van Mieghem C, et al. Diagnostic accuracy of fractional flow reserve from anatomic CT angiography. JAMA. 2012;308(12):1237-45.

36. Meijboom WB, van Mieghem CA, Mollet NR, Pugliese F, Weustink AC, van Pelt N, et al. 64-slice computed tomography coronary angiography in patients with high, intermediate, or low pretest probability of significant coronary artery disease. J Am Coll Cardiol. 2007;50(15):1469-75.

MANUSCRITO 6

Modified continuity equation using left ventricular outflow tract three-dimensional imaging for aortic valve area estimation.

Pinto Teixeira, P., Ramos, R., Rio, P., Moura Branco, L., Portugal, G., Abreu, A., Galrinho, A., **Marques**, **H**., Figueiredo, L., and Cruz Ferreira, R.

Echocardiography, 2017
34(7): p. 978-985

Manuscrito 6

DOI: 10.1111/echo.13589

WILEY Echocardiography

Modified continuity equation using left ventricular outflow tract three-dimensional imaging for aortic valve area estimation

Pedro Pinto Teixeira MD[1] | Ruben Ramos MD[1] | Pedro Rio MD[1] | Luísa Moura Branco MD[1] | Guilherme Portugal MD[1] | Ana Abreu MD[1] | Ana Galrinho MD[1] | Hugo Marques MD[2] | Luísa Figueiredo MD[2] | Rui Cruz Ferreira MD[1]

[1]Cardiology Department, Hospital de Santa Marta, Lisboa, Portugal

[2]Radiology Department, Hospital de Santa Marta, Lisboa, Portugal

Correspondence
Pedro Pinto Teixeira, Cardiology Department, Hospital de Santa Marta, Lisboa, Portugal.
Email: phpintoteixeira@gmail.com

Purpose: Aortic valve area (AVA) is usually estimated by the continuity equation (CE) in which the left ventricular outflow tract (LVOT) area is calculated assuming a circular shape. This study aimed to compare measurements of LVOT area using standard 2D transthoracic echocardiography (2DTTE), 3D transesophageal echocardiography (3DTEE), and multidetector computed tomography (MDCT) and assess their relative impact on AVA estimated by the CE.

Methods and Results: We prospectively enrolled 60 patients with severe aortic stenosis (AS) referred for transcatheter aortic valve replacement (TAVR) who systematically underwent 2DTTE, 3DTEE, and MDCT. Mean LVOT areas obtained by 2DTTE (3.28±0.66 cm^2) and 3DTEE (3.95±0.90 cm^2) were significantly underestimated when compared to the mean MDCT LVOT area (4.31±0.99 cm^2). LVOT was rather elliptical than round, with a mean eccentricity index of 1.47 (ratio of maximum to minimum LVOT diameters) assessed by MDCT. Mean TTE AVA estimated by the CE was 0.62±0.20 cm^2. Substitution of 2DTTE LVOT area by 3DTEE LVOT area in the CE resulted in AVA of 0.74±0.24 cm^2, while using MDCT LVOT area held an AVA of 0.80±0.24 cm^2. MDCT-derived AVA was similar to MDCT planimetric AVA and allowed 24% of patients to be reclassified from severe to moderate AS.

Conclusions: 2DTTE and 3DTEE underestimate LVOT area when compared to MDCT with significant impact on AVA estimation. Assessment through MDCT fusion AVA may be of incremental value in patients with discrepant severity criteria for AS.

KEYWORDS
aortic stenosis, aortic valve replacement, computed tomography, three-dimensional echocardiography

1 | INTRODUCTION

Accurate estimation of aortic valve area (AVA) is crucial to identify patients with severe aortic stenosis (AS) who might be eligible for aortic valve replacement treatment.[1–3] The measurement of AVA using two-dimensional (2D) transthoracic echocardiography (TTE) is based on the widely accepted continuity equation, which assumes a circular geometry of the left ventricular outflow tract (LVOT).[1–5] However, preceding studies using three-dimensional (3D) imaging methods such as multidetector computed tomography (MDCT), magnetic resonance

cont.

Manuscrito 6

imaging, or 3D echocardiography have shown the LVOT shape is often elliptical, leading to a potential underestimation of LVOT area and AVA by 2DTTE.[6–12] In addition to AVA estimation, other echocardiographic criteria are taken into consideration to assess the AS severity such as transaortic gradients, dimensionless index, and planimetry AVA.[1–3] However, there are often discrepancies between these criteria and continuity equation 2DTTE-derived AVA, raising concerns about the accuracy of AVA estimation through this method.[11,13]

Multidetector computed tomography and 3D transesophageal echocardiography (3DTEE) are already routinely used in the preprocedural assessment of the aortic valve root and apparatus in the setting of transcatheter aortic valve replacement (TAVR).[14,15] Moreover, these 3D imaging techniques allow direct LVOT area measurement by planimetry with high spatial resolution and image quality, which could then be introduced into the continuity equation for AVA calculation, avoiding the error associated with 2DTTE-derived LVOT area estimation.[16,17] The incremental value of 3DTEE and MDCT with regard to LVOT and AVA evaluation is still scarcely explored in the literature.

The aim of this study was to (i) compare measurements of LVOT area acquired by 2DTTE, 3DTEE, and MDCT in patients with AS being assessed for TAVR; (ii) assess the impact of a modified multimodality continuity equation incorporating either 3DTEE or MDCT-derived LVOT areas; (iii) evaluate the congruence between 3D-derived AVA and various echocardiographic severity criteria for AS.

2 | METHODS

From April 2014 to December 2015, we prospectively enrolled 60 patients with severe aortic stenosis (defined by 2DTTE estimated AVA <0.6 cm^2/m^2 using the continuity equation) who were referred for TAVR assessment. Patients were included if they had performed 2DTTE, 3DTEE, and MDCT at our institution within 1 week of each other. Patients with previous surgery of the aortic valve or ascending aorta were excluded. The study protocol was approved by the local ethics committee, with waiver of individual informed consent.

2.1 | Echocardiography

Echocardiography studies were executed using a commercially available echocardiographic system (iE33 Philips Medical Systems, Andover, MA, USA) using an S5-1 array probe for 2D echocardiography. All measurements were performed according to recommendations of the American Society of Echocardiography.[1] From the apical long-axis or five-chamber views, continuous-wave (CW) Doppler spectral recordings were collected, enabling assessment of peak and mean transaortic gradients, as well as of velocity-time integrals (VTI) across the aortic valve.[1] The highest aortic valve velocity was systematically sought in all patients and was found in nonapical locations (right parasternal or suprasternal) in nine patients. LVOT area was derived in a standard fashion from the LVOT sagittal diameter [$(\text{LVOT diameter}/2)^2 \times \pi$], obtained on a zoomed parasternal long-axis view, 5 mm below the aortic annulus, in mid-systole.[1] The VTI of the LVOT was assessed by spectral pulsed-wave (PW) Doppler with the sample volume positioned at the same level of the LVOT diameter measurement.[1] Two-dimensional transthoracic AVA (2DTTE AVA) was calculated using the continuity equation in accordance with the current guidelines: (LVOT area x LVOT_{VTI})/AV_{VTI}, where LVOT_{VTI} is the velocity-time integral of LVOT flow, and AV_{VTI} is the velocity-time integral of aortic valve flow.[1–3]

3DTEE was performed with the same echocardiographic system using a X7-2t xMATRIX probe. The examination was undertaken with minimal patient sedation. From the mid-esophageal position, real time 3D imaging of a pyramidal volume (60°×30°) of the aortic valve and LVOT was obtained. Settings were optimized using narrow-angled acquisition mode to ensure frame rates around 25 Hz. A total of three different cycles were recorded in each patient. All volumetric images were analyzed offline by trained readers using a commercially available software package (3D Q-Lab, Philips Medical Systems). After choosing the mid-systolic frame, from the long-axis aortic view, perpendicular 2D planes were shifted and rotated to find the cross-sectional LVOT 5 mm below the aortic annulus, where LVOT area was planimetered (Figure 1). LVOT minimum and maximum diameters were also measured at this level to calculate the eccentricity index (maximum LVOT diameter/minimum LVOT diameter). The eccentricity index values ranged from 1 to 2, with a value of 1 indicating a perfect circle and greater values indicating a progressively more elliptical shape.

Intra-observer variability and inter-observer variability for LVOT diameter on 2DTTE and for LVOT area measurement on 3DTEE were assessed using a randomly selected subset of 15 patients. Measurements were repeated by the same observer after an interval ≥1-month and by a second independent blinded reader. Reproducibility was estimated by intra-class correlation coefficient, with good agreement defined as >0.80.

2.2 | Multidetector computed tomography (MDCT)

Multidetector computed tomography scans were performed using a 64-detector scanner (VCT Lightspeed, GE Healthcare, Milwaukee, WI, USA) after administration of iodinated contrast agent (90–110 mL of Ultravist 370) at 4–5 mL/s followed by 30–50 mL of normal saline at the same rate. Data were acquired using a retrospective ECG-controlled tube current modulation technique, where the highest tube current (450–500 mA) was applied only during the systolic phase of the cardiac cycle. Images were reconstructed from phase 20% to 50% of the RR interval, with 5% interval increments. Mean radiation dose for the entire protocol (which comprehends thoracic and abdominal scan for vascular access study for TAVR) was 19±5 mSv.

Multidetector computed tomography images were analyzed on a dedicated CT workstation (iNtuition, TeraRecon, San Mateo, CA, USA) by an experienced cardiac CT reader who was blinded to all echocardiographic data. The largest cross-sectional area of the LVOT was measured manually at mid-systole (20%–40% of the RR interval depending on the heart rate) just below the level of the aortic valve "hinge points" and using double oblique images to identify the true short-axis (Figure 2).[17] LVOT minimum and maximum diameters were also collected at this level for determination of the eccentricity index.

cont.

Manuscrito 6

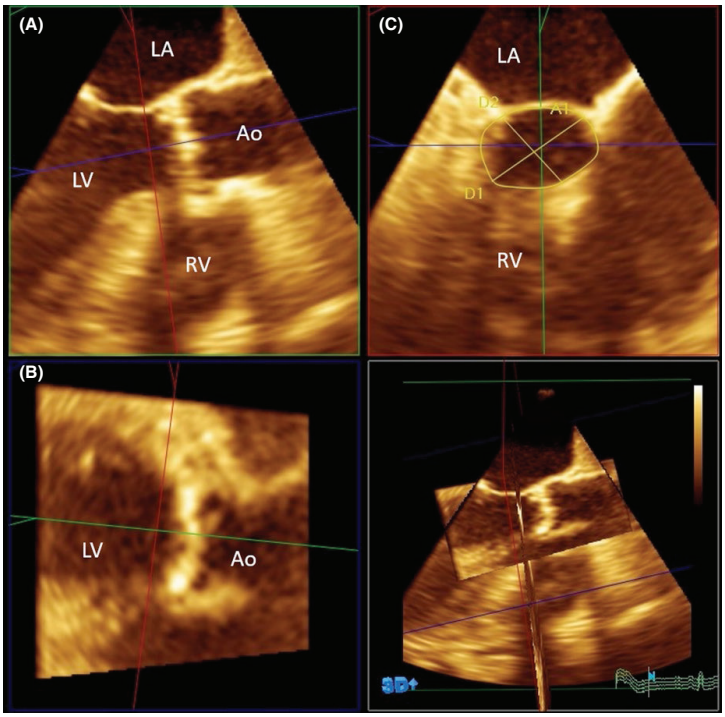

FIGURE 1 Measurement of LVOT area and minimum and maximum LVOT diameters using 3D transesophageal echocardiography. A. Parasternal long-axis plane. B. Transverse plane. C. LVOT short-axis plane. LVOT area (A1) was 6.2 cm^2. LVOT maximum diameter (D1) was 3.24 cm, and LVOT minimum diameter (D2) was 2.60 cm. LA=left atrium; LV=left ventricle; Ao=ascending aorta; RV=right ventricle

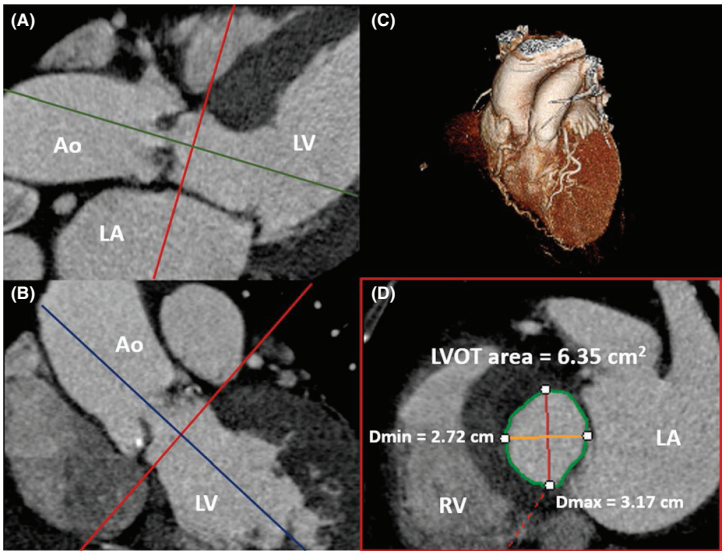

FIGURE 2 Measurement of the left ventricular outflow tract (LVOT) area and minimum (Dmin) and maximum (Dmax) diameters using multidetector computed tomography. The LVOT short-axis view (D) is obtained from two orthogonal views (A and B). Three-dimensional whole heart is depicted in (C). LA=left atrium; LV=left ventricle; Ao=ascending aorta; RV=right ventricle

Planimetry AVA was assessed manually at maximal aortic valve opening by scrolling through the short-axis images toward the tip of the cusps until the smallest orifice was found. AVA was then traced at the inside borders of the coronary cusps (Figure 3).[17,18]

Intra-observer variability and inter-observer variability for LVOT area quantification on MDCT were evaluated using a random subset of 15 patients, with measurements repeated by the same observer after an interval ≥1-month and by a second independent blinded reader.

cont.

Manuscrito 6

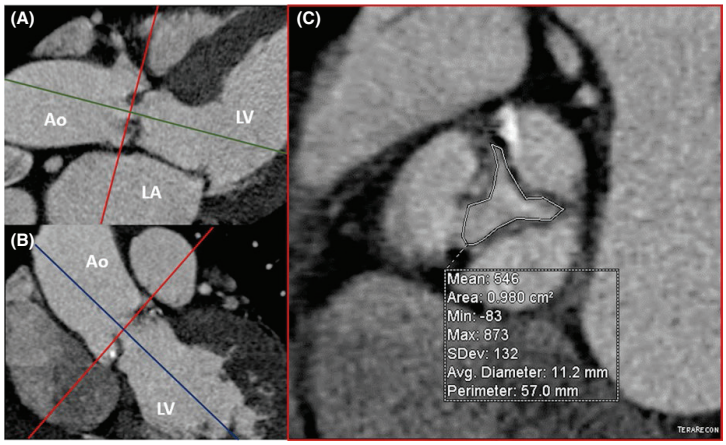

FIGURE 3 Measurement of AVA by planimetry using MDCT. AVA (0.98 cm^2) was measured in mid-systole at the tip of the aortic valve leaflets. Short-axis view (C) of the aortic valve is obtained from 2 orthogonal views (A and B). LA=left atrium; LV=left ventricle; Ao=ascending aorta

Reproducibility was estimated by intra-class correlation coefficient, with good agreement defined as >0.80.

2.3 | Modified continuity equation for AVA estimation

We replaced the conventional 2DTTE LVOT area in the continuity equation by either the 3DTEE LVOT area or the MDCT LVOT area to generate a modified multimodality continuity equation as follows: (3DTEE LVOT area or MDCT LVOT area x LVOT VTI)/Aortic valve VTI. Pulsed-wave and continuous-wave VTI through the LVOT and aortic valve were constant and assessed in a standard fashion by 2DTTE. AVAs estimated through this modified continuity equation were labeled as 3DTEE fusion AVA and MDCT fusion AVA.

2.4 | Statistical analysis

Continuous variables are presented as mean value±standard deviation and categorical variables as absolute numbers and percentages. LVOT and AVA data were compared using two-sided paired *t* test, after checking normal distribution of data and homogeneity of variances. Pearson correlation coefficient was used to test associations between continuous variables. Bland-Altmann analysis was performed to systematically assess the differences between the LVOT areas measured by 2DTTE, 3DTEE, and MDCT.[19] A probability value of <.05 was accepted as statistically significant. Statistical analysis was performed using SPSS Statistics, version 21.

3 | RESULTS

Of the 60 consecutive patients enrolled, five were excluded due to inadequate echocardiographic or tomographic images and three due to concomitant conditions that rendered invalid the continuity equation (two patients with significant aortic regurgitation and one patient with LVOT flow velocity >2 m/s). The final sample consisted of 52 patients, aged 81.5±5.3 years, and 28 were women (54%). Table 1 summarizes the 2DTTE measurements for this population.

3.1 | Assessment of LVOT area and shape

Left ventricular outflow tract diameter on 2DTTE was 2.04±0.20 cm, while the mean LVOT diameter on 3DTEE was 2.13±0.25 cm and on MDCT was 2.32±0.27 cm (*P*<.001). Further findings from 3DTEE and MDCT are depicted in Table 2.

2DTTE LVOT area, estimated from the equation (LVOT diameter/2)^2×∏, was 3.28±0.66 cm^2. On the other hand, 3D imaging methods measured planimetered LVOT areas: Mean 3DTEE LVOT area was 3.95±0.90 cm^2, and mean MDCT LVOT area was 4.31±0.99 cm^2. The

TABLE 1 Transthoracic echocardiography data of the study sample (n=52)

Variable	Value
Left ventricular ejection fraction (%)	59.8±13.9
Left ventricular diastolic volume index (mL/m^2)	58.3±18.4
Left ventricular systolic volume index (mL/m^2)	25.1±14.2
Stroke volume index (mL/m^2)	39.8±13.7
Interventricular wall thickness (cm)	12.9±2.3
Left ventricular posterior wall thickness (cm)	11.1±2.0
LVOT diameter (cm)	2.04±0.20
LVOT area (cm^2)	3.28±0.66
Aortic valve peak velocity (m/s)	4.4±0.6
Transaortic peak systolic gradient (mm Hg)	78.9±21.6
Transaortic mean systolic gradient (mm Hg)	49.4±14.4
Aortic valve velocity-time integral (cm)	109.7±22.8
LVOT velocity-time integral (cm)	20.4±6.0
Dimensionless index ($LVOT_{VTI}/AV_{VTI}$)	0.19±0.06
Aortic valve area (cm^2) by the continuity equation	0.62±0.20
Aortic valve area index (cm^2/m^2)	0.36±0.12

cont.

Manuscrito 6

TABLE 2 3DTEE and MDCT imaging characteristics of the study sample (n=52)

Variable	3DTEE value	MDCT value	*P*-value
Maximum LVOT diameter (cm)	2.41±0.33	2.83±0.33	<.001
Minimum LVOT diameter (cm)	1.98±0.32	1.93±0.27	.26
Mean LVOT diameter (cm)	2.13±0.25	2.35±0.27	<.001
Eccentricity index	1.23±0.16	1.47±0.14	<.001
LVOT area (cm^2)	3.95±0.90	4.31±0.98	<.001
AVA planimetry (cm^2)	0.80±0.19*	0.84±0.17	<.05

*n=36 for AVA planimetry by 3DTEE. MDCT=multidetector computed tomography; LVOT=left ventricular outflow tract

LVOT areas were all significantly different from each other (*P*<.001). 3DTEE and MDCT LVOT areas showed very good correlation (*r*=.83; *P*<.001). 2DTTE LVOT area had only moderate correlation with 3DTEE LVOT area (*r*=.44; *P*<.001) or MDCT LVOT area (*r*=.48; *P*<.001). Compared to MDCT, 2DTTE systematically underestimates LVOT area by a mean of 1.02±0.89 cm^2 (95% confidence interval 0.78–1.27) as shown by the Bland-Altman analysis (Figure 4). This difference corresponds to an underestimation of AVA by 33±30% when using the continuity equation.

The LVOT eccentricity index derived from 3DTEE (1.23±0.16) was significantly different from the one derived from MDCT (1.47±0.14), *P*<.001. No significant correlation was found amidst the eccentricity index and the LVOT areas obtained by each method or the differences between areas. Moreover, eccentricity was not associated with age, gender, body surface area, LVOT area, left ventricular diastolic or systolic volumes, LV ejection fraction, interventricular wall thickness, or aortic valve peak velocity (all with p=NS).

The intra-observer and inter-observer agreement for LVOT diameter and area measurements using the intra-class correlation coefficients were as follows: 2DTTE LVOT diameter (intra-observer 0.93 and inter-observer 0.91), 3DTEE LVOT area (intra-observer 0.96 and inter-observer 0.92), and MDCT LVOT area (intra-observer 0.97 and inter-observer 0.94).

3.2 | AVA and modified continuity equation

2DTTE AVA estimated by the continuity equation was 0.62±0.20 cm^2. Substituting the LVOT area in the continuity equation by the LVOT area acquired by 3DTEE held a mean 3DTEE fusion AVA of 0.74±0.24 cm^2. When adopting the LVOT area from MDCT to the continuity equation, we obtained a mean MDCT fusion AVA of 0.80±0.24 cm^2. All AVAs differed significantly among each other (*P*<.001). 3DTEE fusion AVA showed stronger correlation with MDCT fusion AVA (*r*=.91; *P*<.001) than with 2DTTE AVA (*r*=.75; *P*<.001). MDCT fusion AVA was statistically equivalent to MDCT planimetry AVA (0.84±0.17 cm^2; *P*=.12; *r*=.74) (Figure 5).

Measurements of planimetric AVA by echocardiography were unattainable in several patients because of suboptimal imaging of the aortic valve opening due to heavy calcification of the cusps. We obtained planimetric AVA in 32 patients (mean AVA 0.70±0.18 cm^2) performing 2DTTE and in 36 patients (mean AVA 0.80±0.19 cm^2) using 3DTEE. These planimetric AVAs differed significantly between each other and from fusion AVAs (*P*<.05).

3.3 | Patient reclassification and congruence between echocardiographic parameters and fusion AVA

The dimensionless index (DI), derived from the ratio of $LVOT_{VTI}/AV_{VTI}$, is independent of the LVOT area measurement and is suggestive of

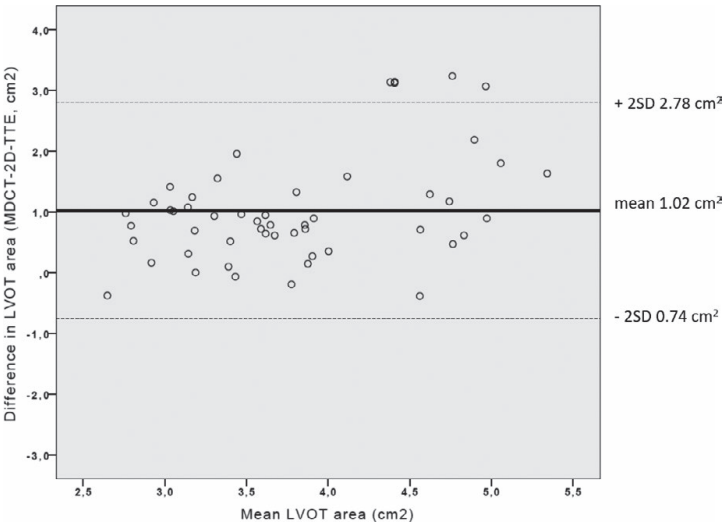

FIGURE 4 Bland-Altman plot showing the difference in LVOT area using 2DTTE versus MDCT. Solid line represents the mean difference and broken lines±2 standard deviations

cont.

Manuscrito 6

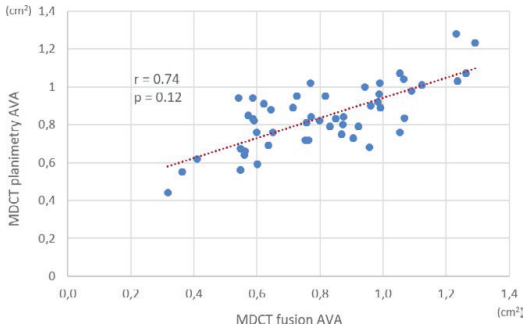

FIGURE 5 Scatter plot of correlation between MDCT fusion AVA and MDCT planimetry AVA

severe aortic stenosis when <0.25. In our sample, where all patients were classified as having severe aortic stenosis based on TTE AVA <0.6 cm^2/m^2 by the continuity equation, only 79% of patients had DI <0.25. In contrast, when using MDCT fusion AVA the correspondence between DI <0.25 and AVA <0.6 cm^2/m^2 was nearly perfect (98% of patients had congruence on both parameters). Furthermore, when adopting MDCT fusion AVA a total of 12 patients (24%) would be reclassified from severe to moderate aortic stenosis. This percentage increases when analyzing the subgroup of patients with mean transaortic gradient <40 mm Hg despite a preserved ejection fraction, where five of nine patients were reclassified into moderate aortic stenosis. The impact of using 3DTEE fusion AVA was less pronounced with a percentage of reclassification over the whole sample of 15% (eight patients).

To improve AVA assessment by 2DTTE, we estimated a corrected 2DTTE AVA using a correction factor of 1.33, derived from the mean ratio of MDCT LVOT area/TTE LVOT area and consistent with the percentage of underestimation of AVA. The corrected TTE AVA (0.83±0.27 cm^2) held identical values to MDCT fusion AVA (*P*=.36) and MDCT planimetry AVA (*P*=.64).

4 | DISCUSSION

In the present study, we found that both 2DTTE and 3DTEE underestimated LVOT area when compared to MDCT and therefore AVA estimation by echocardiography alone was significantly undervalued. Incorporating the planimetric area of the LVOT measured by MDCT into a modified multimodality continuity equation yielded significantly larger AVA values, with nearly one in four patients being reclassified from severe to moderate AS.

Moreover, we confirmed the LVOT shape is rather oval than round, which is supported by the mean eccentricity index obtained by MDCT (1.46±0.14) and is in accordance with the findings of previous studies.[6–12] MDCT allows planimetric measurement of the LVOT area and is therefore independent of geometric assumptions. In contrast, 2DTTE assumes a circular LVOT and relies on a single sagittal diameter mensuration which, in the setting of an eccentric LVOT, may more often correspond to the minimum diameter than to the mean diameter of the ellipse. Furthermore, the squaring of that diameter to derive the area [(LVOT diameter/2)^2×∏] exponentiates even small errors.

Our findings have shown that replacing 2DTTE LVOT area in the continuity equation by MDCT LVOT area resulted in a mean increase of 0.18 cm^2 in AVA values. Yet performing an MDCT scan to assess the LVOT area would be impractical for most patients. 3D echocardiography which also provides threedimensional imaging of the LVOT could dismiss the need for an MDCT scan. However, previous publications have suggested that 3D transthoracic echocardiography also underestimates LVOT area when compared to MDCT.[9–11] Insufficient spatial resolution, especially lateral resolution, to accurately delineate the LVOT borders has been appointed as the primary reason for the underestimation.[9] The current study sought to overcome the image quality issue using TEE, routinely performed in our center for pre-TAVR assessment.

Despite improved echocardiographic window, our results showed that 3DTEE still underestimates LVOT area by a mean of 0.36 cm^2 when compared to MDCT. When applying the modified continuity equation, this resulted in a mean difference of 0.06 cm^2 between 3DTEE fusion AVA and MDCT fusion AVA. Although this difference is significant, 3DTEE fusion AVA correlates much strongly with MDCT fusion AVA (*r*=.91) than with 2DTTE AVA (*r*=.75). It remains unclear the reason for the discrepancy in the LVOT area measurements among the 3D dimensional methods. The mean LVOT eccentricity index derived from 3DTEE is inferior to the one obtained by MDCT, which could suggest 3DTEE fails to recognize more elliptical LVOTs. However, we could not establish any significant correlation between the difference of the areas and the eccentricity index or other factors. Preceding studies have also been unable to predict LVOT eccentricity or to establish a relation between it and discrepancies in the LVOT area measurements.[9,12]

Multimodality imaging is playing an increasingly more important role in the setting of patients with moderate-to-severe AS and prospective aortic valve replacement treatment.[11,20–22] Following the results of the current and previous research, it appears that in patients with discordant calculated AVA, transaortic gradients and DI, a precise assessment of the LVOT area by MDCT, may be useful to accurately classify the severity of the AS.[11,20,23] In the present study, MDCT fusion AVA was similar to MDCT planimetry AVA and MDCT fusion AVA <0.6 cm^2/m^2 held perfect congruence with DI <0.25, whereas 3DTEE fusion AVA failed to accomplish such concordance of parameters.

If the criteria of severe AS as AVA <0.6 cm^2/m^2 was applied to patients assessed by MDCT fusion AVA, 24% of our cohort would be reclassified from severe to moderate AS. However, the cut-point value of 0.6 cm^2/m^2 was validated for patients studied exclusively by 2D echocardiography. Hence, reclassification of patients evaluated by MDCT fusion AVA according to that criteria should be discouraged. Nevertheless, once more data become available, the use of a hybrid or modified continuity equation accounting for the true area of the LVOT might become a useful tool for a more accurate assessment of patients with discrepant echocardiographic criteria for AS severity or poor acoustic windows.

cont.

Manuscrito 6

Bearing in mind that MDCT, 3DTEE or even 3DTTE may not be readily available or clinically indicated, we sought to establish a correction factor to compensate for LVOT ovality. We found that applying a correction factor of 1.33 to AVA measurements by 2DTTE would result in a corrected AVA that is identical to MDCT fusion AVA and MDCT planimetry AVA. In their study, Gaspar et al.[9] proposed a correction factor of 1.17. However, only half of the study population had AS and, interestingly, their mean LVOT eccentricity index was also inferior to what we found. In the same study, they validate their findings on a small group of patients with severe AS. In this particular group, the LVOT mean eccentricity index (1.32±0.1) was higher and closer to what we describe. The inconsistency of values regarding correction factor and eccentricity index underlines the need for further and larger studies in this area.

Our study had important limitations. First and more critical is the absence of a true "gold standard" for AVA. The constraints of AVA estimation using cardiac catheterization and Gorlin formula are well known.[24,25] The role of MDCT on LVOT assessment has been comprehensively described in recent publications, and we acknowledged MDCT as the most reliable method for LVOT area measurement.[7,9–11,15,16,20,23] Second, not all measurements in our study were subject to intra- and inter-observer agreement. Despite this, both echocardiography and MDCT data were collected by experienced operators and the excellent intraclass correlation coefficients obtained for the LVOT areas were reassuring of the overall data quality. Third, the present research focused exclusively on patients with severe AS, and, as such, the findings might not be applicable to patients with mild-to-moderate AS, in whom the ellipticity of the LVOT might be less accentuated. Fourth, the prognostic implications of fusion AVA need to be evaluated in prospective studies and a proper cut-point value for severe AS when using fusion AVA needs to be established. In a recent study, Clavel et al.[26] have suggested that cut-point at a value of 1.2 cm^2, but further research is needed.

5 | CONCLUSIONS

Three-dimensional imaging confirms the LVOT is elliptical in most patients, resulting in underestimation of LVOT area and hence AVA when assessed by 2DTTE. Although 3DTEE approximated its LVOT measurements to those of MDCT, it still failed to recognize larger areas. Incorporating the planimetric area of the LVOT measured by MDCT into a modified continuity equation yielded significantly larger AVA values, with 24% of the patients in our study being reclassified from severe to moderate AS. In patients with discrepant echocardiographic criteria for AS severity, multimodality imaging may be useful for a more accurate assessment.

REFERENCES

1. Baumgartner H, Hung J, Bermejo J, et al. Echocardiographic assessment of valve stenosis: EAE/ASE recommendations for clinical practice. *J Am Soc Echocardiogr*. 2009;22:1–23.
2. Vahanian A, Alfieri O, Andreotti F, et al. Guidelines on the management of valvular heart disease (version 2012). *Eur Heart J*. 2012;33:2451–2496.
3. Nishimura RA, Otto CM, Bonow RO, et al. 2014 AHA/ACC guideline for the management of patients with valvular heart disease: a report of the American College of Cardiology/American Heart Association Task Force on Practice Guidelines. *J Am Coll Cardiol*. 2014;63:e57–e185.
4. Harrison MR, Gurley JC, Smith MD, Grayburn PA, DeMaria AN. A practical application of Doppler echocardiography for the assessment of severity of aortic stenosis. *Am Heart J*. 1988;115:622–628.
5. Oh JK, Taliercio CP, Holmes DR Jr, et al. Prediction of the severity of aortic stenosis by Doppler aortic valve area determination: prospective Doppler-catheterization correlation in 100 patients. *J Am Coll Cardiol*. 1988;11:1227–1234.
6. Doddamani S, Bello R, Friedman MA, et al. Demonstration of left ventricular outflow tract eccentricity by real time 3D echocardiography: implications for the determination of aortic valve area. *Echocardiography*. 2007;24:860–866.
7. Doddamani S, Grushko MJ, Makaryus AN, et al. Demonstration of left ventricular outflow tract eccentricity by 64-slice multi-detector CT. *Int J Cardiovasc Imaging*. 2009;25:175–181.
8. Burgstahler C, Kunze M, Loffler C, Gawaz MP, Hombach V, Merkle N. Assessment of left ventricular outflow tract geometry in non-stenotic and stenotic aortic valves by cardiovascular magnetic resonance. *J Cardiovasc Magn Reson*. 2006;8:825–829.
9. Gaspar T, Adawi S, Sachner R, et al. Threedimensional imaging of the left ventricular outflow tract: impact on aortic valve area estimation by the continuity equation. *J Am Soc Echocardiogr*. 2012;25:749–757.
10. Ng AC, Delgado V, van der Kley F, et al. Comparison of aortic root dimensions and geometries before and after transcatheter aortic valve implantation by 2- and 3-dimensional transesophageal echocardiography and multislice computed tomography. *Circ Cardiovasc Imaging*. 2010;3:94–102.
11. O'Brien B, Schoenhagen P, Kapadia SR, et al. Integration of 3D Imaging data in the assessment of aortic stenosis: impact on classification of disease severity. *Circ Cardiovasc Imaging*. 2011;4:566–573.
12. Saitoh T, Shiota M, Izumo M, et al. Comparison of left ventricular outflow geometry and aortic valve area in patients with aortic stenosis by 2- dimensional versus 3-dimensional echocardiography. *Am J Cardiol*. 2012;109:1626–1631.
13. Minners J, Allgeier M, Gohlke-Baerwolf C, Kienzle RP, Neumann FJ, Jander N. Inconsistent grading of aortic valve stenosis by current guidelines: haemodynamic studies in patients with apparently normal left ventricular function. *Heart*. 2010;96:1463–1468.
14. Tops LF, Delgado V, van der Kley F, Bax JJ. Percutaneous aortic valve therapy: clinical experience and the role of multi-modality imaging. *Heart*. 2009;95:1538–1546.
15. Vaquerizo B, Spaziano M, Alali J, et al. Three-dimensional echocardiography vs. Computed tomography for transcatheter aortic valve replacement sizing. *Eur Heart J Cardiovasc Imaging*. 2016;17:15–23.
16. De Vecchi C, Caudron J, Dubourg B, et al. Effect of the ellipsoid shape of the left ventricular outflow tract on the echocardiographic assessment of aortic valve area in aortic stenosis. *J Cardiovasc Comput Tomogr*. 2014;8:52–57.
17. Tops LF, Krishnan SC, Schuijf JD, Schalij MJ, Bax JJ. Noncoronary applications of cardiac multidetector row computed tomography. *JACC Cardiovasc Imaging*. 2008;1:94–106.
18. Feuchtner GM, Muller S, Bonatti J, et al. Sixty-four slice CT evaluation of aortic stenosis using planimetry of the aortic valve area. *AJR Am J Roentgenol*. 2007;189:197–203.
19. Bland JM, Altman DG. Statistical methods for assessing agreement between two methods of clinical measurement. *Lancet*. 1986;1:307–310.

cont.

Manuscrito 6

20. Kamperidis V, van Rosendael PJ, Katsanos S, et al. Low gradient severe aortic stenosis with preserved ejection fraction: reclassification of severity by fusion of Doppler and computed tomographic data. *Eur Heart J*. 2015;36:2087–2096.
21. Bloomfield GS, Gillam LD, Hahn R, et al. A practical guide to multimodality imaging of transcatheter aortic valve replacement. *JACC Cardiovasc Imaging*. 2012;4:441–455.
22. Ramineni R, Almomani A, Kumar A, Ahmad M. Role of multimodality imaging in transcatheter aortic valve replacement. *Echocardiography*. 2015;32:677–698.
23. Utsunomiya H, Yamamoto H, Horiguchi J, et al. Underestimation of aortic valve area in calcified aortic valve disease: effects of left ventricular ellipticity. *Int J Cardiol*. 2012;157:347–353.
24. Skjaerpe T, Hegrenaes L, Hatle L. Noninvasive estimation of valve area in patients with aortic stenosis by Doppler ultrasound and two-dimensional echocardiography. *Circulation*. 1985;72:810–818.
25. Cannon SR, Richards KL, Crawford M. Hydraulic estimation of stenotic orifice area: a correction of the Gorlin formula. *Circulation*. 1985;71:1170–1178.
26. Clavel MA, Malouf J, Messika-Zeitoun D, Araoz P, Michelena H, Enriquez-Sarano M. Aortic valve area calculation in aortic stenosis by CT and Doppler echocardiography. *JACC Cardiovasc Imaging*. 2015;8:248–257.

How to cite this article: Pinto Teixeira P, Ramos R, Rio P, et al. Modified continuity equation using left ventricular outflow tract three-dimensional imaging for aortic valve area estimation. *Echocardiography*. 2017;34:978–985. https://doi.org/10.1111/echo.13589

MANUSCRITO 7

Left ventricular diverticulum: a finding by cardiac CT angiography

Dourado, R., Goncalves, P.A., **Marques**, **H**., Gaspar, A., Machado, F.P., and Roquette, J.

Rev Port Cardiol, 2009
28(3): p. 341-4

Manuscrito 7

IMAGEM EM CARDIOLOGIA

Divertículo do ventrículo esquerdo: um achado por Angio TC cardíaca [32]

RAQUEL DOURADO, PEDRO ARAÚJO GONÇALVES, HUGO MARQUES, AUGUSTO GASPAR, FRANCISCO PEREIRA MACHADO, JOSÉ ROQUETTE

Hospital da Luz, Lisboa, Portugal

Rev Port Cardiol 2009; 28 (3): 341-344

Palavras-Chave
Divertículo do ventrículo esquerdo; Angio TC de 64 cortes de dupla ampola; Achados em angio TC.

Left ventricular diverticulum: a finding by cardiac CT angiography

Key words
Left ventricular diverticulum; 64-slice dual source computed tomographic angiography; Incidental findings by CT.

INTRODUÇÃO

Os autores apresentam o caso clínico de uma doente de 72 anos, com estenose mitral moderada, submetida a angio Tomografia Computorizada (TC) cardíaca, para avaliação pré-operatória de doença coronária.

A angio TC foi realizada num aparelho de 64 cortes de dupla ampola, (Dual source CT - Somaton Definition®, Siemens-medical). A aquisição do *scan* demorou 10 segundos, foram administrados 96 ml de contraste isoosmolar (Iodixanol 320 mgI/ml- Visipaque®) e a dose de radiação foi 12 mSv.

Figura1. **ECG durante a aquisição da Angio TC cardíaca. Frequência cardíaca média 52 bpm (37- 68bpm).**

INTRODUCTION

We present the case of a 72-year-old woman with moderate mitral stenosis who underwent cardiac computed tomographic (CT) angiography for preoperative assessment of coronary artery disease.

The scan was performed on a 64-slice dual source system (Somatom Definition®, Siemens Medical Solutions) and took 10 seconds. Iodixanol (Visipaque®) 320 mgI/ml iso-osmolar contrast (96 ml) was administered and the radiation dose was 12 mSv.

During the scan the patient developed atrial fibrillation, with a ventricular response of between 37 and 68 bpm (*Figure 1*).

Figure 1. **ECG during cardiac CT angiography. Mean heart rate 52 bpm (37-68).**

Recebido para publicação: Maio de 2008 • Aceite para publicação: Novembro de 2008
Received for publication: May 2008 • Accepted for publication: November 2008

cont.

Manuscrito 7

Rev Port Cardiol
Vol. 28 Março 09 / March 09

Durante a aquisição a doente apresentava fibrilhação auricular, com uma resposta ventricular entre 37 e 68 bpm (*Figura 1*).

A qualidade de imagem permitiu a avaliação de todos os segmentos, excluindo-se doença coronária significativa (*Figuras 2 e 3*).

The image quality was sufficiently good to assess all segments and significant coronary disease was excluded (*Figures 2 and 3*).

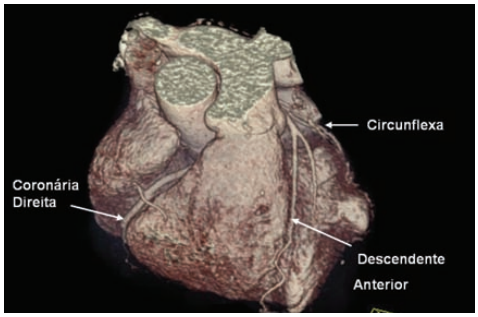

Figura 2. **Reconstrução 3D "volume-rendered".**

Figure 2. **3D volume-rendered reconstruction.**

Coronária Direita: right coronary artery; Circunflexa: circumflex artery; Descendente Anterior: anterior descending artery.

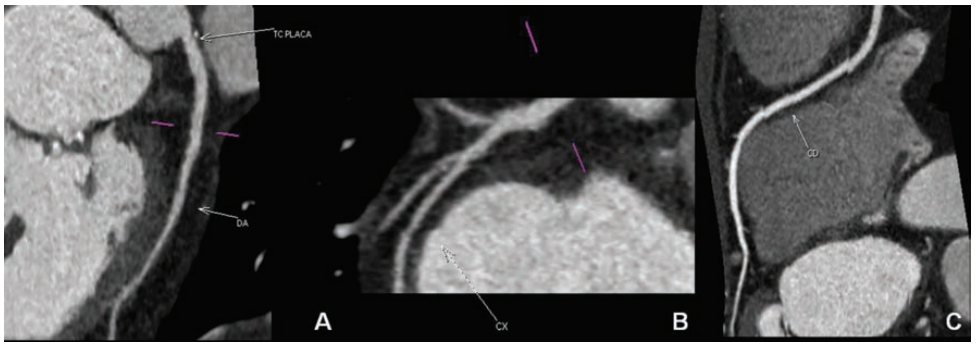

Figura 3. **Reconstrução curva multiplanar. A – Visualização do tronco comum (TC) com placa calcificada não significativa e descendente anterior (DA) sem placas significativas. B e C - Circunflexa (CX) e Coronária direita (CD) respectivamente sem placas significativas.**

Figure 3. **Curved multiplanar reconstruction. A: Left main artery (TC) showing an insignificant calcified plaque and the anterior descending artery (DA) with no significant plaques. B and C: Circumflex (CX) and right coronary (CD) arteries, respectively, with no significant plaques.**

Na avaliação cardíaca, para além da ausência de doença coronária significativa, documentou-se aurícula esquerda dilatada, válvula mitral de folhetos espessados e calcificados, com restrição da sua abertura e normal função sistólica ventricular esquerda (*Figura 4 B*).

No ventrículo esquerdo visualizou-se uma imagem de contornos bem definidos, de pequenas dimensões, fazendo protusão da parede lateral, através de uma conexão estreita. Esta imagem era compatível com a presença de um divertículo do ventrículo esquerdo (*Figuras 4 e 5*).

Besides the absence of significant coronary disease, cardiac assessment revealed a dilated left atrium, thickened and calcified mitral valve leaflets with restricted opening, and normal left ventricular systolic function (*Figure 4B*).

A small, well-defined image was observed in the left ventricle protruding from the lateral wall with a narrow connection, compatible with a left ventricular diverticulum (*Figures 4 and 5*).

cont.

Manuscrito 7

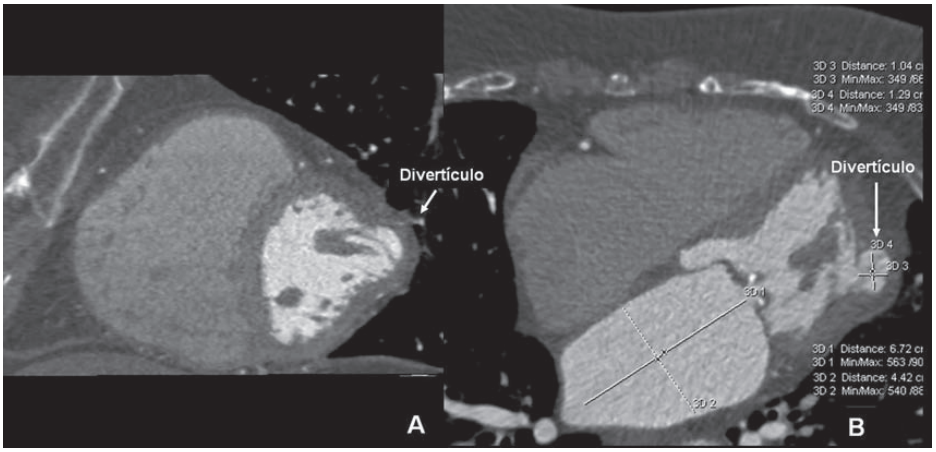

Figura 4. **Visualização do divertículo do ventrículo esquerdo (A) em curto eixo e (B) em longo eixo. B - aurícula esquerda dilatada, válvula mitral com folhetos espessados e calcificados.**

Figure 4. **Left ventricle in short-axis (A) and long-axis (B) view showing diverticulum. B: dilated left atrium and mitral valve with thickened and calcified leaflets.**

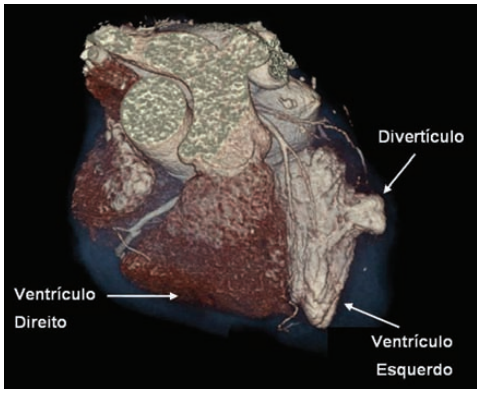

Figura 5. **Reconstrução 3D "volume-rendered" do divertículo do ventrículo esquerdo.**

Figure 5. **3D volume-rendered reconstruction of the left ventricular diverticulum.**

Ventrículo Direito: right ventricle; Divertículo: diverticulum; Ventrículo Esquerdo: left ventricle

O divertículo apresenta contractilidade síncrona com o ventrículo esquerdo, esvaziando quase na totalidade em sístole (*Figura 6*).

The diverticulum contracted in synchrony with the left ventricle, almost completely emptying in systole (*Figure 6*).

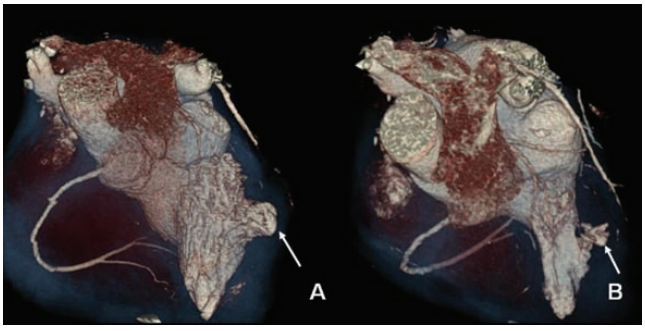

Figura 6. **Reconstrução 3D "volume-rendered" do divertículo do ventrículo esquerdo (seta) em diástole (A) e em sístole (B).**

Figure 6. **3D volume-rendered reconstruction of the left ventricular diverticulum (arrow) in diastole (A) and in systole (B).**

cont.

Manuscrito 7

Rev Port Cardiol
Vol. 28 Março 09 / March 09

Os divertículos ventriculares congénitos são raros, particularmente os diagnosticados em adultos[1-3].

Os divertículos podem cursar com fenómenos embólicos, insuficiência cardíaca, regurgitação valvular, rotura da parede ventricular, taquicardia ventricular ou morte súbita. Na maioria dos casos os divertículos são assintomáticos e constituem achados incidentais nos métodos de imagem[1,4]. O diagnóstico faz-se pela visualização por eco-cardiograma, ventriculografia, tomografia computorizada ou ressonância magnética cardíaca de uma protusão da parede ventricular, com conexão estreita e contractilidade síncrona com a cavidade ventricular[1,5]. Os divertículos são constituídos pelas 3 camadas cardíacas. O diagnóstico diferencial faz-se com aneurismas, sendo que estes habitualmente são formações saculares, de tecido fibroso, com conexão larga e movimento paradoxal[5].

O tratamento dos divertículos varia de acordo com a forma de apresentação, das anomalias associadas e possíveis complicações. Nos doentes sintomáticos com fenómenos embólicos o tratamento é cirúrgico associado a anticoagulação oral. Embora seja controverso alguns autores preconizam a ressecção cirúrgica nos doentes assintomáticos, atendendo ao elevado risco de morte por rotura da parede ou eventos arrítmicos graves[5].

Congenital left ventricular diverticula are rare, especially when diagnosed in adulthood[1-3]. They can be associated with embolism, heart failure, valve regurgitation, ventricular wall rupture, ventricular tachycardia and sudden death. In most cases they are asymptomatic and are incidental findings on imaging studies[1,4]. Diagnosis is obtained by echocardiography, ventriculography, CT scan or magnetic resonance imaging of a protrusion from the ventricular wall, with a narrow connection and contracting in synchrony with the ventricular chamber[1,5]. Diverticula are composed of all three cardiac layers. Differential diagnosis is with aneurysms, which are usually saccular in form and consist of fibrous tissue, with a wide connection and paradoxical motion[5].

Treatment varies according to the form of presentation, associated anomalies and possible complications. In symptomatic patients with embolic phenomena, treatment is surgical associated with oral anticoagulation therapy. Although controversial, surgical resection is recommended by some authors even in asymptomatic patients, given the high risk of death due to wall rupture or severe arrhythmias[5].

Pedido de separatas para:
Address for reprints:

Raquel Dourado
Av. Prof. Reynaldo dos Santos
2795-523 Carnaxide – Portugal
Tel: +351.214241380
Fax: +351.214241388
E-mail: raqueldourado@yahoo.com

BIBLIOGRAFIA / REFERENCES

1. Ohlow MA. Congenital left ventricular aneurysms and diverticula: definition, pathophysiology, clinical relevance and treatment. Cardiology, 2006. 106(2): p. 63-72.

2. Suilen C, Friedli B, Rutishauser W. Congenital intrathoracic left ventricular diverticulum in an adult. Chest, 1990. 98(3): p. 750-751.

3. Mahnken AH et al. Cardiac CT: Beyond the coronaries. Eur Radiol, 2007. 17(4): p. 994-1008.

4. Yazici M et al. Left ventricular diverticulum in two adult patients. Int Heart J, 2005. 46(1): p. 161-165.

5. Shauq AV, Agarwal V, Crawley C. Congenital left ventricular diverticulum. Heart Lung Circ, 2006. 15(4): p. 272-274.

MANUSCRITO 8

White-coat hypertension during coronary computed tomography angiography is associated with higher coronary atherosclerotic burden

Costa, C., de Araujo Goncalves, P., Ferreira, A., Pitta, M.L., Dores, H., Cardim, N., and **Marques**, **H**.,

Coron Artery Dis, 2017
28(1): p. 57-62

Manuscrito 8

Original research 57

White-coat hypertension during coronary computed tomography angiography is associated with higher coronary atherosclerotic burden

Cátia Costa[a,d], Pedro de Araújo Gonçalves[a,b,c], António Ferreira[a,b], Maria L. Pitta[d], Hélder Dores[a,b,c], Nuno Cardim[a] and Hugo Marques[a]

Introduction **White-coat hypertension (WCH) is a prevalent entity, which has been associated with an increased cardiovascular risk.**

Aim **Assess whether WCH is associated with a higher coronary atherosclerotic burden, evaluated by coronary computed tomography angiography (CCTA) and coronary artery calcium (CAC) scoring.**

Methods **A total of 1362 patients who performed CCTA and simultaneous CAC for the assessment of coronary artery disease (CAD) were prospectively enrolled in a single-center registry and divided into three groups: (A) patients with normal blood pressure (BP) ($n = 386$); (B) patients with WCH ($n = 174$; without a history of hypertension or antihypertensive medication, but with systolic BP ≥ 140 and/or diastolic BP ≥ 90 mmHg before examination acquisition); and (C) patients with hypertension ($n = 802$). The following coronary atherosclerotic markers were evaluated: CAC above the 50th percentile (CAC > p50), prevalence of CAD (any plaque), and obstructive CAD (plaque with > 50% stenosis).**

Results **Patients with WCH had a higher coronary atherosclerotic burden compared with patients with normal BP for all markers (30.5 vs. 19.4%, $P = 0.004$ for CAC > p50; 50.6 vs. 36.8%, $P = 0.002$ for CAD, any plaque; and 13.8 vs. 8.3%, $P = 0.045$ for obstructive CAD). On multivariate analysis, WCH was an independent predictor of a CAC > p50 [odds ratio (OR) 1.563, 95% confidence interval 1.018–2.400, $P = 0.041$], but not of the presence of CAD (any plaque) (OR 1.335, $P = 0.169$) or obstructive CAD (OR 1.376, $P = 0.301$).**

Conclusion **In this registry of patients, WCH was an independent predictor of a CAC above the p50. It was also associated with higher other markers of coronary atherosclerotic burden, such as the presence of CAD on CCTA, compared with patients with normal BP.** ***Coron Artery Dis*** **28:57–62**

Coronary Artery Disease 2017, **28**:57–62

Keywords: coronary artery calcium scoring, coronary artery disease, coronary computed tomography angiography, hypertension, white-coat hypertension

[a]Hospital da Luz, [b]Hospital de Santa Cruz, [c]CEDOC, Nova Medical School, Lisbon and [d]Hospital Santarém, Santarém, Portugal

Correspondence to Pedro de Araújo Gonçalves, MD, Hospital Luz, Av. Lusiada, 1500-650 Lisbon, Portugal
Tel: +351 966 866 455; fax: +351 214 241 388;
e-mail: paraujogoncalves@yahoo.co.uk

Received 20 May 2016 **Revised** 23 June 2016 **Accepted** 8 August 2016

Introduction

White-coat hypertension (WCH) is defined as an office blood pressure (BP) up to 140/90 mmHg, but with home BP less than 140/90 mmHg and no evidence of hypertensive target organ damage, and occurs in 15–30% of patients presenting with an elevated BP at the office [1,2]. This entity carries a risk of progression to established hypertension [3,4] and therefore it is recommended that patients with WCH should be followed up to confirm the diagnosis and be advised on lifestyle changes [1,2,5].

It has been shown that WCH is an independent predictor of both renal damage and increased aortic stiffness [6,7] and is also associated with markers of carotid atherosclerosis (both intima-media thickness and stenosis) [8,9], which is in agreement with the higher stroke risk of these patients, as evidenced in recent publications [10,11]. The subclinical damage is also extended to the heart as suggested by a recent large meta-analysis that found WCH to be associated with higher left ventricular mass index, lower mitral E/A ratio, and a larger left atrium [12].

Taken together, these studies support the concept that WCH is not a benign condition and the relation between WCH and several cardiovascular outcomes, including myocardial infarction, stroke, heart failure, the need for revascularization, pacemaker implantation rates and cardiovascular death, has also been highlighted [4,10,11,13,14].

All the published evidence suggests that WCH is in fact a masked cardiovascular risk factor, but for coronary artery disease (CAD) there are not much data available, with only one small study from Kostandonis *et al.* [15] describing an association between WCH with more severe CAD, assessed with conventional invasive angiography.

DOI: 10.1097/MCA.0000000000000424

cont.

Manuscrito 8

58 **Coronary Artery Disease** 2017, Vol 28 No 1

Coronary artery calcium (CAC) scoring provides a noninvasive evaluation of the burden of calcified lesions in the coronary tree, which has been documented extensively as a strong prognostic marker [16,17]. Coronary computed tomography angiography (CCTA) provides a comprehensive evaluation of the total burden of atherosclerotic disease (all plaque compositions types – both calcified as well as noncalcified or mixed, and degree of stenosis – both obstructive and nonobstructive), which has also been linked to future cardiovascular events [18–21].

To the best of our knowledge, this is the first study to examine the association between WCH and the presence and extent of the coronary atherosclerotic burden evaluated noninvasively by both CAC scoring and CCTA.

Methods

Study and design

Between May 2013 and March 2015, 1778 consecutive patients undergoing CCTA for assessment of possible CAD were prospectively included in this single-center registry. Patients referred from the emergency department for possible acute coronary syndrome ($n = 36$), those with indications other than assessment for possible CAD, such as for ablation of atrial fibrillation or implantation of a percutaneous aortic valve ($n = 115$), those without CAC scoring assessment ($n = 95$), and patients with a history of myocardial infarction, coronary artery bypass graft surgery, or percutaneous coronary intervention ($n = 170$) were excluded from the present analysis. For the purpose of this study, 1362 patients were included and the population was divided into three groups according to the BP profile: group A, including patients with normal BP; group B, including WCH patients; and group C, of patients with established hypertension. Patient selection and study design are shown in Fig. 1.

Cardiovascular risk factor assessment

A detailed medical history, including a cardiovascular risk factor questionnaire, was obtained from all patients to assess the presence of: (a) diabetes (defined as fasting plasma glucose ≥ 7.0 mmol/l or use of oral hypoglycemic agents or insulin); (b) dyslipidemia (defined as total cholesterol ≥ 5 mmol/l or treatment with lipid-lowering drugs); (c) hypertension (defined as BP $\geq 140/90$ mmHg or the use of antihypertensive medication); (d) family history of premature CAD [defined as the presence of CAD in first-degree relatives younger than 55 (men) or 65 (women) years]; and (e) smoking (defined as previous, less than 1 year, or current smoker) and ex-smoking (defined as previous, more than 1 year). WCH was defined as the absence of known hypertension or the use of antihypertensive medication, associated with the measurement of systolic BP up to 140 mmHg and/or diastolic BP up to 90 mmHg before the CT scan, a variation of the conventional definition, which considers the measurement of BP at the office. The local ethics committee approved the study and all patients provided their written informed consent.

Scan protocol, image reconstruction, calcium score, and coronary disease assessment

Scans were performed with a dual-source scanner (SOMATOM Definition; Siemens Medical Systems, Germany), with the patient in dorsal decubitus and in deep inspiration breath hold. All patients received sublingual nitroglycerin, except when contraindicated, and β-blockers were administered to lower the heart rate when indicated. During the scan acquisition, a bolus of iodinated contrast (Visipaque; GE Healthcare Inc., Princeton, New Jersey, USA) was infused at 6 ml/s, followed by a 50 ml saline flush. The contrast dose was calculated according to the following formula: (acquisition time + 6 s delay) × flow (6 ml/s). Contrast administration was timed to optimize uniform enhancement of the coronary arteries. Dose-reduction strategies – including ECG-gated tube current modulation, reduced tube voltage, and prospective axial triggering – were used whenever feasible. Transaxial images were reconstructed with a temporal resolution of 83 ms and a slice thickness of 0.75 mm with 0.4 mm increments. Postprocessing was carried out using Aquarius iNtuition Viewer software (TeraRecon Inc., Foster City, California, USA), with multiplanar reconstructions, maximum intensity projection, and volume rendering. All scans were analyzed in the same session by both a cardiologist and a radiologist with level III-equivalent experience. The CAC scoring was calculated by summing the number of coronary segments with calcium, and a higher than expected atherosclerotic burden was defined as a CAC above the 50th percentile (CAC > p50), according to age-adjusted and sex-adjusted monograms, similar to what we have described recently [22]. The presence of CAD, including the presence of plaque (any degree of stenosis) and of obstructive CAD (defined by the presence of a stenosis equal or superior to 50%), was also evaluated.

Statistical analysis

Continuous variables were expressed as medians and interquartile range (IQR) in line with their non-normal distribution. Normality was tested using the Kolmogorov–Smirnov test. Categorical variables were expressed as frequencies and percentages. Statistical comparisons were performed using the χ^2-test or Fisher's exact test, as appropriate, for categorical variables and the Mann–Whitney test for continuous variables. The ability of WCH to predict a CAC > p50, the presence of coronary plaque, and obstructive CAD was assessed in a customized logistic regression model. Two-tailed tests of significance are reported. For all the comparisons, a P value less than 0.05 was considered statistically significant. When appropriate, 95% confidence intervals were

cont.

Manuscrito 8

Fig. 1

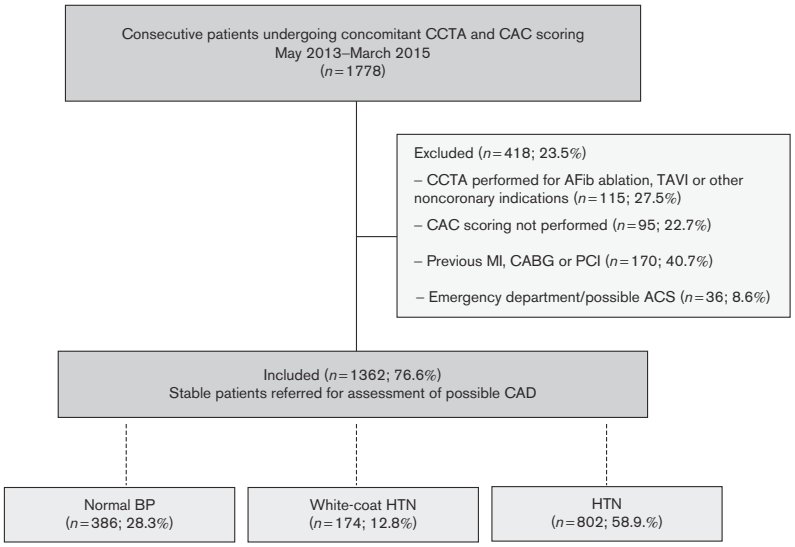

Patient selection and study design. ACS, acute coronary syndrome; AFib, atrial fibrillation; BP, blood pressure; CABG, coronary artery bypass grafting; CAC, coronary artery calcium; CAD, coronary artery disease; CCTA, coronary computed tomography angiography; HTN, hypertension; MI, myocardial infarction; PCI, percutaneous coronary intervention; TAVI, transcatheter aortic valve implantation.

Table 1 Demographical, clinical characteristics, and coronary atherosclerotic burden of the study population

Variables [*n* (%)]	All patients (*n* = 1362)	Normal BP (*n* = 386)	White-coat hypertension (*n* = 174)	Hypertension (*n* = 802)	*P* value
Demographic					
Age [median (IQR)] (years)	58 (50–66)	53 (45–60)	57 (49–64)	61 (54–68)	< 0.001
Male	703 (51.6)	206 (53.4)	105 (60.3)	392 (48.9)	0.017
Cardiovascular risk factors					
Hypertension	802 (58.9)	0 (0)	0 (0)	802 (100)	–
Diabetes	174 (12.8)	17 (4.4)	15 (8.6)	142 (17.7)	< 0.001
Dyslipidemia	781 (57.3)	173 (44.8)	82 (47.1)	526 (65.6)	< 0.001
Smoking or ex-smoking	433 (31.8)	141 (36.5)	56 (32.2)	236 (29.4)	0.048
Family history of CAD	626 (46.0)	163 (42.2)	75 (43.1)	388 (48.4)	0.099
BP profile					
Systolic [median (IQR)]	139 (127–152)	125 (117–132)	150 (144–158)	144 (132–158)	< 0.001
Diastolic [median (IQR)]	79 (71–88)	74 (67–80)	86 (79–93)	81 (71–89)	< 0.001
Calcium score					
Median (IQR)	1 (0–58)	0 (0–11)	0 (0–54)	9 (0–108)	< 0.001
CAC > p50	389 (28.6)	75 (19.4)	53 (30.5)	261 (32.5)	< 0.001
CAD					
Any plaque	745 (54.7)	142 (36.8)	88 (50.6)	515 (64.2)	< 0.001
Obstructive	197 (14.5)	32 (8.3)	24 (13.8)	141 (17.6)	< 0.001

BP, blood pressure; CAC, coronary artery calcium; CAD, coronary artery disease; IQR, interquartile range; p50, 50th percentile.

calculated. The statistical analysis was carried out using SPSS, version 20.0 (SPSS Inc., Chicago, Illinois, USA).

Results

Baseline demographic and clinical characteristics

The baseline demographic and clinical characteristics are shown in Table 1. Briefly, the median age of the 1362 studied patients was 58 (IQR 50–66) years and 51.6% were men. The most prevalent risk factor was hypertension (58.9%), followed by dyslipidemia (57.3%), family history of premature CAD (46%), smoking or ex-smoking (31.8%), and diabetes (12.8%). The median CAC was 1.0 (IQR 0.0–58.0), with 28.6% patients having a CAC higher than the p50, a value lower than what was verified in other populations [23]. As expected, most of the risk factors, with the exception of smoking, were more prevalent in patients with established hypertension, followed by patients in the WCH group.

cont.

Manuscrito 8

60 **Coronary Artery Disease** 2017, Vol 28 No 1

White-coat hypertension and coronary atherosclerotic burden

When groups were compared in terms of the presence and extent of the coronary atherosclerotic burden, patients in the WCH group had a significantly higher prevalence of all the three markers – CAC > p50 and CAD (any plaque and obstructive CAD) – compared with patients with normal BP (Fig. 2). As expected, patients in the established hypertension group showed the highest values for all the coronary atherosclerotic markers, but interestingly, when compared with the WCH group, only the marker 'CAD-any plaque' reached statistical significance and the prevalence of obstructive CAD was only numerically higher (17.6 vs. 13.8%, P = NS).

A multivariate analysis was carried out after evaluation of the correlation between all the demographic and clinical characteristics and the coronary atherosclerotic burden markers. WCH was an independent predictor of a CAC higher than p50 [odds ratio (OR) 1.563, 95% confidence interval 1.018–2.400, $P = 0.041$] (Table 2), but not of the presence of CAD (OR 1.335, $P = 0.169$) or obstructive CAD (OR 1.376, $P = 0.301$) (Tables 3 and 4).

Discussion

The main findings of our study were as follows: (a) WCH, defined as an elevated BP before CT scan, in patients without known hypertension or using antihypertensive medication, was an independent predictor of a calcium score above the p50 for age and sex; and (b) it was also associated with other markers of coronary atherosclerotic burden evaluated by CCTA, such as nonobstructive and obstructive CAD, compared with patients with normal BP.

Fig. 2

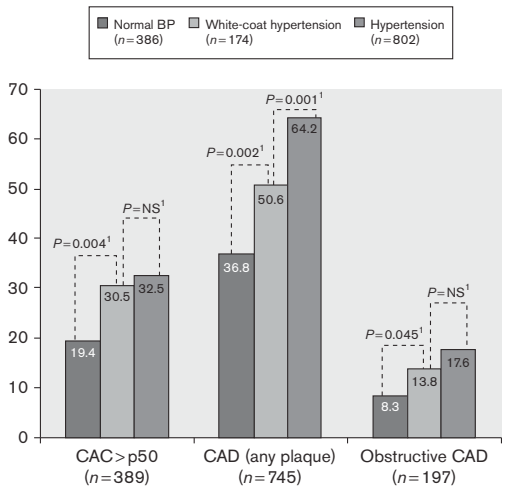

Differences between groups in the different coronary atherosclerotic parameters evaluated. [1]χ^2 or Fisher's exact test. BP, blood pressure; CAC, coronary artery calcium; CAD, coronary artery disease; p50, 50th percentile.

WCH has been associated consistently not only with subclinical organ damage but also with adverse clinical outcomes. In a recent meta-analysis including 3478 patients (of which 666 with WCH), Cuspidi *et al.* [9] reported a higher carotid intima-media thickness, a recognized marker of vascular damage, in patients with WCH compared with patients with normal BP, supporting the concept that WCH is not, effectively, a benign condition. This association was also found for carotid stenosis in the Hisayama study, independent of the other traditional risk factors [8]. This is in agreement with a higher risk of stroke of these patients, as evidenced in the recent publication from the Ohasama study [10] and other studies linking WCH to adverse cardiovascular outcomes [4,10,11,13].

However, for CAD, there are not much data available. Kostandonis *et al.* [15] reported an association between WCH and CAD severity, assessed by the Gensini score, in a small cohort of patients undergoing invasive coronary angiography. In our study, we aimed to study the relation between WCH and CAD using both the nonenhanced (CAC scoring) as well as the enhanced (CCTA) scans, given their documented ability to provide a comprehensive evaluation of the total coronary atherosclerotic burden. Interestingly, recently, several authors documented the prognostic value of disease burden beyond obstructive lesions and therefore in our study, we aimed to evaluate both obstructive and nonobstructive disease [18–20]. We found that WCH was associated with a higher coronary atherosclerotic burden compared with patients with normal BP for all three markers evaluated. Interestingly, the difference between WCH and patients with normal BP was higher than that between WCH and established hypertension (only reaching statistical significance in the marker 'CAD-any plaque'), in line with what has been reported previously for other markers, namely, carotid intima-media thickness [8,9] and left ventricle mass index [12].

The protocol of our institution with a detailed questionnaire and BP measurement before the examination, coupled with an almost routine nonenhanced scan before CCTA acquisition, allowed the design of the current study, providing one opportunity to relate WCH before the examination to the presence and extent of CAD, although with an unconventional definition of WCH.

By multivariate analysis, we found that WCH was an independent predictor of a CAC higher than that expected for sex and age (above the p50), but we could not find the same independent association with the presence of obstructive CAD. The reason for this might be related, on the one hand, to the fact that obstructive

cont.

Manuscrito 8

Table 2 Multivariate analysis – independent predictors of a calcium score more than 50th percentile

Variables	Odds ratio	95% confidence interval	*P* value
Age	1.018	1.001–1.037	**0.042**
Male	1.783	1.158–2.745	**0.009**
White-coat hypertension	1.563	1.018–2.400	**0.041**
Diabetes	1.432	0.650–3.154	0.372
Dyslipidemia	1.193	0.790–1.800	0.402
Smoking or ex-smoking	1.564	1.030–2.376	**0.036**
Family history of premature CAD	1.303	0.863–1.967	0.208

Bold *P* values are significant. CAD, coronary artery disease.

Table 3 Multivariate analysis – independent predictors of the presence of coronary plaque

Variables	Odds ratio	95% confidence interval	*P* value
Age	1.082	1.061–1.104	**0.000**
Male	3.514	2.330–5.299	**0.000**
White-coat hypertension	1.335	0.885–2.015	0.169
Diabetes	2.454	1.053–5.719	**0.038**
Dyslipidemia	0.937	0.638–1.377	0.741
Smoking or ex-smoking	1.508	1.011–2.249	**0.044**
Family history of premature CAD	1.451	0.983–2.144	0.061

Bold *P* values are significant. CAD, coronary artery disease.

Table 4 Multivariate analysis – independent predictors of obstructive coronary artery disease

Variables	Odds ratio	95% confidence interval	*P* value
Age	1.029	1.003–1.056	**0.031**
Male	4.680	2.196–9.976	**0.000**
White-coat hypertension	1.376	0.752–2.519	0.301
Diabetes	2.908	1.206–7.015	**0.017**
Dyslipidemia	0.967	0.536–1.744	0.910
Smoking or ex-smoking	2.014	1.123–3.611	**0.019**
Family history of premature CAD	1.337	0.743–2.406	0.333

Bold *P* values are significant. CAD, coronary artery disease.

CAD was only present in a minority of patients but also that WCH might be a relevant marker for the earlier atherosclerotic disease process in the continuum spectrum of cardiovascular disease.

On the basis of our results and the already available evidence in the literature on the carotid territory and structural heart changes, WCH seems to be an independent risk factor for cardiovascular diseases. This reinforces the current recommendations of the international societies to consider WCH not as a benign entity with close follow-up of these patients and the need for advice on lifestyle changes [1,2,5]. In addition, it has also been shown that there is a high probability of progression to sustained hypertension over a 10-year time period [3,4].

Limitations

The present study has several limitations that should be acknowledged: (a) this is a single-center medium-size prospective registry; (b) other markers of target organ damage (such as intima-media thickness and left ventricle mass) were not evaluated; (c) the definition of WCH in our study differs from the traditional definition used by other studies as we used BP values measured before the CT scan because we believed that a medical exam also corresponds to a time of increased anxiety experienced by the patient, similar to what occurs in office BP; and (d) no data on ambulatory BP monitoring are provided, although many of these patients were closely followed in cardiology outpatient clinics that referred the patients for CCTA for clinical reasons. Therefore, because of the lack of systematic ambulatory BP monitoring data, there is the possibility that some patients included in the WCH group could have had masked hypertension. However, in line with the rationale of CCTA referral being a general marker of good access to health surveillance, it is unlikely that this represents the majority of the cases.

Conclusion

In this registry of patients referred to CCTA, WCH was associated with a higher coronary atherosclerotic burden evaluated by both CAC and CCTA compared with patients without hypertension, but lower than that of patients with established hypertension. WCH was an independent predictor of a calcium score above the p50 for age and sex.

Acknowledgements

Conflicts of interest

There are no conflicts of interest.

References

1 Mancia G, Fagard R, Narkiewicz K, Redon J, Zanchetti A, Bohm M, *et al.* ESH/ESC Guidelines for the management of arterial hypertension: the Task Force for the management of arterial hypertension of the European Society of Hypertension (ESH) and of the European Society of Cardiology (ESC). *J Hypertens* 2013; **31**:1281–1357.
2 Franklin SS, Thijs L, Hansen TW, O'Brien E, Staessen JA. White-coat hypertension: new insights from recent studies. *Hypertension* 2013; **62**:982–987.
3 Sivén SS, Niiranen TJ, Kantola IM, Jula AM. White-coat and masked hypertension as risk factors for progression to sustained hypertension: the Finn-Home study. *J Hypertens* 2016; **34**:54–60.
4 Mancia G, Bombelli M, Brambilla G, Facchetti R, Sega R, Toso E, Grassi G. Long-term prognostic value of white-coat hypertension: an insight from diagnostic use of both ambulatory and home blood pressure measurements. *Hypertension* 2013; **62**:168–174.
5 Cloutier L, Daskalopoulou SS, Padwal RS, Lamarre-Cliche M, Bolli P, McLean D, *et al.* A new algorithm for the diagnosis of hypertension in Canada. *Can J Cardiol* 2015; **31**:620–630.
6 Tientcheu D, Ayers C, Das SR, McGuire DK, de Lemos JA, Khera A, *et al.* Target organ complications and cardiovascular events associated with masked hypertension and white-coat hypertension: analysis from the Dallas Heart Study. *J Am Coll Cardiol* 2015; **66**:2159–2169.
7 Aznaouridis K, Vlachopoulos C, Masoura K, Pietri P, Vyssoulis G, Ioakeimidis N, *et al.* Office blood pressure is a predictor of aortic elastic properties and urinary protein excretion in subjects with white-coat hypertension. *Int J Cardiol* 2016; **203**:98–103.

cont.

Manuscrito 8

8 Fukuhara M, Arima H, Ninomiya T, Hata J, Hirakawa Y, Doi Y, *et al*. White-coat and masked hypertension are associated with carotid atherosclerosis in a general population: the Hisayama study. *Stroke* 2013; **44**:1512–1517.
9 Cuspidi C, Sala C, Tadic M, Rescaldani M, Grassi G, Mancia G. Is white-coat hypertension a risk factor for carotid atherosclerosis? A review and meta-analysis. *Blood Press Monit* 2015; **20**:57–63.
10 Satoh M, Asayama K, Kikuya M, Inoue R, Metoki H, Hosaka M, *et al*. Long-term stroke risk due to partial white-coat or masked hypertension based on home and ambulatory blood pressure measurements: The Ohasama Study. *Hypertension* 2016; **67**:48–55.
11 Stergiou GS, Asayama K, Thijs L, Kollias A, Niiranen TJ, Hozawa A, *et al*. International Database on HOme blood pressure in relation to Cardiovascular Outcome (IDHOCO) Investigators. Prognosis of white-coat and masked hypertension: International Database of HOme blood pressure in relation to cardiovascular outcome. *Hypertension* 2014; **63**:675–682.
12 Cuspidi C, Rescaldani M, Tadic M, Sala C, Grassi G, Mancia G. White-coat hypertension, as defined by ambulatory blood pressure monitoring, and subclinical cardiac organ damage: a meta-analysis. *J Hypertens* 2015; **33**:24–32.
13 Mancia G, Facchetti R, Grassi G, Bombelli M. Adverse prognostic value of persistent office blood pressure elevation in white-coat hypertension. *Hypertension* 2015; **66**:437–444.
14 Bombelli M, Seravalle G, Dell'Oro R, Trevano FQ, Facchetti R, Grassi G, Mancia G. 3C.01: adverse prognostic value of persistent office blood pressure elevation in white-coat hypertension. *J Hypertens* 2015; **33** (Suppl 1): e37.
15 Kostandonis D, Papadopoulos V, Toumanidis S, Papamichael C, Kanakakis I, Zakopoulos N. Topography and severity of coronary artery disease in white-coat hypertension. *Eur J Intern Med* 2008; **19**:280–284.
16 Detrano R, Guerci AD, Carr JJ, Bild DE, Burke G, Folsom AR, *et al*. Coronary calcium as a predictor of coronary events in four racial or ethnic groups. *N Engl J Med* 2008; **358**:1336–1345.
17 Yeboah J, McClelland RL, Polonsky TS, Burke GL, Sibley CT, O'Leary D, *et al*. Comparison of novel risk markers for improvement in cardiovascular risk assessment in intermediate-risk individuals. *JAMA* 2012; **308**: 788–795.
18 Min JK, Dunning A, Lin FY, Achenbach S, Al-Mallah M, Budoff MJ, *et al*. Age- and sex-related differences in all-cause mortality risk based on coronary computed tomography angiography findings results from the International Multicenter CONFIRM (Coronary CT Angiography Evaluation for Clinical Outcomes: An International Multicenter Registry) of 23 854 patients without known coronary artery disease. *J Am Coll Cardiol* 2011; **58**:849–860.
19 Bittencourt MS, Hulten E, Ghoshhajra B, O'Leary D, Christman MP, Montana P, *et al*. Prognostic value of nonobstructive and obstructive coronary artery disease detected by coronary computed tomography angiography to identify cardiovascular events. *Circ Cardiovasc Imaging* 2014; **7**:282–291.
20 Mushtaq S, de Araújo Gonçalves P, Garcia-Garcia HM, Pontone G, Bartorelli AL, Bertella E, *et al*. Long-term prognostic effect of coronary atherosclerotic burden: validation of the computed tomography-Leaman score. *Circ Cardiovasc Imaging* 2015; **8**:e002332.
21 De Araújo Gonçalves P, Campos CA, Serruys PW, Garcia-Garcia HM. Computed tomography angiography for the interventional cardiologist. *Eur Heart J Cardiovasc Imaging* 2014; **15**:842–854.
22 Dores H, de Araújo Gonçalves P, Ferreira AM, Carvalho MS, Sousa PJ, Cardim N, *et al*. Performance of traditional risk factors in identifying a higher than expected coronary atherosclerotic burden. *Rev Port Cardiol* 2015; **34**:247–253.
23 Pereira AC, Gomez LM, Bittencourt MS, Staniak HL, Sharovsky R, Foppa M, *et al*. Age, gender, and race-based coronary artery calcium score percentiles in the Brazilian longitudinal study of adult health (ELSA-Brasil). *Clin Cardiol* 2016; **39**:352–359.

cont.

MANUSCRITO 9

Diabetes as an independent predictor of high atherosclerotic burden assessed by coronary computed tomography angiography: the coronary artery disease equivalent revisited.

de Araujo Goncalves, P., Garcia-Garcia, H. M., Carvalho, M.S., Dores, H., Sousa, P. J., **Marques**, **H**., Ferreira, A., Cardim, N., Teles, R. C., Raposo, L., Gabriel, H. M., Almeida, M., Aleixo, A., Carmo, M. M., Machado, F.P., and Mendes, M.

Int J Cardiovasc Imaging, 2013
29(5): p. 1105-14

Manuscrito 9

Diabetes as an independent predictor of high atherosclerotic burden assessed by coronary computed tomography angiography: the coronary artery disease equivalent revisited

Pedro de Araújo Gonçalves, Hector M. Garcia-Garcia, Maria Salomé Carvalho, Helder Dores, Pedro Jeronimo Sousa, Hugo Marques, et al.

The International Journal of Cardiovascular Imaging
X-Ray Imaging, Echocardiography, Nuclear Cardiology Computed Tomography and Magnetic Resonance Imaging

ISSN 1569-5794
Volume 29
Number 5

Int J Cardiovasc Imaging (2013)
29:1105-1114
DOI 10.1007/s10554-012-0168-4

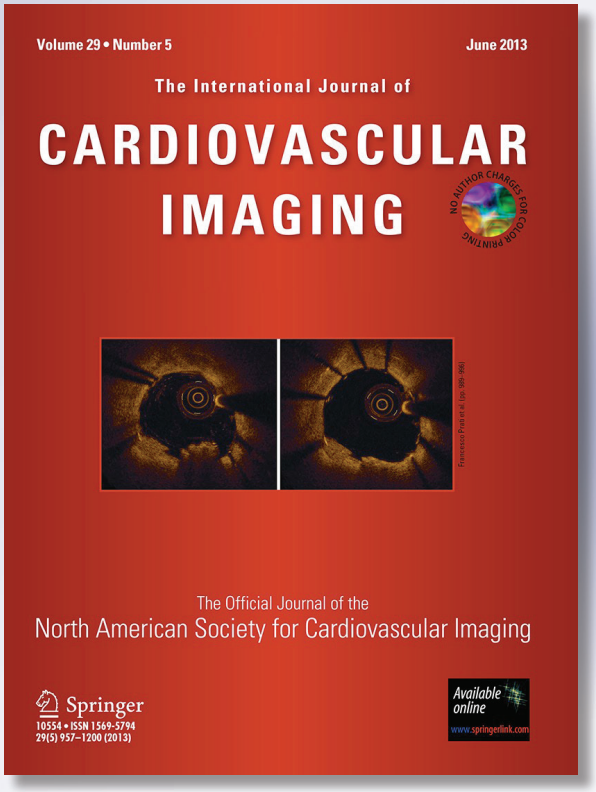

Springer

cont.

Manuscrito 9

cont.

Manuscrito 9

Int J Cardiovasc Imaging (2013) 29:1105–1114
DOI 10.1007/s10554-012-0168-4

ORIGINAL PAPER

Diabetes as an independent predictor of high atherosclerotic burden assessed by coronary computed tomography angiography: the coronary artery disease equivalent revisited

Pedro de Araújo Gonçalves · Hector M. Garcia-Garcia · Maria Salomé Carvalho · Helder Dores · Pedro Jeronimo Sousa · Hugo Marques · Antonio Ferreira · Nuno Cardim · Rui Campante Teles · Luís Raposo · Henrique Mesquita Gabriel · Manuel Almeida · Ana Aleixo · Miguel Mota Carmo · Francisco Pereira Machado · Miguel Mendes

Received: 10 October 2012 / Accepted: 5 December 2012 / Published online: 13 December 2012

Abstract (1) To study the prevalence and severity of coronary artery disease (CAD) in diabetic patients. (2) To provide a detailed characterization of the coronary atherosclerotic burden, including the localization, degree of stenosis and plaque composition by coronary computed tomography angiography (CCTA). Single center prospective registry including a total of 581 consecutive stable patients (April 2011–March 2012) undergoing CCTA (Dual-source CT) for the evaluation of suspected CAD without previous myocardial infarction or revascularization procedures. Different coronary plaque burden indexes and plaque type and distribution patterns were compared between patients with (n = 85) and without diabetes (n = 496). The prevalence of CAD (any plaque; 74.1 vs. 56 %; $p = 0.002$) and obstructive CAD (≥50 % stenosis; 31.8 vs. 10.3 %; $p < 0.001$) were significantly higher in diabetic patients. The remaining coronary atherosclerotic burden indexes evaluated (plaque in LM-3v-2v with prox. LAD; SIS; SSS; CT-LeSc) were also significantly higher in diabetic patients. In the *per segment* analysis, diabetics had a higher percentage of segments with plaque in every vessel (2.6/13.1/7.5/10.5 % for diabetics vs. 1.4/7.1/3.3/4.4 % for nondiabetics for LM, LAD, LCx, RCA respectively; $p < 0.001$ for all) and of both calcified (19.3 vs. 9.2 %, $p < 0.001$) and noncalcified or mixed types (14.4 vs. 7.0 %; $p < 0.001$); the ratio of proximal-to-distal relative plaque distribution (calculated as LM/proximal vs. mid/distal/branches) was lower for diabetics (0.75 vs. 1.04; $p = 0.009$). Diabetes was an independent predictor of CAD and was also associated with more advanced CAD, evaluated by indexes of coronary atherosclerotic burden. Diabetics had a significantly higher prevalence of plaques in every anatomical subset and for the different plaque composition. In this report, the relative geographic distribution of the plaques within each subgroup, favored a more mid-to-distal localization in the diabetic patients.

Keywords Diabetes · Coronary artery disease · Atherosclerotic burden · Coronary CT angiography

P. de Araújo Gonçalves (✉) · M. S. Carvalho · H. Dores · P. J. Sousa · A. Ferreira · R. C. Teles · L. Raposo · H. M. Gabriel · M. Almeida · A. Aleixo · M. Mendes
Cardiology Department, Centro Hospitalar Lisboa Ocidental, Av. Prof. Reinaldo dos Santos, 2790-134 Carnaxide, Lisbon, Portugal
e-mail: paraujogoncalves@yahoo.co.uk

P. de Araújo Gonçalves · H. Marques · A. Ferreira · N. Cardim · F. P. Machado
Hospital da Luz, Lisbon, Portugal

P. de Araújo Gonçalves · A. Aleixo · M. M. Carmo
CEDOC—Chronic Diseases Research Center—FCM-NOVA, Lisbon, Portugal

H. M. Garcia-Garcia
Thoraxcenter, Erasmus MC, Rotterdam, The Netherlands

Introduction

Patients with diabetes are considered to be at an increased risk of cardiovascular events and therefore it has been recommended by many guidelines a more aggressive management of this subset of patients, especially for those with established cardiovascular disease [1, 2].

By contrast, on a primary prevention unselected population level, some of the preventive measures for diabetic patients, like the use of antiplatelets, have failed to demonstrate a clear clinical benefit [3] and are no longer recommended in the absence of clinical evidence of atherosclerotic disease [4]. The reason for the lack of

cont.

benefit of aspirin in diabetic patients is likely related to the fact that diabetic patients represents an heterogeneous subset in what concerns the prevalence and severity of atherosclerotic coronary burden.

This illustrates the need for risk stratification of diabetic patients to identify the ones that can benefit from a more aggressive management at earlier stages. This is an opportunity for noninvasive imaging modalities, such as coronary computed tomography angiography (CCTA), which provides a detailed and comprehensive evaluation of the presence and extent of coronary artery disease (CAD), and can play an important role identifying the diabetic patients that could benefit from a more aggressive prevention of cardiovascular events.

Since CCTA is used mainly as a gatekeeper for the exclusion of significant CAD [5], most of the referred patients are at low to intermediate risk, this provides a good setting to study atherosclerotic disease at an earlier stage.

Therefore the aim of this study is two-folded:

1. To study the prevalence and severity of CAD in diabetic patients at earlier stages of CAD, to further evaluate the concept of CAD equivalent.
2. To provide a detailed characterization of the coronary atherosclerotic burden in diabetic patients, using the comprehensive information derived from CCTA on the localization, degree of stenosis and plaque composition.

Methods

Population

Single center prospective registry, including a total of 772 consecutive patients undergoing CCTA (with Dual source CT), from April 2011 to March 2012.

Patients were excluded if: (1) previous history of myocardial infarction and/or revascularization procedures (n = 70); (2) referred for Cardiac CT for other indications than the evaluation of possible CAD (cardiac CT for atrial fibrillation ablation or transcatheter aortic valve implantation procedures; n = 88); (3) referred for suspected acute coronary syndromes (n = 24); (4) with atrial fibrillation or other significant arrhythmias during scan acquisition that compromised image quality (n = 9). This resulted in a 24.7 % of the total population being excluded.

For the purpose of this study, 581 stable patients referred for suspected CAD were included in the context of: (1) Previous equivocal or inconclusive stress tests or discordant with the clinical evaluation (n = 417, 71.8 %); (2) Cardiac CT as 1st line investigation of possible CAD (n = 136, 23.4; %); 3) Preoperative CAD assessment prior to noncoronary valvular or aortic surgery (n = 17; 2.9 %); (4) Evaluation of possible CAD in cardiomyopathies (Dilated or Hypertrophic) (n = 11; 1.9 %) (Fig. 1: Patient selection and study design).

The study was approved by the local ethics committee and all patients gave a written informed consent.

A detailed medical history by means of a risk factors questionnaire was obtained from the patients to assess for the presence of: (1) Diabetes mellitus (defined as a fasting glucose level of ≥7 mmol/l or the need for insulin or oral hypoglycemic agents) [6]; (2) Dyslipidemia (defined as a total cholesterol level ≥5 mmol/l or treatment with lipid-lowering drugs) [7]; (3) Hypertension (defined as blood pressure ≥140/90 mm Hg or the use of antihypertensive medication) [8]; (4) Obesity (body mass index ≥30 kg/m^2); (5) positive family history of premature CAD [defined as the presence of CAD in first-degree relatives younger than 55 (male) or 65 (female) years of age] [9]; (6) smoking (defined as previous <1 year) or current smoker.

Pre-test probability of CAD was determined using both the Diamond and Forrester extended CAD consortium method (DF–CAD consortium model) [10] and the Morise score [11]. The cardiovascular risk was assessed with the HeartScore [4]. For the DF–CAD consortium probability model, as the CAD probability and CV risk of our population was shifted to lower probability (less that 2 % had a ≥70 % DF probability), the DF–CAD consortium model categories ≥30–70 % and ≥70 % were gathered in a intermediate to high (≥30 %) probability group. For the Morise, the original described cut-off points (for low, intermediate and high probability) were used, and for the HeartScore the established high risk cut-off of ≥5 % was used.

Scan protocol and image reconstruction

All scans were performed with a dual-source scanner (Somatom Definition, Siemens Medical, Germany), with the patient in dorsal decubitus and in deep inspiration breath-hold. Sublingual nitroglycerin was administered to all patients except when contraindicated and intravenous metoprolol (5 mg, with a titration dose up to 20 mg) was administered in patients with heart rate >65 beats/min.

During the scan acquisition, a bolus of iodinated contrast (Visipaque, GE Healthcare, USA) was injected at a 6 ml/s infusion rate, followed by a 50-ml saline flush. The dose of contrast was calculated according to the following formula: (acquisition time + 6 s delay) x flow (6 ml/s). Contrast timing was performed to optimize uniform contrast enhancement of the coronary arteries.

Dose reduction strategies—including electrocardiogram-gated tube current modulation, reduced tube voltage, and prospective axial triggering—were used whenever

cont.

Manuscrito 9

Int J Cardiovasc Imaging (2013) 29:1105–1114

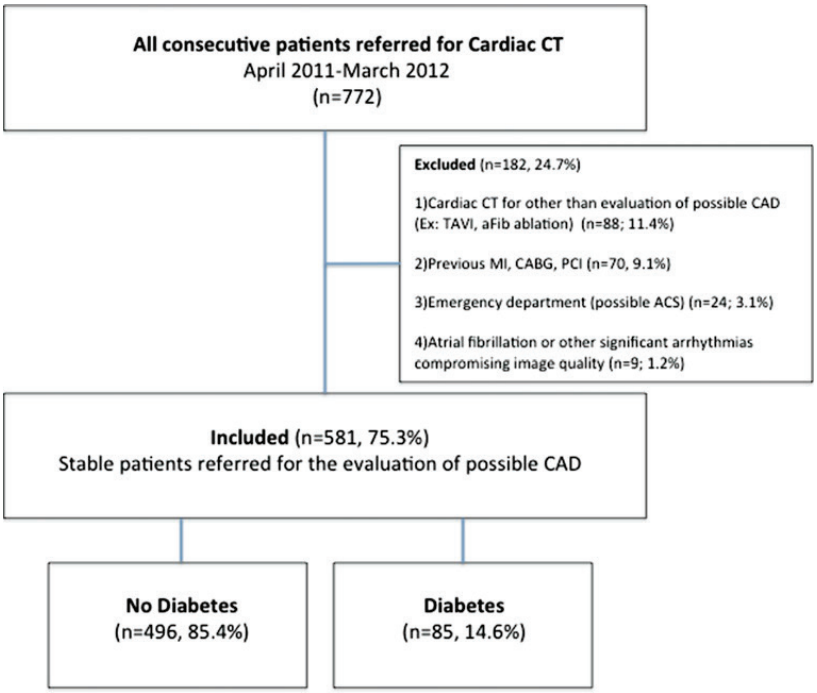

Fig. 1 Patient selection and study design. *CAD* coronary artery disease, *TAVI* transcatheter aortic valve implantation, *aFib* atrial fibrillation, *MI* myocardial infarction, *CABG* coronary artery bypass grafting, *PCI* percutaneous coronary intervention, *ACS* acute coronary syndromes

feasible. Mean estimated radiation dose was 4.6 ± 3.7 mSv, contrast dose was 98.9 ± 14.4 ml and heart rate was 65.6 ± 10.6 bpm.

Transaxial images were reconstructed with a temporal resolution of 83 ms and slice thickness of 0.75 mm with 0.4 mm increments.

Post-processing was carried out using Circulation® software, with multiplanar reconstructions, maximum intensity projection and volume rendering technique.

Coronary artery analysis

All scans were analyzed in the same session by both a cardiologist and a radiologist with Level III—equivalent experience. The Society of Cardiovascular Computed Tomography (SCCT) recommended classification was used regarding segmentation (16 segments), stenosis severity (<25; 25–49; 50–69; 70–99; 100 %) and plaque composition (calcified, noncalcified, mixed plaque) [12]. In each coronary artery segment, coronary atherosclerosis was defined as tissue structures >1 mm^2 that existed either within the coronary artery lumen or adjacent to the coronary artery lumen that could be discriminated from surrounding pericardial tissue, epicardial fat, or the vessel lumen itself. [13] Coronary atherosclerotic lesions were quantified for stenosis by visual estimation. Percent obstruction of coronary artery lumen was based on a comparison of the luminal diameter of the segment exhibiting obstruction to the luminal diameter of the most normal-appearing site immediately proximal to the plaque.

In the detailed *per segment* analysis, for the distribution of plaque on the 3 main coronary vessels, this rules were applied: plaques in the diagonal branches were counted as belonging to the left anterior descending (LAD); plaques in the obtuse marginal an intermediate branch were counted as belonging to the LCx; plaques in the posterior descending and right postero-lateral were counted as belonging to the right coronary artery (RCA). For the last two, coronary dominance was taking into account. The ratio of "proximal-to-distal relative plaque distribution" was calculated as the proportion of plaques between these two subgroups: (1) Left main and proximal segments of the LAD, LCx and RCA; (2) Mid and distal segments of LAD and RCA, distal LCx and all evaluable coronary branches.

Definition of the coronary atherosclerotic burden indexes

The following coronary atherosclerotic burden indexes were evaluated and compared between patients with and

cont.

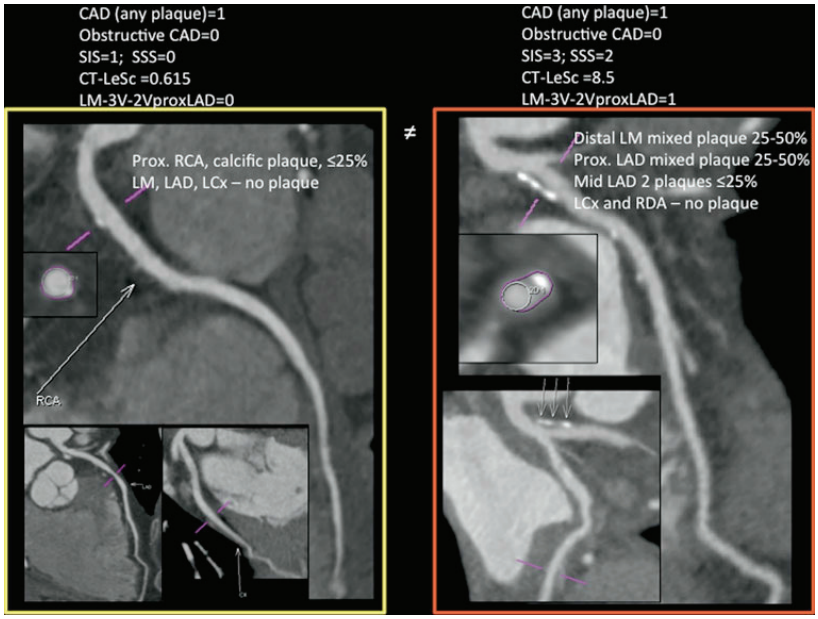

Fig. 2 Two case examples of diabetic patients with nonobstructive CAD. The different plaque burden indexes are shown. *CAD* coronary artery disease, *SIS* segment involvement score, *SSS* segment stenosis score, *CT-LeSc* CT Leaman score, *LM* left main, *LAD* left anterior descending, *LCx* left circunflex, *RCA* right coronary artery, *LM-3 V-2VproxLAD* plaque in left main or 3 vessels or 2 vessels with proximal LAD

without diabetes: (1) Coronary artery disease (CAD)—presence of any plaque in the coronary tree; (2) "Obstructive CAD"—presence of at least one plaque with ≥50 % stenosis; (3) "LM-3v-2v with proximal LAD"—Plaque in the left main or in the 3 main epicardial vessels or in 2 main epicardial vessels including the proximal left anterior descending (LAD); (4) "SIS"—segment involvement score, obtained as the total number of segments with plaque; (5) "SSS"—segment stenosis score, obtained by grading the stenosis severity of each segment with plaque, as was previously described [13]. For these last two, the prognostically validated cut-offs (>5) were used [13]

(6) "Calcium score (CaSc) ≥100"; (7) "CaSc ≥75th percentile" (according to published nomograms [14]; (8) CCTA-adapted Leaman score (CT-LeSc)—this score was calculated taking in account 3 weighting factors (localization, plaque composition and stenosis severity) according to previously described methodology and the same cut-off for high plaque burden (≥8.3) was used (provided as additional information to the reviewers, since the manuscript, where it is originally described, is under consideration elsewhere). In Fig. 2, two case examples of diabetic patients with nonobstructive CAD are shown, with the different plaque burden indexes.

Statistical analysis

Continuous variables are presented as mean ± SD or medians (interquartile range) and categorical variables as frequencies with percentages.

The non-parametric Mann–Whitney or Kruskal–Wallis tests were used to compare continuous variables. Chi square test was used to evaluate differences in frequencies. Differences were regarded significant when $p < 0.05$ (two-tailed).

Multivariate analyses (binary logistic regression model—enter method) were performed to identify independent predictors of CAD (any plaque and obstructive) using the demographic and clinical variables presented in Table 1, that were significant in univariate analysis ($p < 0.05$). A second multivariable analyses was performed to identify independent predictors among the clinical scores of CAD probability (Diamond-Forrester CAD consortium model and Morise score) and the CV risk score HeartScore. For the detailed *per segment* analysis, the unit of measure was each segment and there were no adjustments or corrections made for the serial correlation between segments.

SPSS version 17.0 (SPSS Inc., Chicago, IL, USA) was used for all statistical analyses.

cont.

Manuscrito 9

Results

Study population

In the final study population (n = 581), 85 patients were diabetics (14.6 %).

Regarding the demographic and clinical variables, diabetic patients were older (mean age 61.4 ± 8.7 vs. 56.9 ± 11.3) and had a higher prevalence of obesity (28.6 % vs. 17.4 %) and hypertension (84.7 vs. 58.9 %). This was predominantly a population with low to intermediate CAD probability, more so in the nondiabetic population since 61.7 % had a DF–CAD consortium <30 and 90.7 % had a Morise score <16. The cardiovascular risk, as estimated with the HeartScore (≥5 %), was significantly higher in the patients with diabetes (42.4 vs. 22.6 %) (Table 1).

Independent predictors of CAD

Diabetes was an independent predictor of both the presence of plaque (OR 1.81; 95 % CI 1.02–3.21; $p = 0.041$) and of obstructive CAD (OR 3.69; 95 % CI 2.08–6.53; $p < 0.001$). The other independent predictors of the *presence of plaque* were age ≥65 years (OR 3.42; 95 % CI 2.15–5.45; $p < 0.001$), male sex (OR 2.72; 95 % CI 1.85–4.01; $p < 0.001$), hypertension (OR 1.82; 95 % CI 1.23–2.67; $p = 0.002$), dyslipidemia (OR 1.89; 95 % CI 1.29–2.77; $p = 0.001$), chest pain (OR 0.62; 95 % CI 0.42–0.91; $p = 0.014$) an DF–CAD consortium ≥30 % (OR 2.62; 95 % CI 1.70–4.05; $p < 0.001$), a Morise score ≥16 (OR 2.55; 95 % CI 1.57–4.14; $p < 0.001$), and an HeartScore ≥5 % (OR 3.90; 95 % CI 2.19–6.94; $p < 0.001$). The other independent predictors of *obstructive CAD* were age ≥65 years (OR 1.98; 95 % CI 1.16–3.37; $p = 0.012$), male sex (OR 2.94; 95 % CI 1.68–5.15; $p < 0.001$), an DF–CAD consortium ≥30 % (OR 1.88; 95 % CI 1.04–3.42; $p = 0.038$), a Morise score ≥16 (OR 1.84; 95 % CI 1.06–3.20; $p = 0.031$), and an HeartScore ≥5 % (OR 2.71; 95 % CI 1.50–4.88; $p = 0.001$).

Table 1 Demographic and clinical characteristics of the study population

	No diabetes (n = 496)	Diabetes (n = 85)	*p*
Demographic			
Age	56.9 ± 11.3	61.4 ± 8.7	<0.001
Male sex	277 (55.8)	47 (55.3)	1.000
Risk factors			
Obesity (BMI ≥30)	85 (17.4)	24 (28.6)	0.023
Hypertension	292 (58.9)	72 (84.7)	<0.001
Dyslipidemia	301 (60.7)	59 (69.4)	0.147
Smoking	118 (23.8)	20 (23.5)	1.000
Family history of premature CAD	168 (33.9)	26 (30.6)	0.619
Chest pain	265 (54.3)	46 (54.1)	1.000
CAD probability			
DF–CAD consortium ≥30 %	189 (38.1)	42 (49.4)	0.049
DF–CAD consortium <30 %	307 (61.9)	43 (50.6)	
Morise score ≥16	46 (9.3)	26 (30.6)	<0.001
Morise score 9–15	316 (63.7)	53 (62.4)	
Morise score 0–8	134 (27.0)	6 (7.1)	
CV risk			
HeartScore ≥5 %	112 (22.6)	36 (42.4)	<0.001

Values are mean ± SD or n (%)

CAD coronary artery disease, *BMI* body mass index, *DF–CAD* consortium diamond-forrester CAD consortium model, *CV* cardiovascular

Coronary artery disease prevalence, severity and coronary atherosclerotic burden indexes—*per patient* analysis

The prevalence of plaques in the coronary arteries was high in the overall study population, but this was significantly higher for diabetic patients, as almost 3 out of 4 diabetic patients (74.1 %) had plaques in the coronary arteries.

Table 2 Calcium score and CCTA characteristics of the study population

	No diabetes (n = 496)	Diabetes (n = 85)	*p*
Calcium score			
Median	0 (0-67)	68 (0-311)	<0.001
CaSc ≥100	96 (19.4)	40 (47.1)	<0.001
CaSc ≥75th percentile	60 (12.1)	23 (27.1)	0.001
CCTA			
Normal/No plaque	217 (43.8)	22 (25.9)	<0.001
Nonobstructive CAD	228 (46.0)	36 (42.4)	
Obstructive CAD	51 (10.3)	27 (31.8)	
Coronary atherosclerotic burden indexes			
Plaque in LM-3v-2v with prox. LAD	178 (35.9)	53 (62.4)	<0.001
Segment involvement score >5	66 (13.3)	31 (36.5)	<0.001
Segment stenosis score >5	25 (5.0)	21 (24.7)	<0.001
CT-Leaman Score ≥8.3	79 (15.9)	35 (41.2)	<0.001
Technical data			
Heart rate (bpm)	65.3 ± 10.6	67.0 ± 10.2	0.172
Contrast dose (ml)	99.3 ± 14.7	96.7 ± 12.3	0.119
Radiation dose (mSv)	4.7 ± 4.9	5.7 ± 3.8	0.069

Values are mean ± SD, median (IQR) or n (%)

CaSc calcium score, *CCTA* coronary computed tomography angiography, *CAD* coronary artery disease, *LM-3v-2v* left main, 3 vessel, 2 vessel, *LAD* left anterior descending, *bpm* beats per minute, *mSv* milisievert

cont.

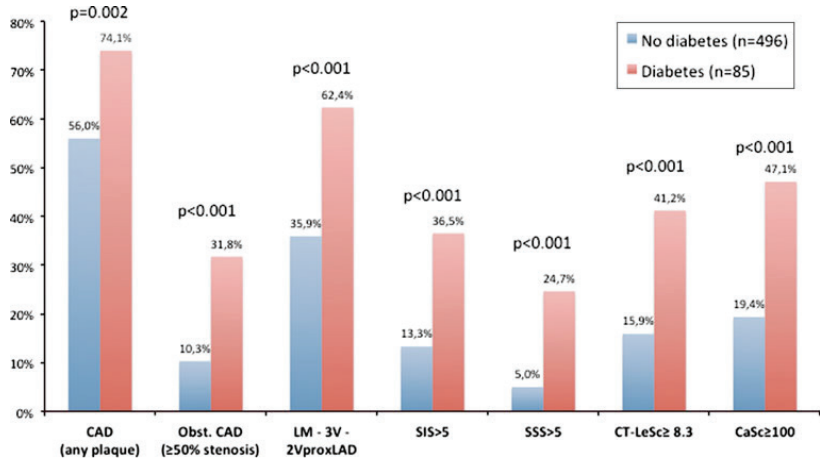

Fig. 3 Diabetes and indexes of coronary atherosclerotic burden. *CAD* coronary artery disease, *LM* left main, *LAD* left anterior descending, *LCx* left circunflex, *LM-3 V-2VproxLAD* plaque in left main or 3 vessels or 2 vessels with proximal LAD, *SIS* segment involvement score, *SSS* segment stenosis score, *CT-LeSc* CT Leaman score

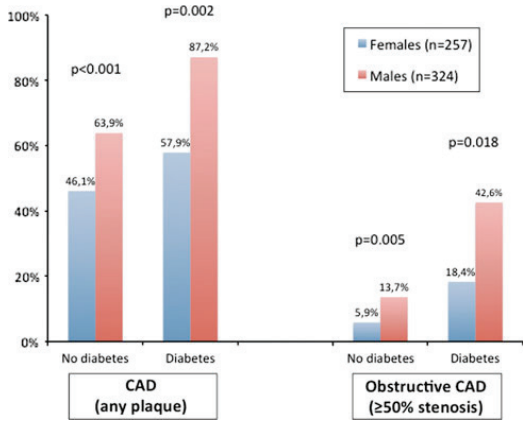

Fig. 4 Prevalence of coronary artery disease (any plaque and obstructive) across the different diabetes and sex subgroups. *CAD* coronary artery disease

All the indexes of coronary atherosclerotic burden were significantly higher in diabetics as compared to nondiabetics (Table 2; Fig. 3).

For some of these indexes, like the presence of obstructive disease, and the SSS, the prevalence was 3–5 times higher in diabetics.

By gender, male diabetics had more often coronary artery disease (any plaque and obstructive), as compared to their counterparts (Fig. 4).

Prevalence, localization and type of plaques—*per segment* analysis

For the analysis of the atherosclerotic burden indexes, 8,136 coronary segments were evaluated for the presence of plaque, degree of stenosis and type of plaque. Because of small size (<2 mm) or insufficient image quality related to artifacts or severe calcification, 866 (10.6 %) segments were excluded (n = 723–10.4 % in nondiabetics; n = 143–12.0 % in diabetics).

On a *"per evaluable segment"* analysis, diabetics had significantly more segments with plaque and this was observed in the left main as well as in the other 3 coronary territories and in both more proximal and more distal locations (Table 3; Fig. 5). The prevalence of obstructive plaque was also significantly higher in patients with, as compared to patients without diabetes (11.6 vs. 6.9 %, $p < 0.001$).

On a *"per segment with plaque"* analysis, nondiabetics had an almost equal distribution of plaques between more proximal (LM/proximal segments) and more mid-to-distal (Mid/distal/branches) localization (ratio of 1.04), but the opposite was seen in patients with diabetes, in whom more plaques were found in the more mid-to-distal segments, as reflected by a ratio of "proximal-to-distal relative plaque distribution" of 0.75 (Table 3).

Regarding plaque composition, diabetics had also a higher percentage of all types of plaques (both calcified and noncalcified or mixed plaques) per evaluable segment (Table 4).

Discussion

The main findings of this study are:

1. Although diabetic patients had a higher prevalence of coronary artery disease, coronary atherosclerotic plaques were commonly observed in both patients with and without diabetes.

cont.

Manuscrito 9

Table 3 Prevalence, and localization of plaques—*per segment* analysis

	No diabetes (n = 496; 6,957 segments)	Diabetes (n = 85; 1,187 segments)	*p*
All evaluable segments	6,234 (89.6)	1,044 (88.0)	0.093
Segments with any plaque	1,008 (16.2)	352 (33.7)	<0.001
Coronary artery distribution			
Any plaque in the LM	87 (1.4)	27 (2.6)	0.007
Any plaque in the RCA	276 (4.4)	110 (10.5)	<0.001
Any plaque in the LAD	441 (7.1)	137 (13.1)	<0.001
Any plaque in the LCx/Ramus	204 (3.3)	78 (7.5)	<0.001
Proximal versus distal distribution			
Any plaque in LM/Proximal	514 (8.2)	151 (14.5)	<0.001
Any plaque in Mid/Distal/Branches	494 (7.9)	201 (19.3)	<0.001
"Ratio of proximal-to-distal relative plaque distribution"	1.04 (514/494)	0.75 (151/201)	0.009

"Ratio of proximal-to-distal relative plaque distribution"—proportion of plaques in the "LM/Proximal" versus "Mid/Distal/branches"

LM left main, *RCA* right coronary artery, *LAD* left anterior descending, *LCx* left circunflex, *Ramus* intermediate branch, "*LM/Prox*" left main or proximal segments of the LAD, LCx or RCA, "*Mid/Distal/Branches*" mid or distal segments of the LAD and RCA, distal segment of the LCx, and branches

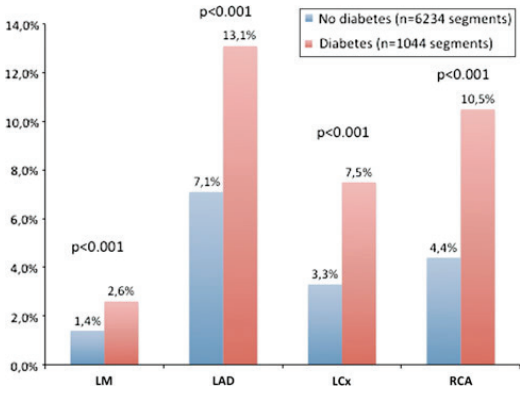

Fig. 5 Prevalence and localization of plaques (any plaque) on a *per segment* analysis. *LM* left main, *LAD* left anterior descending, *LCx* left circunflex, *RCA* right coronary artery

2. Several different coronary atherosclerotic burden indexes were more prevalent in diabetics, indicating more diffuse and severe CAD, and this was especially true for males.
3. In the detailed per segment analysis, diabetics had a higher percentage of segments with plaque in every vessel and of both calcified and noncalcified or mixed types; ratio of proximal-to-distal relative plaque distribution suggested an anatomical gradient in the geographic distribution, with higher proportion of disease involvement in the mid/distal/branches segments in diabetic patients.

Diabetes as an heterogeneous group—not all diabetics have the same CV risk

For many years, diabetic patients have been considered as a subset at higher risk of cardiovascular events. Nevertheless,

Table 4 Type of plaques—*per segment* analysis

	No diabetes (n = 496; 6,957 segments)	Diabetes (n = 85; 1,187 segments)	*p*
All evaluable segments	6,234 (89.6)	1,044 (88.0)	0.093
Segments with any plaque	1,008 (16.2)	352 (33.7)	<0.001
Calcified plaque			
All segments	571 (9.2)	202 (19.3)	<0.001
LM/Proximal	291 (4.7)	83 (8.0)	<0.001
Mid/Distal/Branches	280 (4.5)	119 (11.4)	<0.001
Noncalcified or mixed plaques			
All segments	437 (7.0)	150 (14.4)	<0.001
LM/Proximal	223 (3.6)	68 (6.5)	<0.001
Mid/Distal/Branches	214 (3.4)	82 (7.9)	<0.001

LM left main, *RCA* right coronary artery, *LAD* left anterior descending, *LCx* left circunflex, *Ramus* intermediate branch, "*LM/Proximal*" left main or proximal segments of the LAD, LCx or RCA, "*Mid/Distal/Branches*" Mid or distal segments of the LAD and RCA, distal segment of the LCx, and branches

cont.

it has been difficult to prove a clear benefit of some primary prevention measures, like is the case of aspirin in the primary prevention of cardiovascular events. This inconsistent benefit of aspirin in the absence of clinical manifestations of cardiovascular disease, can be related to the fact that it is less effective in these patients [15] or more likely that diabetic patients are an heterogeneous group in terms of cardiovascular disease presence and extent. This way, without risk stratification, we could be overtreating some low risk diabetic patients, exposing them to the risk of side effects that could offset the reduction in expected atherothrombotic events rate.

Of note, there has been a more consistent beneficial effect of aspirin as primary preventive measure in males, for reducing the risk of myocardial infarction [3] and this is in line with our findings of higher prevalence of coronary plaques and obstructive CAD in this subgroup, as compared to females.

Recently, Saely et al. [16] revisited the concept of diabetes as a CAD equivalent in a study comparing the vascular event rate of patients according to the presence of diabetes and/or CAD. In this study, diabetes was not per se a CAD risk equivalent, since diabetic patients without significant CAD had a lower event rate than nondiabetic patients with significant CAD.

CCTA derived coronary atherosclerotic burden indexes

Scores derived from invasive angiography have previously demonstrated to further stratify diabetic patients with more advanced CAD [17]. We hypothesized that this could also be the case for diabetics with less severe CAD, using the comprehensive information derived from CCTA on the presence, localization, degree of stenosis and plaque composition.

Several different aspects of coronary disease are reflected in these scores: prevalence and severity (*any plaque and obstructive CAD*), number of plaques (*SIS*), number and distribution (*plaque in LM-3v-2v with prox. LAD*), number and stenosis severity (*SSS*), absolute and relative amount of calcified plaque (CaSc ≥100 and ≥75th percentile) and localization, stenosis severity and type of plaque (CT-Le score). All the coronary atherosclerotic burden indexes were significantly higher in diabetics as compared to nondiabetics, reflecting the higher prevalence as well as the more severe coronary disease of this subset of patients and they can be useful as noninvasive imaging tools for risk stratification. Some of these indexes have already been prognostically validated and demonstrated a good correlation with major cardiovascular events [13, 18, 19]. In our view, since the prevalence of plaque is very high, even in this predominantly low-to-intermediate CAD probability population, these coronary atherosclerotic burden indexes can help risk stratify patients and should ideally be included in the CCTA report. However, since they convey information on different aspects of CAD, with some overlap in the information they provide and, in clinical practice, reporting on all of them is not suitable, ideally we should be able to decide in the future which one(s) should be routinely used, based on their prognostic performance.

Anatomical distribution and plaque composition

In this report, the higher prevalence of plaques in diabetic patients was seen in the left main as well as in the other 3 coronary territories and in both proximal and distal locations. Regarding the left main and the other proximal locations, we observed a higher percentage of plaques in diabetics as compared to nondiabetics. This is in line with previous studies linking the geographic distribution of myocardial infarction culprit lesions to more proximal locations in the coronary tree [20] and could explain the higher incidence of coronary events experienced by diabetic patients.

One interesting finding in our study is related to the relative geographic localization of plaques in diabetics as compared to patients without diabetes.

Although in prevalence of evaluable segments, diabetics had more plaques in every location (both proximal and distal) compared to nondiabetics, the relative geographic plaque distribution was different in the two subgroups of patients, since diabetics had a ratio of "proximal-to-distal relative plaque distribution" of 0.75 (vs. 1.04 for nondiabetics), suggesting a higher predisposition to disease involvement of the more distal segments. This finding, on a *per segment* analysis, together with the higher prevalence of a SIS >5 on the *per patient* analysis reflects the more diffuse nature of coronary atherosclerotic burden of diabetic patients.

As diabetic patients are considered to be a model of more advanced CAD, this could suggest that as the coronary atherosclerosis progresses, distal segments become more involved by disease, although serial measurements in time would be the ideal setting to evaluate this hypothesis.

The *per segment* analysis allowed also the evaluation of the plaque composition. Diabetic patients had a significantly higher prevalence of segments with both calcified and noncalcified or mixed plaques, in both more proximal or more distal locations. The proportion of calcified to noncalcified or mixed plaques was the same for both subgroups of patients.

Limitations

There are a number of limitations related to this report:

1. This is a single center data with medium size cohort;

cont.

Manuscrito 9

2. The population included in our study was mainly composed of patients with low to intermediate CAD probability and CV risk, as this reflects daily practice of CCTA being used as a gatekeeper to exclude obstructive CAD and are in line with the recommendations. Since coronary plaques were present in nearly 60 % of the patients, this was an opportunity to evaluate the coronary atherosclerotic burden pattern of DM patients at earlier stages.
3. There were some differences in the baseline characteristics of the two subgroups of patients, that could have contributed to the higher disease extent observed in diabetic patients. Nevertheless, after adjusting for those differences, diabetes remained an independent predictor of both the presence and severity of CAD.
4. Since patients were referred for CCTA because of symptoms and/or the results of stress tests, some referral bias has to be acknowledged.

Conclusions

Diabetes was an independent predictor of CAD and was also associated with more advanced CAD, evaluated by indexes of coronary atherosclerotic burden.

The comprehensive information regarding the presence, severity and type of plaque noninvasively provided by CCTA, has made possible a detailed characterization of the coronary disease pattern of diabetic patients at an earlier stage of disease.

Diabetics had a significantly higher prevalence of plaques in every anatomical subset (type of vessel and both proximal or distal localizations) and for the different plaque composition (both calcified and noncalcified or mixed). In this report, the relative geographic distribution of the plaques within each subgroup, favored a more mid-to-distal localization in the diabetic patients.

Conflict of interest None.

References

1. Buse JB, Ginsberg HN, Bakris GL, Clark NG, Costa F, Eckel R et al (2007) Primary prevention of cardiovascular diseases in people with diabetes mellitus: a scientific statement from the American Heart Association and the American Diabetes Association. Circulation 115(1):114–126
2. Ryden L, Standl E, Bartnik M, Van den Berghe G, Betteridge J, de Boer MJ et al (2007) Guidelines on diabetes, pre-diabetes, and cardiovascular diseases: executive summary. The task force on diabetes and cardiovascular diseases of the European Society of Cardiology (ESC) and of the European Association for the Study of Diabetes (EASD). Eur Heart J 28(1):88–136
3. De Berardis G, Sacco M, Strippoli GF, Pellegrini F, Graziano G, Tognoni G et al (2009) Aspirin for primary prevention of cardiovascular events in people with diabetes: meta-analysis of randomised controlled trials. BMJ 339:b4531
4. Perk J, De Backer G, Gohlke H, Graham I, Reiner Z, Verschuren M et al (2012) European Guidelines on cardiovascular disease prevention in clinical practice (version 2012). The Fifth Joint Task Force of the European Society of Cardiology and Other Societies on Cardiovascular Disease Prevention in Clinical Practice (constituted by representatives of nine societies and by invited experts). Developed with the special contribution of the European Association for Cardiovascular Prevention & Rehabilitation (EACPR). Eur Heart J 33(13):1635–1701
5. Taylor AJ, Cerqueira M, Hodgson JM, Mark D, Min J, O'Gara P et al (2010) ACCF/SCCT/ACR/AHA/ASE/ASNC/NASCI/SCAI/SCMR 2010 appropriate use criteria for cardiac computed tomography. A report of the American College of Cardiology Foundation Appropriate Use Criteria Task Force, the Society of Cardiovascular Computed Tomography, the American College of Radiology, the American Heart Association, the American Society of Echocardiography, the American Society of Nuclear Cardiology, the North American Society for Cardiovascular Imaging, the Society for Cardiovascular Angiography and Interventions, and the Society for Cardiovascular Magnetic Resonance. J Am Coll Cardiol 56(22):1864–1894
6. (1997) Report of the Expert Committee on the Diagnosis and Classification of Diabetes Mellitus. Diabetes Care 20(7): 1183–1197
7. Expert Panel on Detection E (2001) Treatment of high blood cholesterol in A. Executive summary of the third report of the national cholesterol education program (NCEP) expert panel on detection, evaluation, and treatment of high blood cholesterol in adults (adult treatment panel III). JAMA 285(19):2486–2497
8. European Society of Hypertension-European Society of Cardiology Guidelines C (2003) European Society of Hypertension-European Society of Cardiology guidelines for the management of arterial hypertension. J Hypertens 21(6):1011–1053
9. Taylor AJ, Bindeman J, Feuerstein I, Cao F, Brazaitis M, O'Malley PG (2005) Coronary calcium independently predicts incident premature coronary heart disease over measured cardiovascular risk factors: mean three-year outcomes in the prospective army coronary calcium (PACC) project. J Am Coll Cardiol 46(5):807–814
10. Genders TS, Steyerberg EW, Alkadhi H, Leschka S, Desbiolles L, Nieman K et al (2011) A clinical prediction rule for the diagnosis of coronary artery disease: validation, updating, and extension. Eur Heart J 32(11):1316–1330
11. Morise AP, Haddad WJ, Beckner D (1997) Development and validation of a clinical score to estimate the probability of coronary artery disease in men and women presenting with suspected coronary disease. Am J Med 102(4):350–356
12. Raff GL, Abidov A, Achenbach S, Berman DS, Boxt LM, Budoff MJ et al (2009) SCCT guidelines for the interpretation and reporting of coronary computed tomographic angiography. J Cardiovasc Comput Tomogr 3(2):122–136
13. Min JK, Shaw LJ, Devereux RB, Okin PM, Weinsaft JW, Russo DJ et al (2007) Prognostic value of multidetector coronary computed tomographic angiography for prediction of all-cause mortality. J Am Coll Cardiol 50(12):1161–1170
14. Hoff JA, Chomka EV, Krainik AJ, Daviglus M, Rich S, Kondos GT (2001) Age and gender distributions of coronary artery calcium detected by electron beam tomography in 35,246 adults. Am J Cardiol 87(12):1335–1339
15. Evangelista V, Totani L, Rotondo S, Lorenzet R, Tognoni G, De Berardis G et al (2005) Prevention of cardiovascular disease in

cont.

type-2 diabetes: how to improve the clinical efficacy of aspirin. Thromb Haemost 93(1):8–16
16. Saely CH, Aczel S, Koch L, Schmid F, Marte T, Huber K et al (2010) Diabetes as a coronary artery disease risk equivalent: before a change of paradigm? Eur J Cardiovasc Prev Rehabil 17(1):94–99
17. Mack MJ, Banning AP, Serruys PW, Morice MC, Taeymans Y, Van Nooten G et al (2011) Bypass versus drug-eluting stents at three years in SYNTAX patients with diabetes mellitus or metabolic syndrome. Ann Thorac Surg 92(6):2140–2146
18. Andreini D, Pontone G, Mushtaq S, Bartorelli AL, Bertella E, Antonioli L et al (2012) A long-term prognostic value of coronary CT angiography in suspected coronary artery disease. JACC Cardiovasc Imaging 5(7):690–701
19. Min JK, Dunning A, Lin FY, Achenbach S, Al-Mallah M, Budoff MJ et al (2011) Age- and sex-related differences in all-cause mortality risk based on coronary computed tomography angiography findings results from the international multicenter CONFIRM (coronary CT angiography evaluation for clinical outcomes: an international multicenter registry) of 23,854 patients without known coronary artery disease. J Am Coll Cardiol 58(8):849–860
20. Wang JC, Normand SL, Mauri L, Kuntz RE (2004) Coronary artery spatial distribution of acute myocardial infarction occlusions. Circulation 110(3):278–284

MANUSCRITO 10

Prevalence and predictors of coronary artery disease in patients with a calcium score of zero

de Carvalho, M. S., de Araujo Goncalves, P., Garcia-Garcia, H. M., de Sousa, P. J., Dores, H., Ferreira, A., Cardim, N., Carmo, M. M., Aleixo, A., Mendes, M., Machado, F. P., Roquette, J., and **Marques**, **H**.,

Int J Cardiovasc Imaging, 2013
29(8): p. 1839-46

Manuscrito 10

Int J Cardiovasc Imaging (2013) 29:1839–1846
DOI 10.1007/s10554-013-0267-x

ORIGINAL PAPER

Prevalence and predictors of coronary artery disease in patients with a calcium score of zero

Maria Salomé Leal de Carvalho · Pedro de Araújo Gonçalves · Hector M. Garcia-Garcia · Pedro Jerónimo de Sousa · Helder Dores · António Ferreira · Nuno Cardim · Miguel Mota Carmo · Ana Aleixo · Miguel Mendes · Francisco Pereira Machado · José Roquette · Hugo Marques

Received: 15 March 2013 / Accepted: 19 July 2013 / Published online: 26 July 2013

Abstract The absence of coronary calcification is associated with an excellent prognosis. However, a calcium score of zero does not exclude the presence of coronary artery disease (CAD) or the possibility of future cardiovascular events. Our aim was to study the prevalence and predictors of coronary artery disease in patients with a calcium score of zero. Prospective registry consisted of 3,012 consecutive patients that underwent cardiac CT (dual source CT). Stable patients referred for evaluation of possible CAD that had a calcium score of zero (n = 864) were selected for this analysis. The variables that were statistically significant were included in a multivariable logistic regression model. From 864 patients with a calcium score of zero, 107 (12.4 %) had coronary plaques on the contrast CT (10.8 %, n = 93 with nonobstructive CAD and 1.6 %, n = 14 with obstructive CAD). By logistic regression analysis, the independent predictors of CAD in this population were age >55 years [odds ratio (OR) 1.63 (1.05–2.52)], hypertension [OR 1.64 (1.05–2.56)] and dyslipidemia [OR 1.54 (1.00–2.36)]. In the presence of these 3 variables, the probability of having coronary plaques was 21 %. The absence of coronary artery calcification does not exclude the presence of coronary artery disease, but the prevalence of obstructive disease is very low. In this population, the independent predictors of CAD in the setting of a calcium score of zero were hypertension, dyslipidemia, and age above 55 years. In the presence of these 3 predictors, the probability of having CAD was almost 2 times higher than in the general population.

Keywords Zero calcium score · Coronary artery disease · Noncalcified plaque

M. S. L. de Carvalho (✉) · P. de Araújo Gonçalves · P. J. de Sousa · H. Dores · A. Aleixo · M. Mendes
Centro Hospitalar Lisboa Ocidental, Lisboa, Portugal
e-mail: mariasalomecarvalho@gmail.com

P. de Araújo Gonçalves · A. Ferreira · N. Cardim · F. P. Machado · J. Roquette · H. Marques
Hospital da Luz, Lisboa, Portugal

P. de Araújo Gonçalves · M. M. Carmo · A. Aleixo
CEDOC – Chronic Diseases Research Center – FCM-Nova, Lisboa, Portugal

H. M. Garcia-Garcia
Thoraxcenter, Erasmus MC, Rotterdam, The Netherlands

Introduction

Coronary artery disease (CAD) is a major cause of death in developed countries and it is expected to remain the most important disease in the upcoming years [1].

Quantification of coronary artery calcium [calcium scoring (CaSc)] can provide a measure of the atherosclerotic plaque burden, since coronary arterial calcification occurs almost exclusively in atherosclerotic plaques [2, 3]. Also, it has been demonstrated in many large clinical trials, that CaSc is a strong predictor of cardiovascular events [4–7].

On the other hand, the absence of calcium in the coronary arteries, although it does not rule out atherosclerotic disease, is consistent with an excellent long-term prognosis [8] and has a high sensitivity and negative predictive value for excluding obstructive CAD. This fact prompted some recent guidelines to suggest that a calcium score of zero might exclude the need for coronary angiography in symptomatic patients [9]. Nevertheless, in previous studies, a high variation was reported in the incidence of obstructive CAD in patients with a CaSc of zero, ranging from 2 to 32 % [10–15]. For instance, in the recent CONFIRM registry, it was shown that in patients with a CaSc of zero, obstructive CAD is

cont.

Manuscrito 10

possible and is associated with increased cardiovascular events [16]. The aim of this study was to assess the prevalence and predictors of coronary artery disease in a population of stable patients referred for evaluation of possible CAD who had a calcium score of zero.

Methods

Study design and patient population

Single center prospective registry including 3,012 consecutive patients undergoing dual source coronary CT angiography (CCTA) from February 2007 to March 2012. For this analysis, 864 stable patients (with symptoms and/or positive or inconclusive stress tests) referred for evaluation of possible CAD that had a calcium score of zero were included.

Exclusion criteria included: (1) preoperative CAD assessment prior to noncoronary valvular or aortic surgery (n = 51); (2) evaluation of possible CAD in cardiomyopathies (dilated cardiomyopathy or hypertrophic cardiomyopathy) (n = 162); (3) cardiac CT for atrial fibrillation ablation (n = 330); (4) previous myocardial infarction and/or revascularization procedures (n = 257); (5) suspected ACS (n = 70); (6) other indications (n = 102). Patients with atrial fibrillation or other significant arrhythmias during scan acquisition or artifacts that significantly compromised image quality were also excluded, as every patient with a CaSc >0 (Fig. 1).

The study was approved by the local ethics committee and all patients gave a written informed consent.

A detailed medical history with a questionnaire investigating risk factors was obtained from the patients to assess for the presence of: (1) Diabetes mellitus (defined as a fasting glucose level of ≥126 mg/dl or the need for insulin or oral hypoglycemic agents) [17]; (2) Dyslipidemia (defined as a total cholesterol level ≥200 mg/dl or treatment with lipid-lowering drugs) [18]; (3) Hypertension (defined as blood pressure ≥140/90 mmHg or the use of antihypertensive medication) [19]; (4) Obesity (body mass index ≥30 kg/m^2); (5) positive family history of premature CAD (defined as the presence of CAD in first-degree relatives younger than 55 (male) or 65 (female) years of age) [20]; (6) smoking (defined as previous (less <1 year) or current smoker).

Pre-test probability of CAD was determined using both the modified Diamond and Forrester [21] and the Morise score [22]. The cardiovascular risk was assessed with the Heart Score [23]. In the modified Diamond–Forrester, patients were classified into very low (<5 %), low (<10 %), intermediate (10–90 %) and high probability (>90 %). For the Morise score, patients were classified into low (scores 0–8), intermediate (scores 9–15) and high probability (scores ≥16). For the Heart Score, the cut-off of ≥5 % (high-risk) was used.

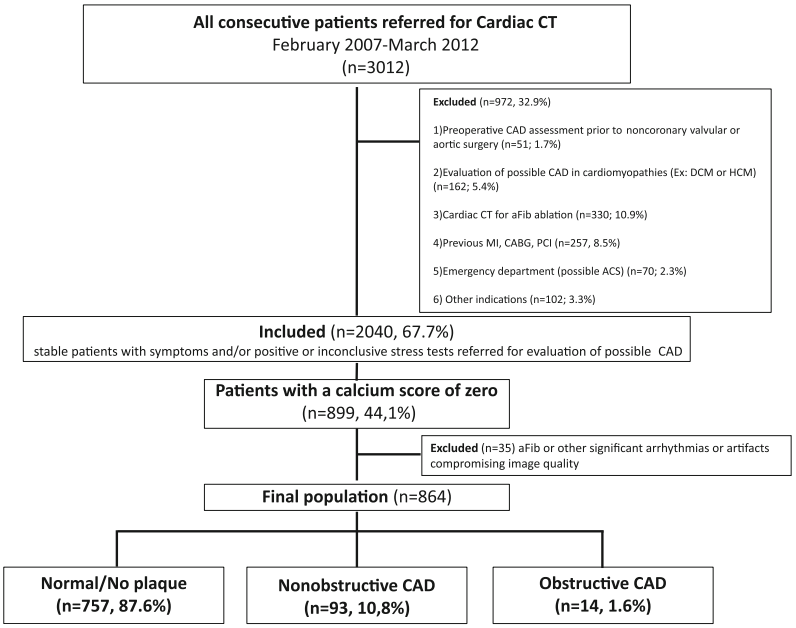

Fig. 1 Patient selection and study design

cont.

Manuscrito 10

Scan protocol and image reconstruction

All scans were performed with the first generation of dual-source scanner (Somatom Definition, Siemens Medical, Germany), with the patient in dorsal decubitus and in deep inspiration breath-hold.

The calcium score acquisition consisted of step and shoot—prospective ECG triggering at 70 % of the R–R interval if the heart rate was below 80 beats per min (bpm) or at 40 % of the R–R interval if the heart rate was higher. From the topogram, a cranio-caudal scan was obtained from the carina to the plane just below the heart *silhouette*, with 120 kV and 128 mAs/rot tube current, with CARE-Dose 4D mAs modulation. The value of the calcium score was obtained with the analysis of consecutive non-contrast 3 mm slices, with a reconstruction b35f Kernel and a small (cardiac) FOV, with a dedicated software (CaSc–Siemens), where every area at least with 3 mm^2 within a coronary vessel with a density above 130 HU (Hounsfield Units) was selected.

For CCTA, sublingual nitroglycerin was administered to all patients, except when contraindicated, and intravenous metoprolol (5 mg, with a titration dose up to 20 mg) was administered in patients with heart rate >70 bpm.

During the scan acquisition, a bolus of iodinated contrast was injected at a 6 ml/s infusion rate, followed by a 50-ml saline flush. The dose of contrast was calculated according to the following formula: (acquisition time + 6 s delay) × flow (6 ml/s). A ROI was defined in the ascending aorta for the bolus trigger technique, set at 120 HU.

Dose reduction strategies—including electrocardiogram-gated tube current modulation, reduced tube voltage, and prospective axial triggering—were used whenever feasible.

Mean estimated radiation dose was 0.8 ± 0.5 mSv for CaSc and 4.6 ± 3.8 mSv for CT scan. Mean contrast dose was 96.2 ± 13.6 ml and heart rate was 67.8 ± 12.9 bpm.

Transaxial images were reconstructed with a temporal resolution of 83 ms and slice thickness of 0.75 mm with 0.4 mm increments. Post-processing was carried out using Circulation® software, with multiplanar reconstructions, maximum intensity projection and volume rendering technique. All scans were analysed independently in the same session by both a cardiologist and a radiologist with level III equivalent experience by the Society of Cardiovascular Computed Tomography. In case of disagreement, a joint reading was performed and a consensus decision was reached.

In each coronary artery segment, coronary atherosclerosis was defined as tissue structures >1 mm^2 that existed either within the coronary artery lumen or adjacent to the coronary artery lumen that could be discriminated from surrounding pericardial tissue, epicardial fat, or the vessel lumen itself [24]. Coronary atherosclerotic lesions were quantified for stenosis by visual estimation. Percent obstruction of coronary artery lumen was based on a comparison of the luminal diameter of the segment exhibiting obstruction to the luminal diameter of the most normal-appearing site immediately proximal to the plaque. Obstructive CAD was defined by presence of at least one plaque with ≥50 % stenosis.

Statistical analysis

Continuous variables with normal distribution were expressed as mean ± standard deviation. Categorical variables were expressed as percentages and their frequencies were compared with the Chi square test.

Binary logistic regression models were built to elucidate independent predictors of CAD without coronary calcification.

The objective of this model was the assessment of clinical variables that aid to predict the presence of CAD in patients with a calcium score of zero. All the demographic, risk factors and clinical variables present in Table 2 that had a p <0.1 in univariate analysis were included in a multivariate logistic regression model (Enter method).

Statistical analysis was performed with SPSS 17.0 software for Windows (SPSS Inc., Chicago, IL, USA).

Results

Baseline and procedural characteristics

In the final study population of 864 patients, most of the patients were female (55 %) and mean age was 53.8 ± 11.0 years. The prevalence of traditional risk factors was low, with only 9.0 % of patients with diabetes. This was predominantly a low risk population with few high risk patients (only 9.0 % with the Morise score and 3.1 % with the modified Diamond–Forrester had a high CAD probability). Likewise, most of the patients were not considered as high cardiovascular risk, as assessed by the Heart Score (only 11.9 % had a Heart Score ≥5 %)—Table 1.

Coronary plaques were detected on CCTA in 107 patients (12.4 %): 10.8 % (n = 93) with nonobstructive CAD and 1.6 % (n = 14) with obstructive CAD—Fig. 2. Considering the degree of stenosis of the obstructive CAD group, 64 % (n = 9) had a 50–70 % stenosis and 36 % (n = 5) a >70 % stenosis. Considering the extent of disease, all these patients had obstructive CAD in only 1 vessel and 93 % had a single lesion. Regarding the distribution, most of the obstructive CAD lesions were found in proximal or mid segment locations (87 %), and the most affected artery was the right coronary artery 50 % (n = 7).

cont.

Manuscrito 10

Table 1 Demographic, clinical and CCTA characteristics of the study population

	All patients (n = 864)
Demographic	
Age	53.8 ± 11.0
Male sex	389 (45.0)
Risk factors	
Obesity (BMI ≥ 30)	160 (18.5)
Diabetes	78 (9.0)
Hypertension	459 (53.1)
Dyslipidemia	454 (52.5)
Smoking	206 (23.8)
Family history of premature CAD	284 (32.9)
Chest pain	
Asymptomatic	441 (51.0)
Noncardiac	194 (22.5)
Atypical	182 (21.1)
Typical	47 (5.4)
CAD probability—Morise	
Score ≥16	78 (9.0)
Score 9–15	446 (51.6)
Score 0–8	340 (39.4)
CAD probability—modified Diamond Forrester	
Very low	188 (21.8)
Low	391 (45.3)
Intermediate	257 (29.7)
High	27 (3.1)
CV risk	
Heart Score ≥5 %	103 (11.9)
CCTA	
Normal/no plaque	757 (87.6)
Non obstructive CAD	93 (10.8)
Obstructive CAD	14 (1.6)
Technical data	
Heart rate (bpm)	67.8 ± 12.9
Contrast dose (ml)	96.2 ± 13.6
Radiation dose—CTA (mSv)	4.6 ± 3.8
Radiation dose—CaSc (mSv)	0.8 ± 0.5

Values are mean ± SD or n (%)

BMI body mass index, *CAD* coronary artery disease, *CV* cardiovascular, *CCTA* coronary computed tomography angiography, *bpm* beats per minute, *mSv* milisievert

Left anterior descendent was affected in 5 patients, while left main was affected in one patient and the circumflex artery in other patient.

There were no significant differences in the prevalence of CAD in patients referred for CCTA because of positive/inconclusive stress tests (93/722 = 12.9 %) versus patients referred without previous stress tests (14/142 = 9.9 %), $p = 0.403$.

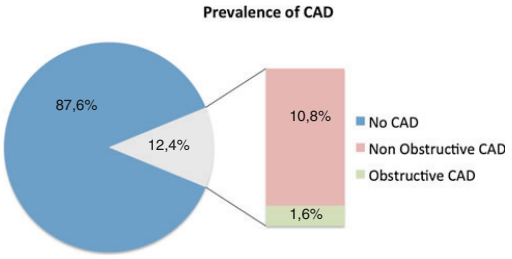

Fig. 2 Distribution of CT angiographic findings

Table 2 Prevalence of CAD according to the pretest probability (Morise)

Pretest probability	Nonobstructive CAD	Obstructive CAD
Low (n = 340)	27 (7.9 %)	6 (1.8 %)
Intermediate (n = 446)	64 (14.3 %)	6 (1.3 %)
High (n = 78)	16 (20.5 %)	2 (2.6 %)
p	0.002	0.708

We further analyzed the distribution of CAD in the different pretest probability subgroups. Using those defined by Morise, the prevalence of CAD (any plaque) was 7.9, 14.3 and 20.5 % in low, intermediate and high pretest probability patients, respectively. Regarding obstructive CAD, a higher prevalence was also found in patients with high pretest probability, but this increase was not statistically significant (Table 2).

Univariate analysis

Patients with CAD were older (prevalence of age ≥55 years 64 vs. 47 %, $p = 0.001$) than patients without CAD and had a higher prevalence of dyslipidemia (65 vs. 51 %, $p = 0.010$) and hypertension (67 vs. 51 %, $p = 0.002$).

The pre-test CAD probability assessed both by the Morise score and the modified Diamond–Forrester was higher in the CAD group and these patients had a 2–4 times higher probability of being of a high CAD probability group. Cardiovascular risk, estimated by the Heart Score, was also significantly higher in patients with CAD. Although there was a trend in this group towards a higher prevalence of diabetes and male gender, these differences were not statistically significant—Table 3.

Multivariate analysis

By multivariate analysis, the independent predictors of CAD in patients with a calcium score of zero were age ≥55 (OR 1.631, 95 % CI 1.054–2.524, $p = 0.028$), hypertension (OR

cont.

Table 3 Univariate analysis

	No CAD (n = 757)	CAD (n = 107)	*p*
Demographic			
Age ≥55 years	355 (47.0)	68 (63.6)	**0.001**
Male gender	335 (44.3)	54 (50.5)	0.254
Risk factors			
Diabetes	64 (8.5)	14 (13.1)	0.147
Obesity (BMI ≥ 30)	139 (18.4)	21 (19.6)	0.790
Hypertension	387 (51.1)	72 (67.3)	**0.002**
Dyslipidemia	385 (50.9)	69 (64.5)	**0.010**
Smoking	184 (24.3)	22 (20.6)	0.467
Family history of premature CAD	248 (32.8)	36 (33.6)	0.913
Symptoms			
Chest pain	371 (49.0)	52 (48.6)	1.000
CAD probability—Morise			
Score ≥16	62 (8.2)	16 (15.0)	**0.002**
Score 9–15	382 (50.5)	64 (59.8)	
Score 0–8	313 (41.3)	27 (25.2)	
CAD probability—modified Diamond Forrester			
Very low	171 (22.6 %)	17 (15.9)	**0.005**
Low	342 (45.2)	49 (45.8)	
Intermediate	225 (29.8)	32 (29.9)	
High	18 (2.4)	9 (8.4)	
CV risk			
Heart Score ≥5	79 (10.4)	24 (22.4)	**0.001**

Values are mean ± SD or n (%)

CAD coronary artery disease, *BMI* body mass index, *CV* cardiovascular

Bold indicates *p* value with statistical significance

1.641, 95 % CI 1.051–2.560, $p = 0.029$) and dyslipidemia (OR 1.538, 95 % CI 1.002–2.361, $p = 0.049$) (Fig. 3). In the presence of these 3 variables (n = 176 patients, 20.4 % of the population), the probability of having coronary plaques was 21 % (vs. 12.4 % in the total studied population). We also analyzed the prevalence of CAD according to the presence of none, one, two or three of these risk factors. The results are shown in Table 4.

Discussion

In this single center cohort of stable patients without known CAD, referred for cardiac CT angiography, we found a very low prevalence of obstructive CAD (1.6 %) in the subset with a CaSc of zero. When considering the degree of stenosis, only 0.6 % had a stenosis >70 %.

The prevalence and clinical significance of obstructive CAD on coronary CT angiography among patients with a

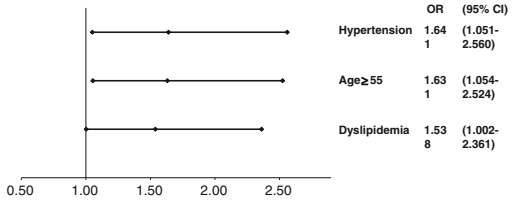

Fig. 3 Independent predictors of CAD in patients with a CaSc of zero

calcium score of zero has been evaluated in several cohorts, but with conflicting results, depending on the population included. Data from Nieman et al. [14], the CONFIRM registry [16], Rubinshtein et al. [13] and Akram et al. [11], are in line with our results, with a low prevalence of obstructive CAD (2, 3.5, 7.2 and 8.2 %, respectively). Our prevalence was even lower, and this might be explained by a high prevalence of patients with a low pretest probability of CAD.

In contrast, in the work of Harberl et al. [10] and Gottlieb et al. [12], there was a high prevalence of CAD (32 and 19.4 %, respectively), which can be related to the fact that these studies included patients referred for conventional angiography, including patients with possible acute coronary syndromes.

In our population, the prevalence of CAD in patients with positive/inconclusive stress tests (exercise electrocardiography in most cases) was not significantly different from that of patients referred to CCTA without previous tests, as in the study from Nieman et al. [14].

Calcium scoring enables a noninvasive quantification of the total coronary atherosclerotic burden, although it underestimates the burden of disease, by not measuring noncalcified plaques [25]. Nevertheless, it has been shown to outperform traditional risk stratification tools, such as clinical risk factor assessment, ankle-brachial index, carotid intima-media thickness and high-sensitivity C-reactive protein, as a predictor of cardiovascular events [4, 5].

Our data suggests that, although the absence of calcium does not exclude the presence of CAD, it was associated with a very low probability of obstructive lesions. This was especially true in cases of low and intermediate pretest CAD probability, as in the study from Werkhoven et al. [15] in which the prevalence of obstructive CAD, in the absence of calcium, was only 3.4 and 3.8 % in patients with low and intermediate pretest CAD probability, respectively. This is in line with the excellent prognosis that has been demonstrated for patients with a calcium score of zero [8].

In our population, older age (≥55 years), hypertension and dyslipidemia were independent predictors of CAD in

cont.

Manuscrito 10

Table 4 Prevalence of CAD according to the presence of risk factors found to be independent predictors

Independent preditors	No CAD	Nonobstructive CAD	Obstructive CAD	Total	*p*
0	158 (96.9 %)	5 (3.1 %)	0 (0 %)	163	<0.001
1	210 (86.8 %)	25 (10.3 %)	7 (2.9 %)	242	
2	250 (88.3 %)	28 (9.9 %)	5 (1.8 %)	283	
3	139 (79.0 %)	35 (19.9 %)	2 (1.1 %)	176	
	757	93	14	864	

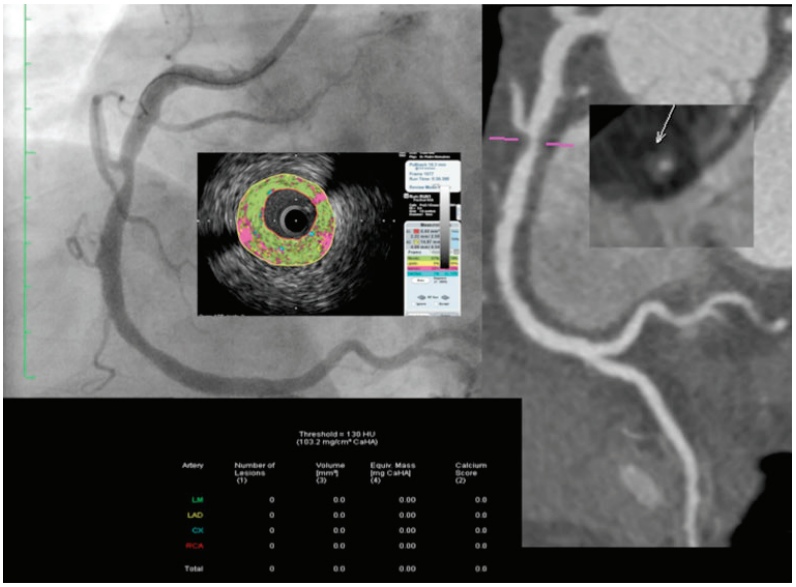

Fig. 4 Non-calcified plaque on cardiac CT (on the *right*) in a patient with a CaSc of zero; the angiography (on the *left*) confirmed the presence of a 50–70 % stenosis in the mid-RCA; intravascular ultrasound with virtual histology (in the *middle*) suggests the presence of microcalcifications

this subset of patients without calcium, and in the presence of these 3 predictors, the probability of having CAD was almost 2 times higher than in the general population. Nevertheless, the odds ratios for the independent predictors were rather modest and other traditional CAD risk factors were not found to be independent predictors. This way, we could hypothesize that coronary plaques without calcium could be a different phenotypical subset of CAD. Another possibility could be that these patients with coronary plaques in the absence of calcium represent CAD at earlier stages, since calcium is considered to be associated with more advanced forms of atherosclerotic lesions [2]. In fact, in our population, all the patients with obstructive CAD had only 1 vessel disease, most (93 %) with a single lesion, and only a minority (36 %) had >70 % stenosis.

One last hypothesis could be that these plaques can have microcalcifications below the threshold of cardiac CT spacial resolution, as in the case example (Fig. 4), in which small spots of calcium were only detected by intravascular ultrasound (IVUS) virtual histology.

Limitations

There are a number of limitations related to this report: (1) this is a single center retrospective study with medium size cohort; (2) our population in mainly of low CAD probability and CV risk; the very low percentage of obstructive CAD found can not be extrapolated to cohorts with more patients with higher CAD probability and CV risk (3) the definition of CAD was made using CCTA and not invasive angiography, which may lead to false-positive findings, although this is unlikely in the absence of calcium; (4) lack of prognostic information, since we did not evaluate the prognostic importance of obstructive CAD in patients with a CaSc of zero.

Manuscrito 10

Conclusions

In this population of stable patients referred for evaluation of possible CAD that had a calcium score of zero, 12.4 % had coronary plaques and 1.6 % had obstructive (≥50 %) CAD.

Therefore, and despite the known high negative predictive value of CaSc for coronary events, the absence of coronary artery calcification does not exclude the presence of coronary artery disease, but the prevalence of obstructive disease is very low.

In this population, we found that age ≥55, hypertension, dyslipidemia were independent predictors of CAD in the setting of a calcium score of zero. In the presence of these 3 predictors, the probability of having CAD was almost 2 times higher than in the total studied population.

Conflict of interest All the authors declare that they have no conflict of interest.

References

1. Lloyd-Jones D, Adams R, Carnethon M, De Simone G, Ferguson TB, Flegal K et al (2009) Heart disease and stroke statistics—2009 update: a report from the American heart association statistics committee and stroke statistics subcommittee. Circulation 119(3):480–486
2. Stary HC, Chandler AB, Dinsmore RE, Fuster V, Glagov S, Insull W Jr et al (1995) A definition of advanced types of atherosclerotic lesions, a histological classification of atherosclerosis. A report from the committee on vascular lesions of the council on arteriosclerosis, American heart association. Arterioscler Thromb Vasc Biol 15:1512–1531
3. Budoff M, Jollis JG, Dowe D, Min J for the VCT study group (2013) Diagnostic accuracy of coronary artery calcium for obstructive disease: results from the ACCURACY trial. Int J Cardiol 166(2):505–508
4. Detrano R, Guerci AD, Carr JJ, Bild DE, Burke G, Folsom AR et al (2008) Coronary calcium as a predictor of coronary events in four racial or ethnic groups. N Engl J Med 358:1336–1345
5. Yeboah J, McClelland RL, Polonsky TS, Burke GL, Sibley CT, O'Leary D et al (2012) Comparison of novel risk markers for improvement in cardiovascular risk assessment in intermediate-risk individuals. JAMA 308:788–795
6. Shaw LJ, Raggi P, Schisterman E, Berman DS, Callister TQ (2003) Prognostic value of cardiac risk factors and coronary artery calcium screening for all-cause mortality. Radiology 228(3):826–833
7. Petretta M, Daniele S, Acampa W, Imbriaco M, Pellegrino T, Messalli G et al (2012) Prognostic value of coronary artery calcium score and coronary CT angiography in patients with intermediate risk of coronary artery disease. Int J Cardiovasc Imaging 28(6):1547–1556
8. Sarwar A, Shaw LJ, Shapiro MD, Blankstein R, Hoffmann U, Cury RC et al (2009) Diagnostic and prognostic value of absence of coronary artery calcification. J Am Coll Cardiol Imaging 2:675–688
9. National Institute for Health and Clinical Excellence (2010) Chest pain of recent onset. Assessment and diagnosis of recent onset chest pain or discomfort of suspected cardiac origin. London: NICE. Available from: http://www.nice.org.uk/guidance/CG95
10. Haberl R, Tittus J, Böhme E, Czernik A, Richartz BM, Buck J et al (2005) Multislice spiral computed tomographic angiography of coronary arteries in patients with suspected coronary artery disease: an effective filter before catheter angiography? Am Heart J 149:1112–1119
11. Akram K, O'Donnell RE, King S, Superko HR, Agatston A, Voros S (2009) Influence of symptomatic status on the prevalence of obstructive coronary artery disease in patients with zero calcium score. Atherosclerosis 203:533–537
12. Gottlieb I, Miller JM, Arbab-Zadeh A, Dewey M, Clouse ME, Sara L et al (2009) The absence of coronary calcification does not exclude obstructive coronary artery disease or the need for revascularization in patients referred for conventional coronary angiography. J Am Coll Cardiol 44:627–634
13. Rubinshtein R, Gaspar T, Halon DA, Goldstein J, Peled N, Lewis BS (2007) Prevalence and extent of obstructive coronary artery disease in patients with zero or low calcium score undergoing 64-slice cardiac multidetector computed tomography for evaluation of a chest pain syndrome. Am J Cardiol 99:472–475
14. Nieman K, Galema TW, Neefjes LA, Weustink AC, Musters P, Moelker AD et al (2009) Comparison of the value of coronary calcium detection to computed tomographic angiography and exercise testing in patients with chest pain. Am J Cardiol 104(11): 1499–1504
15. van Werkhoven J, de Boer S, Schuijf J, Cademartiri F, Maffei E, Jukema J et al (2010) Impact of clinical presentation and pretest likelihood on the relation between calcium score and computed tomographic coronary angiography. Am J Cardiol 106(12): 1675–1679
16. Villines TC, Hulten EA, Shaw LJ, Goyal M, Dunning A, Achenbach S et al (2011) Prevalence and severity of coronary artery disease and adverse events among symptomatic patients with coronary artery calcification scores of zero undergoing coronary computed tomography angiography: results from the CONFIRM (coronary CT angiography evaluation for clinical outcomes: an international multicenter) registry. J Am Coll Cardiol 58:2533–2540
17. Gavin J, Alberti K, Davidson M, DeFronzo R, Drash A, Gabbe S et al (1997) Report of the expert committee on the diagnosis and classification of diabetes mellitus. Diabet Care 20(7):1183–1197
18. Grundy S, Becker D, Clark L, Cooper R, Denke M, Howard W et al (2001) Expert panel on detection Evaluation and treatment of high blood cholesterol in Adults. Executive summary of the third report of the National Cholesterol Education Program (NCEP) expert panel on detection, evaluation, and treatment of high blood cholesterol in adults (adult treatment panel III) JAMA 285(19):2486–2497
19. European Society of Hypertension-European Society of Cardiology Guidelines C (2003) European Society of Hypertension-European Society of Cardiology guidelines for the management of arterial hypertension (2003). J Hypertens 21(6):1011–1053
20. Taylor AJ, Bindeman J, Feuerstein I, Cao F, Brazaitis M, O'Malley PG (2005) Coronary calcium independently predicts incident premature coronary heart disease over measured cardiovascular risk factors: mean 3-year outcomes in 18 the prospective army coronary calcium (PACC) project. J Am Coll Cardiol 46(5):807–814
21. Gibbons RJ, Balady GJ, Bricker JT, Chaitman BR, Fletcher GF, Froelicher VF et al (2002) American college of cardiology/American heart association task force on practice guidelines (committee to update the 1997 exercise testing guidelines). ACC/AHA, guideline update for exercise testing: summary article: a report of the American college of cardiology/American heart association task force on practice guidelines. Circulation 106(14):1883–1892

cont.

Manuscrito 10

22. Morise AP, Haddad WJ, Beckner D (1997) Development and validation of a clinical score to estimate the probability of coronary artery disease in men and women presenting with suspected coronary disease. Am J Med 102(4):350–356
23. Perk J, De Backer G, Gohlke H, Graham I, Reiner Z, Verschuren M et al (2012) European Guidelines on cardiovascular disease prevention in clinical practice (version 2012): the fifth joint Task Force of the European society of cardiology and other societies on cardiovascular disease prevention in clinical practice (constituted by representatives of nine societies and by invited experts) Developed with the special contribution of the European association for cardiovascular prevention and rehabilitation (EACPR). Eur Heart J 33(13):1635–1701
24. Min JK, Shaw LJ, Devereux RB, Okin PM, Weinsaft JW, Russo DJ et al (2007) Prognostic value of multidetector coronary computed tomographic angiography for prediction of all-cause mortality. J Am Coll Cardiol 50(12):1161–1170
25. Rumberger JA, Simons DB, Fitzpatrick LA, Sheedy PF, Schwartz RS (1995) Coronary artery calcium area by electron-beam computed tomography and coronary atherosclerotic plaque area. Circulation 92:2157–2162

MANUSCRITO 11

Relationship of Hypertension to Coronary Atherosclerosis and Cardiac Events in Patients With Coronary Computed Tomographic Angiography

Nakanishi, R., Baskaran, L., Gransar, H., Budoff, M. J., Achenbach, S., Al-Mallah, M., Cademartiri, F., Callister, T.Q., Chang, H. J., Chinnaiyan, K., Chow, B. J. W., DeLago, A., Hadamitzky, M., Hausleiter, J., Cury, R., Feuchtner, G., Kim, Y. J., Leipsic, J., Kaufmann, P. A., Maffei, E., Raff, G., Shaw, L. J., Villines, T. C., Dunning, A., **Marques**, **H**., Pontone, G., Andreini, D., Rubinshtein, R., Bax, J., Jones, E., Hindoyan, N., Gomez, M., Lin, F. Y., Min, J.K., and Berman, D. S.

Hypertension, 2017
70(2): p. 293-299

Manuscrito 11

Peer Reviewed

Title:
Relationship of Hypertension to Coronary Atherosclerosis and Cardiac Events in Patients With Coronary Computed Tomographic Angiography

Journal Issue:
HYPERTENSION, 70(2)

Author:
Nakanishi, R
Baskaran, L
Gransar, H
Budoff, MJ
Achenbach, S
Al-Mallah, M
Cademartiri, F
Callister, TQ
Chang, H-J
Chinnaiyan, K
Chow, BJW
DeLago, A
Hadamitzky, M
Hausleiter, J
Cury, R
Feuchtner, G
Kim, Y-J
Leipsic, J
Kaufmann, PA
Maffei, E
Raff, G
Shaw, LJ
Villines, TC
Dunning, A
Marques, H
Pontone, G
Andreini, D
Rubinshtein, R
Bax, J
Jones, E

cont.

Manuscrito 11

Hindoyan, N
Gomez, M
Lin, FY
Min, JK
Berman, DS

Publication Date:
08-01-2017

Series:
UCLA Previously Published Works

Permalink:
http://escholarship.org/uc/item/35c5c4bg

DOI:
https://doi.org/10.1161/HYPERTENSIONAHA.117.09402

Keywords:
angiography, atherosclerosis, coronary artery disease, hypertension, risk factors

Local Identifier(s):
UCPMS ID: 2157741

Abstract:
Hypertension is an atherosclerosis factor and is associated with cardiovascular risk. We investigated the relationship between hypertension and the presence, extent, and severity of coronary atherosclerosis in coronary computed tomographic angiography and cardiac events risk. Of 17 181 patients enrolled in the CONFIRM registry (Coronary CT Angiography Evaluation for Clinical Outcomes: An International Multicenter Registry) who underwent ≥64-detector row coronary computed tomographic angiography, we identified 14 803 patients without known coronary artery disease. Of these, 1434 hypertensive patients were matched to 1434 patients without hypertension. Major adverse cardiac events risk of hypertension and non-hypertensive patients was evaluated with Cox proportional hazards models. The prognostic associations between hypertension and no-hypertension with increasing degree of coronary stenosis severity (nonobstructive or obstructive ≥50%) and extent of coronary artery disease (segment involvement score of 1-5, >5) was also assessed. Hypertension patients less commonly had no coronary atherosclerosis and more commonly had nonobstructive and 1-, 2-, and 3-vessel disease than the no-hypertension group. During a mean follow-up of 5.2±1.2 years, 180 patients experienced cardiac events, with 104 (2.0%) occurring in the hypertension group and 76 (1.5%) occurring in the no-hypertension group (hazard ratios, 1.4; 95% confidence intervals, 1.0-1.9). Compared with no-hypertension patients without coronary atherosclerosis, hypertension patients with no coronary atherosclerosis and obstructive coronary disease tended to have higher risk of cardiac events. Similar trends were observed with respect to extent of coronary artery disease. Compared with no-hypertension patients, hypertensive patients have increased presence, extent, and severity of coronary atherosclerosis and tend to have an increase in major adverse cardiac events.

cont.

Manuscrito 11

Original Article

Relationship of Hypertension to Coronary Atherosclerosis and Cardiac Events in Patients With Coronary Computed Tomographic Angiography

Rine Nakanishi, Lohendran Baskaran, Heidi Gransar, Matthew J. Budoff, Stephan Achenbach, Mouaz Al-Mallah, Filippo Cademartiri, Tracy Q. Callister, Hyuk-Jae Chang, Kavitha Chinnaiyan, Benjamin J.W. Chow, Augustin DeLago, Martin Hadamitzky, Joerg Hausleiter, Ricardo Cury, Gudrun Feuchtner, Yong-Jin Kim, Jonathon Leipsic, Philipp A. Kaufmann, Erica Maffei, Gilbert Raff, Leslee J. Shaw, Todd C. Villines, Allison Dunning, Hugo Marques, Gianluca Pontone, Daniele Andreini, Ronen Rubinshtein, Jeroen Bax, Erica Jones, Niree Hindoyan, Millie Gomez, Fay Y. Lin, James K. Min, Daniel S. Berman

Abstract—Hypertension is an atherosclerosis factor and is associated with cardiovascular risk. We investigated the relationship between hypertension and the presence, extent, and severity of coronary atherosclerosis in coronary computed tomographic angiography and cardiac events risk. Of 17 181 patients enrolled in the CONFIRM registry (Coronary CT Angiography Evaluation for Clinical Outcomes: An International Multicenter Registry) who underwent ≥64-detector row coronary computed tomographic angiography, we identified 14 803 patients without known coronary artery disease. Of these, 1434 hypertensive patients were matched to 1434 patients without hypertension. Major adverse cardiac events risk of hypertension and non-hypertensive patients was evaluated with Cox proportional hazards models. The prognostic associations between hypertension and no-hypertension with increasing degree of coronary stenosis severity (nonobstructive or obstructive ≥50%) and extent of coronary artery disease (segment involvement score of 1–5, >5) was also assessed. Hypertension patients less commonly had no coronary atherosclerosis and more commonly had nonobstructive and 1-, 2-, and 3-vessel disease than the no-hypertension group. During a mean follow-up of 5.2±1.2 years, 180 patients experienced cardiac events, with 104 (2.0%) occurring in the hypertension group and 76 (1.5%) occurring in the no-hypertension group (hazard ratios, 1.4; 95% confidence intervals, 1.0–1.9). Compared with no-hypertension patients without coronary atherosclerosis, hypertension patients with no coronary atherosclerosis and obstructive coronary disease tended to have higher risk of cardiac events. Similar trends were observed with respect to extent of coronary artery disease. Compared with no-hypertension patients, hypertensive patients have increased presence, extent, and severity of coronary atherosclerosis and tend to have an increase in major adverse cardiac events. **(*Hypertension*. 2017;70:00-00. DOI: 10.1161/HYPERTENSIONAHA.117.09402.)**

Key Words: angiography ■ atherosclerosis ■ coronary artery disease ■ hypertension ■ risk factors

Received March 16, 2017; first decision March 25, 2017; revision accepted May 14, 2017.

From the Los Angeles BioMedical Research Institute at Harbor UCLA Medical Center, Torrance, CA (R.N., M.J.B.); Departments of Imaging and Medicine, Cedars-Sinai Medical Center, Los Angeles, CA (R.N., H.G., D.S.B.); Department of Radiology, Dalio Institute of Cardiovascular Imaging, NewYork-Presbyterian Hospital and Weill Cornell Medicine (L.B., E.J., N.H., M.G., F.Y.L., J.K.M.); Department of Medicine, University of Erlangen, Germany (S.A.); King Saudbin Abdulaziz University for Health Sciences, King Abdullah International Medical Research Center, King AbdulAziz Cardiac Center, Ministry of National Guard, Health Affairs, Riyadh, Saudi Arabia (M.A.-M.); Department of Radiology, Montreal Heart Institute, Quebec, Canada (F.C., E.M.); Department of Radiology, Erasmus University Medical Center, Rotterdam, The Netherlands (F.C., E.M.); Tennessee Heart and Vascular Institute, Hendersonville (T.Q.C.); Division of Cardiology, Severance Cardiovascular Hospital and Severance Biomedical Science Institute, Yonsei University College of Medicine, Yonsei University Health System, Seoul, South Korea (H.-J.C.); William Beaumont Hospital, Royal Oaks, MI (K.C., G.R.); Department of Medicine and Radiology, University of Ottawa, Ontario, Canada (B.J.W.C.); Capitol Cardiology Associates, Albany, New York (A.D.); Department of Radiology and Nuclear Medicine, German Heart Center Munich, Germany (M.H.); Medizinische Klinik und Poliklinik I, Ludwig-Maximilians-Universität München, Germany (J.H.); Baptist Cardiac and Vascular Institute, Miami, FL (R.C.); Department of Radiology, Medical University of Innsbruck, Austria (G.F.); Department of Medicine and Radiology, Seoul National University Hospital, South Korea (Y.-J.K.); Department of Medicine and Radiology, University of British Columbia, Vancouver, Canada (J.L.); Department of Nuclear Cardiology, Cardiovascular Center, University Hospital, Zurich, Switzerland (P.A.K.); Department of Cardiology, Emory University School of Medicine, Atlanta, GA (L.J.S.); Department of Medicine, Walter Reed National Military Medical Center, Bethesda, MD (T.C.V.); Duke Clinical Research Institute, Durham, NC (A.D.); UNICA, Cardiac CT and MRI Unit, Hospital da Luz, Lisbon, Portugal (H.M.); Department of Clinical Sciences and Community Health, University of Milan, Italy (G.P., D.A.); Centro Cardiologico Monzino, IRCCS, Italy (G.P., D.A.); Department of Cardiology at the Lady Davis Carmel Medical Center, The Ruth and Bruce Rappaport School of Medicine, Technion-Israel Institute of Technology, Haifa, Israel (R.R.); and Department of Cardiology, Leiden University Medical Center, HARTZ, The Netherlands (J.B.).

Correspondence to Daniel S. Berman, Cedars-Sinai Medical Center, 8700 Beverly Blvd, Los Angeles, CA 90048. E-mail Bermand@cshs.org

Hypertension **is available at http://hyper.ahajournals.org** **DOI: 10.1161/HYPERTENSIONAHA.117.09402**

cont.

Manuscrito 11

Hypertension affects almost one third of adults, including >7 million patients in the United States[1–3] and is strongly associated with cardiovascular morbidity and mortality.[4–9] Although hypertension is a well-established risk factor for coronary artery disease (CAD),[10] the relationships between hypertension and coronary atherosclerotic plaque stenosis, extent, characteristics, and major adverse cardiac events (MACE) risk have not been examined. Coronary computed tomographic angiography (CTA) has emerged as an accurate noninvasive modality to evaluate coronary atherosclerotic plaque and assess the risk of patients with suspected CAD.[11–14] In this study, we used coronary CTA to investigate the relationship between hypertension and the presence, extent, and severity of CAD and to explore whether hypertension adds to the assessment of atherosclerosis in prediction of MACE.

Methods

Study Population

From 17 181 patients enrolled in the CONFIRM (Coronary CT Angiography Evaluation for Clinical Outcomes: An International Multicenter Registry) registry between 2002 and 2011 who underwent ≥64-detector row coronary CTA at 17 centers, we identified 14 803 patients without known CAD who underwent coronary CTA. Of those, we sequentially excluded patients without information on MACE (n=6889), early revascularization <3 months after coronary CTA (n=1212), and any risk factors used for matching (n=2272), resulting in a population of 4430 patients. Hypertensive and nonhypertensive subjects were matched for age, sex, all other CAD risk factors, including diabetes mellitus, dyslipidemia, current smoking, family history, chest pain symptoms (asymptomatic, atypical, noncardiac, and typical chest pain), and dyspnea using propensity scores.[15] The resulting propensity score was then applied 1:1 to match every hypertensive subject (n=2791) to a corresponding nonhypertensive subject (n=1639) using a Mahalanobis nearest-neighbor matching algorithm with caliper <0.01.[15] After matching, 2868 patients (age 56.4±11.1 years, male 60.8%) comprised the final study population, with 1434 patients with hypertension and 1434 patients without hypertension. The study was followed by Declaration of Helsinki Guidelines, and each institution obtained Institutional Review Board approval. All patients had signed informed consent.

Prescan Risk Factor Assessment

All CAD risk factors were prospectively ascertained before the coronary CTA examination by direct patient interview by a physician or nurse research coordinator and by standardized site surveys. Hypertension was defined as a history of physician-diagnosed high blood pressure or treatment with blood pressure medications. Dyslipidemia was defined as physician-diagnosed dyslipidemia or current treatment with lipid-lowering medications. Diabetes mellitus was defined by physician-diagnosed diabetes mellitus or use of insulin or oral hypoglycemic agents. A smoking history was defined as current smoking or cessation of smoking within 3 months of testing. Family history of CAD was determined by self-report. Chest symptom characteristics (asymptomatic, atypical, noncardiac, and typical chest pain and dyspnea) were recorded.[16]

Imaging Analysis

Coronary CTA was performed using multidetector CT scanners with ≥64 slices detector rows as previously described.[14,17] CT data sets were evaluated for the presence of any plaque and plaque composition (stenosis and extent) on coronary CTA, using a modified 16-segment American Heart Association coronary tree model in accordance with the Society of Cardiovascular Computed Tomographic guidelines.[18] Coronary plaque was identified as hyperdense structure adjacent to lumen of any size or hypodense structure distinct from lumen and per-arterial tissue >1 mm^2 in largest area. Severity of luminal stenosis was classified into 3 groups: none (0% luminal stenosis), nonobstructive (1%–49% luminal stenosis), and obstructive stenosis (≥50% luminal stenosis). For per-vessel analysis, we used a 5-group categorization: no plaque, nonobstructive CAD, and presence of obstructive CAD in 1, 2, or 3 vessels. Left main disease was categorized as a 3-vessel CAD equivalent. For measures of CAD extent and distribution, the segment involvement score (SIS) was defined as the total number of coronary artery segments involved with any plaque.[13] For per-location analysis, we used a 5-group categorization: left main, proximal, mid and distal coronary segments, and side branches, including diagonal branches, obtuse marginal branches, posterior descending artery, and posterior lateral branch. Detected plaques were visually classified as noncalcified plaque (containing no calcification), partially calcified plaque (containing calcification and noncalcified plaque), or calcified plaque (containing only calcification).

Statistical Analysis

Continuous variables were expressed as the mean±SD. The Wilcoxon rank-sum test (for nonparametrically distributed variables) was used to conduct intergroup comparisons between no-hypertension and hypertension groups. Categorical variables were compared using Pearson χ^2 tests.

MACE was defined as all-cause death or nonfatal myocardial infarction. Myocardial infarction was defined by site physicians in accordance with American College of Cardiology/American Heart Association guidelines and the World Health Organization Universal Definition of Myocardial Infarction.[19,20] The log-rank test was used for comparing MACE event rates between the hypertension and no-hypertension groups, and MACE-free survival was further assessed using Cox proportional hazards models and Kaplan–Meier survival curves. We also assessed MACE risk by Cox proportional hazards models in men and women.

In addition, degrees of stenosis severity (normal, nonobstructive, and obstructive CAD ≥50%) and extent of CAD (SIS of 0, 1–5, and >5) were assessed among no-hypertension and hypertension groups in relation to time to MACE by Cox proportional hazards models. Scaled Schoenfeld residuals were used to verify the assumption of proportional hazards of the Cox models.[21] Hazard ratios (HRs) and 95% confidence intervals (CIs) were calculated from the Cox models. Area under the curves (AUC) by receiver operator characteristics for prediction of MACE were used to evaluate the added value of hypertension over assessment of coronary atherosclerosis alone (≥50% stenosis or SIS) or the combination of coronary atherosclerosis and clinical factors other than hypertension (other clinical factors [age, sex, diabetes mellitus, dyslipidemia, current smoking, family history, and all chest symptoms]). We also calculated continuous net reclassification index (cNRI)[22] between the models to investigate whether hypertension reclassified patients with respect to MACE risk over the combination of other clinical risk factors and atherosclerosis variables.

All statistical calculations were performed using STATA (Version 11.2; StataCorp LP, College Station, TX) for Windows.

Results

Patient Characteristics

Table 1 demonstrates the baseline characteristics among patients with and without hypertension. Propensity matching resulted in no differences between the groups in age, male sex, other CAD risk factors, and all chest symptoms (P>0.05 for all).

CAD Characteristics on Coronary CTA

Extent and severity of CAD as observed on coronary CTA in patients with and without hypertension are shown in Table 2. About plaque extent and severity stenosis, compared with the no-hypertension patients, hypertension patients manifested a greater SIS and a lower prevalence of absent

cont.

Manuscrito 11

Table 1. Clinical Characteristics (n=2868)

Clinical Characteristics	No Hypertension (n=1434)	Hypertension (n=1434)	*P* Value
Age	56.3±11.0	56.6±11.1	0.47
Male sex (%)	60.8	60.8	1.00
Diabetes mellitus (%)	7.5	8.5	0.30
Dyslipidemia (%)	48.0	49.0	0.60
Smoking (%)	16.5	18.3	0.20
Family history (%)	33.3	34.8	0.41
Chest pain status (%)			
Asymptomatic	39.8	37.7	0.17
Noncardiac	14.2	15.8	
Atypical	37.3	35.9	
Typical	8.8	10.7	
Dyspnea	12.8	14.6	0.44

Table 2. CAD Characteristics on Coronary CTA (n=2868)

CAD Characteristics on Coronary CTA	No Hypertension (n=1434)	Hypertension (n=1434)	*P* Value
SIS (median; IQR)	0 (0–2)	1 (0–3)	<0.0001
No. of vessels with plaque and ≥50% stenosis (%)			
No plaque	53.0	43.7	<0.001
Nonobstructive plaque (1%–49%)	33.3	37.7	
1-vessel disease (≥50%)	9.5	12.1	
2-vessel disease (≥50%)	2.6	4.4	
3-vessel disease (≥50%)/ Left main	1.6	2.2	
Distribution for any coronary artery disease (%)			
Left main	12.6	14.1	0.24
Proximal	38.2	46.6	<0.001
Mid	29.3	36.0	<0.001
Distal	14.1	18.6	0.002
Side branches	14.7	18.4	0.01
Distribution for coronary artery disease with ≥50% stenosis (%)			
Left main	0.3	0.6	0.18
Proximal	7.5	10.0	0.02
Mid	8.2	10.3	0.06
Distal	3.4	4.6	0.12
Side branches	4.7	7.0	0.01
Plaque characteristics (%)			
Noncalcified plaque	13.2	17.8	0.001
Partially calcified plaque	19.5	22.2	0.08
Calcified plaque	24.3	28.2	0.02

CAD indicates coronary artery disease; CTA, computed tomographic angiography; IQR, interquartile range; and SIS, segment involvement score.

plaque. Hypertension patients possessed greater prevalence of obstructive lesions in 1, 2, or 3 vessels (*P*<0.001). Hypertension patients had more ≥50% stenosis in the proximal and mid coronary arteries and side branches. On plaque characteristics, any noncalcified plaque or calcified plaque was more observed in hypertension patients compared with no-hypertension patients (Table 2).

MACE Risk

One-hundred eighty patients (6.3% of study population) experienced MACE at a mean follow-up of 5.2±1.2 years, occurring in 104 patients of the hypertension group and 76 patients of the no-hypertension group (42 deaths, 34 nonfatal myocardial infarction; 7.3% versus 5.3%, *P*=0.03; Tables 3 and 4). Kaplan–Meier curve demonstrated that MACE were more common in the hypertension versus the no-hypertension subjects (*P*<0.01; Figure 1). By Cox proportional analysis, hypertension subjects experienced higher MACE risk than no-hypertension subjects (HR, 1.4; 95% CI, 1.0–1.9; *P*=0.03). On a subanalysis by sex, in both of men and women, MACE tended to be more common in the hypertension versus the no-hypertension subjects (HR, 1.4; 95% CI, 0.9–2.0; *P*=0.12 for men, and HR, 1.4; 95% CI, 0.9–2.3; *P*=0.14 for women).

Considering the CTA findings, the risk of MACE was progressively higher in the subjects with nonobstructive CAD and those with obstructive CAD when compared with those with no-CAD (Figure 2A). A trend toward a higher odds ratio was observed among hypertension patients with normal coronary arteries; however, it did not reach statistical significance (HR, 1.9; 95% CI, 1.0–3.6; *P*=0.06). In patients with nonobstructive CAD, the HRs of the hypertension and no-hypertension groups were similar. In the obstructive CAD group, the HR in the hypertension group was only slightly higher than that in the no-hypertension group (Figure 2A).

On the extent of CAD, similar findings were observed. The risk of MACE was also progressively higher in the subjects with SIS of 1 to 5 and those with SIS of >5 when compared with those with no-CAD. The HRs of the hypertension group in the SIS of 1 to 5 and SIS of >5 groups were only slightly higher than the no-hypertension group (Figure 2B).

The incremental added value of hypertension in prediction of MACE over clinical and CTA variables is shown in Table 4. The presence of obstructive CAD was predictive of MACE (model 1; AUC, 0.648). The combination of other clinical factors increased this prediction (model 2; *P*<0.0001 for cNRI and *P*<0.0001 for AUC). When hypertension was then added (model 3), there was a significant increase in cNRI (*P*=0.03), and a trend toward increase in the AUC (*P*=0.055). Similar

Table 3. MACE Risk

MACE Risk			
MACE	No Hypertension (n=1434)	Hypertension (n=1434)	*P* Value
MACE (%, n)	5.3 (76)	7.3 (104)	0.03
Deaths (%, n)	2.9 (42)	3.9 (56)	
Nonfatal MI (%, n)	2.4 (34)	3.4 (48)	

MACE indicates major adverse cardiac events; and MI, myocardial infarction.

cont.

Manuscrito 11

Table 4. Predictors of MACE

Predictors of MACE						
Models	cNRI (95% CI)	*P* Value	% Events Reclassified	% Nonevents Reclassified	AUC	AUC *P* Value
Stenosis severity of CAD						
Model 1	…	…	…	…	0.648	
Model 2 (vs model 1)	0.39 (0.24–0.54)	<0.0001	14%, *P*=0.053	24%, *P*<0.0001	0.729	<0.0001
Model 3 (vs model 2)	0.17 (0.02–0.32)	0.03	16%, *P*=0.04	1%, *P*=0.59	0.734	0.055
Extent of CAD						
Model 4	…	…	…	…	0.678	
Model 5 (vs model 4)	0.41 (0.26–0.56)	<0.0001	17%, *P*=0.03	24%, *P*<0.0001	0.721	0.001
Model 6 (vs model 5)	0.17 (0.02–0.32)	0.03	16%, *P*=0.04	1%, *P*=0.59	0.726	0.052

Model 1: Stenosis severity ≥50%. Model 2: Age, sex, and other risk factors+stenosis severity ≥50%. Model 3: Age, sex, and other risk factors+stenosis severity ≥50%+HT. Model 4: SIS. Model 5: Age, sex, and other risk factors+SIS. Model 6: Age, sex, and other risk factors+SIS+HT. Other risk factors are diabetes mellitus, dyslipidemia, smoking, family history, and chest symptoms. AUC indicates area under the curve; CAD, coronary artery disease; CI, confidence interval; cNRI, continuous net reclassification index; HT, hypertension; MACE, major adverse cardiac events; MI, myocardial infarction; and SIS, segment involvement score.

results were observed with respect to the extent of CAD. The SIS alone was predictive MACE (model 4; AUC, 0.678). The combination of other clinical factors increased this prediction (model 5; *P*<0.0001 for cNRI and *P*=0.0001 for AUC). When hypertension was added (model 6), a significant increase in cNRI (*P*=0.03) and an increase in the AUC were observed (*P*=0.052).

Discussion

This study demonstrated that patients with hypertension had more advanced coronary atherosclerosis by coronary CTA and future MACE risk compared with those without hypertension. When stratifying by sex, there was a trend toward increased MACE risk in hypertension in both men and women. Patients with hypertension more frequently had any CAD, with higher prevalence of any CAD and of 1-, 2-, and 3-vessel obstructive CAD in each category, as well as CAD ≥50% stenosis in the proximal, mid, and side branches. Hypertension patients also had greater prevalence of any noncalcified plaque and calcified plaque. When stratifying by the extent and severity of CAD, MACE risk in the hypertension group was slightly higher than that in the non-hypertension group across the CAD categories. There was a trend toward incremental predictive value of hypertension over other risk factors and the extent or severity of CAD.

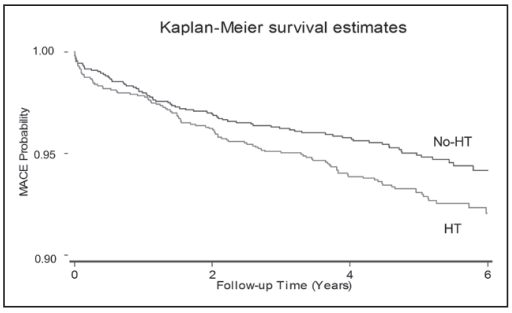

Figure 1. Kaplan–Meier curve for major adverse cardiac events (MACE) in patients with no known coronary artery disease (CAD) among the absence and presence of hypertension (HT).

It is well known that hypertension is a main cardiovascular risk factor and related to worsening prognosis.[4,5,7–9] To our knowledge, however, no previous studies have shown the direct relation of hypertension to CAD characteristics, including the presence, extent, and severity of CAD on coronary CTA and MACE risk that is described in this article.

Using the current registry, our group previously reported the relationship between diabetes mellitus and current smoking and the presence, extent, and severity of coronary atherosclerosis on coronary CTA, as well as the relationship of the coronary CTA findings to future adverse outcomes.[23,24] The findings of this study suggest that the presence of hypertension per se may not add as much incremental prognostic value as these other risk factors after taking into account the presence, extent, and severity of coronary CTA.

Hypertension has been previously shown to be a predictor of the extent of coronary atherosclerosis as assessed by coronary artery calcium.[25] Both diabetes mellitus and smoking were found to be stronger predictors of coronary atherosclerosis than hypertension. Extensive epidemiological data have also demonstrated that hypertension is an independent risk factor for coronary atherosclerosis and for future cardiac events,[26,27] but that it is less strong a predictor than diabetes mellitus and smoking.[25] Our findings are concordant with the previous data with respect to coronary atherosclerosis, including a relationship to increasing amounts of obstructive CAD and with showing a trend toward association with MACE events.

How hypertension results in increase in coronary atherosclerosis has been extensively studied. The principal underlying pathophysiologic mechanism is considered to be a mechanical one related to pulse pressure.[28] Wide pulse pressure has been reported to be associated with increased cardiac events.[29–33] Both increased pulse pressure and systolic pressure contribute to endothelial dysfunction, which facilitates the entry of low-density lipid cholesterol into the blood vessel

cont.

Manuscrito 11

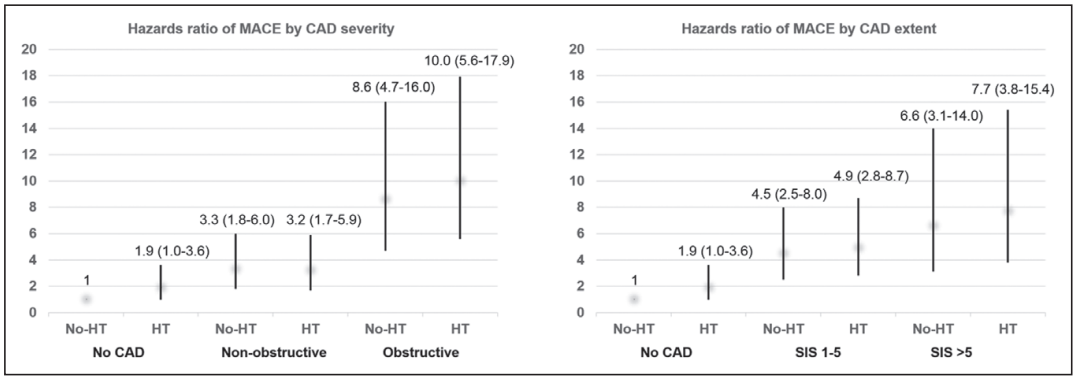

Figure 2. A, **Left**, Cox proportional hazard models by normal, nonobstructive, and obstructive coronary artery disease (CAD) among no-hypertension (no-HT) and hypertension (HT) groups. **B**, **Right**, Cox proportional hazard models by segment involvement score (SIS) 0, 1 to 5, and >5 among no-HT and HT groups.

wall, initiating the atherosclerotic process.[34] Hypertension also is a cause of left ventricular hypertrophy (LVH),[35,36] which has been implicated as a cause of coronary atherosclerosis, myocardial infarction, arrhythmia, cardiac failure, or cardiac death.[34,37–39] LVH is associated with collagen deposition within the left ventricle.[34] This process is considered to explain the frequent association of LVH with midmyocardial scarring on cardiovascular magnetic resonance, which is associated with increase in cardiac events.[40]

Of interest, in this study, in patients with no evidence of CAD on coronary CTA, those with hypertension had a >2-fold MACE risk compared to those with no-hypertension. An increased risk of events in these patients could have been related to LVH; however, information on LVH was not present in the CONFIRM database.

Limitations

There are several limitations in this study. Data on duration and severity of hypertension, as well as information on LVH, did not exist in the current registry. Information was not uniformly available on specific antihypertensive medications at the time of testing. Further, no information was available on the effectiveness of blood pressure control after testing which may have affected MACE risk.[41] We have included various CAD descriptors, including the extent, stenosis severity, basic characteristics, and location of CAD. However, other variables, such as vulnerable plaque features or bifurcation lesions, that might be associated with MACE risk were not available in this study. The number of events by sex was small and may have led to the finding that a trend toward increased MACE divided by sex was not statistically significant.

Perspectives

Compared with patients without hypertension, hypertensive patients have increased presence, extent, and severity of coronary atherosclerosis and tend to have an increase in MACE events. The findings support the concept of lifestyle modification regardless of sex to optimize CAD risk factors, including hypertension, to reduce future cardiovascular events as suggested by current guidelines.[42]

Conclusions

Hypertensive patients had greater amount of coronary atherosclerosis and greater risk of MACE compared with nonhypertensive patients, independent of other clinical risk factors and of the presence of obstructive CAD or extent of CAD. Further, hypertensive individuals with an increasing degree of CAD stenosis severity and extent of CAD experienced modestly increase rates of MACE compared with nonhypertensive patients.

Disclosures

J.K. Min received modest speakers' bureau medical advisory board compensation and significant research support from GE Healthcare. D.S. Berman received grant funding from Siemens and GE Healthcare. S. Achenbach received grant support from Siemens and Bayer Schering Pharma and has served as a consultant for Servier. M. Al-Mallah received support from the American Heart Association, BCBS Foundation of Michigan, and Astellas. F. Cademartiri has served on the Speakers' Bureau of Guerbet and is a consultant for Guerbet, Servier, and Somahlution. K. Chinnaiyan received grant support from Bayer Pharma and Blue Cross Blue Shield Blue Care MI. B.J.W. Chow received research and fellowship support from GE Healthcare, research support from Pfizer and AstraZeneca, and educational support from TeraRecon. G. Pontone received grant support from GE Healthcare and Heartflow, and has served on the Speakers' Bureau of GE Healthcare, Bracco, and Medtronic. J. Hausleiter received a research grant from Siemens Medical Systems. P.A. Kaufmann received institutional research support from GE Healthcare and grant support from Swiss National Science Foundation. G. Raff received grant support from Siemens, Blue Cross Blue Shield Blue Care MI, and Bayer Pharma. All other authors report no conflicts.

References

1. Ostchega Y, Yoon SS, Hughes J, Louis T. Hypertension awareness, treatment, and control–continued disparities in adults: United States, 2005–2006. *NCHS Data Brief*. 2008;3:1–8.
2. Centers for Disease Control and Prevention (CDC). Vital signs: prevalence, treatment, and control of hypertension–United States, 1999–2002 and 2005–2008. *MMWR Morb Mortal Wkly Rep*. 2011;60:103–108.
3. Roger VL, Go AS, Lloyd-Jones DM, et al; American Heart Association Statistics Committee and Stroke Statistics Subcommittee. Heart disease and stroke statistics–2012 update: a report from the American Heart Association. *Circulation*. 2012;125:e2–e220. doi: 10.1161/CIR.0b013e31823ac046.

cont.

Manuscrito 11

4. Ezzati M, Lopez AD, Rodgers A, Vander Hoorn S, Murray CJ; Comparative Risk Assessment Collaborating Group. Selected major risk factors and global and regional burden of disease. *Lancet*. 2002;360:1347–1360. doi: 10.1016/S0140-6736(02)11403-6.
5. Staessen JA, Gasowski J, Wang JG, Thijs L, Den Hond E, Boissel JP, Coope J, Ekbom T, Gueyffier F, Liu L, Kerlikowske K, Pocock S, Fagard RH. Risks of untreated and treated isolated systolic hypertension in the elderly: meta-analysis of outcome trials. *Lancet*. 2000;355:865–872.
6. Ezzati M, Vander Hoorn S, Lawes CM, Leach R, James WP, Lopez AD, Rodgers A, Murray CJ. Rethinking the "diseases of affluence" paradigm: global patterns of nutritional risks in relation to economic development. *PLoS Med*. 2005;2:e133. doi: 10.1371/journal.pmed.0020133.
7. Messerli FH. Hypertension and sudden cardiac death. *Am J Hypertens*. 1999;12:181S–188S.
8. Koyanagi S, Eastham C, Marcus ML. Effects of chronic hypertension and left ventricular hypertrophy on the incidence of sudden cardiac death after coronary artery occlusion in conscious dogs. *Circulation*. 1982;65:1192–1197.
9. Zipes DP, Wellens HJ. Sudden cardiac death. *Circulation*. 1998;98:2334–2351.
10. Kaplan NM, Opie LH. Controversies in hypertension. *Lancet*. 2006;367:168–176. doi: 10.1016/S0140-6736(06)67965-8.
11. Budoff MJ, Dowe D, Jollis JG, Gitter M, Sutherland J, Halamert E, Scherer M, Bellinger R, Martin A, Benton R, Delago A, Min JK. Diagnostic performance of 64-multidetector row coronary computed tomographic angiography for evaluation of coronary artery stenosis in individuals without known coronary artery disease: results from the prospective multicenter ACCURACY (Assessment by Coronary Computed Tomographic Angiography of Individuals Undergoing Invasive Coronary Angiography) trial. *J Am Coll Cardiol*. 2008;52:1724–1732. doi: 10.1016/j.jacc.2008.07.031.
12. Meijboom WB, Meijs MF, Schuijf JD, et al. Diagnostic accuracy of 64-slice computed tomography coronary angiography: a prospective, multicenter, multivendor study. *J Am Coll Cardiol*. 2008;52:2135–2144. doi: 10.1016/j.jacc.2008.08.058.
13. Min JK, Shaw LJ, Devereux RB, Okin PM, Weinsaft JW, Russo DJ, Lippolis NJ, Berman DS, Callister TQ. Prognostic value of multidetector coronary computed tomographic angiography for prediction of all-cause mortality. *J Am Coll Cardiol*. 2007;50:1161–1170. doi: 10.1016/j.jacc.2007.03.067.
14. Min JK, Dunning A, Lin FY, et al; CONFIRM Investigators. Age- and sex-related differences in all-cause mortality risk based on coronary computed tomography angiography findings results from the International Multicenter CONFIRM (Coronary CT Angiography Evaluation for Clinical Outcomes: An International Multicenter Registry) of 23,854 patients without known coronary artery disease. *J Am Coll Cardiol*. 2011;58:849–860. doi: 10.1016/j.jacc.2011.02.074.
15. Imbens G. The role of propensity score in estimating dose-response functions. 2000;87:706–710.
16. Abidov A, Rozanski A, Hachamovitch R, Hayes SW, Aboul-Enein F, Cohen I, Friedman JD, Germano G, Berman DS. Prognostic significance of dyspnea in patients referred for cardiac stress testing. *N Engl J Med*. 2005;353:1889–1898. doi: 10.1056/NEJMoa042741.
17. Min JK, Dunning A, Lin FY, et al. Rationale and design of the CONFIRM (COronary CT Angiography EvaluatioN For Clinical Outcomes: An InteRnational Multicenter) Registry. *J Cardiovasc Comput Tomogr*. 2011;5:84–92. doi: 10.1016/j.jcct.2011.01.007.
18. Abbara S, Arbab-Zadeh A, Callister TQ, Desai MY, Mamuya W, Thomson L, Weigold WG. SCCT guidelines for performance of coronary computed tomographic angiography: a report of the Society of Cardiovascular Computed Tomography Guidelines Committee. *J Cardiovasc Comput Tomogr*. 2009;3:190–204. doi: 10.1016/j.jcct.2009.03.004.
19. Anderson JL, Adams CD, Antman EM, et al; American College of Cardiology; American Heart Association Task Force on Practice Guidelines (Writing Committee to Revise the 2002 Guidelines for the Management of Patients With Unstable Angina/Non-ST-Elevation Myocardial Infarction); American College of Emergency Physicians; Society for Cardiovascular Angiography and Interventions; Society of Thoracic Surgeons; American Association of Cardiovascular and Pulmonary Rehabilitation; Society for Academic Emergency Medicine. ACC/AHA 2007 guidelines for the management of patients with unstable angina/non-ST-Elevation myocardial infarction: a report of the American College of Cardiology/American Heart Association Task Force on Practice Guidelines (Writing Committee to Revise the 2002 Guidelines for the Management of Patients With Unstable Angina/Non-ST-Elevation Myocardial Infarction) developed in collaboration with the American College of Emergency Physicians, the Society for Cardiovascular Angiography and Interventions, and the Society of Thoracic Surgeons endorsed by the American Association of Cardiovascular and Pulmonary Rehabilitation and the Society for Academic Emergency Medicine. *J Am Coll Cardiol*. 2007;50:e1–e157. doi: 10.1016/j.jacc.2007.02.013.
20. Thygesen K, Alpert JS, White HD; Joint ESC/ACCF/AHA/WHF Task Force for the Redefinition of Myocardial Infarction. Universal definition of myocardial infarction. *J Am Coll Cardiol*. 2007;50:2173–2195. doi: 10.1016/j.jacc.2007.09.011.
21. Grambsch P. Proportional hazards tests and diagnostics based on weighted residuals. 1994;81:515–526.
22. Pencina MJ, D'Agostino RB Sr, Steyerberg EW. Extensions of net reclassification improvement calculations to measure usefulness of new biomarkers. *Stat Med*. 2011;30:11–21. doi: 10.1002/sim.4085.
23. Rana JS, Dunning A, Achenbach S, et al. Differences in prevalence, extent, severity, and prognosis of coronary artery disease among patients with and without diabetes undergoing coronary computed tomography angiography: results from 10,110 individuals from the CONFIRM (COronary CT Angiography EvaluatioN For Clinical Outcomes): an InteRnational Multicenter Registry. *Diabetes Care*. 2012;35:1787–1794. doi: 10.2337/dc11-2403.
24. Nakanishi R, Berman DS, Budoff MJ, et al. Current but not past smoking increases the risk of cardiac events: insights from coronary computed tomographic angiography. *Eur Heart J*. 2015;36:1031–1040. doi: 10.1093/eurheartj/ehv013.
25. Kronmal RA, McClelland RL, Detrano R, Shea S, Lima JA, Cushman M, Bild DE, Burke GL. Risk factors for the progression of coronary artery calcification in asymptomatic subjects: results from the Multi-Ethnic Study of Atherosclerosis (MESA). *Circulation*. 2007;115:2722–2730. doi: 10.1161/CIRCULATIONAHA.106.674143.
26. Goff DC Jr, Lloyd-Jones DM, Bennett G, et al; American College of Cardiology/American Heart Association Task Force on Practice Guidelines. 2013 ACC/AHA guideline on the assessment of cardiovascular risk: a report of the American College of Cardiology/American Heart Association Task Force on Practice Guidelines. *J Am Coll Cardiol*. 2014;63(25 pt B):2935–2959. doi: 10.1016/j.jacc.2013.11.005.
27. Conroy RM, Pyörälä K, Fitzgerald AP, et al; SCORE project group. Estimation of ten-year risk of fatal cardiovascular disease in Europe: the SCORE project. *Eur Heart J*. 2003;24:987–1003. doi: 10.1016/S0195-668X(03)00114-3.
28. Lee TM, Lin YJ, Su SF, Chien KL, Chen MF, Liau CS, Lee YT. Relation of systemic arterial pulse pressure to coronary atherosclerosis in patients with mitral stenosis. *Am J Cardiol*. 1997;80:1035–1039.
29. Verdecchia P, Schillaci G, Reboldi G, Franklin SS, Porcellati C. Different prognostic impact of 24-hour mean blood pressure and pulse pressure on stroke and coronary artery disease in essential hypertension. *Circulation*. 2001;103:2579–2584.
30. Benetos A, Safar M, Rudnichi A, Smulyan H, Richard JL, Ducimetieère P, Guize L. Pulse pressure: a predictor of long-term cardiovascular mortality in a French male population. *Hypertension*. 1997;30:1410–1415.
31. Madhavan S, Ooi WL, Cohen H, Alderman MH. Relation of pulse pressure and blood pressure reduction to the incidence of myocardial infarction. *Hypertension*. 1994;23:395–401.
32. Mitchell GF, Moyé LA, Braunwald E, Rouleau JL, Bernstein V, Geltman EM, Flaker GC, Pfeffer MA. Sphygmomanometrically determined pulse pressure is a powerful independent predictor of recurrent events after myocardial infarction in patients with impaired left ventricular function. SAVE investigators. Survival and Ventricular Enlargement. *Circulation*. 1997;96:4254–4260.
33. Blacher J, Staessen JA, Girerd X, Gasowski J, Thijs L, Liu L, Wang JG, Fagard RH, Safar ME. Pulse pressure not mean pressure determines cardiovascular risk in older hypertensive patients. *Arch Intern Med*. 2000;160:1085–1089.
34. Frohlich ED. State of the Art lecture. Risk mechanisms in hypertensive heart disease. *Hypertension*. 1999;34:782–789.
35. Khattar RS, Acharya DU, Kinsey C, Senior R, Lahiri A. Longitudinal association of ambulatory pulse pressure with left ventricular mass and vascular hypertrophy in essential hypertension. *J Hypertens*. 1997;15:737–743.
36. Pannier B, Brunel P, el Aroussy W, Lacolley P, Safar ME. Pulse pressure and echocardiographic findings in essential hypertension. *J Hypertens*. 1989;7:127–132.
37. Haider AW, Larson MG, Benjamin EJ, Levy D. Increased left ventricular mass and hypertrophy are associated with increased risk for sudden death. *J Am Coll Cardiol*. 1998;32:1454–1459.

cont.

Manuscrito 11

38. Vasan RS, Levy D. The role of hypertension in the pathogenesis of heart failure. A clinical mechanistic overview. *Arch Intern Med*. 1996;156:1789–1796.
39. Dunn FG, McLenachan J, Isles CG, Brown I, Dargie HJ, Lever AF, Lorimer AR, Murray GD, Pringle SD, Robertson JW. Left ventricular hypertrophy and mortality in hypertension: an analysis of data from the Glasgow Blood Pressure Clinic. *J Hypertens*. 1990;8:775–782.
40. O'Hanlon R, Grasso A, Roughton M, et al. Prognostic significance of myocardial fibrosis in hypertrophic cardiomyopathy. *J Am Coll Cardiol*. 2010;56:867–874. doi: 10.1016/j.jacc.2010.05.010.
41. Wright JT Jr, Williamson JD, Whelton PK, et al. A randomized trial of intensive versus standard blood-pressure control. *N Engl J Med*. 2015;373:2103–2116.
42. Eckel RH, Jakicic JM, Ard JD, et al; American College of Cardiology/American Heart Association Task Force on Practice Guidelines. 2013 AHA/ACC guideline on lifestyle management to reduce cardiovascular risk: a report of the American College of Cardiology/American Heart Association Task Force on Practice Guidelines. *J Am Coll Cardiol*. 2014;63(25 pt B):2960–2984. doi: 10.1016/j.jacc.2013.11.003.

Novelty and Significance

What Is New?

- This study is the first study showing the relation of hypertension to the presence, extent, and severity of coronary artery disease on coronary computed tomographic angiography and to risk of major adverse cardiac events among patients without known coronary artery disease.

What Is Relevant?

- The presence of hypertension per se may not add as much incremental prognostic value as other risk factors after taking into account the presence, extent, and severity of coronary computed tomographic angiography.

Summary

Patients with hypertension had greater prevalence of extent and stenosis severity of coronary artery disease and modestly increased major adverse cardiac events risk compared with those without hypertension.

cont.

Manuscrito 11

Hypertension
Journal of the American Heart Association

American Heart Association®

Relationship of Hypertension to Coronary Atherosclerosis and Cardiac Events in Patients With Coronary Computed Tomographic Angiography

Rine Nakanishi, Lohendran Baskaran, Heidi Gransar, Matthew J. Budoff, Stephan Achenbach, Mouaz Al-Mallah, Filippo Cademartiri, Tracy Q. Callister, Hyuk-Jae Chang, Kavitha Chinnaiyan, Benjamin J.W. Chow, Augustin DeLago, Martin Hadamitzky, Joerg Hausleiter, Ricardo Cury, Gudrun Feuchtner, Yong-Jin Kim, Jonathon Leipsic, Philipp A. Kaufmann, Erica Maffei, Gilbert Raff, Leslee J. Shaw, Todd C. Villines, Allison Dunning, Hugo Marques, Gianluca Pontone, Daniele Andreini, Ronen Rubinshtein, Jeroen Bax, Erica Jones, Niree Hindoyan, Millie Gomez, Fay Y. Lin, James K. Min and Daniel S. Berman

Hypertension. published online June 12, 2017;
Hypertension is published by the American Heart Association, 7272 Greenville Avenue, Dallas, TX 75231

Print ISSN: 0194-911X. Online ISSN: 1524-4563

MANUSCRITO 12

Sex-Specific Associations Between Coronary Artery Plaque Extent and Risk of Major Adverse Cardiovascular Events: The CONFIRM Long-Term Registry

Schulman-Marcus, J., Hartaigh, B. O., Gransar, H., Lin, F., Valenti, V., Cho, I., Berman, D., Callister, T., DeLago, A., Hadamitzky, M., Hausleiter, J., Al-Mallah, M., Budoff, M., Kaufmann, P., Achenbach, S., Raff, G., Chinnaiyan, K., Cademartiri, F., Maffei, E., Villines, T., Kim, Y. J., Leipsic, J., Feuchtner, G., Rubinshtein, R., Pontone, G., Andreini, D., **Marques**, **H**., Shaw, L., and Min, J. K.

JACC Cardiovasc Imaging, 2016
9(4): p. 364-372

Manuscrito 12

JACC: CARDIOVASCULAR IMAGING
VOL. 9, NO. 4, 2016

ISSN 1936-878X/$36.00
PUBLISHED BY ELSEVIER
http://dx.doi.org/10.1016/j.jcmg.2016.02.010

Sex-Specific Associations Between Coronary Artery Plaque Extent and Risk of Major Adverse Cardiovascular Events

The CONFIRM Long-Term Registry

Joshua Schulman-Marcus, MD,[a] Bríain ó Hartaigh, PhD,[a] Heidi Gransar, MS,[b] Fay Lin, MD,[a] Valentina Valenti, MD,[a] Iksung Cho, MD,[a] Daniel Berman, MD,[b] Tracy Callister, MD,[c] Augustin DeLago, MD,[d] Martin Hadamitzky, MD,[e] Joerg Hausleiter, MD,[e] Mouaz Al-Mallah, MD,[f] Matthew Budoff, MD,[g] Philipp Kaufmann, MD,[h] Stephan Achenbach, MD,[i] Gilbert Raff, MD,[j] Kavitha Chinnaiyan, MD,[j] Filippo Cademartiri, MD,[k] Erica Maffei, MD,[k] Todd Villines, MD,[l] Yong-Jin Kim, MD,[m] Jonathon Leipsic, MD,[n] Gudrun Feuchtner, MD,[o] Ronen Rubinshtein, MD,[p] Gianluca Pontone, MD,[q] Daniele Andreini, MD,[q] Hugo Marques, MD,[r] Leslee Shaw, MD,[s] James K. Min, MD[a]

ABSTRACT

OBJECTIVES The purpose of this study was to examine sex-specific associations, if any, between per-vessel coronary artery disease (CAD) extent and the risk of major adverse cardiovascular events (MACE) over a 5-year study duration.

BACKGROUND The presence and extent of CAD diagnosed by coronary computed tomography angiography (CTA) is associated with increased short-term mortality and MACE. Nevertheless, some uncertainty remains regarding the influence of sex on these findings.

METHODS 5,632 patients (mean age 60.2 ± 11.8 years, 36.5% women) from the CONFIRM (Coronary CT Angiography Evaluation for Clinical Outcomes: An International Multicenter) registry were followed for 5 years. Obstructive CAD was defined as ≥50% luminal stenosis in a coronary vessel. Using Cox proportional hazards models, we calculated the hazard ratio (HR) for incident MACE among women and men, defined as death or myocardial infarction.

RESULTS Obstructive CAD was more prevalent in men (42% vs. 26%; $p < 0.001$), whereas women were more likely to have normal coronary arteries (43% vs. 27%; $p < 0.001$). There were a total of 798 incident MACE events. After adjustment, there was a strong association between increased MACE risk and nonobstructive CAD (HR: 2.16 for women, 2.56 for men; $p < 0.001$ for both), obstructive 1-vessel CAD (HR: 3.69 and 2.66; $p < 0.001$), 2-vessel CAD (HR: 3.92 and 3.55; $p < 0.001$), and 3-vessel/left main CAD (HR: 5.94 and 4.44; $p < 0.001$). Further exploratory analyses of atherosclerotic burden did not identify sex-specific patterns predictive of MACE.

CONCLUSIONS In a large prospective coronary CTA cohort followed long-term, we did not observe an interaction of sex for the association between MACE risk and increased per-vessel extent of obstructive CAD. These findings highlight the persistent prognostic significance of anatomic CAD subsets as detected by coronary CTA for the risk of MACE in both women and men. (J Am Coll Cardiol Img 2016;9:364–72) © 2016 by the American College of Cardiology Foundation.

From the [a]Dalio Institute of Cardiovascular Imaging, Weill Cornell Medical College and New York Presbyterian Hospital, New York, New York; [b]Department of Imaging, Cedars-Sinai Medical Center, Los Angeles, California; [c]Tennessee Heart and Vascular Institute, Hendersonville, Tennessee; [d]Capital Cardiology Associates, Albany, New York; [e]Division of Cardiology, Deutsches Herzzentrum Munchen, Munich, Germany; [f]Research Center, King Abdul Aziz Cardiac Center, National Guard Health Affairs, Riyadh, Saudi Arabia; [g]Department of Medicine, Harbor UCLA Medical Center, Los Angeles, California; [h]University Hospital, Zurich, Switzerland; [i]Department of Medicine, University of Erlangen, Erlangen, Germany; [j]William Beaumont Hospital, Royal Oaks, Michigan; [k]Cardiovascular Imaging Unit, Giovanni XXIII Hospital, Monastier, Treviso, Italy; [l]Department of Medicine, Walter Reed Medical Center, Washington, DC; [m]Seoul National University Hospital, Seoul, South Korea; [n]Department of Medicine and Radiology, University of British Columbia, Vancouver, British Columbia, Canada; [o]Department of Radiology, Medical University of Innsbruck, Innsbruck, Austria; [p]Department of Cardiology at the Lady Davis Carmel Medical Center, The Ruth and Bruce Rappaport School of Medicine, Technion-Israel Institute of Technology, Haifa, Israel; [q]Department of Clinical Sciences and Community Health, University of Milan, Centro Cardiologico Monzino, IRCCS, Milan, Italy; [r]Department of Surgery,

cont.

Manuscrito 12

JACC: CARDIOVASCULAR IMAGING, VOL. 9, NO. 4, 2016
APRIL 2016:364–72

Sex disparities in coronary artery disease (CAD) outcomes are well documented (1–4). Although women tend to have a lower prevalence of obstructive CAD, prior evidence indicates that women are more likely to be admitted for angina pectoris and experience worsened outcomes after myocardial infarction (MI) (5). Likewise, women with symptomatic CAD are more likely to suffer worse clinical outcomes, a finding present even among women with apparently normal or nonobstructive coronary arteries as evaluated by invasive coronary angiography (6,7). In light of the considerable burden of CAD in women, further improvements in risk stratification are essential for guiding preventive strategies and public health initiatives.

SEE PAGE 373

Coronary computed tomography angiography (CTA) is a noninvasive imaging modality that enables accurate detection and exclusion of CAD. Prior epidemiological studies have demonstrated that the presence and extent of anatomic CAD are associated with a heightened risk of death as well as major adverse cardiovascular events (MACE) within a 2-year follow-up period (8–13). A chief limitation, however, is the lack of certainty regarding the influence of sex on these findings. One study reported that nonobstructive CAD was associated with increased mortality risk in women but not in men (8). A subsequent propensity-matched study derived from similar data documented an equivalent risk of mortality and MI for nonobstructive CAD between sexes (13); however, the latter study failed to examine the sex-specific relationship between obstructive CAD and MACE. Further still, most of the available published reports have been unable to account for the risk beyond 3 years. Thus, an additional question is whether sex-specific differences in risk persist or attenuate over a longer duration of follow-up. Using data from a large prospective coronary CTA registry, we therefore set out to determine the sex-specific relationships, if any, between the extent of CAD and risk of MACE over a 5-year study period.

METHODS

STUDY POPULATION. Study patients were identified from the CONFIRM (Coronary CT Angiography Evaluation for Clinical Outcomes: An International Multicenter) registry, a dynamic, international, multicenter, observational cohort study that prospectively collects clinical, procedural, and follow-up data on patients undergoing ≥64-detector row coronary CTA. The rationale, design, site-specific patient characteristics, and follow-up durations have been described previously (14). In brief, this study screened 12,086 patients with 5-year follow-up data who underwent coronary CTA at 17 centers in 9 countries (Austria, Canada, Germany, Israel, Italy, Portugal, South Korea, Switzerland, and the United States) between 2002 and 2009. Individuals with known CAD at the time of coronary CTA, as defined by prior MI or coronary revascularization or cardiac transplantation, were excluded (n = 1,593). Patients with incomplete follow-up of all clinical events (n = 4,585), with adverse events on the day of the coronary CTA (n = 50), with missing plaque severity data (n = 224), or those who were missing age and sex information (n = 2) were also omitted. Thus, the analytic sample comprised 5,632 patients. Each study site received institutional review board approval for all registry procedures, including follow-up methodologies, and each participant provided written informed consent.

CLINICAL DATA COLLECTION. Standardized data collection methods were used at the participating study sites. Data were systematically collected for each consecutive patient while applying consistent definitions for suspected cardiac symptoms, risk factors, and angiographic CAD extent and severity. Patient information was gathered for traditional cardiac risk factors, including hypertension, diabetes, dyslipidemia, current smoking, and a family history of premature CAD. Patients who were treated for hypertension, diabetes, or dyslipidemia, or who otherwise had a prior diagnosis for these conditions

ABBREVIATIONS AND ACRONYMS

ACEi/ARB = angiotensin-converting enzyme/angiotensin receptor blocker
CTA = computed tomographic angiography
CP = calcified plaque
HR = hazard ratio
LM = left main
MACE = major adverse clinical events
MI = myocardial infarction
NCP = noncalcified plaque
PCP = partially calcified plaque

Curry Cabral Hospital, Lisbon, Portugal; and the [S]Division of Cardiology, Emory University School of Medicine, Atlanta, Georgia.
Research reported in this publication was supported by the Heart Lung and Blood Institute of the National institutes of Health under award number R01 HL115150, and funded, in part, by a generous gift from the Dalio Institute of Cardiovascular Imaging and the Michael Wolk Foundation. Dr. Min has received the following grants, NIH/NIHLBI R01HL111141, NIH/NIHLBI R01HL115150, NIH/NIHLBI R01HL118019, NIH/NIHLBI, U01HL105907, NPRP09-370-3-089. Dr. Min has served as a consultant with HeartFlow; has served on the scientific advisory board of Arineta; has partial ownership in MDDX and Autoplaq; and has received research support from GE Healthcare. All other authors have reported that they have no relationships relevant to the contents of this paper to disclose. Drs. Schulman-Marcus and ó Hartaigh contributed equally to this work. John Mahmarian, MD, served as Guest Editor for this article.

Manuscript received February 15, 2016; revised manuscript received February 19, 2016, accepted February 22, 2016.

cont.

Manuscrito 12

JACC: CARDIOVASCULAR IMAGING, VOL. 9, NO. 4, 2016
APRIL 2016:364–72

TABLE 1 Study Demographics

	Overall (n = 5,632)	Women (n = 2,056)	Men (n = 3,576)	p Value
Age, yrs	60.2 ± 11.8	62.4 ± 11.4	58.9 ± 11.8	<0.001
Cardiac risk factors				
Hypertension	3,079 (54.9)	1,234 (60.3)	1,845 (51.9)	<0.001
Hyperlipidemia	3,031 (54.1)	1,133 (55.3)	1,898 (53.3)	0.15
Diabetes	961 (17.1)	358 (17.5)	603 (16.9)	0.61
Current smoker	1,193 (21.4)	306 (15.0)	887 (25.0)	<0.001
Family history of premature CAD	1,662 (29.9)	674 (33.2)	988 (28.0)	<0.001
Chest pain				<0.001
Typical	739 (14.8)	292 (15.8)	447 (14.1)	
Atypical	1,625 (32.4)	651 (35.3)	974 (30.8)	
Noncardiac	664 (13.3)	298 (16.2)	366 (11.6)	
Asymptomatic	1,983 (39.6)	603 (32.7)	1,380 (43.6)	
Dyspnea	734 (16.8)	328 (20.2)	406 (14.7)	<0.001
Baseline medication use				
ASA	1,443 (32.6)	491 (30.5)	952 (33.8)	0.02
Beta blocker	1,289 (29.1)	498 (30.9)	791 (28.1)	0.05
ACEI/ARB	1,273 (28.8)	439 (27.3)	834 (29.6)	0.1
Statin	1,603 (36.0)	588 (36.3)	1,015 (35.9)	0.78
Extent of CAD by coronary CTA				
Normal	1,844 (32.7)	878 (42.7)	966 (27.0)	<0.001
Nonobstructive CAD	1,690 (30.0)	611 (29.7)	1,079 (30.2)	0.72
1-vessel obstructive CAD	1,094 (19.4)	318 (15.5)	776 (21.7)	<0.001
2-vessel obstructive CAD	544 (9.7)	135 (6.6)	409 (11.4)	<0.001
3-vessel/LM obstructive CAD	460 (8.2)	114 (5.5)	346 (9.7)	<0.001
Early revascularization (<90 days)	1,243 (22.1)	345 (16.8)	898 (25.1)	<0.001

Values are mean ± SD or n (%).

ACEI = angiotensin-converting enzyme inhibitor; ARB = angiotensin receptor blocker; ASA = acetylsalicylic acid; CAD = coronary artery disease; CTA = computed tomography angiography; LM = left main.

were categorized as having that risk factor. Family history of premature CAD was defined as a primary relative with a diagnosis early in life (i.e., mother <65 years of age or father <55 years of age). Chest pain was defined and categorized by the interviewing physician as nonanginal, atypical angina, or typical angina pectoris. The presence of excessive dyspnea as a reason for referral was also noted. The baseline use of cardiac medications (aspirin, beta blockers, angiotensin-converting enzyme/angiotensin receptor blocker, statin) were also collected.

CORONARY CTA PERFORMANCE AND INTERPRETATION. Standardized protocols for image acquisition, as defined by the Society of Cardiovascular Computed Tomography, were used at all participating sites (15). Specific details of coronary CTA procedures have been defined in detail elsewhere (14). Each site applied the standard anatomic segmental analysis for image interpretation. Plaque composition was defined as noncalcified, partially calcified, or calcified. All segments were coded for the presence and severity of coronary stenosis and were scored as normal (0% luminal stenosis), mild-moderate (1% to 49% luminal stenosis), moderate (50% to 69% luminal stenosis), or severe (≥70% luminal stenosis). For the primary analysis, CAD extent was defined by ≥50% stenosis in 0, 1, 2, or 3 coronary artery vessels. As reported in prior studies (8,9,16), given its prognostic significance, left main disease (50% luminal stenosis) was grouped with 3-vessel obstructive CAD.

Limited exploratory analyses of plaque composition and per-segment severity were also performed using previously reported methods (8). A segment involvement score was calculated as the total number of coronary artery segments exhibiting plaque, irrespective of the degree of luminal stenosis within each segment (minimum = 0; maximum = 16). A segment stenosis score was used as a measure of overall coronary artery plaque extent. Each individual coronary segment was graded as having no to severe plaque (i.e., scores from 0 to 3) based on extent of obstruction of coronary luminal diameter. Then the extent scores of all 16 individual segments were summed to yield a total score ranging from 0 to 48.

STUDY OUTCOME. Patients were followed prospectively for 5 years. The primary outcome measure for the present study was MACE, which included a combination of all-cause mortality and nonfatal MI. Secondary exploratory outcomes were all-cause mortality and nonfatal MI. Cause of death was not obtained in the CONFIRM registry. Late revascularization was not included as an outcome owing to insufficient data. Follow-up procedures were approved by all study centers' institutional review boards. All-cause mortality was adjudicated by trained study personnel or by querying of national medical databases. Other events were collected through a combination of direct questioning of patients using a scripted interview and examination of the patients' medical records as previously described (14). Acute MI was further ascertained using biomarker quantification during patients' hospital stays.

STATISTICAL METHODS. Demographic characteristics were summarized according to sex, with categorical variables presented as counts with proportions and continuous variables as mean ± SD, unless specified otherwise. Categorical variables were compared with the chi-square test, whereas continuous variables were compared with Student unpaired *t* test or Wilcoxon nonparametric tests where appropriate. Kaplan-Meier curves with log-rank tests were used to assess the sex-specific relationship between CAD extent and MACE. Next, we attempted to select the most relevant candidate risk factors for

cont.

Manuscrito 12

JACC: CARDIOVASCULAR IMAGING, VOL. 9, NO. 4, 2016
APRIL 2016:364–72

multivariate adjustment using a stepwise Cox regression procedure, reporting hazard ratios (HRs) with 95% confidence intervals (CIs). Initially, we modeled associations between each clinical risk factor and MACE, selecting a subset of covariates with a p value <0.25 in univariate analyses. We then used a backward multivariate regression model with a covariant retention threshold set at a p value of <0.10. We chose a less-conservative p value of 0.10 to permit inclusion of covariates that are traditionally associated with cardiovascular risk but were not deemed significant at the conventional threshold p value of <0.05. Categorical variables were retained if 1 component was significant. As a sensitivity check, and to conform to prior studies reported from the CONFIRM registry (9), patients who underwent early revascularization procedures ≤90 days previous were excluded from all survival analyses (n = 1,245). Variables retained in the final Cox model were also used as covariates during exploratory analyses of various plaque characteristics. For the purpose of this study, we also tested for an interaction between sex and each of the coronary CTA characteristics with the study outcomes. A 2-tailed p value <0.05 was considered statistically significant. All statistical analyses were conducted using STATA version 12 (StataCorp, College Station, Texas).

TABLE 2 Predictors of MACE

	Univariate		Multivariate*	
	HR (95% CI)	p Value	HR (95% CI)	p Value
Age	1.04 (1.03–1.05)	<0.001	1.03 (1.02–1.04)	<0.001
Women	0.97 (0.84–1.12)	0.68		
Hypertension	1.51 (1.31–1.75)	<0.001	1.24 (1.02–1.51)	0.035
Hyperlipidemia	0.93 (0.81–1.07)	0.32		
Diabetes	1.92 (1.64–2.25)	<0.001	1.42 (1.16–1.74)	0.001
Smoking	1.20 (1.03–1.41)	0.03	1.48 (1.21–1.82)	<0.001
Family history of premature CAD	0.90 (0.77–1.06)	0.21		
Typical angina	1.52 (1.25–1.85)	<0.001	1.30 (1.01–1.66)	0.038
Atypical angina	0.98 (0.83–1.16)	0.82	0.99 (0.79–1.24)	0.904
Noncardiac chest pain	0.84 (0.67–1.05)	0.12	1.12 (0.85–1.66)	0.396
Dyspnea	1.50 (1.22–1.84)	<0.001		
Aspirin	1.63 (1.37–1.94)	<0.001		
Beta blocker	1.25 (1.04–1.50)	0.02		
ACE/ARB	1.58 (1.32–1.88)	<0.001	1.26 (1.04–1.52)	0.017
Statin	1.36 (1.14–1.62)	<0.001		
Nonobstructive disease	0.95 (0.81–1.10)	0.47	2.25 (1.66–3.05)	<0.001
1-vessel obstructive disease	1.65 (1.40–1.93)	<0.001	2.86 (2.08–3.94)	<0.001
2-vessel obstructive disease	1.73 (1.41–2.11)	<0.001	3.46 (2.44–4.91)	<0.001
3-vessel obstructive disease	2.42 (1.99–2.95)	<0.001	4.68 (3.31–6.61)	<0.001
Early revascularization	2.41 (2.07–2.80)	<0.001		

*HRs shown only for variables retained.

ACE = angiotensin-converting enzyme; CI = confidence interval; HR = hazard ratio; MACE = major adverse cardiovascular events; other abbreviations as in Table 1.

RESULTS

BASELINE CHARACTERISTICS. Of 5,632 patients included in the study, 2,056 (36.5%) were women. The mean age of the cohort was 60.2 ± 11.8 years; women were significantly older than men (mean 62.4 vs. 58.9, p < 0.001). Demographic data are displayed in Table 1. Men were more likely to be smokers, whereas women were more likely to have hypertension, a family history of premature CAD, symptoms of chest pain, and excessive dyspnea (p < 0.001 for all). With regard to the extent of visualized atherosclerosis, men had an increased number of vessels with obstructive CAD, whereas women were more likely to have normal coronary arteries (p < 0.001 for all). There were a total of 371 deaths and 484 MIs in the cohort; 798 first MACE events were used for analyses. No sex-specific differences in the number of deaths or MIs were observed.

CLINICAL CHARACTERISTICS ASSOCIATED WITH MACE. The results of the multivariate model construction procedures are reported in Table 2. All variables were entered into the backward regression except for female sex (p = 0.68) and family history (p = 0.32). Of candidate risk factors, age, hypertension, diabetes, tobacco use, angiotensin-converting enzyme/angiotensin receptor blocker use, angina typicality, and per-vessel CAD severity were retained as important predictors of MACE. Sex was not a significant predictor of MACE when forced into the final multivariate model (HR: 0.86; 95% CI: 0.71 to 1.04; p = 0.12). All variables remained significantly associated with MACE in the multivariate Cox proportional hazards model with the exception of some angina variants.

CAD EXTENT AND MACE. In multivariate regression analyses, an increasing number of vessels with obstructive CAD was associated with increased MACE risk in a dose-response relationship (Figure 1). As displayed in Figure 2, increased per-vessel CAD extent was associated with MACE risk over time in both women and men (p < 0.001 by log-rank test for both). After adjustment, increasing per-vessel CAD extent was significantly associated with increased MACE risk in a manner similar to the overall cohort in both women and men (Table 3) (p for interaction = 0.98).

In exploratory analyses of secondary outcomes, there was no clear stepwise relationship between the number of diseased vessels and all-cause mortality in either sex (p for interaction = 0.58). Notably, in both women and men, the adjusted point estimates trended toward increased hazard of death

cont.

Manuscrito 12

JACC: CARDIOVASCULAR IMAGING, VOL. 9, NO. 4, 2016
APRIL 2016:364–72

FIGURE 1 Multivariate Cox Regression Model for Risk of MACE

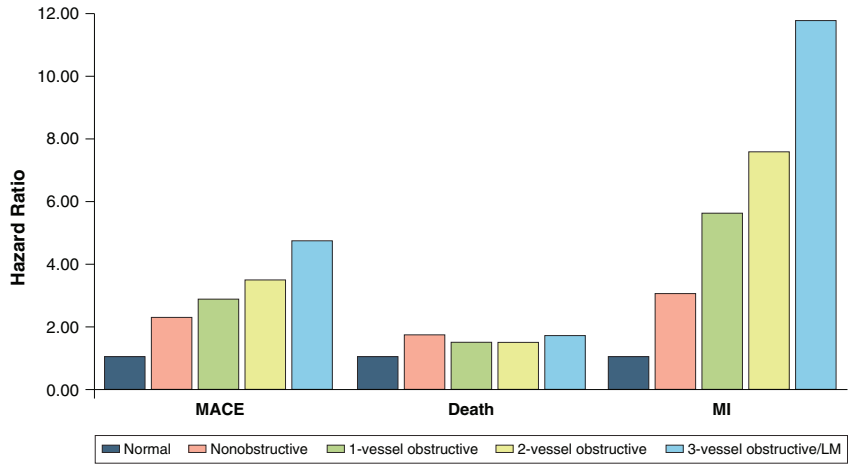

	MACE		Death		MI	
	Adjusted HR (95% CI)	P-value	Adjusted HR (95% CI)	P-value	Adjusted HR (95% CI)	P-value
Normal	Ref	Ref	Ref	Ref	Ref	Ref
Nonobstructive	2.25 (1.66 - 3.05)	<0.001	1.71 (1.19 - 2.46)	0.004	3.03 (1.85 - 4.96)	<0.001
1-vessel obstructive	2.86 (2.08 - 3.94)	<0.001	1.48 (0.97 - 2.23)	0.064	5.57 (3.41 - 9.10)	<0.001
2-vessel obstructive	3.46 (2.44 - 4.91)	<0.001	1.46 (0.91 - 2.36)	0.117	7.55 (4.50 - 12.67)	<0.001
3-vessel obstructive/LM	4.68 (3.31 - 6.61)	<0.001	1.70 (1.05 - 2.75)	0.030	11.71 (7.04 - 19.48)	<0.001

Increasing number of vessels with obstructive coronary artery disease associated with a monotonic rise in major adverse cardiovascular events (MACE) risk. CI = confidence interval; HR = hazard ratio; LM = left main; MI = myocardial infarction; Ref = reference.

for both nonobstructive and obstructive disease. Conversely, in both women and men, there appeared to be a stepwise relationship between the secondary outcome of nonfatal MI and number of diseased vessels after adjustment for covariates (p for interaction = 0.93). These findings were not materially different when patients with early revascularization (≤90 days after the index coronary CTA) were removed as a sensitivity check (data not shown).

SEX-SPECIFIC PLAQUE PATTERNS AND MACE. In exploratory analyses of other per-patient and per-segment measures, men had a higher prevalence of atherosclerotic plaque and obstructive CAD (Table 4). After adjustment, all measures of increased atherosclerotic severity and extent were associated with increased MACE risk in women and men. There were no significant sex-specific interactions, with the exception that increased segments of calcified plaque were associated with increased MACE risk in women but not in men (p for interaction = 0.004).

DISCUSSION

In the present study, we observed a strong and independent association between increased extent of per-vessel obstructive CAD by coronary CTA and heightened risk of MACE over a 5-year period among women and men. Similar findings were observed for the secondary outcome of nonfatal MI in both sexes, whereas increased mortality risk was more uniform across the spectrum of anatomic CAD. These findings highlight the persistent prognostic significance of increased CAD extent as detected by coronary CTA for both women and men.

The current study observations are fitting with previous observations; that is, although obstructive CAD detected by coronary CTA is less common in women than in men, its presence is associated with equal if not worse adverse outcomes. In an analysis of 24,775 patients followed over a mean of 2.3 years, Min et al. (8) found that although increased mortality risk was noted in both men and women with

cont.

Manuscrito 12

JACC: CARDIOVASCULAR IMAGING, VOL. 9, NO. 4, 2016
APRIL 2016:364–72

nonobstructive, 1-vessel, and 2-vessel obstructive disease, in women 3-vessel/left main obstructive disease was associated with an even higher mortality risk compared with men (HR: 4.21 compared with 3.27). In a smaller single-center cohort of 1,127 patients (57% women), Shaw et al. (16) also observed that although higher obstructive CAD burden by coronary CTA was associated with increased mortality in both sexes, women with 3-vessel obstructive/left main disease had a higher risk of death compared with men. These findings are in concord with prior registry data demonstrating higher rates of in-hospital mortality in women with obstructive CAD (17). Our study extends the prior published reports by observing the attenuation of the aforementioned sex-specific differences in MACE over a longer duration. However, our study emphasizes the core finding of the prior published reports that the extent of obstructive CAD detected by coronary CTA, regardless of sex, is the most significant predictor of increased MACE risk.

The present study findings are also in line with those of Leipsic et al. (13), who observed an association between increased risk of MACE and nonobstructive CAD by coronary CTA and no significant disparity between women and men. In that study, over the course of 2.3 years, the authors made use of propensity analysis to match patients with normal coronary arteries and nonobstructive CAD by coronary CTA for age and CAD risk factors. Following this approach, the annual death, MI, or MACE rates for both women and men with nonobstructive CAD were equivalent. This analysis stands in contrast to other coronary CTA and retrospective invasive studies suggesting a unique adverse prognosis for nonobstructive CAD by coronary CTA in women compared with men (1,6,7,18). Our study re-enforces the findings of Leipsic et al. (13) by observing a similar attenuation in sex-specific MACE risk for nonobstructive CAD over a longer time frame and with a larger number of events available for analysis. Further still, the present study highlights that nonobstructive CAD is associated with increased risk of MACE in men as well as women (19), and its presence in the former category should not be overlooked.

Although this study did not identify sex differences in MACE risk for several measures of CAD severity and extent, it must be emphasized that our findings do not exclude sex differences in the pathophysiology and functional importance of atherosclerosis. For example, an intriguing study of early atherosclerosis using intravascular ultrasound reported that women have lower measures of

FIGURE 2 Kaplan-Meier Event-Free Survival Curves

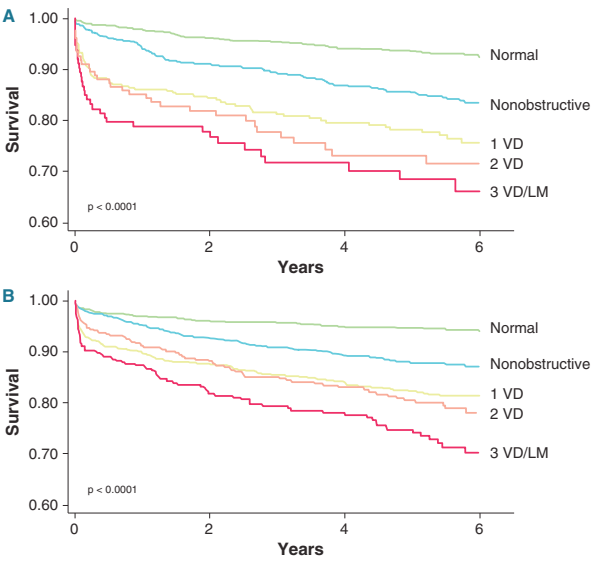

Increased per-vessel coronary artery disease extent was associated with greater major adverse cardiovascular event risk over time in **(A)** women and **(B)** men ($p < 0.001$ by log-rank test for both). VD = vessel disease; other abbreviation as in Figure 1.

TABLE 3 Adjusted Hazards of MACE and MACE Components by CAD Extent, Stratified by Sex

	Women		Men	
	Adjusted HR (95% CI)	p Value	Adjusted HR (95% CI)	p Value
Total MACE				
Normal	Ref	Ref	Ref	Ref
Nonobstructive	2.16 (1.41-3.29)	<0.001	2.56 (1.62-4.04)	<0.001
1-vessel obstructive	3.69 (2.35-5.78)	<0.001	2.66 (1.66-4.26)	<0.001
2-vessel obstructive	3.92 (2.24-6.85)	<0.001	3.55 (2.17-5.79)	<0.001
3-vessel obstructive/LM	5.94 (3.47-10.17)	<0.001	4.44 (2.73-7.22)	<0.001
Death				
Normal	Ref	Ref	Ref	Ref
Nonobstructive	1.89 (1.14-3.16)	0.013	1.74 (1.02-2.97)	0.042
1-vessel obstructive	1.96 (1.07-3.58)	0.028	1.33 (0.75-2.38)	0.314
2-vessel obstructive	2.06 (0.95-4.45)	0.066	1.35 (0.71-2.56)	0.346
3-vessel obstructive/LM	1.66 (0.70-3.98)	0.253	1.76 (0.94-3.29)	0.064
MI				
Normal	Ref	Ref	Ref	Ref
Nonobstructive	2.38 (1.22-4.61)	0.011	4.58 (2.02-10.35)	<0.001
1-vessel obstructive	5.96 (3.11-11.40)	<0.001	6.79 (3.01-15.32)	<0.001
2-vessel obstructive	6.26 (2.86-13.69)	<0.001	10.42 (4.57-23.80)	<0.001
3-vessel obstructive/LM	14.04 (6.89-28.61)	<0.001	13.57 (5.96-30.89)	<0.001

MI = myocardial infarction; Ref = reference; other abbreviations as in Tables 1 and 2.

cont.

Manuscrito 12

JACC: CARDIOVASCULAR IMAGING, VOL. 9, NO. 4, 2016
APRIL 2016:364–72

TABLE 4 Plaque Patterns and Adjusted Risk of MACE, Stratified by Sex

	Demographics			Adjusted HR* (95% CI)			
	Women	Men	p Value	Women	p Value	Men	p Value
Per patient							
CACS			<0.001				
None	766 (55.3)	760 (37.1)		1.00	1.00	1.00	1.00
1–400	470 (33.9)	901 (44.0)		1.76 (1.11–2.78)	0.02	1.93 (1.18–3.16)	0.01
≥400	149 (10.8)	388 (18.9)		2.86 (1.65–4.95)	<0.001	2.41 (1.41–4.13)	0.001
Maximal CAD stenosis severity			<0.001				
No plaque	878 (42.7)	966 (27.0)		1.00	1.00	1.00	1.00
Mild (1%–49%)	611 (29.7)	1,079 (30.2)		2.14 (1.40–3.26)	<0.001	2.56 (1.62–4.03)	<0.001
Moderate (50%–69%)	215 (10.5)	538 (15.0)		3.64 (2.25–5.88)	<0.001	2.62 (1.61–4.28)	<0.001
Severe (≥70%)	352 (17.1)	993 (27.8)		4.50 (2.89–7.01)	<0.001	3.74 (2.38–5.87)	<0.001
Location of any obstructive CAD							
RCA	258 (13.0)	726 (21.1)	<0.001	1.99 (1.39–2.84)	<0.001	1.62 (1.27–2.07)	<0.001
LAD artery	436 (21.5)	1,176 (33.2)	<0.001	2.54 (1.86–3.47)	<0.001	1.45 (1.15–1.83)	0.002
LCX artery	184 (9.5)	631 (18.6)	<0.001	2.58 (1.78–3.74)	<0.001	1.83 (1.43–2.33)	<0.001
LM	32 (1.6)	95 (2.8)	0.006	1.99 (0.92–4.30)	0.08	1.21 (0.70–2.09)	0.49
Per segment							
CAD severity and extent							
Log segment involvement score	0.8 (0.0–1.4)	1.1 (0.0–1.8)	<0.001	2.04 (1.68–2.49)	<0.001	1.59 (1.36–1.87)	<0.001
Log segment stenosis score	0.9 (0.0–1.6)	1.3 (0.0–2.1)	<0.001	1.88 (1.60–2.21)	<0.001	1.53 (1.34–1.74)	<0.001
No. of segments with NCP			<0.001				
0	1,668 (82.8)	2,535 (74.5)		1.00	1.00	1.00	1.00
1	205 (10.2)	415 (12.2)		1.14 (0.75–1.74)	0.53	1.09 (0.79–1.52)	0.59
2	72 (3.6)	195 (5.7)		1.21 (0.62–2.39)	0.58	1.34 (0.89–2.01)	0.17
≥3	69 (3.4)	257 (7.6)		1.12 (0.54–2.30)	0.77	1.02 (0.69–1.49)	0.93
No. of segments with PCP			<0.001				
0	1,632 (81.0)	2,289 (67.3)		1.00	1.00	1.00	1.00
1	189 (9.4)	401 (11.8)		1.24 (0.81–1.90)	0.32	1.02 (0.73–1.42)	0.93
2	76 (3.8)	259 (7.6)		1.45 (0.81–2.60)	0.21	1.13 (0.78–1.65)	0.51
≥3	117 (5.8)	453 (13.3)		2.09 (1.35–3.25)	0.001	1.12 (0.83–1.50)	0.46
No. of segments with CP†			<0.001				
0	1,526 (75.8)	2,148 (63.1)		1.00	1.00	1.00	1.00
1	199 (9.9)	436 (12.8)		1.52 (0.99–2.36)	0.06	0.94 (0.67–1.34)	0.74
2	94 (4.7)	265 (7.8)		1.76 (1.02–3.05)	0.04	0.93 (0.62–1.39)	0.72
≥3	195 (9.7)	553 (16.2)		2.39 (1.66–3.45)	<0.001	1.11 (0.84–1.47)	0.47

Values are n (%) or median (interquartile range), unless otherwise indicated. *Adjusted for age, hypertension, diabetes, smoking, symptoms, and use of ACEI/ARB. †p for interaction = 0.004.

CACS = coronary artery calcium score; CP = calcified plaque; IQR = interquartile range; LAD = left anterior descending; LCX = left circumflex; NCP = noncalcified plaque; PCP = partially calcified plaque; RCA = right coronary artery; other abbreviations as in Tables 1 to 3.

microvascular dysfunction, whereas men tend to have a higher burden of atheroma and endothelial dysfunction in epicardial arteries (20). In addition, prior research has shown that women with nonobstructive CAD but who present with chest pain and apparently normal invasive angiograms have increased rates of microvascular dysfunction, which is associated with a higher burden of clinical outcomes (18). Differing mechanisms of plaque disruption in acute MI have been noted between men and women (3). Finally, although rigorous and clinically relevant, the measures of CAD extent used in the present study are relatively crude. Given these considerations, further studies are needed to distinguish whether there are sex-specific plaque characteristics detected by coronary CTA, and whether these are associated with a higher risk of clinical events.

STUDY LIMITATIONS. Although CONFIRM represents the largest consecutive cohort of patients undergoing coronary CTA, as a registry it is subject to potential selection and referral bias. Many of the patients with long-term follow-up had incomplete outcomes data regarding MI and were excluded from this study. Thus, in spite of a lengthy follow-up and a relatively high number of events, the analyses relative to several sex-specific subgroups may have been underpowered, which likely explains the wide 95% CIs

cont.

Manuscrito 12

JACC: CARDIOVASCULAR IMAGING, VOL. 9, NO. 4, 2016
APRIL 2016:364–72

observed for some of the risk estimates reported in this study. A further and important limitation is that data were not collected on post-coronary CTA modifications of pharmacotherapy or behavior. Studies in other cohorts have demonstrated variable changes in post-test medical therapy by degree of anatomic CAD (21,22). It is unknown whether such treatment choices are affected by sex, and this is a matter worthy of further study. Data were also unavailable regarding any stress testing, and so the functional significance of stenoses was unknown. Other clinically relevant outcomes (e.g., cause-specific mortality, stroke) were not collected. In light of these limitations, however, this study is the largest consecutive cohort of patients undergoing coronary CTA with long-term outcomes data available.

CONCLUSIONS

The present study emphasized the clear prognostic significance of per-vessel obstructive CAD extent as detected by coronary CTA over a 5-year period. During this time, there were no distinct sex-specific differences in the risk of MACE. Though our findings await confirmation through forthcoming studies, as an initial step preventive strategies should be encouraged for men and women who present with any atherosclerosis as detected by coronary CTA.

REPRINT REQUESTS AND CORRESPONDENCE: Dr. James K. Min, Dalio Institute of Cardiovascular Imaging, Weill Cornell Medical College and the New York-Presbyterian Hospital, 413 East 69th Street, Suite 108, New York, New York 10021. E-mail: jkm2001@med.cornell.edu.

PERSPECTIVES

COMPETENCY IN MEDICAL KNOWLEDGE: Greater per-vessel extent of obstructive CAD as detected by coronary CTA is associated with greater MACE risk over a 5-year duration. Because there was no observed interaction for this association, this holds true of CAD detected in both women and men.

TRANSLATIONAL OUTLOOK: Although rigorous and clinically relevant, the measures of CAD extent used in the present study are relatively crude. Further studies are needed to distinguish whether there are sex-specific plaque characteristics detected by coronary CTA and whether these are associated with a higher risk of clinical events.

REFERENCES

1. Shaw LJ, Bugiardini R, Merz CN. Women and ischemic heart disease: evolving knowledge. J Am Coll Cardiol 2009;54:1561–75.

2. Hochman JS, Tamis JE, Thompson TD, et al. Sex, clinical presentation, and outcome in patients with acute coronary syndromes. Global Use of Strategies to Open Occluded Coronary Arteries in Acute Coronary Syndromes IIb Investigators. N Engl J Med 1999;341:226–32.

3. Della Rocca DG, Pepine CJ. What causes myocardial infarction in women without obstructive coronary artery disease? Circulation 2011;124:1404–6.

4. Vaccarino V, Parsons L, Peterson ED, Rogers WJ, Kiefe CI, Canto J. Sex differences in mortality after acute myocardial infarction: changes from 1994 to 2006. Arch Intern Med 2009;169:1767–74.

5. Johnson BD, Shaw LJ, Pepine CJ, et al. Persistent chest pain predicts cardiovascular events in women without obstructive coronary artery disease: results from the NIH-NHLBI-sponsored Women's Ischaemia Syndrome Evaluation (WISE) study. Eur Heart J 2006;27:1408–15.

6. Gulati M, Cooper-DeHoff RM, McClure C, et al. Adverse cardiovascular outcomes in women with nonobstructive coronary artery disease: a report from the Women's Ischemia Syndrome Evaluation Study and the St James Women Take Heart Project. Arch Intern Med 2009;169:843–50.

7. Sedlak TL, Lee M, Izadnegahdar M, Merz CN, Gao M, Humphries KH. Sex differences in clinical outcomes in patients with stable angina and no obstructive coronary artery disease. Am Heart J 2013;166:38–44.

8. Min JK, Dunning A, Lin FY, et al. Age- and sex-related differences in all-cause mortality risk based on coronary computed tomography angiography findings results from the International Multicenter CONFIRM (Coronary CT Angiography Evaluation for Clinical Outcomes: An International Multicenter Registry) of 23,854 patients without known coronary artery disease. J Am Coll Cardiol 2011;58:849–60.

9. Nakazato R, Arsanjani R, Achenbach S, et al. Age-related risk of major adverse cardiac event risk and coronary artery disease extent and severity by coronary CT angiography: results from 15 187 patients from the International Multisite CONFIRM Study. Eur Heart J Cardiovasc Imaging 2014;15:586–94.

10. Chow BJ, Small G, Yam Y, et al. Incremental prognostic value of cardiac computed tomography in coronary artery disease using CONFIRM: COro-Nary computed tomography angiography evaluation for clinical outcomes: an InteRnational Multicenter registry. Circ Cardiovasc Imaging 2011;4:463–72.

11. Hadamitzky M, Achenbach S, Al-Mallah M, et al. Optimized prognostic score for coronary computed tomographic angiography: results from the CONFIRM registry (COronary CT Angiography EvaluatioN For Clinical Outcomes: An InteRnational Multicenter Registry). J Am Coll Cardiol 2013;62:468–76.

12. Leipsic J, Taylor CM, Grunau G, et al. Cardiovascular risk among stable individuals suspected of having coronary artery disease with no modifiable risk factors: results from an international multicenter study of 5262 patients. Radiology 2013;267:718–26.

13. Leipsic J, Taylor CM, Gransar H, et al. Sex-based prognostic implications of nonobstructive coronary artery disease: results from the International Multicenter CONFIRM Study. Radiology 2014;273:393–400.

14. Min JK, Dunning A, Lin FY, et al. Rationale and design of the CONFIRM (COronary CT Angiography EvaluatioN For Clinical Outcomes: An InteRnational Multicenter) Registry. J Cardiovasc Comput Tomogr 2011;5:84–92.

15. Abbara S, Arbab-Zadeh A, Callister TQ, et al. SCCT guidelines for performance of coronary computed tomographic angiography: a report of the Society of Cardiovascular Computed Tomography Guidelines Committee. J Cardiovasc Comput Tomogr 2009;3:190–204.

16. Shaw LJ, Min JK, Narula J, et al. Sex differences in mortality associated with computed tomographic angiographic measurements of obstructive and nonobstructive coronary artery disease: an exploratory analysis. Circ Cardiovasc Imaging 2010;3:473–81.

17. Shaw LJ, Shaw RE, Merz CNB, et al. Impact of ethnicity and gender differences on angiographic coronary artery disease prevalence and in-hospital

cont.

Manuscrito 12

JACC: CARDIOVASCULAR IMAGING, VOL. 9, NO. 4, 2016
APRIL 2016:364–72

mortality in the American College of Cardiology-National Cardiovascular Data Registry. Circulation 2008;117:1787–801.

18. Bairey Merz CN, Shaw LJ, Reis SE, et al. Insights from the NHLBI-Sponsored Women's Ischemia Syndrome Evaluation (WISE) Study: part II: gender differences in presentation, diagnosis, and outcome with regard to gender-based pathophysiology of atherosclerosis and macrovascular and microvascular cor. J Am Coll Cardiol 2006;47:S21–9.

19. Maddox TM, Stanislawski MA, Grunwald GK, et al. Nonobstructive coronary artery disease and risk of myocardial infarction. JAMA 2014;312:1754–63.

20. Han SH, Bae JH, Holmes DR Jr., et al. Sex differences in atheroma burden and endothelial function in patients with early coronary atherosclerosis. Eur Heart J 2008;29:1359–69.

21. Hulten E, Bittencourt MS, Singh A, et al. Coronary artery disease detected by coronary computed tomographic angiography is associated with intensification of preventive medical therapy and lower low-density lipoprotein cholesterol. Circ Cardiovasc Imaging 2014;7:629–38.

22. Pursnani A, Celeng C, Schlett CL, et al. Use of coronary computed tomographic angiography findings to modify statin and aspirin prescription in patients with acute chest pain. Am J Cardiol 2016;117:319–24.

KEY WORDS CAD, CT coronary angiography, sex differences

MANUSCRITO 13

Long-term prognostic impact of CT-Leaman score in patients with non-obstructive CAD: Results from the COronary CT Angiography EvaluatioN For Clinical Outcomes InteRnational Multicenter (CONFIRM) study

Andreini, D., Pontone, G., Mushtaq, S., Gransar, H., Conte, E., Bartorelli, A.L., Pepi, M., Opolski, M. P., B, O.H., Berman, D. S., Budoff, M. J., Achenbach, S., Al-Mallah, M., Cademartiri, F., Callister, T. Q., Chang, H. J., Chinnaiyan, K., Chow, B. J., Cury, R., Delago, A., Hadamitzky, M., Hausleiter, J., Feuchtner, G., Kim, Y. J., Kaufmann, P. A., Leipsic, J., Lin, F. Y., Maffei, E., Raff, G., Shaw, L. J., Villines, T. C., Dunning, A., **Marques**, **H**., Rubinshtein, R., Hindoyan, N., Gomez, M., and Min, J.K.,

Int J Cardiol, 2017
231: p. 18-25

Manuscrito 13

International Journal of Cardiology 231 (2017) 18–25

Contents lists available at ScienceDirect

International Journal of Cardiology

journal homepage: www.elsevier.com/locate/ijcard

Long-term prognostic impact of CT-Leaman score in patients with non-obstructive CAD: Results from the COronary CT Angiography EvaluatioN For Clinical Outcomes InteRnational Multicenter (CONFIRM) study☆

Daniele Andreini [i,*], Gianluca Pontone [i], Saima Mushtaq [i], Heidi Gransar [d], Edoardo Conte [i], Antonio L. Bartorelli [i], Mauro Pepi [i], Maksymilian P. Opolski [a], Bríain ó Hartaigh [b], Daniel S. Berman [d], Matthew J. Budoff [e], Stephan Achenbach [f], Mouaz Al-Mallah [g], Filippo Cademartiri [j,y], Tracy Q. Callister [k], Hyuk-Jae Chang [l], Kavitha Chinnaiyan [m], Benjamin J.W. Chow [n], Ricardo Cury [o], Augustin Delago [q], Martin Hadamitzky [r], Joerg Hausleiter [s], Gudrun Feuchtner [t], Yong-Jin Kim [u], Philipp A. Kaufmann [v], Jonathon Leipsic [w], Fay Y. Lin [b], Erica Maffei [y], Gilbert Raff [m], Leslee J. Shaw [z], Todd C. Villines [aa], Allison Dunning [c], Hugo Marques [h], Ronen Rubinshtein [p], Niree Hindoyan [x], Millie Gomez [x], James K Min [b]

[a] Department of Interventional Cardiology and Angiology, Institute of Cardiology, Warsaw, Poland
[b] Department of Radiology, The New York-Presbyterian Hospital and the Weill Cornell Medical College, New York, NY, USA
[c] Department of Healthcare Policy and Research, Weill Cornell Medical College, New York, NY, USA
[d] Department of Imaging and Division of Cardiology, Department of Medicine, Cedars-Sinai Heart Institute, Cedars-Sinai Medical Center, Los Angeles, CA, USA
[e] Department of Medicine, Harbor UCLA Medical Center, Los Angeles, CA, USA
[f] Department of Medicine, University of Erlangen, Erlangen, Germany
[g] King Saud bin Abdulaziz University for Health Sciences, King Abdullah International Medical Research Center, King Abdul Aziz Cardiac Center, Ministry of National Guard, Health Affairs, Saudi Arabia
[h] Department of Surgery, Curry Cabral Hospital, Lisbon, Portugal
[i] Department of Clinical Sciences and Community Health, University of Milan, Centro Cardiologico Monzino, IRCCS Milan, Italy
[j] Department of Radiology, Erasmus Medical Center, Rotterdam, The Netherlands
[k] Tennessee Heart and Vascular Institute, Hendersonville, TN, USA
[l] Division of Cardiology, Severance Cardiovascular Hospital, Seoul, South Korea
[m] William Beaumont Hospital, Royal Oaks, MI, USA
[n] Department of Medicine and Radiology, University of Ottawa Heart Institute, Ontario, Canada
[o] Baptist Cardiac and Vascular Institute, Miami, FL, USA
[p] Department of Cardiology at the Lady Davis Carmel Medical Center, The Ruth and Bruce Rappaport School of Medicine, Technion-Israel Institute of Technology, Haifa, Israel
[q] Capitol Cardiology Associates, Albany, NY, USA
[r] Division of Cardiology, Deutsches Herzzentrum München, Munich, Germany
[s] Medizinische Klinik I der Ludwig-Maximilians-Universität München, Munich, Germany
[t] Department of Radiology, Medical University of Innsbruck, Innsbruck, Austria
[u] Department of Medicine and Radiology, Seoul National University Hospital, Seoul, South Korea
[v] Department of Nuclear Cardiology, Cardiovascular Center, University Hospital Zurich, Zurich, Switzerland
[w] Department of Medical Imaging and Division of Cardiology, St. Paul's Hospital, University of British Columbia, Vancouver, BC, Canada
[x] Dalio Institute of Cardiovascular Imaging, Weill Cornell Medical College and New York-Presbyterian Hospital, New York, NY, USA
[y] Cardiovascular Imaging Unit, Giovanni XXIII Hospital, Monastier, Italy
[z] Department of Medicine, Emory University School of Medicine, Atlanta, GA, USA
[aa] Department of Medicine, Walter Reed National Medical Center, Bethesda, MD, USA

ARTICLE INFO

Article history:
Received 7 September 2016
Received in revised form 13 December 2016
Accepted 19 December 2016
Available online 28 December 2016

ABSTRACT

Background: Non-obstructive coronary artery disease (CAD) identified by coronary computed tomography angiography (CCTA) demonstrated prognostic value. CT-adapted Leaman score (CT-LeSc) showed to improve the prognostic stratification. Aim of the study was to evaluate the capability of CT-LeSc to assess long-term prognosis of patients with non-obstructive (CAD).

Methods: From 17 centers, we enrolled 2402 patients without prior CAD history who underwent CCTA that showed non-obstructive CAD and provided complete information on plaque composition. Patients were divided

☆ **Relationships with industry**. Dr. Min has served on the medical advisory boards Arineta; He is a consultant to Heart Flow and Cardiovascular Research Foundation; and has received research support from GE Healthcare.

* Corresponding author at: Via C. Parea 4, 20138 Milan, Italy.
E-mail address: daniele.andreini@ccfm.it (D. Andreini).

http://dx.doi.org/10.1016/j.ijcard.2016.12.137

cont.

Manuscrito 13

Keywords:
Coronary CT angiography
CT-adapted Leaman score
Non-obstructive CAD
Prognosis
Patients reclassification

into a group without CAD and a group with non-obstructive CAD (<50% stenosis). Segment-involvement score (SIS) and CT-LeSc were calculated. Outcomes were non-fatal myocardial infarction (MI) and the combined end-point of MI and all-cause mortality.
Results: Patient mean age was 56 ± 12 years. At follow-up (mean 59.8 ± 13.9 months), 183 events occurred (53 MI, 99 all-cause deaths and 31 late revascularizations). CT-LeSc was the only multivariate predictor of MI (HRs 2.84 and 2.98 in two models with Framingham and risk factors, respectively) and of MI plus all-cause mortality (HR 2.48 and 1.94 in two models with Framingham and risk factors, respectively). This was confirmed by a net reclassification analysis confirming that the CT-LeSc was able to correctly reclassify a significant proportion of patients (cNRI 0.28 and 0.23 for MI and MI plus all-cause mortality, respectively) vs. baseline model, whereas SIS did not.
Conclusion: CT-LeSc is an independent predictor of major acute cardiac events, improving prognostic stratification of patients with non-obstructive CAD.

1. Introduction

In recent years, studies supporting the prognostic value of coronary CT angiography (CCTA), including single-center studies and a large multicenter registry, have been published [1,2]. According to these data, while the absence of identifiable plaques in the coronary tree is associated with an excellent prognosis, it has also been consistently demonstrated that the identification of non-obstructive lesions, a unique feature of CCTA as a non-invasive coronary imaging modality, has prognostic value. This has clinical implications because many patients fall in this category, as reflected by the high proportion of patients with atherosclerotic plaques in many CCTA databases [2–5]. Nevertheless, as non-obstructive CAD is a very heterogeneous and prevalent condition, there is the need for tools to quantify total coronary atherosclerotic burden in order to better stratify these patients. Recently, a new developed score, the CT-adapted Leaman score (CT-LeSc), using the comprehensive information on lesion localization, plaque composition and degree of stenosis provided by CCTA, resulted in a relatively small, single-center setting, to be an independent long-term predictor of hard cardiac events and to improve the CCTA prognostic stratification of non-obstructive CAD [6].

In the present prospective international multicenter study, we evaluated the capability of the CT-LeSc to stratify the long-term prognosis of a large cohort of patients with non-obstructive CAD at CCTA evaluation.

2. Methods

2.1. Study population

The design and rationale of the CONFIRM (COronary CT Angiography EvaluatioN For Clinical Outcomes: An InteRnational Multicenter) registry has been described previously [7]. For the current study, we utilized the data from the CONFIRM long-term follow-up registry that included only patients who had a follow-up duration of more than three years. Overall, 17,181 patients who underwent CCTA at 17 centers in 9 countries (Austria, Canada, Germany, Israel, Italy, Portugal, South Korea, Switzerland, and United States) were enrolled between February 2003 and May 2011 for long-term follow-up. Inclusion criteria were age >18 years, a CCTA performed with a scanner equipped with at least 64-detectors, and CCTA images of interpretable quality. Among the 5010 patients in whom MACE data at follow-up and complete plaque characteristics data were collected we excluded those with prior history of CAD ($n = 1741$), myocardial revascularization performed early after CCTA (<90 days) ($n = 377$) and presence of obstructive coronary lesions (>50%) ($n = 490$). The analytic sample comprised 2402. patients. Informed consent was obtained from each patient and [2] the study protocol conforms to the ethical guidelines of the 1975 Declaration of Helsinki as reflected in a priori approval by the institution's human research committee.

2.2. Risk factor assessment

Clinical CAD risk factors including smoking, hypertension, dyslipidemia, diabetes, and family history were collected prior to CCTA examination by direct patient interview performed by a physician or nurse research coordinator and/or with standardized site questionnaires [7].

2.3. Imaging analysis

CCTA data were acquired using multi-detector row CT scanners consisting of 64-rows or greater. Expert readers analyzed all CCTA images according to the guidelines of the Society of Cardiovascular Computed Tomography (SCCT) [8,9]. We defined coronary atherosclerosis in CCTA images as any tissue structure larger than 1 mm^2, which was either within the lumen of the coronary artery or adjacent to the coronary artery lumen and could be distinguished from the adjacent epicardial fat, pericardial tissue, or the artery lumen. We used a modified American Heart Association 16-segment coronary artery tree model for analysis [10]. Coronary artery luminal narrowing was defined as the presence of any plaque resulting in a % diameter reduction >0. Non-obstructive lesions were defined as coronary artery segments showing plaques with a luminal diameter stenosis <50%. Normal CCTA was defined as the absence of any coronary artery luminal narrowing. The SIS, ranging from 0 to 16, was calculated as the total number of segments with plaques (any degree of stenosis). The methodology for the CT-LeSc has been previously described [11]. Briefly, three sets of weighting factors are used for this score: 1) localization of the coronary plaques, accounting for dominance; 2) type of plaque, with a multiplication factor of 1 for calcified plaques and of 1.5 for non-calcified and mixed plaques; and 3) degree of stenosis, with a multiplication factor of 0.615 for non-obstructive (<50% stenosis) and a multiplication factor of 1 for obstructive (≥50% stenosis) lesions. The CT-LeSc was calculated on a patient level as the sum of the partial CT-LeSc of all evaluable coronary segments. For both the SIS and the CT-LeSc, prognostically validated cut-off values (>5) were used [4,6]. Analysis of coronary artery calcium score was performed when available. The total mean dose length product for CCTA was estimated to be 938 ± 379 mGy × cm, corresponding to an estimated radiation dose of 13 ± 5 mSv.

2.4. Patient follow-up

The primary outcomes of the current study were non-fatal myocardial infarction (MI) and the combined end-point of MI and all-cause mortality. As previously reported [7], the outcomes were assessed at each institution by direct interview, telephone contact, review of medical records, or using a mailed standardized questionnaire. In the USA, all-cause mortality was additionally searched by the Social Security Death Index. Site physicians defined MI according to ACC/AHA guidelines and the World Health Organization Universal Definition of Myocardial Infarction [12]. All revascularizations were recorded and patients with elective myocardial revascularization were censored at follow-up.

cont.

Manuscrito 13

2.5. Statistical analysis

Categorical variables are presented as counts and proportions. Continuous variables are presented as means ± SD. A one-way ANOVA or the Kruskal–Wallis test was used to conduct continuous variables intergroup comparisons among patients without CAD, non-obstructive CAD but a LS < 5 and non-obstructive CAD but a LS > 5. Pearson's chi-square test (χ^2) was used for categorical variables comparison. Time-to-event analysis for the study endpoints were calculated using univariable Cox proportional-hazards models reporting hazard ratios (HR) with 95% confidence intervals (95% CI). Multivariable Cox proportional hazards models were also constructed with variables based on clinical judgment univariate analysis results. All the analyses were performed evaluating combined endpoints (MI, MI plus all cause of death,). To avoid overfitting and multicollinearity issues, we developed four different models, for all different combined endpoints. The first model was adjusted for the CT-LeSc and the Framingham risk score. The second model was adjusted for the SIS and the Framingham risk score. The third model was adjusted for the CT-LeSc and baseline clinical characteristics. The fourth model was adjusted for the SIS and baseline clinical characteristics.

A sub-analysis were performed in patients in which CACS was available; a prognostically validated cut-off >400 was used as previously suggested [13]. Moreover we performed a separate sub-analysis for patients with and without chest pain at baseline. Of note, in the analysis of symptomatic subjects the Morise score was included in model 1 and 2, instead of the Framingham score.

Survival curves were calculated using the Kaplan–Meier method for population stratified by the presence of non-obstructive CAD and the CT-LeSc, with each survival curve compared using the log-rank test. A two-tailed p value of <0.05 was considered statistically significant. The comparison between performance of the CT-LeSc and SIS added to a baseline model was further quantified by a continuous net reclassification index (cNRI) [14].

3. Results

3.1. Patient characteristics and MACE

Indications for CCTA were chest pain (1200 patients, 49.9%), multiple CAD risk factors (595 patients, 24.7%), and equivocal or abnormal stress test results (607 patients, 25.3%). Mean pre-test probability of CAD was low-to-intermediate (mean Morise score 11.6 ± 4.2). The mean duration of follow-up was 59.8 ± 13.9 months, up to 96 months (Table 1). One-hundred and eighty-three patients exhibited events during follow-up (53 MI, 99 all-cause deaths and 31 late revascularizations).

3.2. Univariate predictors of events

Among clinical characteristics, therapy with aspirin was the only predictor of MI, whereas hypertension and diabetes were predictors of MI plus all-cause death. Among CCTA data, a SIS > 5 and non-obstructive CAD with a CT-LeSc > 5 were predictors of MI, whereas a SIS > 5, non-obstructive CAD with a CT-LeSc ≤ 5 and non-obstructive CAD with a CT-LeSc > 5 were predictors of MI plus all-cause death (Table 2).

3.3. Multivariate predictors of events

The only significant independent predictor of MI was non-obstructive CAD with a CT-LeSc > 5 (HR 2.84 and 2.98 in model 1 and model 3, respectively). The independent predictors of MI plus all-cause death were the Framingham score (HR 1.02 and 1.03 in model 1 and model 2, respectively), age (HR 1.04 and 1.05 in model 3 and model 4, respectively), diabetes (HR 1.84 and 1.86 in model 3 and model 4, respectively), a SIS > 5 (HR 1.95 in model 2, HR not significant in model 4), non-obstructive CAD with a CT-LeSc ≤ 5 (HR 2.05 and 1.55 in model 1 and model 3, respectively) and non-obstructive CAD with a CT-LeSc > 5 (HR 2.48 and 1.94 in model 1 and model 3, respectively) (Table 3).

Table 1
Clinical and CCTA baseline characteristics.

	All patients (n = 2402)	No CAD (n = 1450)	Non-obstructive CAD with LS ≤ 5 (n = 611)	Non-obstructive CAD with LS > 5 (n = 341)
Clinical characteristics				
Age	56 ± 12	53 ± 12	61 ± 10*	63 ± 11*,ς
Male	1208 (50.3)	657 (45.3)	346 (56.7)*	205 (60.1)*
BMI	28 ± 5.49	27.79 ± 5.39	28.09 ± 5.11	28.61 ± 6.40
Hypertension	1302 (54.2)	674 (46.5)	394 (64.5)*	234 (68.6)*
Diabetes	252 (10.5)	116 (8)	74 (12.1)§	62 (18.1)*,ς
Current smoking	425 (17.7)	250 (17.2)	105 (17,2)	70 (20.53)
Family history	798 (33.2)	492 (33.9)	188 (30,8)	118 (34.6)
Dyslipidemia	1207 (50.3)	641 (44.2)	342 (56)*	224 (65.7)*,ς
Morise	11.57 ± 4.16	10.70 ± 4.42	12.68 ± 3.37*	13.19 ± 3.31*
Framingham	11.99 ± 9.63	9.74 ± 7.78	14.83 ± 10.46*	16.27 ± 11.98*
Chest pain at baseline				
No chest pain	1053 (43.8)	590 (40.7)	308 (50.4)	155 (45.4)
Non-cardiac/unspecified pain	418 (17.4)	296 (20.4)	79 (12.9)	43 (12.6)
Atypical chest pain	737 (30.7)	436 (30.1)	184 (30.1)	117 (34.3)
Typical chest pain	194 (8.1)	128 (8.8)	40 (6.5)	26 (7.6)
Therapy				
ASA	503 (20.9)	265 (18.3)	137 (22.4)§	101 (29.6)*,ς
Statin	506 (21.1)	226(15.6)	161 (26.4)*	119 (34.8)*,ς
CCTA characteristics				
SIS	1.08 ± 1.89	0	1.61 ± 0.88*	4.64 ± 2.36*,o

Continuous variable are expressed as mean ± SD; Ordinal variables are expressed as n (%); BMI: body mass index; SIS: segment involvement score; LS: Leaman score; CAD: coronary artery disease.

* p < 0,0001 vs no CAD.
o p < 0,0001 vs LS < 5.
§ p < 0,05 vs no CAD.
ς p < 0,05 vs LS < 5.

cont.

Manuscrito 13

Table 2
Univariate analysis.

	MI		MI + all-cause death	
	HR (95% CI)	*p*	HR (95% CI)	*p*
Clinical characteristics				
Age	1 (0.98–1.02)	0.871	1.04 (1.02–1.05)	<0.0001
Male	0.78 (0.46–1.32)	0.343	1.1 (0.79–1.51)	0.5731
BMI	1.03 (0.99–1.07)	0.128	1.01 (0.98–1.04)	0.596
Hypertension	1.52 (0.87–2.67)	0.143	1.97 (1.39–2.79)	<0.0001
Diabetes	1.85 (0.9–3.79)	0.095	1.95 (1.29–2.96)	0.002
Current smoking	1.68 (0.91–3.1)	0.096	1.33 (0.91–1.95)	0.144
Family history	1.46 (0.84–2.52)	0.182	0.86 (0.1–1.23)	0.417
Dyslipidemia	1.17 (0.68–2.01)	0.573	0.9 (0.65–1.24)	0.505
Morise	0.98 (0.92–1.05)	0.629	1.03 (0.99–1.07)	0.168
Framingham	1.01 (0.99–104)	0.366	1.03 (1.02–1.04)	<0.0001
Chest pain at baseline				
No chest pain	1		1	
Non-cardiac pain/unspecified	1.34 (0.69–2.64)	0.388	0.80 (0.52–1.24)	0.325
Atypical chest pain	0.82 (0.42–1.57)	0.547	0.50 (0.33–0.75)	0.001
Typical chest pain	1.07 (0.41–2.80)	0.886	0.60 (0.31–1.16)	0.130
Therapy				
ASA	1.84 (1.01–3.34)	0.046	1.42 (0.98–2.05)	0.063
Statin	1.2 (0.63–2.27)	0.585	1.12 (0.77–1.63)	0.563
CCTA characteristics				
SIS > 5	1.13 (1.02–1.26)	0.022	1.18 (1.12–1.25)	<0.001
No CAD	1		1	
Non-Ob CT-LeSc ≤ 5	1.18 (0.62–2.23)	0.618	1.88 (1.3–2.72)	0.0008
Non-OB CT-LeSc > 5	2.11 (1.11–3.99)	0.023	2.37 (1.58–3.57)	<0.001

BMI: body mass index; SIS: segment involvement score; CT-LeSc: CT-Adapted Leaman Score; Non-Ob: non-obstructive coronary artery disease (stenosis <50%); MI: non-fatal myocardial infarction; CAD: coronary artery disease.

Table 3
Multivariate analysis.

	MI		MI + all-cause death	
	HR (95% CI)	*p*	HR (95% CI)	*p*
Model 1				
Framingham	1.01 (0.98–1.04)	0.4316	1.02 (1.01–1.04)	0.0006
ASA	1.51 (0.82–2.77)	0.1860	1.32 (0.91–1.93)	0.1402
Non-Ob CT-LeSc < 5	1.70 (0.84–3.47)	0.1444	2.05 (1.36–3.01)	0.0006
Non-Ob CT-LeSc > 5	2.84 (1.38–5.85)	0.0049	2.48 (1.58–3.90)	0.0001
Model 2				
ASA	1.67 (0.91–3.05)	0.0995	1.41 (0.98–2.06)	0.0672
Framingham	1.02 (0.99–1.05)	0.1011	1.03 (1.02–1.04)	<0.0001
SIS > 5	0.85 (0.20–3.35)	0.8252	1.95 (1.09–3.49)	0.0244
Model 3				
Age	0.99 (0.96–1.02)	0.7768	1.04 (1.02–1.06)	<0.0001
Male	0.67 (0.35–1.28)	0.2363	0.91 (0.62–1.34)	0.6515
BMI	0.98 (0.93–1.04)	0.6053	0.99 (0.95–1.02)	0.6837
Hypertension	1.13 (0.57–2.26)	0.7140	1.39 (0.89–2.14)	0.1414
Diabetes	1.41 (0.60–3.32)	0.4242	1.84 (1.13–2.99)	0.0138
Current smoking	1.11 (0.50–2.43)	0.7914	1.42 (0.89–2.26)	0.1342
Dyslipidemia	1.10 (0.57–2.11)	0.7719	0.74 (0.50–1.09)	0.1342
Family history	1.23 (0.65–2.31)	0.5184	1.06 (0.71–1.59)	0.7598
ASA	1.42 (0.73–2.76)	0.2937	1.08 (0.71–1.65)	0.6983
Non-Ob CT-LeSc < 5	1.64 (0.73–3.65)	0.2252	1.55 (0.97–2.45)	0.0627
Non-Ob CT-LeSc > 5	2.98 (1.35–6.58)	0.0070	1.94 (1.18–3.12)	0.0095
Model 4				
Age	1.01 (0.98–1.03)	0.5466	1.05 (1.03–1.07)	<0.0001
Male	0.79 (0.42–1.49)	0.4813	0.99 (0.68–1.46)	0.9953
BMI	0.98 (0.93–1.04)	0.7247	0.99 (0.95–1.03)	0.7503
Hypertension	1.19 (0.59–2.37)	0.6170	1.46 (0.94–2.25)	0.0900
Diabetes	1.52 (0.65–3.55)	0.3278	1.86 (1.14–3.02)	0.0125
Current smoking	1.20 (0.55–2.64)	0.6413	1.49 (0.93–2.35)	0.0957
Dyslipidemia	1.21 (0.63–2.32)	0.5568	0.77 (0.52–1.13)	0.1878
Family history	1.28 (0.68–2.39)	0.4402	1.08 (0.72–1.61)	0.7032
ASA	1.54 (0.79–2.96)	0.2001	1.13 (0.74–1.72)	0.5560
SIS > 5	0.83 (0.19–3.52)	0.8043	1.38 (0.74–2.56)	0.3083

3.4. Survival analysis

When MI only was considered as outcome, the event-free survival rates were 98% in patients without CAD, 98% in patients with non-obstructive CAD and a CT-LeSc ≤ 5 and 95% in patients with non-obstructive CAD and a CT-LeSc > 5 (log-rank *p* value = 0.01) (Figure 1A). When the end-point of MI plus all-cause mortality was used, event-free survival rates were 97%, 92% and 88% in patients without CAD, with non-obstructive CAD and a CT-LeSc ≤ 5 and with non-obstructive CAD and a CT-LeSc > 5, respectively (log-rank *p* value < 0.0001) (Figure 1B).

3.5. Reclassification index

The net reclassification analysis (Table 4) showed that a CT-LeSc > 5 is able to correctly reclassify a significant proportion of patients (0.28 and 0.23for MI and MI plus all-cause mortality, respectively), in comparison with the baseline model including age, male gender, diabetes, hypertension, smoking, dyslipidemia, and family history of premature CAD. Conversely, reclassification using a SIS > 5 was not statistically significant in any models.

3.6. Coronary artery calcium score sub-analysis

Coronary artery calcium score (CACS) was available in 1537 patients (64%). CACS > 400 was identified in 67 patients (4.4%) in the entire cohort; CACS > 400 was present in 6 patients (1.6%) with CT LeSc ≤ 5 and in 61 subjects (22.9%) among those with CT LeSc > 5. At univariate analysis neither CACS > 400 or SIS > 5 was associated with MI (HR 1.85; 95% CI 0.57–5.98, $p = 0.306$ and 0.89; 0.22–3.68, $p = 0.896$), while only CT-LeSc > 5 was a significantly predictors of MI (HR 2.09; 95% CI 1.02–4.30, $p = 0.04$). When the composite endpoint including MI and all cause of death was considered, CACS > 400, SIS > 5 and CT-LeSc > 5

cont.

Manuscrito 13

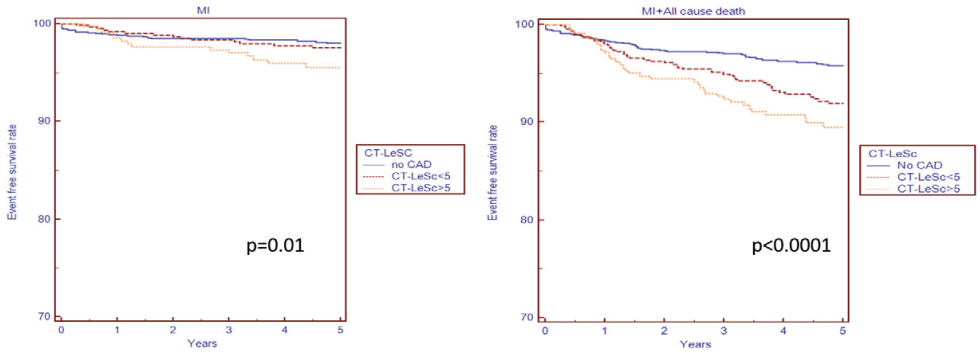

Fig. 1. Kaplan-Meier survival curves for MI (A) showing the event-free survival rates of 98% in patients with non-obstructive CAD and a CT-LeSc ≤ 5 and 95% in patients with non-obstructive CAD and a CT-LeSc > 5 (log-rank *p* value = 0.01). When the end point was MI plus all-cause mortality (B), event-free survival rates were 97%, 92% and 88% in patients without CAD, with non-obstructive CAD and a CT-LeSc ≤ 5 and with non-obstructive CAD and a CT-LeSc > 5, respectively (log-rank *p* value < 0.0001). MI: myocardial infarction; CAD: coronary artery disease; CT-LeSc: computed tomography adapted Leaman score.

were all significative predictors of events (HR 3.99, HR 2.38 and HR 2.73, respectively; $p < 0.001$).

At multivariate analysis CACS > 400 remains a significantly predictor of MI + all cause of death when adjusted for Framingham risk score (HR 3.04; 95% CI 1.72–5.36, $p < 0.001$) and for baseline clinical characteristics (HR 2.05; 95% CI 1.14–3.68, $p = 0.017$); SIS > 5 remains significantly associated to MI + all cause of death only when adjusted for Framingham risk score (HR 1.96; 95% CI 1.09–3.55, $p = 0.027$), but not when adjusted for clinical baseline characteristics.

Of note, only CT-LeSc > 5 was significantly associated to MI when adjusted both for Framingham risk score (HR 2.68; 95% CI 1.18–6.12, $p = 0.019$) and for baseline clinical characteristics (HR 3.13; 95% CI 1.29–7.53, $p = 0.012$) at multivariate analysis. When the composite endpoint including MI + all cause of death was considered CL-LeSc > 5 was still associated to events both when adjusted for Framingham risk score (HR 2.52; 95% CI 1.52–4.16, $p < 0.001$) and for baseline characteristics (HR 1.79, 95% CI 1.05–3.05, $p = 0.038$).

In this subgroup of patients with CACS reported, the event free survival rates were 98% in those with CT-LeSc < 5 and 95% in those with CT-LeSc > 5 (log-rank $p = 0.0289$) (Figure 2B); on the contrary CACS > 400 score was not significantly associated to worst survival rates (Figure 2A).

3.7. Asymptomatic patients vs symptomatic patients

Among the entire cohort 1053 patients (43.8%) did not report chest pain at baseline, while 1349 patients (56.2%) were symptomatic at the time of CCTA.

A separate sub-analysis in asymptomatic subjects showed that at univariate analysis there were no predictor of MI; on the contrary, age, hypertension, diabetes and the Framingham score were the clinical characteristics associated to MI + all cause of death, while among CT parameters both SIS > 5 and CT-LeSc > 5 were associated to MI + all cause of death (Table 5).

Table 4
Net Reclassification Index for SIS > 5 and CT-LeSc > 5 for prediction of composite endpoints.

	MI			MI + all-cause death		
	cNRI	cNRI 95% CI	*p*	cNRI	cNRI 95% CI	*p*
BL	–	–	–	–	–	–
BL + SIS > 5	0.15	−0.09–0.40	0.271	−0.039	−0.19–0.11	0.648
BL + CT-LeSc > 5	0.28	0.02–0.54	0.046	0.23	0.07–0.39	0.006

In the subgroups of patients with chest pain at baseline only CT-LeSc > 5 was associated to MI at univariate (HR 2.5; 95% CI 1.13–5.75, $p = 0.025$), while age, hypertension and the Morise score were associated to MI + all cause of death, but only CT-LeSc > 5 (HR 2.53; 95% CI 1.42–4.48, $p = 0.002$) was found to be associated to this composite end-point among CCTA variables (Table 6).

At multivariate analysis SIS > 5 was not associated to endpoints both in asymptomatic and symptomatic patients. On the contrary CT-LeSc > 5 was found to be a predictor of MI in symptomatic patients (HR 2.63 and 2.76 in Model 1 and 3, respectively) and to be associated with MI + All cause of death both in asymptomatic and symptomatic patients only when adjusted for Framingham or Morise score (HR 2.56 and 2.39 in asymptomatic and symptomatic patients, respectively), but not when clinical baseline characteristics were evaluated separately (Table 7).

4. Discussion

Coronary CTA has been demonstrated to be accurate for the detection of non-obstructive CAD and coronary atherosclerosis when compared to coronary intravascular ultrasound [15]. Detection of non-obstructive CAD, which may be considered an unique feature of CCTA among other non-invasive imaging modalities, has relevant prognostic implications. Indeed, it may identify a population that has an higher event-free survival rate as compared to that of patients with obstructive disease but lower than that of patients with normal coronaries [4,5,16,17]. In order to better stratify the prognosis among the large and heterogeneous cohort of patients with non-obstructive CAD, different coronary plaque scores have been proposed. Among them, the SIS and SSS demonstrated a remarkable prognostic value [4,18]. Particularly, a single-center study by Bittencourt et al. demonstrated that among patients with obstructive CAD, a greater extent of non-obstructive plaques, as quantified by SIS, was associated with a higher event rate [16].

4.1. CT adapted-Leaman score

A recently proposed plaque score, the CT-LeSc based on lesion localization, plaque composition and degree of stenosis, demonstrated to improve the prognostic stratification of non-obstructive CAD in an another single-center study [6]. To the best of our knowledge, this is the first prospective international multicenter study finalized to evaluate if the CT-LeSc is able to stratify the long-term prognosis in a selected but large patient cohort with non-obstructive lesions. The main findings of the study are that the CT-LeSc allows to distinguish within patients with non-obstructive CAD those with a cardiac event risk similar to that shared by patients without plaques from those with a less favorable

cont.

Manuscrito 13

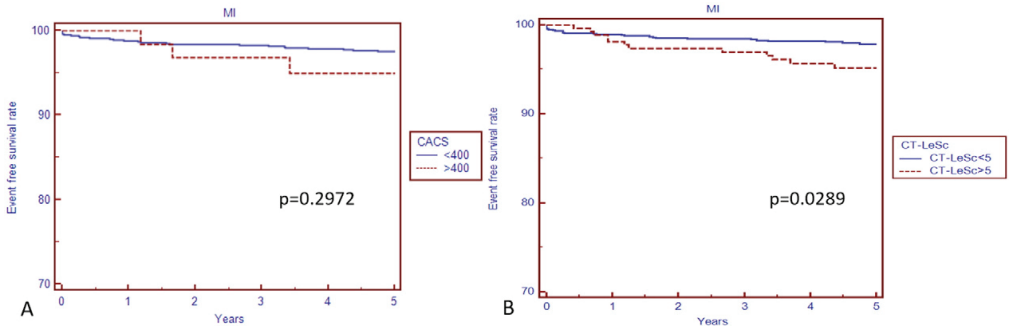

Fig. 2. Kaplan Meyer survival curves for MI using CACS (A) and CT-LeSc (B). CACS > 400 was not able to stratify patients at higher risk of MI. On the contrary, patients with CT-LeSc > 5 was associated to an event free survival rate of 95%, that was found to be significantly lower than patients with CT-LeSc < 5 (log-rank $p = 0.0289$). MI: myocardial infarction; CACS: coronary artery calcium score; CT-LeSc: computed tomography adapted Leaman score.

prognosis. Moreover, the CT-LeSc appears to be superior to the SIS, despite the latter already showed to possess a good prognostic value. In particular, analyzing the primary outcomes of the study we found that a CT-LeSc > 5 was an univariate predictor of MI and MI plus all-cause death and the only multivariate predictor of MI.

4.2. CT-LeSc vs SIS

The CT-LeSc appears to be superior to the SIS that exhibited HR systematically lower than the CT-LeSc at both univariate and multivariate analysis. This is confirmed by the net reclassification analysis showing that the CT-LeSc, but not the SIS, was able to correctly reclassify a significant proportion of patients vs. a baseline model including age, gender and risk factors for both primary and secondary endpoints.

4.3. CACS and CT-LeSc

In the sub-group of patients with calcium score, CACS > 400 has been confirmed to be a predictor of composite end-point including all cause of death, but only CT-LeSc appeared to correctly identify patients at higher risk of MI. These findings could be explained by recent studies, suggesting that non-calcified plaques may be associated to higher risk of acute coronary syndrome when compared to calcified ones [19].

4.4. Asymptomatic and symptomatic patients

Approximately half of the patients included in this study were asymptomatic for chest pain at the time of CCTA. In order to better clarify the possible role of CCTA in the evaluation of asymptomatic patients we performed a specific separate analysis in asymptomatic vs symptomatic patients. Of note we have found no clinical or CCTA parameters resulting to be significantly associated to MI in asymptomatic patients. On the contrary in symptomatic patients only CT-LeSc > 5 was associated to MI both at univariate and multivariate analyses. This findings suggest that CT-LeSc could be an important tool to discriminate patients at higher risk of MI among those symptomatic for chest pain, even if CCTA results to be negative for significative stenosis (>50%).

4.5. Survival analysis

Analyzing the survival curves for primary endpoints, we found that MI-free survival rate was 98% for patients with normal coronary arteries and for those with non-obstructive CAD and a CT-LeSc ≤ 5. Conversely, the survival rate fell to 95% in the presence of a CT-LeSc > 5, confirming the power of the CT-LeSc in stratifying the prognosis of patients with non-obstructive lesions. Adding all-cause mortality to MI in the survival analysis, patients with non-obstructive stenosis and a low CT-LeSc

Table 5
Univariate analysis for asymptomatic patients.

	MI		MI + all-cause death	
	HR (95% CI)	*p*	HR (95% CI)	*p*
Clinical characteristics				
Age	1.01 (0.98–1.04)	0.578	1.03 (1.01–1.05)	0.001
Male	0.68 (0.31–1.52)	0.356	0.93 (0.60–1.43)	0.717
BMI	1.04 (0.98–1.09)	0.182	1.02 (0.98–1.05)	0.424
Hypertension	1.63 (0.70–3.78)	0.261	1.83 (1.15–2.94)	0.011
Diabetes	1.43 (0.43–4.79)	0.556	2.05 (1.15–3.63)	0.015
Current smoking	0.99 (0.34–2.89)	0.996	0.98 (0.55–1.75)	0.962
Family history	1.26 (0.54–2.93)	0.597	0.77 (0.46–1.29)	0.333
Dyslipidemia	0.62 (0.27–1.42)	0.263	0.67 (0.40–1.01)	0.052
Framingham	0.98 (0.93–1.03)	0.404	1.02 (1.01–1.03)	0.048
Therapy				
ASA	1.50 (0.56–3.99)	0.411	1.69 (1.03–2.77)	0.038
Statin	0.70 (0.20–2.40)	0.572	0.97 (0.55–1.72)	0.931
CCTA characteristics				
No CAD	1		1	
SIS > 5	1.94 (0.46–8.22)	0.367	2.02 (1.06–4.56)	0.034
Non-Ob CT-LeSc ≤ 5	1.12 (0.44–2.85)	0.807	2.11 (1.29–3.42)	0.003
Non-OB CT-LeSc > 5	1.61 (0.56–4.53)	0.376	2.17 (1.22–3.86)	0.009

Table 6
Univariate analysis for symptomatic patients.

	MI		MI + All-cause death	
	HR (95% CI)	*p*	HR (95% CI)	*p*
Clinical characteristics				
Age	1.01 (0.97–1.03)	0.921	1.04 (1.02–1.07)	<0.001
Male	0.86 (0.43–1.74)	0.862	0.74 (0.46–1.22)	0.246
BMI	1.02 (0.95–1.08)	0.641	1.01 (0.96–1.05)	0.754
Hypertension	1.15 (0.57–2.31)	0.696	1.76 (1.06–2.95)	0.031
Diabetes	1.93 (0.9–4.67)	0.149	1.83 (0.98–3.42)	0.059
Current smoking	1.49 (0.67–3.32)	0.323	1.39 (0.79–2.44)	0.249
Family history	1.38 (0.68–2.79)	0.373	1.05 (0.63–1.72)	0.866
Dyslipidemia	1.51 (0.74–3.08)	0.259	1.40 (0.87–2.29)	0.181
Morise	1.01 (0.92–1.09)	0.946	1.08 (1.02–1.16)	0.016
Therapy				
ASA	1.82 (0.84–3.93)	0.129	1.18 (0.66–2.08)	0.571
Statin	1.31 (0.59–2.87)	0.513	1.29 (0.76–2.18)	0.354
CCTA characteristics				
No CAD	1		1	
SIS	–	–	2.03 (1.01–5.31)	0.051
Non-Ob CT-LeSc ≤ 5	1.20 (0.49–2.92)	0.677	1.43 (0.80–2.57)	0.229
Non-OB CT-LeSc > 5	2.54 (1.13–5.75)	0.025	2.53 (1.42–4.48)	0.002

cont.

Manuscrito 13

Table 7
Multivariate analysis for asymptomatic and asymptomatic patients.

	MI HR (95% CI)	p	MI + all-cause death HR (95% CI)	p
Asymptomatic patients				
Model 1*				
Non-Ob CT-LeSc > 5	3.34 (0.97–11.44)	0.059	2.56 (1.31–4.99)	0.006
Model 2*				
SIS > 5	2.42 (0.55–10.73)	0.248	1.80 (0.82–3.95)	0.144
Model 3§				
Non-Ob CT-LeSc > 5	3.15 (0.84–11.78)	0.089	1.50 (0.73–2.94)	0.227
Model 4§				
SIS > 5	1.19 (0.26–5.51)	0.821	0.98 (0.41–2.35)	0.967
Symptomatic patients				
Model 1#				
Non-Ob CT-LeSc > 5	2.63 (1.07–6.46)	0.035	2.39 (1.29–4.42)	0.006
Model 2#				
SIS > 5	–	–	2.03 (0.85–4.82)	0.110
Model 3§				
Non-Ob CT-LeSc > 5	2.76 (1.06–7.25)	0.040	1.81 (0.94–3.51)	0.075
Model 4§				
SIS > 5	–	–	1.54 (0.64–1.86)	0.807

§ Adjusted for ASA and baseline clinical characteristics.
# Adjusted for ASA and Morise score.
* Adjusted for ASA and Framingham score.

exhibited a prognosis that was halfway between that of patients without plaques and that of patients with a CT-LeSc > 5.

4.6. Future strategies for early detection of non-obstructive CAD

Previous studies have proposed that early identification of non-obstructive CAD with CCTA may lead to a more aggressive strategy to control cardiovascular risk factors and to improve clinical follow-up [4,20]. Recently, a sub-study of CONFIRM performed in a cohort of patients receiving baseline statin and aspirin treatment showed that statin therapy was associated with a significant mortality reduction in patients with non-obstructive CAD but had no impact on patients without CAD [18]. These are valid arguments in support of the identification of parameters, such as the CT-LeSc allowing to stratify the long-term prognosis of the large and heterogeneous group of patients in whom CCTA shows non-obstructive CAD. Moreover, recent studies demonstrated the prognostic value of plaque characterization by CCTA. Indeed, this non-invasive imaging modality is able to identify some features, such as vessel positive remodeling and low-attenuation plaques, that have been associated with a higher risk of cardiac events [19]. High-risk plaques can be detected by CCTA and are independent predictors of fatal and non-fatal acute coronary syndrome, while positive remodeling has been observed in coronary stenoses that, regardless of the degree of narrowing, were found to be functionally important by invasive fractional flow reserve [21]. Therefore, additional studies are needed to integrate the CT-LeSc with other features such as positive remodeling or eventually with non-invasive FFR by CCTA for improving the prognostic characterization of patients without obstructive coronary lesions.

4.7. Study limitations

In interpreting these data some limitations should be considered. First, management decisions in all patient, such as medical therapies or revascularization, were left to the discretion of the referring physicians. Because some therapies (i.e. aspirin, statin) may have a positive effect on patient outcomes and were commonly used in patients with and without plaques, we expect that differences between subgroups would be even greater in the absence of such treatments. Second, we included all-cause mortality in the primary and secondary endpoints given its unparalleled clinical importance and freedom from ascertainment bias. However, as specific causes of death for each patient were not uniformly available at all sites, the true proportion of deaths that could attributable to cardiovascular events in our patients is unknown. Third, this study included a cohort of patients who were referred for CCTA because of suspected CAD and were often symptomatic. Although it is unlikely that our patient symptoms were related to non-obstructive CAD, generalization of this study findings to asymptomatic patients remains uncertain. Fourth, data on coronary calcium score were not included in the analysis because they were available for two third only of the study population.

5. Conclusion

The CT-adapted Leaman score is an independent predictor of major acute cardiac events and allows to distinguish, among a population with non-obstructive CAD, patients with risk of cardiac events similar to those without plaques from patients with a less favorable prognosis.

Conflict of interest

The authors report no relationships that could be construed as a conflict of interest.

References

[1] F. Bamberg, W.H. Sommer, V. Hoffmann, et al., Meta-analysis and systematic review of the long-term predictive value of assessment of coronary atherosclerosis by contrast-enhanced coronary computed tomography angiography, J. Am. Coll. Cardiol. 57 (24) (2011) 2426–2436.
[2] A. Pen, Y. Yam, L. Chen, et al., Discordance between Framingham risk score and atherosclerotic plaque burden, Eur. Heart J. 34 (14) (2013) 1075–1082.
[3] G.P. de Araújo, H.M. Garcia-Garcia, M.S. Carvalho, et al., Diabetes as an independent predictor of high atherosclerotic burden assessed by coronary computed tomography angiography: the coronary artery disease equivalent revisited, Int. J. Cardiovasc. Imaging 29 (5) (2013) 1105–1114.
[4] D. Andreini, G. Pontone, S. Mushtaq, et al., A long-term prognostic value of coronary CT angiography in suspected coronary artery disease, JACC Cardiovasc. Imaging 5 (7) (2012) 690–701.
[5] J.K. Min, A. Dunning, F.Y. Lin, et al., Age- and sex-related differences in all-cause mortality risk based on coronary computed tomography angiography findings results from the International Multicenter CONFIRM, J. Am. Coll. Cardiol. 58 (8) (2011) 849–860.
[6] S. Mushtaq, G.P. De Araujo, H.M. Garcia-Garcia, et al., Long-term prognostic effect of coronary atherosclerotic burden: validation of the computed tomography-Leaman score, Circ. Cardiovasc. Imaging 8 (2) (2015) e002332.
[7] J.K. Min, A. Dunning, F.Y. Lin, et al., Rationale and design of the CONFIRM (COronary CT Angiography EvaluatioN For Clinical Outcomes: An InteRnational Multicenter) Registry, J. Cardiovasc. Comput. Tomogr. 5 (2) (2011) 84–92.
[8] J. Leipsic, S. Abbara, S. Achenbach, et al., SCCT guidelines for the interpretation and reporting of coronary CT angiography: a report of the Society of Cardiovascular Computed Tomography Guidelines Committee, J. Cardiovasc. Comput. Tomogr. 8 (5) (2014) 342–358.
[9] S. Abbara, A. Arbab-Zadeh, T.Q. Callister, et al., SCCT guidelines for performance of coronary computed tomographic angiography: a report of the Society of Cardiovascular Computed Tomography Guidelines Committee, J. Cardiovasc. Comput. Tomogr. 3 (2) (2009) 190–204.
[10] W.G. Austen, J.E. Edwards, R.L. Frye, et al., A reporting system on patients evaluated for coronary artery disease. Report of the Ad Hoc Committee for Grading of Coronary Artery Disease, Council on Cardiovascular Surgery, American Heart Association, Circulation 51 (4Suppl) (1975) 5–40.
[11] G.P. de Araújo, H.M. Garcia-Garcia, H. Dores, et al., Coronary computed tomography angiography-adapted Leaman score as a tool to noninvasively quantify total coronary atherosclerotic burden, Int. J. Cardiovasc. Imaging 29 (7) (2013) 1575–1584.
[12] K. Thygesen, J.S. Alpert, H.D. White, et al., Joint ESC/ACCF/AHA/WHF Task Force for the Redefinition of Myocardial. Universal definition of myocardial infarction, J. Am. Coll. Cardiol. 50 (22) (2007) 2173–2195.
[13] H.S. Hecht, Coronary artery calcium scanning: past, present, and future, JACC Cardiovasc. Imaging 5 (8) (2015) 579–596.
[14] M.J. Pencina, R.B. D'Agostino Sr., E.W. Steyerberg, Extensions of net reclassification improvement calculations to measure usefulness of new biomarkers, Stat. Med. 30 (1) (2011) 11–21.
[15] J.E. van Velzen, J.D. Schuijf, F.R. de Graaf, et al., Diagnostic performance of noninvasive multidetector computed tomography coronary angiography to detect coronary artery disease using different endpoints: detection of significant stenosis vs. detection of atherosclerosis, Eur. Heart J. 32 (5) (2011) 637–645.
[16] M.S. Bittencourt, E. Hulten, B. Ghoshhajra, et al., Prognostic value of nonobstructive and obstructive coronary artery disease detected by coronary computed tomography angiography to identify cardiovascular events, Circ. Cardiovasc. Imaging 7 (2) (2014) 282–291.
[17] F.Y. Lin, L.J. Shaw, A.M. Dunning, et al., Mortality risk in symptomatic patients with nonobstructive coronary artery disease: a prospective 2-center study of 2,583

cont.

Manuscrito 13

patients undergoing 64-detector row coronary computed tomographic angiography, J. Am. Coll. Cardiol. 58 (5) (2011) 510–519.
[18] B.J. Chow, G. Small, Y. Yam, et al., Prognostic and therapeutic implications of statin and aspirin therapy in individuals with nonobstructive coronary artery disease: results from the CONFIRM registry, Arterioscler. Thromb. Vasc. Biol. 35 (4) (2015) 981–989.
[19] S. Motoyama, H. Ito, M. Sarai, et al., Plaque characterization by coronary computed tomography angiography and the likelihood of acute coronary events in mid-term follow-up, J. Am. Coll. Cardiol. 66 (4) (2015) 337–346.
[20] D. Andreini, G. Pontone, S. Mushtaq, et al., Prognostic value of multidetector computed tomography coronary angiography in diabetes: excellent long-term prognosis in patients with normal coronary arteries, Diabetes Care 36 (7) (2013) 1834–1841.
[21] Park HB, Heo R, ó Hartaigh B et al. Atherosclerotic plaque characteristics by CT angiography identify coronary lesions that cause ischemia: a direct comparison to fractional flow reserve. JACC Cardiovasc. Imaging 2015;8(1):1-10.

MANUSCRITO 14

Coronary computed tomography angiography-adapted Leaman score as a tool to noninvasively quantify total coronary atherosclerotic burden

de Araujo Goncalves, P., Garcia-Garcia, H.M., Dores, H., Carvalho, M.S., Jeronimo Sousa, P., **Marques**, **H**., Ferreira, A., Cardim, N., Campante Teles, R., Raposo, L., Mesquita Gabriel, H., Sousa Almeida, M., Aleixo, A., Mota Carmo, M., Pereira Machado, F., and Mendes, M.

Int J Cardiovasc Imaging, 2013
29(7): p. 1575-84

Manuscrito 14

Int J Cardiovasc Imaging (2013) 29:1575–1584
DOI 10.1007/s10554-013-0232-8

ORIGINAL PAPER

Coronary computed tomography angiography-adapted Leaman score as a tool to noninvasively quantify total coronary atherosclerotic burden

Pedro de Araújo Gonçalves · Hector M. Garcia-Garcia · Helder Dores · Maria Salomé Carvalho · Pedro Jerónimo Sousa · Hugo Marques · Antonio Ferreira · Nuno Cardim · Rui Campante Teles · Luís Raposo · Henrique Mesquita Gabriel · Manuel Sousa Almeida · Ana Aleixo · Miguel Mota Carmo · Francisco Pereira Machado · Miguel Mendes

Received: 19 April 2013 / Accepted: 24 April 2013 / Published online: 1 May 2013

Abstract To describe a coronary computed tomography angiography (CCTA)-adapted Leaman score (CT-LeSc) as a tool to quantify total coronary atherosclerotic burden with information regarding localization, type of plaque and degree of stenosis and to identify clinical predictors of a high coronary atherosclerotic burden as assessed by the CT-LeSc. Single center prospective registry including a total of 772 consecutive patients undergoing CCTA (Dual-source CT) from April 2011 to March 2012. For the purpose of this study, 581 stable patients referred for suspected coronary artery disease (CAD) without previous myocardial infarction or revascularization procedures were included. Pre-test CAD probability was determined using both the Diamond–Forrester extended CAD consortium method (DF-CAD consortium model) and the Morise score. Cardiovascular risk was assessed with the HeartScore. The cut-off for the 3rd tercile (CT-LeSc $\geq$8.3) was used to define a population with a high coronary atherosclerotic burden. The median CT-LeSc in this population (n = 581, 8,136 coronary segments evaluated; mean age 57.6 $\pm$ 11.1; 55.8 % males; 14.6 % with diabetes) was 2.2 (IQR 0–6.8). In patients with CAD (n = 341), the median CT-LeSc was 5.8 (IQR 3.2–9.6). Among patients with nonobstructive CAD, most were classified in the lowest terciles (T1, 43.0 %; T2, 36.1 %), but 20.9 % were in the highest tercile (T3). The majority of the patients with obstructive CAD were classified in T3 (78.2 %), but 21.8 % had a CT-LeSc in lower terciles (T1 or T2). The independent predictors of a high CT-LeSc were: Male sex (OR 1.73; 95 % CI 1.04–2.90) diabetes (OR 2.91; 95 % CI 1.61–5.23), hypertension (OR 2.54; 95 % CI 1.40–4.63), Morise score $\geq$16 (OR 1.97; 95 % CI 1.06–3.67) and HeartScore $\geq$5 (OR 2.42; 95 % CI 1.41–4.14). We described a cardiac CT adapted Leaman score as a tool to quantify total (obstructive and nonobstructive) coronary atherosclerotic burden, reflecting the comprehensive information about localization, degree of stenosis and type of plaque provided by CCTA. Male sex, hypertension, diabetes, a HeartScore $\geq$5 % and a Morise score $\geq$16 were associated with a high coronary atherosclerotic burden, as assessed by the CT-LeSc. About one fifth of the patients with nonobstructive CAD had a CT-LeSc in the highest tercile, and this could potentially lead to a reclassification of the risk profile of this subset of patients identified by CCTA, once the prognostic value of the CT-LeSc is validated.

Keywords CCTA · Coronary artery disease · Atherosclerotic burden · Risk scores

P. de Araújo Gonçalves (✉) · H. Dores · M. S. Carvalho · P. Jerónimo Sousa · A. Ferreira · R. Campante Teles · L. Raposo · H. Mesquita Gabriel · M. Sousa Almeida · A. Aleixo · M. Mendes
Cardiology Department, Centro Hospitalar Lisboa Ocidental, Lisbon, Portugal
e-mail: paraujogoncalves@yahoo.co.uk

P. de Araújo Gonçalves · H. Marques · A. Ferreira · N. Cardim · F. Pereira Machado
Hospital da Luz, Lisbon, Portugal

P. de Araújo Gonçalves · A. Aleixo · M. Mota Carmo
CEDOC, Chronic Diseases Research Center, FCM-NOVA, Lisbon, Portugal

H. M. Garcia-Garcia
Thoraxcenter, Erasmus MC, Rotterdam, The Netherlands

cont.

Introduction

Coronary atherosclerosis is the leading cause of mortality and it is expected to remain the most important disease in the upcoming years [1]. Frequently, the first manifestation of coronary disease is an acute coronary syndrome (ACS), and many patients were previously asymptomatic [2]. An early detection of coronary disease is of utmost relevance and a non-invasive diagnostic test is desirable.

In the recent years, coronary computed tomography angiography (CCTA) has become widely available and adopted. The main reason for this is the high predictive accuracy of detection of obstructive coronary artery disease (CAD) compared to conventional invasive coronary angiography [3, 4]. In addition, CCTA allows also the identification of nonobstructive CAD and in this way it can provide a noninvasive quantification of the total coronary atherosclerotic burden. Since the percentage of patients with nonobstructive CAD is very high, there is a need for tools to stratify cardiovascular risk by the degree of plaque burden [5]. The information regarding the localization, severity and composition of coronary plaques identified with CCTA can be collected in scores to reflect the total coronary plaque burden, and some have been already developed and validated [6].

Conventional cardiovascular (CV) risk factors relate to the risk of subsequent CV events and they can be combined in tools as it has been done in the Heart Score [7]. Notwithstanding these observations, accurate prediction of major coronary events on the individual patient level, as opposed to population based studies, remains challenging.

Therefore the aim of this study is two folded: (1) To describe a CCTA-adapted Leaman score (CT-LeSc) as a tool to quantify total coronary atherosclerotic burden including information regarding localization, type of plaque and degree of stenosis and; (2) To identify clinical predictors of a high coronary atherosclerotic burden as assessed by CT-LeSc in a population of stable patients referred for CCTA for suspected CAD.

Methods

Population

Single center prospective registry including a total of 772 consecutive patients undergoing CCTA (with Dual source CT) from April 2011 to March 2012. Patients were excluded if: (1) previous myocardial infarction and/or revascularization procedures (n = 70); (2) referred for Cardiac CT for other indications than the evaluation of possible CAD (cardiac CT for atrial fibrillation ablation or transcatheter aortic valvular implantation procedures; n = 88); (3) referred for suspected ACS (n = 24); (4) with atrial fibrillation or other significant arrhythmias during scan acquisition that compromised image quality (n = 9). This resulted in a 24.7 % of the total population being excluded.

For the purpose of this study, 581 stable patients referred for suspected CAD were included in the context of: (1) Previous equivocal or inconclusive stress tests or discordant with the clinical evaluation (n = 417; 71.8 %); (2) Cardiac CT as 1st line investigation of possible CAD (n = 136; 23.4 %); (3) Preoperative CAD assessment prior to noncoronary valvular or aortic surgery (n = 17; 2.9 %); (4) Evaluation of possible CAD in cardiomyopathies (DCM or HCM; n = 11; 1.9 %; Fig. 1: Patient selection and study design).

The study was approved by the local ethics committee and all patients gave a written informed consent.

A detailed medical history with a risk factors questionnaire was obtained from the patients to assess for the presence of: (1) Diabetes mellitus (defined as a fasting glucose level of ≥7 mmol/l or the need for insulin or oral hypoglycemic agents) [8]; (2) Dyslipidemia (defined as a total cholesterol level ≥5 mmol/l or treatment with lipid-lowering drugs) [9]; (3) Hypertension (defined as blood pressure ≥140/90 mm Hg or the use of antihypertensive medication) [10]; (4) Obesity (body mass index ≥30 kg/m^2); (5) positive family history of premature CAD (defined as the presence of CAD in first-degree relatives younger than 55 [male] or 65 [female] years of age) [11]; (6) smoking (defined as previous [less <1 year] or current smoker.

Pre-test probability of CAD was determined using both the Diamond and Forrester extended CAD consortium method (DF-CAD consortium model) [12] and the Morise score [13]. The cardiovascular risk was assessed with the HeartScore [7]. As the CAD probability and CV risk of our population was shifted to lower probability and risk, the cut-offs used were: (1) for DF-CAD consortium model categories ≥30–70 and ≥70 % were gathered in a Intermediate to High (≥30 %) probability group.

For the Morise, the population was divided in terciles, and for the HeartScore the established high risk cut-off of ≥5 % was used.

Scan protocol and image reconstruction

All scans were performed with a dual-source scanner (Somatom Definition, Siemens Medical, Germany), with the patient in dorsal decubitus and in deep inspiration breath-hold. Sublingual nitroglycerin was administered to all patients except when contraindicated and intravenous metoprolol (5 mg, with a titration dose up to 20 mg) was administered in patients with heart rate >65 beats/min.

During the scan acquisition, a bolus of iodinated contrast (Visipaque, GE Healthcare, USA) was injected at a

cont.

Manuscrito 14

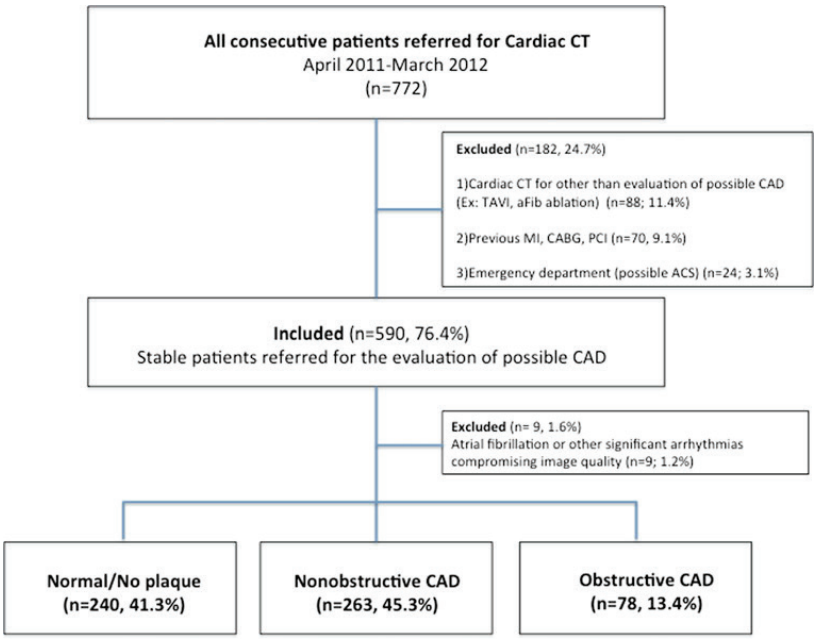

Fig. 1 Patient selection and study design. *CAD* coronary artery disease, *TAVI* transcatheter aortic valve implantation, *aFib* atrial fibrillation, *MI* myocardial infarction, *CABG* coronary artery bypass grafting, *PCI* percutaneous coronary intervention, *ACS* acute coronary syndromes

6 ml/s infusion rate, followed by a 50-ml saline flush. The dose of contrast was calculated according to the following formula: (acquisition time +6 s delay) × flow (6 ml/s). Contrast timing was performed to optimize uniform contrast enhancement of the coronary arteries.

Dose reduction strategies—including electrocardiogram-gated tube current modulation, reduced tube voltage, and prospective axial triggering—were used whenever feasible. Mean estimated radiation dose was 4.6 ± 3.7 mSv, contrast dose was 98.9 ± 14.4 ml and heart rate was 65.6 ± 10.6 bpm.

Transaxial images were reconstructed with a temporal resolution of 83 ms and slice thickness of 0.75 mm with 0.4 mm increments.

Post-processing was carried out using Circulation® software, with multiplanar reconstructions, maximum intensity projection and volume rendering technique.

Coronary artery analysis

All scans were analyzed in the same session by both a cardiologist and a radiologist with Level III-equivalent experience. The Society of Cardiovascular Computed Tomography recommended classification was used regarding segmentation (16 segments), stenosis severity (<25, 25–49, 50–69, 70–99, 100 %) and plaque composition (calcified, non calcified, mixed plaque) [14].

In each coronary artery segment, coronary atherosclerosis was defined as a tissue structure >1 mm^2 that existed either within the coronary artery lumen or adjacent to the coronary artery lumen that could be discriminated from surrounding pericardial tissue, epicardial fat, or the vessel lumen itself [6]. Coronary atherosclerotic lesions were quantified for stenosis by visual estimation. Percent obstruction of coronary artery lumen was based on a comparison of the luminal diameter of the segment exhibiting obstruction to the luminal diameter of the most normal-appearing site immediately proximal to the plaque.

CCTA adapted Leaman score (CT-LeSc)

For the CT adaptation of the LeSc, we used three sets of weighting factors, all noninvasively provided by CCTA: (1) *localization* of the coronary plaques as originally described [15]. In this study, a modification was made to account for balanced dominance. In cases of balanced dominance, not taken in account in the original Leaman or in the Syntax scores, we assumed an intermediate value between right and left dominance which changed the values for the posterior descending and the proximal, mid and

cont.

distal RCA segments as well as for the left main and proximal and distal segments of the circumflex; (2) *type of plaque* (i.e. noncalcified, calcified or mixed plaques). To take in account the cardiac CT added information related to plaque composition, an additional weighting factor of 1.5 was added to predominantly noncalcified of mixed plaques and a factor of 1 to predominantly calcified plaques, reflecting the assumption of less plaque vulnerability of the later ones [16, 17]; (3) *degree of stenosis* (<50 ≥% stenosis). In the presence of obstructive CAD (≥50 % stenosis), the score in each segment was multiplied by 1 and for nonobstructive CAD it was multiplied by a factor of 0.615. This factor reflects the relative proportion in the published hazard ratios for mortality in the large CONFIRM registry [5] for obstructive versus nonobstructive CAD (2.6 vs 1.6 respectively) and it was assumed to reflect the relative prognostic impact of nonobstructive CAD (Table 1).

Table 1 CT-adapted Leaman Score (CT-LeSc) weighting factors

Segment	Right dominance	Left dominance	Balanced
Coronary segments			
RCA proximal	1	0	0.5
RCA mid	1	0	0.5
RCA distal	1	0	0.5
PDA	1	na	0.5
Left main	5	6	5.5
LAD proximal	3.5	3.5	3.5
LAD mid	2.5	2.5	2.5
LAD distal	1	1	1
1st diagonal	1	1	1
2nd diagonal	0.5	0.5	0.5
LCx proximal	1.5	2.5	2.0
1st obtuse marginal	1	1	1
LCx distal	0.5	1.5	1
2nd obtuse marginal	1	1	1
PDA from LCA	na	1	na
PL branch from LCA	na	0.5	0.5
PL branch from RCA	0.5	na	na
Intermediate branch	1	1	1
Stenosis severity			
Obstructive CAD	1		
Nonobstructive CAD	0.615		
Plaque composition			
Non-calcified or mixed	1.5		
Calcified	1		

RCA right coronary artery, *PDA* posterior descending artery, *LAD* left anterior descending, *LCx* left circumflex, *PL* postero-lateral, *CAD* coronary artery disease

The CT-LeSc on a patient level was calculated as the sum of the partial CT-LeSc of all evaluable coronary segments. Two cases examples are shown in Fig. 2.

Statistical analysis

Continuous variables are presented as mean ± SD or medians (interquartile range) and categorical variables as frequencies with percentages.

The non-parametric Mann–Whitney or Kruskal–Wallis tests were used to compare continuous variables, and the Chi square test to evaluate differences in frequencies. Differences were regarded significant when $p < 0.05$ (two-tailed).

Since there are no previous validated cut-offs for the presently described CCTA score, the population with CAD was divided in terciles. A high CT-LeSc was defined with the cut-off for the 3rd tercile (a score ≥8.3, n = 116; 34.8 % of the CAD population) and patients in this group were compared with the remaining population.

Multivariate analyses (binary logistic regression model—enter method) were performed to identify independent predictors of a high CT-LeSc using the demographic and clinical variables presented in Table 2 that had a p value <0.2 at univariate analyses. A second multivariable analyses was performed to identify independent predictors among the clinical scores of CAD probability (Diamond–Forrester CAD consortium model and Morise score) and the CV risk score HeartScore.

SPSS version 17.0 (SPSS Inc., Chicago, IL, USA) was used for all statistical analyses.

Results

In the final study population of 581 patients, 8,136 coronary segments were evaluated. Segments <2 mm (n = 742; 9.1 %) or with suboptimal image quality related to artefacts or severe calcification (n = 120; 1.5 %) were excluded.

Most of patients were male (55.8 %) and mean age was 57.6 ± 11.1, and 14.6 % were diabetics. This was predominantly a population with low to intermediate CAD probability since 60.1 % had a DF-CAD consortium <30 and 87.6 % had a Morise score <16. A high cardiovascular risk, as assessed by an HeartScore ≥5 %, was present in 25.5 % of the patients. In this population, the median calcium score was 1 (IQR 0–93), 23.4 % had a calcium score (CaSc) ≥100 and 14.3 % had a CaSc ≥75th percentile. In the population with CAD, the median CaSc was 64 (IQR 8–200; Table 2).

CT-LeSc

Overall (n = 581), the median CT-LeSc in this population was 2.2 (IQR 0–6.8). In patients with CAD (n = 341), the

Manuscrito 14

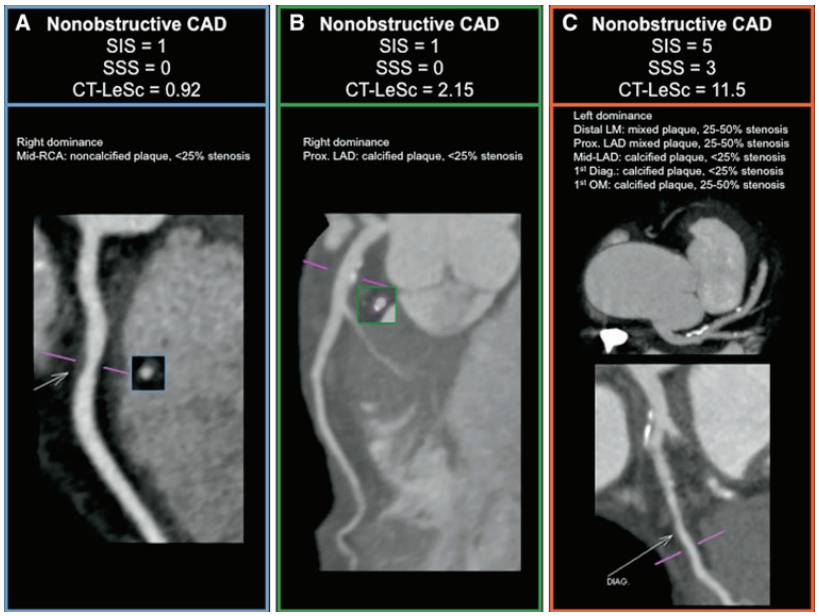

Fig. 2 Three cases examples of patients with nonobstructive CAD stratified by different coronary atherosclerotic burden scores. In panel *A*, a patient with a single lesion in the mid-RCA (weighting for localization × type of plaque × stenosis severity = 1 × 1.5 × 0.615 = 0.92); In panel *B*, a patient with a single proximal LAD lesion (CT-LeSc = 3.5 × 1 × 0.615 = 2.15). In panel *C*, a patient with left dominance and 5 nonobstructive lesions with a total CT-LeSc = LM (6 × 1.5 × 0.615) + prox. LAD (3.5 × 1.5 × 0.615) + mid-LAD (2.5 × 1 × 0.615) + 1st Diag. (1 × 1 × 0.615) + 1st OM (1 × 1 × 0.615) = 11.5. *CAD* coronary artery disease, *CT-LeSc* CT Leaman score, *SIS* segment involvement score, *SSS* segment stenosis score, *LM* left main, *LAD* left anterior descending, *LCx* left circunflex, *RCA* right coronary artery, *1st Diag.* first diagonal branch, *1st OM* first obtuse marginal branch

median CT-LeSc was 5.8 (IQR 3.2–9.6). Within this population the median CT-LeSc in patients with non-obstructive disease (n = 263) was 4.6 (IQR 2.9–7.7) and in patients with obstructive disease (n = 78) it was 11.7 (IQR 8.7–14.4). The terciles in population with CAD were: *T1 ≤3.7 (0.3–3.7)*; *T2 (3.8–8.3)*; *T3* ≥8.3 (8.3–24.1).

Regarding the distribution of patients with nonobstructive versus obstructive CAD across the CT-LeSc terciles, most of the patients with nonobstructive CAD were in T1 (n = 113, 43.0 %) or T2 (n = 95, 36.1 %), but about one fifth (n = 55, 20.9 %) were in the highest tercile (T3, CT-LeSc ≥8.3). On the other hand, although most of the patients with obstructive CAD were classified in T3, 21.8 % had a CT-LeSc in lower terciles (T1, 2.6 %; T2, 19.2 %; Fig. 3).

The median CT-LeSc was significantly higher in males and in the presence of diabetes and hypertension, as well as in patients with a high cardiovascular risk assessed by an HeartScore ≥5 %. The median CT-LeSc was also significantly higher in patients with a CaSc ≥100 and CaSc ≥75th percentile (Fig. 4: Median CT-LeSc in different patient subgroups).

Univariate predictors

In the univariate analysis, a high CT-LeSc was associated with older age (≥60 years), diabetes and hypertension. The percentage of male patients and patients with dyslipidemia was also higher in the high CT-LeSc group, but not statistically significant. Patients in the high CT group had also a higher pre-test CAD probability (DF-CAD consortium ≥30 % and Morise score ≥16) as well as higher CV risk, reflected in the significantly higher percentage of patients with a HeartScore ≥5 %. Of note, some traditional risk factor as obesity, smoking status and family history of premature CAD were not differently distributed in the two groups, and this was also the case for chest pain (Table 3).

Multivariate predictors

By multivariate analysis, the independent predictors of a high CT-LeSc were: male sex; diabetes, hypertension, Morise score ≥16 and HeartScore ≥5 (Table 4; Fig. 5). Of note, regarding the modifiable risk factors, patients with

cont.

Table 2 Demographic, clinical and CCTA characteristics of the study population

	All patients (n = 581)
Demographic	
Age	57.6 ± 11.1
Male sex	324 (55.8)
Risk factors	
Obesity (BMI ≥30)	109 (18.8)
Diabetes	85 (14.6)
Hypertension	364 (62.7)
Dyslipidemia	360 (62.0)
Smoking	138 (23.8)
Family history of premature CAD	194 (33.4)
Chest pain	
Asymptomatic	270 (46.5)
Noncardiac	169 (29.1)
Atypical	109 (18.8)
Typical	33 (5.7)
CAD probability	
DF-CAD consortium ≥70 %	11 (1.9)
DF-CAD consortium 30–70 %	221 (38.0)
DF-CAD consortium <30 %	349 (60.1)
Morise score ≥16	72 (12.4)
Morise score 9–15	369 (63.5)
Morise score 0–8	140 (24.1)
CV risk	
Heart score ≥5 %	148 (25.5)
Calcium score	
Median	1 (0–93)
Median in patients with CAD	64 (8–200)
CaSc ≥100	136 (23.4)
CaSc ≥75th percentile	83 (14.3)
CCTA	
Normal/no plaque	240 (41.3)
Nonobstructive CAD	263 (45.3)
Obstructive CAD	78 (13.4)
Technical data	
Heart rate (bpm)	65.6 ± 10.6
Contrast dose (ml)	98.9 ± 14.4
Radiation dose (mSv)	4.6 ± 3.7

Values are mean ± SD, median (IQR) or n (%)

CAD coronary artery disease, *BMI* body mass index, *DF-CAD consortium* Diamond–Forrester CAD consortium model, *CV* cardiovascular, *CCTA* coronary computed tomography angiography, *CaSc* calcium score, *bpm* beats per minute, *mSv* milisievert

diabetes had a threefold and patients with hypertension a 2.5-fold higher probability of having a high CT-LeSc.

A high HeartScore (≥5 %) and a high Morise score (≥16) were associated respectively with a 2.5 and twofold higher probability of having a high coronary atherosclerotic burden, as assessed by the CT-LeSc.

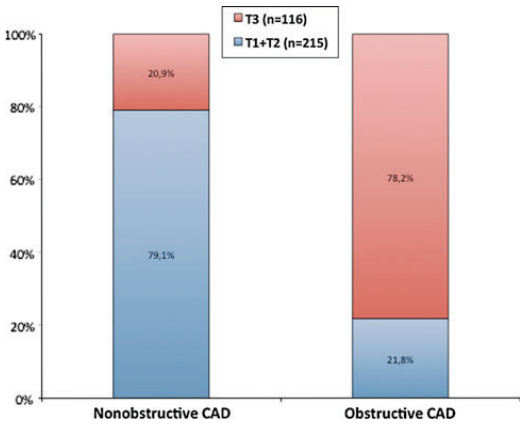

Fig. 3 Distribution of the two subgroups of patients (nonobstructive and obstructive CAD), according to CT-LeSc terciles (T1 + T2 vs T3). *CAD* coronary artery disease, *T1* 1st tercile, *T2* 2nd tercile, *T3* 3rd tercile

Discussion

The main findings of this study are: (1) Calculation of a cardiac CT adapted Leaman score as a tool to quantify total (obstructive and nonobstructive) coronary atherosclerotic burden, reflecting the comprehensive information about localization, degree of stenosis and type of plaque provided by CCTA is feasible; (2) There was a significant association between the CT-LeSc and diabetes, a well recognized subset of advanced coronary atherosclerotic burden. A high CV risk (HeartScore) and a high CAD probability (Morise score) were also both associated with nearly a 2–2.5 fold higher probability of having a high coronary atherosclerotic burden, as assessed by the CT-LeSc.

Although the exclusion of obstructive CAD remains presently the main indication to refer a patient for CCTA, this noninvasive diagnostic tool can also provide information regarding the presence of nonobstructive plaques, detecting CAD at earlier disease stages. Although on a *per lesion* basis, vulnerability is positively associated with the degree of stenosis, on a *per patient* level most of the acute events come from nonobstructive lesions [18–20]. It is also recognized that many of the nonstenotic lesions can have a high plaque burden, underestimated by luminal angiograms, since they undergo expansive or positive outward enlargement, and such remodeling is a potential surrogate marker of plaque vulnerability [21]. In the multicenter virtual histology intravascular ultrasound (VH-IVUS) PROSPECT study [22], a large plaque burden, a small lumen area and the presence of a thin cap fibroatheroma were independent predictors of future nonculprit lesion major adverse cardiac events (MACE). In this study, lesions that led to MACE had a high plaque burden by

cont.

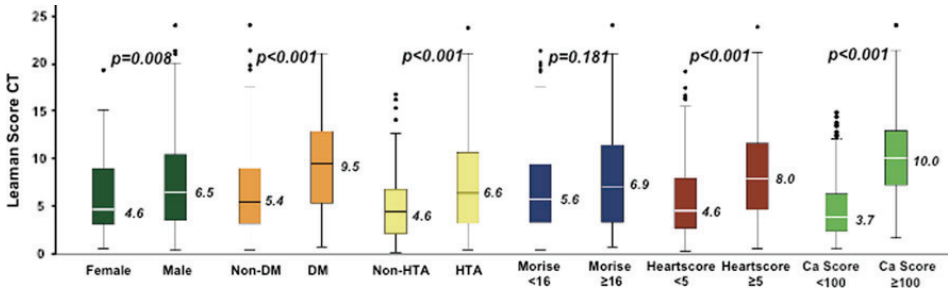

Fig. 4 Median CT-LeSc in different patient subgroups. *DM* diabetes mellitus, *HTA* hypertension, *CA score* calcium score, *CT-LeSc* CT Leaman score

Table 3 Univariate analysis

	CT LeSc T1 + 2 (<8.3)	CT LeSc ≥ T3 (≥8.3)	*p*
Age ≥60	126 (56.0)	79 (68.1)	0.031
Male sex	138 (61.3)	81 (69.8)	0.121
BMI ≥30	41 (18.3)	25 (22.1)	0.404
Diabetes	26 (11.6)	36 (31.0)	<0.001
Hypertension	144 (64.0)	98 (84.5)	<0.001
Dyslipidemia	146 (64.9)	87 (75.0)	0.057
Smoking	53 (23.6)	31 (26.7)	0.520
Family history of premature CAD	77 (34.2)	37 (31.9)	0.666
Chest pain	106 (47.3)	59 (51.3)	0.487
DF-CAD consortium ≥30 %	66 (29.3)	64 (55.2)	<0.001
Morise score ≥16	105 (46.7)	78 (67.2)	<0.001
Heart score ≥5	29 (12.9)	24 (20.7)	0.060

Values are n (%); *CAD* coronary artery disease, *BMI* body mass index, *DF-CAD* consortium-diamond–Forrester CAD consortium model

Table 4 Multivariate analysis—independent predictors of a high CT-LeSc (3rd tercile, score ≥8.3)

	OR	(95 % CI)	*p*
Demographic and clinical variables			
Age ≥60	1.370	0.819–2.291	0.230
Male sex	1.732	1.035–2.901	0.037
Diabetes	2.905	1.612–5.234	<0.001
Hypertension	2.543	1.395–4.634	0.002
Dyslipidemia	1.563	0.919–2.660	0.099
Clinical scores			
Heart score ≥5	2.416	1.411–4.135	0.001
DF-CAD consortium ≥30 %	1.590	0.918–2.754	0.098
Morise ≥16	1.971	1.060–3.666	0.032

OR odds ratio, *DF-CAD consortium* Diamond–Forrester CAD consortium model

IVUS, but were mild by baseline angiography (mean diameter stenosis 32 %). The prognostic value of nonobstructive CAD has also been recently reinforced from large cardiac CT registries (CONFIRM) and meta-analysis [23].

In the large international multicenter CONFIRM registry, all-cause mortality was significantly higher for patients with nonobstructive CAD, as compared with patients without coronary atherosclerosis. One notable finding in this registry is the superimposed survival curves of nonobstructive and 1 vessel obstructive CAD, reinforcing the prognostic impact of nonobstructive coronary lesions [6].

Why a plaque burden CT score?

The main reason is because CAD represents a very heterogeneous condition and there is a need to structure the quantification of the plaque burden and to integrate the most important information collected by CT and finally to homogenize the reporting of CT findings.

There are already some CT scores developed and prognostically validated namely the segment involvement score (SIS) and the segment stenosis score (SSS), but they only reflect some aspects of the coronary atherosclerotic burden, the former only takes into account the number of segments with plaque and the latter the degree of stenosis [6]. The CT-LeSc reflects some of the aspects that are partially included in the SIS (number of segments with plaque) and the SSS (degree of stenosis), and combines these two aspects, and also the localization, on a more comprehensive score.

Why these three components?

Individually, *localization* of the plaque within the coronary tree, *the type of plaques* and *degree of stenosis* are strong predictors of future coronary events.

Since CCTA is able to reliably collect information on these three aspects, a comprehensive score should be able to integrate these components.

cont.

Manuscrito 14

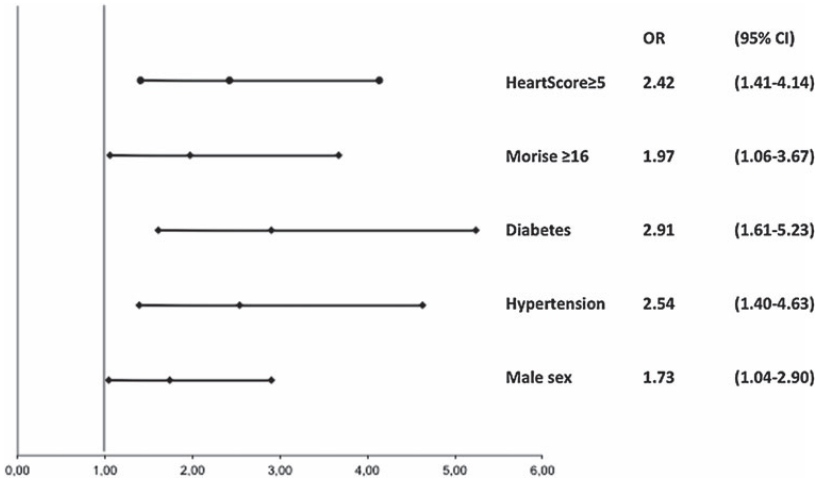

Fig. 5 Independent predictors of a high CT-LeSc (score ≥8.3). *CT-LeSc* CT Leaman score

Regarding *localization*, the original Leaman score was developed as a score to quantify obstructive coronary disease identified with invasive angiography [15]. In this score, with the rational of relative blood supply to the left ventricle, all coronary segments were given a weighting factor, reflecting the relative contribution of blood flow to the left ventricle of each vessel segment, taking also in account the specific right or left dominance systems. Recently, this score was used as the segment weighting factor for the development of the syntax score [24] which has been proven to have a strong prognostic value in different clinical scenarios [25, 26]. In our score, values were also provided for balanced dominance, reflecting more adequately the anatomical variants of the coronary tree.

Plaque composition has been found in both pathological and clinical studies associated with cardiac events [22, 27]. CCTA has shown to be able to characterize plaque composition [28]. Thin cap fibroatheroma is the most common pathological substrate of ACS and in CCTA these plaques appear as noncalcified or mixed plaques [16]. In a recent study by Maurovich-Horvat et al. [16], the frequency of a napkin-ting sign, a CCTA feature of advanced lesions by histology, was similar between noncalcified and mixed plaques, which also reinforces our weighting factor in the CT-LeSc for plaque composition that was the same between these two types (a factor of 1.5), and different from predominantly calcified plaques (a factor of 1).

Regarding the *degree of stenosis*, we assumed in our scoring system a factor reflecting the proportion of the hazard ratios for obstructive versus nonobstructive observed in the recently large scale CONFIRM registry. By gathering all the nonobstructive (<25, 25–49 %) and obstructive (50–69, 70–99, 100 %) in the same risk categories, this scoring system is expected to have a good intra and inter-observer correlation, since the other two weighting factors (localization and plaque calcification) have also an excellent reproducibility and are usually described in CCTA reporting.

Clinical implications

Many tools are already available to help stratifying patients at risk of a CV event and some scores have been already developed gathering the information provided by the different traditional risk factors, like the Framingham score or the HeartScore. Notwithstanding these observations, accurate prediction of major coronary events on the individual patient level, as opposed to population based studies, remains challenging.

The clinical implications of a score that reflect the extent of coronary atherosclerotic burden is related to the fact that this way we can have a tool to quantify and compare this burden, which is particularly useful when reporting a CCTA of a patient without obstructive CAD, but in whom the extent of nonobstructive CAD could lead to a reclassification of his risk profile and thereby his cardiovascular treatment.

Of note in our study is the fact that although the CT-LeSc, by having the degree of stenosis in its composition, tends to favour patients with obstructive CAD, we were able to demonstrate that a significant percentage (20.9 %) of patients with nonobstructive CAD had in fact a CT-LeSc in the highest tercile (T3). Conversely, among patients with obstructive CAD, about one fifth had a coronary

cont.

atherosclerotic burden, as assessed by the CT-LeSc, in lower terciles.

The CT-LeSc, by having a weight related to the localization, it reflects not only the extent of CAD but also the expected clinical consequences in case that the more proximal lesions evolve to a significant stenosis or become unstable and trigger a coronary event.

In our study, a high HeartScore and a high Morise score were both associated with nearly a 2–2.5 fold higher probability of having a high coronary atherosclerotic burden, as assessed by the CT-LeSc. This could be expected for the HeartScore, as it was develop as a tool to predict cardiovascular risk. In the case of the Morise score, is was developed and validated as a clinical tool to estimate the probability of CAD, but it has also been linked to cardiovascular outcomes [29]. The Diamond–Forrester was not an independent predictor of a high CT-LeSc and although we used the recently calibrated CAD consortium model [12], is has been developed and calibrated for obstructive CAD identified with invasive angiography and doesn't take in account the cardiovascular risk factors in its composition.

Limitations

There are a number of limitations related to this report: (1) This is a single center data with medium size cohort; (2) High prevalence of low CAD probability/CV risk patients. The population included in our study was mainly composed of patients with low to intermediate CAD probability and CV risk. Nevertheless, CAD was present in nearly 60 % of the patients and this reflects the daily practice and the recommendations that high CAD probability patients have not an appropriate indication for CCTA [30]; (3) For the weighting factor of plaque composition, we used a multiplication factor of 1.5 for mixed and noncalcified plaques. Although this was an arbitrary factor, this is in line with several CCTA prognostic studies that demonstrated lower hazard ratios for calcified plaques and reflects an assumption of less plaque vulnerability of calcified plaques. (4) Lack of prognostic validation: the aim of this study was to describe a CCTA score to quantify total coronary atherosclerotic burden and to identify its clinical predictors. Future studies will be needed to provide a prognostic validation of this described CT-LeSc.

Conclusions

The calculation of the CCTA-adapted Leaman score as a tool to quantify total (obstructive and nonobstructive) coronary atherosclerotic burden, reflecting the comprehensive information about localization, degree of stenosis and type of plaque provided by CCTA is feasible. There was a significant association between the CT-LeSc and some traditional demographic and clinical risk factors. In face of this association, we expect this score to be a useful tool to quantify the coronary atherosclerotic burden evaluated by CCTA and it is expected to convey prognostic information, and this should be evaluated in future studies.

About one fifth of the patients with nonobstructive CAD had a CT-LeSc in the highest tercile, which could potentially lead to a reclassification of the risk profile of these subset of patients identified by CCTA, once the prognostic value of the CT-LeSc is validated.

Conflict of interest There were no sources of funding and the authors have no conflicts of interest related to this manuscript.

References

1. Lloyd-Jones D, Adams R, Carnethon M, De Simone G, Ferguson TB, Flegal K et al (2009) Heart disease and stroke statistics—2009 update: a report from the American Heart Association Statistics Committee and Stroke Statistics Subcommittee. Circulation 119(3):480–486
2. Braunwald E (2006) Epilogue: what do clinicians expect from imagers? J Am Coll Cardiol 47(8 Suppl):C101–C103
3. Meijboom WB, van Mieghem CA, Mollet NR, Pugliese F, Weustink AC, van Pelt N et al (2007) 64-slice computed tomography coronary angiography in patients with high, intermediate, or low pretest probability of significant coronary artery disease. J Am Coll Cardiol 50(15):1469–1475
4. Weustink AC, Mollet NR, Neefjes LA, van Straten M, Neoh E, Kyrzopoulos S et al (2009) Preserved diagnostic performance of dual-source CT coronary angiography with reduced radiation exposure and cancer risk. Radiology 252(1):53–60
5. Chow BJ, Small G, Yam Y, Chen L, Achenbach S, Al-Mallah M et al (2011) Incremental prognostic value of cardiac computed tomography in coronary artery disease using CONFIRM: COro-Nary computed tomography angiography evaluation for clinical outcomes: an InteRnational Multicenter registry. Circ Cardiovasc Imaging 4(5):463–472
6. Min JK, Shaw LJ, Devereux RB, Okin PM, Weinsaft JW, Russo DJ et al (2007) Prognostic value of multidetector coronary computed tomographic angiography for prediction of all-cause mortality. J Am Coll Cardiol 50(12):1161–1170
7. Perk J, De Backer G, Gohlke H, Graham I, Reiner Z, Verschuren M et al (2012) European Guidelines on cardiovascular disease prevention in clinical practice (version 2012): the Fifth Joint Task Force of the European Society of Cardiology and Other Societies on Cardiovascular Disease Prevention in Clinical Practice (constituted by representatives of nine societies and by invited experts) * Developed with the special contribution of the European Association for Cardiovascular Prevention & Rehabilitation (EACPR). Eur Heart J 33(13):1635–1701
8. Report of the Expert Committee on the Diagnosis and Classification of Diabetes Mellitus (1997) Diabetes Care 20(7):1183–1197
9. Expert Panel on Detection E, Treatment of High Blood Cholesterol in A (2001) Executive summary of the third report of the National Cholesterol Education Program (NCEP) expert panel on detection, evaluation, and treatment of high blood cholesterol in adults (adult treatment panel III). JAMA 285(19):2486–2497
10. European Society of Hypertension-European Society of Cardiology Guidelines C (2003) 2003 European Society of Hypertension-European Society of Cardiology guidelines for the management of arterial hypertension. J Hypertens 21(6):1011–1053

cont.

11. Taylor AJ, Bindeman J, Feuerstein I, Cao F, Brazaitis M, O'Malley PG (2005) Coronary calcium independently predicts incident premature coronary heart disease over measured cardiovascular risk factors: mean three-year outcomes in the Prospective Army Coronary Calcium (PACC) project. J Am Coll Cardiol 46(5):807–814
12. Genders TS, Steyerberg EW, Alkadhi H, Leschka S, Desbiolles L, Nieman K et al (2011) A clinical prediction rule for the diagnosis of coronary artery disease: validation, updating, and extension. Eur Heart J 32(11):1316–1330
13. Morise AP, Haddad WJ, Beckner D (1997) Development and validation of a clinical score to estimate the probability of coronary artery disease in men and women presenting with suspected coronary disease. Am J Med 102(4):350–356
14. Raff GL, Abidov A, Achenbach S, Berman DS, Boxt LM, Budoff MJ et al (2009) SCCT guidelines for the interpretation and reporting of coronary computed tomographic angiography. J Cardiovasc Comput Tomogr 3(2):122–136
15. Leaman DM, Brower RW, Meester GT, Serruys P, van den Brand M (1981) Coronary artery atherosclerosis: severity of the disease, severity of angina pectoris and compromised left ventricular function. Circulation 63(2):285–299
16. Maurovich-Horvat P, Schlett CL, Alkadhi H, Nakano M, Otsuka F, Stolzmann P et al (2012) The napkin-ring sign indicates advanced atherosclerotic lesions in coronary CT angiography. JACC Cardiovasc Imaging 5(12):1243–1252
17. Andreini D, Pontone G, Mushtaq S, Bartorelli AL, Bertella E, Antonioli L et al (2012) A long-term prognostic value of coronary CT angiography in suspected coronary artery disease. JACC Cardiovasc Imaging 5(7):690–701
18. Little WC, Downes TR, Applegate RJ (1991) The underlying coronary lesion in myocardial infarction: implications for coronary angiography. Clin Cardiol 14(11):868–874
19. Falk E, Shah PK, Fuster V (1995) Coronary plaque disruption. Circulation 92(3):657–671
20. Libby P, Theroux P (2005) Pathophysiology of coronary artery disease. Circulation 111(25):3481–3488
21. Naghavi M, Libby P, Falk E, Casscells SW, Litovsky S, Rumberger J et al (2003) From vulnerable plaque to vulnerable patient: a call for new definitions and risk assessment strategies: part I. Circulation 108(14):1664–1672
22. Stone GW, Maehara A, Lansky AJ, de Bruyne B, Cristea E, Mintz GS et al (2011) A prospective natural-history study of coronary atherosclerosis. N Engl J Med 364(3):226–235
23. Bamberg F, Sommer WH, Hoffmann V, Achenbach S, Nikolaou K, Conen D et al (2011) Meta-analysis and systematic review of the long-term predictive value of assessment of coronary atherosclerosis by contrast-enhanced coronary computed tomography angiography. J Am Coll Cardiol 57(24):2426–2436
24. Sianos G, Morel MA, Kappetein AP, Morice MC, Colombo A, Dawkins K et al (2005) The SYNTAX score: an angiographic tool grading the complexity of coronary artery disease. EuroIntervention 1(2):219–227
25. Serruys PW, Morice MC, Kappetein AP, Colombo A, Holmes DR, Mack MJ et al (2009) Percutaneous coronary intervention versus coronary-artery bypass grafting for severe coronary artery disease. N Engl J Med 360(10):961–972
26. Brito J, Teles R, Almeida M, de Araujo Goncalves P, Raposo L, Sousa P et al (2011) Predictive value of SYNTAX score in risk stratification of patients undergoing unprotected left main coronary artery angioplasty. J Invasive Cardiol 23(12):494–499
27. Virmani R, Kolodgie FD, Burke AP, Farb A, Schwartz SM (2000) Lessons from sudden coronary death: a comprehensive morphological classification scheme for atherosclerotic lesions. Arterioscler Thromb Vasc Biol 20(5):1262–1275
28. Pundziute G, Schuijf JD, Jukema JW, Decramer I, Sarno G, Vanhoenacker PK et al (2008) Head-to-head comparison of coronary plaque evaluation between multislice computed tomography and intravascular ultrasound radiofrequency data analysis. JACC Cardiovasc Interv 1(2):176–182
29. Morise AP, Jalisi F (2003) Evaluation of pretest and exercise test scores to assess all-cause mortality in unselected patients presenting for exercise testing with symptoms of suspected coronary artery disease. J Am Coll Cardiol 42(5):842–850
30. Taylor AJ, Cerqueira M, Hodgson JM, Mark D, Min J, O'Gara P et al (2010) ACCF/SCCT/ACR/AHA/ASE/ASNC/NASCI/SCAI/SCMR 2010 appropriate use criteria for cardiac computed tomography. A report of the American College of Cardiology Foundation Appropriate Use Criteria Task Force, the Society of Cardiovascular Computed Tomography, the American College of Radiology, the American Heart Association, the American Society of Echocardiography, the American Society of Nuclear Cardiology, the North American Society for Cardiovascular Imaging, the Society for Cardiovascular Angiography and Interventions, and the Society for Cardiovascular Magnetic Resonance. J Am Coll Cardiol 56(22):1864–1894

MANUSCRITO 15

Machine learning for prediction of all-cause mortality in patients with suspected coronary artery disease: a 5-year multicentre prospective registry analysis.

Motwani, M., Dey, D., Berman, D. S., Germano, G., Achenbach, S., Al-Mallah, M. H., Andreini, D., Budoff, M. J., Cademartiri, F., Callister, T. Q., Chang, H. J., Chinnaiyan, K., Chow, B. J., Cury, R. C., Delago, A., Gomez, M., Gransar, H., Hadamitzky, M., Hausleiter, J., Hindoyan, N., Feuchtner, G., Kaufmann, P. A., Kim, Y. J., Leipsic, J., Lin, F. Y., Maffei, E., **Marques**, **H**., Pontone, G., Raff, G., Rubinshtein, R., Shaw, L. J., Stehli, J., Villines, T. C., Dunning, A., Min, J. K., and Slomka, P. J.

Eur Heart J, 2017
38(7): p. 500-507

Manuscrito 15

European Heart Journal (2017) **38**, 500–507
doi:10.1093/eurheartj/ehw188

CLINICAL RESEARCH
Coronary artery disease

Machine learning for prediction of all-cause mortality in patients with suspected coronary artery disease: a 5-year multicentre prospective registry analysis

Manish Motwani[1], Damini Dey[1], Daniel S. Berman[1], Guido Germano[1], Stephan Achenbach[2], Mouaz H. Al-Mallah[3], Daniele Andreini[4], Matthew J. Budoff[5], Filippo Cademartiri[6,7], Tracy Q. Callister[8], Hyuk-Jae Chang[9], Kavitha Chinnaiyan[10], Benjamin J.W. Chow[11], Ricardo C. Cury[12], Augustin Delago[13], Millie Gomez[14], Heidi Gransar[1], Martin Hadamitzky[15], Joerg Hausleiter[16], Niree Hindoyan[14], Gudrun Feuchtner[17], Philipp A. Kaufmann[18], Yong-Jin Kim[19], Jonathon Leipsic[20], Fay Y. Lin[14], Erica Maffei[21], Hugo Marques[22], Gianluca Pontone[23], Gilbert Raff[10], Ronen Rubinshtein[24], Leslee J. Shaw[25], Julia Stehli[18], Todd C. Villines[26], Allison Dunning[27], James K. Min[28], and Piotr J. Slomka[1]*

[1]Departments of Imaging and Medicine and the Cedars-Sinai Heart Institute, and the Biomedical Imaging Research Institute, Department of Biomedical Sciences, Cedars-Sinai Medical Center, Los Angeles, CA, USA; [2]Department of Cardiology, Friedrich Alexander Universität Erlangen-Nürnberg, Germany; [3]King Saud bin Abdulaziz University for Health Sciences, King Abdullah International Medical Research Center, King AbdulAziz Cardiac Center Saudia Arabia; [4]Department of Clinical Sciences and Community Health, University of Milan, Centro Cardiologico Monzino, IRCCS, Milan, Italy; [5]Department of Medicine, Harbor UCLA Medical Center, Los Angeles, CA, USA; [6]Department of Radiology, Montréal Heart Institute/Université de Montréal, Montréal, Quebec, Canada; [7]Department of Radiology, Erasmus Medical Center, Rotterdam, The Netherlands; [8]Tennessee Heart and Vascular Institute, Hendersonville, TN, USA; [9]Division of Cardiology, Severance Cardiovascular Hospital, Seoul, South Korea; [10]William Beaumont Hospital, Royal Oaks, MI, USA; [11]Department of Medicine and Radiology, University of Ottawa Heart Institute, ON, Canada; [12]Miami Cardiac and Vascular Institute, Miami, FL, USA; [13]Capitol Cardiology Associates, Albany, NY, USA; [14]Dalio Institute of Cardiovascular Imaging, Weill Cornell Medical College and New York-Presbyterian Hospital, New York, NY, USA; [15]Department of Radiology and Nuclear Medicine, German Heart Center Munich, Munich, Germany; [16]Medizinische Klinik I der Ludwig-Maximilians-Universität München, Munich, Germany; [17]Department of Radiology, Medical University of Innsbruck, Innsbruck, Austria; [18]Department of Nuclear Medicine, Cardiac Imaging, University Hospital Zurich, Zurich, Switzerland; [19]Department of Medicine and Radiology, Seoul National University Hospital, Seoul, South Korea; [20]Department of Medical Imaging and Division of Cardiology, St. Paul's Hospital, University of British Columbia, Vancouver, BC, Canada; [21]Montréal Heart Institute, Montréal, Quebec, Canada; [22]Department of Radiology, UNICA - Hospital da LUZ, Lisbon, Portugal; [23]Centro Cardiologico Monzino, IRCCS, Milan, Italy; [24]Department of Cardiology at the Lady Davis Carmel Medical Center, The Ruth and Bruce Rappaport School of Medicine, Technion-Israel Institute of Technology, Haifa, Israel; [25]Department of Medicine, Emory University School of Medicine, Atlanta, GA, USA; [26]Department of Medicine, Walter Reed National Medical Center, Bethesda, MD, USA; [27]Duke Clinical Research Institute, Durham, NC, USA; and [28]Departments of Radiology and Medicine, Weill Cornell Medical College, Dalio Institute of Cardiovascular Imaging, New York-Presbyterian Hospital, New York, NY, USA

Online publish-ahead-of-print 1 June 2016

See page 508 for the editorial comment on this article (doi:10.1093/eurheartj/ehw217)

Aims Traditional prognostic risk assessment in patients undergoing non-invasive imaging is based upon a limited selection of clinical and imaging findings. Machine learning (ML) can consider a greater number and complexity of variables. Therefore, we investigated the feasibility and accuracy of ML to predict 5-year all-cause mortality (ACM) in patients undergoing coronary computed tomographic angiography (CCTA), and compared the performance to existing clinical or CCTA metrics.

Methods and results The analysis included 10 030 patients with suspected coronary artery disease and 5-year follow-up from the COronary CT Angiography EvaluatioN For Clinical Outcomes: An InteRnational Multicenter registry. All patients underwent CCTA as their standard of care. Twenty-five clinical and 44 CCTA parameters were evaluated, including segment stenosis score (SSS), segment involvement score (SIS), modified Duke index (DI), number of segments with non-calcified, mixed or calcified plaques, age, sex, gender, standard cardiovascular risk factors, and Framingham risk score (FRS). Machine learning involved automated feature selection by information gain ranking, model building with a boosted ensemble algorithm, and 10-fold stratified cross-validation. Seven hundred and forty-five patients died during 5-year follow-up.

* Corresponding author. Artificial Intelligence in Medicine Program, Departments of Imaging and Medicine, and Cedars-Sinai Heart Institute, Cedars-Sinai Medical Center, 8700 Beverly Boulevard, A047N, Los Angeles, CA 90048, USA. Tel: +1 310 423 4348, Email: piotr.slomka@cshs.org

cont.

Manuscrito 15

	Machine learning exhibited a higher area-under-curve compared with the FRS or CCTA severity scores alone (SSS, SIS, DI) for predicting all-cause mortality (ML: 0.79 vs. FRS: 0.61, SSS: 0.64, SIS: 0.64, DI: 0.62; $P < 0.001$).
Conclusions	Machine learning combining clinical and CCTA data was found to predict 5-year ACM significantly better than existing clinical or CCTA metrics alone.

Keywords Coronary artery disease • Coronary CT angiography • Prognosis • Machine learning

Introduction

Coronary computed tomography angiography (CCTA) is an accurate non-invasive technique for the diagnosis and exclusion of obstructive coronary artery disease (CAD).[1] In addition to coronary stenosis, CCTA also allows for evaluation of coronary atherosclerosis extent, severity, distribution, and composition. Beyond clinical variables, these imaging findings add incremental utility for prediction of future adverse events.[2–4]

Machine learning (ML) is a field of computer science that uses computer algorithms to identify patterns in large datasets with a multitude of variables, and can be used to predict various outcomes based on the data. Machine learning algorithms typically build a model from test inputs in order to make data-driven predictions or decisions. In recent years, ML techniques have emerged as highly effective methods for prediction and decision-making in a multitude of disciplines, including internet search engines, customized advertising, natural language processing, finance trending, and robotics.[5,6] There is consensus in the ML community on the superior performance of aggregation approaches, known as ensemble methods such as 'boosting', and therefore we have chosen a boosting approach for this study.[7] To date, the benefit of utilizing ML with data from CCTA to predict hard-prognostic endpoints has not been evaluated on a large scale. Therefore, the aim of this study was to utilize a large, prospective multinational registry of patients undergoing CCTA to assess the feasibility and accuracy of ML to predict 5-year all-cause mortality (ACM), and then compare the performance to existing clinical or CCTA metrics.

Methods

Study population

Ten thousand and thirty stable patients with suspected CAD and with 5-year follow-up from the COronary CT Angiography EvaluatioN For Clinical Outcomes: An InteRnational Multicenter (CONFIRM) registry were studied.[2,8] COronary CT Angiography EvaluatioN For Clinical Outcomes: An InteRnational Multicenter is an international, multicentre, observational registry collecting clinical, procedural, and follow-up data of patients undergoing clinically indicated CCTA (enrolled 2004–10).[2] The study complies with the Declaration of Helsinki, all patients provided informed consent for inclusion in the registry, and institutional review board approval was obtained at each centre. Individuals with known CAD (defined as prior myocardial infarction (MI) or revascularization) or those with early revascularization after the index CCTA (defined as within 90 days) were excluded from the present study.

Clinical data

A structured interview was conducted before CCTA to collect information on symptoms and the presence of cardiovascular risk factors (*Figure 1*). Hypertension was defined as a history of blood pressure >140 mmHg or treatment with antihypertensive medications. Diabetes mellitus was defined by a diagnosis made previously by a physician and/or use of insulin or oral hypoglycaemic agents. Smoking history was defined as current smoking, or cessation of smoking within the last 3 months. Family history of premature CAD was defined as MI in a first-degree relative <55 years (male) or <65 years (female). Dyslipidaemia was defined as known but untreated dyslipidaemia, or current treatment with lipid-lowering medications. In addition, blood cholesterol levels of the lipid test nearest to the index examination were recorded. The primary outcome of the study was ACM recorded as a binary variable, and the study end-point was time to ACM. In U.S. sites, death status was ascertained by querying the Social Security Death Index. In non-U.S. sites, follow-up data were collected by mail or telephone contact with the patients or their families; events were verified by hospital records or contacts with the attending physician.

Coronary computed tomographic angiography data

Image acquisition

Coronary computed tomographic angiography investigations were performed on ≥64-detector row scanners from a variety of vendors (Lightspeed VCT, GE Healthcare, Milwaukee, WI, USA; Somatom Definition CT, Siemens, Erlangen, Germany). The imaging protocol adhered to Society of Cardiovascular Computed Tomography guidelines.[9] Detailed methodology has been previously published.[2]

Image analysis

All scans were analysed by level III-equivalent cardiologists or radiologists. Images were evaluated by an array of post-processing techniques, including axial, multi-planar reformat, maximum intensity projection, and short-axis cross-sectional views.

Coronary segments were scored visually for the presence and composition of coronary plaque, and degree of luminal stenosis using a 16-segment coronary artery model.[9] In each segment, plaques were classified as non-calcified, mixed, or calcified. The presence of coronary calcification was determined visually in contrast-enhanced datasets. Non-calcified plaque was defined as a tissue structure >1 mm^2 that could be clearly discriminated from the vessel lumen and surrounding tissue, with a density below the blood-pool. Plaques meeting this definition and in addition showing any calcified areas were classified as mixed. Severity of luminal stenosis in each segment was scored visually: 0 (none, 0%), 1 (mild, 1–49%), 2 (moderate, 50–69%), or 3 (severe, ≥70%).

For purposes of classification for per-vessel analyses, we considered four arterial territories: left main (LM), left anterior descending (LAD) and its diagonal branches, left circumflex (LCx) and its obtuse marginal branches, and the right coronary artery (RCA). The posterior descending artery and posterolateral branch were considered as part of the RCA or LCx system, depending on recorded dominance.

cont.

Manuscrito 15

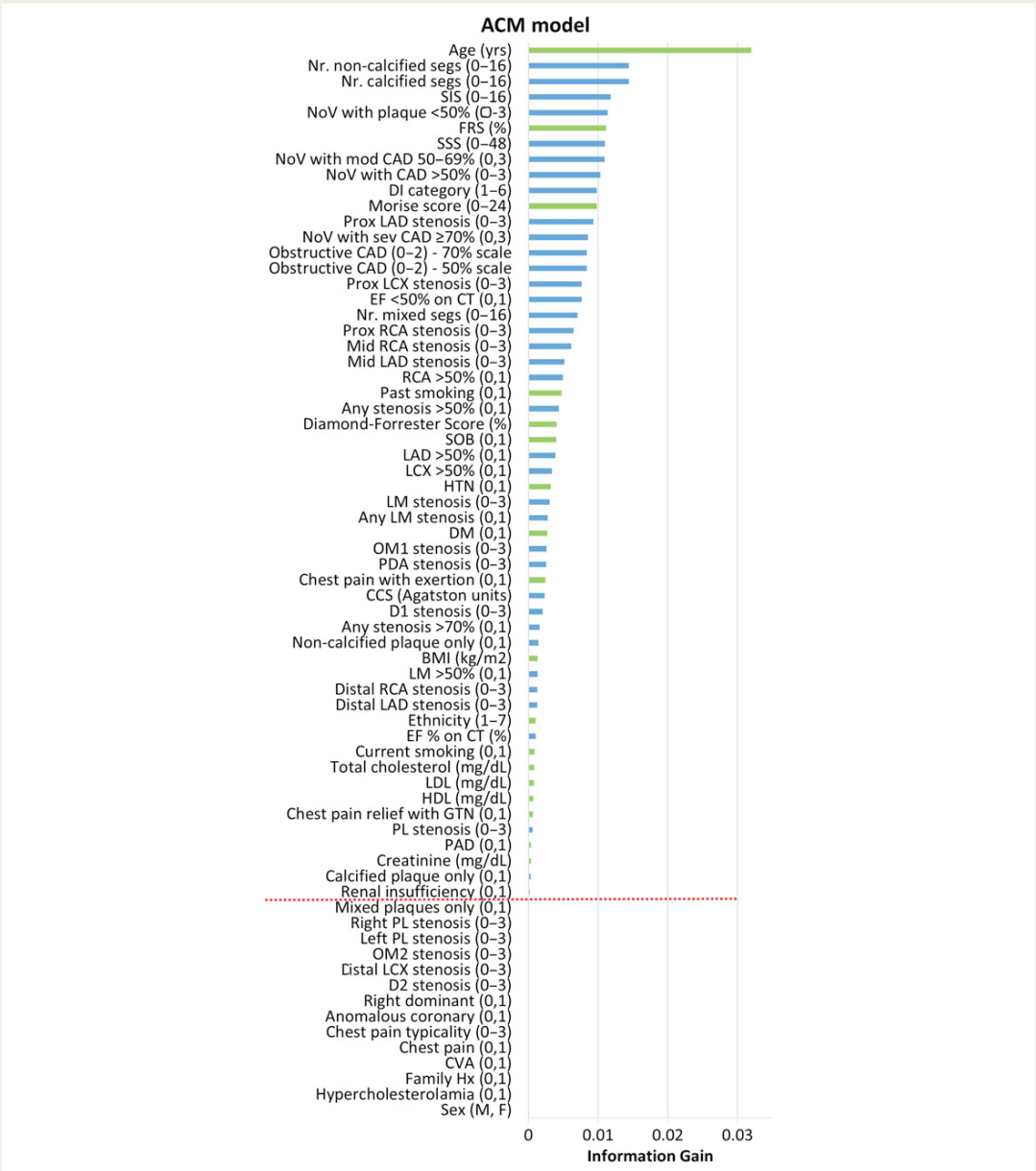

Figure 1 Feature selection. Forty-four coronary computed tomographic angiography variables (blue) and 25 clinical variables (green) were available. Information gain ranking was used to evaluate the worth of each variable by measuring the entropy gain with respect to the outcome, and then rank the attributes by their individual evaluations (top to bottom). Only attributes resulting in information gain >0 (above red line) were subsequently used in boosting. This figure shows the results from one representative fold of the cross-validation procedure. Variables are followed by units, or categorical range in parentheses—full details in Supplementary material online, Appendix. ACM, all-cause mortality; BMI, body mass index; CAD, coronary artery disease; CCS, coronary calcium score; CVA, cerebrovascular accident; D, diagonal; DM, diabetes mellitus; EF, ejection fraction; F, female; FRS, Framingham risk score; HDL, high-density lipoprotein; HTN, hypertension; LM, left main; LAD, left anterior descending artery; LCX, left circumflex; LDL, low-density lipoprotein M, male; NoV, number of vessels; Nr., number of; OM, obtuse marginal; PAD, peripheral arterial disease; PL, posterolateral branch; RCA, right coronary artery; sev, severe; SSS, segment stenosis score; SIS, segment involvement score.

cont.

Manuscrito 15

Comparative metrics

Clinical and CCTA parameters were summarized with a number of existing metrics to allow direct comparison with the ML method.

Clinical data

Framingham risk score (FRS) was used as a comparative summary metric for clinical parameters. Framingham risk score was calculated with the established categorical model using low-density lipoprotein cholesterol according to Wilson *et al.*[10] Although, FRS was originally validated for the 10-year risk of coronary heart disease in asymptomatic patients, this is a commonly adopted strategy given the absence of any more suitable clinical risk score for symptomatic patients or shorter follow-up periods. Moreover, it frames the accuracy of the ML-model in the context of a widely used and understood clinical score.[2–4]

Coronary computed tomographic angiography data

Three composite CCTA-based scores assessing overall plaque burden and severity of CAD were derived. First, the segment stenosis score (SSS) was employed as an overall measure of coronary plaque extent.[2] For each patient, individual coronary segments were scored 0–3 based on luminal diameter stenosis, and then summed to yield a total SSS (0–48). Second, the segment involvement score (SIS) was calculated as a measure of overall coronary plaque distribution, by summation of the absolute number of coronary segments with plaque (0–16).[2] Third, the modified Duke prognostic CAD index (DI) was used, which categorizes patients into the following subsets, each with an increasing risk of 5-year death: (1) <50% stenosis, (2) ≥2 stenoses 30–49% (including 1 artery with proximal disease) or 1 vessel with 50–69% stenosis, (3) 2 stenoses 50–69% or 1 vessel with ≥70% stenosis, (4) 3 stenoses 50–69% or 2 vessels with ≥70% stenosis or proximal left anterior descending stenosis ≥70%, (5) 3 vessels ≥70% stenoses or 2 vessels ≥70% stenosis with proximal LAD, and (6) LM stenosis ≥50%.[2]

Machine learning

Forty-four CCTA parameters and 25 clinical parameters were available (*Figure 1*). Machine learning involved automated feature selection by information gain ranking, model building with a boosted ensemble algorithm, and 10-fold stratified cross-validation for the entire process (*Figure 2*).[11–14] Machine learning techniques were implemented in the open-source Waikato Environment for Knowledge Analysis platform (3.7.12).[14,15]

Feature selection

Feature selection was performed using a technique known as 'information gain attribute ranking'.[11] Information gain is defined as a measure of the effectiveness of an attribute in classifying the training data. It is measured as the amount by which the entropy of the class decreases, which reflects the additional information about the class provided by the attribute. Only attributes resulting in information gain >0 were subsequently used in model building (*Figure 1*).

Model building

Predictive classifiers for ACM prediction were developed by an ensemble classification approach ('boosting'), employing an iterative LogitBoost algorithm using decision stumps (single-node decision trees) for each feature-selected variable as base classifiers.[12,16] The principle behind ML ensemble boosting is that a set of weak base classifiers can be combined to create a single strong classifier by iteratively adjusting their appropriate weighting according to misclassifications. A series of base classifier predictions and an updated weighting distribution are produced with each iteration. These predictions are then combined by weighted majority voting to derive an overall classifier—the 'LogitBoost score' or risk probability estimate (%).

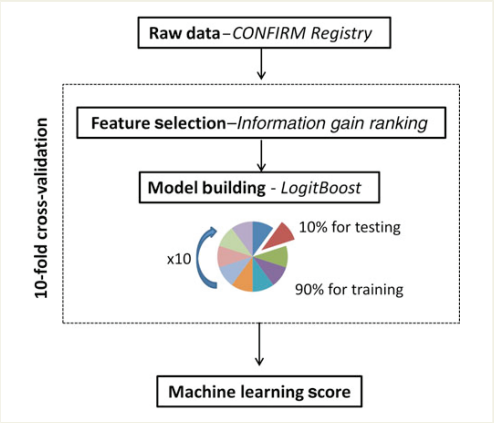

Figure 2 Computational methods. Machine learning involved automated feature selection by information gain ranking, model building with a boosted ensemble algorithm (LogitBoost), and 10-fold stratified cross-validation.

Cross-validation

The performance and general error estimation of the entire ML process (feature selection and LogitBoost) was assessed using stratified 10-fold cross-validation which is currently the preferred technique in data mining.[13,17] The main advantages of this validation technique compared with the conventional split-sample (test and validation) approach are: (i) it reduces the variance in prediction error leading to a more accurate estimate of model prediction performance; (ii) it maximizes the use of data for both training and validation, without overfitting or overlap between test and validation data; and (iii) guards against testing hypotheses suggested by arbitrarily split data (Type III errors).[13]

Briefly, the dataset is randomly divided into 10 equal folds, each with approximately the same number of events; 10 validation experiments are then performed, with each fold used in turn as the validation set, and the remaining 9 folds as the training set. Therefore, each data point is used once for testing and 9 times for training, and the result is 10 experimental LogitBoost models trained on 90% fractions. The validation results from 10 experimental models are then combined to provide a measure of the overall performance (*Figure 2*).[13]

Statistical analysis

Continuous variables are presented as mean ± SD. The performance of ML to predict ACM was compared with CCTA severity scores (SSS, SIS, and DI) and FRS, using receiver-operating characteristic (ROC) analysis and pairwise comparisons according to Delong *et al.*[18] For ML scores, the optimal thresholds for three risk categories (low, intermediate, and high) were defined using the two-graph-ROC (TG-ROC) technique at the 90% accuracy level.[19] Calibration of the LogitBoost model was assessed using the Brier score method (range: 0–1)—lower scores being consistent with better model calibration.[20] Calibration was also assessed graphically with plots showing the observed and predicted proportion of events, grouped by decile of risk.[21] For all analyses, surviving

cont.

patients were right censored to their follow-up date. All statistical tests were two tailed and $P < 0.05$ was considered significant.

Results

Study population

Table 1 describes the baseline characteristics of the study population. There was no drop-out in this analysis and primary outcome data were determined for all patients. Seven hundred and forty-five patients died during the mean follow-up time of 5.4 ± 1.4 years.

Feature selection

Figure 1 shows the results from one representative fold of the 10-fold cross-validation procedure. In this representative fold, using the information gain ranking criteria, 54 of the available 69 variables were selected for the LogitBoost model (19 clinical and 35 from CCTA). As expected, age was the highest ranked feature for ACM prediction, but 8 of the top 10 ranked features were CCTA-derived factors rather than clinical.

Prediction all-cause mortality

Machine learning exhibited a higher area-under-the-curve (AUC) compared with FRS or CCTA data alone for prediction of 5-year ACM (ML: 0.79 vs. FRS: 0.61, SSS: 0.64, SIS: 0.64, DI: 0.62; $P <$ 0.001 for all) (*Figure 3*). Segment stenosis score and SIS were superior to FRS for predicting ACM ($P < 0.05$).

Risk categorization by machine learning

Based on TG-ROC analysis, the intermediate-risk range for the LogitBoost model was a risk probability estimate of between 3.8 and 14%, corresponding to 90% sensitivity and specificity, respectively.

Table 1 Baseline patient characteristics

Characteristic	Data (n = 10 030)
Age (years ± SD)	59 ± 13
Sex, *n* (%)	
Male	5628 (56)
Female	4402 (44)
CAD risk factors, *n* (%)	
Diabetes	1783 (18)
Hypercholestoraemia	5415 (54)
Hypertension	5477 (55)
Current smoker	2432 (24)
Family history	3936 (39)
Chest pain, *n* (%)	
Non-cardiac	1615 (16)
Atypical angina	2967 (30)
Typical angina	1820 (18)
Dyspnoea on exertion, *n* (%)	3224 (32)

CAD, coronary artery disease.

Low- and high-risk ranges were considered as either side of the intermediate range. With this categorization, the number of patients assigned to low-, intermediate-, and high-risk groups in the study population by the LogitBoost model were: 3960 (39%), 4768 (48%), and 1302 (13%), respectively. The corresponding observed 5-year ACM event rates in these risk-groups were 1.8, 6.7, and 27%, respectively.

Calibration of machine learning scores

The Brier score for the LogitBoost model predicting ACM was 0.08 indicating good calibration between LogitBoost scores (estimated predicted risk) and observed 5-year risk. A calibration plot also confirmed good agreement between LogitBoost scores and the observed 5-year risk of ACM (*Figure 4*).

Discussion

In this study, we observed ML methods to be an effective method for the prediction of 5-year ACM. The ML method performed superiorly to clinical and CCTA summary metrics alone. To our knowledge, this is the first large-scale evaluation of ML for prognostic risk assessment using CCTA data. The observed efficacy suggests ML has an important clinical role in evaluating prognostic risk in individual patients with suspected CAD.

The ability to correctly identify high-risk patients who may benefit from intensified preventative measures is a major challenge in

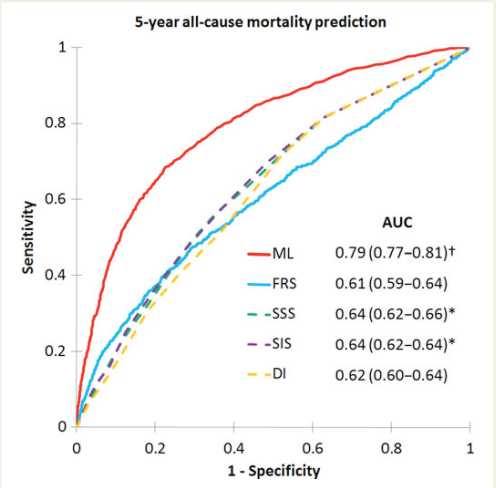

Figure 3 Receiver-operating characteristic curves for prediction of 5-year all-cause mortality. Machine learning using feature selection and a LogitBoost model had a significantly higher area-under-the-curve for all-cause mortality prediction than all other scores ($P < 0.001$)†. Area-under-the-curves for segment stenosis score and segment involvement score were greater than Framingham risk score ($P < 0.05$)‡. FRS, Framingham risk score; SSS, segment stenosis score; SIS, segment involvement score; DI, modified Duke index.

cont.

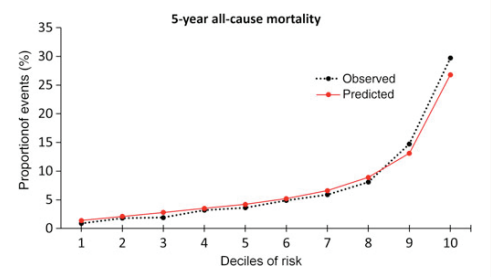

Figure 4 Calibration plot for LogitBoost model. The calibration plot shows the relationship between the observed and predicted proportion of events, grouped by decile of risk. The LogitBoost model showed good calibration with the observed 5-year risk of all-cause mortality.

cardiovascular medicine.[22,23] Although traditional risk factors for CAD offer general guidance and are effective tools for population-based comparisons, they are ineffective for individual risk assessments.[23,24] Even when combined into global summary scores for easy usage, the use of clinical variables alone is associated with substantial over- or under-treatment, emphasizing the need for more precise assessment through patient-specific imaging.[10,23]

Appreciating and integrating the myriad risk predictors in an individual patient is a challenge for the clinician. To date, efforts to improve risk-stratification by using CCTA have largely relied upon luminal stenosis severity. The emphasis placed on this variable over others is in alignment with prior studies using invasive coronary angiography, but ignores an array of other variables important in the CAD pathogenic process, including coronary calcium content, plaque composition, and plaque burden.[2,25] As an increasing number of CCTA variables along with all clinical variables affecting risk need to be considered, the complexity of assessment increases, making it more difficult for a clinician to draw an overall conclusion regarding risk in an individual patient. Furthermore, the potential influence of unexpected interactions between several weaker predictors in an individual patient is often overlooked. In this study, we demonstrate that ML is able to overcome these challenges, by providing deep integration of the comprehensive CCTA and clinical data.

We performed risk assessment using state-of-the-art ML methods, a form of artificial intelligence that distinguishes itself from traditional prognostic methods by making no *priori* assumptions about causative factors. This characteristic allows for an agnostic exploration of all available data for non-linear patterns that may predict a particular individual's risk, i.e. precision risk-stratification. This important concept represents a divergence from a 'hypothesis-driven' approach conventional in traditional prognostic risk assessments. As observed in the present study, the lack of any required hypothesis avoids overlooking important but unexpected predictor variables or interactions, as well as enabling the recognition of clinically important risk among patients with several marginal risk factors (or no risk factors at all). Further, by its nature, any given ML algorithm requires only minimal input during its model-building phase and none after that. This feature of ML methods is particularly important, given the ease with which the machine can seamlessly incorporate new data to continually update and optimize its algorithm—and thus continually improve its predictive performance over time.[5,26]

In a prior study, our group employed a traditional logistic regression approach to predict 2-year ACM, also based on data from the CONFIRM registry.[2] The resulting model comprised three clinical and CCTA variables, and exhibited an AUC of 0.68. In the current study, which extends follow-up to 5 years, ML methods offered an incremental gain in prognostic performance while handling over 60 variables and a vast number of variable–variable interactions in each patient. The latter effectively individualizes risk assessment and overcomes many of the limitations of a standard statistical approach.

The results of this study have considerable clinical import. Prior large-scale studies have documented the inadequacies of current limited-variable methods for prediction of disease prevalence, severity, and prognosis; and highlight the need for more accurate methods to perform these important clinical tasks.[27–29] As observed in other fields that require accurate prediction and decision-making in the presence of large amounts of data, ML may offer an improved alternative to current cardiovascular risk-stratification in the individual patient. These improvements may be furthered by the emergence of standard electronic health records and software capable of automated atherosclerotic plaque characterization and quantification—both of which may improve any given ML algorithm.

A limitation of the ML approach is that by using an increasing number of variables and interactions to predict risk, it can subsequently be difficult to identify the specific therapeutic targets that will reduce risk in that individual patient. However, the current therapeutic approach to CAD is very similar across all risk groups, and the benefit of an incremental improvement in risk-stratification in this context, even if a specific causative risk factor or interaction cannot be identified, is that it may allow physicians to move away from this 'one-size fits all' approach with confidence—with the advantage of cost-savings and reduced adverse effects in those that currently receive unnecessary treatments. Furthermore, in time those patients in whom ML re-classifies risk different from traditional approaches can be prospectively studied in greater depth to identify the causative factors and interactions—and this may finally unlock new therapeutic targets.

Study limitations

In the current study, we have only been able to discuss the feasibility and performance of ML, but not its prospective practical implementation. The ability of any ML approach to handle a large number of variables is only advantageous if these variables are actually inputted into the ML algorithm—and this can be a time-consuming process, depending on the mode of data entry. However, we envisage ML working in the background of standard electronic health records or clinical reporting systems, gathering its variables automatically without additional burden on the physician—allowing on-the-fly risk score computation. This is the same principle already adopted by many ML applications—for example, the personalized advertisements that appear in real-time while web-browsing are all based on the passive collection of variables and their seamless input into ML algorithms. In this regard, the feature selection component is particularly important to future practical implementation as it

cont.

minimizes the amount of data needed to be handled by such an on-the-fly ML application without compromising on accuracy.

Although prospectively collected, the CONFIRM registry data used to derive the LogitBoost model was nevertheless observational, and the influence of selection bias cannot be discounted. Observational cohort studies, however, are the best suited to assess the initial feasibility of ML algorithms, given the requirement to both develop and validate their efficacy. Once validated, prospective randomized controlled treatment trials based upon ML risk-stratification can then be considered. Whether an objective ML approach without prior hypothesis is more effective than subjective but flexible human thinking is an issue that future prospective studies may explore. Future prospective studies may also allow comparison of our ML approach integrating CCTA and clinical data, to the alternative strategy in this study population of clinical assessment with stress-testing.

Although alternative, more cardiac-specific endpoints than ACM may have been utilized, these data were not available for all centres in the CONFIRM registry. For the current study which had the aim of demonstrating feasibility of the ML approach, ACM was the most definitive end-point, with the maximal amount of patients to facilitate the best trained and validated ML model.

Although we evaluated 69 distinct variables with ML, along with variable–variable interactions, we did not consider the totality of features that may offer improved risk prediction, as we were limited to those collected for the CONFIRM registry. In particular, more detailed clinical data such as duration, magnitude and control of risk factors, as well more advanced plaque characterization with % aggregate plaque volume, arterial remodelling, or Hounsfield-unit-based plaque composition classification, may augment the current ML model.

Another limitation is the use of FRS as the summary metric for evaluation of clinical parameters as it was originally validated for 10-year outcomes in asymptomatic patients. However, this is a commonly adopted strategy given the absence of any more suitable clinical risk score for symptomatic patients or shorter follow-up periods, and moreover, it frames the accuracy of the ML-model in the context of a widely used and understood clinical score.[2–4] Finally, while numerous ML methods exist, we evaluated the efficacy of only a single ensemble method (LogitBoost). In particular, boosting is also available for Cox-based models (CoxBoost) which leads to the possibility of time-to-event prediction using such alternative analysis.[30]

Conclusions

In a large, prospective 5-year multinational study of patients with suspected CAD, ML was an effective method for the prediction of ACM, and performed superiorly to the use of clinical and CCTA variables alone.

Authors' contributions

M.M., P.J.S., H.G. performed statistical analysis; J.K.M., D.S.B., P.J.S. handled funding and supervision; M.M., D.D., S.A., M.A.-M., D.A.M.J.B., F.C., T.Q.C., H.-J.C., K.C., B.J.W.C., R.C., A.D., M.G., H.G., M.H., J.H., N.H., G.F., P.A.K., Y.-J.K.; J.L., F.Y.L., E.M., H.M., G.P., G.R., R.R., L.J.S., J.S., T.C.V., A.D., D.S.B., J.K.M., P.J.S. acquired the data; P.J.S., M.M., D.S.B., J.K.M. conceived and designed the research; M.M., P.J.S. drafted the manuscript; D.D., D.S.B., J.K.M. made critical revision of the manuscript for key intellectual content.

Supplementary material

Supplementary material is available at *European Heart Journal* online.

Acknowledgements

We thank all staff at the participating sites for their effort to collect data for the CONFIRM registry.

Funding

This work was supported by research grants from the National Heart Lung and Blood Institute: R01-HL111141, R01-HL115150, R01-HL118019 (J.K.M.), R01-2R01HL089765 (P.J.S.); the Dowager Countess Eleanor Peel Trust, Manchester, UK, and the Dickinson Trust, Manchester, UK (M.M.); National Research Foundation of Korea (Leading Foreign Research Institute Recruitment Program 2012027176) (H.J.C); Adelson Family Foundation (D.S.B) as well as a generous gift from the Dalio Foundation, New York, NY and the Michael Wolk Foundation, New York, NY (J.K.M.).

Conflict of interest: none declared.

References

1. Budoff MJ, Dowe D, Jollis JG, Gitter M, Sutherland J, Halamert E, Scherer M, Bellinger R, Martin A, Benton R, Delago A, Min JK. Diagnostic performance of 64-multidetector row coronary computed tomographic angiography for evaluation of coronary artery stenosis in individuals without known coronary artery disease: results from the prospective multicenter ACCURACY (Assessment by Coronary Computed Tomographic Angiography of Individuals Undergoing Invasive Coronary Angiography) trial. *J Am Coll Cardiol* 2008;**52**:1724–1732.
2. Hadamitzky M, Achenbach S, Al-Mallah M, Berman D, Budoff M, Cademartiri F, Callister T, Chang HJ, Cheng V, Chinnaiyan K, Chow BJW, Cury R, Delago A, Dunning A, Feuchtner G, Gomez M, Kaufmann P, Kim YJ, Leipsic J, Lin FY, Maffei E, Min JK, Raff G, Shaw LJ, Villines TC, Hausleiter J. Optimized prognostic score for coronary computed tomographic angiography: Results from the CONFIRM registry (COronary CT angiography evaluation for clinical outcomes: An international multicenter registry). *J Am Coll Cardiol* 2013;**62**:468–476.
3. Hadamitzky M, Freißmuth B, Meyer T, Hein F, Kastrati A, Martinoff S, Schömig A, Hausleiter J. Prognostic value of coronary computed tomographic angiography for prediction of cardiac events in patients with suspected coronary artery disease. *JACC Cardiovasc Imaging* 2009;**2**:404–411.
4. Chow BJ, Small G, Yam Y, Chen L, Achenbach S, Al-Mallah M, Berman DS, Budoff MJ, Cademartiri F, Callister TQ, Chang H-J, Cheng V, Chinnaiyan K, Delago A, Dunning A, Hadamitzky M, Hausleiter J, Kaufmann P, Lin F, Maffei E, Raff GL, Shaw LJ, Villines TC, Min JK. Incremental prognostic value of cardiac CT in CAD using CONFIRM (COroNary computed tomography angiography evaluation for clinical outcomes: an InteRnational Multicenter registry). *Circ Cardiovasc Imaging* 2011;**4**:463–472.
5. Waljee AK, Higgins PDR. Machine learning in medicine: a primer for physicians. *Am J Gastroenterol* 2010;**105**:1224–1226.
6. Deo RC. Machine learning in medicine. *Circulation*. 2015;**132**:1920–1930.
7. Dietterich TG. Ensemble methods in machine learning. *Lect Notes Comput Sci* 2000; **1857**:1–15.
8. Min JK, Dunning A, Lin FY, Achenbach S, Al-Mallah MH, Berman DS, Budoff MJ, Cademartiri F, Callister TQ, Chang H-J, Cheng V, Chinnaiyan KM, Chow B, Delago A, Hadamitzky M, Hausleiter J, Karlsberg RP, Kaufmann P, Maffei E, Nasir K, Pencina MJ, Raff GL, Shaw LJ, Villines TC. Rationale and design of the CONFIRM (COronary CT Angiography EvaluatioN For Clinical Outcomes: An InteRnational Multicenter) Registry. *J Cardiovasc Comput Tomogr* 2011;**5**:84–92.
9. Abbara S, Arbab-Zadeh A, Callister TQ, Desai MY, Mamuya W, Thomson L, Weigold WG. SCCT guidelines for performance of coronary computed tomographic angiography: a report of the Society of Cardiovascular Computed Tomography Guidelines Committee. *J Cardiovasc Comput Tomogr* 2009;**3**:190–204.
10. Wilson PWF, D'Agostino RB, Levy D, Belanger AM, Silbershatz H, Kannel WB. Prediction of coronary heart disease using risk factor categories. *Circulation* 1998;**97**: 1837–1847.

cont.

Manuscrito 15

11. Hall M, Holmes G. Benchmarking attribute selection techniques for discrete class data mining. *IEEE Trans Knowledge Data Eng* 2003;**15**:1437–1447.
12. Friedman J, Hastie T, Tibshirani R. Additive logistic regression: a statistical view of boosting (with discussion and a rejoinder by the authors). *Ann Stat* 2000;**28**: 337–407.
13. Molinaro AM, Simon R, Pfeiffer RM. Prediction error estimation: a comparison of resampling methods. *Bioinformatics* 2005;**21**:3301–3307.
14. Arsanjani R, Dey D, Khachatryan T, Shalev A, Hayes S, Fish M, Nakanishi R, Germano G, Berman D, Slomka P. Prediction of revascularization after myocardial perfusion SPECT by machine learning in a large population. *J Nucl Cardiol* 2015;**22**: 877–884.
15. Hall M, Frank E, Holmes G, Pfahringer B, Reutemann P, Witten IH. The WEKA data mining software: an update. *ACM SIGKDD Explor Newsl* 2009;**11**:10–18.
16. Kanamori T, Takenouchi T, Eguchi S, Murata N. Robust loss functions for boosting. *Neural Comput.* 2007;**19**:2183–2244.
17. Witten IH, Frank E, Hall MA. *Data Mining: Practical Machine Learning Tools and Techniques*, 3rd ed. Boston: Morgan Kaufman; 2011.
18. DeLong ER, DeLong DM, Clarke-Pearson DL. Comparing the areas under two or more correlated receiver operating characteristic curves: a nonparametric approach. *Biometrics* 1988;**44**:837–845.
19. Greiner M, Sohr D, Göbel P. A modified ROC analysis for the selection of cut-off values and the definition of intermediate results of serodiagnostic tests. *J Immunol Methods* 1995;**185**:123–132.
20. Brier GW. Verification of forecasts expressed in terms of probability. *Mon Weather Rev* 1950;**78**:1–3.
21. Selvarajah S, Kaur G, Haniff J, Cheong KC, Hiong TG, van der Graaf Y, Bots ML. Comparison of the Framingham Risk Score, SCORE and WHO/ISH cardiovascular risk prediction models in an Asian population. *Int J Cardiol* 2014;**176**:211–218.
22. Franco M, Cooper RS, Bilal U, Fuster V. Challenges and opportunities for cardiovascular disease prevention. *Am J Med* 2015;**124**:95–102.
23. Arbab-Zadeh A, Fuster V. The myth of the "vulnerable plaque". *J Am Coll Cardiol* 2015;**65**:846–855.
24. Greenland P, Knoll MD, Stamler J, Neaton JD, Dyer AR, Garside DB, Wilson PW. Major risk factors as antecedents of fatal and nonfatal coronary heart disease events. *JAMA* 2003;**290**:891–897.
25. Budoff MJ, Shaw LJ, Liu ST, Weinstein SR, Mosler TP, Tseng PH, Flores FR, Callister TQ, Raggi P, Berman DS. Long-term prognosis associated with coronary calcification: observations from a registry of 25,253 patients. *J Am Coll Cardiol* 2007; **49**:1860–1870.
26. Mjolsness E, DeCoste D. Machine learning for science: state of the art and future prospects. *Science* 2001;**293**:2051–2055.
27. Patel MR, Peterson ED, Dai D, Brennan JM, Redberg RF, Anderson HV, Brindis RG, Douglas PS. Low diagnostic yield of elective coronary angiography. *N Engl J Med* 2010;**362**:886–895.
28. Meijboom WB, Mieghem CA, van Pelt N, Weustink A, Pugliese F, Mollet NR, Boersma E, Regar E, van Geuns RJ, de Jaegere PJ, Serruys PW, Krestin GP, de Feyter PJ. Comprehensive assessment of coronary artery stenoses computed tomography coronary angiography versus conventional coronary angiography and correlation with fractional flow reserve in patients with stable angina. *J Am Coll Cardiol* 2008;**52**:636–643.
29. Kang X, Berman DS, Lewin HC, Cohen I, Friedman JD, Germano G, Hachamovitch R, Shaw LJ. Incremental prognostic value of myocardial perfusion single photon emission computed tomography in patients with diabetes mellitus. *Am Heart J* 1999;**138**:1025–1032.
30. Binder H, Allignol A, Schumacher M, Beyersmann J. Boosting for high-dimensional time-to-event data with competing risks. *Bioinformatics* 2009;**25**:890–896.

CAPÍTULO IV

Objetivos

4.1. OBJETIVOS

1. Criar um normograma para caracterização da avaliação volumétrica da aurícula esquerda, na fase cardíaca mais frequentemente utilizada para avaliação coronária — diástole média — 70% do intervalo entre ondas R. Determinar uma medida que seja prática (rápida e fácil de se obter) e apresente boa correlação com o volume auricular, por forma a tornar eficiente a avaliação volumétrica da aurícula esquerda.

2. Caracterização anatómica e funcional dos doentes com FA que realizaram exame de TC em contexto prévio à realização de ablação de fibrilhação auricular e a seu contributo prognóstico para determinar o sucesso da terapêutica ablativa percutânea.

3. Otimização dos exames de TC cardíaca realizados em contexto prévio à realização de ablação de fibrilhação auricular.

CAPÍTULO V

População

SUMÁRIO

5.1. INTRODUÇÃO

Neste trabalho de investigação foram constituídas cinco populações de estudo num total de 693 doentes, tendo por base um registo prospetivo de doentes consecutivos que realizaram TC cardíaca no Hospital da Luz.
No âmbito do registo não houve condicionamento da referenciação dos doentes.

5.2. DEFINIÇÃO DOS GRUPOS POPULACIONAIS:

5.2.1. Normograma e caracterização anátomo-funcional e correlação prognóstica dos doentes com FA

Para criação do normograma (**Capítulo VIII**) e caracterização anátomo-funcional e sua correlação prognóstica nos doentes com FA (**Capítulo IX**), foi criado o grupo A e suas divisões A1 e A2, bem como o grupo B (ver **Tabela 1**) num total de 423 doentes.

Grupo A — grupo "doentes com FA" — n=277

De um registo prospetivo de 2062 indivíduos que realizaram TC cardíaca de Maio de 2009 a final de Abril de 2012 — 3 anos, foram selecionados todos aqueles que a indicação foi a avaliação prévia a ablação de fibrilhação auricular (com diagnóstico prévio de FA) — 277 doentes. Assim foi constituído o **grupo A.**

A subconstituição sucessiva deste grupo A em grupo A1 e posteriormente em grupo A2 deveu-se aos seguintes critérios:

- O **grupo A1** é constituído por todos os doentes do grupo A em que a TC permitia avaliar função (aquisição de TC em modo retrospetivo e em ritmo sinusal durante o TC) — foi o grupo base de doentes com FA utilizado no capítulo VIII.
- Do grupo A1 foram selecionados apenas os doentes com FA paroxística, que realizaram ablação e em que foi possível obter informação de seguimento clínico, formando assim o **grupo A2**.

FIGURA 1

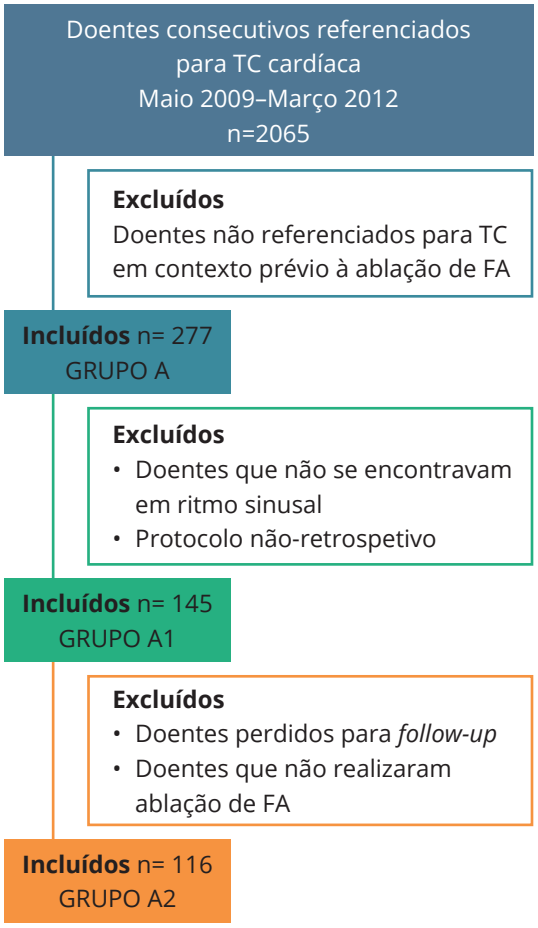

A caracterização mais pormenorizada da população do grupo A1 é efetuada no **Capítulo VIII** e a do grupo A2 no **Capítulo IX**.

Grupo B — grupo controlo (representativo da população normal) — n=146

De um registo prospetivo de 2062 indivíduos que realizaram TC cardíaca de Maio de 2009 a final de Abril de 2012 — 3 anos, foram selecionados todos os indivíduos que seriam representativos de uma população "normal", por reunirem todas as seguintes condições:

- Sem doença cardíaca conhecida, incluindo doença valvular e doença coronária
- Sem hipertensão arterial — sem história de HTA, sem medicação para HTA e com a tensão arterial medida antes da realização da TC com valores sistólicos inferiores a 140mmHg e valores diastólicos inferiores a 90 mmHg
- Sem obesidade — com IMC <30kg/m^2

TABELA 1

Descrição populacional grupo A e B

	Grupo A	**Grupo B**
N	**277**	**146**
Sexo masculino (n, %)	**199 (72%)**	**74 (51%)**
Idade (anos)*	56,23 +/- 12,31	45,41+/-12,97
Altura (cm)*	171,26 +/- 10,68	167,59+/-10,21
Peso (kg)*	79,94 +/-14,14	71,73+/-14,07
Área de superficie corporal (m^2)*	1,95 +/- 0,2	1,82+/-0,22
ìndice de massa corporal (kg/m^2)*	27,07 +/- 3,98	25,43+/-3,75
Tensão arterial sistólica (mmHg)*	134,6 +/- 19,96	123,44+/-13,47
Tensão arterial diastólica (mmHg)*	78,74 +/- 10,44	73,43+/-9,56
Hipertensos#	47%	0.00%
Ritmo sinusal durante o exame#	69%	100%
VAEsqMax (ml)	81+/- 30,14	49,1+/-14,4

**média e desvio padrão*

 # percentagem

- Sem história de arritmia cardíaca e em ritmo sinusal durante a aquisição da TC
- Ecocardiograma normal, realizado num prazo inferior a 60 dias da data da TC (incluindo menção de : normal dimensão da aurícula esquerda, ausência de disfunção diastólica do VEsq e ausência de patologia valvular mitral)
- Com resultados da TC cardíaca que revelaram:
  - Ausência de doença coronária obstrutiva (estenoses máximas <50%)
  - Sem doença valvular na TC
  - Fração de ejeção do VEsq preservada e sem disfunção segmentar.
  - Aurícula esquerda com volume máximo normal

No grupo resultante só haviam 74 mulheres pelo que, para manter o grupo com representação similar entre sexos, se selecionaram os primeiros 74 homens incluídos. Da população resultante, 148 doentes, excluíram-se dois doentes (mulheres) por informação incompleta no arquivo de imagem.

A caracterização mais pormenorizada da população do grupo B é efetuada no **Capítulo VIII**.

5.2.2. Otimização dos exames de TC cardíaco prévio à ablação de FA

Para a avaliação da otimização dos exames de TC cardíaca realizados num contexto prévio à ablação de FA (Capítulo X) foram criados os grupos 1, 2 e 3, independentes, num total de 270 doentes (ver **Tabela 2**).

Grupo 1 — n=150

De um registo prospetivo de doentes consecutivos que realizaram TC cardíaca no Hospital da Luz, selecionaram-se todos cuja indicação foi a avaliação prévia a ablação de fibrilhação auricular. Desses foram selecionados para este grupo os primeiros 150 doentes consecutivos incluídos no registo.

Grupo 2 — n=60

De um registo prospetivo de doentes consecutivos que realizaram TC cardíaca no Hospital da Luz, selecionaram-se todos cuja indicação foi a avaliação prévia a ablação de fibrilhação auricular. Desses foram selecionados para este grupo os últimos 60 doentes consecutivos incluídos no registo que realizaram o exame no aparelho de TC inicial (TC dupla-ampola 1ªgeração) .

Grupo 3 — n=60

De um registo prospetivo de doentes consecutivos que realizaram TC cardíaca no Hospital da Luz, selecionaram-se todos cuja indicação foi a avaliação prévia a ablação de fibrilhação auricular. Desses foram selecionados para este grupo os primeiros 60 doentes consecutivos incluídos no registo que realizaram o exame no novo aparelho de TC (TC dupla-ampola de 3.ª geração).

TABELA 2

Descrição populacional dos grupos 1, 2 e 3

	Grupo 1	Grupo 2	Grupo 3
n	150	60	60
Idade (anos)	59 (48-65)	63 (53-69)	65 (56-70)
Sexo masculino	74% (n=111)	72% (n=43)	73% (n=44)
IMC (Kg/m²)	26,6 (24,2-29,1)	27,1 (24,0-28,6)	26,3 (24,5-28,9)
Doentes com FA (%)	100%	100%	100%

CAPÍTULO VI

TC Cardíaca

Aspetos técnicos e protocolos de aquisição

RESUMO

Neste capítulo é feita uma revisão dos aspetos técnicos dos aparelhos de TC relevantes no contexto de avaliação cardíaca e a forma como influenciam a preparação do doente (inclui-se artigo sobre a utilização de beta-bloqueantes para modulação da frequência cardíaca — **Manuscrito 16**) [1].

Atribui-se especial destaque à espantosa evolução da dose de radiação dos exames de TC cardíaco. Em relação a este aspeto são incluídos dois manuscritos (**Manuscritos 17** e **18**) [2, 3].

Faz-se igualmente uma descrição dos diversos exames englobados sob a denominação lata: "TC cardíaca".

Terminamos por definir os protocolos de aquisição de TC efetuados em cada uma das populações de estudo desta tese.

MANUSCRITOS

Manuscrito 16

Bailout intravenous esmolol for heart rate control in cardiac computed tomography angiography.

Aguiar Rosa, S., Ramos, R., **Marques**, **H**., Santos, R., Leal, C., Casado, H., Saraiva, M., Figueiredo, L., and Cruz Ferreira, R., Rev Port Cardiol, 2016. **35**(12): p. 673-678.

Manuscrito 17

Effective radiation dose of three diagnostic tests in cardiology: single photon emission computed tomography, invasive coronary angiography and cardiac computed tomography angiography.

de Araujo Goncalves, P., Jeronimo Sousa, P., Cale, R., **Marques**, **H**., Borges dos Santos, M., Dias, A., Dores, H., Carvalho, M.S., Ventosa, A., Martins, T., Campante Teles, R., Almeida, M., and Mendes, M., Rev Port Cardiol, 2013. **32**(12): p. 981-6.

Manuscrito 18

Radiation in cardiac CT: predictors of higher dose and its reduction over time.

Sousa, P.J., Goncalves, P.A., **Marques**, **H**., Raposo, L., Cale, R., Brito, J., Gaspar, A., Machado, F.P., and Roquette, J., Rev Port Cardiol, 2010. **29**(11): p. 1655-65.

SUMÁRIO

6.1. INTRODUÇÃO

A impressionante evolução tecnológica dos aparelhos de TC tem tido paralelo no aumento de indicações apropriadas dos exames conhecidos como TC cardíaca.
São abordados sumariamente neste capítulo as evoluções técnicas dos aparelhos de TC e o seu contributo na avaliação dos doentes das populações de estudo desta tese.

6.2. ASPETOS TÉCNICOS

6.2.1. Cobertura crâneo-caudal

Desde a realização dos primeiros exames de TC multidetetor (4 detetores) com capacidade de sincronização eletrocardiográfica, que se assistiu ao intensificar da corrida ao maior número de detetores.
O acréscimo do número de detetores permite uma maior cobertura crâneo-caudal, o que significa menor número de ciclos cardíacos para completar a aquisição volumétrica do coração por menor tempo de aquisição, logo menor dependência de frequências cardíacas estáveis e menor tempo de apneia necessária para obter bons exames.
Atualmente já existem dois aparelhos de TC no mercado cujo o número de detetores permite numa só rotação com a mesa parada a cobertura volumétrica total de um coração.
Outra forma desenvolvida para aumentar artificialmente a cobertura crâneo-caudal são as aquisições de *pitch* muito elevado em TC com dupla-ampola, permitindo também a aquisição volumétrica de todo o coração apenas num batimento cardíaco.

6.2.2. Resolução de sinal, contraste, espacial e temporal

Contrastes com maior concentração de iodo por mililitro, novos detetores aliados a novas reconstruções (iterativas) e a softwares automáticos (ou semi-automáticos) de otimização de dose permitem otimizar os rácios sinal/ruído e contraste/ruído. A resolução espacial beneficiou sobretudo do desenvolvimento de novos detetores (mais finos e com menor latência), com resoluções máximas atuais de 0,23mm (Revolution CT®- GE healthcare) praticamente isotrópicas. No entanto, apesar das melhorias, não atingiram ainda os valores de 0,16mm da angiografia convencional, 0,15mm do Intravascular UltraSound (IVUS) e os 0,015mm do Optic Coerence Tomography (OCT). Estes aspetos contribuíram para a melhor definição do cálcio e a melhor definição do lúmen e parede dos vasos.

A resolução temporal talvez se mantenha atualmente como a principal limitação da avaliação coronária, sendo frequentemente necessária a diminuição da frequência cardíaca do doente antes da aquisição do exame (esta questão foi abordada no **Manuscrito 16**)[1]. Ainda assim sofreu grande evolução com velocidades de rotação maiores e com o desenvolvimento de aparelhos de dupla-ampola (resolução temporal duas vezes melhor do que aparelho com a mesma velocidade de rotação e só uma ampola). A melhor resolução temporal nativa (sem técnicas de aquisição segmentada) é de 66ms (Somatom Force ®, Siemens Healthcare), ainda aquém dos 33ms da angiografia convencional, mas já aproximada dos 33 a 66ms das técnicas ecocardiográficas. Há, no entanto, formas indiretas de aumentar a resolução temporal, sendo a mais promissora o desenvolvimento de softwares para o realizar ainda no espaço da reconstrução [4]. Com a evolução da resolução temporal, os artefactos de movimento foram grandemente diminuídos permitindo estudos com frequências cardíacas mais elevadas (ver **Figura 1**).

6.2.3. Técnicas de energia espetral

As técnicas de energia espetral podem ser utilizadas para otimização do contraste da imagem, permitindo significativa redução do volume de contraste iodado necessário por reconstrução de imagem utilizando informação apenas dos menor keV.

Estas técnicas podem ainda ser utilizadas para a codificação de substâncias na imagem, como o cálcio, o ácido úrico e até mesmo o iodo. Assim permitem fazer a avaliação quantitativa e por mapa de cores do volume de iodo por *voxel*.

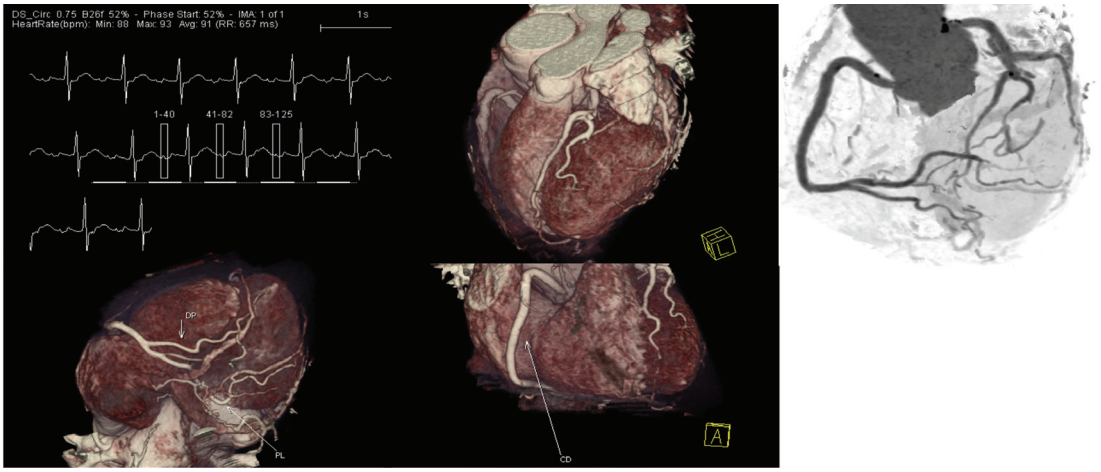

FIGURA 1

Angio-TC coronário em doente com frequência cardíaca média de 91bpm.
Imagens sem artefacto de movimento. Exame realizado em 2008, com TC dupla ampola primeira geração no Hospital da Luz, com resolução temporal nativa de 83ms.
(Imagens Hugo Marques — UNICA — Hospital da Luz.)

As técnicas de energia espetral têm igualmente utilidade na avaliação de isquémia e na avaliação de realce tardio.

Futuramente poderão servir para retirar o cálcio das imagens e mostrar a angiografia coronária como se fosse apenas uma técnica luminográfica (sem perda de qualidade).

6.2.4. Dose de radiação

No início, a TC cardíaca era considerada um exame de dose de radiação ionizante elevada, tendo sido esta limitação um dos maiores *drivers* para a evolução tecnológica. O risco da radiação ionizante utilizada na imagem médica deve-se aos seus efeitos estocásticos, pela possibilidade de doses pequenas de radiação poderem provocar mutações genéticas que por sua vez aumentariam o risco de cancro.

Se a associação entre radiação e efeitos cancerígenos foi observada para doses elevadas nos sobreviventes das bombas atómicas ou na população sujeita a radiação no desastre de Chernobyl, em que uma exposição a uma dose de radiação de 100mSv aumenta a probabilidade de morte por cancro em 0,5%[5], este efeito e relação carece de informação científica suficiente para doses menores [6, 7].

Assim existem diversas teorias propostas para cálculo de risco oncogénico para doses de radiação baixa (inferiores a 100mSv), desde a teoria da Hormese que defende que

doses baixas poderão ter efeito protector , até à teoria "linear sem *threshold*" que serve de base para o modelo "ALARA" (*as low as reasonably achievable*) que rege a utilização dos meios complementares diagnósticos com radiação. Esta teoria diz que para cada dose de radiação (mesmo as baixas doses) existe um maior risco de desenvolvimento de cancro e que esta relação é direta [8, 9].
De todas as teorias propostas, esta é a que resulta num maior risco carcinogénico dos exames imagiológicos com radiação X.
O primeiro estudo multicêntrico prospetivo sobre dose de radiação da TC cardíaca para avaliação coronária foi publicado em 2009, com valores muito diferentes de dose média entre centros e com doses de radiação médias de 12mSv [10].
Desde então as doses de radiação têm sistematicamente diminuído devido a diversos fatores contributivos, nomeadamente: aquisições mais rápidas (num só batimento cardíaco), o desenvolvimento de ampolas que permitem maior miliamperagem com menores KV e o desenvolvimento da reconstrução iterativa.
Atualmente conseguem-se exames com doses inferiores a 1mSv (ver **Figura 2**).

Durante este período publicámos um trabalho em 2010 em que avaliamos a evolução temporal da dose de radiação (sendo a dose média do nosso centro para TC cardíaca para avaliação das artérias coronárias: 6,6mSv) e onde foi possível identificar preditores de dose mais alta, nomeadamente um índice de massa corporal (IMC) elevado (que não permitia utilizar menores kV na aquisição), a história de cirurgia cardíaca prévia (pela necessidade de aumentar a aquisição crâneo-caudal para observar pontagens) e a presença de arritmia (que diminui a capacidade de modulação da radiação ao longo do intervalo RR) [3].
Num outro trabalho em que participámos e publicámos: numa população de 6196 doentes comparámos a dose de radiação dos três exames mais utilizados no diagnóstico de doença coronária, a angiografia convencional (dose média de 8,1mSv), a cintigrafia de perfusão miocárdica (10,7mSv) e a angio-TC coronária (5,4mSv) [2].

Está em fase de publicação o estudo PROTECTION VI (do qual o autor desta tese é o investigador responsável do nosso centro), que irá atualizar os dados do primeiro estudo PROTECTION I [10], antevendo-se reduções da dose média em cerca de nove a dez vezes, sem diminuição da qualidade de imagem.
A otimização da dose de radiação nos exames de TC cardíaca pré-ablação de FA foi âmbito desta investigação e é descrita no Capítulo X.

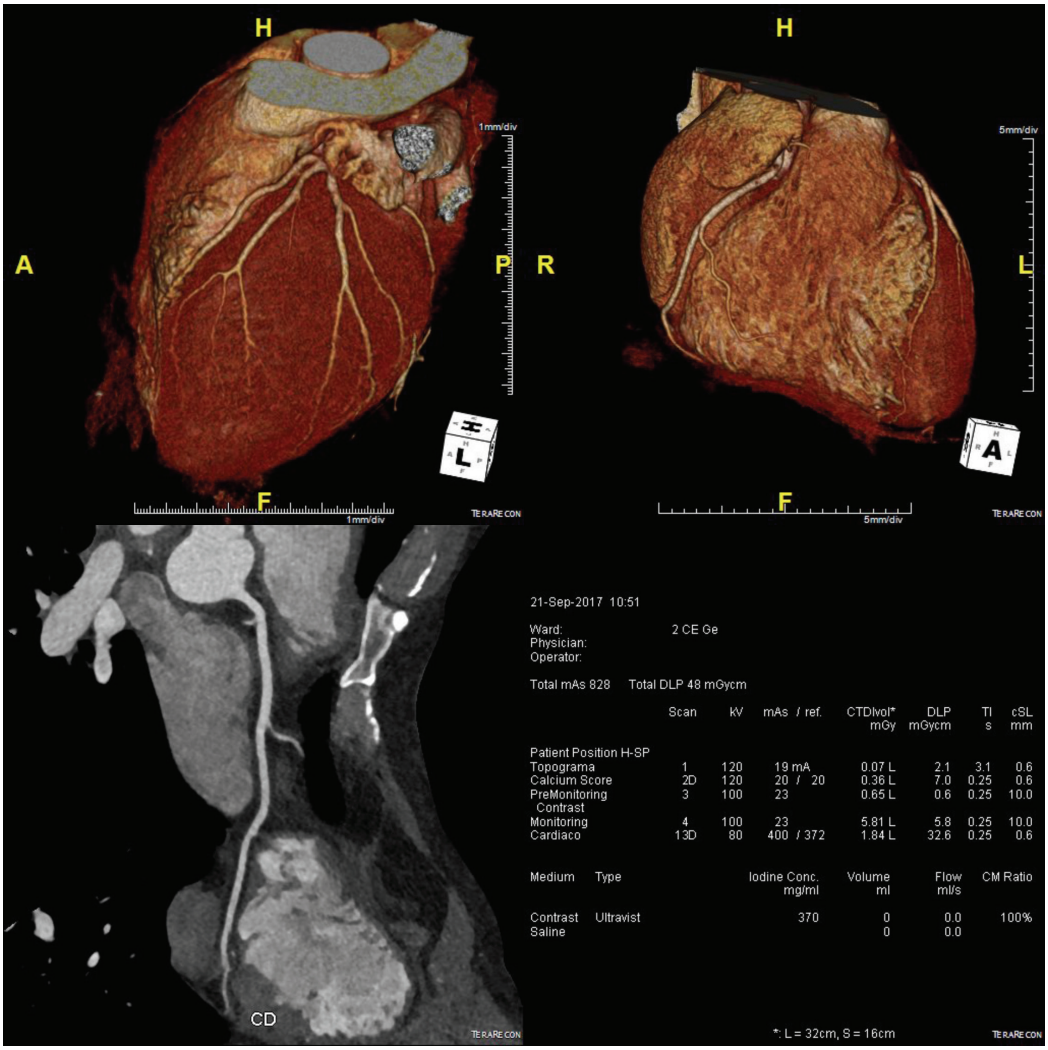

FIGURA 2

TC cardíaco realizado no aparelho de TC Force — Hospital da Luz; Dose de radiação do "Score" de cálcio = 0,1mSv; Dose de radiação da Angio-TC coronária = 0,6mSv.

(Imagens Hugo Marques — UNICA — Hospital da Luz.)

De qualquer forma, importa realçar que:

- O efeito carcinogénio da radiação ionizante de baixa dose, a utilizada em imagiologia médica, é uma extrapolação do risco observado para doses de pelo menos 100mSv.
- A dose média de um exame de TC cardíaco em 2009 era de 12mSv e atualmente é provavelmente cerca de 9 a 10 vezes menor.
- Na avaliação desta problemática não pode ser excluído o benefício da informação obtida pela realização de um exame apropriado e o risco basal atual de morte por cancro na população ocidental

6.3. TC CARDÍACA — UM OU VÁRIOS ESTUDOS?

Esta denominação engloba diferentes estudos para avaliar o coração que têm em comum a utilização de sincronização eletrocardiográfica.

Podem ser realizados sem contraste para:

- avaliar e quantificar placas calcificadas nas artérias coronárias – *score* de cálcio
- avaliar e quantificar o cálcio valvular — *score* de cálcio valvular
- obter imagens antes da administração de contraste para poder avaliar a captação de contraste por uma massa
- avaliar a presença de áreas espontaneamente densas em situações agudas, como, por exemplo, os hematomas murais.

Podem ser realizados com contraste para:

- detetar e avaliar estenoses coronárias — Angio-TC coronário — a indicação mais frequente
- avaliação de patência de pontagens
- avaliação de perfusão miocárdica — com técnicas de primeira passagem ou avaliação da perfusão estática em equilíbrio
- avaliação cardíaca extra-coronária — miocárdio, válvulas, pericárdio, massas
- ser combinado com outros exames de angiografia, nomeadamente nos estudos de duplo e triplo *rule out* (exclusão de doença coronária, tromboembolismo pulmonar e dissecção aórtica) ou para avaliar o restante leito vascular pré-intervenção percutânea.

No contexto dos doentes com FA, a TC cardíaca inclui os seguintes exames:

- avaliação coronária
- avaliação anatómica e exclusão de trombo pré-ablação de fibrilhação auricular ou pré-oclusão do AAESQ
- avaliação de complicações pós ablação ou pós-oclusão.

6.4. TC CARDÍACA — PROTOCOLOS DE AQUISIÇÃO NOS DIFERENTES GRUPOS POPULACIONAIS ÂMBITO DESTA TESE (DEFINIDOS NO CAPÍTULO V)

Grupo A — grupo "doentes com FA"

TC dupla-ampola 1ª geração — 64 detetores — SOMATOM Definition®, com resolução temporal nativa de 83ms e velocidade de mesa máximo de 45,7mm/s

- Aquisição: depois de disponível optou-se por avaliação prospetiva, de acordo com o referido no protocolo de aquisição do grupo 2 (ver abaixo). Antes dessa disponibilidade realizámos exames com aquisição de acordo com o protocolo do grupo 1 (ver abaixo)
- Reconstrução — *filtered back projection*, com espessura de corte de 1,5mm, incremento 0,7mm e matriz 512x512
- Contraste — 320mgI/ml — injecção trifásia a 6ml/seg.
  - Primeira fase de contraste puro com volume calculado segundo a fórmula = (tempo de aquisição +tempo de espera) x6. O tempo de espera foi fixado em 7 segundos.
  - Segunda fase de 30 ml de contraste diluído (30% contraste e 70%s oro).
  - Terceira fase de 30ml de soro.
- Técnica de *bolus tracking* com região de interesse na aorta ascendente e início de aquisição 7 segundos após atingir a densidade de 150UH (unidades *Hounsfield*).

Grupo B — grupo controlo (representativo da população normal)

TC dupla-ampola 1ª geração — 64 detetores — SOMATOM Definition®, com resolução temporal nativa de 83ms e velocidade de mesa máximo de 45,7mm/s

- Medicação:
  - 5mg de nitroglicerina sublingual se TArt sistólica >100mmHg
  - Metoprolol endovenoso aos doentes com FC superior a 70bpm (5mg a cada 3min até FC alvo de 70bpm até uma dose máxima de 25mg)
  - Prévia a administração de fármacos confirmadas ausências de contra-indicações ou alergias.
- Aquisição: retrospetiva, com modulação da miliamperagem — com 20% da miliamperagem fora dos intervalos de dose máxima escolhidos da seguinte forma:
  - Se rítmico e FC <70bpm — dose máxima 70-80% do intervalo RR

  - Se rítmico com FC 70-80 — dose máxima de 40 a 80% do intervalo RR
  - Se rítmico e FC >80 — dose máxima a 40-50% do intervalo RR.
- Determinação da kV — 100kV, excepto se IMC<18,5 quando se utilizava 80kV
- Reconstrução — *filtered back projection*, com espessura de corte de 1,5mm, incremento 0,7mm e matriz 256x256, com reconstruções de 10 em 10% de todo o intervalo RR
- Contraste — 320mgI/ml — injeção trifásica a 7ml/seg.
  - Primeira fase de contraste puro com volume calculado segundo a fórmula = (tempo de aquisição +tempo de espera) x7. O tempo de espera foi fixado em 7 segundos.
  - Segunda fase de 30 ml de contraste diluído (30% contraste e 70% soro).
  - Terceira fase de 30ml de soro.
- Técnica de *bolus tracking* com região de interesse na aorta ascendente e início de aquisição 7 segundos após atingir a densidade de 120UH (unidades *Hounsfield*)

Grupo 1

TC dupla-ampola 1ª geração — 64 detetores — SOMATOM Definition®, com resolução temporal nativa de 83ms e velocidade de mesa máximo de 45,7mm/s

- Aquisição: retrospetiva, com modulação da miliamperagem — com 20% da miliamperagem fora dos intervalos de dose máxima escolhidos da seguinte forma:
  - Se rítmico e FC <70bpm — dose máxima 70% do intervalo RR
  - Se arrítmico ou rítmico com FC 70-80 — dose máxima de 40 a 80% do intervalo RR
  - Se rítmico e FC >80 — dose máxima a 40-50% do intervalo RR.
- Determinação da kV — 100kV., se BMI<30, caso contrario 120kV
- Reconstrução — *filtered back projection*, com espessura de corte de 1,5mm, incremento 0,7mm e matriz 512x512
- Contraste — 320mgI/ml — injeção trifásica a 6ml/seg.
  - Primeira fase de contraste puro com volume calculado segundo a fórmula = (tempo de aquisição +tempo de espera) x6. O tempo de espera foi fixado em 7 segundos.
  - Segunda fase de 30 ml de contraste diluído (30% contraste e 70% soro).
  - Terceira fase de 30ml de soro.

> Técnica de *bolus tracking* com região de interesse na aorta ascendente e início de aquisição 7 segundos após atingir a densidade de 150UH (unidades *Hounsfield*)

Grupo 2

TC dupla-ampola 1ª geração — 64 detetores — SOMATOM Definition®, com resolução temporal nativa de 83ms e velocidade de mesa máximo de 45,7mm/s

> Aquisição: prospetiva se rítmico ou arrítmico com pequena variabilidade RR. Noutros casos aquisição retrospetiva com modulação da miliamperagem (3% da miliamperagem fora dos intervalos de dose máxima (minimal dose manual), com dose máxima de 40 a 80% do intervalo RR).
> Determinação da kV — 80kV se BMI<30, caso contrario 100kV se peso inferior a 100kg e 120kV se peso superior a 100kg
> Reconstrução — FBP, com espessura de corte de1,5mm, incremento 0,7mm e matriz 512x512.
> Contraste — 370 mg I /ml — Injecção trifásia a 5ml/seg.
  - Primeira fase de contraste puro com volume calculado segundo a fórmula = (tempo de aquisição +tempo de espera) x5. O tempo de espera foi fixado em 10 segundos.
  - Segunda fase de 30 ml de contraste diluído (30% contraste e 70%s oro).
  - Terceira fase de 30ml de soro.
> Técnica de "bolus tracking" com região de interesse na aorta ascendente e início de aquisição 10segundos após atingir a densidade de 150UH (unidades *Hounsfield*)

Grupo 3

TC dupla-ampola 3ªgeração — 192 detetores — SOMATOM Force® com resolução temporal nativa de 66ms e velocidade de mesa (*pitch*) máximo em modo FLASH de 737mm/seg.

> Aquisição: em modo FLASH (aquisição em batimento cardíaco único com método de velocidade de mesa muito elevado 737mm/s), excepto se doentes com FC média superior a 80 bpm onde se opta pela aquisição em método prospetivo. Aquisição retrospetiva apenas em doentes com marcada variabilidade do intervalo RR.
> Determinação da kV e miliamperagem — por referência 80Kv com 200mAs/rot,com indicação de realização de angio-TC. Apenas se BMI>30, os kV de

referência passam a 100. No entanto, o novo aparelho apresenta a capacidade de avaliar a densidade do doente no topograma realizado, servindo os valores de referência, como um guia para o ruído admissível/máximo que se pretende ter na imagem, fazendo o aparelho uma modificação dos valores por forma a otimizar a dose de radiação, mantendo a qualidade da imagem.

- Reconstrução — iterativa — SAFFIRE força 3, com espessura de corte de1,5mm, incremento 0,7mm e matriz 512x512
- Contraste — 370mg I / ml — injecção trifásia a 4ml/seg.
  - Primeira fase de contraste puro com volume calculado segundo a fórmula = (tempo de aquisição +tempo de espera) x4. O tempo de espera foi fixado em 15 segundos, dado a aquisição preferencialmente utilizada (modo FLASH) durar menos de 1 segundo.
  - Segunda fase de 30 ml de contraste diluído (30% contraste e 70% soro).
  - Terceira fase de 30ml de soro.
- Técnica de *bolus tracking* com região de interesse na aorta ascendente e início de aquisição 15segundos após atingir a densidade de 150UH (unidades *Hounsfield*)

Em jeito de conclusão, salientamos que a modulação da aquisição a cada doente e a cada indicação permite otimizar a dose de contraste, a dose de radiação e a acuidade do exame.

BIBLIOGRAFIA

1. Aguiar Rosa, S., Ramos, R., Marques, H., Santos, R., Leal, C., Casado, H., Saraiva, M., Figueiredo, L., and Cruz Ferreira, R., *Bailout intravenous esmolol for heart rate control in cardiac computed tomography angiography.* Rev Port Cardiol, 2016. **35**(12): p. 673-678.
2. de Araujo Goncalves, P., Jeronimo Sousa, P., Cale, R., Marques, H., Borges dos Santos, M., Dias, A., Dores, H., Carvalho, M.S., Ventosa, A., Martins, T., Campante Teles, R., Almeida, M., and Mendes, M., *Effective radiation dose of three diagnostic tests in cardiology: single photon emission computed tomography, invasive coronary angiography and cardiac computed tomography angiography.* Rev Port Cardiol, 2013. **32**(12): p. 981-6.
3. Sousa, P.J., Goncalves, P.A., Marques, H., Raposo, L., Cale, R., Brito, J., Gaspar, A., Machado, F.P., and Roquette, J., *Radiation in cardiac CT: predictors of higher dose and its reduction over time.* Rev Port Cardiol, 2010. **29**(11): p. 1655-65.
4. Min, J.K., Arsanjani, R., Kurabayashi, S., Andreini, D., Pontone, G., Choi, B.W., Chang, H.J., Lu, B., Narula, J., Karimi, A., Roobottom, C., Gomez, M., Berman, D.S., Cury, R.C., Villines, T., Kang, J., and Leipsic, J., *Rationale and design of the ViCTORY (Validation of an Intracycle CT Motion CORrection Algorithm for Diagnostic AccuracY) trial.* J Cardiovasc Comput Tomogr, 2013. **7**(3): p. 200-6.
5. Gerber, T.C., Carr, J.J., Arai, A.E., Dixon, R.L., Ferrari, V.A., Gomes, A.S., Heller, G.V., McCollough, C.H., McNitt-Gray, M.F., Mettler, F.A., Mieres, J.H., Morin, R.L., and Yester, M.V., *Ionizing radiation in cardiac imaging: a science advisory from the American Heart Association Committee on Cardiac Imaging of the Council on Clinical Cardiology and Committee on Cardiovascular Imaging and Intervention of the Council on Cardiovascular Radiology and Intervention.* Circulation, 2009. **119**(7): p. 1056-65.
6. Muirhead, C.R., *Studies on the Hiroshima and Nagasaki survivors, and their use in estimating radiation risks.* Radiat Prot Dosimetry, 2003. **104**(4): p. 331-5.
7. Preston, D.L., Ron, E., Tokuoka, S., Funamoto, S., Nishi, N., Soda, M., Mabuchi, K., and Kodama, K., *Solid cancer incidence in atomic bomb survivors: 1958-1998.* Radiat Res, 2007. **168**(1): p. 1-64.
8. Einstein, A.J., *Effects of radiation exposure from cardiac imaging: how good are the data?* J Am Coll Cardiol, 2012. **59**(6): p. 553-65.
9. Einstein, A.J., Henzlova, M.J., and Rajagopalan, S., *Estimating risk of cancer associated with radiation exposure from 64-slice computed tomography coronary angiography.* JAMA, 2007. **298**(3): p. 317-23.
10. Hausleiter, J., Meyer, T., Hermann, F., Hadamitzky, M., Krebs, M., Gerber, T.C., McCollough, C., Martinoff, S., Kastrati, A., Schomig, A., and Achenbach, S., *Estimated radiation dose associated with cardiac CT angiography.* JAMA, 2009. **301**(5): p. 500-7.

ANEXOS

MANUSCRITO 16

Bailout intravenous esmolol for heart rate control in cardiac computed tomography angiography.

Aguiar Rosa, S., Ramos, R., **Marques**, **H**., Santos, R., Leal, C., Casado, H., Saraiva, M., Figueiredo, L., and Cruz Ferreira, R.

Rev Port Cardiol, 2016
35(12): p. 673-678

Manuscrito 16

Rev Port Cardiol. 2016;35(12):673–678

Portuguese Society of CARDIOLOGY

Revista Portuguesa de
Cardiologia
Portuguese Journal of Cardiology
www.revportcardiol.org

ORIGINAL ARTICLE

Bailout intravenous esmolol for heart rate control in cardiac computed tomography angiography

Sílvia Aguiar Rosa[a,*], Ruben Ramos[a], Hugo Marques[b], Rosana Santos[b], Cecília Leal[b], Helena Casado[b], Márcia Saraiva[b], Luísa Figueiredo[b], Rui Cruz Ferreira[a]

[a] *Cardiology Department, Santa Marta Hospital, Lisbon, Portugal*
[b] *Radiology Department, Santa Marta Hospital, Lisbon, Portugal*

Received 9 February 2016; accepted 8 July 2016
Available online 17 November 2016

KEYWORDS
Coronary computed tomography angiography;
Esmolol;
Heart rate control

Abstract
Objective: To evaluate the efficacy and safety of a heart rate (HR) reduction protocol using intravenous esmolol as bailout for failed oral metoprolol regimens in patients undergoing coronary computed tomography angiography (CCTA) with 64-slice multidetector computed tomography (64-MDCT).
Methods: Patients who underwent cardiac 64-MDCT in a single institution between 2011 and 2014 were analyzed. Those with HR above 60 beats per minute (bpm) on presentation received oral metoprolol (50-200 mg) at least one hour before CCTA. Intravenous esmolol 1-2 mg/kg was administered as a bolus whenever HR remained over 65 bpm just before imaging. The primary efficacy endpoint was HR <65 bpm during CCTA. The primary safety endpoint was symptomatic hypotension or bradycardia up to hospital discharge.
Results: During the study period CCTA was performed in 947 cases. In 86% of these, oral metoprolol was the only medication required to successfully reduce HR <60 bpm. Esmolol was used in the remaining 130 patients (14%). For esmolol-treated patients mean baseline and acquisition HR were 74±14 bpm and 63±9 bpm, respectively ($p<0.001$). The target HR of <65 bpm was achieved in 82 of the 130 esmolol-treated patients (63%). Considering the whole population, esmolol use led to a significant increase in the primary efficacy endpoint from 86% to 95% ($p<0.001$). Esmolol also resulted in a statistically, but not clinically, significant reduction in systolic blood pressure (144±22 to 115±17 mmHg; $p<0.001$). The combined primary safety endpoint was only observed in two (1.5%) patients.
Conclusion: Despite optimal use of oral beta-blockers, 14% of patients needed intravenous esmolol for HR control. The pre-medication combination of oral metoprolol and on-demand administration of intravenous esmolol was safe and effective and enabled 95% of patients to be imaged with HR below 65 bpm.

* Corresponding author.
E-mail address: silviaguiarosa@gmail.com (S. Aguiar Rosa).

http://dx.doi.org/10.1016/j.repc.2016.07.004

cont.

PALAVRAS-CHAVE
Angiografia coronária por tomografia computorizada;
Esmolol;
Controlo de frequência cardíaca

Esmolol endovenoso em regime *bail out* para controlo de frequência cardíaca na tomografia computorizada cardíaca

Resumo
Objetivo: Avaliar a eficácia e segurança de um protocolo de redução de frequência cardíaca (FC) utilizando esmolol endovenoso após falência de metoprolol oral, em doentes submetidos a angiografia coronária por tomografia computorizada (CCTA) de 64 cortes.
Métodos: De 2011 a 2014 foram avaliados os indivíduos submetidos a CCTA num único centro. Os indivíduos com FC >60 bpm à admissão receberam 50-200 mg de metoprolol oral pelo menos uma hora antes da CCTA. Esmolol endovenoso em bólus (1-2 mg/kg) foi administrado se FC >65 bpm imediatamente antes da aquisição de imagem. O *endpoint* primário de eficácia foi FC <65 bpm durante a aquisição de imagem com contraste. O *endpoint* primário de segurança foi hipotensão ou bradicardia sintomática durante a permanência no hospital.
Resultados: Foram efetuadas 947 CCTA durante o período de estudo. Em 86% dos casos, metoprolol oral foi o único fármaco utilizado. Foi necessária a administração de esmolol em 130 (14%) doentes. Nos doentes que receberam esmolol, a FC basal reduziu em média de 74±14 bpm para 63±9 bpm (p<0,001). O objetivo primário de FC <65 bpm foi alcançado em 82 desses 130 doentes (63%). Considerando toda a população, o recurso a esmolol permitiu um aumento significativo da proporção de CCTA realizados com FC <65 bpm (86% para 95% [p<0,001]). A administração de esmolol esteve associada a redução estatisticamente, mas não clinicamente, significativa da pressão arterial sistólica (144±22 para 115±17 mmHg; p<0,001). O *endpoint* combinado de segurança foi observado em dois (1,5%) dos doentes.
Conclusão: Apesar da utilização sistemática de betabloqueante oral, 14% dos casos necessitaram de esmolol endovenoso para controlo adequado de FC. Pré-medicação combinada de metoprolol oral e esmolol endovenoso quando necessária foi segura e eficaz, e permitiu que 95% dos doentes apresentassem FC <65 bpm no momento da aquisição de imagem.

Introduction

Adequate heart rate (HR) control is paramount for optimal cardiac imaging using single-source 64-slice multidetector computed tomography (64-MSDT).[1–5] For these scanners, HR during image acquisition should be below 65 beats per minute (bpm) and preferably lower than 60 bpm for optimal image quality.[6] However, commonly used pre-medication regimens with oral or intravenous metoprolol are frequently unsatisfactory.[7–9] Side effects, including hypotension and bradycardia, are also points of concern.

Intravenous esmolol, due to its rapid onset and short half-life, has been reported as a valuable option for adequate HR control, either alone or in combination with oral beta-blockers.[10–12]

The aim of the present study is to evaluate the efficacy and safety of an HR reduction protocol using intravenous esmolol as bailout for failed oral metoprolol regimens in patients undergoing coronary computed tomography (CT) angiography (CCTA).

Methods

Study population

Patients undergoing CCTA in a tertiary academic medical center between August 2011 and June 2014 were analyzed. Those presenting in sinus rhythm and without contraindications for beta-blockers were included. All patients had indication for coronary anatomy assessment. Nineteen patients also had associated secondary indications: percutaneous aortic valve implantation (two), paroxysmal atrial fibrillation ablation (sinus rhythm during CCTA) (three), assessment of left ventricular morphology (two), evaluation of valve heart disease (three) or ascending aorta (two), and morphological studies for congenital heart disease (seven).

Patient preparation

Oral metoprolol was not used for patients presenting with HR <60 bpm, who proceeded directly to the CT table. Individuals with baseline HR of 60-65 bpm or >65 bpm received 50 mg or 100 mg oral metoprolol, respectively. An additional dose of 100 mg metoprolol was administered one hour later if HR was still above 65 bpm. After repeated oral metoprolol administration another 60 min interval was allowed. Patients were then moved to the CT table. After sublingual nitrate administration and just after scouting or calcium score image acquisition (Figure 1), an intravenous (IV) bolus of esmolol 1 or 2 mg/kg was administered if HR was >65 bpm or >70 bpm, respectively. A second bolus of esmolol was administered 1 min later if HR remained above 65 bpm using the same dosage.

cont.

Manuscrito 16

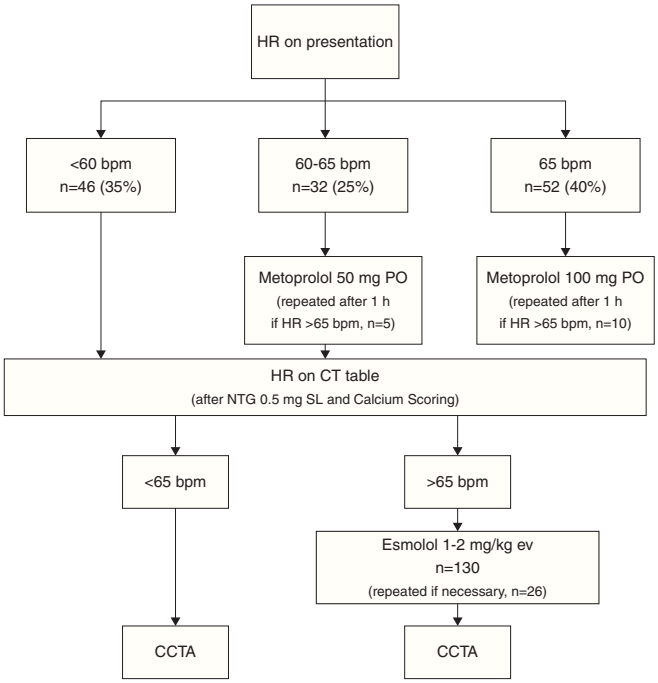

Figure 1 Protocol flowchart. CCTA: cardiac computed tomography angiography; CT: computed tomography; HR: heart rate; IV: intravenous.

Blood pressure and HR were assessed at baseline, in the CT room before and after scanning, and before discharge until systolic blood pressure (SBP) was >100 mmHg and HR >50 bpm or had returned to baseline.

Scan protocol and image reconstruction

A single scanner was used for all cases (LightSpeed VCT XT, GE Healthcare, Milwaukee, USA). First, unenhanced prospective heart rate-triggered axial scanning of the heart was performed for calcium scoring (slice thickness 2.5 mm; voltage 120 kV, tube current 70 mA; 0.35 s partial rotation) just after sublingual nitrate administration. In view of the requirement for esmolol administration (HR on the CT table >65 bpm) a conservative acquisition approach was used and retrospective gating with dose modulation was selected for all these patients. The contrast-enhanced scan was obtained using Visipaque™ (iodixanol) 320 mg injected through a peripheral vein at 5 ml/s followed by a saline bolus chase. The scan parameters used were 0.625 mm collimation, rotation time 350 ms, pitch adjusted to each patient's HR, tube voltage 80-120 mV, and effective mA 100-600.

Estimated effective radiation dose was calculated by applying a factor of 0.014 to the volumetric CT dose. Calcium scoring was included in the total effective radiation dose. Electrocardiographically gated datasets were reconstructed from 40% to 80% of the R-R cycle length in 10% increments.

Endpoints

The primary efficacy endpoint was HR <65 bpm during contrast image acquisition and the secondary efficacy endpoint was HR <60 bpm during contrast image acquisition.

The primary safety endpoint was symptomatic hypotension (SBP <90 mmHg) or bradycardia (heart rate <45 bpm) up to hospital discharge, while the secondary safety endpoints were SBP <90 mmHg or HR <45 bpm (with or without symptoms) up to hospital discharge.

Statistical analysis

The statistical analysis was performed using IBM SPSS Statistics (version 22; IBM SPSS, Chicago, IL). Continuous variables were expressed as mean ± standard deviation or median ± interquartile range. Normality was tested by the Kolmogorov-Smirnov test. Study group characteristics were compared using the Student's t test or the Wilcoxon-Mann-Whitney test for continuous variables, and Pearson's chi-square test or Fisher's exact test for categorical measures, as appropriate.

cont.

Table 1 Clinical characteristics of patients receiving and not receiving esmolol.

	Esmolol	No esmolol
Age (years)	60.9±13.8	61.5±13.7
Male	54.0%	52.9%
Weight (kg)	73.9±13.7	75.4±14.3
BMI (kg/m^2)	27.40±4.42	23.7±2.7
Hypertension	69.6%	73.5%
Diabetes	27.7%	26.5%
Dyslipidemia	68.6%	66.9%
Current smoker	14.5%	12.5%
Previous MI	18.7%	12.5%
Previous PCI	17.9%	14.0%
Previous CABG	16.9%	8.1%
Previous beta-blockers	55.3%	45.6%

BMI: body mass index; CABG: coronary artery bypass grafting; MI: myocardial infarction; PCI: percutaneous coronary intervention.

Results

Of the 947 CCTAs performed (76% of all CCTAs performed in the study period), HR <65 bpm during CCTA acquisition was achieved in 830 cases (86%) using the oral metoprolol regimen alone. Intravenous esmolol was necessary in the other 130 patients (54% male, mean age 60.9±13.8 years and body mass index 27.40±4.42 kg/m^2) (Table 1). Nearly half (53%) of the esmolol-treated patients had been pre-medicated before admission with oral beta-blockers in accordance with the indications of the referring physician.

In about one third (35%) of esmolol-treated patients, HR on presentation was <60 bpm and thus they received no oral metoprolol, but on the CT table HR increased to >65 bpm requiring IV esmolol as per protocol. The remaining 65% (84 patients) had received in-hospital oral metoprolol (mean dose 0.69 mg/kg) according to the predefined study protocol. The mean time between first oral dose of metoprolol and intravenous esmolol administration was 82±39 min. The mean esmolol dose administered was 1.54 mg/kg.

Initial mean HR in esmolol-treated patients was 74±14 bpm, which decreased to 63±9 bpm during CCTA acquisition (p<0.001), corresponding to a significant mean reduction in HR of 15±13% (Figure 2). During CCTA HR variability, defined as (maximum HR - minimum HR)/mean HR, was 6.3±7.1 in esmolol patients.

HR <65 bpm was achieved in 82 of the 130 esmolol-treated patients (63%). Thus, considering the entire CCTA population, the combined metoprolol/esmolol regimen led to a significant increase in the primary efficacy endpoint, from 86% to 95% (p<0.001) (Figure 3).

The secondary efficacy endpoint (HR <60 bpm) was reached in 47 of the 130 esmolol patients (36%).

Four of the esmolol-treated patients (3%) had minimum HR below 45 bpm. Mean time to HR recovery to >60 bpm in these patients was 37.8±32.3 min. During CCTA, HR above 80 bpm was observed in five (4%) patients. Mean HR at discharge was 64±7 bpm (Figure 2) in the esmolol group.

Esmolol use resulted in a significant reduction in mean SBP (143±21 to 115±17 mmHg; p<0.001). In 11 patients (8%) SBP decreased to levels below 90 mmHg. Mean SBP

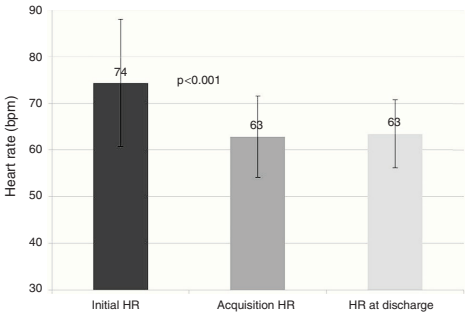

Figure 2 Changes in heart rate after esmolol administration. HR: heart rate.

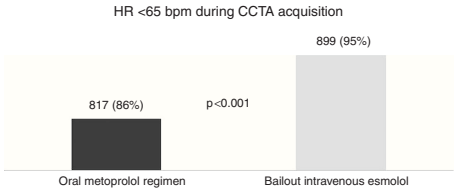

Figure 3 Improvement in primary efficacy endpoint (heart rate <65 bpm) when intravenous esmolol was added to the heart rate reduction protocol. CCTA: cardiac computed tomography angiography; HR: heart rate.

at discharge was 119±18 mmHg (Figure 4A). Initial diastolic blood pressure was 80±12 mmHg, decreasing to 62±11 mmHg after intravenous esmolol (p<0.001). Diastolic blood pressure at discharge was 69±10 mmHg (Figure 4B).

The combined primary safety endpoint (symptomatic hypotension or symptomatic bradycardia) was only observed in two patients (1.5%). Both cases resolved with supine positioning, intravenous fluids and atropine (1 mg) administration, without further complications.

In esmolol-treated patients 113 scans (87%) were of good image quality, 10 (8%) were of moderate quality, and seven (5%) were of poor quality and considered non-diagnostic. In the latter group HR during CCTA was 75±9 bpm and HR variability was 5.3 (42.6).

Retrospective gating with dose modulation was selected for all esmolol-treated patient due to high baseline HR. Mean estimated radiation dose was 9.8±10.6 mSv.

Discussion

HR while scanning should be less than 65 bpm and ideally less than 60 bpm for optimal image quality when a 64-slice MDCT scanner is to be used.[6] Despite this recommendation, in 2007 an American survey showed that there were differences in beta-blocker protocols and that a cutoff higher than 65 bpm was used by 80% of centers.[13]

Metoprolol is the most common beta-blocker agent used to achieve HR control during CCTA. However, due to its low oral bioavailability, variable metabolism and inter-subject

cont.

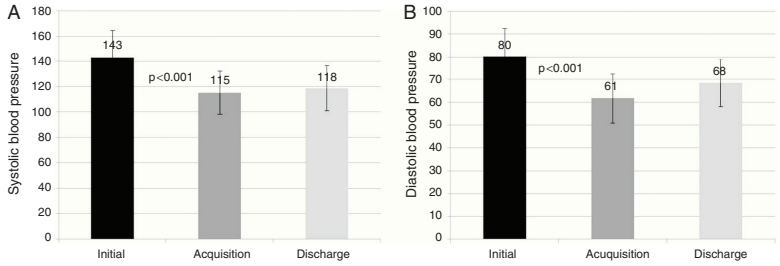

Figure 4 Changes in (A) systolic and (B) diastolic blood pressure after esmolol administration.

variability, the results are often suboptimal. This has led to the use of several alternate regimens including intravenous metoprolol, other beta-blockers such as atenolol, ivabradine, or calcium channel blockers.[14,15] Nevertheless intravenous metoprolol, the most commonly used parenteral beta-blocker, has demonstrated limited efficacy in lowering HR.

Ivabradine has been suggested as an alternative to beta-blockers. Regimens of oral ivabradine proved more effective in reducing HR than oral metoprolol[16] and an intravenous protocol demonstrated efficacy and safety in patients ineligible for intravenous beta-blockers.[17]

Esmolol may be at least as efficacious as intravenous metoprolol to achieve optimal HR.[12] However, to our knowledge there are no studies reporting on esmolol use as bailout when previous oral HR regimens have failed.

In our study the oral metoprolol regimen used enabled 86% of patients to achieve target HR <65 bpm. This percentage is higher than described in previous studies. De Graaf et al. demonstrated optimal beta-blockade in 73% of CCTA patients using oral metoprolol.[18] Intravenous metoprolol, also commonly used, again demonstrated limited efficacy in lowering HR. In a study by Jimenez-Juan et al. only 42% of patients who did not achieve HR <60 bpm with oral metoprolol reached target HR with additional intravenous metoprolol.[19] These findings highlight the need for a more effective protocol for HR control. In addition, the rapid action and short half-life of esmolol make it an attractive drug in this setting. Similarly to data reported by Degertekin et al.,[10] in our study bolus esmolol produced HR below 65 bpm in 63% (82/130) of patients. Thus, the introduction of bailout intravenous esmolol enabled 95% of the entire cohort to be imaged with HR below 65 bpm. The mean HR reduction was 11 bpm, 4% of patients were imaged with HR greater than 80 bpm and only 5% of CCTA exams were considered to be non-diagnostic.

Our study suggests that despite an aggressive beta-blocker strategy, the risk of side effects was relatively small. Only 1.5% of patients had symptomatic hypotension or bradycardia. Wang et al. reported 0.4% incidence of adverse events in a Chinese population treated with intravenous esmolol only.[11] In our cohort, however, esmolol was used on top of oral metoprolol in 64% of cases, which could explain the higher incidence of side effects. Contraindications for beta-blockers are often considered a limitation for CCTA in patients with relatively high HR. Esmolol's short half-life could make it useful for patients who cannot tolerate prolonged beta-blockade.

We reported a higher effective radiation dose than some real-world registries.[20] Unlike these studies, in which both prospective and retrospective acquisition protocols are reported, herein we report on a specific population subset in which only a retrospective acquisition protocol was chosen for all patients (because of high baseline HR). Also, in our registry about 15% of esmolol-treated patients had secondary indications for scanning, such as study for transcatheter aortic valve implantation, in which the scan range is significantly greater.

The introduction of high temporal resolution (83 ms) dual-source CT in clinical practice in 2005 has enabled high image quality diagnostic CCTA studies at increased HR with less dependency on HR lowering agents.[21] However, the latest generation of dual-source scanners has introduced a new scan mode, prospectively ECG-triggered helical data acquisition with very high pitch values. The high pitch enables acquisition with very low radiation exposure (<1 mSv) but low and regular HR is critical for this technique. Consequently, effective HR reduction strategies are yet again pivotal if such very low dose acquisition protocols are to be followed.[22]

Study limitations

This is a retrospective study with inherent limitations including potential selection bias. However, the HR control protocol was prospectively designed and uniformly applied to all eligible patients. Also, this was a single-center experience with a relatively small sample of esmolol-treated patients. Larger multicenter trials using placebo or intravenous metoprolol as active controls will be needed to clearly establish the role of intravenous esmolol in this setting.

Conclusion

Despite optimal use of oral metoprolol for HR control before CCTA, 14% of cases still required intravenous esmolol for HR control. Bailout administration of intravenous esmolol on the CT table was safe and effective and enabled 95% of patients to be imaged with HR below 65 bpm.

cont.

Ethical disclosures

Protection of human and animal subjects. The authors declare that no experiments were performed on humans or animals for this study.

Confidentiality of data. The authors declare that they have followed the protocols of their work center on the publication of patient data.

Right to privacy and informed consent. The authors have obtained the written informed consent of the patients or subjects mentioned in the article. The corresponding author is in possession of this document.

Conflicts of interest

The authors have no conflicts of interest to declare.

References

1. Leschka S, Wildermuth S, Boehm T, et al. Noninvasive coronary angiography with 64-section CT: effect of average heart rate and heart rate variability on image quality. Radiology. 2006;241:378–85.
2. Brodoefel H, Reimann A, Burgstahler C, et al. Noninvasive coronary angiography using 64-slice spiral computed tomography in an unselected patient collective: effect of heart rate, heart rate variability and coronary calcifications on image quality and diagnostic accuracy. Eur J Radiol. 2008;66:134–41.
3. Hoffmann MH, Shi H, Manzke R, et al. Noninvasive coronary angiography with 16-detector row CT: effect of heart rate. Radiology. 2005;234:86–97.
4. Khan M, Cummings KW, Gutierrez FR, et al. Contraindications and side effects of commonly used medications in coronary CT angiography. Int J Cardiovasc Imaging. 2011;27:441–9.
5. Shim SS, Kim Y, Lim SM. Improvement of image quality with beta-blocker premedication on ECG-gated 16-MDCT coronary angiography. AJR Am J Roentgenol. 2005;184:649–54.
6. Schroeder S, Kopp AF, Kuettner A, et al. Influence of heart rate on vessel visibility in noninvasive coronary angiography using new multislice computed tomography: experience in 94 patients. Clin Imaging. 2002;26:106–11.
7. Mahabadi AA, Achenbach S, Burgstahler C, et al., Working group ''Cardiac CT'' of the German Cardiac Society. Safety, efficacy, and indications of beta-adrenergic receptor blockade to reduce heart rate prior to coronary CT angiography. Radiology. 2010;257:614–23.
8. Shapiro MD, Pena AJ, Nichols JH, et al. Efficacy of pre-scan beta-blockade and impact of heart rate on image quality in patients undergoing coronary multidetector computed tomography angiography. Eur J Radiol. 2008;66:37–41.
9. Pannu HK, Sullivan C, Lai S, et al. Evaluation of the effectiveness of oral beta-blockade in patients for coronary computed tomographic angiography. J Comput Assist Tomogr. 2008;32:247–51.
10. Degertekin M, Gemici G, Kaya Z, et al. Safety and efficacy of patient preparation with intravenous esmolol before 64-slice computed tomography coronary angiography. Coron Artery Dis. 2008;19:33–6.
11. Wang JD, Zhang HW, Xin Q, et al. Safety and efficacy of intravenous esmolol before prospective electrocardiogram-triggered high-pitch spiral acquisition for computed tomography coronary angiography. J Geriatr Cardiol. 2014;11:39–43.
12. Maurovich-Horvat P, Károlyi M, Horváth T, et al. Esmolol is noninferior to metoprolol in achieving a target heart rate of 65 beats/min in patients referred to coronary CT angiography: a randomized controlled clinical trial. J Cardiovasc Comput Tomogr. 2015;9:139–45.
13. Johnson PT, Eng J, Pannu HK, et al. 64-MDCT angiography of the coronary arteries: nationwide survey of patient preparation practice. AJR Am J Roentgenol. 2008;190:743–7.
14. Raju VM, Gosling OE, Morgan-Hughes G, et al. High-dose intravenous metoprolol usage for reducing heart rate at CT coronary angiography: efficacy and safety. Clin Radiol. 2014;69:739–44.
15. Maffei E, Palumbo AA, Martini C, et al. ''In-house'' pharmacological management for computed tomography coronary angiography: heart rate reduction, timing and safety of different drugs used during patient preparation. Eur Radiol. 2009;19:2931–40.
16. Adile KK, Kapoor A, Jain SK, et al. Safety and efficacy of oral ivabradine as a heart rate-reducing agent in patients undergoing CT coronary angiography. Br J Radiol. 2012;85:e424–8.
17. Cademartiri F, Garot J, Tendera M, et al. Intravenous ivabradine for control of heart rate during coronary CT angiography: a randomized, double-blind, placebo-controlled trial. J Cardiovasc Comput Tomogr. 2015;9:286–94.
18. de Graaf FR, Schuijf JD, van Velzen JE, et al. Evaluation of contraindications and efficacy of oral beta blockade before computed tomographic coronary angiography. Am J Cardiol. 2010;105:767–72.
19. Jiménez-Juan L, Nguyen ET, Wintersperger BJ, et al. Failed heart rate control with oral metoprolol prior to coronary CT angiography: effect of additional intravenous metoprolol on heart rate, image quality and radiation dose. Int J Cardiovasc Imaging. 2013;29:199–206.
20. de Araújo Gonçalves P, Jerónimo Sousa P, Calé R, et al. Effective radiation dose of three diagnostic tests in cardiology: single photon emission computed tomography, invasive coronary angiography and cardiac computed tomography angiography. Rev Port Cardiol. 2013;32:981–6.
21. Fang XM, Chen HW, Hu XY, et al. Dual-source CT coronary angiography without heart rate or rhythm control in comparison with conventional coronary angiography. Int J Cardiovasc Imaging. 2010;26:323–31.
22. Achenbach S, Marwan M, Ropers D, et al. Coronary computed tomography angiography with a consistent dose below 1 mSv using prospectively electrocardiogram-triggered high-pitch spiral acquisition. Eur Heart J. 2010;31:340–6.

MANUSCRITO 17

Effective radiation dose of three diagnostic tests in cardiology: single photon emission computed tomography, invasive coronary angiography and cardiac computed tomography angiography.

de Araujo Goncalves, P., Jeronimo Sousa, P., Cale, R., **Marques**, **H**., Borges dos Santos, M., Dias, A., Dores, H., Carvalho, M. S., Ventosa, A., Martins, T., Campante Teles, R., Almeida, M., and Mendes, M.,

Rev Port Cardiol, 2013
32(12): p. 981-6

Manuscrito 17

Rev Port Cardiol. 2013;32(12):981–986

Revista Portuguesa de Cardiologia
Portuguese Journal of Cardiology
www.revportcardiol.org

ORIGINAL ARTICLE

Effective radiation dose of three diagnostic tests in cardiology: Single photon emission computed tomography, invasive coronary angiography and cardiac computed tomography angiography

Pedro de Araújo Gonçalves[a,b,c,*], Pedro Jerónimo Sousa[a,c], Rita Calé[d], Hugo Marques[e], Miguel Borges dos Santos[a], André Dias[f], Hélder Dores[a], Maria Salomé Carvalho[a], António Ventosa[a], Teresa Martins[f], Rui Campante Teles[a], Manuel Almeida[a], Miguel Mendes[a]

[a] *Serviço de Cardiologia, Hospital de Santa Cruz – Centro Hospitalar de Lisboa Ocidental, Lisboa, Portugal*
[b] *CEDOC – Chronic Diseases Research Center – Faculdade de Ciências Médicas-UNL, Lisboa, Portugal*
[c] *Centro Cardiovascular, Hospital da Luz, Lisboa, Portugal*
[d] *Serviço de Cardiologia, Hospital Garcia de Orta, Almada, Portugal*
[e] *Centro de Imagiologia, Hospital da Luz, Lisboa, Portugal*
[f] *Serviço de Medicina Nuclear, Hospital de Santa Cruz – Centro Hospitalar de Lisboa Ocidental, Lisboa, Portugal*

Received 30 January 2013; accepted 29 May 2013
Available online 25 November 2013

KEYWORDS
Ionizing radiation;
Single photon emission computed tomography;
Invasive coronary angiography;
Cardiac computed tomography;
Obesity

Abstract
Introduction: Diagnostic tests that use ionizing radiation play a central role in cardiology and their use has grown in recent years, leading to increasing concerns about their potential stochastic effects.

The aims of this study were to compare the radiation dose of three diagnostic tests: single photon emission computed tomography (SPECT), invasive coronary angiography (ICA) and cardiac computed tomography (cardiac CT) and their evolution over time, and to assess the influence of body mass index on radiation dose.
Methods: We assessed consecutive patients included in three prospective registries (SPECT, ICA and cardiac CT) over a period of two years. Radiation dose was converted to mSv and compared between the three registries. Differences over time were evaluated by comparing the first with the fourth semester.
Results: A total of 6196 exams were evaluated: 35% SPECT, 53% ICA and 22% cardiac CT. Mean radiation dose was 10.7±1.2 mSv for SPECT, 8.1±6.4 mSv for ICA, and 5.4±3.8 mSv for cardiac CT ($p<0.001$ for all). With regard to the radiation dose over time, there was a very small

* Corresponding author.
E-mail address: paraujogoncalves@yahoo.co.uk (P. de Araújo Gonçalves).

http://dx.doi.org/10.1016/j.repce.2013.05.010

cont.

Manuscrito 17

reduction in SPECT (10.7 to 10.5 mSv, p=0.004), a significant increase (25%) in ICA (7.0 to 8.8 mSv; p<0.001), and a significant reduction (29%) in cardiac CT (6.5 to 4.6 mSv, p<0.001). Obesity was associated with a significantly higher radiation dose in all three exams.

Conclusions: Cardiac CT had a lower mean effective radiation dose than invasive coronary angiography, which in turn had a lower mean effective dose than SPECT.

There was a significant increase in radiation doses in the ICA registry and a significant decrease in the cardiac CT registry over time.

PALAVRAS-CHAVE
Radiação;
Cintigrafia de perfusão miocárdica;
Coronariografia invasiva;
Tomografia computorizada cardíaca;
Obesidade

Dose efetiva de radiação de três exames de diagnóstico em cardiologia: cintigrafia de perfusão miocárdica, coronariografia invasiva e tomografia computorizada cardíaca

Resumo

Introdução: Os exames diagnósticos que usam radiação ionizante têm um papel central na cardiologia e a par do seu uso crescente, tem aumentado a preocupação pelos seus potenciais efeitos estocásticos.

Os objetivos deste estudo foram: 1) Comparar a dose de radiação de três exames: Cintigrafia de perfusão miocárdica (SPECT), coronariografia invasiva (CAT) e tomografia computorizada cardíaca (AngioTC) e a sua evolução temporal. 2) Avaliar o impacto do índice de massa corporal na dose de radiação.

Métodos: Doentes consecutivos incluídos em três registos prospetivos (SPECT, CAT e AngioTC) durante dois anos. A dose de radiação foi convertida a mSv e comparada entre os três registos. A evolução temporal foi avaliada por comparação do 1.° e 4.° semestres.

Resultados: Foram avaliados 6196 exames: 35% SPECT, 53% CAT e 22% AngioTC. A dose de radiação foi: 10,7 ± 1,2 mSv para o SPECT; 8,1 ± 6,4 mSv para o CAT; 5,4 ± 3,8 mSv para a AngioTC (p < 0,001 todas comparações).

Evolução temporal da dose de radiação: redução muito ligeira no SPECT (10,7 para 10,5 mSv; p = 0,004); aumento significativo (25%) no CAT (7,0 para 8,8 mSv; p < 0,001); redução significativa (29%) na AngioTC (6,5 para 4,6 mSv; p < 0,001). A obesidade associou-se a níveis de radiação significativamente mais elevados nos três exames.

Conclusão: O exame associado a uma menor dose de radiação foi a AngioTC, seguida do CAT que, por sua vez, foi menor que a do SPECT. Houve um aumento significativo da dose de radiação no registo CAT e uma redução significativa no registo da AngioTC ao longo do tempo.

List of abbreviations

BMI	Body mass index
CAD	coronary artery disease
CT	computed tomography
ICA	invasive coronary angiography
SPECT	single photon emission computed tomography

Introduction

In recent years, the development of imaging techniques using ionizing radiation has resulted in considerable progress in the diagnosis and treatment of heart disease. Three commonly used diagnostic modalities that involve ionizing radiation are used for assessing patients with possible coronary artery disease (CAD): single photon emission computed tomography (SPECT), cardiac computed tomography (cardiac CT) and invasive coronary angiography (ICA), the latter being considered the gold standard for the diagnosis of CAD.[1]

Different radiation doses have been reported for each of these exams, ranging from 5 to 10 mSv for ICA, 6 to 15 mSv for SPECT, and 4 to 21 mSv for cardiac CT.[2–5] With more frequent use of these exams, there have been growing concerns about the radiation's potential secondary effects, especially the stochastic effects of high cumulative doses over time.[6,7]

We have previously reported on the effective radiation dose associated with cardiac CT in a single-center registry, documenting a significant decrease in dose over time, and were able to identify the predictors of higher dose.[8]

New scanners and acquisition protocols have recently been developed which lead to significant reductions in radiation dose associated with cardiac CT.[9,10]

The aims of this study were to evaluate and compare the radiation dose used in three diagnostic tests – SPECT, ICA and cardiac CT – and their evolution over time, and to assess the influence of body mass index on radiation dose.

cont.

Manuscrito 17

Table 1 Demographic and clinical characteristics of the study population.

	Cardiac CT (n=1344)	ICA (n=3267)	SPECT (n=1585)
Age (years, mean ± SD)	59±12	66±12	64±9
Male (%)	60%	61%	63%
BMI (kg/m^2)	27.3±4.3	27.3±4.2	27.5±4.4
Diabetes (%)	16%	29%	N/A
Hypertension (%)	57%	72%	N/A
Dyslipidemia (%)	54%	57%	N/A
Smoking (%)	27%	31%	N/A
Previous MI (%)	3%	17%	N/A
Previous PCI (%)	7%	18%	N/A
Previous CABG (%)	3%	7%	N/A

Values are means (SD) or percentages. BMI: body mass index; CABG: coronary artery bypass grafting; CT: computed tomography; ICA: invasive coronary angiography; MI: myocardial infarction; N/A: not available; PCI: percutaneous coronary intervention; SPECT: single photon emission computed tomography.

Methods

From three prospective registries of SPECT, ICA and cardiac CT, we selected for this analysis the exams performed during a two-year period (October 1, 2008 to September 30, 2010) in which the indication was assessment of possible CAD.

The exams were performed with an SMV DST-XL gamma camera using 99m Tc-tetrofosmin with stress/rest or rest/stress protocols (SPECT registry), a Siemens Coroskop TOP/ARTIS dFC system (ICA registry), and a Siemens Somatom Definition dual-source scanner (cardiac CT registry). The effective radiation dose was converted to mSv in accordance with current literature and the manufacturer's product information and compared between the registries. Briefly, a factor of 0.014 mSv/Gy cm was used for the conversion of cardiac CT dose-length product,[9,11] a factor of 0.183 mSv/Gy cm^2 was used for the conversion of ICA dose-area product,[12,13] and factors of 0.0060 mSv/MBq^{-1} (after exercise) and 0.0071 mSv/MBq^{-1} (at rest) were used for the conversion of injected activity in SPECT.[14–16] To evaluate the evolution of radiation doses over time, the study period was divided into four semesters according to the date of the exam and effective radiation dose was compared between the first and last semesters in each registry. All prospectively collected variables in the respective registries were analyzed, looking for predictors of dose change over time.

Statistical analysis

Continuous variables are presented as mean ± standard deviation (unless otherwise specified), and categorical variables as number (n) or frequency (%).

Continuous variables were analyzed using the Mann–Whitney or Kruskal–Wallis nonparametric tests. The chi-square test was used to assess differences in frequencies.

Statistical significance was accepted for two-sided p values <0.05.

The statistical analysis was performed using SPSS Statistics 17.0 for Windows.

Results

During the two-year period of this analysis, 6196 exams were performed: 3267 (52.7%) ICA, 1585 (25.6%) SPECT and 1344 (21.7%) cardiac CT. The demographic and clinical characteristics of the study population are presented in Table 1.

Mean effective radiation dose was 8.2±5.6 mSv for the whole population, 10.7±1.2 mSv for SPECT, 8.1±6.4 mSv for ICA and 5.4±3.8 mSv for cardiac CT (p<0.001 for all comparisons, Figure 1).

Division of the study period into semesters showed that there was a small but significant reduction in mean effective radiation dose over time for SPECT (10.7 to 10.5 mSv; p<0.01). In cardiac CT there was a significant 29% decrease in mean effective radiation dose (6.5 to 4.6 mSv, p<0.001) and in ICA a significant 25% increase (7.0 to 8.8 mSv; p<0.001) (Table 2 and Figure 2).

The factors associated with the 25% increase in mean effective radiation dose with ICA from the first to the fourth semester were the higher proportions of positive exams, radial vascular access and exams performed by fellows in

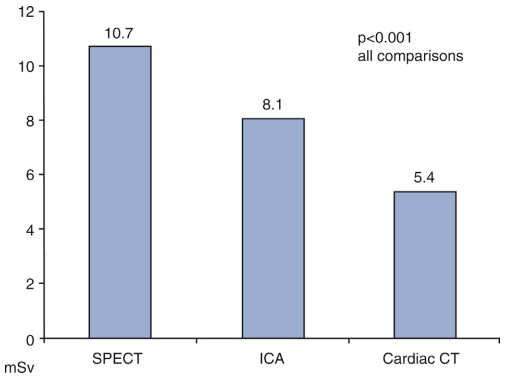

Figure 1 Mean effective radiation dose used in each exam studied. CT: computed tomography; ICA: invasive coronary angiography; SPECT: single photon emission computed tomography.

cont.

Table 2 Mean effective radiation dose for each exam over the four semesters.

	1st semester	2nd semester	3rd semester	4th semester	p (1st vs. 4th)
SPECT	10.7 ± 1.1	10.7 ± 1.4	10.7 ± 1.3	10.5 ± 0.9	0.004
ICA	7.0 ± 6.0	7.6 ± 5.6	9.0 ± 6.9	8.7 ± 6.9	<0.001
Cardiac CT	6.5 ± 3.7	6.2 ± 4.2	5.0 ± 4.1	4.6 ± 3.0	<0.001

CT: computed tomography; ICA: invasive coronary angiography; SPECT: single photon emission computed tomography.

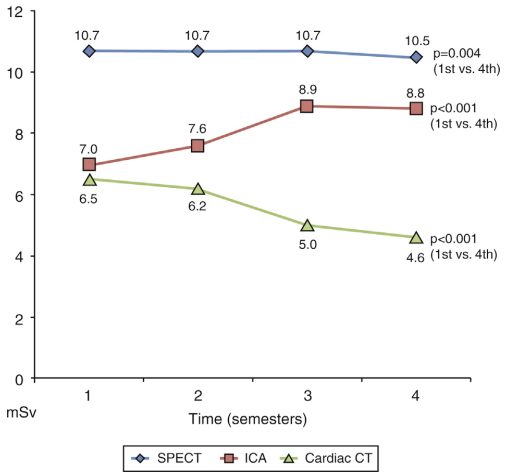

Figure 2 Time trends in mean effective radiation dose used in each exam. CT: computed tomography; ICA: invasive coronary angiography; SPECT: single photon emission computed tomography.

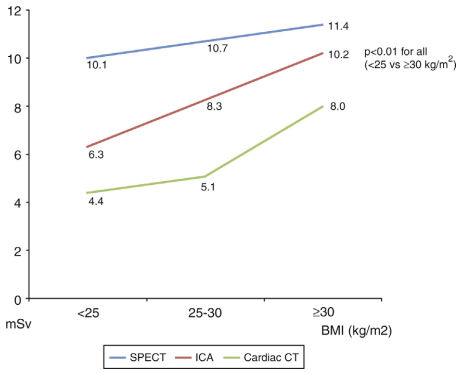

Figure 3 Mean effective radiation doses for each exam and different body mass index classes. BMI: body mass index; CT: computed tomography; ICA: invasive coronary angiography; SPECT: single photon emission computed tomography.

training (Table 3). In the first semester 39% of ICA progressed to percutaneous coronary intervention, while in the fourth semester this proportion increased to 42% (p<0.001). Regarding vascular access, in the first semester only 1% of ICA were performed by radial access, which increased to 46% in the fourth semester. In our population, the use of radial vascular access was associated with a mean increase of 15% in effective radiation dose (from 7.8 mSv with femoral access to 9.0 with radial access, p<0.001). Finally, the proportion of exams performed by trainee operators increased from 26% in the first semester to 52% in the fourth. In this registry, when the exam was performed by a trainee operator there was a mean increase of 29% in effective radiation dose (from 7.3 mSv with a senior operator to 9.4 mSv with a trainee operator, p<0.001).

The only variable associated with the decrease in effective radiation dose for cardiac CT was the use of prospective (step-and-shoot) acquisition: the use of a prospective acquisition protocol was associated with a decrease of 60% in effective radiation dose. In the first semester no exams were performed with this protocol, while in the fourth semester 45% were acquired prospectively (Table 3).

The influence of body mass index on mean effective radiation dose was also evaluated. There was a significantly higher dose in obese patients (BMI ≥30 kg/m^2) compared to overweight patients, which in turn was higher that in patients with normal weight (BMI <25 kg/m^2) (Figure 3).

Discussion

In this analysis, we found significantly different effective radiation doses associated with common diagnostic tests used in cardiology. The dose was highest for SPECT, followed by ICA and lowest for cardiac CT. Furthermore, we found

Table 3 Variables associated with increase in ICA radiation dose and decrease in cardiac CT radiation dose.

		ΔmSv	1st semester	4th semester
ICA	Proportion of patients undergoing PCI	ND	39%	42%
	Exams performed by fellows in training	↑29%	26%	52%
	Proportion of radial vascular access	↑15%	1%	46%
Cardiac CT	Prospective acquisition	↓60%	0%	45%

CT: computed tomography; ICA: invasive coronary angiography.

cont.

some time trends in the mean effective radiation dose associated with ICA and cardiac CT related to particular clinical and procedural methodologies.

The biological effects of ionizing radiation are related to the cumulative effective dose, and doses above 100 mSv have been linked to stochastic effects including the development of cancer, while the effects of lower radiation levels, common in diagnostic X-ray imaging, are much less clear.[4,17] Although other theoretical models based on dose-threshold and hormetic effects have been proposed, the more conservative linear no-threshold model, which assumes that no level of radiation is without risk, is widely accepted.[4,17]

On this basis, procedures that use ionizing radiation should be performed in accordance with the ''as low as reasonably achievable'' philosophy, and physicians ordering and performing cardiac imaging diagnostic tests should be familiar with the associated radiation doses and with ways in which they can be minimized.

The mean effective radiation dose we found for each exam is in agreement with previous studies.[3,4,6,18] Furthermore, we confirmed that certain variables influence the effective radiation dose delivered by these exams. For ICA, the effective radiation dose increased with the use of radial access and with less experienced operators, which is in line with published data.[13,19] The higher radiation dose in the ICA registry over time was also associated with a higher proportion of positive exams; although we did not quantify the difference between positive and negative ICA, we can assume that positive tests needed more cine angiograms of the coronary arteries, with a consequent increase in the radiation dose used.

For cardiac CT, the introduction and increasingly frequent use of a prospective protocol during the study period was associated in our experience with a significant decrease in the effective radiation dose for this exam, as has been demonstrated by other authors.[20–22] Finally, for SPECT, the dose change over time was very small, which is to be expected since there were no changes in protocol during the study period.

It is worth noting that during the same period, doses associated with stress-only and rest-only SPECT studies were significantly lower (with mean effective doses of 2.3±0.9 mSv and 5.8±1.0 mSv, respectively) but they were not considered for the purpose of this study, and the small number of patients involved (n=49 and n=63, respectively) would not have had a significant impact on the overall SPECT radiation dose.

Mean effective radiation doses were significantly higher for obese patients in all the exams analyzed. This was especially true for cardiac CT and ICA, with an almost two-fold increase in radiation dose compared to their normal-weight counterparts. In the SPECT registry, the effect of BMI was less pronounced. This should be taken in consideration when selecting the appropriate diagnostic exam, especially for those at higher risk from radiation exposure, like women and younger patients.[23] In line with this, particular attention should be paid to cardiac CT dose, since patients in our registry undergoing cardiac CT were significantly younger than those in the ICA and SPECT registries.

Although the present study focuses on comparison of the radiation dose between three different diagnostic exams, other features should be taken into account when comparing different imaging modalities. As cardiac CT and ICA require the administration of iodinated contrast, care should be taken in the presence of impaired renal function or history of allergies; likewise, the probability of CAD is also an important factor, as SPECT and ICA are more appropriate for patients with higher probability of CAD.[24,25] Thus, all these features (radiation dose, need for iodinated contrast and CAD probability) should be taken into consideration when selecting the most appropriate exam for each patient.

Conclusions

In these registries of diagnostic tests commonly used in cardiology, the mean effective radiation dose used in cardiac CT was lower than that used in ICA, which in turn was lower than the doses used in SPECT. There was a significant increase over time in the mean effective radiation dose associated with ICA, mainly related to the increased use of radial access, and a decrease in cardiac CT doses as a consequence of the implementation of a prospective protocol. Obesity was associated with a significantly higher radiation dose in all three exams.

Ethical disclosures

Protection of human and animal subjects. The authors declare that the procedures followed were in accordance with the regulations of the relevant clinical research ethics committee and with those of the Code of Ethics of the World Medical Association (Declaration of Helsinki).

Confidentiality of data. The authors declare that they have followed the protocols of their work center on the publication of patient data and that all the patients included in the study received sufficient information and gave their written informed consent to participate in the study.

Right to privacy and informed consent. The authors have obtained the written informed consent of the patients or subjects mentioned in the article. The corresponding author is in possession of this document.

Conflicts of interest

The authors have no conflicts of interest to declare.

References

1. Task Force on Myocardial Revascularization of the European Society of Cardiology (ESC), the European Association for Cardio-Thoracic Surgery (EACTS), European Association for Percutaneous Cardiovascular Intervention (EAPCI), Wijns W, et al. Guidelines on myocardial revascularization. Eur Heart J. 2010;31:2501–55.
2. Hirshfeld Jr JW, Balter S, Brinker JA, et al. ACCF/AHA/HRS/SCAI clinical competence statement on physician knowledge to optimize patient safety and image quality in fluoroscopically guided invasive cardiovascular procedures: a report of the American College of Cardiology Foundation/American Heart Association/American College of Physicians Task Force on Clinical Competence and Training. Circulation. 2005;111:511–32.

cont.

3. Einstein AJ, Moser KW, Thompson RC. Radiation dose to patients from cardiac diagnostic imaging. Circulation. 2007;116:1290–305.
4. Gerber TC, Carr JJ, Arai AE, et al. Ionizing radiation in cardiac imaging: a science advisory from the American Heart Association Committee on Cardiac Imaging of the Council on Clinical Cardiology and Committee on Cardiovascular Imaging and Intervention of the Council on Cardiovascular Radiology and Intervention. Circulation. 2009;119:1056–65.
5. Fazel R, Shaw LJ. Radiation exposure from radionuclide myocardial perfusion imaging: concerns and solutions. J Nucl Cardiol. 2011;18:562–5.
6. Fazel R, Krumholz HM, Wang Y, et al. Exposure to low-dose ionizing radiation from medical imaging procedures. N Engl J Med. 2009;361:849–57.
7. Almeida AG. Cardiac computed tomography and radiation: balancing benefit and risk. Rev Port Cardiol. 2010;29: 1677–82.
8. Sousa PJ, Goncalves PA, Marques H, et al. Radiation in cardiac CT: predictors of higher dose and its reduction over time. Rev Port Cardiol. 2010;29:1655–65.
9. Achenbach S, Marwan M, Ropers D, et al. Coronary computed tomography angiography with a consistent dose below 1 mSv using prospectively electrocardiogram-triggered high-pitch spiral acquisition. Eur Heart J. 2010;31:340–6.
10. Duarte R, Bettencourt N, Costa JC, et al. Coronary computed tomography angiography in a single cardiac cycle with a mean radiation dose of approximately 1 mSv: initial experience. Rev Port Cardiol. 2010;29:1667–76.
11. Hausleiter J, Meyer T, Hermann F, et al. Estimated radiation dose associated with cardiac CT angiography. JAMA. 2009;301:500–7.
12. Betsou S, Efstathopoulos EP, Katritsis D, et al. Patient radiation doses during cardiac catheterization procedures. Br J Radiol. 1998;71:634–9.
13. Neill J, Douglas H, Richardson G, et al. Comparison of radiation dose and the effect of operator experience in femoral and radial arterial access for coronary procedures. Am J Cardiol. 2010;106:936–40.
14. Cerqueira MD, Allman KC, Ficaro EP, et al. Recommendations for reducing radiation exposure in myocardial perfusion imaging. J Nucl Cardiol. 2010;17:709–18.
15. Hesse B, Tagil K, Cuocolo A, et al. EANM/ESC procedural guidelines for myocardial perfusion imaging in nuclear cardiology. Eur J Nucl Med Mol Imaging. 2005;32:855–97.
16. Myoview package insert. European Prescribing Information. Available at http://www.gehealthcare.com/euen/molecular-imaging/congress/pdf/myoview-pi.pdf
17. Einstein AJ. Effects of radiation exposure from cardiac imaging: how good are the data? J Am Coll Cardiol. 2012;59:553–65.
18. Kaufmann PA, Knuuti J. Ionizing radiation risks of cardiac imaging: estimates of the immeasurable. Eur Heart J. 2011;32:269–71.
19. Jolly SS, Yusuf S, Cairns J, et al. Radial versus femoral access for coronary angiography and intervention in patients with acute coronary syndromes (RIVAL): a randomised, parallel group, multicentre trial. Lancet. 2011;377:1409–20.
20. Gopal A, Mao SS, Karlsberg D, et al. Radiation reduction with prospective ECG-triggering acquisition using 64-multidetector computed tomographic angiography. Int J Cardiovasc Imaging. 2009;25:405–16.
21. Stolzmann P, Leschka S, Scheffel H, et al. Dual-source CT in step-and-shoot mode: noninvasive coronary angiography with low radiation dose. Radiology. 2008;249:71–80.
22. Ferreira AM, Lopes R, Correia Mda G, et al. Low-dose cardiac CT. Rev Port Cardiol. 2010;29:459–62.
23. Einstein AJ, Henzlova MJ, Rajagopalan S. Estimating risk of cancer associated with radiation exposure from 64-slice computed tomography coronary angiography. JAMA. 2007;298:317–23.
24. Taylor AJ, Cerqueira M, Hodgson JM, et al. ACCF/SCCT/ACR/AHA/ASE/ASNC/NASCI/SCAI/SCMR 2010 appropriate use criteria for cardiac computed tomography. A report of the American College of Cardiology Foundation Appropriate Use Criteria Task Force, the Society of Cardiovascular Computed Tomography, the American College of Radiology, the American Heart Association, the American Society of Echocardiography, the American Society of Nuclear Cardiology, the North American Society for Cardiovascular Imaging, the Society for Cardiovascular Angiography and Interventions, and the Society for Cardiovascular Magnetic Resonance. J Am Coll Cardiol. 2010;56:1864–94.
25. NICE clinical guideline 95. Chest pain of recent onset: assessment and diagnosis of recent onset chest pain or discomfort of suspected cardiac origin. Available from: http://www.nice.org.uk/guidance/CG95

MANUSCRITO 18

Radiation in cardiac CT:
predictors of higher dose and its reduction over time.

Sousa, P.J., Goncalves, P. A., **Marques**, **H**., Raposo, L., Cale, R., Brito, J., Gaspar, A., Machado, F. P., and Roquette, J.

Rev Port Cardiol, 2010
29(11): p. 1655-65

Manuscrito 18

ARTIGOS ORIGINAIS

Radiação na AngioTC cardíaca: preditores de maior dose utilizada e sua redução ao longo do tempo [115]

PEDRO JERÓNIMO SOUSA[1], PEDRO ARAÚJO GONÇALVES[1], HUGO MARQUES[2], LUÍS RAPOSO[1], RITA CALÉ[1], JOÃO BRITO[1], AUGUSTO GASPAR[2], FRANCISCO PEREIRA MACHADO[11], JOSÉ ROQUETTE[1]

[1] Centro Cardiovascular, Hospital da Luz, Lisboa, Portugal
[2] Centro de Imagiologia, Hospital da Luz, Lisboa, Portugal

Rev Port Cardiol 2010; 29 (11): 1655-1665

RESUMO

A tomografia computorizada cardíaca é um método não invasivo de obter informação da anatomia cardíaca, permitindo avaliar a doença coronária. No entanto, uma das limitações que tem vindo a ser apontada a este exame é a utilização de radiação. O objectivo deste trabalho foi avaliar a variação da dose de radiação ao longo do tempo e identificar variáveis que se associassem ao seu aumento.

Foi analisado um registo prospectivo de 643 doentes submetidos a TC cardíaca com 64 cortes e dupla ampola (Dual source CT - Somaton Definition®, Siemens-medical) durante os anos de 2007 e 2008.

A amostra foi dividida em quartis, segundo a ordem cronológica de realização dos exames. Verificou-se uma redução progressiva da mediana da dose de radiação ao longo dos quartis analisados [Q1: 8,9 (5,9-14,1), Q2: 6,6 (5,5-10,7), Q3: 6,4 (5,3-8,7), Q4: 6,1 (5,2-7,9)], significativa quando o primeiro quartil foi comparado com os restantes (p<0,05). Paralelamente a este decréscimo, verificou-se uma utilização progressivamente maior de uma voltagem da ampola de 100Kv (p<0,001). Os predictores

Radiation in cardiac CT: predictors of higher dose and its reduction over time

ABSTRACT

Introduction: Cardiac CT provides noninvasive information on cardiac anatomy, particularly in coronary artery disease. However, exposure to radiation has been identified as a limitation of this exam. The aim of this study was to evaluate variations in radiation dose over time and to identify variables associated with use of higher radiation doses.

Methods: A prospective registry of 643 patients who underwent 64-slice dual source cardiac CT scan (Dual souce CT - Somaton Definition®, Siemens-Medical) during 2007 and 2008 was analyzed.

Results: The sample was divided into quartiles according to the chronological order of the exams. There was a progressive reduction in median radiation dose in the quartiles analyzed (Q1: 8.9 [5.9-14.1], Q2: 6.6 [5.5-10.7], Q3: 6.4 [5.3-8.7], Q4: 6.1 [5.2-7.9] mSv), significant when the first quartile was compared with the others

Recebido para publicação: Março de 2010 • Aceite para publicação: Julho de 2010
Received for publication: March 2010 • Accepted for publication: July 2010

cont.

Manuscrito 18

Rev Port Cardiol
Vol. 29 Novembro 10 / November 10

de uma dose de radiação alta foram: IMC>32, cirurgia cardíaca prévia, presença de fibrilhação auricular na aquisição, maior tempo de aquisição e o uso 120 kV como voltagem da ampola. Quando pelo menos uma destas características estava presente (um terço da população), a dose de radiação foi significativamente superior [12,1 (9,5-14,8) *versus* 5,7 (5,0-6,7) mSv. p<0,001].

Palavras Chave:
AngioTC Cardíaco; Radiação

(p<0.05). Along with this reduction, there was a progressive increase in the use of a tube voltage of 100 kV (p<0.001).
Predictors of a higher radiation dose were higher body mass index, previous cardiac surgery, atrial fibrillation during acquisition, longer acquisition time and use of a tube voltage of 120 kV. When one or more of these variables were present (one third of the population), the radiation dose was significant higher (12.1 [9.5-14.8] vs. 5.7 [5.0-6.7] mSv, p<0.001).

Key words
Cardiac CT; Radiation

INTRODUÇÃO

A coronariografia invasiva é considerada o *gold standard* para o diagnóstico de doença coronária. Contudo, exames não invasivos, tais como a prova de esforço, a cintigrafia de perfusão miocárdica, o ecocardiograma de sobrecarga, a tomografia computorizada e a ressonância magnética nuclear cardíaca são uma alternativa na avaliação da anatomia e fisiologia cardíacas.

Nas três últimas décadas, a tomografia computorizada (TC) tem demonstrado um papel importante na avaliação diagnóstica. A era moderna da angiotomografia computorizada cardíaca (AngioTC cardíaca) iniciou-se aproximadamente em 1997, com a introdução na prática clínica dos sistemas helicoidais de corte único[1]. Com as gerações sucessivas de aparelhos de TC, até aos sistemas de 64 cortes, verificou-se uma melhoria progressiva da resolução espacial e temporal, bem como uma diminuição importante do tempo de aquisição. Assim, desde 2004, com a introdução da TC de 64 cortes na prática clínica, a coronariografia não invasiva por TC cardíaca tem despertado interesse particular, nomeadamente pela sua utilidade na exclusão da presença de doença coronária, fruto do seu elevado valor preditivo negativo[2] (*Figura 1*).

INTRODUCTION

Invasive coronary angiography is considered the gold standard for diagnosis of coronary artery disease. However, noninvasive exams such as exercise testing, myocardial perfusion scintigraphy, stress echocardiography, computed tomography (CT) and cardiac magnetic resonance imaging are alternative methods of assessing cardiac anatomy and physiology.

Over the last thirty years, CT has come to play an important role in diagnostic evaluation. The modern era of CT angiography began around 1997 with the introduction into clinical practice of single-slice spiral systems[1]. The development of new generations of CT scanners led to progressive improvements in spatial and temporal resolution and significant reductions in acquisition time. Since the introduction of 64-slice systems in 2004, noninvasive coronary CT angiography has aroused particular interest for its ability to exclude the presence of coronary artery disease due to its high negative predictive value[2] (*Figure 1*).

In parallel with these technological advances, the radiation doses used to acquire CT images has increased in the most recent systems, with exposure rising from 5-8 mSv (four-slice) to 15-20 mSv (64-slice)[3]. However, it is hoped that the better image quality of the

cont.

Manuscrito 18

Pedro Jerónimo Sousa, et al.
Rev Port Cardiol 2010; 29: 1655-1665

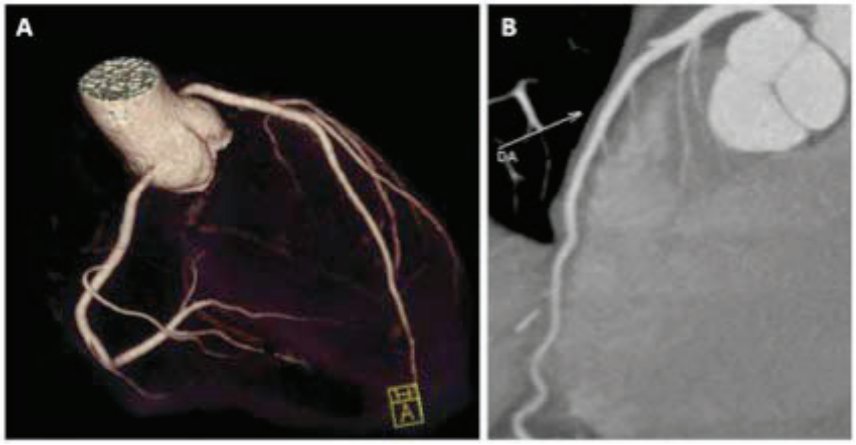

Figura 1. Coronariografia virtual (A) e reconstrução multiplantar (B) em exame com boa qualidade de imagem documentando coronárias sem placas significativas

Figure 1. Virtual coronary angiography (A) and multiplane reconstruction (B) in good-quality cardiac CT images showing coronaries without significant plaques

Paralelamente a esta evolução tecnológica, a dose de radiação utilizada na aquisição de imagens de TC tem vindo a aumentar com os aparelhos mais recentes. A exposição estimada aumentou de 5-8 mSv (TC de quatro cortes) para 15-20 mSv (TC de 64 cortes)[3]. Com os sistemas de última geração, em particular com os aparelhos de dupla ampola e os de 320 cortes, espera-se que a melhoria da qualidade de imagem seja acompanhada por uma redução da dose de radiação.

Existe igualmente uma grande variabilidade nesta dose entre os vários centros e os vários aparelhos, com medianas de doses de radiação que variam entre 4,9 e 29,1 mSv[4].

No entanto, esta dose de radiação elevada, apontada como uma limitação para esta técnica, pode ser eficazmente reduzida tanto pela optimização dos protocolos de aquisição existentes, como pelo desenvolvimento de novos *softwares* e protocolos.

O objectivo deste trabalho foi avaliar a evolução temporal da dose de radiação na TC cardíaca e identificar variáveis associadas a doses mais elevadas de radiação.

MÉTODOS

Todos os doentes submetidos a TC cardíaca

latest generation scanners, particularly dual-source and 320-slice machines, will be accompanied by a reduction in radiation dose.

There are also considerable variations between different centers and systems, with median radiation doses ranging between 4.9 and 29.1 mSv [4].

This high radiation dose has been identified as a limitation of the technique, but it can be significantly reduced by optimization of existing acquisition protocols and by the development of new software and protocols.

The aim of this study was to evaluate variations in radiation dose in cardiac CT over time and to identify variables associated with use of higher radiation doses.

METHODS

All patients who underwent cardiac CT with a dual-source 64-slice scanner (Somatom Definition® - Siemens Medical Systems) during 2007 and 2008 were enrolled in a prospective single-center registry. This population of 643 patients was divided into quartiles (Q1-Q4) according to the chronological order of the exams, in order to analyze radiation dose over time.

Demographic (age and gender) and clinical

cont.

Manuscrito 18

Rev Port Cardiol
Vol. 29 Novembro 10 / November 10

de 64 cortes de dupla ampola (*Somaton Definition® - Siemens Medical*) de 2007 e 2008 foram incluídos num registo prospectivo de centro único. Esta população (643 doentes) foi dividida em quartis, de acordo com a ordem cronológica dos exames, para estudar a dose de radiação ao longo do tempo.

Variáveis demográficas (idade, sexo), clínicas [presença de factores de risco cardiovascular, índice de massa corporal (IMC), cirurgia cardíaca prévia, enfarte de miocárdio prévio e presença de fibrilhação auricular] e de protocolo (tempo de aquisição, dose de contraste, frequência cardíaca e uso de voltagem da ampola de 120 kVs) foram avaliadas de modo a identificar os preditores de uma dose de radiação mais elevada (definida como presente quando superior à mediana da população). As variáveis identificadas como preditores por análise univariada foram combinadas num modelo de regressão logística para apurar os preditores independentes da utilização de elevada dose de radiação.

Procotocolo de aquisição e reconstrução de imagens

Todas as TC cardíacas foram efectuadas com um aparelho de 64 cortes com dupla ampola (*Somatom Definition, Siemens Medical®, Forchheim, Germany*), com o doente em decúbito dorsal e em apneia após inspiração profunda. Foi administrada nitroglicerina sublingual em todos os doentes (salvo contra-indicações). Não foi administrado beta-bloqueante especificamente para a realização do exame.

A voltagem da ampola foi definida para 100 ou 120 kVs, de acordo com o IMC. Utilizou-se modulação por ECG da corrente da ampola, reduzindo-a a 20% nas fases do ciclo cardíaco não utilizadas para avaliação das coronárias. Esta modulação não foi utilizada nos doentes em fibrilhação auricular. O *pitch* – velocidade de movimento da mesa – foi variável com a frequência cardíaca, aspecto regulado automaticamente pelo equipamento dependendo da frequência cardíaca, sendo este ajuste feito automaticamente. Foram reconstruídas imagens transaxiais, sendo a resolução

variables (cardiovascular risk factors, body mass index [BMI], previous cardiac surgery, previous myocardial infarction [MI] and atrial fibrillation) and protocol parameters (acquisition time, contrast dose, heart rate and use of 120-kV tube voltage), were analyzed in order to identify predictors of a higher radiation dose (defined as higher than the median in the population). Variables identified as predictors on univariate analysis were combined in a logistic regression model to determine independent predictors of use of higher radiation doses.

Acquisition protocol and image reconstruction

All scans were performed with a dual-source 64-slice scanner (Somatom Definition, Siemens Medical Systems, Forchheim, Germany), with the patient in dorsal decubitus and in deep inspiration breath-hold. Sublingual nitroglycerin was administered to all patients except when contraindicated. No beta-blockers were administered specifically for the exam.

Tube voltage was 100 or 120 kV, depending on BMI. ECG-gated tube current, which reduces current by 20% in phases of the cardiac cycle that are not used for assessment of the coronary arteries, was used except for patients in atrial fibrillation. Pitch was varied according to heart rate, this adjustment being carried out automatically by the equipment. Transaxial images were reconstructed with a temporal resolution of 83 ms and slice thickness of 0.75 mm with 0.4 mm increments. Post-processing was carried out using Circulation® software, with multiplane reconstructions, maximum intensity projection and volume rendering technique.

The contrast medium used was intravenous iodixanol (320 mg/ml – Visipaque®) in a 6 ml/s infusion. The quantity of contrast was calculated according to the following formula: (acquisition time + 6 s delay) x flow (6 ml/s).

Contrast administration was followed by flushing with 50 ml saline (6 ml/s).

Statistical analysis

SPSS version 17.0 was used for the statistical analysis. Continuous variables are pre-

cont.

Manuscrito 18

temporal de 83ms, a espessura dos cortes de 0,75mm, com incrementos de 0,4mm. Foi feito o pós-processamento numa consola com o *software Circulation*, sendo utilizadas reconstruções multiplanares (MPR), de projecção de intensidade máxima (MIP) e de volume (VRT).

Foi utilizado meio de contrastre (Iodixanol 320 mg/mL – Visipaque®) endovenoso, a uma infusão de 6 ml/seg. A quantidade de contraste dependeu da duração da aquisição e foi calculada pela seguinte fórmula: (duração da aquisição + *delay* 6 seg) x fluxo (6ml/seg) .

A injecção de contraste foi seguida de um *flush* de 50 mL de soro fisiológico (6 mL/seg).

ANÁLISE ESTATÍSTICA

A análise estatística foi efectuada utilizando a aplicação SPSS Statistics 17,0 para Windows. As variáveis contínuas apresentam-se como mediana (intervalo interquartil) e as categóricas como número (n) ou frequência (%).

Para comparar diferenças entre variáveis contínuas, utilizaram-se os testes não paramétricos de Mann-Whitney ou Kruskal-Wallis e o Chi quadrado foi aplicado para testar diferenças em frequências. A análise multivariada foi efectuada através de um modelo de regressão logística.

Aceitou-se existir diferença significativa quando p<0,05 (duas caudas).

RESULTADOS

Os resultados apresentam-se na Tabela I.

A mediana da idade foi de 59 (52-66) anos, 60% dos indivíduos eram do sexo masculino e o IMC foi de 26 (24-29) kg/m². O tempo de aquisição foi de 8 (7-10) segundos, foi administrado 84 (78-96) mL de contraste e a dose de radiação foi de 6,6 (5,4-10,7) mSv. A frequência cardíaca durante a aquisição foi 65 (56-75) bpm, não tendo sido efectuada redução adicional da frequência cardíaca para a aquisição. Não se verificaram diferenças entre os quartis analisados relativamente a estas variáveis.

A mediana da dose de radiação foi de 6,6

sented as medians (interquartile range) and categorical variables as frequencies (n) or percentages (%).

The non-parametric Mann-Whitney or Kruskal-Wallis tests were used to compare continuous variables, and the chi-square test to test differences in frequencies. Multivariate analysis was performed using a logistic regression model.

Differences were taken to be significant when p<0.05 (two-tailed).

RESULTS

The results are presented in Table I.

The patients' median age was 59 (52-66) years, 60% were male and BMI was 26 (24-29) kg/m². Acquisition time was 8 (7-10) s, 84 (78-96) ml of contrast was administered and the radiation dose was 6.6 (5.4-10.7) mSv. Heart rate during acquisition was 65 (56-75) bpm, with no additional heart rate lowering being carried out. No differences were observed between quartiles in terms of these variables.

There was a progressive reduction in the median radiation dose over time (Q1: 8.9 [5.9-14.1], Q2: 6.6 [5.5-10.7], Q3: 6.4 [5.3-8.7], Q4: 6.1 [5.2-7.9] mSv). This difference was significant when the first quartile was compared with the others (*Figure 2*).

A tube voltage of 100 kV was used in 78% of the exams. There was a progressive increase in the use of this voltage over time (Q1: 54%, Q2: 79%, Q3: 87%, Q4: 91%; p<0.001) (*Figure 2*).

On univariate analysis, predictors of a higher radiation dose (above the median) were male gender, higher BMI, previous cardiac surgery, previous MI, atrial fibrillation during acquisition, longer acquisition time and use of a tube voltage of 120 kV (*Table II*).

On multivariate analysis, predictors of a higher radiation dose were higher BMI, previous cardiac surgery, atrial fibrillation during acquisition, longer acquisition time and use of a tube voltage of 120 kV (*Table III*).

Patients with one or more of the following:

cont.

Manuscrito 18

Rev Port Cardiol
Vol. 29 Novembro 10 / November 10

Tabela I. Resultados da população total e após divisão em quartis das variáveis estudadas

	Total	Q1	Q2	Q3	Q4	p
n	643	161	161	161	160	NS
Idade (anos)	59 (52-66)	58 (52-64)	59 (51-68)	61 (51-67)	59 (52-67)	NS
% sexo masculino	60	69	53	63	56	NS
IMC (kg/m^2)	26 (24-29)	27 (24-29)	26 (24-29)	26 (24-28)	27 (24-29)	NS
FRCV (n)	2 (1-3)	2 (1-3)	2 (1-3)	1 (1-3)	2 (1-3)	0,01
Dose de contraste (mL)	84 (78-96)	84 (78-96)	84 (78-90)	84 (78-96)	84,0 (72-90)	NS
Duração aquisição (seg)	8 (7-10)	8 (7-10)	8 (7-9)	8 (7-10)	8 (6-10)	NS
FC média (bpm)	65 (56-75)	65 (56-75)	64 (54-72)	65 (57-76)	66 (57-76)	NS
Dose de radiação (mSv)	6,6 (5,4-10,7)	8,9 (5.9-14,1)	6,6 (5.5-10,7)	6,4 (5.3-8,7)	6,1 (5,2-7,9)	<0,05
% 100 Kv	78	54	79	87	91	<0,01

FC: frequência cardíaca; FRCV: índice de RFCV; IMC: Índice de massa corporal

Table I. Variables studied for the total study population and divided into quartiles

	Total	Q1	Q2	Q3	Q4	p
n	643	161	161	161	160	NS
Age (years)	59 (52-66)	58 (52-64)	59 (51-68)	61 (51-67)	59 (52-67)	NS
% male	60	69	53	63	56	NS
BMI (kg/m^2)	26 (24-29)	27 (24-29)	26 (24-29)	26 (24-28)	27 (24-29)	NS
CVRF (n)	2 (1-3)	2 (1-3)	2 (1-3)	1 (1-3)	2 (1-3)	0.01
Contrast dose (ml)	84 (78-96)	84 (78-96)	84 (78-90)	84 (78-96)	84,0 (72-90)	NS
Acquisition time (s)	8 (7-10)	8 (7-10)	8 (7-9)	8 (7-10)	8 (6-10)	NS
Mean HR (bpm)	65 (56-75)	65 (56-75)	64 (54-72)	65 (57-76)	66 (57-76)	NS
Radiation dose (mSv)	6.6 (5.4-10.7)	8,9 (5.9-14.1)	6.6 (5.5-10.7)	6.4 (5.3-8.7)	6.1 (5.2-7.9)	<0.05
% 100 kV tube voltage	78	54	79	87	91	<0.01

BMI: body mass index; CVRF: cardiovascular risk factors; HR: heart rate

(5,4-10,7) mSv e verificou-se uma redução progressiva ao longo do tempo [Q1: 8,9 (5,9-14,1), Q2: 6,6 (5,5-10,7), Q3: 6,4 (5,3-8,7), Q4: 6,1 (5,2-7,9)]. Esta diferença foi significativa quando o primeiro quartil foi comparado com os restantes (*Figura 2*).

Em 78% dos exames utilizou-se uma voltagem da ampola de 100 kVs. Houve um aumento progressivo da selecção desta voltagem com o tempo (Q1: 54%, Q2: 79%, Q3: 87%, Q4: 91%; p<0,001 – *Figura 2*).

Por análise univariada, os preditores de uma dose de radiação alta (acima da mediana) foram: sexo masculino, maior IMC, cirurgia cardíaca prévia, enfarte de miocárdio prévio, ritmo de fibrilhação auricular na aquisição, maior tempo de aquisição ou dose de contraste administrada, menor frequência cardíaca e utilização de uma voltagem da ampola de 120 kV (*Tabela II*).

Por análise multivariada, os preditores de uma dose de radiação alta foram: maior IMC, cirurgia cardíaca prévia, presença de fibrilhação auricular na aquisição, maior tempo de

BMI >32.4 kg/m^2 (the best cutoff to predict high radiation dose), previous cardiac surgery, atrial fibrillation during acquisition or acquisition time >10 s (the best cutoff to predict high radiation dose) made up 38% of the population. Radiation dose was higher in this subgroup than in patients without any of these characteristics (12.1 [9.5-14.8] vs. 5.7 [5.0-6.7] mSv, p<0.001).

DISCUSSION

In this study we set out to identify the factors associated with a higher radiation dose in cardiac CT angiography. The use of a 120-kV tube voltage was a predictor of a higher radiation dose, as was higher BMI, since this meant the voltage could not be reduced. Longer acquisition time and higher contrast dose (which, as it depends on the former, lost its predictive value on multivariate analysis) were also associated with higher radiation dose.

cont.

Manuscrito 18

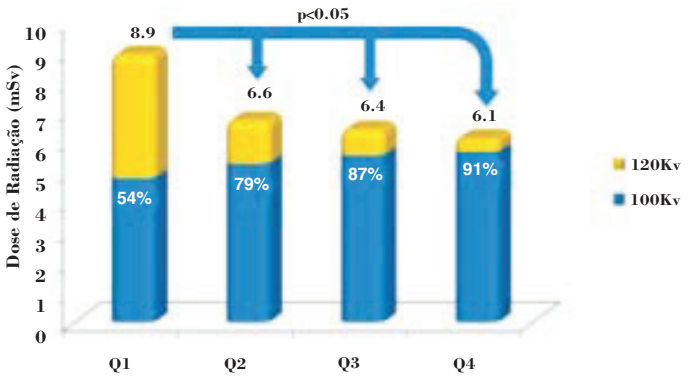

Figura 2. Representação gráfica da evolução da dose de radiação de acordo com os quartis de tempo. A percentagem incluída nas colunas representa a proporção de utilização de 100 kV como voltagem da ampola (*versus* 120 kV)

Figure 2. Chart showing changes in radiation dose by quartiles of time. The percentages in the columns represent the proportion of use 100 kV tube voltage (vs. 120 kV)

Tabela II. Variáveis testadas para preditores de dose de radiação elevada por análise univariada

	Dose de radiação		
	Abaixo da mediana (6,6mSv)	Acima da mediana (6,6mSv)	p
Variáveis demográficas			
Idade (anos)	58 (52-65)	60 (51-68)	0,202
Sexo masculino (%)	50	68	<0,001
Variáveis clínicas			
≥ 1 FRCV (%)	83%	87%	0,
IMC (k^s/m^2)	26 (24-28)	27 (25-30)	<0,001
Cirurgía cardiaca prévia (%)	1%	11%	<0,001
Enfarte de miocárdio prévio (%)	5%	10%	0,010
FA (%)	0%	11%	<0,001
Variáveis do protocolo			
Tempo de aquisição (seg)	7 (6-8)	9 (7-11)	<0,001
Dose de contraste	78 (72-84)	90 78-102)	<0,001
Frequência cardíaca	68 (60-77)	63 (54-73)	<0,001
Voltagem da ampola120 kV	2%	41%	<0,001

FA: Fibrilhação auricular; FRCV: Factores de Risco Cardiovasculars; IMC: Índice de Massa Corporal;

Table II. Variables tested to identify predictors of higher radiation dose on univariate analysis.

	Radiation dose		
	Below median (6.6mSv)	Above median (6.6mSv)	p
Demographic variables			
Age (years)	58 (52-65)	60 (51-68)	0,202
% male	50	68	<0.001
Clinical variables			
≥ 1 CVRF (%)	83%	87%	0.170
BMI (kg/m^2)	26 (24-28)	27 (25-30)	<0.001
Previous cardiac surgery (%)	1%	11%	<0.001
Previous MI (%)	5%	10%	0.010
AF (%)	0%	11%	<0.001
Protocol parameters			
Acquisition time (s)	7 (6-8)	9 (7-11)	<0.001
Contrast dose	78 (72-84)	90 78-102)	<0.001
Heart rate	68 (60-77)	63 (54-73)	<0.001
120 kV tube voltage	2%	41%	<0.001

AF: atrial fibrillation; BMI: body mass index; CVRF: cardiovascular risk factor; MI: myocardial infarction

cont.

Manuscrito 18

Rev Port Cardiol
Vol. 29 Novembro 10 / November 10

aquisição e o uso 120 kV como voltagem da ampola (*Tabela III*).

Doentes com pelo menos uma das seguintes variáveis de: IMC >32,4 kg/m² (melhor limiar para discriminar radiação alta), cirurgia cardíaca prévia, aquisição em fibrilhação auricular ou duração da aquisição >10s (melhor limiar para discriminar radiação alta) constituíram 38% da população. Neste subgrupo, a dose de radiação foi superior, quando comparados com a ausência de todas estas características [12,1 (9,5-14,8) *versus* 5,7 (5,0-6,7), p<0,001].

DISCUSSÃO

Neste trabalho procurámos identificar os factores associados a uma dose de radiação superior, na AngioTC cardíaca. A utilização de uma voltagem da ampola de 120 kV foi um preditor de maior dose de radiação. Em concordância com este achado, um elevado IMC, pela impossibilidade de se reduzir a voltagem da ampola, associou-se a uma maior dose de radiação. Um maior tempo de aquisição e maior dose de contraste (que, dependendo da anterior, perdeu o valor preditor por análise multivariada) associaram-se igualmente a uma dose de radiação superior.

O tempo de aquisição maior aumenta a dose de radiação, por traduzir uma maior área corporal adquirida ou por estarmos na presença de frequências cardíacas mais lentas, aumentando o tempo de diástole e a duração da aquisição nesta fase do ciclo cardíaco. A frequência cardíaca baixa, quando analisada isoladamente, também foi um preditor de maior dose de radiação. Igualmente, a presença de cirurgia cardíaca prévia, associou-se a uma maior dose de radiação. Isto resulta de uma maior prevalência de doentes com revascularização miocárdica cirúrgica, o que aumenta a janela de aquisição, para incluir as pontagens. Já a presença de enfarte de miocárdio prévio, que também foi preditor de maior dose de radiação, perdeu este valor na análise multivariada, possivelmente pelo efeito de incluir neste grupo doentes com

Longer acquisition time increases radiation dose and may reflect a larger body surface area scanned or lower heart rate causing prolonged diastole and hence acquisition time. Low heart rate, when analyzed in isolation, also predicted higher radiation dose, as did previous cardiac surgery (due to the high proportion of patients with previous CABG who required a longer acquisition window in order to include the grafts). Previous MI, which was a predictor of higher radiation dose on univariate analysis, lost its predictive value on multivariate analysis, possibly because this group included patients with previous CABG. Finally, atrial fibrillation during acquisition was associated with higher radiation dose, since it prevented ECG pulsing (see below).

Other studies have likewise found that greater body weight and absence of a stable sinus rhythm are associated with higher radiation doses [4].

After excluding the main predictors of higher radiation dose (BMI >32.4 kg/m2, previous cardiac surgery, atrial fibrillation during acquisition, and acquisition time >10 s), a subgroup of two-thirds of the population was identified in whom the radiation dose was significantly lower (5.7 mSv), a reduction of 53%.

As well as identifying the variables associated with higher radiation dose, we found that there was a progressive reduction in radiation dose over time, due to the increasing availability of low-radiation protocols, such as limiting tube voltage to 100 kV, which did not exist when our center began operating. There has also been progressive optimization of acquisition protocols to individual patient characteristics, which also helps reduce radiation dose.

There have been few studies analyzing changes in radiation dose over time. A study by Hausleiter et al. showed that a 12-month increase in experience in cardiac CT angiography was associated with a reduction of 1% in radiation dose [4]. Another, presented by Bettencourt de Sousa et al. at the 2008 Congress of the European Society of Cardiac Radiology, demonstrated an inverse relation-

cont.

Manuscrito 18

Tabela III. Preditores independentes de dose de radiação elevada por análise multivariada

Variável	HR	IC (95%)	p
IMC	1,129	1,038-1,229	0,045
Cirurgia cardíaca prévia	5,776	1,042-32,28	0,003
FA	30,874	3,247-293,617	<0,001
Duração da aquisição	1,975	1,672-2,334	<0,001
120 kV	71,394	23,363-218,170	<0,001

FA: Fibrilhação Auricular; HR: *Hazard Ratio*; IC: Intervalos de Confiança; K: Índice de Massa Corporal

Table III. Independent predictors of higher radiation dose on multivariate analysis.

Variable	HR	CI (95%)	p
BMI	1.129	1.038-1.229	0.045
Previous cardiac surgery	5.776	1.042-32.28	0.003
AF	30,874	3.247-293.617	<0.001
Acquisition time	1.975	1.672-2.334	<0.001
120 kV tube voltage	71.394	23.363-218.170	<0.001

AF: atrial fibrillation; BMI: body mass index; CI: confidence interval; HR: hazard ratio

revascularização miocárdica cirúrgica prévia. Finalmente, a presença de fibrilhação auricular na aquisição associou-se a maior dose de radiação administrada por prejudicar a aquisição com "ECG *gating*" (descrito abaixo).

Em concordância com o encontrado, outros estudos verificaram que maior peso e a ausência de um ritmo sinusal estável, se associava a uma maior dose de radiação utilizada[4].

Após exclusão dos principais preditores de elevada dose de radiação (IMC>32,4 kG/m^2, cirurgia cardíaca prévia, aquisição em fibrilhação auricular, duração da aquisição >10seg), foi identificado um subgrupo, correspondente a 2/3 da população, em que a dose de radiação foi significativamente menor (5,7 mSv, redução de 53%).

Além de apurarmos as variáveis que se associaram a uma dose superior de radiação, verificámos que esta foi sendo progressivamente menor ao longo do tempo. Contribuíu para este efeito o facto de terem surgido uma maior disponibilidade de protocolos de baixa radiação, como a limitação da voltagem da ampola a 100 kV, que não estava presente no início do funcionamento deste centro. Por outro lado, houve uma progressiva optimização dos protocolos de aquisição às características dos doentes, com consequente redução da dose de radiação.

A informação disponível no que respeita à

ship between a center's experience and radiation dose, with a 22% reduction after 1000 exams[5].

Reductions can be achieved by tailoring the acquisition protocol to individual patient characteristics[6]. Firstly, instead of rigidly scanning from carina to diaphragm, the scan range can be adjusted to the patient's anatomy, according to a prior low-dose scan for calcium scoring [4]. This is a simple way to reduce the radiation used, since each 1 cm increase in scan range is associated with an increase of 5% in radiation dose[4]. Secondly, the tube voltage should be reduced to the lowest value that will allow image quality to be maintained for a given patient's anatomic shape and for the equipment used[4]. Reducing tube voltage from 120 to 100 kV considerably reduces radiation dose, since this varies with the square of the tube voltage[7]. In suitable patients (nonobese), this measure can lead to a reduction of 40-46% in radiation dose without compromising image quality[4, 8]. Finally, since cardiac motion is least during diastole, diastolic image reconstructions are most likely to be free of motion artifacts, and so restricting maximum tube current to a predefined time window during diastole and decreasing it during the rest of the cycle (ECG pulsing) can reduce total radiation while maintaining image quality [4, 9, 10]. In the extreme form of this

cont.

Manuscrito 18

Rev Port Cardiol
Vol. 29 Novembro 10 / November 10

análise da variação da dose de radiação com a evolução temporal é escassa. Um trabalho de Hausleiter demonstrou que um aumento de 12 meses de experiência na realização de AngioTC cardíaca se associou a uma diminuição da dose de radiação de 1%[4]. Um outro trabalho, apresentado por Bettencourt de Sousa no Congresso da Sociedade Europeia de Radiologia Cardíaca 2008, demonstrou a presença de uma relação inversa entre a experiência do centro e a dose de radiação utilizada (redução de 22% após 1000 exames)[5].

Esta redução na dose de radiação pode conseguir-se ajustando os parâmetros do protocolo de aquisição às características individuais dos doentes[6]. Em primeiro lugar, em vez da aquisição de imagens se estender sistematicamente da carina ao diafragma, esta deve ser ajustada de acordo com a anatomia de cada doente, de acordo com uma primeira passagem com baixa dose de radiação para *score* de cálcio[4]. Esta é uma técnica fácil para reduzir a radiação utilizada, já que por cada centímetro a mais na extensão de aquisição de imagens há um aumento de 5% na dose de radiação[4]. Em segundo lugar, a corrente da ampola deve ser reduzida para o valor mais baixo que se espere manter uma boa qualidade de imagem para determinado biótipo de doente e aparelho de AngioTC. Uma redução da voltagem da ampola de 120 kV para 100 kV diminui consideravelmente a dose de radiação, já que esta varia com o quadrado da voltagem[7]. Em doentes apropriados (IMC não elevado) esta medida pode levar a uma redução de 40-46% da dose de radiação sem comprometer a qualidade da imagem[4,8]. Finalmente, tendo em conta que o movimento cardíaco é menor durante a diástole, as reconstruções de imagem efectuadas nesta fase serão, com maior probabilidade, livres de artefactos de movimento. Assim, limitando a corrente máxima da ampola a uma porção predefinida da diástole e diminuindo-a no restante ciclo cardíaco, pode diminuir-se a radiação total utilizada, mantendo a possibilidade de obter imagens de qualidade (técnica denominada "ECG *pulsing*")[4, 9, 10]. Levando este protocolo ao extremo, pode ligar-se ape-

protocol, prospective gating, the X-ray tube is only switched on during part of diastole and is switched off for the rest of the cardiac cycle, resulting in sequential rather than spiral scanning. This protocol requires a stable heart rate below 65 bpm and hence intravenous beta-blockers are often needed [8]. Although it results in a substantial reduction in radiation dose, this technique does not provide functional information such as ventricular or valve function [8, 9]. A combination of 100 kV tube voltage and prospective gating can achieve an impressive reduction of 90% [8].

Although the debate on the use of radiation in imaging studies has focused on cardiac CT angiography, it should be remembered that other common techniques use radiation. In 2006, cardiac CT angiography accounted for only 3% of the collective radiation exposure resulting from medical exams in the US [11]. Considering only cardiological exams, the mean radiation dose in coronary angiography is 7 mSv, while for myocardial perfusion scintigraphy it is 15.7 mSv. The latter exam accounted for 22.1% of radiation exposure resulting from diagnostic exams (cardiac or non-cardiac) in the US [12].

CONCLUSION

In this study of consecutive patients undergoing cardiac CT angiography, independent predictors of higher radiation dose were higher body mass index, previous cardiac surgery, atrial fibrillation during acquisition, longer acquisition time and use of a tube voltage of 120 kV. In two-thirds of the study population, none of these characteristics was present and radiation dose was significantly lower (5.7 mSv). Over time, it has been possible to reduce the radiation dose used in these exams, as a result of the development of new protocols and progressive optimization of existing protocols and by adapting them to individual patient characteristics.

cont.

nas a ampola durante parte da diástole e desligá-la no restante ciclo cardíaco com aquisição não helicoidal ("*gating* prospectivo"). Este protocolo requer uma frequência cardíaca estável e inferior a 65 batimentos por minuto, com necessidade frequente da utilização de betabloqueantes endovenosos[8]. Apesar de diminuir bastante a dose de radiação utilizada, não permite obter informação funcional (ex: função ventricular ou valvular)[8, 9]. A combinação da utilização de uma voltagem da ampola de 100 kV e a aquisição prospectiva podem conseguir uma impressionante redução de 90%[8].

Embora o debate sobre o uso de radiação em exames de imagem se tenha centrado na AngioTC cardíaca, deve referir-se que outras técnicas frequentemente utilizadas usam radiação. Em 2006, a AngioTC cardíaca correspondeu apenas a cerca de 3% da dose colectiva de radiação recebida em consequência de exames médicos[11]. Considerando apenas os exames na área da cardiologia, referimos que a dose de radiação usada numa coronariografia 7 mSv e de uma cintigrafia de perfusão miocárdica é de 15,6 mSv. Este último exame foi responsável por 22,1% da exposição de radiação em consequência da realização de exames complementares de diagnóstico (cardíacos ou não cardíacos)[12].

CONCLUSÃO

Nesta análise de doentes consecutivos submetidos a AngioTC cardíaco, foram preditores independentes de maior dose de radiação um elevado índice de massa corporal, antecedentes de cirurgia cardíaca, presença de fibrilhação auricular na aquisição, maior tempo de aquisição e o uso 120 kV como voltagem da ampola. Em 2/3 da nossa população, nenhuma destas características está presente e a dose de radiação é significativamente mais baixa (5,7mSv). Ao longo do tempo tem sido possível diminuir a dose de radiação utilizada nestes exames, resultante do aparecimento de novos protocolos e por uma progressiva optimização dos já disponíveis, adaptando-os às características individuais de cada doente.

Pedido de Separatas para:
Address for Reprints:

Pedro Jerónimo Sousa
Centro Cardiovascular
Hospital da Luz
Av. Lusíada
1500-650 Lisboa
e-mail: p965675551@gmail.com

BIBLIOGRAFIA / REFERENCES

1. Hurlock GS, Higashino H, Mochizuki T. History of cardiac computed tomography: single to 320-detector row multislice computed tomography. Int J Cardiovasc Imaging 2009;25 Suppl 1:31-42

2. Schroeder S., Achenbach S., Bengel F et al. Cardiac computed tomography: indications, applications, limitations, and training requirements. Eur Heart J 2008;29(4), 531-56.

3. Pugliese F, Mollet NR, Hunink MG et al. Diagnostic performance of coronary CT angiography by using different generations of multisection scanners: single-center experience. Radiology 2008;246(2):384-93.

4. Hausleiter J, Meyer T, Hermann F et al. Estimated radiation dose associated with cardiac CT angiography. JAMA 2009;301(5):500-7

5. Bettencourt de Sousa N, Sampaio F, Mateus P et al. Multislice computed tomography coronary angiography – radiation dose is inversely related to experience. European Radiology 2008;18(S3):C74

6. Alkadhi H, Stolzmann P, Scheffel H et al. Radiation dose of cardiac dual-source CT: the effect of tailoring the protocol to patient-specific parameters. Eur J Radiol 2008;68(3):385-91.

7. Hausleiter J, Meyer T, Hadamitzky M et al. Radiation dose estimates from cardiac multislice computed tomography in daily practice: impact of different scanning protocols on effective dose estimates. Circulation 2006;113(10):1305-10

8. Gopal A, Mao SS, Karlsberg D et al. Radiation reduction with prospective ECG-triggering acquisition using 64-multidetector Computed Tomographic angiography. Int J Cardiovasc Imaging 2009;25(4):405-16

9. Alkadhi H. Radiation dose of cardiac CT - what is the evidence? Eur Radiol 2009;19(6):1311-5.

10. Jakobs TF, Becker CR, Ohnesorge B et al. Multislice helical CT of the heart with retrospective ECG gating: reduction of radiation exposure by ECG-controlled tube current modulation. Eur Radiol 2002;12(5):1081-6.

11. Mettler FA Jr, Thomadsen BR, Bhargavan M et al. Medical radiation exposure in the U.S. in 2006: preliminary results. Health Phys 2008;95(5):502-7.

12. Fazel R, Krumholz HM, Wang Y et al. Exposure to low-dose ionizing radiation from medical imaging procedures. N Engl J Med 2009;361(9):849-57.

CAPÍTULO VII

Avaliação dimensional 2D, volumétrica, funcional e classificação anatómica

Base de dados e análise estatística

RESUMO

Neste capítulo definem-se as medições efetuadas, por forma a torná-las reprodutíveis noutros trabalhos de investigação.
Faz-se a avaliação da variabilidade intra-observador, inter-obervador e inter-fases do ciclo cardíaco.
Definimos as classificações anatómicas utilizadas para a caracterização do AAEsq e da drenagem das veias pulmonares.
O pós-processamento foi efetuado em consola Terarecon®.
Por fim descrevemos a forma de colher, registar e analisar estatisticamente os dados obtidos.

SUMÁRIO

7.1. INTRODUÇÃO

Neste capitulo descrevem-se as formas estandardizadas de obtenção da informação dimensional 2D, volumétrica e funcional da AEsq e do AAEsq.
Avaliamos a variabilidade intra-observador, inter-observador e inter-fases cardíacas.
Descrevem-se as classificações utilizadas para caracterização morfológica do AAEsq e da drenagem das veias pulmonares.
Por fim descrevemos a forma de colher, registar e analisar estatisticamente os dados.

7.2. AVALIAÇÃO DIMENSIONAL 2D, VOLUMÉTRICA, FUNCIONAL E CLASSIFICAÇÃO ANATÓMICA

7.2.1. Avaliação dimensional 2D

No decorrer desta tese foram diversas as avaliações dimensionais 2D que foram efetuadas, segue-se a definição da sua obtenção:

Avaliação das dimensões de um *ostium*:

- Utilizado para avaliar a dimensão dos *ostiae* das veias pulmonares e do AAEsq.
- Após obter a imagem *en face* do *ostium* pela obtenção de um plano bi-perpendicular (ver **Figura 1**), mede-se o maior diâmetro e o diâmetro perpendicular a esse. A divisão dos diâmetros permite avaliar o grau de ovalidade do *ostium*.

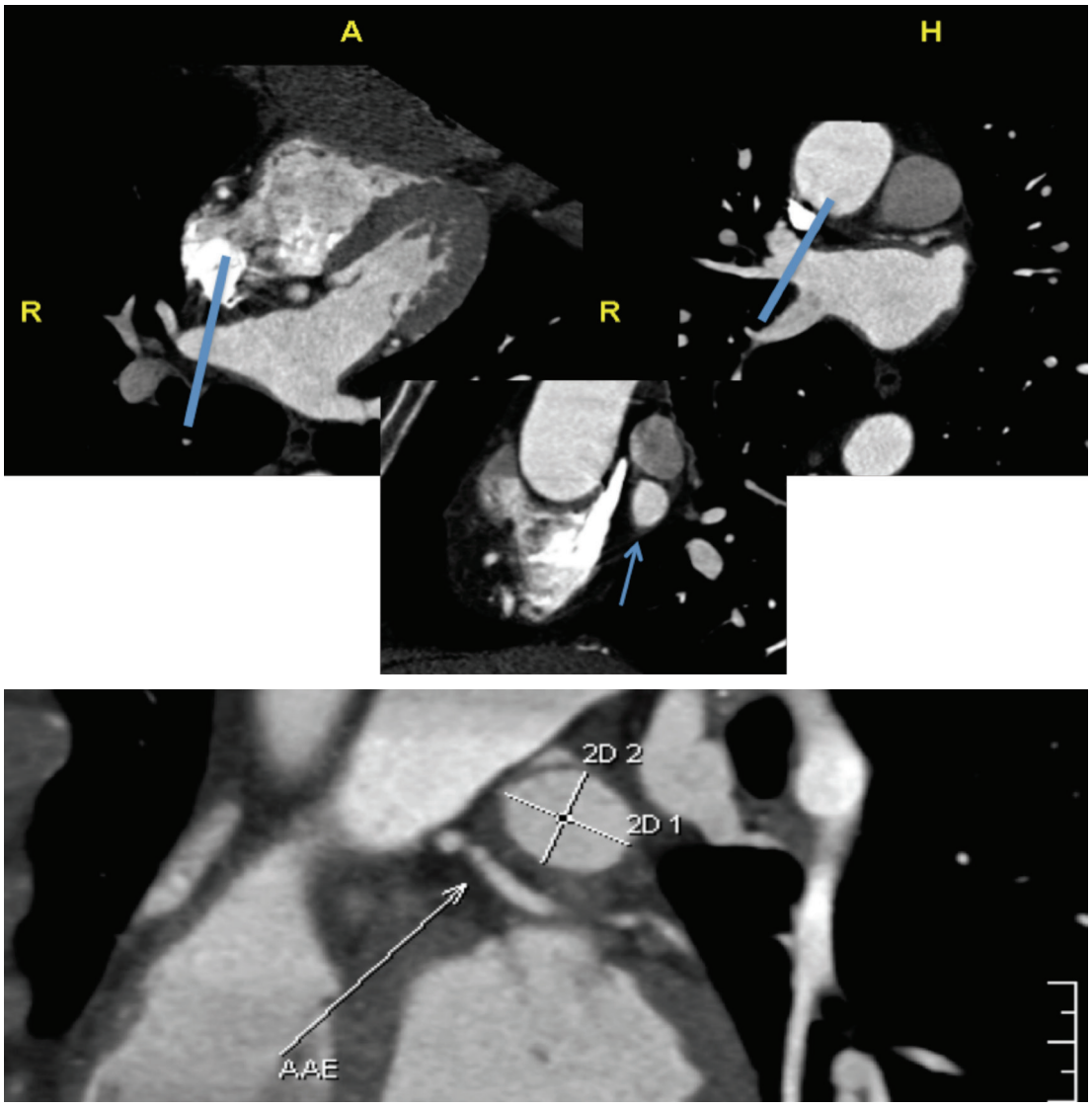

FIGURA 1

A avaliação das dimensões dos *ostiae* é efetuada em plano 2D, bi-perpendicular (em cima) obtendo-se o maior diâmetro e traçando-se o menor perpendicular ao primeiro (em baixo).
(Imagens Hugo Marques — UNICA — Hospital da Luz.)

Avaliação da área máxima da aurícula esquerda em plano axial direto e obtenção dos diâmetros nesse plano (ver **Figura 2**):

- Faz-se avaliação visual da maior área da AEsq (excluindo o AAEsq e as veias pulmonares) visualizando consecutivamente a AEsq em plano axial transversal.
- Após a sua determinação, obtêm-se a área ao desenhar uma região de interesse com limites coincidentes com a parede da aurícula, excluindo o AAEsq e as veias pulmonares (se estiverem no plano), unindo em curva os dois pontos

da parede da AEsq de cada lado dessa(s) estrutura(s) por forma a manter a curvatura da parede da AEsq.

> Os diâmetros máximos são medidos em latero-lateral e ântero-posterior estrito.

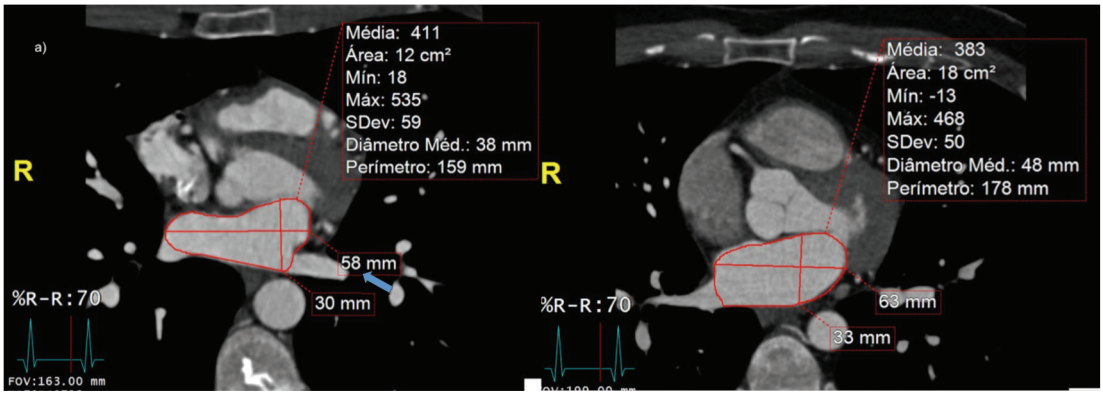

FIGURA 2

Dois doentes, mostrando os locais habituais do plano de maior área (o mais frequente é visualizar o plano da VPIEsq (seta)).

(Imagens Hugo Marques — UNICA — Hospital da Luz.)

Avaliação do diâmetro máximo crâneo-caudal em plano sagital (ver **Figura 3**):

> Faz-se avaliação visual da maior área da AEsq em plano sagital, excluindo o AAEsq e as veias pulmonares. Na maioria das vezes este plano encontra-se muito próximo do bordo vertebral esquerdo.

> Após a sua determinação obtêm-se o diâmetro máximo crâneo-caudal estrito.

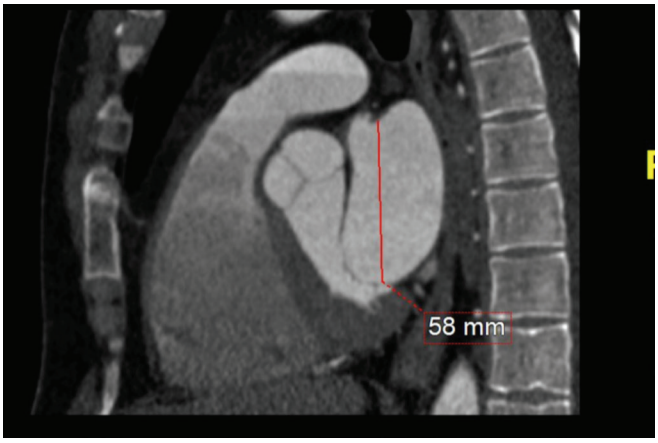

FIGURA 3

Maior diâmetro crâneo-caudal em plano sagital direto.

(Imagens Hugo Marques — UNICA — Hospital da Luz.)

7.2.2. Avaliação volumétrica

Os volumes foram obtidos pela soma dos vóxeis das áreas desenhadas.

Na obtenção da volume da AEsq, excluíram-se as veias pulmonares e o AAEsq, utilizando a forma de desenho de área referido acima.

Descreve-se abaixo a obtenção dos diversos volumes da AEsq, com os mesmos princípios utilizados para a avaliação volumétrica do AAEsq.

Escolha das fases do ciclo cardíaco para avaliação do volume da AEsq:

> avaliação qualitativa da dimensão da aurícula esquerda nos 2 planos cardíacos (eixo longo do VEsq e 4 câmaras) em fases consecutivas, com observação do movimento da válvula mitral. Escolha da fase do ciclo de volume máximo (normalmente aos 40% do intervalo RR), do volume mínimo (normalmente aos 100% do intervalo RR) e do volume pré-sístole AEsq (frequentemente aos 80% do intervalo RR) (ver **Figura 4** e **5**).

7.2.3. Avaliação funcional da AEsq

Após os cálculos dos diversos volumes, a avaliação funcional seguiu as definições internacionais nomeadamente:

TABELA 1

Avaliação funcional da AEsq — definições e fórmula de cálculo.

Função reservatório	Índice de expansibilidade	(VAEsqMax –VAEsqMin) / VAEsqMin
Função conduto	Fração de Ejeção Passiva	**Volume sistólico passivo da AEsq** (VAEsqMax –VAEsqPS) / VAEsqMax
Função ativa	Fração de Ejeção ativa (FejACT)	**Volume sistólico ativo da AEsq** (VAEsqPS –VAEsqMin) / VAEsqPS
Função AEsq	Fração de Ejeção (Fej)	(VAEsqMax –VAEsqMin) / VAEsqMax

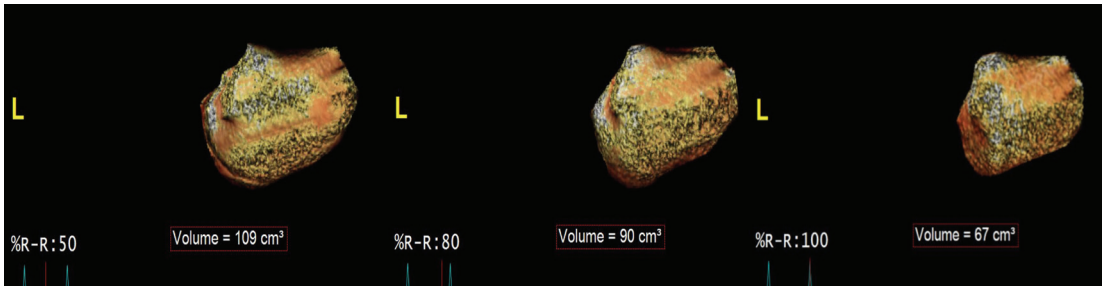

FIGURA 4

A avaliação funcional da aurícula esquerda é efetuada com medição do volume máximo da aurícula esquerda antes da abertura da válvula mitral (neste caso a 50% do intervalo RR), do volume após esvaziamento passivo – volume pré-sístole auricular (neste caso a 80% do intervalo RR) e do volume mínimo (após esvaziamento ativo) após o fecho da válvula mitral (neste caso 100% do intervalo RR).

(Imagens Hugo Marques — UNICA — Hospital da Luz.)

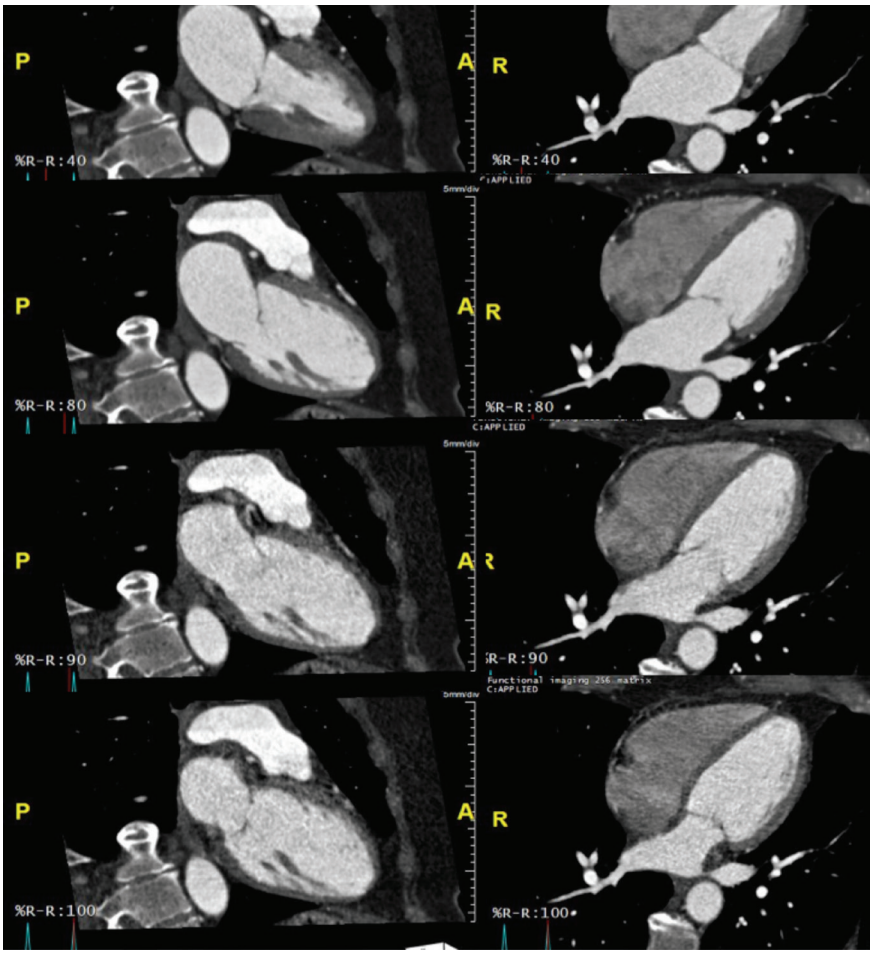

FIGURA 5

Nos planos cardíacos longo eixo e 4 câmaras observamos as diferentes fases do ciclo que nos permitem definir a fase de volume máximo 40% do intervalo RR (1ª linha de imagens); fase pré-sístole da AEsq (2ª linha de imagens); inicio da sístole auricular (3.ª linha de imagens), o que faz com que a fase anterior seja a do volume pré-sístole auricular; volume mínimo (4.ª linha de imagens).

(Imagens Hugo Marques — UNICA — Hospital da Luz.)

7.2.4. Avaliação da variabilidade intra-observador, inter-observador e inter-fase

Para avaliação da variabilidade intra-observador, foram medidas três vezes os volumes auriculares de 30 doentes, em tempos diferentes e sem acesso aos resultados anteriores.

Para avaliação da variabilidade inter-observador, mediram-se uma vez os volumes auriculares de 30 doentes, quer pelo autor da tese, quer por um técnico de radiologia com experiência em TC cardíaca.

A variabilidade inter-fase foi testada pela medição de volumes de 30 doentes consecutivos a 70% do intervalo RR e numa reconstrução adicional a 75% do intervalo RR.

7.3. CLASSIFICAÇÃO ANATÓMICA DO APÊNDICE AURICULAR ESQUERDO E DAS VEIAS PULMONARES

7.3.1. Classificação das Veias Pulmonares

A classificação das veias pulmonares adotada foi a publicada por Marom(1), dada a sua simplicidade e utilização frequente noutras séries: letra maiúscula representa o lado ("R" – *right* – direita; "L" – *left* – esquerda), seguindo-se um número que representa o número de *ostiae* das veias pulmonares do lado em questão. Associando-se ainda uma letra minúscula que pode ter diferentes significados, como é perceptível na esquematização representada na **Figura 6** (1).

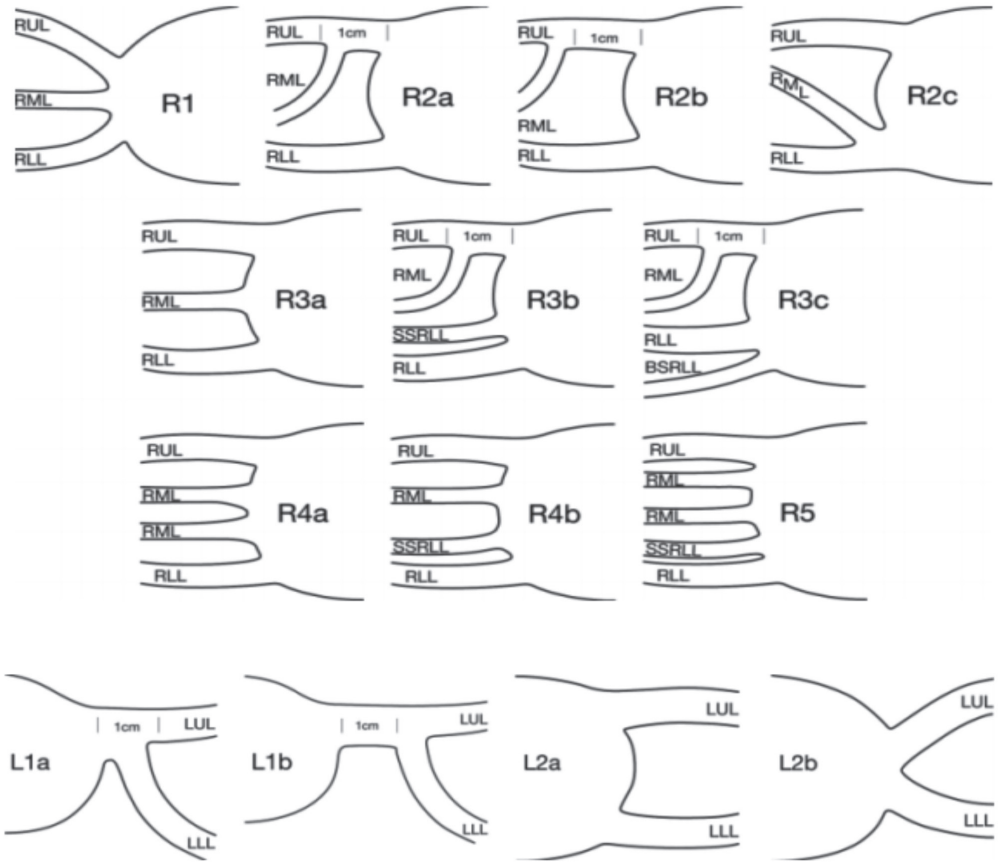

FIGURA 6

Classificação dao padrão de drenagem das veias pulmonares proposto por Marom (Radiology. 2004 Mar;230(3):824-9). R — direita; L — esquerda

7.3.2. Classificação do Apêndice Auricular Esquerdo

Foram utilizadas duas classificações:

- para a avaliação do tipo de AAEsq adotámos a classificação descrita por Wang e Di Biase (2) (ver **Figura 7**).
- Para a avaliação do número de lobos utilizámos a classificação de Erol(3) que representa o número de câmaras principais/lobos do AAEsq, mas com uma modificação. Erol descreve três como o número máximos de câmaras máximo e nós verificámos que havia conjunto relevante de AAEsq que apresentavam mais do que três câmaras. Assim Erol definiu para o AAEsq, um número de lobos de 1 a 3 e nós descrevemos de 1 a 5 (ver **Figura 8**).

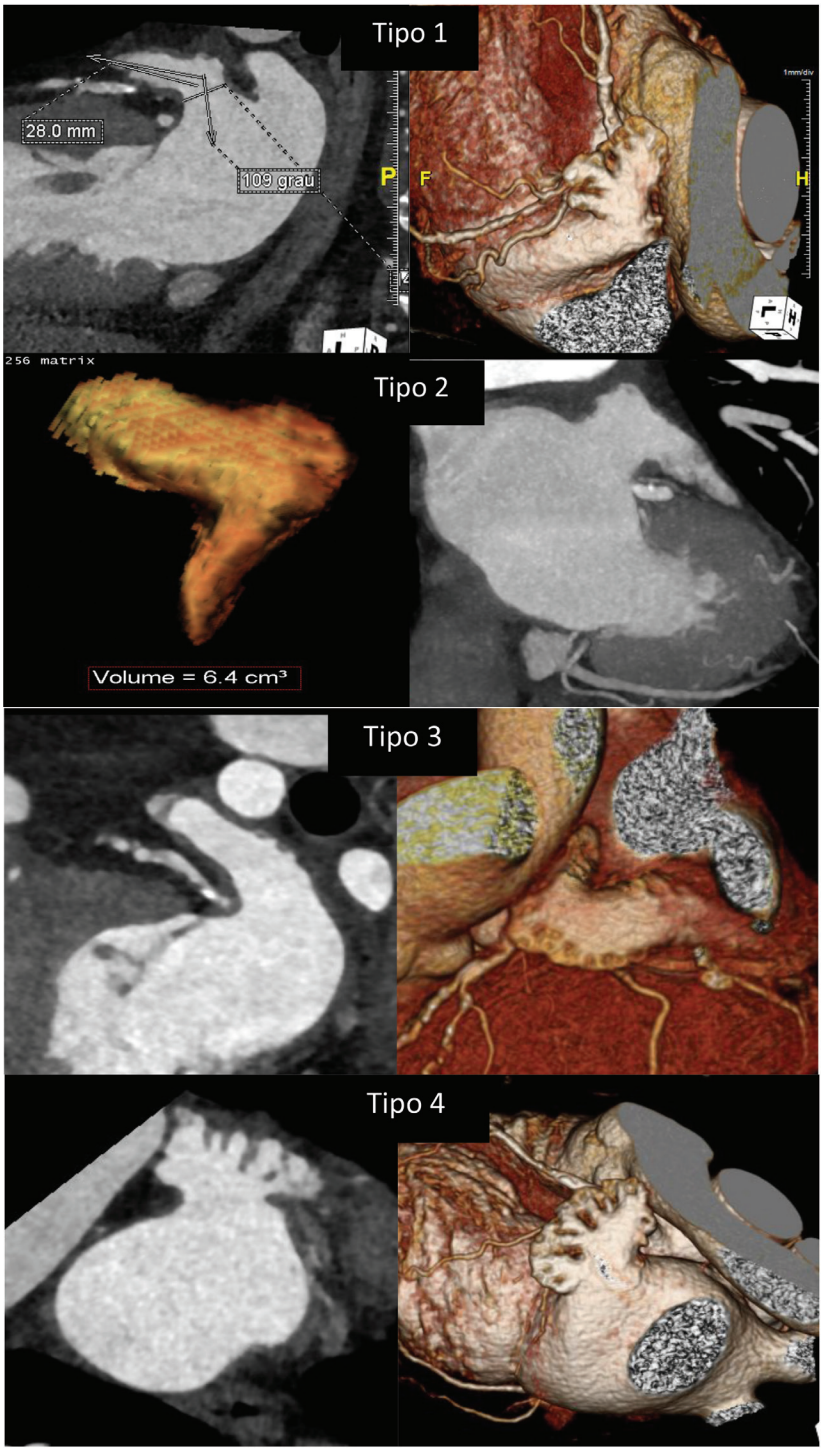

FIGURA 7

Classificação morfológica dos AAEsq baseada em Wang e Di Biase. Com correlação dimensional de Kimura. **Tipo 1** — Cactus; **Tipo 2** — Chicken Wing; **Tipo 3** — Windsock; **Tipo 4** — Cauliflower.

(Imagens Hugo Marques — UNICA — Hospital da Luz.)

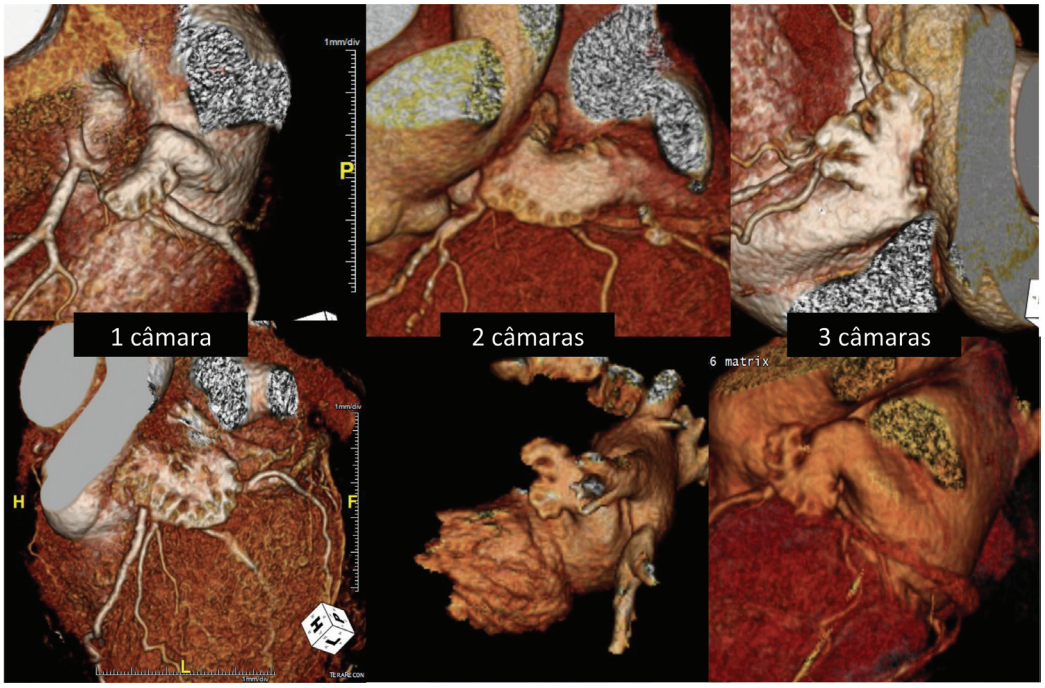

FIGURA 8
Classificação dos AAEsq de acordo com Erol.
(Imagens Hugo Marques — UNICA — Hospital da Luz.)

7.4. BASES DE DADOS E ANÁLISE ESTATISTICA

Os dados demográficos, fatores de risco, antecedentes cardiovasculares, indicação para a realização da angio TC, dados técnicos respeitantes à aquisição do exame, bem como do seu resultado após processamento das imagens adquiridas (incluindo parâmetros morfológicos, dimensionais e funcionais dos doentes com FA) foram colhidos numa folha especificamente elaborada para este motivo, que sofreu evolução adaptativa de acordo com a utilização de novo aparelho de TC. Estes dados foram posteriormente introduzidos numa base de dados.

A análise estatística foi realizada no programa IBM SPSS STATISTICS SUBSCIPTION. As variáveis contínuas são apresentadas como médias e desvio padrão e as variáveis categóricas como frequências e percentagens.
Foram usados testes não paramétricos (Mann-Whitney ou Kruskal-Wallis) para comparar as variáveis contínuas e o teste Qui Quadrado para comparar variáveis categóricas. As diferenças foram consideradas significativas para um valor de $p<0,05$.

No capítulo VIII para obter um envelope de confiança a 95% do grupo "normal" (grupo B) no espaço volume e idade, foi utilizada a distância de Mahalanobis.
Foi realizada análise multivariável (regressão *logistic and linear*, com seleção "*stepwise*") para identificar os preditores independentes de recidiva após ablação percutânea de FA, usando as variáveis do *score* ATLAS.
Foram efetuada curvas de sobrevida Kaplan-Meier para detetar diferenças no prognóstico após ablação de diferentes grupos de doentes para variáveis discretas. Para as variáveis contínuas utilizámos a regressão de Cox.

BIBLIOGRAFIA

1. Marom EM, Herndon JE, Kim YH, et al. Variations in pulmonary venous drainage to the left atrium: implications for radiofrequency ablation. Radiology. 2004;230(3):824-9.
2. Wang Y, Di Biase L, Horton RP, et al. Left atrial appendage studied by computed tomography to help planning for appendage closure device placement. J Cardiovasc Electrophysiol. 2010;21(9):973-82.
3. Erol B, Karcaaltincaba M, Aytemir K, et al. Analysis of left atrial appendix by dual-source CT coronary angiography: morphologic classification and imaging by volume rendered CT images. European journal of radiology. 2011;80(3):e346-50.

CAPÍTULO VIII

Normograma volumétrico da aurícula esquerda em fase médio-diastólica

Aplicabilidade a doentes com fibrilhação auricular

RESUMO

Este capítulo aborda um dos objetivos desta tese: a criação de um normograma que permita a caracterização da avaliação volumétrica da aurícula esquerda, na fase cardíaca mais frequentemente utilizada para avaliação coronária — diástole média — 70% do intervalo RR. Procurámos ainda determinar uma medida prática (rápida e fácil de se obter mesmo sem software dedicado), que apresente boa correlação com o volume auricular, por forma a tornar eficiente a avaliação volumétrica da aurícula esquerda em qualquer TC cardíaco.

O normograma foi testado nos dados obtidos nos doentes com fibrilhação auricular, tendo sido construído uma regressão entre o volume em fase médio-diastólica (a 70% do intervalo RR) e o volume máximo.

Este trabalho resultou num artigo original submetido a uma revista indexada internacional, incluído em anexo neste capítulo.

ARTIGO SUBMETIDO

Reference mid-diastolic left atrium volume by ECG gated computed tomography angiography (CTA) and its utility in atrial fibrillation patients.

Marques, **H**; Ferreira, AM; Adragão, P; Lopes, J.; Radu, L.; Goyri O'Neill, JE; Pisco, JM; Araújo Gonçalves, P.

submetido ao *The International Journal of Cardiovascular Imaging*

SUMÁRIO

8.1. INTRODUÇÃO

A dimensão e a função da AEsq variam com a disfunção diastólica VEsq, com a cardiopatia isquémica, com diversos tipos de miocardiopatias e com a patologia valvular.

São poucas as medições em Cardiologia com um impacto tão amplo como o da dimensão da AEsq, que está independentemente associada ao risco de:

- FA e à sua recorrência;
- eventos tromboembólicos;
- insuficiência cardíaca;
- enfarte do miocárdio;
- causa de morte cardiovascular.

Assim sendo, uma adequada avaliação da AEsq é importante para o diagnóstico clínico, estratificação de risco e monitorização terapêutica.
O seu valor prognóstico em relação à população geral, aplica-se também a doentes com patologia cardíaca (1-13).
Em doentes com FA, o volume da aurícula esquerda é mais importante preditor de sucesso da terapêutica ablativa percutânea do que o próprio tipo de fibrilhação.

A avaliação dimensional da AEsq é geralmente efetuada por ecocardiografia com dimensões bidimensionais (14) usadas para extrapolar o volume.
Apesar das diversas técnicas de medição da AEsq, esta foi sempre considerada problemática. Atualmente a avaliação volumétrica por RM é tida como *gold standard*, correlacionando-se, em modo decrescente, com a TC, a ecografia 3D e a ecografia 2D sendo que a ecografia tende a subestimar a verdadeira dimensão (5, 15).

Os padrões da normalidade definidos para a AEsq têm por base o seu volume máximo, que se atinge na porção terminal do tempo sistólico do VEsq (normalmente próximo dos 40% do intervalo entre ondas R consecutivas — RR).

Tem havido um rápido crescimento do número de exames de TC cardíaco, sobretudo para avaliação de doença coronária, acompanhando o evoluir das indicações tidas como apropriadas, havendo *guidelines,* como por exemplo as do NICE (*National institute for health and care excellence*) do Reino Unido, que consideram a TC cardíaca para avaliação coronária (em aparelho com pelo menos 64 cortes) como o exame de primeira linha em todos os doentes com dor torácica que possa ser de etiologia cardíaca (independentemente da probabilidade pré-teste de doença cardíaca) (16).
Nos exames de TC é possível avaliar outras estruturas cardíacas e extra-cardíacas, sendo possível medir a aurícula esquerda. No entanto, a tecnologia de TC mais avançada, associada aos novos protocolos, permite obter a informação necessária para avaliar as artérias coronárias com elevada acuidade apenas numa fase do ciclo (normalmente na diástole média — cerca de 70% do intervalo RR). Sem informação em telediástole e telesístole, não se pode fazer avaliação funcional, nem caracterizar dimensionalmente a aurícula esquerda por ausência de normogramas em fase médio-diastólica (igualmente ausentes para outras técnicas imagiológicas como a ecocardiografia e a ressonância magnética).

Neste capítulo tivemos por objetivo

- Definir o padrão da normalidade da dimensão da AEsq para a fase médio-diastólica (MD) do ciclo cardíaco
- Determinar uma medida prática (rápida e fácil de se obter mesmo sem software dedicado), que apresente boa correlação com o volume auricular, por forma a tornar eficiente a avaliação volumétrica da aurícula esquerda em qualquer TC cardíaco.
- Determinar a correlação entre o volume da AEsq em tempo MD e o volume máximo
- Determinar se o normograma e a correlação podem ser aplicados nos doentes com FA

8.2. MÉTODOS

As populações de estudo foram definidas no **Capítulo V**; o protocolo de aquisição definidos no **Capítulo VI** e a forma de avaliação dimensional no **Capítulo VII**.
Resumidamente:
Foram constituídos dois grupos: um constituído com doentes com FA (Grupo A1 — 145 doentes) e outro representativo da população normal (grupo B — 146 indivíduos saudáveis).

A **Figura 1** sumariza a constituição da população de doentes com FA

FIGURA 1

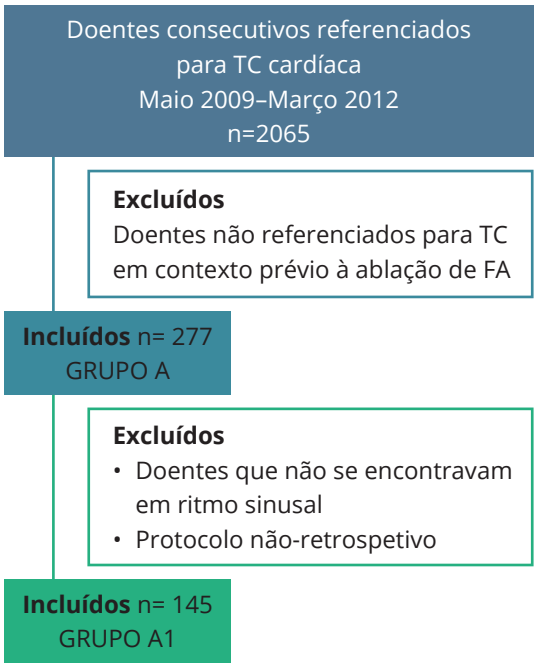

O Grupo B foi constituído da seguinte forma:
De um registo prospetivo de 2062 indivíduos que realizaram TC cardíaca de Maio de 2009 a final de Abril de 2012 — 3 anos, foram selecionados todos os indivíduos que seriam representativos de uma população "normal", por reunirem todas as seguintes condições:

> Sem doença cardíaca conhecida, incluindo doença valvular e doença coronária

- Sem hipertensão arterial — sem história de HTA, sem medicação para HTA e com a tensão arterial medida antes da realização da TC com valores sistólicos inferiores a 140mmHg e valores diastólicos inferiores a 90 mmHg
- Sem obesidade — com IMC <30kg/m^2
- Sem história de arritmia cardíaca e em ritmo sinusal durante a aquisição da TC
- Ecocardiograma normal, realizado num prazo inferior a 60 dias da data da TC (incluindo menção de : normal dimensão da aurícula esquerda, ausência de disfunção diastólica do VEsq e ausência de patologia valvular mitral)
- Com resultados da TC cardíaca que revelaram:
  - Ausência de doença coronária obstrutiva (estenoses máximas <50%)
  - Sem doença valvular na TC
  - Fracção de ejeção do VEsq preservada e sem disfunção segmentar.
  - Aurícula esquerda com volume máximo normal

No grupo resultante só haviam 74 mulheres pelo que, para manter o grupo com representação similar entre sexos, se selecionaram os primeiros 74 homens incluídos. Da população resultante 148, excluiram-se dois doentes (mulheres) por informação incompleta no arquivo de imagem.

A forma de obtenção das medidas de volume e das medidas de áreas e diâmetros relevantes para este estudo estão definidas no **Capítulo VII**.

A avaliação estatística utilizada está referenciada no **Capítulo VII**.

A variabilidade intra-observador, inter-obervador e inter-fases do ciclo cardíaco foi avaliada da forma definida no **Capítulo VII**.

8.3. RESULTADOS

Na tabela 1 estão reunidos os dados demográficos dos grupos de estudo

TABELA 1

Descrição da população em estudo.

	Grupo A1	**Grupo B**
N	145	146
Homens (n, %)	107 (73,8%)	74 (51%)
Idade na altura do procedimento (anos)*	57,04+/-12,42	45,41+/-12,97
Altura (cm)*	172,02+/-8,27	167,59+/-10,21
Peso (kg)*	79,41+7-12,95	71,73+7-14,07
ASC (m^2)*	1,94+7-0,19	1,82+/-0,22
IMC (kg/m^2)*	26,78+/-3,74	25,43+7-3,75

** média e desvio padrão*

No **Gráfico 1** (abaixo) visualizamos: em cima, as curvas do normograma do volume da aurícula esquerda a 70% do intervalo RR (intervalo de confiança a 95); nas curvas que se encontram a meio visualizamos as curvas por género; e na região inferior as curvas do volume indexado. O **Gráfico 2** (abaixo) é semelhante mas para a avaliação do volume máximo.

GRÁFICO 1

Avaliação gráfica em envelope do intervalo de confiança
a 95% do volume da AEsq a 70% do RR para a população normal

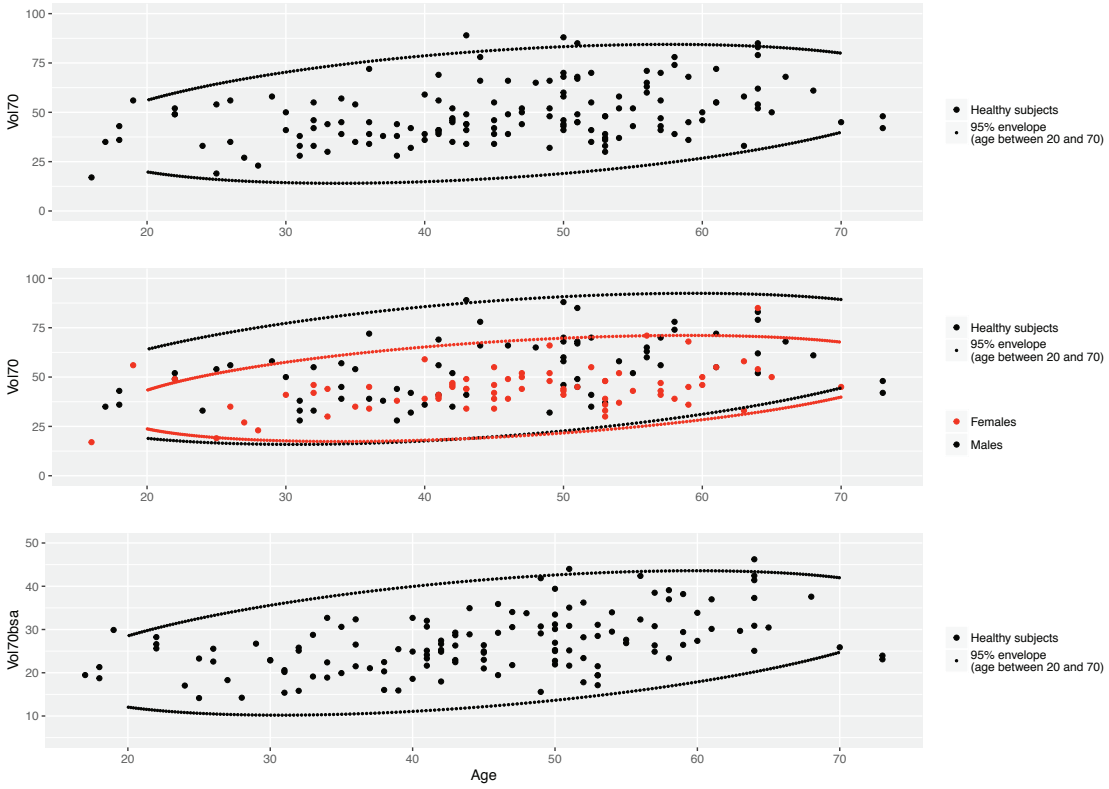

GRÁFICO 2

Avaliação gráfica em envelope do intervalo de confiança
a 95% do volume da AEsq máximo para a população normal

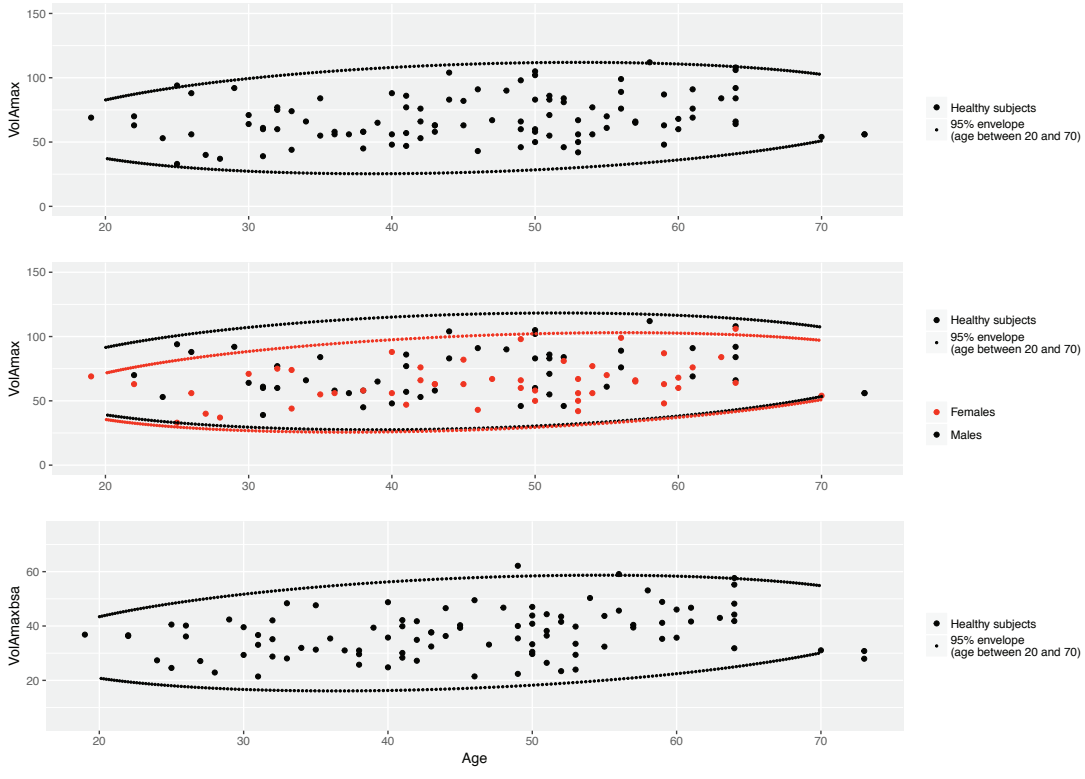

A **Tabela 2** apresenta o normograma do volume da AEsq a 70% por grupo etário dos 20 aos 70 anos e a **Tabela 3** o normograma do volume máximo da AEsq para o mesmo grupo.

TABELA 2

Apresenta os valores dos limites superiores e inferiores (intervalo de confiança 95) para o volume da AEsq médio-diastólico para toda a população normal e divididos por género. As últimas colunas apresentam os valores para o volume indexado à área de superfície corporal

Idade	VAEsq (70% do intervalo RR) U	VAEsq (70% do intervalo RR) L	VAEsq (70% do intervalo RR) Homens U	VAEsq (70% do intervalo RR) Homens L	VAEsq (70% do intervalo RR) Mulheres U	VAEsq (70% do intervalo RR) Mulheres L	VAEsq indexado (70% do intervalo RR) U	VAEsq indexado (70% do intervalo RR)L
20-29	70	14.3	76.9	15.8	57.3	17.6	35.5	10.2
30-39	78.5	14	85.4	15.8	65.1	17.3	39.8	10.1
40-49	83.1	14.8	90.7	17.7	69.6	18	42.5	11
50-59	84.4	19.1	92.4	22.8	71.1	21.6	43.5	13.6
60-69	84.2	26.9	92.4	31.3	71	28.5	43.5	17.9

U = limite superior do intervalo confiança 95%

L = limite inferior do intervalo confiança 95%

TABELA 3

Apresenta os valores dos limites superiores e inferiores (intervalo de confiança 95) para o volume da AEsq máximo para toda a população normal e divididos por género. As últimas colunas apresentam os valores para o volume indexado à área de superfície corporal

Idade	VAEsqMax U	VAEsqMax L	VAEsqMax Homens U	VAEsqMax Homens L	VAEsqMax Mulheres U	VAEsqMax Mulheres L	VAEsqMaxi U	VAEsqMaxi L
20-29	99.1	27.3	106.8	29.5	88.1	26.8	51.5	16.6
30-39	107.8	25.3	115.1	27.4	97.3	25.6	56.1	16.1
40-49	111.6	25.4	118.2	27.5	102	25.8	58.4	16.3
50-59	111.9	28.3	118.3	30.4	102.9	29.5	58.6	18.2
60-69	110.5	36.3	116.3	38.3	102.5	37.2	58.3	22.6

U = limite superior do intervalo confiança 95%

L = limite inferior do intervalo confiança 95%

Por forma a estimar os volumes máximos a partir de dados obtidos a 70% do intervalo RR, criámos 3 regressões da seguinte forma:

No Grupo B – representante de indivíduos normais

1 — Prever o VAEsqMax a partir do VAEsq a 70%, incluindo a idade em anos, o sexo (0=masculino; 1 = feminino) e a ASC (m^2). Por regressão linear multivariável e seleção *stepwise*, o sexo e a ASC forma excluídos do modelo.

VAEsqMAx = 1,211xVAEsq a 70% - 0,216xidade + 18,992

R square = 0,876 e VAEsq a 70% e Idade correlacionados com o VAEsqMax com p<0,000.

Standard error of estimate – 6,375

2 — Prever o VAEsqMax a partir da idade em anos, o sexo (0=masculino; 1 = feminino) e a ASC (m^2); a maior área da AEsq em plano axial estrito, o maior diâmetro ântero-posterior e látero-lateral da AEsq no plano da área axial máxima; a altura máxima no plano sagital; a área da AEsq em plano 4 câmaras e os maiores diâmetros bi-perpendiculares da AEsq no plano 4 câmaras.

Por regressão linear multivariável e seleção *stepwise*, todos os fatores foram excluídos excepto a maior área em plano axial, a altura em plano sagital e a idade.

VAEsqMAx = 3,688xárea máxima axial + 1,174xaltura máxima sagital – 0,166xidade – 41,750

R square = 0,770 e a área axial máxima e a altura máxima sagital, correlacionados com o VAEsqMax com p<0,000.

Standard error of estimate — 8,628

No Grupo A1 – doentes com FA

3 — Prever o VAEsqMax a partir do VAEsq a 70%, incluindo a idade em anos, o sexo (0=masculino; 1 = feminino) e a ASC (m^2). Por regressão linear multivariável e seleção *stepwise*, o sexo e a ASC forma excluídos do modelo.

VAEsqMAx = 0,867xVAEsq a 70% - 0,112xidade + 29,632

R square = 0,856 e VAEsq a 70% e Idade correlacionados com o VAEsqMax com p<0,000.

Standard error of estimate — 12,556

Para avaliar a utilidade da aplicabilidade dos normogramas criados na população normal nos doentes com FA fizemos a avaliação da sensibilidade e especificidade tendo por base a classificação real pelo volume máximo *vs* a classificação efetuada com base no volume a 70% do RR de forma dicotómica (acima e abaixo do limite superior do intervalo de confiança a 95%).

Utilizando os valores das tabelas obtivemos uma sensibilidade de 98% e uma especificidade de 66%

Ao utilizar os dados do **Gráfico 1** — a sensibilidade é de 100% e a especificidade de 81,5%.

Variabilidade intra-observador, inter-obervador e inter-fases do ciclo cardíaco

Esta avaliação foi efetuada por *average measure correlation*, tendo-se verificado mínima variabilidade, com coeficientes de *reliability* altos de 0,999; 0,998; 0,998.

8.4. DISCUSSÃO

A dilatação da AEsq tem valor prognóstico independente e a sua dilatação poderá estar relacionado com diagnóstico alternativo que poderia explicar os sintomas dos doentes referenciados para TC cardíaca para avaliação das coronárias. Assim e como cada vez mais estes exames contêm informação cardíaca apenas em fase MD, a possibilidade da caracterização dimensional da aurícula esquerda nesta fase do ciclo é importante e efetuada sem radiação ou custo adicionais.
Há apenas um estudo que define um normograma para a aurícula esquerda na fase de MD, no entanto tem por base uma amostra 40% menor; não apresenta indexação etária da população referência (tida como normal); não foi excluída doença valvular latente ou disfunção diastólica do VEsq por ecocardiografia; não foi estudada a aplicabilidade do normograma em doentes com FA (aspeto que apresenta maior relevância nestes doentes, dado o volume da AEsq ser marcador independente de prognóstico e ser o principal fator que se correlaciona com o risco de recidiva da terapêutica ablativa percutânea) (17).
O nosso normograma apresenta intervalos de confiança menores e valores de limite máximo mais aproximados com os do *gold standard* — RM (15), reflectindo muito provavelmente uma maior "normalidade" da nossa amostra.

Foi possível criar uma regressão com boa precisão para estimar o volume máximo a partir de dados obtidos a 70% do intervalo RR, quer tendo por base o volume, quer dados mais fáceis de obter como a idade, a área axial máxima e a altura sagital máxima da AEsq. Esta regressão é um contributo para, de forma eficiente e sem necessitar de softwares de pós-processamento, ser possível avaliar o volume auricular máximo em todo e qualquer estudo de TC cardíaco para avaliar coronárias.

Verificámos ainda a aplicabilidade do nosso normograma a 70% do RR nos doentes com FA (ainda não avaliado em publicações prévias). Verificámos uma ótima capacidade para identificar doentes com FA com AEsq dilatadas com sensibilidades de 98% (utilizando a tabela 2) e de 100% (utilizando o gráfico 1).

8.5. CONCLUSÃO

Estabelecemos, com base na maior amostra analisada, o padrão de normalidade do volume da aurícula esquerda em fase médio-diastólica e verificámos uma ótima relação entre esses volumes e os volumes máximos.

Desenvolvemos uma forma eficiente de estimar o volume máximo da AEsq com base em medidas facilmente obtidas na fase médio-diastólica, como a área axial máxima e a altura sagital máxima, podendo ser utilizado para avaliar dimensionalmente a AEsq em qualquer exame de coronariografia por TC.

Verificámos que o normograma proposto identifica adequadamente indivíduos com FA que apresentem volumes auriculares aumentados, aspeto que tem relevância clínica e prognóstica.

BIBLIOGRAFIA

1. Beinart R, Boyko V, Schwammenthal E, et al. Long-term prognostic significance of left atrial volume in acute myocardial infarction. J Am Coll Cardiol. 2004;44(2):327-34.
2. Dini FL, Cortigiani L, Baldini U, et al. Prognostic value of left atrial enlargement in patients with idiopathic dilated cardiomyopathy and ischemic cardiomyopathy. Am J Cardiol. 2002;89(5):518-23.
3. Hoit BD. Left atrial size and function: role in prognosis. J Am Coll Cardiol. 2014;63(6):493-505.
4. Kizer JR, Bella JN, Palmieri V, et al. Left atrial diameter as an independent predictor of first clinical cardiovascular events in middle-aged and elderly adults: the Strong Heart Study (SHS). Am Heart J. 2006;151(2):412-8.
5. Kuhl JT, Lonborg J, Fuchs A, et al. Assessment of left atrial volume and function: a comparative study between echocardiography, magnetic resonance imaging and multi slice computed tomography. Int J Cardiovasc Imaging. 2012;28(5):1061-71.
6. Melenovsky V, Borlaug BA, Rosen B, et al. Cardiovascular features of heart failure with preserved ejection fraction versus nonfailing hypertensive left ventricular hypertrophy in the urban Baltimore community: the role of atrial remodeling/dysfunction. J Am Coll Cardiol. 2007;49(2):198-207.
7. Meris A, Amigoni M, Uno H, et al. Left atrial remodelling in patients with myocardial infarction complicated by heart failure, left ventricular dysfunction, or both: the VALIANT Echo study. Eur Heart J. 2009;30(1):56-65.
8. Moller JE, Hillis GS, Oh JK, et al. Left atrial volume: a powerful predictor of survival after acute myocardial infarction. Circulation. 2003;107(17):2207-12.
9. Nistri S, Olivotto I, Betocchi S, et al. Prognostic significance of left atrial size in patients with hypertrophic cardiomyopathy (from the Italian Registry for Hypertrophic Cardiomyopathy). Am J Cardiol. 2006;98(7):960-5.
10. Reed D, Abbott RD, Smucker ML, et al. Prediction of outcome after mitral valve replacement in patients with symptomatic chronic mitral regurgitation. The importance of left atrial size. Circulation. 1991;84(1):23-34.
11. Rossi A, Cicoira M, Florea VG, et al. Chronic heart failure with preserved left ventricular ejection fraction: diagnostic and prognostic value of left atrial size. Int J Cardiol. 2006;110(3):386-92.

12. Rossi A, Cicoira M, Zanolla L, et al. Determinants and prognostic value of left atrial volume in patients with dilated cardiomyopathy. J Am Coll Cardiol. 2002;40(8):1425.
13. Takx RAP, Vliegenthart R, Schoepf UJ, et al. Prognostic value of CT-derived left atrial and left ventricular measures in patients with acute chest pain. European journal of radiology. 2017;86:163-8.
14. Costa FM, Ferreira AM, Oliveira S, et al. Left atrial volume is more important than the type of atrial fibrillation in predicting the long-term success of catheter ablation. Int J Cardiol. 2015;184:56-61.
15. Maceira AM, Cosin-Sales J, Roughton M, et al. Reference left atrial dimensions and volumes by steady state free precession cardiovascular magnetic resonance. J Cardiovasc Magn Reson. 2010;12:65.
16. Moss AJ, Williams MC, Newby DE, et al. The Updated NICE Guidelines: Cardiac CT as the First-Line Test for Coronary Artery Disease. Current cardiovascular imaging reports. 2017;10(5):15.
17. Walker JR, Abadi S, Solomonica A, et al. Left-sided cardiac chamber evaluation using single-phase mid-diastolic coronary computed tomography angiography: derivation of normal values and comparison with conventional end-diastolic and end-systolic phases. European radiology. 2016;26(10):3626-34.

ANEXOS

ARTIGO SUBMETIDO

Reference mid-diastolic left atrium volume by ECG gated computed tomography angiography (CTA) and its utility in atrial fibrillation patients.

Marques, **H**; Ferreira, AM; Adragão, P; Lopes, J.; Radu, L.; Goyri O'Neill, JE; Pisco, JM; Araújo Gonçalves, P.

submetido ao *The International Journal of Cardiovascular Imaging*

Artigo submetido ao *The International Journal of Cardiovascular Imaging*

The International Journal of Cardiovascular Imaging

Reference mid-diastolic left atrium volume by ECG gated computed tomography angiography (CTA) and its utility in atrial fibrillation patients.

--Manuscript Draft--

Manuscript Number:	
Full Title:	Reference mid-diastolic left atrium volume by ECG gated computed tomography angiography (CTA) and its utility in atrial fibrillation patients.
Article Type:	Original Article
Keywords:	Cardiac computed tomography; left atrium; mid-diastole; volume; reference values; atrial fibrillation; nomogram
Corresponding Author:	Hugo Marques, M.D. Hospital da Luz Lisboa, PORTUGAL
Corresponding Author Secondary Information:	
Corresponding Author's Institution:	Hospital da Luz
Corresponding Author's Secondary Institution:	
First Author:	Hugo Marques, M.D.
First Author Secondary Information:	
Order of Authors:	Hugo Marques, M.D.
	António Miguel Ferreira
	Pedro Adragão
	João Lopes
	Lucian Radu
	João Goyri ONeill
	João Pisco
	Pedro Araújo Gonçalves
Order of Authors Secondary Information:	
Funding Information:	
Abstract:	Purpose With newer scanner technology, image acquisition in coronary CT angiography (CCTA) tends to be performed only at mid-diastole. The aims of this study were 1) to provide reference values for left atrium (LA) mid-diastolic volume (MDV); 2) to assess whether and how can LA end-systolic volume (ESV) be derived from simple MD measurements; 3) assess the diagnostic accuracy of the resulting reference values in a population of patients with atrial fibrillation (AF). Methods The study group consisted of 146 individuals without know cardiovascular disease and normal findings on CCTA, and 145 patients with AF undergoing CCTA prior to ablation. End-diastolic, ES and MD LA volumes were measured. Mahalanobis distance was used to create a 95% envelop of the normal group in a space age by volume and determine upper and lower limits of normal. Results The mean LAMDV in normal subjects was 27.0 ml/m2 (95% limits 12.5-41.5) and 26.7 ml/m2 (95% limits 14.7-38.7) for men and women, respectively. LAMDV correlated closely to ESV and could accurately predicted LAESV by a regression equation both in

cont.

Artigo submetido ao *The International Journal of Cardiovascular Imaging*

	normal and AF populations (R2>0.8, p<0,001). LAMDV indexed nomogram by age can predict LAESV enlargement in AF population with a sensibility of 100%. Conclusions This study provides reference values for mid-diastolic LA volume adjusted by age, gender and BSA. End-systolic LA volume can be accurately predicted from simple mid-diastolic measurements both in normal subjects and AF patients. This benchmark can accurately be used to access LA volume enlargement in AF patients.

cont.

Artigo submetido ao *The International Journal of Cardiovascular Imaging*

Introduction:

Left atrium (LA) size provides important prognostic information, both in general population and in the setting of heart disease [1-6]. LA size is usually assessed by echocardiography, using 2D measures in specific cardiac planes at end-systolic (ES) phase, with LA volume often extrapolated from these measurements.

Coronary CT angiography (CCTA) has become a fast growing non-invasive test for ruling out coronary artery disease. CCTA allows for extra-coronary cardiac evaluation, with very accurate chamber size measurements when compared to MRI [7] [8]. Current reference values for LA volumes in CCTA were determined for ES and end-diastolic (ED) phases. However, with newer scanner technology, image acquisition tends to be performed only at mid-diastole (MD) in order to minimize radiation exposure [9]. So, with no ES and ED images, chamber function cannot be assessed and LA measurements lack suitable reference values.

The aims of this study were 1) to provide reference values for mid-diastolic LA volume (at 70% of the cardiac cycle) relative to gender, age and body surface area (BSA); 2) to assess whether and how can ES LA volume be accurately derived from simple MD measurements; 3) assess the diagnostic accuracy of the resulting reference values in a population of patients with atrial fibrillation (AF).

cont.

Artigo submetido ao *The International Journal of Cardiovascular Imaging*

Materials and Methods:

Study Population

Normal subjects group:

From a population of 2062 consecutive subjects undergoing CCTA for suspected coronary artery disease (CAD) between May 2009 and April 2012, we selected consecutive individuals who fulfilled the inclusion criteria and had the exam done with retrospective ECG gating.

The criteria that defined our "normal" group were: 1) normal echocardiogram less than 60 days before CCTA (including no LA enlargement, no left ventricular diastolic dysfunction and no mitral valve disease); 2) no known heart disease (including valvular diseases or CAD); 3) no know history of hypertension or anti-hypertensive medication (including systolic blood pressure <140mmHg and diastolic blood pressure <90 mmHg at the time of CCTA); 4) body mass index < 30 kg/m2; 5) no history of arrhythmias; 6) sinus rhythm during CCTA; 7) no evidence of structural heart disease or obstructive CAD (> 50% stenosis) on CCTA. Two of the patients were excluded because of incomplete imaging archive data, yielding a final population of 146 normal subjects.

AF patients group (AF Group):

From 277 consecutive patients undergoing CCTA prior to AF ablation between May 2009 and April 2012, we selected 145 who were in sinus rhythm during image acquisition and had the exam performed with retrospective ECG gating.

The study was approved by the local ethics committee and all patients gave written informed consent.

CCTA acquisition

CCTA was performed on a dual-source 64-slice first generation scanner (Somatom Definition ®, Siemens, Germany), with a native temporal resolution of 83ms.

Normal Group CT protocol:

In the absence of contra-indications, IV metoprolol was used prior to image acquisition whenever the heart rate was above 70 bpm (5mg every 3 min until target heart rate (HR) of 70bpm or total metoprolol dose of 25 mg). All patients whose systolic blood pressure was above 100mmHg received 5mg of sublingual nitroglycerine. Image acquisition was done with retrospective gating with tube current modulation to reduce radiation outside 40-80% of the RR interval if HR was between 70-80 beats per minute (bpm), outside 70-80% of the RR interval if HR below 70bpm and outside 40-50% of the RR interval if HR >80bpm.

Tube voltage was set to 100kV, except for patients with BMI < 18.5 Kg/m^2, where tube voltage was changed to 80kV. We used a "bolus tracking" technique, with trigger set at 120HU on the ascending

cont.

Artigo submetido ao *The International Journal of Cardiovascular Imaging*

aorta. A triphasic IV contrast protocol was used (320mgI/ml) with volumes calculated as follows: 1st phase of 100% contrast with volume = (time of acquisition + 7seconds - waiting time between bolus tracking and breathing instructions) x 7 (flow rate); 2nd phase with 30 ml of a mix with 30% contrast and 70% saline; 3rd phase with 30 ml of 100% saline.

AF Group CT protocol:

No beta-blockers or nitroglycerine were used. Acquisition was done with retrospective gating with tube current modulation to reduce radiation. If HR<70bpm, maximal dose at 70% of the RR, if HR 70-80bpm maximal dose between 40-80% of the RR interval, and if HR >80bpm, maximal dose between 40-50% of the RR interval.

Tube voltage was set to 100kV, except for patients with BMI < 18.5 Kg/m^2 or > 30 Kg/m^2, where 80kV and 120kV were used, respectively. We used a "bolus tracking" technique, with trigger set at 150 HU on the ascending aorta, together with a triphasic IV contrast protocol defined as above, but with a lower flow rate of 6ml/s.

Calculation of LA size

Images were reconstructed at every 10% of the RR interval (10 phases of axial data from 0-90% of the RR interval) with 1.5 mm thickness and 0.7mm increment, 256x256 matrix, using filtered back projection reconstruction and a medium smooth convolution kernel (B25f). The phase showing maximal atrial volume was identified from visual assessment of the different series (mitral valve opening and LA size). Mid diastolic phase was set at 70% of the RR interval. Volumes were generated by voxel count by manually drawn left atrium endocardial contours in contiguous axial planes, excluding the left atrium appendage and the pulmonary veins.

We also measured LA areas in the 4-chamber and transverse axial planes. The largest LA diameters were also measured in transverse axial plane (latero-lateral and antero-posterior) and in the sagittal plane (largest craniocaudal diameter – maximal height in sagittal plane). These measurements in axial and sagittal planes were chosen for their simplicity, since they can be easily done very quickly and without need for special software. (figure 1). A radiologist with large experience in CCTA (HM) analyzed all scans on an Aquarius workstation (Terarecon Inc., Foster City, California, USA) according to current Society for Cardiovascular Computed Tomography and European Society for Cardiovascular Radiology guidelines.

Inter-observer, intra-observer, and interphase variability

To test inter-observer variability two readers (the radiologist and a radiology technician with experience in cardiac CT) both measured, independently, the LA volumes of 30 patients. To test intra-observer variability, the radiologist measured the LA volumes of 10 patients 3 times (2 days apart and blinded for previous results). Interphase variability was assessed by measuring LA volumes of 30 consecutive patients both on 70% and on an additional reconstruction made at 75% of the RR interval.

cont.

Artigo submetido ao *The International Journal of Cardiovascular Imaging*

Categorical variables are presented as number and percentage, andcontinuous variables as mean ± SD. Unpaired t test and Fisher exact test were used to compare continuous and categoricaldata, respectively. Mahalanobis` distance was used to create a 95% envelop of LA volumes (mid-diastolic and end-systolic) for the normal group in the age-volume space and determine upper and lower limits of normal.

The ability to predict end-systolic LA volume from mid-diastolic LA volume was assessed using multivariable linear regression analysis further including age, BSA, and a stepwise selection for gender. The capability of extrapolating end-systolic LA volumes using 2D measures (area and diameters in the axial and 4-chamber planes, and LA height in the sagittal plane) was evaluated by multivariable linear regression including these measurements, age, and gender, in a stepwise selection with $p<0.10$ as criterion.. The correlation between predicted and observed LA volumes was assessed by Pearson's correlation coefficient. Finally, indexed mid-diastolic and end-systolic LA volumes of AF patients were categorized into dichotomous variables (above or below the upper limit of reference in normal subjects), allowing the calculation of sensitivity, specificity, positive and negative predictive values for the mid-diastolic cut-offs. The level of agreement between categorized mid-diastolic and end-systolic indexed LA volumes was also assessed using Cohens K coefficient.

All analyses were performed with Statistical Pack for Social Sciences version 12.0 (SPSS Inc., Chicago, Illinois). Statistical significance was set at two-tailed $p<0.05$.

cont.

Artigo submetido ao *The International Journal of Cardiovascular Imaging*

RESULTS

Baseline characteristics of "normal" and AF groups are summarized in table 1.

Normal values

We depicted the MD nomogram both on graph (figure2) and on table (table 2 and 3) with normal reference absolute and indexed (to BSA) values by age and gender.

The mean left atrium MD volume indexed (LAMDVI) was 26,9ml/m2 with 6,8ml/m2 of standard deviation, with a 95% confidence interval of (13,6 – 40,2)

We also created a nomogram for maximal left atrium volume based on the same population. This results are presented in the same way as above, in figure 3 and table 2 and 3., with mean ES volume indexed (LAESVI) of 37,5ml/m2 with 8,7ml/m2 of standard deviation, with a 95% confidence interval of (20,4 – 54,6).

Relationship between mid –diastole data and maximum volumes

For the normal group we estimated maximum volumes from MD data in two different ways:

One included the MD volume information and age. The other included only maximal area in axial plane and maximal craniocaudal diameter in sagittal plane, as well as age.

For the AF group we estimated ES volumes based on MD volumes and age.

All multivariable linear regressions showed a strong relationship between MD and ES volumes, with high correlation coefficients (R = 0,876; 0,770 and 0,856 respectively) and small standard error of the estimate (SEE) (6.375ml; 8,628ml and 12.556ml, respectively (table 4).

Estimated volumes were compared with actual ES volumes with Blant-Altman analysis demonstrating a tight fit with no evidence of a systematic difference between Measured and Predicted LAESV for all groups (figure 4-6), and 95% confidence interval of +/- 12,3ml for normal population including MD volume information; +/- 16,4ml for normal population without including MD volume information and +/- 25,7ml for AF patients including MD volume information on the regression

Ability of MD nomogram to detect left atrium ES volume enlargement in AF patients

Indexed volumes LAMDVI and lAESVI for all FA subjects were categorized into dichotomous variables, above or below the upper limit reference values form table 2

With this method increased LAMDVI detected increased LAESVI in 53/54 cases, giving a sensitivity of 98% and specificity of 66% (50/76).

cont.

Artigo submetido ao *The International Journal of Cardiovascular Imaging*

(88/108).

Using our nomogram we over predicted LAESVI in AF patients, that resulted in some false positives but very few or none (depending on the method used) false negative

Interobserver, intraobserver, and interphase variability.

Interobserver, intraobserver and interphase variability was accessed by average measure correlation, with very good results, with measured reliability coefficient of 0,998, 0,999 and 0,998, respectively

cont.

Artigo submetido ao *The International Journal of Cardiovascular Imaging*

DISCUSSION

The increased utilization of prospective CCTA, with acquisition only at MD, hampers the ability of functional and chamber size evaluation, sacrificing its potential prognostic information.
Prospective gating (which includes several types of acquisitions such as single heart beat with full heart coverage detector or with very high pitch – "FLASH acquisition") has resulted in significant less radiation exposure [10] with no impact in the exam accuracy [11], so this type of scan protocols with lower radiation and without information on all RR interval are now recommended whenever possible [12], and by far the most used.

Left atrium size has independent prognostic value, and left atrium dilatation may be related to alternative diagnosis (in the absence of obstructive CAD by CCTA) that could help explain the symptoms that prompted the CT in the first place.
So the ability of assessing LA size with measures done only in MD would be clinically relevant, and at no extra cost.

We have provided a left atrium volume nomograms at MD and ES, both absolute and indexed to BSA, as well as by age and gender.

Lin et al [13] published normal left atrium ES volumes are higher and with a wider confidence interval than ours, probably due to inclusion of left atrium appendage on the atrium volume, and a less strict "normality" definition of the normal subjects studied.

A recent study by Walker et al [14] assessed normal values for MD left atrium volumes and its ability to detect chamber enlargement, but there was no age group indexation and latent valvular disease and left ventricular diastolic dysfunction were not excluded by cardiac ultrasound. "Normal" group size was 40% smaller. The applicability of that information to AF patients was not tested.
Our results are consistent with CT and CMR reference values for normal maximum size of the left atrium [15,13] and similar to those for mid diastole reported by Walker[14]. Nevertheless, being MR the gold standard for volume, our results correlate closely to that of MR published by Maceira et al (23) than the ones previously published by Walker and the confidence intervals are smaller, probably because of a better definition of "normality" of the normal group.
As far as we know our study is the largest to date to provide normal values and upper limits for left atrium size at MD in gated CTA, and the only one to provide it by age group.

We demonstrated that MD volumes correlate very well to ES volumes, both on the normal subjects group and in AF patients. This correlation in the AF population has special value as maximum volume is the main driver for AF ablation therapy failure [16,17].

cont.

Artigo submetido ao *The International Journal of Cardiovascular Imaging*

We also provided a accurate, easy and time-efficient way to determine LA ES volume from axial and sagittal MD reconstruction. This facilitates quantitative assessment of left atrium for the great majority of patients that undergo coronary CTA.

Lastly we tested the ability to use the nomogram in AF population to detect left atrium enlargement in AF patients and found a very high sensitivity 98-100%, with some false positives due to overestimation. When using the data by age group (table) specificity increased from 66% to 81,5%, probably because age is important in this estimation.

.

Limitations

Our MD volumes are gathered from 70% RR interval. We tested and found no significant variability between measures made at 70% to the ones at 75%, and this part of the cardiac cycle is used because of less cardiac motion, so measuring volumes in a slightly different MD phase reconstruction should incur significant differences in values.

Our normal subjects group were given sublingual nitroglycerin immediately before the CT scan that might reduce the preload, which might affect the LA size.

Conclusions

This study established normal LA dimensions at MD cardiac phase, adjusted by age, gender and BSA and creates a regression to predict maximum LA volume from MD data.

This benchmark can accurately be used to access LA dilation in AF patients with very high sensitivity.

BIBLIOGRAFIA

1. Beinart R, Boyko V, Schwammenthal E, Kuperstein R, Sagie A, Hod H, Matetzky S, Behar S, Eldar M, Feinberg MS (2004) Long-term prognostic significance of left atrial volume in acute myocardial infarction. J Am Coll Cardiol 44 (2):327-334. doi:10.1016/j.jacc.2004.03.062

2. Dini FL, Cortigiani L, Baldini U, Boni A, Nuti R, Barsotti L, Micheli G (2002) Prognostic value of left atrial enlargement in patients with idiopathic dilated cardiomyopathy and ischemic cardiomyopathy. Am J Cardiol 89 (5):518-523

3. Hoit BD (2014) Left atrial size and function: role in prognosis. J Am Coll Cardiol 63 (6):493-505. doi:10.1016/j.jacc.2013.10.055

cont.

Artigo submetido ao *The International Journal of Cardiovascular Imaging*

4. Kizer JR, Bella JN, Palmieri V, Liu JE, Best LG, Lee ET, Roman MJ, Devereux RB (2006) Left atrial diameter as an independent predictor of first clinical cardiovascular events in middle-aged and elderly adults: the Strong Heart Study (SHS). Am Heart J 151 (2):412-418. doi:10.1016/j.ahj.2005.04.031
5. Takx RAP, Vliegenthart R, Schoepf UJ, Nance JW, Bamberg F, Abro JA, Carr CM, Litwin SE, Apfaltrer P (2017) Prognostic value of CT-derived left atrial and left ventricular measures in patients with acute chest pain. European journal of radiology 86:163-168. doi:10.1016/j.ejrad.2016.11.013
6. Tsang TS, Abhayaratna WP, Barnes ME, Miyasaka Y, Gersh BJ, Bailey KR, Cha SS, Seward JB (2006) Prediction of cardiovascular outcomes with left atrial size: is volume superior to area or diameter? J Am Coll Cardiol 47 (5):1018-1023. doi:10.1016/j.jacc.2005.08.077
7. Grothues F, Smith GC, Moon JC, Bellenger NG, Collins P, Klein HU, Pennell DJ (2002) Comparison of interstudy reproducibility of cardiovascular magnetic resonance with two-dimensional echocardiography in normal subjects and in patients with heart failure or left ventricular hypertrophy. Am J Cardiol 90 (1):29-34
8. Koka AR, Gould SD, Owen AN, Halpern EJ (2012) Left atrial volume: comparison of 2D and 3D transthoracic echocardiography with ECG-gated CT angiography. Academic radiology 19 (1):62-68. doi:10.1016/j.acra.2011.08.017
9. Sun Z, Ng KH (2012) Prospective versus retrospective ECG-gated multislice CT coronary angiography: a systematic review of radiation dose and diagnostic accuracy. European journal of radiology 81 (2):e94-100. doi:10.1016/j.ejrad.2011.01.070
10. Sousa PJ, Goncalves PA, Marques H, Raposo L, Cale R, Brito J, Gaspar A, Machado FP, Roquette J (2010) Radiation in cardiac CT: predictors of higher dose and its reduction over time. Rev Port Cardiol 29 (11):1655-1665
11. Abbara S, Blanke P, Maroules CD, Cheezum M, Choi AD, Han BK, Marwan M, Naoum C, Norgaard BL, Rubinshtein R, Schoenhagen P, Villines T, Leipsic J (2016) SCCT guidelines for the performance and acquisition of coronary computed tomographic angiography: A report of the society of Cardiovascular Computed Tomography Guidelines Committee: Endorsed by the North American Society for Cardiovascular Imaging (NASCI). Journal of cardiovascular computed tomography 10 (6):435-449. doi:10.1016/j.jcct.2016.10.002
12. Maruyama T, Takada M, Hasuike T, Yoshikawa A, Namimatsu E, Yoshizumi T (2008) Radiation dose reduction and coronary assessability of prospective electrocardiogram-gated computed tomography coronary angiography: comparison with retrospective electrocardiogram-gated helical scan. J Am Coll Cardiol 52 (18):1450-1455. doi:10.1016/j.jacc.2008.07.048
13. Lin FY, Devereux RB, Roman MJ, Meng J, Jow VM, Jacobs A, Weinsaft JW, Shaw LJ, Berman DS, Callister TQ, Min JK (2008) Cardiac Chamber Volumes, Function, and Mass as Determined by 64-Multidetector Row Computed Tomography: Mean Values Among Healthy Adults Free of Hypertension and Obesity. JACC: Cardiovascular Imaging 1 (6):782-786. doi:https://doi.org/10.1016/j.jcmg.2008.04.015
14. Walker JR, Abadi S, Solomonica A, Mutlak D, Aronson D, Agmon Y, Lessick J (2016) Left-sided cardiac chamber evaluation using single-phase mid-diastolic coronary computed tomography angiography: derivation of normal values and

cont.

Artigo submetido ao *The International Journal of Cardiovascular Imaging*

comparison with conventional end-diastolic and end-systolic phases. European radiology 26 (10):3626-3634. doi:10.1007/s00330-016-4211-z
15. Maceira AM, Cosin-Sales J, Roughton M, Prasad SK, Pennell DJ (2010) Reference left atrial dimensions and volumes by steady state free precession cardiovascular magnetic resonance. J Cardiovasc Magn Reson 12:65. doi:10.1186/1532-429x-12-65
16. Costa FM, Ferreira AM, Oliveira S, Santos PG, Durazzo A, Carmo P, Santos KR, Cavaco D, Parreira L, Morgado F, Adragao P (2015) Left atrial volume is more important than the type of atrial fibrillation in predicting the long-term success of catheter ablation. Int J Cardiol 184:56-61. doi:10.1016/j.ijcard.2015.01.060
17. Mesquita JF, A.M.; Cavaco, D.; Costa, F.M.; Carmo, P.; Marques, H.; Morgado, F.; Mendes, Miguel; Adragão, P. (2017) Development and validation of a risk score for predicting atrial fibrillation recurrence after a first catheter ablation procedure – ATLAS score. Europace. doi:doi.org/10.1093/europace/eux265

cont.

Artigo submetido ao *The International Journal of Cardiovascular Imaging*

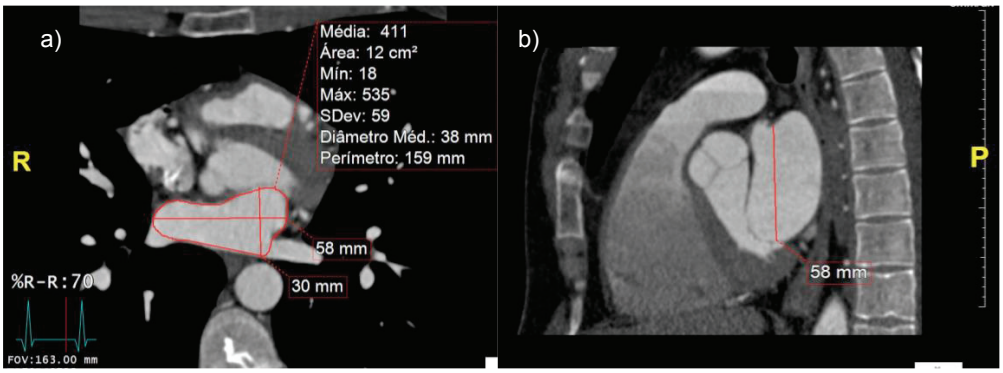

Figure 1 – measures in axial and sagittal planes
a) Drawing of the biggest LA area and maximal antero-posterior and latero-lateral diameters in axial plane.
b) Drawing of the biggest craniocaudal diameter in the sagittal plane

cont.

Artigo submetido ao *The International Journal of Cardiovascular Imaging*

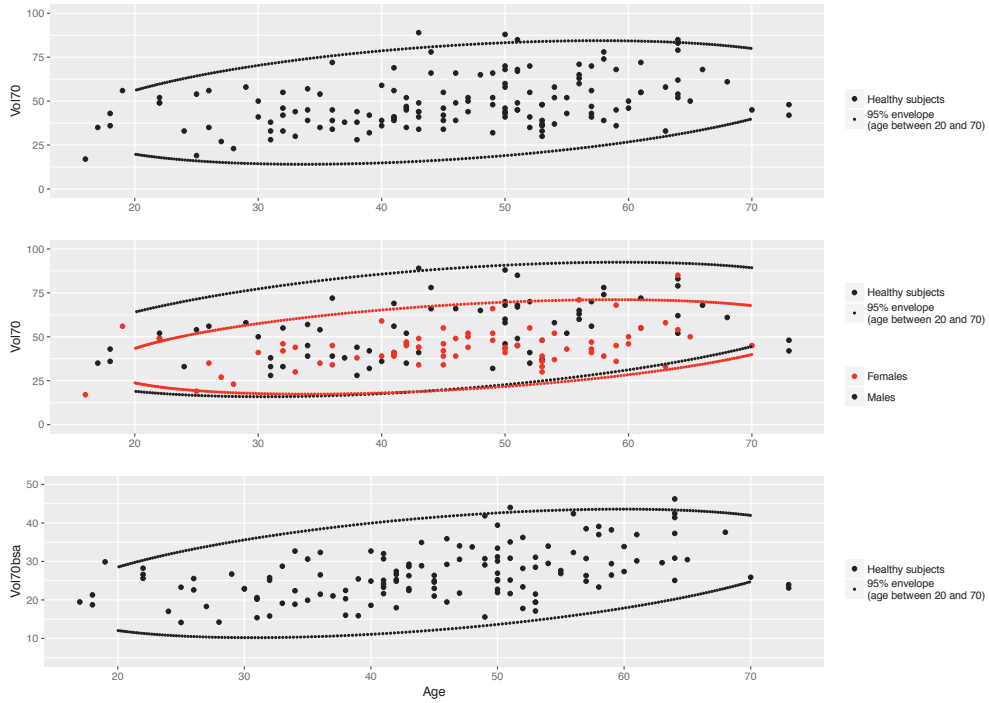

Figure 2 – Graph depicted nomogram for left atrium volume at MD
Above – Absolute LAMDV by age
Middle – Absolute LAMDV by age and gender
Under – LAMDVI (body surface area) by age

cont.

Artigo submetido ao *The International Journal of Cardiovascular Imaging*

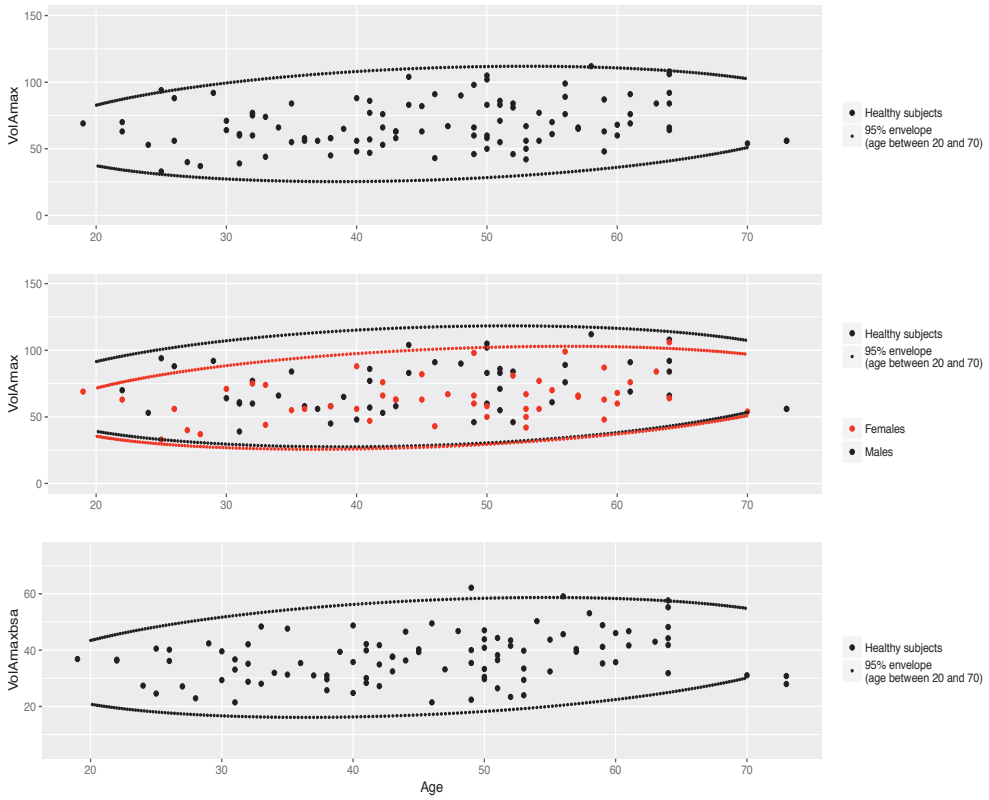

Figure 3 – Graph depicted nomogram for left atrium ES volume
Above – LAESV by age
Middle – LAESV by age and gender
Under – LAESVI by age

cont.

Artigo submetido ao *The International Journal of Cardiovascular Imaging*

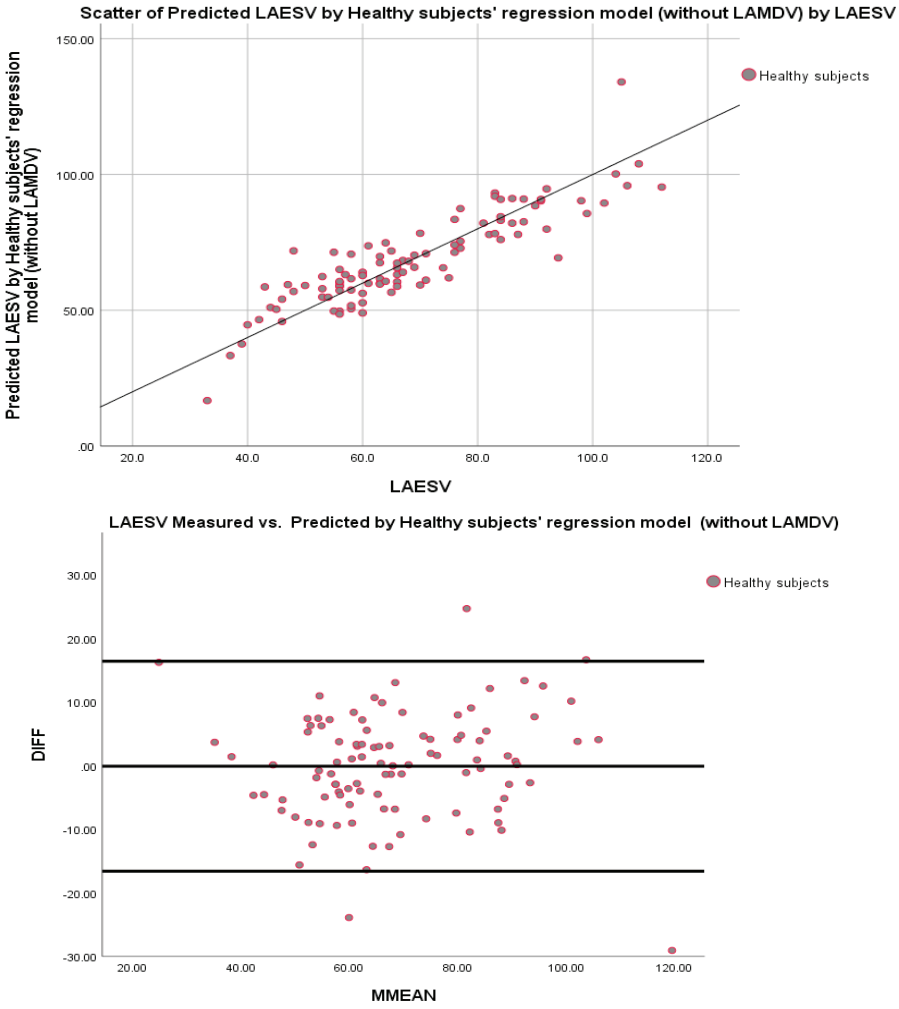

Figure 4 – Refers to the regression equation to predict LAESV from maximal LA area in axial plane and maximal craniocaudal diameter in sagittal plane (without LAMDV information) in the normal group.
The graph below shows a Bland-Altman plot comparing LAESV estimated with the real value

cont.

Artigo submetido ao *The International Journal of Cardiovascular Imaging*

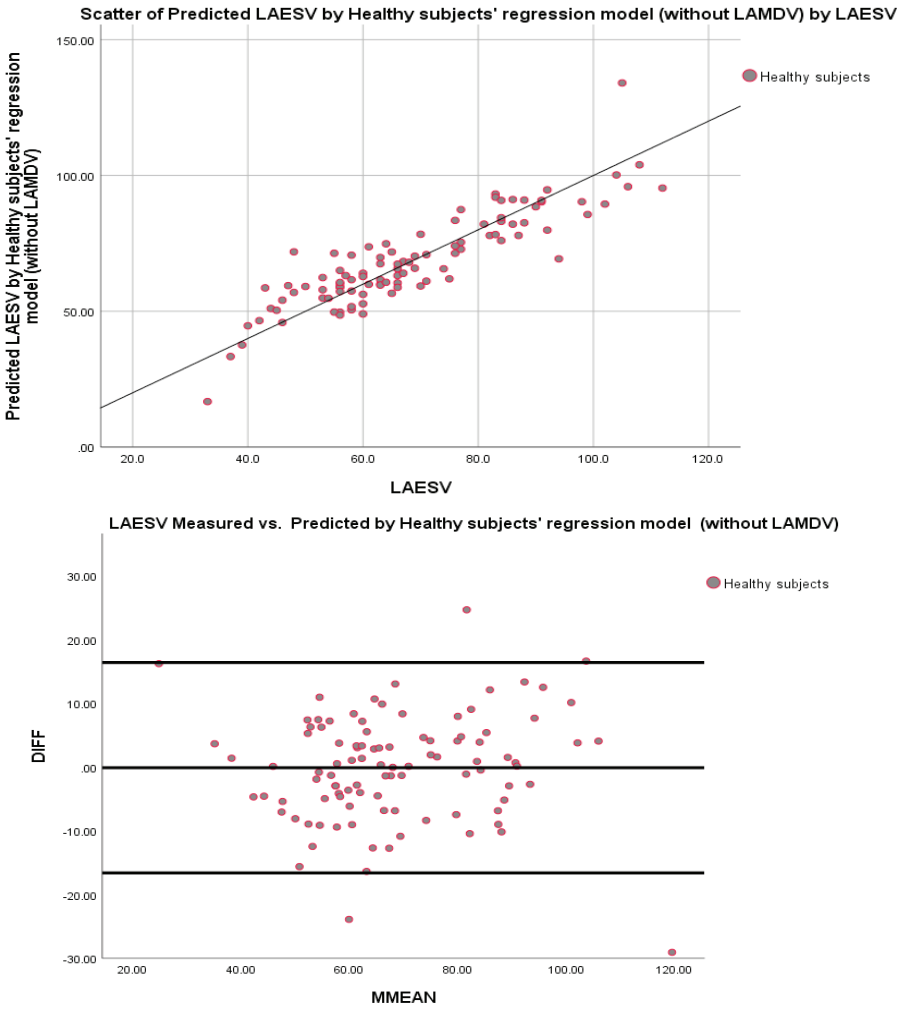

Figure 4 – Refers to the regression equation to predict LAESV from maximal LA area in axial plane and maximal craniocaudal diameter in sagittal plane (without LAMDV information) in the normal group.
The graph below shows a Bland-Altman plot comparing LAESV estimated with the real value

cont.

Artigo submetido ao *The International Journal of Cardiovascular Imaging*

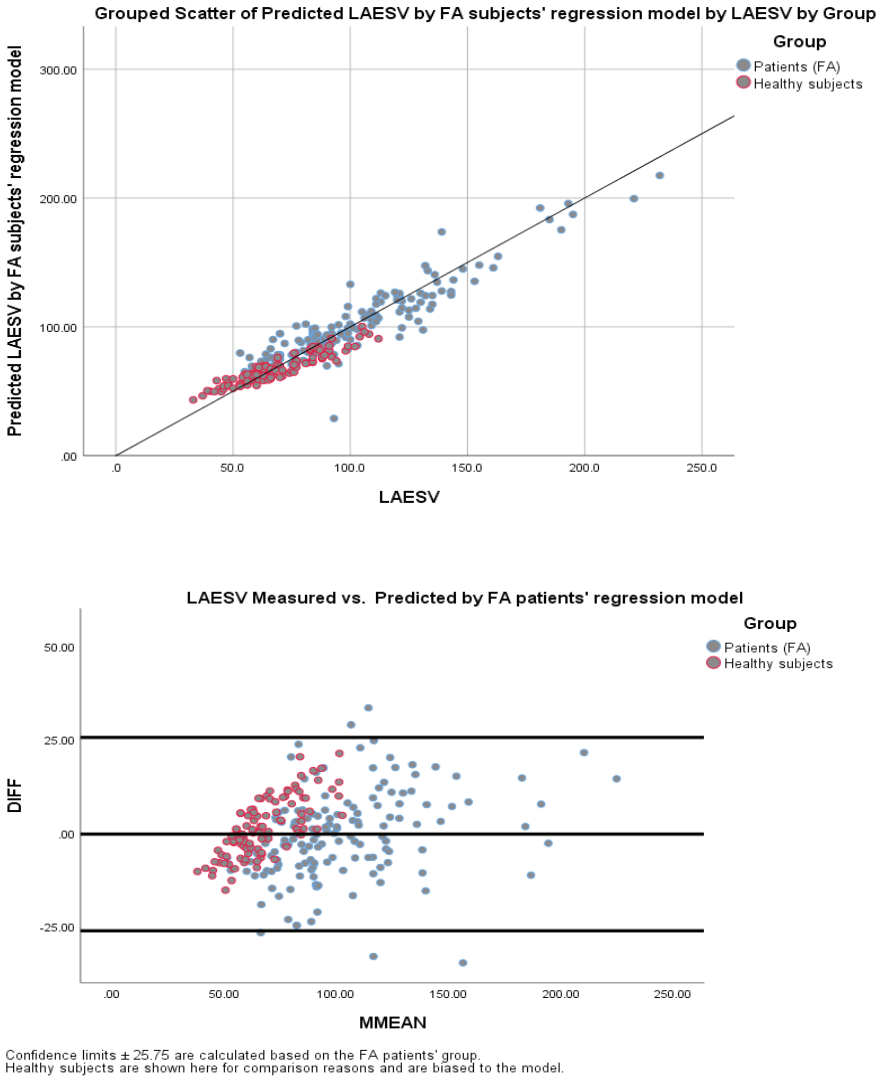

Figure 6 – Refers to the regression equation to predict LAESV from LAMDV in the AF group.
The graph below shows a Bland-Altman plot comparing LAESV estimated with the real value. We superimposed normal population for comparison.

cont.

Artigo submetido ao *The International Journal of Cardiovascular Imaging*

Table 1 – Population Characteristics

	Healthy ("normal") Subjects	AF Subjects
N	**146**	**145**
Males	**74 (51%)**	**107 (73.8%)**
Age (years)	45.41+/-12.97	57.04+/-12.42
Height (cm)	167.59+/-10.21	172.02+/-8.27
Weight (kg)	71.73+/-14.97	79.41+/-12.95
BSA (m^2)	1.82+/-0.22	1.94+/-0.19
BMI (kg/m^2)	25.43+/-3.75	26.78+/-3.74

BMI – body mass index
BSA – body surface area
AF – atrial fibrillation

cont.

Artigo submetido ao *The International Journal of Cardiovascular Imaging*

Table 2 – Normal reference values for LA measures

	All	Females	Males
LAMDV (ml)	49.1 [20.9 - 77.3]	44.2 [22.6 – 65.8]	53.8 [22.8 – 84.8]
Ax area at MD (cm^2)	15.8 [8.4 – 23.2]	14.4 [8.7 – 20.1]	17.1 [9.3 – 24.9]
Sag height at MD (mm)	51.3 [39.5 – 63.1]	50.2 [38.2 – 62.2]	52.4 [41.2 – 63.6]
LAESV (ml)	68.5 [33.8 – 103.2]	64.3 [33.3 – 95.3]	72.5 [36 – 109]
LAMDVI (ml/m^2)	26.9 [13.6 – 40.2]	26.7 [14.7 – 38.7]	27 [12.5 – 41.5]
LAESVI (ml/m^2)	37.5 [20.4 – 54.6]	38.1 [20.9 – 55.3]	36.9 [19.8 – 54]

LAMDV – left atrium mid diastolic volume
Ax area at MD – maximal LA area in axial plane at mid diastolic phase
Sag height at MD – maximal LA craniocaudal diameter in sagittal plane at mid diastolic phase
LAESV – left atrium end systolic volume
LAMDVI - left atrium mid diastolic volume indexed
LAESVI – left atrium end systolic volume indexed

cont.

Artigo submetido ao *The International Journal of Cardiovascular Imaging*

Table 3 – Reference values 95% confidence interval for LA volume

Age	LAMDV U (ml)	LAMDV L (ml)	LAMDV Male U (ml)	LAMDV Male L (ml)	LAMDV Female U (ml)	LAMDV Female L (ml)	LAMDVI U (ml/m2)	LAMDVI L (ml/m2)
20-29	70	14.3	76.9	15.8	57.3	17.6	35.5	10.2
30-39	78.5	14	85.4	15.8	65.1	17.3	39.8	10.1
40-49	83.1	14.8	90.7	17.7	69.6	18	42.5	11
50-59	84.4	19.1	92.4	22.8	71.1	21.6	43.5	13.6
60-69	84.2	26.9	92.4	31.3	71	28.5	43.5	17.9
Age	**LAESV U (ml)**	**LAESV L (ml)**	**LAESV Male U (ml)**	**LAESV Male L (ml)**	**LAESV Female U (ml)**	**LAESV Female L (ml)**	**LAESVI U (ml/m2)**	**LAESVI L (ml/m2)**
20-29	99.1	27.3	106.8	29.5	88.1	26.8	51.5	16.6
30-39	107.8	25.3	115.1	27.4	97.3	25.6	56.1	16.1
40-49	111.6	25.4	118.2	27.5	102	25.8	58.4	16.3
50-59	111.9	28.3	118.3	30.4	102.9	29.5	58.6	18.2
60-69	110.5	36.3	116.3	38.3	102.5	37.2	58.3	22.6

LAMDV – left atrium mid diastolic volume
LAESV – left atrium end systolic volume
LAMDVI - left atrium mid diastolic volume indexed
LAESVI – left atrium end systolic volume indexed
U – upper limit of 95% confidence interval
L – lower limit of 95% confidence interval

cont.

Table 4 – Regression Equations for estimating ESV (maximum volumes) from MD information

	Regression Equation	SEE	R
Normal Population	LAESV = 1.211*LAMDV -0.216*Age +18.992	6.375	0.876
Normal Population	LAESV = 3.688* Axarea +1.174* Sagheight - 0.166*Age - 41.750	8.628	0.770
AF Population	LAESV = 0.867*LAMDV - 0.112*Age +29.632	12.556	0.856

LAMDV – left atrium mid diastolic volume
LAESV – left atrium end systolic volume
Axarea – maximal LA area in axial plane
Sagheight – maximal LA height in sagittal plane

CAPÍTULO IX

Caracterização anatómica e funcional da Aurícula Esquerda nos doentes com FA e seu contributo prognóstico para prever o sucesso da terapêutica ablativa percutânea

RESUMO

Este capítulo faz a descrição da AEsq nos doentes com FA submetidos a realização de TC cardíaca num contexto prévio a ablação de FA. Estes doentes foram seguidos após a terapêutica ablativa e avaliado o seu sucesso.

Nos doentes em que foi possível obter informação funcional no exame de TC (aquisição retrospetiva), fez-se esta caracterização quer a nível da AEsq quer do AAEsq, sendo avaliado o *timing* de recidiva e a sua correlação com os parâmetros anátomo-funcionais disponíveis.

SUMÁRIO

9.1. INTRODUÇÃO E OBJETIVOS

Foi abordado no **Capítulo II** a relevância clínica da AEsq, bem como a sua correlação com a arritmia crónica mais frequente, a FA.
Conhece-se a relevância das alterações estruturais da parede da AEsq, no desenvolvimento da FA, na sua perpetuação e recidiva pós terapêutica (1).

O desenvolvimento embriológico da AEsq, com um componente a originar a "câmara" propriamente dita e as veias pulmonares, e outro a resultar no AAEsq, é o responsável pelas primeiras questões a abordar (2):

- Haverá nestes componentes disparidades de *remodeling* estrutural que condicionem a origem, desenvolvimento e perpetuação da fibrilhação auricular?
  - Haverá boa correlação entre os volumes da AEsq e do AAEsq ?
  - Haverá boa correlação entre a função da AEsq e a do AAEsq?

Esta modificação estrutural poderá ser o fator determinante do sucesso terapêutico, nomeadamente do tratamento ablativo percutâneo.
Assim, estudámos não só morfologia, mas igualmente a função da AEsq e do AAEsq, procurando responder às seguintes questões:

- Será o componente funcional um marcador mais precoce e/ou com maior correlação com o *remodeling* causador de recidiva?
- Haverá outros marcadores anatómicos que se correlacionem com a recidiva?

Por fim e procurando otimizar toda a informação que o exame de TC nos pode transmitir, nomeadamente em relação ao AAEsq, relativamente a aspetos que poderão associar-se a um maior risco de formação de trombo atendendo à tríade de Virchow,

procurámos verificar se existe correlação com o *score* de risco tromboembólico CHA_2DS_2VASc e procurar dar resposta às seguintes questões:

- Estará um *score* de risco CHA_2DS_2VASc não baixo correlacionado com AEsq maiores?
- Estará um *score* de risco CHA_2DS_2VASc não baixo correlacionado com AEsq com menor função ativa?
- Estará um *score* de risco CHA_2DS_2VASc não baixo correlacionado com AAEsq maiores?
- Estará um *score* de risco CHA_2DS_2VASc não baixo correlacionado com AAEsq com menor função ativa?
- Estará um *score* de risco CHA_2DS_2VASc não baixo correlacionado com os tipos de AAEsq?
- Estará um *score* de risco CHA_2DS_2VASc não baixo correlacionado com a necessidade de 2ª aquisição na TC (para exclusão de trombos)?

Para isto tomámos como score de risco CHA_2DS_2VASc baixo o valor de score 0; e como score de risco CHA_2DS_2VASc não baixo o valor de score superior a 0.

9.2. MATERIAL E MÉTODOS

9.2.1. População

De um registo prospetivo de 2062 indivíduos que realizaram TC cardíaca de Maio de 2009 a final de Abril de 2012 – 3 anos, foram selecionados todos aqueles que a indicação para TC foi a avaliação prévia a ablação de fibrilhação auricular – 277 doentes. Assim foi constituído o **grupo A.**

A subconstituição sucessiva deste grupo A em grupo A1 e posteriormente em grupo A2 deveu-se aos seguintes critérios:

- O **grupo A1** é constituído por todos os doentes do grupo A em que a TC permitia avaliar função (aquisição de TC em modo retrospetivo e em ritmo sinusal durante o TC) – foi o grupo base de doentes com FA utilizado no capítulo VIII.
- Do grupo A1 foram selecionados apenas os doentes com FA paroxística, que realizaram ablação e em que foi possível obter informação de seguimento clínico, formando assim o **grupo A2.**

FIGURA 1

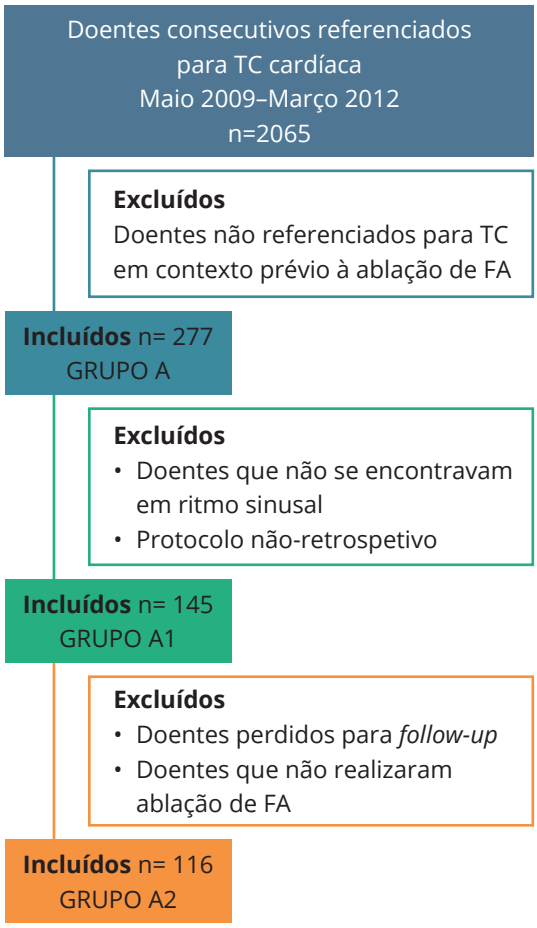

9.2.2. Protocolo de aquisição da Tc

Descrito no **Capítulo VI**.

9.2.3. Classificação das veias pulmonares

A classificação das veias pulmonares adotada foi a publicada por Marom (3) e já descrita em maior detalhe no **Capítulo VII**.

9.2.4. Classificação do apêndice auricular esquerdo

Utilizamos duas classificações, a de Wang e Di Biase (4) para o tipo de AAEsq e a de Erol (5) para o número de câmaras. As classificações estão descritas no **Capítulo VII**.

9.3. RESULTADOS

Na Tabela 1 fazemos a descrição geral da população do grupo A e dos seus dois sub-constituintes A1 e A2.

TABELA 1

Comparação geral da população grupo A, e seus subconstituintes A1 e A2

	Grupo A	Grupo A1	Grupo A2
N	277	145	116
Homens (n, %)	199 (72%)	107 (73,8%)	84 (72,4%)
Idade (anos)*	56,23+/-12,31	57,04 +/- 12,42	58,14 +/11,68
Altura (anos)*	171,26+/-10,68	172,02 +/-8,27	171,94+/-8,74
Peso (kg)*	79,94+/-14,14	79,4 +/-12,951	79,43+/-12,64
ASC (m^2)*	1,95+/-0,2	1,94 +/-0,19	1,94+/-0,19
IMC (kg/m^2)*	27,07+/-3,98	26,78 +/-3,74	26,67+/-3,70
DM#	9.10%	6.20%	2.6%
HTA#	47.40%	46.90%	30.2%
Dislipidémia#	37.20%	35.90%	12.1%
Fumador#	21.40%	22.80%	5.2%

** média e desvio padrão*

 # percentagem

9.3.1. Grupo A

Na Tabela 2 fazemos a descrição dos resultados do protocolo de TC utilizado nos doentes que realizaram o exame num contexto prévio à ablação percutânea.

Inclui-se a média da dose de radiação total: 5,7+/-3,27mSv.

Salientamos a presença de achados extra-cardíacos major em 7% da população, alertando para a importância da leitura de todo o tórax incluído na aquisição (os achados foram considerados major se necessitassem de intervenção diagnóstica subsequente ou terapêutica). Destacam-se nestes 7%: 2 neoplasias do pulmão, 1 metastização hepática, 1 sequestro pulmonar, 5 pneumopatias inflamatórias.

TABELA 2

Grupo A — dados do exame

	Grupo A
Aquisição retrospetiva#	72.00%
FC média (bpm)	70,5 +/-16,9
Ritmo durante aquisição#	
Sinusal	69%
FA	28.20%
outro	2.80%
Aquisição com 100kV#	76.00%
2ª aquisição efetuada#	9.70%
Número de trombos	2.00
Achados extra cardiacos major#	7.00%
dose radiação total (DLP x 0,014) (mSv)	5,7 +/- 3,27 *
Dose contraste (ml)	99,12 +/- 15,96 *

** média e desvio padrão*

 # percentagem

9.3.2. Grupo A2 – Grupo de doentes FA paroxística com FUP

A descrição geral do Grupo A2 encontra-se na tabela 1 (acima).

O risco clinico de episódio isquémico neste grupo foi avaliado pelo *score* de risco CHA_2DS_2VASc, com a distribuição no gráfico abaixo.

GRÁFICO 1

score CHA_2DS_2VASc

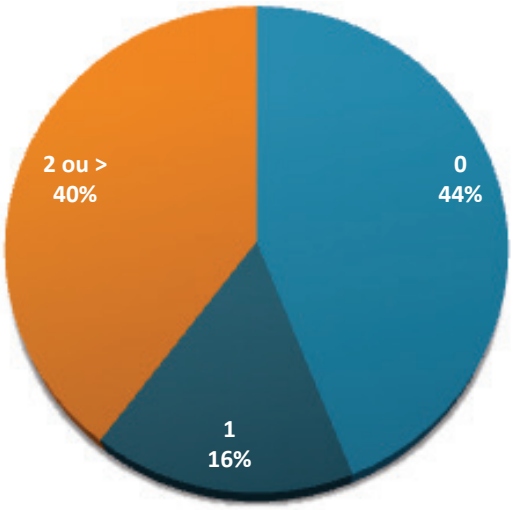

9.3.2.1. Avaliação Morfológica

A descrição morfológica dos doentes do grupo A2 é efetuada no conjunto de gráficos e tabelas que se seguem.

Sumariamente fazemos a sua exposição.

9.3.2.1.1. Avaliação da drenagem das veias pulmonares (Gráfico 2)

À direita o padrão de drenagem dominante, com 2 *ostiae* está presente em 80,2% dos doentes, sendo que quase metade do total dos doentes (49%) têm o padrão R2a – veia média drenando para a veia superior a menos de 1cm do *ostium* (ver **Figura 2**).

Salientamos ainda que em cerca de 5% de doentes, não são possíveis de caracterizar totalmente com a classificação de Marom (ver **Figura 3** e **4**).

À esquerda o padrão de drenagem mais frequente são igualmente os dois *ostiae* (78%) (ver **Figura 5**), com cerca de 62 % da população total a apresentar o padrão L2b, onde não há parede auricular "livre" entre os *ostiae*.

GRÁFICOS 2

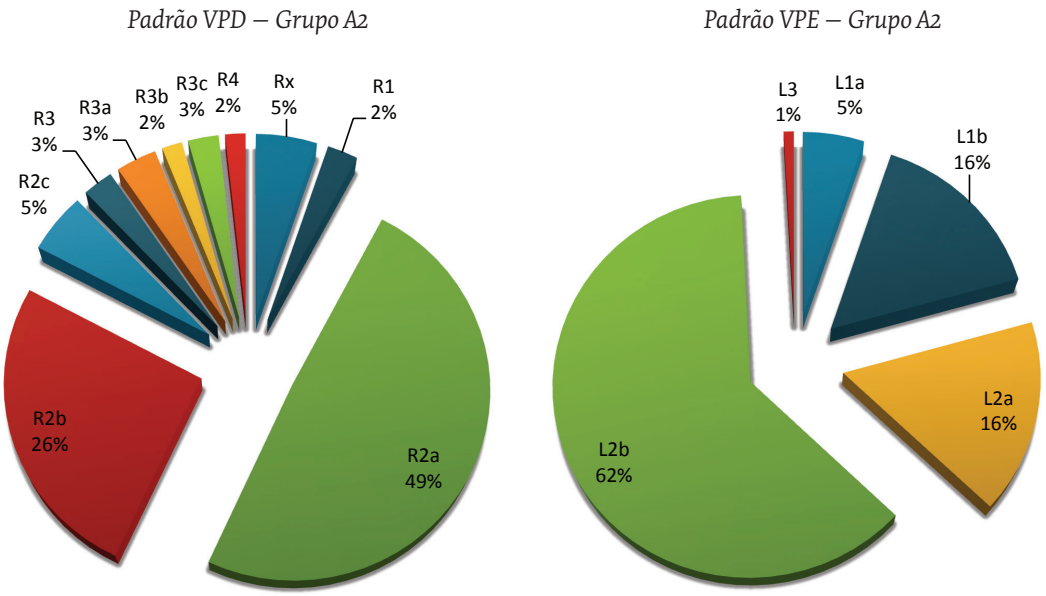

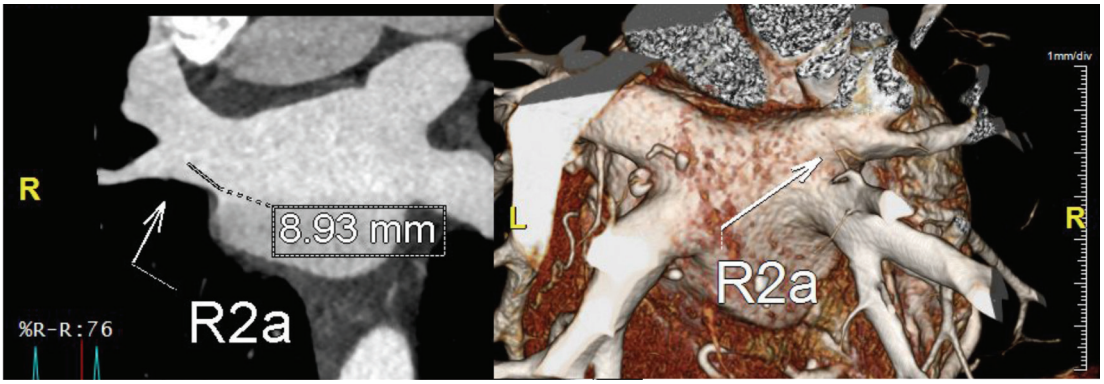

FIGURA 2

Exemplo da forma mais prevalente de drenagem das VP à direita, com 2 *ostiae* e drenagem da VP média na superior a menos de 1cm do *ostium*.

(Imagens Hugo Marques — UNICA — Hospital da Luz.)

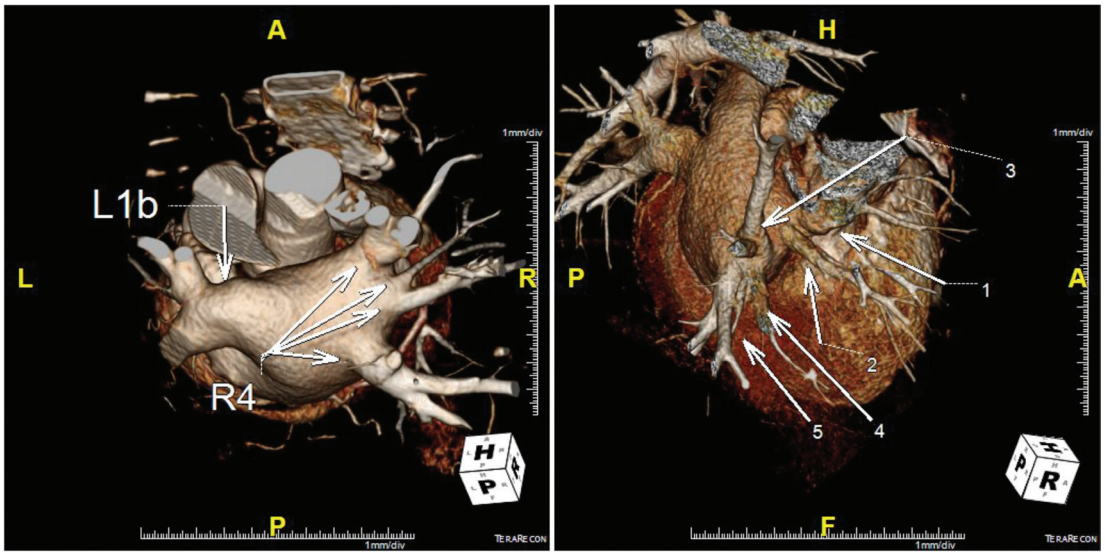

FIGURA 3

Exemplo de variantes anatómicas da drenagem das VP à direita. No caso Rx -"5", 3 dos *ostiae* têm origem na VPIDrt. A drenagem das veias à esquerda exemplificada L1b - padrão de drenagem com tronco comum e comprimento superior a 1cm – foi o 3º mais prevalente na nossa série.

(Imagens Hugo Marques — UNICA — Hospital da Luz.)

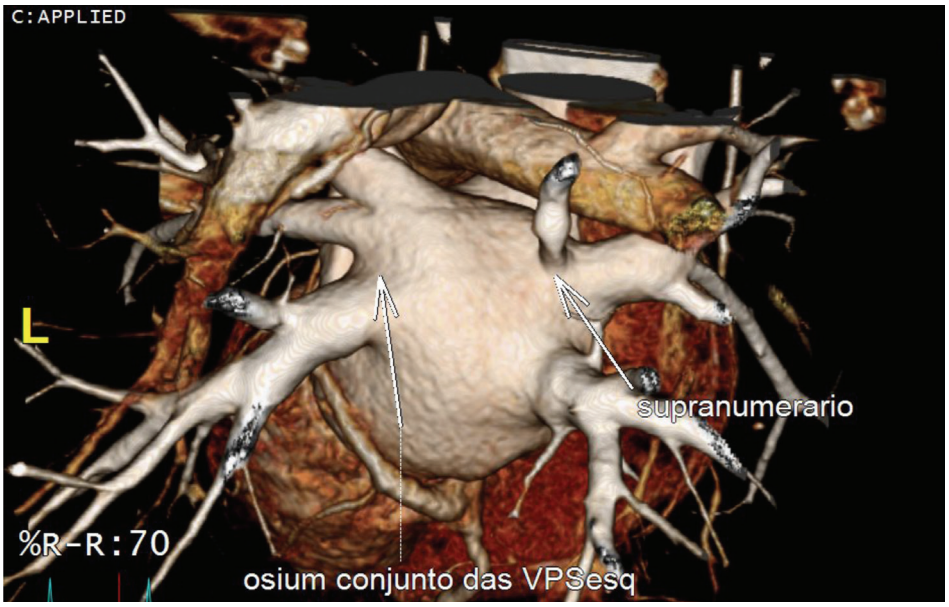

FIGURA 4

Imagem volumetrica 3D de variante anatómica da drenagem das veias pulmonares, com VPSEsq a apresentar *ostium* conjunto e veia supranumerária subsegmentar do lobo superior direito, com drenagem isolada. Este caso é um bom exemplo das vantagens e desvantagens de uma classificação, por um lado permite agrupar doentes para serem estudados, por outro perde a granularidade, aquilo que nos faz muitas vezes únicos. A classificação daquele padrão seria L2a (embora tivesse *ostium* conjunto da VPSEsq) para as veias pulmonares à esquerda e R3 (por haver 3 *ostiae*) para as veias pulmonares à direita, sem determinante de "letra", pela anatomia não coincidir com a descrita na classificação.

(Imagens Hugo Marques — UNICA — Hospital da Luz.)

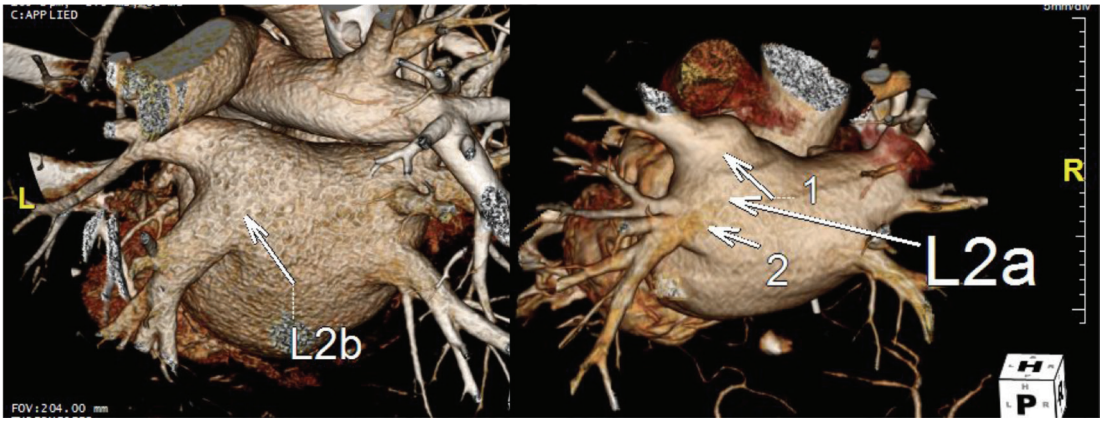

FIGURA 5

Exemplo das duas formas mais prevalentes de drenagem das VP à esquerda, com dois *ostiae* (L2), no caso "b" sem parede auricular livre e no caso "a" com parede auricular livre entre os *ostiae.*
(Imagens Hugo Marques – UNICA – Hospital da Luz.)

9.3.2.1.2. Avaliação do *ostium* das veias pulmonares por padrão dominante

Na **Tabela 3** podemos verificar qual a dimensão do *ostium* das veias pulmonares superiores e inferiores à direita e à esquerda, quando o seu padrão de drenagem é dos mais comuns (R2a; R2b; L2a; L2b).

Verificámos que não há diferença estatística entre a dimensão e ovalidade dos *ostiae* das veias pulmonares, em relação ao seu padrão, nomeadamente entre R2a e R2b; entre L2a e L2b.

TABELA 3

Avaliação do ostium *das veias pulmonares por padrão dominante*

	Padrão VPD				**Padrão VPE**	
	R2a	**R2b**	***p***		**L2a**	**L2b**
VPSD diâmetro max do *ostium**	20,38 +/-3,32	19,48 +/-2,74	0.25	VPSE diâmetro max do *ostium**	17,77 +/-2,94	19,20 +/-3,01
VPSD diâmetro min do *ostium**	15,66 +/-3,38	15,04 +/-2,77	0.81	VPSE diâmetro min do *ostium**	13,00 +/-2,58	13,50 +/-2,39
VPID diâmetro max do *ostium**	18,66 +/-2,71	18,18 +/-3,2	0.68	VPIE diâmetro max do *ostium**	17,64 +/-3,93	18,24 +/-2,70
VPID diâmetro min do *ostium**	15,91 +/-2,19	15,89 +/-2,42	0.85	VPIE diâmetro min do *ostium**	12,05 +/-2,61	13,38 +/-2,29
VPSD ovalidade do *ostium**	1,34 +/-0,27	1,36 +/-0,89	0.82	VPSE ovalidade do *ostium**	1,39 +/-0,32	1,47 +/-0,32
VPID ovalidade do *ostium**	1,19 +/-0,15	1,24 +/-1,24	0.56	VPIE ovalidade do *ostium**	1,50 +/-0,34	1,42 +/-0,31

**média e desvio padrão*

9.3.2.1.3. Avaliação da morfologia do apêndice auricular esquerdo e presença de apêndices acessórios (Gráfico 3)

O tipo de apêndice mais prevalente foi o tipo 2 — *chicken wing* representando 43% dos apêndices estudados.

A maioria dos apêndices tiverem 2 câmaras/lobos, representando 45% do total.

Cerca de 7% dos doentes apresentaram pelo menos um apêndice acessório.

GRÁFICO 3

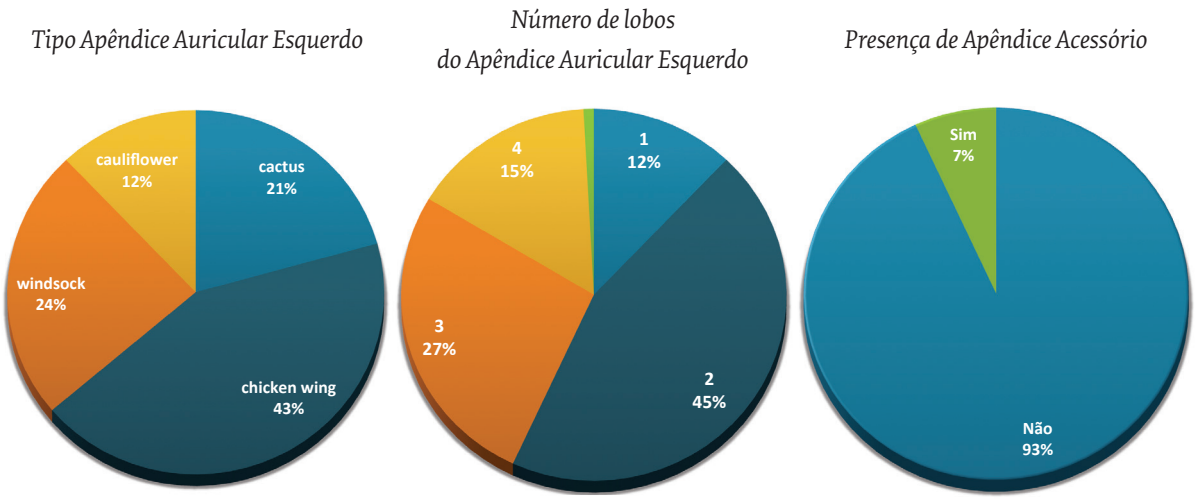

9.3.3. Avaliação Dimensional e Funcional

A informação dimensional e funcional da aurícula da AEsq e do AAEsq está reunida na tabela (ver **Tabela 4**).

9.3.3.1. Avaliação estatística dos dados morfológicos, dimensionais e funcionais

Procurámos avaliar se existem diferenças significativas de acordo com o tipo de AAEsq em relação aos volumes máximos indexados do AAEsq, e AEsq, assim como em relação à função ativa do AAEsq.

Observámos que, nos nossos resultados, apenas o volume auricular máximo indexado (VAEsqMaxi) é significativamente diferente de acordo com o tipo de AAEsq. Os doentes com AAEsq do tipo Chicken Wing têm AEsq com volume máximo indexado significativamente menor (p=0,031 na comparação AAEsq tipo 2 vs não 2; e p=0,057 na comparação individual dos 4 tipos) (ver **Tabela 5**).

TABELA 4

	Média	Desvio Padrão
VAEsqMax (ml)	103.40	33.57
VAEsqMaxi (ml/m²)	53.30	16.54
VAEsqMin (ml)	66.41	35.98
VAEsqPS (ml)	81.88	30.13
AEsq função ativa	0.29	0.14
AEsq função global	0.39	0.16
n = 116		
VAAEsqMax (ml)	9.60	5.00
VAAEsqMaxi (ml/m²)	4.95	2.71
VAAEsqMin (ml)	4.96	2.93
VAAEsqPS (ml)	8.20	4.31
AAEsq função ativa	0.41	0.18
AAEsq função global	0.48	0.19
n = 56		

TABELA 5

		VAEsqMaxi (ml/m²)	
		Média	**Desvio Padrão**
Tipo AAEsq	*not chicken wing*	59.18	19.26
	chicken wing	48.98	11.55
		VAAEsqMaxi (ml/m²)	
		Média	**Desvio Padrão**
Tipo AAEsq	*cactus*	61.42	15.37
	chicken wing	48.98	11.55
	winsock	59.48	21.95
	cauliflower	53.92	24.08

Como forma de avaliar correlação volumétrica e funcional entre os dois componentes embriologicamente diferentes da AEsq – câmara da AEsq e o AAEsq, avaliámos a correlação entre o volume máximo e a fração de ejeção de ambos.
Nos nossos resultados, houve uma moderada correlação positiva entre volumes da AEsq e do AAEsq (r=0,53; p =0,001), com uma correlação semelhante entre as suas funções globais (r=0,51; p=0,002).

Comparámos parâmetros morfológicos, dimensionais e funcionais com a probabilidade de um CHA_2DS_2VASc não baixo (ver **Tabela 6**).
Os parâmetros do AAEsq não mostraram ser significativamente diferentes, nomeadamente o tipo de AAEsq classificados como chicken wing e não chicken wing (r=0,224), o volume máximo e o volume mínimo do AAEsq, e a função ativa do AAEsq.

TABELA 6

	CHA_2DS_2VASc				
	0		**1+**		
	Média	**Desvio Padrão**	**Mean**	**Standard Deviation**	***p***
AEsqFejACT	0.33	0.14	0.26	0.14	0.04
VAEsqMaxi (ml/m²)	49.38	14.97	54.69	17.44	0.08
VAEsqMini (ml/m²)	28.25	13.45	36.27	18.75	0.02
AAEsqFejACT	0.38	0.18	0.44	0.21	0.28
VAAEsqMaxi (ml/m²)	4.43	1.40	5.39	3.29	0.77
VAAEsqMini (ml/m²)	2.31	1.22	2.71	1.71	0.75

No entanto o volume auricular mínimo indexado (VAEsqMini) e a função ativa da AEsq (FEjAct) são significativamente diferentes entre os grupos de risco baixo e não baixo de evento tromboembólico, estando um *score* de zero (risco baixo) associada a um menor volume mínimo indexado e a uma maior função ativa da AEsq.

9.3.4. Avaliação Prognóstica

Estes 116 doentes foram seguidos, em média, durante 4,8 anos, tendo sido avaliada a presença de recidiva após ablação percutânea de fibrilhação auricular por radiofrequência com navegação magnética.

Houve uma percentagem de recidiva de 34,5% (não entrando nesta contabilidade, como convencionado internacionalmente, as recidivas nos 3 primeiros meses após ablação por não serem consideradas falha do tratamento).

9.3.4.1. Análise univariada variáveis contínuas

As informações estão agregadas na **Tabela 7** e **Gráficos 4**.

Como se pode observar, não houve diferenças significativas entre os grupos, para nenhum parâmetro testado.

TABELA 7

	RECIDIVA						
	sem recidiva			**com recidiva**			
	N	**Média**	**Desvio Padrão**	**N**	**Média**	**Desvio Padrão**	***p***
Idade na altura do procedimento (anos)	76	58.54	11.60	40	57.38	11.96	0.762
Altura (cm)	76	171.55	8.57	40	172.57	9.11	0.905
Peso (kg)	76	79.48	12.60	40	79.44	12.92	0.921
IMC (kg/m²)	76	26.72	3.64	40	26.68	3.88	0.943
VAEsqMax (ml)	76	104.28	34.13	40	101.73	32.83	0.693
VAEsqMin (ml)	76	66.40	36.27	40	66.12	35.86	0.947
VAEsqPS (ml)	76	81.98	30.62	40	80.63	29.46	0.832
VAEsqMaxi (ml/m²)	76	52.99	16.63	40	51.37	16.59	0.497
AEsq Função reservatório	76	0.75	0.46	40	0.71	0.43	0.617
AEsq Função conduto	76	0.19	0.09	40	0.19	0.09	0.758
AEsq Função ativa	76	0.28	0.15	40	0.30	0.12	0.641
AEsq Função global	76	0.39	0.16	40	0.38	0.15	0.617
VAAEsqMax (ml)	37	10.48	5.63	19	7.82	2.86	0.27
VAAEsqMin (ml)	37	5.43	3.32	19	4.35	1.90	0.814
VAAEsqPS (ml)	37	9.13	4.98	19	6.98	3.27	0.358
VAAEsqMaxi (ml/m²)	37	5.43	3.02	19	4.06	1.59	0.29

cont.

cont.

	RECIDIVA						
	sem recidiva			com recidiva			
	N	Média	Desvio Padrão	N	Média	Desvio Padrão	*p*
AAEsq Função reservatório	37	1.27	0.96	19	1.17	1.15	0.583
AAEsq Função conduto	37	0.19	0.12	19	0.14	0.14	0.242
AAEsq Função ativa	37	0.42	0.2	19	0.4	0.18	0.64
AAEsq Função global	37	0.48	0.21	19	0.46	0.17	0.583

GRÁFICOS 4

Média +/- DP VAEsq

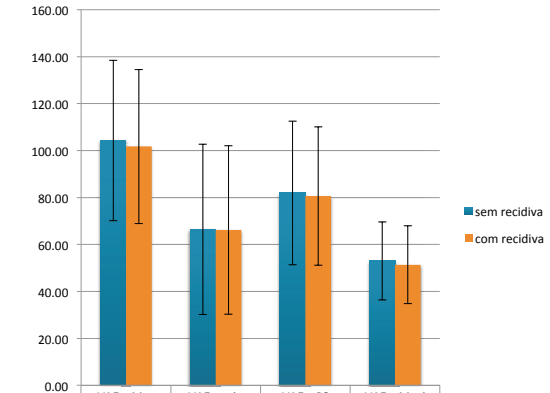

	VAEsqMax	VAEsqmin	VAEsqPS	VAEsqMaxi
sem recidiva	104.28	66.40	81.98	52.99
com recidiva	101.73	66.12	80.63	51.37

Média +/- DP Função AEsq

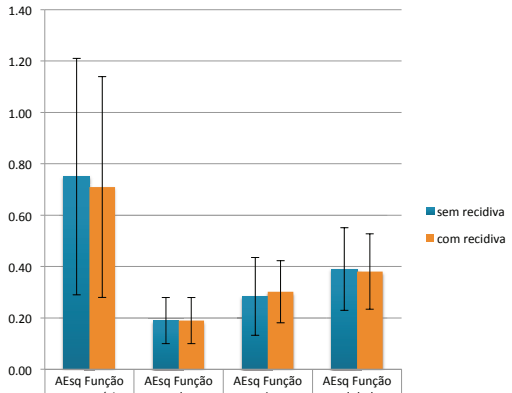

	AEsq Função reservatório	AEsq Função conduto	AEsq Função ativa	AEsq Função global
sem recidiva	0.75	0.19	0.28	0.39
com recidiva	0.71	0.19	0.30	0.38

Média +/- DP VAAEsq

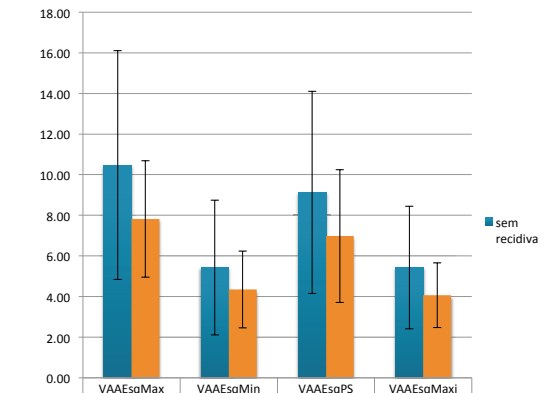

	VAAEsqMax	VAAEsqMin	VAAEsqPS	VAAEsqMaxi
sem recidiva	10.48	5.43	9.13	5.43
com recidiva	7.82	4.35	6.98	4.06

Média +/- DP Função AAEsq

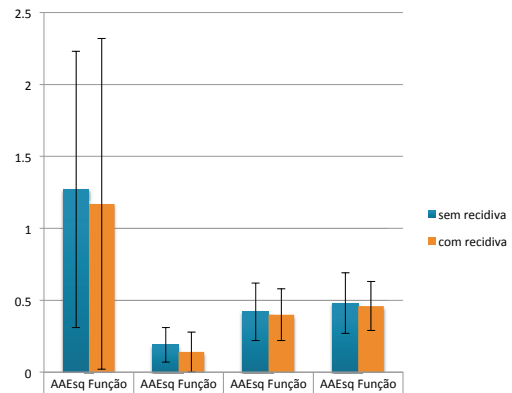

	AAEsq Função reservatório	AAEsq Função conduto	AAEsq Função ativa	AAEsq Função global
sem recidiva	1.27	0.19	0.42	0.48
com recidiva	1.17	0.14	0.4	0.46

9.3.4.2. Análise univariada variáveis discretas

Apenas o padrão de drenagem das veias pulmonares à direita teve impacto prognóstico, como se pode observar nas curvas de "sobrevida" (recidiva) de Kaplan Meier, com o padrão R2a a condicionar um número significativamente menor de recidivas, com a maior diferença a ocorrer até aos 2 anos de seguimento (ver **Gráficos 5** e **6**). No **Gráfico 7**, verificámos não haver diferença relacionável com o padrão de drenagem das veias pulmonares à esquerda.

GRÁFICO 5

Curva de Kaplan Meier, mostrando a diferença significativa de recidiva entre os doentes com padrão de drenagem das VPDrt (R2a *vs* R2b)

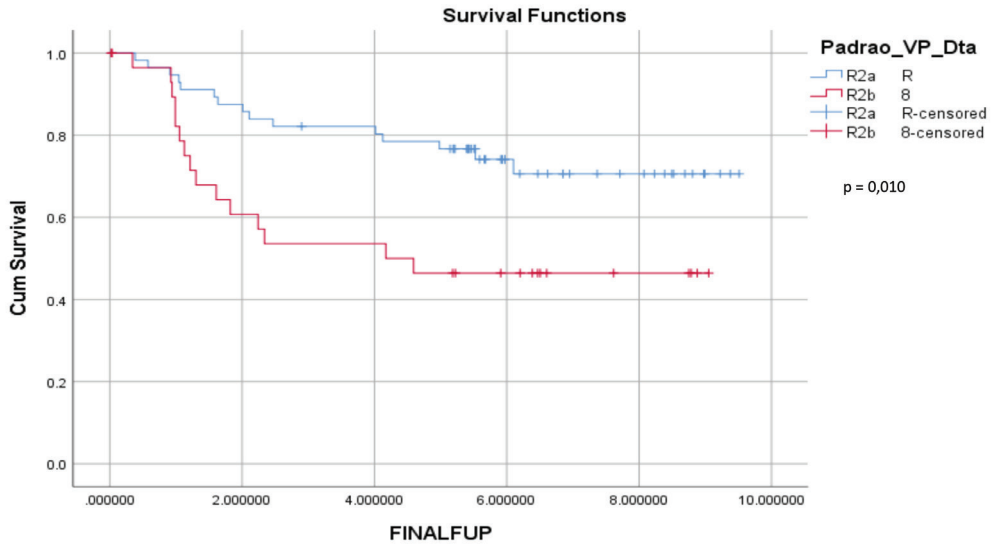

GRÁFICO 6

Curva de Kaplan Meier, mostrando a diferença significativa de recidiva entre os doentes com padrão de drenagem das VPDrt (R2a *vs* R2b e (R3 ou mais *ostiae*))

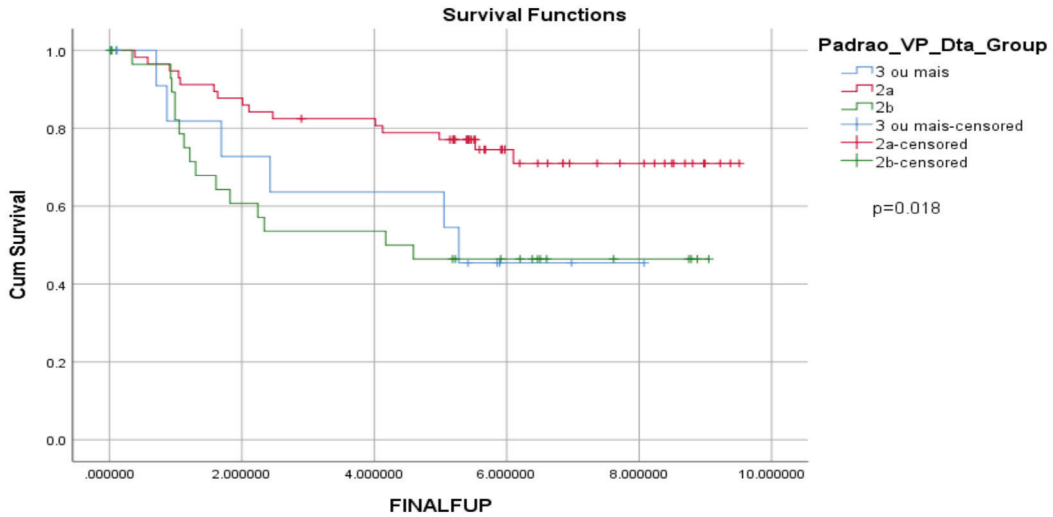

GRÁFICO 7

Curva de Kaplan Meier, não mostrando diferença significativa de recidiva entre os doentes com padrão de drenagem das VPEsq (L2a *vs* L2b)

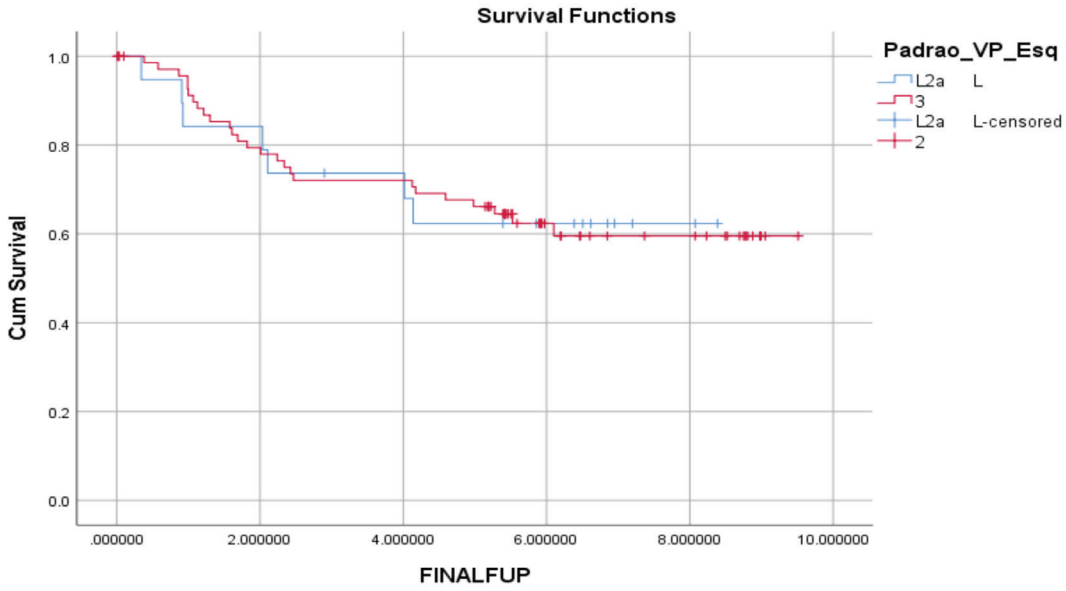

Os parâmetros dimensionais e funcionais não traduziram impacto prognóstico significativo, nem mesmo a comparação entre grupos com aurícula dilatada vs não dilatada (com base no volume máximo indexado) (p= 0.339) (ver **Gráfico 8**).

GRÁFICO 8

Curva de Kaplan Meier, não mostrando diferença significativa de recidiva entre os doentes com aurículas dilatadas *vs* não dilatadas — caracterizadas pelo VAEsq Maxi acima ou abaixo do limite superior do intervalo de confiança a 95%.

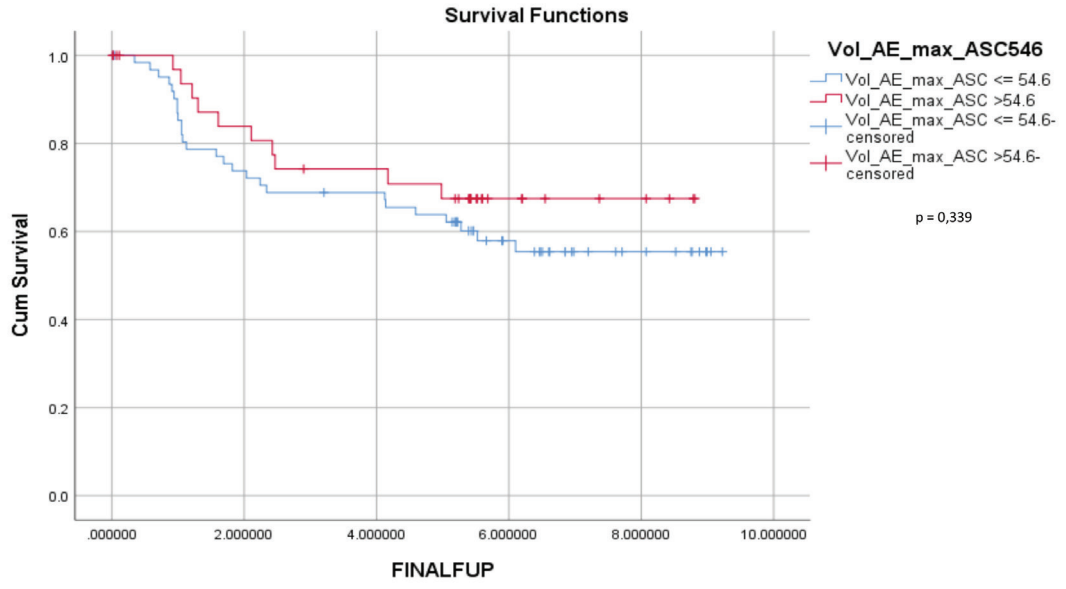

9.3.4.3. Análise multivariável

No entanto, na avaliação multivariável, ajustando para os fatores do *score* ATLAS (idade; tipo de FA sexo; tabagismo;), o volume da aurícula esquerda passou a ter relevância prognóstica significativa, com p=0,022.

Avaliando igualmente o padrão de drenagem das veias pulmonares à direita, incluindo os fatores que participam no *score* ATLAS, verificamos que o padrão R2a é de facto um preditor independente de melhor prognóstico (menor recidiva) após ablação.

9.4. DISCUSSÃO

A constituição do nosso grupo de estudo com informação prognóstica (grupo A2), procurou utilizar todos os doentes a quem tinha sido realizada uma TC cardíaca pré -ablação de FA com capacidade de reconstruções em diferentes fases para avaliação funcional. Procurámos ainda homogeneizar a amostra avaliando apenas doentes com FA paroxística. No entanto, estes são os doentes que mais frequentemente realizam ablação, pelo que a diminuição da dimensão da amostra foi marginal.

Os nossos dados de **avaliação morfológica** estão em linha com séries de outros países, nomeadamente no padrão mais frequente de drenagem das veias pulmonares com dois *ostiae* de cada lado (6, 7) ou na prevalência de todos os tipos de AAEsq. Tal como na série de Di Biase (8), o AAEsq tipo II — *chicken wing* foi o mais prevalente 43% *vs* 48%, sendo o menos frequente em ambas as séries o tipo IV — *cauliflower*, no entanto nos nossos resultados surge como quatro vezes mais prevalente do que na Di Biase 12% vs 3%. Estas diferenças poderão dever-se à variabilidade inter-observador na classificação nos tipos de AAEsq.

Os apêndices acessórios da AEsq apresentam prevalências entre os 5-10 % (9, 10), sendo o nosso resultado de 7% dentro do espectável. Salientamos, no entanto, a importância destas estruturas no contexto do doente com FA, nomeadamente na terapêutica de encerramento do AAEsq, dado estes doentes não fazerem sempre TC prévio à terapêutica percutânea. A ecografia tem baixa acuidade para o seu diagnóstico e a oclusão do AAEsq principal costuma acompanhar-se de redução de medidas

farmacológicas de prevenção de eventos tromboembólicos, não protegendo assim o doente da formação de trombos no apêndice acessório.

Em relação às questões formuladas no início do capítulo, no que concerne a **avaliação dimensional e funcional**, verificámos apenas uma moderada associação entre a função e o volume do AAEsq e a AEsq, provavelmente traduzindo a génese embrionária diferente.

Não houve correlação entre o risco de eventos tromboembólicos calculado pelo *score* CHA_2DS_2VASc (baixo vs não baixo, conforme descrito acima) e a morfologia do AAEsq (mesmo com aquelas que estão associadas a maior estase como o tipo não *chicken wing (15)*) ou o seu volume máximo indexado, o volume mínimo indexado ou a função ativa.
Outro marcador para estase no AAEsq avaliável por TC é a necessidade de segunda aquisição (tardia) por fraca homogeneização contraste-sangue (16). No nossos resultados, não houve correlação entre a necessidade de segunda aquisição e o risco de eventos tromboembólicos.
No entanto, a função ativa da AEsq é significativamente maior no grupo de baixo risco pelo *score* CHA_2DS_2VASc ($p = 0{,}042$), assim como é menor o volume mínimo indexado ($p=0{,}022$), dois marcadores de possível estase auricular.

Em relação ao **contributo prognóstico**, não confirmámos que houvesse, na nossa série, um marcador de prognóstico do resultado da terapêutica ablativa a nível morfológico, dimensional ou funcional no AAEsq.
Muito recentemente (11) foi publicada uma série com 52 doentes e seguimento até 24 meses, que demonstrou o volume máximo do AAESq como marcador independente de recorrência da FA após ablação. Essa série apresenta volumes máximos da AEsq e do AAEsq com médias aproximadas aos nossos resultados. A inclusão de doentes com FA permanente poderá estar na génese das diferenças observadas.

Da avaliação da AEsq, só na avaliação multivariada, se verificou o VAEsqMax como preditor independente de recidiva, não havendo nenhum marcador funcional com relevância prognóstica neste grupo, neste contexto.

Explorando a possibilidade de haver morfologias de drenagem das veias pulmonares que possam dificultar a sua ablação, verificámos que o padrão das veias pulmonares à direita R2a confere um significativo maior tempo livre de recidiva após terapêutica ablativa do que o padrão R2b e de que os outros padrões de drenagem de veias à direita. A avaliação multivariável incluindo os elementos do *score* ATLAS, permitiu verificar e confirmar a importância do padrão R2a, como marcador independente de melhor prognóstico. Outros estudos verificaram que a inclinação das veias pulmonares (12), a dimensão dos *ostiae* (13) e a presença de variantes anatómicas de drenagem (14), têm igualmente valor prognóstico. Nós avaliámos a dimensão dos *ostiae* das veias pulmonares à direita e a sua ovalidade e verificámos que não divergem significativamente entre padrão R2a e R2b, pelo que os resultados na nossa série atribuem-se a outras razões. Ao reparármos que a grande diferença de recidiva ocorre cedo no seguimento (ver gráfico 5, 6 e 9) e que na análise das curvas, as curvas são quase paralelas após dessa primeira fase, leva-nos a especular que a grande diferença entre estes grupos ocorre no procedimento e não no substrato da doença. Ou seja, poderá ser importante intensificar o procedimento de ablação sempre que um doente tiver um padrão de drenagem das veias pulmonares à direita não R2a.

GRÁFICO 9

Análise multivariável em curvas de Kaplan Meier, incluindo para além do padrão das veias pulmonares à direita os elementos que participam no *score* ATLAS (idade, tipo de FA, VAEsqMaxi, sexo, ser fumador). A avaliação por regressão de Cox, demonstra o padrão R2a como preditor independente de menor recidiva.

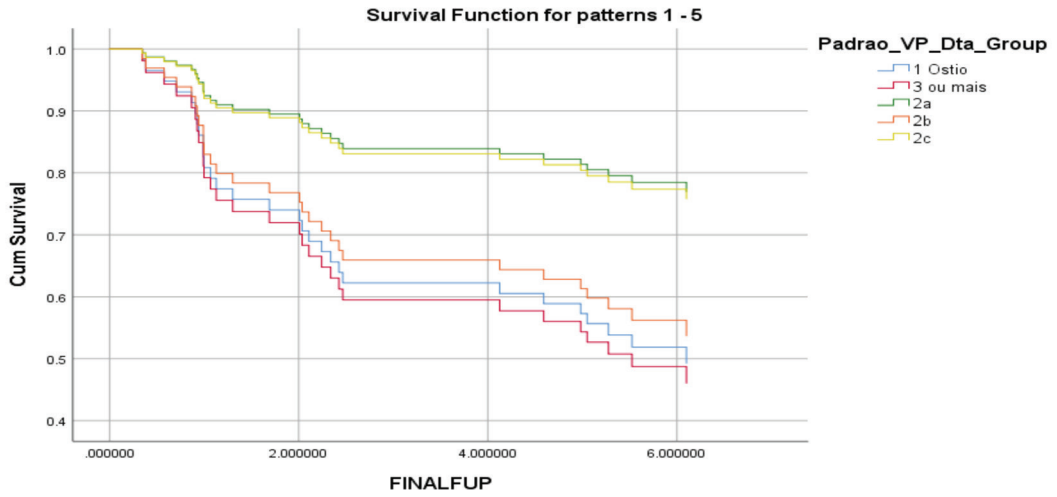

Limitações:

O tamanho da amostra do grupo A2 poderá ter limitado a correlação das variáveis funcionais com o prognóstico após a terapêutica ablativa. No entanto, com a tecnologia atual, não há justificação para a realização de exames retrospetivos no contexto pré-ablação de FA. Portanto ao procurar, como nós, otimizar o exame a todo o doente e não modificando o protocolo considerado adequado por estarmos a realizar estudo investigacional, não será possível aumentar a amostra. Este aspeto foi o principal determinante para que não se aumentasse o tempo de inclusão de doentes neste trabalho investigacional, uma vez que em Abril de 2012 praticamente a totalidade dos doentes em ritmo sinusal que realizaram o exame de TC cardíaca num contexto pré-ablativo foram efetuados com protocolo prospetivo (que não permite a avaliação funcional).

Foi apenas avaliada a função do AAEsq em 56 doentes, a avaliação preliminar dos dados levou-nos a dirigir o nosso trabalho para a avaliação de outros parâmetros.

A escolha de só avaliar doentes com FA paroxística prendeu-se com dois fatores: tornar a amostra homogénea e excluir doentes que, por terem FA não paroxísticas mais "avançadas" no decorrer do *continuum* patogénico, pudessem apesar do reduzido número confundir os resultados do grupo paroxístico.

9.5. CONCLUSÃO

Entre a AEsq e o AAEsq em doentes com FA paroxística existe apenas moderada correlação no que concerne os seus volumes e função.

Identificámos fatores da AEsq, como uma maior fração de ejeção e um menor volume mínimo indexado, que se associam a uma maior probabilidade de *score* CHA_2DS_2VASc baixo.

Nesta população de 116 doentes com seguimento médio de 4,8 anos, a presença de um padrão de drenagem pulmonar direita R2a associa-se a melhor prognóstico, mesmo quando ajustado para os fatores do *score* ATLAS..

O volume auricular em análise multivariada é um preditor independente de recidiva após ablação.

Restantes características volumétricas e funcionais da AEsq e do AAEsq não tiveram relevância prognóstica significativa.

Salientamos dois fatores identificados por TC relevantes no contexto destes doentes, nomeadamente os 7% de apêndices acessórios e os 7% de achados extra-cardíacos major.

BIBLIOGRAFIA

1. Marrouche NF, Wilber D, Hindricks G, et al. Association of atrial tissue fibrosis identified by delayed enhancement MRI and atrial fibrillation catheter ablation: the DECAAF study. JAMA. 2014;311(5):498-506.
2. Kanmanthareddy A, Reddy YM, Vallakati A, et al. Embryology and Anatomy of the Left Atrial Appendage: Why Does Thrombus Form? Interv Cardiol Clin. 2014;3(2):191-202.
3. Marom EM, Herndon JE, Kim YH, et al. Variations in pulmonary venous drainage to the left atrium: implications for radiofrequency ablation. Radiology. 2004;230(3):824-9.
4. Wang Y, Di Biase L, Horton RP, et al. Left atrial appendage studied by computed tomography to help planning for appendage closure device placement. J Cardiovasc Electrophysiol. 2010;21(9):973-82.
5. Erol B, Karcaaltincaba M, Aytemir K, et al. Analysis of left atrial appendix by dual-source CT coronary angiography: morphologic classification and imaging by volume rendered CT images. European journal of radiology. 2011;80(3):e346-50.
6. Chen J, Yang ZG, Xu HY, et al. Assessments of pulmonary vein and left atrial anatomical variants in atrial fibrillation patients for catheter ablation with cardiac CT. European radiology. 2017;27(2):660-70.
7. Thorning C, Hamady M, Liaw JV, et al. CT evaluation of pulmonary venous anatomy variation in patients undergoing catheter ablation for atrial fibrillation. Clinical imaging. 2011;35(1):1-9.
8. Di Biase L, Santangeli P, Anselmino M, et al. Does the left atrial appendage morphology correlate with the risk of stroke in patients with atrial fibrillation? Results from a multicenter study. J Am Coll Cardiol. 2012;60(6):531-8.
9. Abbara S, Mundo-Sagardia JA, Hoffmann U, et al. Cardiac CT assessment of left atrial accessory appendages and diverticula. AJR American journal of roentgenology. 2009;193(3):807-12.
10. Holda MK, Koziej M, Wszolek K, et al. Left atrial accessory appendages, diverticula, and left-sided septal pouch in multi-slice computed tomography. Association with atrial fibrillation and cerebrovascular accidents. Int J Cardiol. 2017;244:163-8.
11. Pinto Teixeira P, Ramos R, Rio P, et al. Modified continuity equation using left ventricular outflow tract three-dimensional imaging for aortic valve area estimation. Echocardiography (Mount Kisco, NY). 2017;34(7):978-85.

12. Buist TJ, Gal P, Ottervanger JP, et al. Association between pulmonary vein orientation and ablation outcome in patients undergoing multi-electrode ablation for atrial fibrillation. Journal of cardiovascular computed tomography. 2016;10(3):251-7.
13. Kiuchi K, Yoshida A, Takei A, et al. Topographic variability of the left atrium and pulmonary veins assessed by 3D-CT predicts the recurrence of atrial fibrillation after catheter ablation. Journal of arrhythmia. 2015;31(5):286-92.
14. Kubala M, Hermida JS, Nadji G, et al. Normal pulmonary veins anatomy is associated with better AF-free survival after cryoablation as compared to atypical anatomy with common left pulmonary vein. Pacing Clin Electrophysiol. 2011;34(7):837-43.
15. Fukushima K, Fukushima N, Kato K, et al. Correlation between left atrial appendage morphology and flow velocity in patients with paroxysmal atrial fibrillation. Eur Heart J Cardiovasc Imaging. 2016;17(1):59-66.
16. Ishiyama M, Akaike G, Matsusako M, et al. Severity of pseudofilling defect in the left atrial appendage on cardiac computed tomography is a simple predictor of the degree of left atrial emptying dysfunction in patients with chronic atrial fibrillation. Journal of computer assisted tomography. 2012;36(4):450-4.

CAPÍTULO X

Otimização dos exames de TC cardíaca prévios a ablação de Fibrilhação Auricular

RESUMO

Este capítulo aborda um dos objetivos da tese: a otimização dos exames de TC cardíaca realizados num contexto prévio à realização de ablação de fibrilhação auricular. Foi efetuada uma avaliação de exames consecutivos em três períodos temporais diferentes, nomeadamente: no início da nossa atividade, no final da nossa atividade com o primeiro aparelho de TC disponível e no início de atividade no novo aparelho de TC, como parte de um controlo de qualidade de uma otimização que se quer constante.

Na comparação entre o primeiro e o segundo períodos temporais é sobretudo avaliado o contributo do aumento da experiência. Na comparação entre o segundo e o terceiro períodos temporais é analisado particularmente o papel da evolução tecnológica.

Esta avaliação sistematizada permitiu objetivar os ganhos em redução da dose de radiação e volume de contraste, associados à avaliação qualitativa e quantitativa da imagem de TC e resultou num artigo original submetido a revista indexada nacional.

ARTIGO SUBMETIDO

Tomografia computorizada cardíaca prévia a ablação de fibrilhação auricular — efeitos da evolução tecnológica e otimização de protocolos

Hugo Marques, Pedro de Araújo Gonçalves, António Miguel Ferreira, Rita Cruz, João Lopes, Rosana dos Santos, Lucian Radu, Francisco Costa, João Mesquita, Pedro Carmo Diogo Cavaco, Leonor Parreira, João Pisco, João Goyri o´Neill, Pedro Adragão

Submetido à Revista Portuguesa de Cardiologia

SUMÁRIO

10.1. INTRODUÇÃO

O campo da TC cardíaca é ainda recente, com experiência que se tem acumulado rapidamente, associado a uma evolução tecnológica vertiginosa, do qual resultou um campo investigacional fértil.

A otimização de protocolos de TC deve ser um trabalho contínuo, com controlo de qualidade periódico, trabalhando-se sob a máxima: "Cada exame é realizado para uma indicação, um doente e numas condicões específicas".

Assim é possível verificar, no desenho do nosso protocolo de aquisição dos exames de TC pré-ablação (informação adicional abaixo e no capítulo VI), um conjunto de componentes variáveis que visam sobretudo esta adaptação ao doente e às suas características – *"one size can fit all but only if it is too large for many"*.

10.2. MÉTODOS

Foram incluídos 270 doentes de um registo prospetivo de doentes consecutivos de centro único de grande volume, que realizaram TC cardíaco num contexto de avaliação prévia a ablação de fibrilhação auricular.

Formaram-se 3 grupos independentes:

- o grupo 1 – os TC cardíacos efetuados aos primeiros 150 doentes
- o grupo 2 - os TC cardíacos efetuados aos últimos 60 doentes efetuados com o mesmo aparelho de TC do grupo 1
- o grupo 3 - os TC cardíacos efetuados aos primeiros 60 doentes do novo aparelho de TC.

Avaliámos a otimização do protocolo com base na dose de radiação, no volume de contraste, na necessidade de aquisição complementar e na avaliação objetiva da

qualidade de imagem, incluindo os rácios sinal/ruído, contraste/ruído, bem como homogeneização de densidade aurícula esquerda/apêndice auricular esquerdo.

10.3. RESULTADOS

Houve uma redução significativa da dose de radiação entre cada um dos grupos e da dose de contraste entre os primeiros e o último grupo (5,6mSv e 100ml contraste para o grupo1; 1,3mSv e 90ml no grupo2; 0,6mSv e 65ml no grupo3).

Realçamos que houve uma redução da dose de radiação de grupo em cerca de 3 vezes em média, o que significa que os exames atuais estão a ser realizados com cerca de 10% da dose inicial.

Apesar desta redução de dose de radiação e de volume de contraste utilizados, o grupo 3 revelou resultados significativamente melhores na avaliação quantitativa da qualidade de imagem, com rácios sinal/ruído de 13,5; contraste/ruído de 14,8 e de homogeneização de densidade de 0,92 (p<0,001).

Houve uma tendência (embora não significativa) para uma menor necessidade de aquisição complementar tardia (2ª aquisição) ao longo das séries, dos 11% no grupo 1 para os 5% no grupo 3 (p=0,057).

TABELA 1

Descrição dos grupos e avaliação comparativa.

	Grupo 1 (G1)	**Grupo 2 (G2)**	**Grupo 3 (G3)**	**P**
n	150	60	60	
Idade, anos	59 (48-65)	63 (53-69)	65 (56-70)	**0.001** †
Sexo masculino	74% (n=111)	72% (n=43)	73% (n=44)	0.805
IMC, Kg/m²	26.6 (24.2-29.1)	27.1 (24.0-28.6)	26.3 (24.5-28.9)	0.987
% ritmo sinusal	75% (n=112)	70% (n=42)	70% (n=42)	0.590
Frequência cardíaca, bpm	68 (59-77)	66 (58-75)	65 (58-80)	0.746
Protocolo				**<0.001** *†¶
% Protocolo Retrospetivo	100% (n=150)	5% (n=3)	3% (n=2)	
% Protocolo Prospetivo	NA	98% (n=59)	5% (n=3)	
% Protocolo FLASH	NA	NA	91.7%(n=55)	

cont.

cont.

	Grupo 1 (G1)	Grupo 2 (G2)	Grupo 3 (G3)	P
Volume de contraste	100 (90-108)	90 (80-100)	65 (60-65)	**<0.001** *†¶
Radiação 1ª aquisição, mGy.cm	402 (286-670)	95 (72-146)	41 (28-50)	**<0.001** *†¶
% 2ª aquisição	11% (n=17)	10% (n=6)	5% (n=3)	0.165
kV				**<0.001** *†¶
% de aquisição 70kv	0	0	33.3% (n=20)	
% de aquisição 80kv	0	82% (n=49)	57% (n=34)	
% de aquisição 90kv	0	0	3% (n=2)	
% de aquisição 100kv	83% (n=125)	20% (n=12)	2% (n=1)	
% de aquisição 120kv	17% (n=25)	2% (n=1)	5% (n=3)	
Presença de trombo	1% (n=1)	2% (n=1)	0	0.556
Acuidade diagnóstica qualitativa	100%	100%	100%	1.00
Vol AEsq a 70% do ciclo cardíaco	83 (65-105)	80 (69-96)	87 (66-99)	0.767

IMC: Índice de massa corporal; FLASH: protocolo de aquisição num só batimento cardíaco utilizando velocidade de mesa muito rápida; kV: quilovoltagem

** Grupo 1 vs. Grupo 2 p < 0.01; † Grupo 1 vs. Grupo 3 < 0.01; ¶ Grupo 2 vs. Grupo 3 < 0.01*

TABELA 2

Avaliação quantitativa da qualidade de imagem

	Grupo 2	Grupo 3	*p*
n	60	60	
Sinal/ruído AEsq	10.0 (8.3-12.1)	13.5 (11.0-16.2)	**<0.001**
Contraste/ruído (densidade AAEsq-VEsq / DP AAEsq)	8.8 (7.1-11.7)	14.8 (12.6-17.0)	**<0.001**
Rácio densidade média AEsq / AAEsq	1.04 (0.93-1.14)	0.92 (0.86-0.99)	**<0.001**

AEsq — Aurícula esquerda; AAEsq — Apêndice auricular esquerdo; VEsq — Ventrículo esquerdo

10.4. DISCUSSÃO

A TC cardíaca, num contexto prévio a ablação de fibrilhação auricular, permite dispensar outros métodos de imagem, sendo capaz de fornecer um excelente mapa anatómico e excluir a presença de trombos intra-cardíacos (1, 2). No entanto, para que a

presença de falsos positivos não diminua a acuidade da técnica e consequentemente o seu valor como "exame único" prévio à técnica ablativa, é necessário diferenciar trombos verdadeiros de imagens referidas como pseudotrombos, que não são infrequentes e resultam de insuficiente homogeneização contraste-sangue entre a AEsq e o AAEsq (3).

Existem diferentes formas de diferenciar estas entidades, nós optámos sempre por avaliar as imagens da primeira aquisição logo após a sua reconstrução e caso a homogeneização de densidade AEsq/AAEsq não permitisse a exclusão de trombo, repetimos a aquisição limitada ao AAEsq sem a administração de mais contraste, dentro de um período temporal de 3 minutos após a primeira aquisição.

O *timing* da aquisição do nosso protocolo, procura, para além de diminuir a necessidade de segundas passagens, otimizar a qualidade de imagem mantendo bons rácios de sinal/ruído e contraste/ruído, sem aumentar a dose de contraste ou a dose de radiação final. Este aspeto foi conseguido com doses de contraste e radiação significativamente menores. Para este resultado, contribuíram, em grande medida, a experiência acumulada e o avanço tecnológico dos equipamentos.

Salientamos ainda que a comparação quantitativa da qualidade de imagem entre os dois aparelhos de TC foi traduzida por uma melhoria da qualidade de imagem apesar da redução da radiação e contraste. Acresce também que todos os exames foram considerados com acuidade diagnóstica para exclusão de trombo, de forma independente, por um radiologista e um cardiologista muito experiente em TC cardíaca, apesar dos 17% de casos (74 exames) realizados em FA.

Como referido anteriormente, existem outras formas de otimizar estes protocolos, sumariamente descritas nesta tabela (ver **Tabela 3**, descrito em maior detalhe no artigo submetido).

Consideramos que a realização deste protocolo de TC, num contexto prévio a ablação de FA, como exame único, representa um protocolo com menor dose de radiação, sem sacrifício da qualidade conforme confirmado pela avaliação quantitativa da qualidade da imagem.

TABELA 3

Comparação com outras publicações

	Marques et al. Protocolo atual - G3	Lazoura et al	Teunissen et al	Iwayama et al	Annoni et al
n do grupo referência (n total do estudo)	60 (270)	122	605	20 (60)	100 (200)
Sincronização eletrocardiográfica	sim	sim	sim	não	não
Dupla administração de contraste	não	não	sim	não	não
Realizado para exclusão de trombo	sim	sim	sim	não	não
% de exames em que não foi possível excluir trombo	0%	0%	0%	NA	NA
% de 2.ª aquisição	5%	100%	4,30%	NA	NA
Necessidade de 2.ª aquisição	5%	16%	4,30%	NA	NA
ETE prévio à ablação de FA	não necessária	não necessária	não necessária	necessária	necessária
Dose de radiação	0,6mSv	3,5mSv	3,1mSv	1,1mSv	0,4mSv
Dose de contraste	64ml	90ml	100ml	28,7ml	80ml

ETE — Ecocardiograma Transesofágico; FA — Fibrilhação Auricular; mSv — milisievert

10.5. CONCLUSÃO

A experiência acumulada e os avanços tecnológicos contribuem para a otimização dos exames de TC cardíaca em contexto de pré-ablação de fibrilhação auricular, sendo possível reduções significativas do volume de contraste utilizado e da dose de radiação, para valores médios submilisievert, sem diminuição da qualidade de imagem.

BIBLIOGRAFIA

1. Hur J, Kim YJ, Lee HJ, et al. Dual-enhanced cardiac CT for detection of left atrial appendage thrombus in patients with stroke: a prospective comparison study with transesophageal echocardiography. Stroke. 2011;42(9):2471-7.
2. Romero J, Husain SA, Kelesidis I, et al. Detection of left atrial appendage thrombus by cardiac computed tomography in patients with atrial fibrillation: a meta-analysis. Circ Cardiovasc Imaging. 2013;6(2):185-94.
3. Feuchtner GM, Dichtl W, Bonatti JO, et al. Diagnostic accuracy of cardiac 64-slice computed tomography in detecting atrial thrombi. Comparative study with transesophageal echocardiography and cardiac surgery. Invest Radiol. 2008;43(11):794-801.

ANEXOS

ARTIGO SUBMETIDO

Tomografia computorizada cardíaca prévia a ablação de fibrilhação auricular — efeitos da evolução tecnológica e otimização de protocolos

Hugo Marques, Pedro de Araújo Gonçalves, António Miguel Ferreira, Rita Cruz, João Lopes, Rosana dos Santos, Lucian Radu, Francisco Costa, João Mesquita, Pedro Carmo Diogo Cavaco, Leonor Parreira, João Pisco, João Goyri o´Neill, Pedro Adragão

Submetido à Revista Portuguesa de Cardiologia

Artigo submetido à Revista Portuguesa de Cardiologia

Manuscript Details

Manuscript number	REPC_2017_404
Title	Tomografia computorizada cardíaca prévia a ablação de fibrilhação auricular – efeitos da evolução tecnológica e optimização de protocolos
Short title	Tomografia computorizada cardíaca prévia a ablação de fibrilhação auricular
Article type	Original article

Abstract

RESUMO: Introdução: A capacidade da TC cardíaca fornecer um mapa anatómico preciso e excluir a presença de trombo intra-cardíaco é conhecida. O objectivo deste estudo foi avaliar o impacto da optimização de protocolos e evolução tecnológica nas doses de radiação e contraste, e na qualidade de imagem dos exames de TC cardíaca previo a ablação de fibrilhação auricular (FA). Métodos: Registo prospectivo de doentes consecutivos de centro único, sendo incluídos os que realizaram TC cardíaca num contexto de avaliação prévia a ablação de FA (n=270), distribuídos em 3 grupos: Grupo1 constituído pelos primeiros 150 doentes; Grupo2 os últimos 60 doentes realizados no mesmo aparelho; Grupo3 os primeiros 60 doentes do novo aparelho. Avaliámos a optimização do protocolo com base na dose de radiação, volume contraste, necessidade de aquisição complementar e na avaliação objectiva da qualidade de imagem (rácios sinal/ruído, contraste/ruído e homogeneização de densidade AE/AAE). Resultados: Houve uma redução significativa da radiação entre cada um dos grupos e da dose de contraste entre o primeiro e último grupo (G1: 5,6mSv e 100ml; G2: 1,3mSv e 90ml; G3: 0,6mSv e 65ml). Apesar das menores doses de radiação e contraste, o Grupo3 apresentou resultados significativamente melhores de qualidade de imagem (racios sinal/ruído 13,5; contraste/ruído 14,8; homogeneização de densidade 0,92). Conclusão: A optimização de protocolos e a evolução tecnológica permitiram reduções significativas nas doses de radiação e de contraste utilizadas na TC cardíaca pré-ablação de FA, sem prejudicar a qualidade de imagem. ABSTRACT: Background: Cardiac computed tomography (CT) can provide a precise tridimentional anatomic map and exclude intra-cardiac thrombus. We aimed to access the impact of CT protocol optimization and technological evolution on the contrast and radiation dose as well as on image quality previous to atrial fibrillation (AF) ablation. Methods: From a prospective registry of consecutive patients who underwent cardiac CT in a single center, we selected 270 patients in whom the CT was done for evaluation prior to AF ablation and they were distributed in 3 groups: Group1: the first 150 patients included; Group2: the last 60 patients performed with the same CT scanner; Group3: the first 60 exams performed with the new CT scanner. Quality of the protocol was access based on radiation dose, contrast volume used, the use of a second (delayed) acquisition, and on quantitative image quality analisis (signal to noise and contrast to noise ratios; density homogeneity racio between LA and LAA). Results: We found a significant radiation dose as well as contrast dose reduction between the first and last subgroups (G1: 5,6mSv and 100ml; G2: 1,3mSv and 90ml; G3: 0,6mSv and 65ml). Even though group 3 had less radiation and contrast used it still had better quantitative image quality (signal/noise of 13,5; contrast/noise 14,8; density homogeneity racio of 0,92). Conclusion: Protocol optimization and technology both contributed to significant lower radiation dose and contrast volume used on cardiac CTs prior to AF ablation, without compromising image quality.

Keywords	Palavras chave: Tomografia computorizada cardíaca; Fibrilhação auricular; dose de radiação; auricula esquerda Keywords: Cardiac computed tomography; Atrial fibrilation; radiation dose; left atrium
Corresponding Author	Pedro de Ara?jo Gon?alves
Order of Authors	Hugo Marques, Pedro de Ara?jo Gon?alves, Antonio Ferreira, Rita Cruz, João Lopes, Rosana dos Santos, Lucian Radu, João Mesquita, Francisco Costa, Pedro Carmo, Diogo Cavaco, Leonor Parreira, Joao Pisco, João Goyri O´Neill, Pedro Adragao

cont.

Artigo submetido à Revista Portuguesa de Cardiologia

Tomografia computorizada cardíaca prévia a ablação de fibrilhação auricular – efeitos da evolução tecnológica e optimização de protocolos

Cardiac computed tomography previous to atrial fibrillation ablation – effects of technological improvements and protocol optimization.

Hugo Marques[1,2,3], Pedro de Araújo Gonçalves[1,3,4,6], António Miguel Ferreira[1,4], Rita Cruz[5], João Lopes[2], Rosana dos Santos[1,2], Lucian Radu, Francisco Costa[4,6], João Mesquita[4,6], Pedro Carmo[4,6], Diogo Cavaco[4,6], Leonor Parreira[6], João Pisco[3], João Goyri 0´Neill[3], Pedro Adragão[4,6]

1 - UNICA – Unidade de Imagem Cardiovascular por TC e RM –Centro de Imagiologia- Hospital da Luz Lisboa

2 - Serviço de Radiologia - Hospital de Santa Marta, CHLC, Lisboa

3 – Nova Medical School, Lisboa

4 - Serviço de Cardiologia, Hospital de Santa Cruz, CHLO, Lisboa

5 – Serviço de Imagiologia - Hospital Beatriz Angelo, Loures

6 – Centro Cardiovascular- Hospital da Luz Lisboa

Corresponding author:
Pedro de Araújo Gonçalves,
Email:paraujogoncalves@yahoo.co.uk
Telemovel: 966866455
Fax: +351214241388
Morada: Hospital de Santa Cruz, Avenida Professor Doutor Reinaldo dos Santos. 2790-134 Carnaxide
Hospital da Luz, Avenida Lusiada. Lisboa.
Nova Medical school, Campo dos Martires da Pátria, Lisboa.

Contagem de palavras: 3064

cont.

Artigo submetido à Revista Portuguesa de Cardiologia

RESUMO:

Introdução:

A capacidade da TC cardíaca fornecer um mapa anatómico preciso e excluir a presença de trombo intra-cardíaco é conhecida.

O objectivo deste estudo foi avaliar o impacto da optimização de protocolos e evolução tecnológica nas doses de radiação e contraste, e na qualidade de imagem dos exames de TC cardíaca previo a ablação de fibrilhação auricular (FA).

Métodos:

Registo prospectivo de doentes consecutivos de centro único, sendo incluídos os que realizaram TC cardíaca num contexto de avaliação prévia a ablação de FA (n=270), distribuídos em 3 grupos: Grupo1 constituído pelos primeiros 150 doentes; Grupo2 os últimos 60 doentes realizados no mesmo aparelho; Grupo3 os primeiros 60 doentes do novo aparelho. Avaliámos a optimização do protocolo com base na dose de radiação, volume contraste, necessidade de aquisição complementar e na avaliação objectiva da qualidade de imagem (rácios sinal/ruído, contraste/ruído e homogeneização de densidade AE/AAE).

Resultados:

Houve uma redução significativa da radiação entre cada um dos grupos e da dose de contraste entre o primeiro e último grupo (G1: 5,6mSv e 100ml; G2: 1,3mSv e 90ml; G3: 0,6mSv e 65ml). Apesar das menores doses de radiação e contraste, o Grupo3 apresentou resultados significativamente melhores de qualidade de imagem (racios sinal/ruído 13,5; contraste/ruído 14,8; homogeneização de densidade 0,92).

Conclusão:

A optimização de protocolos e a evolução tecnológica permitiram reduções significativas nas doses de radiação e de contraste utilizadas na TC cardíaca pré-ablação de FA, sem prejudicar a qualidade de imagem.

Palavras chave: Tomografia computorizada cardíaca; Fibrilhação auricular; dose de radiação; auricula esquerda

cont.

Artigo submetido à Revista Portuguesa de Cardiologia

ABSTRACT:

Background:

Cardiac computed tomography (CT) can provide a precise tridimentional anatomic map and exclude intra-cardiac thrombus.

We aimed to access the impact of CT protocol optimization and technological evolution on the contrast and radiation dose as well as on image quality previous to atrial fibrillation (AF) ablation.

Methods:

From a prospective registry of consecutive patients who underwent cardiac CT in a single center, we selected 270 patients in whom the CT was done for evaluation prior to AF ablation and they were distributed in 3 groups: Group1: the first 150 patients included; Group2: the last 60 patients performed with the same CT scanner; Group3: the first 60 exams performed with the new CT scanner.

Quality of the protocol was access based on radiation dose, contrast volume used, the use of a second (delayed) acquisition, and on quantitative image quality analisis (signal to noise and contrast to noise ratios; density homogeneity racio between LA and LAA).

Results:

We found a significant radiation dose as well as contrast dose reduction between the first and last subgroups (G1: 5,6mSv and 100ml; G2: 1,3mSv and 90ml; G3: 0,6mSv and 65ml). Even though group 3 had less radiation and contrast used it still had better quantitative image quality (signal/noise of 13,5; contrast/noise 14,8; density homogeneity racio of 0,92).

Conclusion:

Protocol optimization and technology both contributed to significant lower radiation dose and contrast volume used on cardiac CTs prior to AF ablation, without compromising image quality.

Keywords: Cardiac computed tomography; Atrial fibrilation; radiation dose; left atrium

cont.

Artigo submetido à Revista Portuguesa de Cardiologia

INTRODUÇÃO E OBJECTIVOS

O isolamento percutâneo das veias pulmonares está bem estabelecido para o tratamento da fibrilhação auricular, sendo uma area de grande desenvolvimento clinico e tecnológico nos últimos anos [1]. Antes da sua realização, é necessária a exclusão de trombo intra-cardíaco, nomeadamente no apêndice auricular esquerdo (AAEsq) [2-4]. A obtenção prévia de mapa anatómico 3D da aurícula esquerda (AEsq) e veias pulmonares facilita o procedimento contribuindo para a sua segurança, reduz a radiação a que o doente é submetido durante a ablação e poderá aumentar a sua acuidade[5-8].

A tomografia computorizada (TC) cardíaca é um método imagiológico com capacidade para fornecer toda esta informação (exclusão de trombo e informação anatómica) de forma não invasiva [9], pelo que tem ganho preponderância nestes doentes (**Figura 1**) [10]. Este trabalho tem por objectivo avaliar a optimização dos protocolos de TC cardíaca prévia a ablação de fibrilhação auricular (pré-ablação), tendo por base a dose de radiação e de contraste e a qualidade diagnóstica, tendo em conta o aumento da experiencia do centro e os avanços tecnológicos disponíveis.

MÉTODOS:

Desenho do estudo e população:

De um registo prospectivo de centro único de grande volume doentes submetidos a avaliação por TC cardíaca já descrito anteriormente[11], selecionaram-se todos aqueles cuja indicação foi a avaliação prévia a ablação de fibrilhação auricular (pré-ablação). Desses foram constituídos 3 grupos de doentes consecutivos, independentes: Grupo 1 - Os primeiros 150 doentes consecutivos incluídos no registo; Grupo 2 - Os últimos 60 doentes efectuados com o mesmo aparelho de TC que tivemos disponível – TC dupla-ampola de 1ª geração, com 64 cortes (SOMATOM Definition®, Siemens Healthcare); Grupo 3 foi constituído com os primeiros 60 doentes efectuados com o novo aparelho de TC dupla-ampola 3ª geração – 192 detectores (SOMATOM Force®, Siemens Healthcare). (**Figura 2).** O grupo 1 serviu de grupo controlo quando comparado com o grupo 2, para avaliação da experiência na optimização dos exames. O grupo 2 serviu de grupo controlo quando comparado com o grupo 3 para avaliação da evolução tecnológica na optimização dos exames.

Protocolo de Aquisição

Todos os exames foram realizados dentro das 24h prévias à realização do procedimento ablativo.

Protocolo de aquisição para o grupo 1 :

Exames realizados em TC dupla-ampola 1ª geração – 64 detectores – SOMATOM Definition®, com resolução temporal nativa de 83ms e velocidade de mesa (“pitch”) máximo de 45,7mm/s.

Aquisição com protocolo retrospectivo, com modulação da miliamperagem - com 20% da miliamperagem fora dos intervalos de dose máxima, escolhidos da seguinte forma: se rítmico e frequência cardíaca (FC) inferior a 70 batimentos por minuto (bpm) – dose máxima apenas aos 70% do intervalo RR; se arrítmico ou

cont.

Artigo submetido à Revista Portuguesa de Cardiologia

rítmico com FC 70-80bpm - dose máxima de 40 a 80% do intervalo RR; se rítmico e FC superior a 80bpm – dose máxima a 40-50% do intervalo RR.

A kilovoltagem (kV) foi determinada da seguinte forma: 100kV se índice de massa corporal (BMI)<30, caso contrario 120Kv.

As imagens forma reconstruídas com protocolo de "filtered back projection" (FBP), com uma espessura de 1,5mm e um incremento de 0,7mm, matriz 512x512.

O contraste utilizado tinha a concentração de 320mgI/ml e foi administrado num protocolo trifásico com um débito de 6ml/seg, da seguinte forma: primeira fase com administração de contraste puro com volume calculado segundo a formula: volume de contraste administrado = (tempo de aquisição +tempo de espera) x 6 (valor do fluxo de administração). O tempo de espera foi fixado em 7 segundos; segunda fase com a administração de 30 ml de contraste diluído (30% contraste e 70% soro); terceira fase com administração de 30ml de soro.

Foi utilizado a técnica de "bolus tracking" com região de interesse na aorta ascendente e início de aquisição 7 segundos após atingir a densidade de 150HU (unidades de Hounsfield).

Protocolo de aquisição para o grupo 2:

Exames realizados em TC dupla-ampola 1ª geração – 64 detectores – SOMATOM Definition®, com resolução temporal nativa de 83ms e velocidade de mesa ("pitch") máximo de 45,7mm/s

Aquisição com protocolo prospectivo se doente rítmico ou arrítmico com pequena variabilidade RR; noutros casos aquisição retrospectiva (modulação da miliamperagem com 20% da miliamperagem fora dos intervalos de dose máxima, com dose máxima de 40 a 80% do intervalo RR).

A kV foi determinada da seguinte forma: 80kV se BMI < 30, caso contrario 100kV se peso inferior a 100kg e 120kV se peso superior a 100kg.

As imagens forma reconstruídas com protocolo de "filtered back projection" (FBP), com uma espessura de 1,5mm e um incremento de 0,7mm, matriz 512x512.

O contraste utilizado tinha a concentração de 370mgI/ml e foi administrado num protocolo trifásico com um débito de 5ml/seg, da seguinte forma: primeira fase com administração de contraste puro com volume calculado segundo a formula: volume de contraste administrado = (tempo de aquisição +tempo de espera) x 5 (valor do fluxo de administração). O tempo de espera foi fixado em 10 segundos; segunda fase com a administração de 30 ml de contraste diluído (30% contraste e 70% soro); terceira fase com administração de 30ml de soro.

Foi utilizado a técnica de "bolus tracking" com região de interesse na aorta ascendente e início de aquisição 10 segundos após atingir a densidade de 150HU (unidades de Hounsfield).

Protocolo de aquisição para o grupo 3:

Exames realizados em TC dupla-ampola 3ªgeração – 192 detectores - SOMATOM Force®, com resolução temporal nativa de 66ms e velocidade de mesa ("pitch") máximo em modo FLASH de 737mm/seg.

cont.

Artigo submetido à Revista Portuguesa de Cardiologia

Aquisição com protocolo FLASH (aquisição em batimento cardíaco único com método de velocidade de mesa muito elevado 737mm/s), excepto se doentes com FC média superior a 80bpm onde se opta pela aquisição em método prospectivo. Aquisição retrospectiva apenas em doentes com marcada variabilidade RR.

A determinação da kV e da miliamperagem (mA) é efectuada de forma automática tendo em conta a densidade do topograma e os parâmetros de referência, os quais optámos por definir 80kV com 200mAs/rot, com indicação de realização de angio-TC. Apenas se BMI>30, os kV de referência passam a 100kV. Os valores de referência, servem como um guia para o ruído admissível/máximo que se pretende ter na imagem, fazendo o aparelho uma modificação dos valores por forma a optimizar a dose de radiação, mantendo a qualidade da imagem.

As imagens foram reconstruídas com protocolo iterativo – SAFFIRE "força" 3, com 1,5mm de espessura e 0,7mm de incremento, com matriz 512x512.

O contraste utilizado tinha a concentração de 370mgI/ml e foi administrado num protocolo trifásico com um débito de 4ml/seg, da seguinte forma: primeira fase com administração de contraste puro com volume calculado segundo a formula: volume de contraste administrado = (tempo de aquisição +tempo de espera) x 4 (valor do fluxo de administração). O tempo de espera foi fixado em 15 segundos (compensa a marcada diminuição do tempo de aquisição que no protocolo FLASH é inferior a 1 segundo); segunda fase com a administração de 30 ml de contraste diluído (30% contraste e 70% soro); terceira fase com administração de 30ml de soro.

Foi utilizado a técnica de "bolus tracking" com região de interesse na aorta ascendente e início de aquisição 15 segundos após atingir a densidade de 150HU (unidades de Hounsfield).

Avaliámos a optimização do protocolo com base em diversos parâmetros:

A) na dose de radiação em mSv, calculada a partir dos DLP (dose lengh product) totais, disponibilizados pelo aparelho, multiplicados pelo factor de conversão 0,014 [12-14]; B) no volume de contraste utilizado em ml; C) na avaliação subjectiva da qualidade diagnóstica, definida por exame com acuidade diagnóstica para excluir trombo na aurícula esquerda e apêndice auricular esquerdo, avaliada por dois médicos diferentes, (com nível III de formação em TC cardíaca), de forma independente, bem como pelo número de doentes em que foi considerado necessário uma segunda aquisição, mais tardia (sem nova administração de contraste, para avaliar adequadamente o apêndice auricular esquerdo e permitir a exclusão de trombo); D) na avaliação objectiva da qualidade do exame, efectuada para avaliação da capacidade de optimização do protocolo entre aparelhos diferentes (aplicada ao grupo 2 e 3), caracterizada pelo rácio sinal/ruído, o rácio contraste/ruído e a homogeneização de densidade entre a AEsq e o AAEsq

Definição dos parâmetros de avaliação quantitativa da qualidade de imagem:

O rácio sinal/ruído é obtido por desenho de uma região de interesse no centro da aurícula esquerda e dividindo a densidade média pelo desvio padrão. (**Figura 3**).

Em relação ao rácio contraste/ruído, neste tipo de exame e tendo em conta a importância de exclusão de trombo, optámos por definir este parâmetro em relação à densidade do miocárdio do ventrículo esquerdo e não em relação à gordura epicárdica, uma vez que o miocárdio do ventrículo esquerdo é a estrutura limítrofe

cont.

Artigo submetido à Revista Portuguesa de Cardiologia

com o AAEsq com menor diferença de densidade em relação ao lúmen do mesmo. Para o cálculo deste parâmetro foram desenhadas regiões de interesse no AAEsq (local de menor densidade visual) e intra-miocárdico, no segmento do miocárdio em maior proximidade do AAE. O rácio foi obtido da seguinte forma (densidade média do AAEsq – densidade média do miocárdio)/ desvio padrão do AAEsq. A homogeneização de densidade entre a AEsq e o AAEsq é obtida pela divisão da densidade média da AEsq obtida na região de interesse desenhada no local visual de maior densidade com a densidade média obtida da região de interesse desenhada no local de menor densidade visual no AAEsq. (**Figura 3**)

Dentro de cada grupo foram ainda registadas características demográficas (género, idade, peso, altura), bem como o ritmo cardíaco e frequência cardíaca (máxima, mínima e média) durante a aquisição, variáveis do protocolo utilizado (retrospectivo, prospectivo, flash; kV da aquisição; DLP do exame), o volume auricular, a presença de trombo intra-cardíaco e a presença de complicações tromboembólicas após o procedimento de ablação até à alta clínica.

Todos os exames foram efectuados com sincronização com ECG, procurando optimizar os parâmetros do protocolo ao doente.

Os exames foram avaliados logo após a sua realização para decisão de necessidade de aquisição complementar (2ª aquisição) quando a opacificação do AAESq era determinada insuficiente para exclusão segura de trombo ou quando, por qualquer outra causa, o exame era considerado não diagnóstico. Esta segunda aquisição era efectuada nos primeiros 3 minutos após a aquisição inicial, sem utilizar mais contraste e limitada ao AAEsq (**Figuras 4-5**).

Análise estatística:

As variáveis contínuas apresentam-se como mediana (intervalo interquartil) e as categóricas como número (n) e frequência (%). Para comparação entre variáveis contínuas utilizaram-se os testes não paramétricos de Mann-Whitney ou Kruskal-Wallis. O teste exacto de Fisher foi usado para testar diferenças nas frequências de variáveis categóricas. Foi utilizado o software Statistical Pack for Social Sciences (IBM SPSS) versão 20 para Mac OSX. Aceitou-se existir diferença significativa quando $p<0,05$ (duas caudas).

RESULTADOS:

Os resultados da avaliação dos 3 grupos e da comparação entre grupos são apresentados na **Tabela 1**.

Dose de Radiação:

Os exames do grupo 1 tiveram radiação mediana de 5,6mSv (402DLP “dose lengh product” x0,014), os do grupo 2 - 1,3mSv (95DLPx0,014) e 0,6mSv para os doentes do grupo 3 (41DLPx0,014).

Salientamos a diferença significativa no tipo de protocolo utilizado e na kV dos exames, aspecto que contribui decisivamente para a diferença significativa na dose média de radiação dos exames.

Dose de Contraste:

A evolução do protocolo permitiu ainda uma redução significativa entre os grupos da dose de contraste, dos 100ml de volume no grupo 1 para os 65ml utilizados no grupo 3.

cont.

Artigo submetido à Revista Portuguesa de Cardiologia

Avaliação qualitativa da imagem:

Todos os exames foram considerados diagnósticos. Apesar de não ter atingido significância, existe uma tendência para a menor necessidade de 2ª aquisição com o evoluir do protocolo, com percentagem de 2ª aquisições de 11% no grupo 1 (destes 17 casos apenas num caso a área de menor densidade traduzia imagem "correcta" dado corresponder a verdadeiro trombo, confirmado por ecocardiografia trans-esofágica) (**figuras 4-5**) e de apenas 5% no grupo 3 (p = 0,057).

Avaliação quantitativa da qualidade da imagem:

Na avaliação quantitativa da qualidade de imagem (**Tabela 2**) entre o grupo 2 e o grupo 3, verificamos que apesar da redução da dose de radiação e do volume de contraste, os exames apresentaram melhor qualidade com rácios sinal/ruído e contraste/ruído significativamente maiores e com maior homogeneização de densidade entre a AEsq e o AAEsq.

Na **tabela 3** verificamos que a necessidade de 2ª aquisição não se correlacionou com o volume auricular (apesar parecer existir uma tendência para ser necessária em auriculas maiores, p=0,087), mas apenas com a aquisição em fibrilhação auricular e com a frequência cardíaca média durante a aquisição.

DISCUSSÃO:

A TC cardíaca num contexto prévio a ablação de fibrilhação auricular, permite dispensar outros métodos de imagem, sendo capaz de fornecer um excelente mapa anatómico e excluir a presença de trombos intra-cardíacos [9, 15]. No entanto, para que a presença de falsos positivos, não diminua a acuidade da técnica e consequentemente o seu valor como "exame único" prévio à técnica ablativa, é necessário diferenciar trombos verdadeiros de imagens referidas como pseudotrombos, que não são infrequentes e resultam de insuficiente homogeneização contraste-sangue entre a AEsq e o AAEsq [16].

Existem diferentes formas de diferenciar estas entidades, optámos por avaliar sempre as imagens da primeira aquisição logo após a sua reconstrução e, caso a homogeneização de densidade AEsq/AAEsq, não permitisse a exclusão de trombo, repetimos a aquisição limitada ao AAEsq sem mais contraste, dentro de um período temporal de 3 minutos após a primeira aquisição. Para diminuir a necessidade de 2ª aquisições, que são infrequentes (11% no Grupo 1 e 5% no Grupo 3), atrasámos o início da aquisição inicial aumentado o valor de densidade para inicio de aquisição ("*trigger*") no "*bolus tracking*", assim como o tempo de espera entre esse "*trigger*" e o início da aquisição propriamente dita.

Apesar destas modificações de protocolo não terem resultado numa diminuição significativa do número de 2ª aquisições necessárias, parece existir uma tendência nesse sentido (de 11% no grupo 1 para 5% no grupo 3, p=0,057).

O *timing* da aquisição do nosso protocolo procura, para além de diminuir a necessidade de segundas passagens, optimizar a qualidade de imagem mantendo bons rácios de sinal/ruído e contraste/ruído, sem aumentar a dose de contraste ou a dose de radiação final. Este aspecto foi conseguido com doses de contraste e radiação significativamente menores (p<0,001). Já anteriormente o nosso grupo publicou que a aquisição em fibrilação auricular era um preditor de maior dose de radiação, pelo que se torna ainda mais

cont.

Artigo submetido à Revista Portuguesa de Cardiologia

relevante a adopção de protocolos que visam reduzir a sua dose, sobretudo em doentes que com frequência necessitam de vários exames seriados com radiação ionizante ao longo da sua vida[17, 18].

Salientamos ainda que a comparação quantitativa da qualidade de imagem entre os dois aparelhos de TC foi traduzida por uma melhoria da qualidade de imagem apesar da redução da radiação e contraste. Acresce também que: todos os exames foram considerados com acuidade diagnóstica para exclusão de trombo, de forma independente, por um radiologista e um cardiologista com larga experiência em TC cardíaca, apesar dos 17% de casos (74 exames) realizados em FA.

Como referido anteriormente existem outras formas de procurar optimizar estes protocolos, nomeadamente:

A) Com protocolo de dupla aquisição, incluindo sempre aquisição tardia, como efectuado por Lazoura et al [19], que estudou 122 doentes, com 16% de defeitos de replecção do AAEsq na primeira aquisição, dos quais todos foram diagnóstico na segunda aquisição (como na nossa série), tendo-se identificado cerca de 3% de trombos. Neste artigo, verifica-se ainda que a necessidade de segunda passagem avaliada através da percentagem de defeitos de replecção do AAEsq era de apenas 16% (5% no Grupo 3 do nosso estudo), pelo que a decisão de segunda aquisição apenas se necessário, como efectuado no nosso estudo, parece-nos a mais acertada. Comparativamente com o nosso estudo, a dose de contraste e radiação foi superior:

B) Com protocolo de dupla injecção de contraste e apenas adquirindo uma vez, após a segunda administração, como efectuado por Teunissen et al [20], que estudou 605 doentes, com doses médias de contraste de 100ml e de radiação de 3,1mSv. A percentagem de necessidade de segunda aquisição foi de 4,3%. Comparativamente com o nosso estudo, este protocolo obteve resultados semelhantes na necessidade de 2ªs aquisições, mas à custa de maiores doses de contraste e radiação.

C) Protocolo sem sincronização electrocardiográfica, como o realizado por Iwayama et al [21], que estudou 60 doentes, mas não avaliou a presença de trombo. Obteve dose de radiação média de 1,1mSv.

No entanto a não exclusão de trombo neste protocolo, não permite a dispensa da realização de ecocardiograma trans-esofágico (ETE), o que acresce custo e fonte de morbilidade aos doentes. Mesmo realizando o exame sem sincronização electrocardiográfica, a dose de radiação foi superior à utilizada no nosso estudo.

Noutro estudo, igualmente com exames realizados sem sincronização electrocardiográfica, Annoni et al [22] estudou 200 doentes, 100 dos quais no grupo de menor dose de radiação. Não avaliou a presença de trombo e obteve uma dose de radiação média de 0,4mSv Tal como no estudo de Iwayama, a não exclusão de trombo não dispensa da realização de ETE. Salientamos que a dose de radiação do estudo de Annoni et al é a mais reduzida com valores médios de 0,4mSv (valores semelhantes aos utilizados no grupo 3 do nosso estudo - 0,6mSv) (**Tabela 4**).

Consideramos que, face aos resultados apresentados, este protocolo de TC num contexto prévio a ablação de FA, como exame único, representa um protocolo com menor dose de radiação, sem sacrifício da qualidade conforme confirmado pela avaliação quantitativa da qualidade da imagem.

Limitações

Como possíveis limitações deste estudo, salientamos:

cont.

Artigo submetido à Revista Portuguesa de Cardiologia

A) Não foi realizado ecocardiograma trans-esofágico sistemático em todos os doentes, mas apenas para confirmação dos trombos identificados na TC cardíaca. No entanto, apesar de poder ser considerada uma limitação, a acuidade para excluir trombo da TC cardíaca é muito elevada e quando acompanhada de aquisição tardia, o número de falsos positivos é igualmente muito baixo [9]; B) Entre o grupo 1 e o grupo 2 houve uma mudança na concentração de iodo do contraste utilizado (320 para 370mgI/ml), mas que foi compensada pelo menor fluxo de administração do mesmo no grupo 2.; C) a nossa série apresenta um número reduzido de trombos, mas este aspecto é uma característica frequente na população que realiza exame de TC pré-ablação de FA; D) apenas foi avaliada quantitativamente a qualidade da imagem do grupo 2 e 3, dado ter coincidido com a introdução de ums tecnologia nova. Houve avaliação subjectiva da qualidade de imagem em todos os grupos; E) Não testámos um protocolo sem sincronização electrocardiografica, que poderia estar associado a menor dose de radiação [22]. No entanto, em aquisição em modo FLASH, a redução de dose não deveria ser significativa, além disso a acuidade para exclusão de trombo não foi ainda estabelecida, o que limitaria a sua adopção como exame único prévio à ablação

.

CONCLUSÕES:

A optimização de protocolos e a evolução tecnológica permitiram reduções significativas nas doses de contraste e de radiação (para valores submilisiviert) na TC cardíaca pré-ablação de fibrilhação auricular, sem diminuição da qualidade de imagem.

cont.

Artigo submetido à Revista Portuguesa de Cardiologia

LEGENDAS DAS FIGURAS:

Figura 1: Avaliação por AngioTC cardíaca da AEsq e do AAEsq.

1. Avaliação a permeabilidade do AAesq.
2. Avaliação da morfologia da AEsq e do padrão de drenagem das veias pulmonares
3. Maior detalhe da drenagem da veia pulmonar inferior direita
4. Detalhe morfológico do AAESq
5. Avaliação volumetrica da AEsq
6. Presença de veia pulmonar supra-numerária com drenagem directa na AEsq.
7. Presença de pequeno apêndice acessório.

Figura 2: População do estudo

Figura 3: Calculo dos indices de sinal/ruído e contraste/ruído.
A) Região de interesse (ROI) na AEsq; B) ROI no AAEsq; C) ROI na parede do VEsq
Cálculo sinal/ruído = Densidade média AEsq / Desvio Padrão AEsq
Cálculo contraste/ruído = (densidade média AAEsq-densidade média da parede Vesq)/ Desvio Padrão AAEsq
Avaliação da homogenização de contraste AEsq/AAEsq = Densidade média AEsq / Densidade média da área de menor densidade no AAEsq

Figura 4: Avaliação do AAEsq – necessidade de 2ª aquisição (mais tardia) para diferenciação entre trombo e pseudotrombo. Exemplo de trombo – com a correspondência no ETE (avaliação dimensional muito aproximada).

Figura 5: Avaliação do AAEsq – necessidade de 2ª aquisição para diferenciação entre trombo e pseudotrombo. Exemplo de pseudotrombo – identificado pelo ganho de contraste na 2ª aquisição (mais tardia), a sua densidade média e a homogenização de densidade com a restante aurícula.

Figura 6: Avaliação do AAEsq – diferenciação entre trombo e pseudotrombo. Exemplo de pseudotrombo que pela densidade média elevada não necessita de segunda aquisição.

cont.

Artigo submetido à Revista Portuguesa de Cardiologia

BIBLIOGRAFIA

1. Adragao P, Carmo P, Cavaco D, Carmo J, Ferreira A, Moscoso Costa F, et al. Relationship between rotors and complex fractionated electrograms in atrial fibrillation using a novel computational analysis. Rev Port Cardiol. 2017;36(4):233-8.
2. Calkins H, Hindricks G, Cappato R, Kim YH, Saad EB, Aguinaga L, et al. 2017 HRS/EHRA/ECAS/APHRS/SOLAECE expert consensus statement on catheter and surgical ablation of atrial fibrillation: executive summary. Journal of interventional cardiac electrophysiology : an international journal of arrhythmias and pacing. 2017.
3. Kalla M, Sanders P, Kalman JM, Lee G. Radiofrequency Catheter Ablation For Atrial Fibrillation: Approaches And Outcomes. Heart, lung & circulation. 2017;26(9):941-9.
4. Kirchhof P, Benussi S, Kotecha D, Ahlsson A, Atar D, Casadei B, et al. 2016 ESC Guidelines for the Management of Atrial Fibrillation Developed in Collaboration With EACTS. Revista espanola de cardiologia (English ed). 2017;70(1):50.
5. Imanli H, Bhatty S, Jeudy J, Ghzally Y, Ume K, Vunnam R, et al. Validation of a novel CARTOSEG segmentation module software for contrast-enhanced computed tomography-guided radiofrequency ablation in patients with atrial fibrillation. Pacing Clin Electrophysiol. 2017.
6. Kanaji Y, Miyazaki S, Iwasawa J, Ichihara N, Takagi T, Kuroi A, et al. Pre-procedural evaluation of the left atrial anatomy in patients referred for catheter ablation of atrial fibrillation. Journal of cardiology. 2016;67(1):115-21.
7. Walters TE, Ellims AH, Kalman JM. The role of left atrial imaging in the management of atrial fibrillation. Progress in cardiovascular diseases. 2015;58(2):136-51.
8. Oude Velthuis B, Molenaar M, Reinhart Dorman HG, Stevenhagen JY, Scholten MF, van der Palen J, et al. Use of three-dimensional computed tomography overlay for real-time cryoballoon ablation in atrial fibrillation reduces radiation dose and contrast dye. Netherlands heart journal : monthly journal of the Netherlands Society of Cardiology and the Netherlands Heart Foundation. 2017;25(6):388-93.
9. Romero J, Husain SA, Kelesidis I, Sanz J, Medina HM, Garcia MJ. Detection of left atrial appendage thrombus by cardiac computed tomography in patients with atrial fibrillation: a meta-analysis. Circ Cardiovasc Imaging. 2013;6(2):185-94.
10. To AC, Flamm SD, Marwick TH, Klein AL. Clinical utility of multimodality LA imaging: assessment of size, function, and structure. JACC Cardiovasc Imaging. 2011;4(7):788-98.
11. Dores H, de Araujo Goncalves P, Ferreira AM, Carvalho MS, Sousa PJ, Cardim N, et al. Performance of traditional risk factors in identifying a higher than expected coronary atherosclerotic burden. Rev Port Cardiol. 2015;34(4):247-53.
12. G. Bongartz SJG, A.G. Jurik, M. Leonardi, E. van Persijn van Meerten, R. Rodríguez, K. Schneider, A. Calzado, J. Geleijns, K.A. Jessen, W. Panzer, P. C.

cont.

Artigo submetido à Revista Portuguesa de Cardiologia

Shrimpton, G. Tosi. European Guidelines for Multislice Computed Tomography. 2004.
13. Christner JA, Kofler JM, McCollough CH. Estimating effective dose for CT using dose-length product compared with using organ doses: consequences of adopting International Commission on Radiological Protection publication 103 or dual-energy scanning. AJR American journal of roentgenology. 2010;194(4):881-9.
14. Hausleiter J, Meyer T, Hermann F, Hadamitzky M, Krebs M, Gerber TC, et al. Estimated radiation dose associated with cardiac CT angiography. JAMA. 2009;301(5):500-7.
15. Hur J, Kim YJ, Lee HJ, Nam JE, Ha JW, Heo JH, et al. Dual-enhanced cardiac CT for detection of left atrial appendage thrombus in patients with stroke: a prospective comparison study with transesophageal echocardiography. Stroke. 2011;42(9):2471-7.
16. Feuchtner GM, Dichtl W, Bonatti JO, Jodocy D, Muller S, Hintringer F, et al. Diagnostic accuracy of cardiac 64-slice computed tomography in detecting atrial thrombi. Comparative study with transesophageal echocardiography and cardiac surgery. Invest Radiol. 2008;43(11):794-801.
17. Sousa PJ, Goncalves PA, Marques H, Raposo L, Cale R, Brito J, et al. Radiation in cardiac CT: predictors of higher dose and its reduction over time. Rev Port Cardiol. 2010;29(11):1655-65.
18. de Araujo Goncalves P, Jeronimo Sousa P, Cale R, Marques H, Borges dos Santos M, Dias A, et al. Effective radiation dose of three diagnostic tests in cardiology: single photon emission computed tomography, invasive coronary angiography and cardiac computed tomography angiography. Rev Port Cardiol. 2013;32(12):981-6.
19. Lazoura O, Ismail TF, Pavitt C, Lindsay A, Sriharan M, Rubens M, et al. A low-dose, dual-phase cardiovascular CT protocol to assess left atrial appendage anatomy and exclude thrombus prior to left atrial intervention. Int J Cardiovasc Imaging. 2016;32(2):347-54.
20. Teunissen C, Habets J, Velthuis BK, Cramer MJ, Loh P. Double-contrast, single-phase computed tomography angiography for ruling out left atrial appendage thrombus prior to atrial fibrillation ablation. Int J Cardiovasc Imaging. 2017;33(1):121-8.
21. Iwayama T, Arimoto T, Ishigaki D, Hashimoto N, Kumagai YU, Koyama YO, et al. The Clinical Value of Nongated Dual-Source Computed Tomography in Atrial Fibrillation Catheter Ablation. J Cardiovasc Electrophysiol. 2016;27(1):34-40.
22. Annoni AD, Andreini D, Pontone G, Formenti A, Petulla M, Consiglio E, et al. Ultra-low-dose CT for left atrium and pulmonary veins imaging using new model-based iterative reconstruction algorithm. Eur Heart J Cardiovasc Imaging. 2015;16(12):1366-73.

cont.

Artigo submetido à Revista Portuguesa de Cardiologia

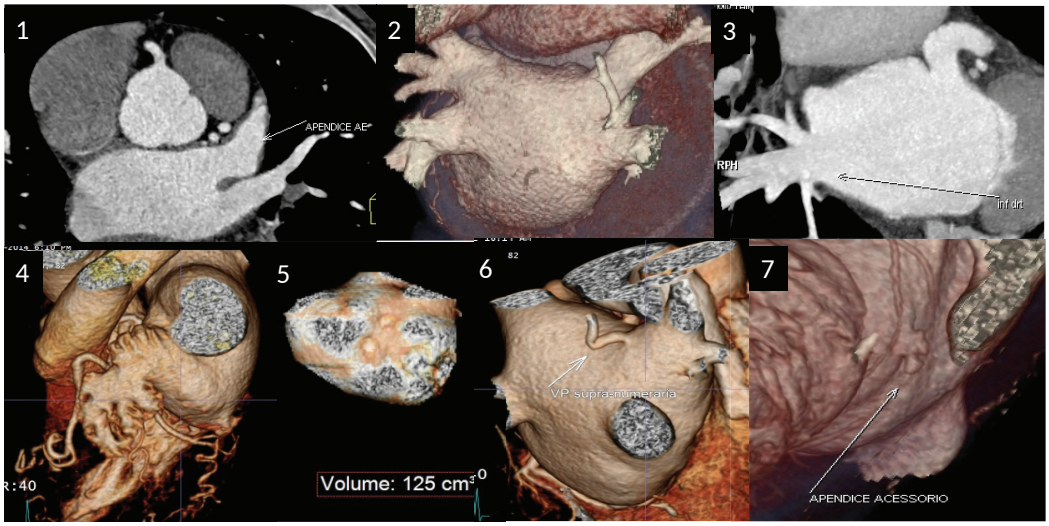

Figura 1

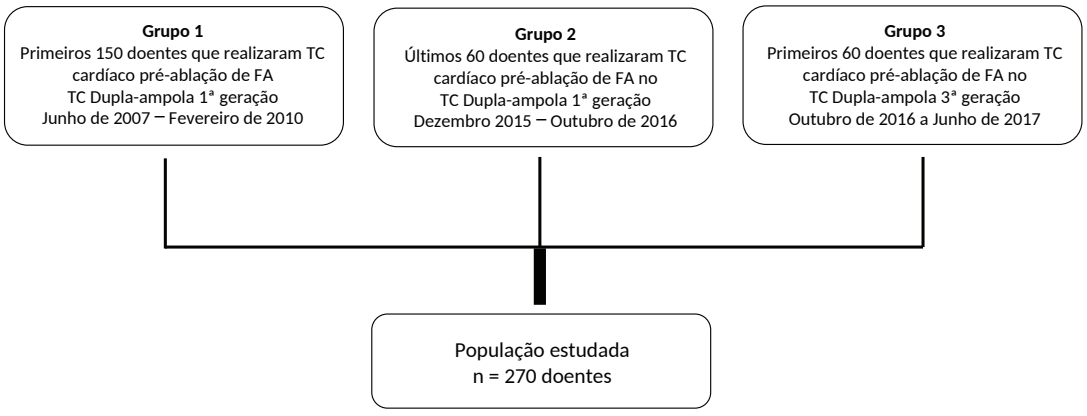

Figura 2

cont.

Artigo submetido à Revista Portuguesa de Cardiologia

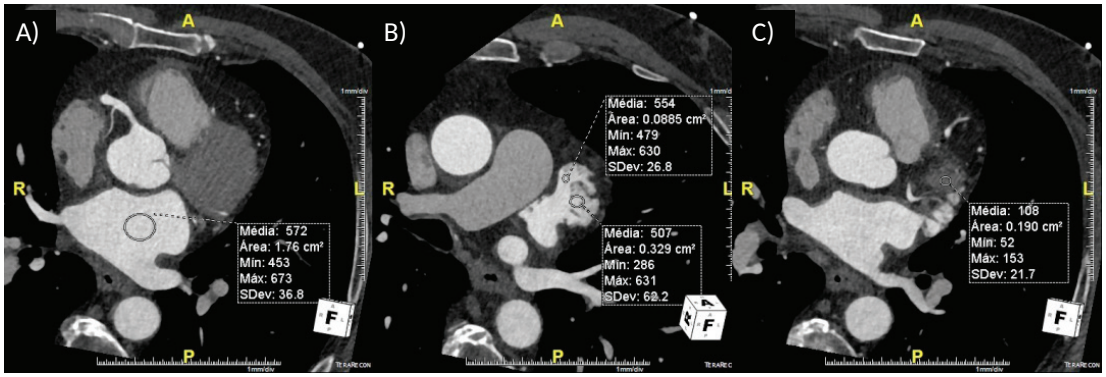

Figura 3

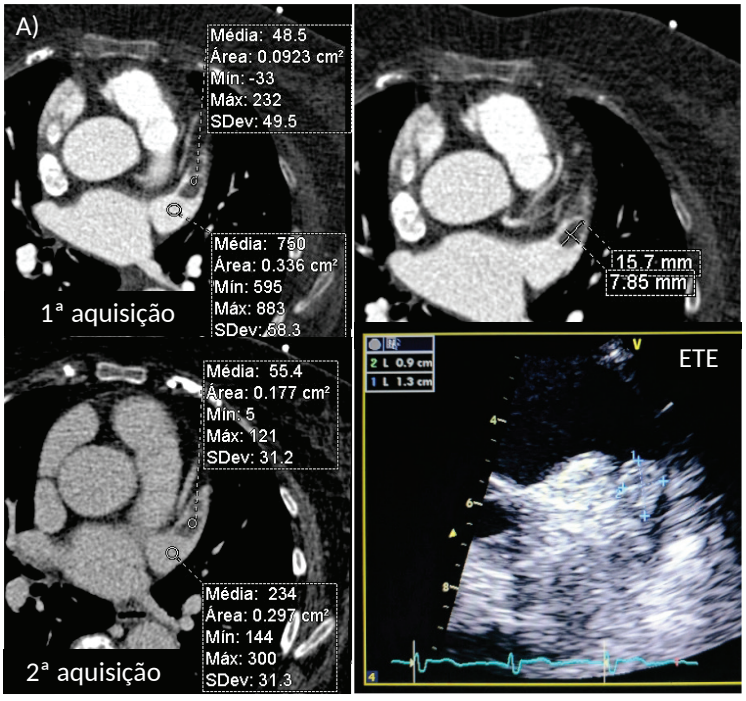

Figura 4

cont.

Artigo submetido à Revista Portuguesa de Cardiologia

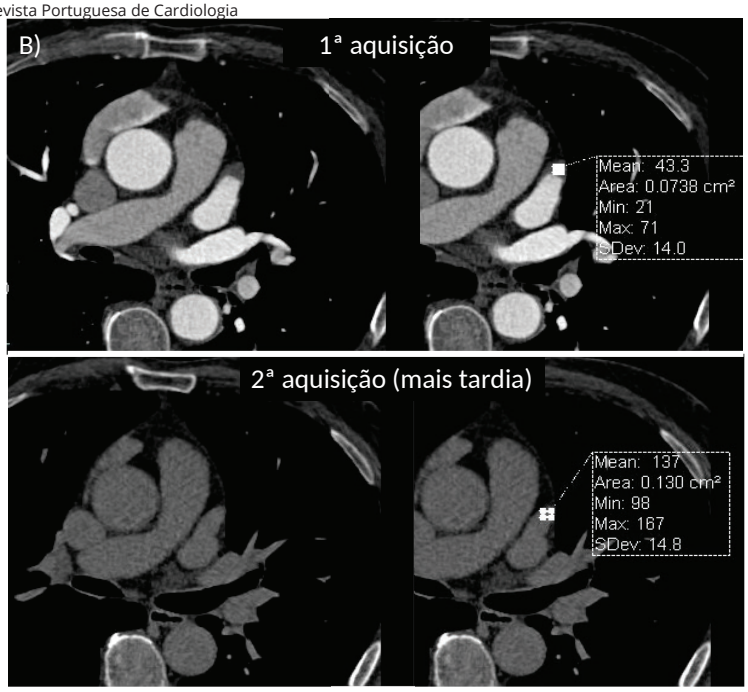

Figura 5

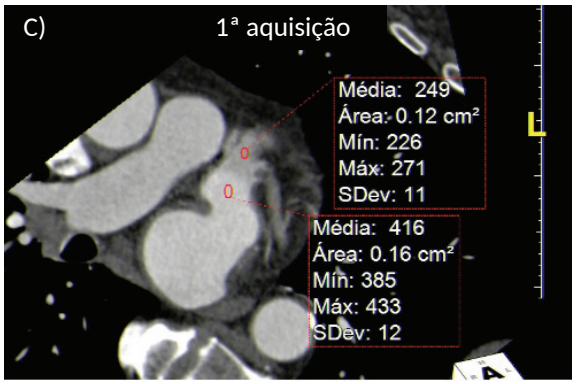

Figura 6

cont.

Artigo submetido à Revista Portuguesa de Cardiologia

Tabela 1: Descrição dos grupos e avaliação comparativa.

	Grupo 1 (G1)	Grupo 2 (G2)	Grupo 3 (G3)	P
n	150	60	60	
Idade, anos	59 (48-65)	63 (53-69)	65 (56-70)	**0.001** †
Sexo masculino	74% (n=111)	72% (n=43)	73% (n=44)	0.805
IMC, Kg/m²	26.6 (24.2-29.1)	27.1 (24.0-28.6)	26.3 (24.5-28.9)	0.987
% ritmo sinusal	75% (n=112)	70% (n=42)	70% (n=42)	0.590
Frequência cardíaca, bpm	68 (59-77)	66 (58-75)	65 (58-80)	0.746
Protocolo				**<0.001** *†¶
% Protocolo Retro	100% (n=150)	5% (n=3)	3% (n=2)	
% Protocolo Prospectivo	NA	98% (n=59)	5% (n=3)	
% Protocolo FLASH	NA	NA	91.7%(n=55)	
Volume de contraste	100 (90-108)	90 (80-100)	65 (60-65)	**<0.001** *†¶
Radiação 1ª aquisição, mGy.cm	402 (286-670)	95 (72-146)	41 (28-50)	**<0.001** *†¶
% 2ª aquisição	11% (n=17)	10% (n=6)	5% (n=3)	0.165
kV				**<0.001** *†¶
% de aquisição 70kv	0	0	33.3% (n=20)	
% de aquisição 80kv	0	82% (n=49)	57% (n=34)	
% de aquisição 90kv	0	0	3% (n=2)	
% de aquisição 100kv	83% (n=125)	20% (n=12)	2% (n=1)	
% de aquisição 120kv	17% (n=25)	2% (n=1)	5% (n=3)	
Presença de trombo	1% (n=1)	2% (n=1)	0	0.556
Acuidade diagnóstica qualitativa	100%	100%	100%	1.00
Vol AEsq a 70% do ciclo cardíaco	83 (65-105)	80 (69-96)	87 (66-99)	0.767

IMC: Índice de massa corporal;
FLASH: protocolo de aquisição num só batimento cardíaco utilizando velocidade de mesa muito rápida;
AE – aurícula esquerda; kV: quilovoltagem
* Grupo 1 vs. Grupo 2 p < 0.01; † Grupo 1 vs. Grupo 3 < 0.01; ¶ Grupo 2 vs. Grupo 3 < 0.01

Tabela: Avaliação quantitativa da qualidade de imagem:

	Grupo 2	Grupo 3	p
n	60	60	
Sinal/ruído AEsq	10.0 (8.3-12.1)	13.5 (11.0-16.2)	**<0.001**
Contraste/ruído (densidade AAEsq-VEsq / DP AAEsq)	8.8 (7.1-11.7)	14.8 (12.6-17.0)	**<0.001**
Rácio densidade média AEsq/AAEsq	1.04 (0.93-1.14)	0.92 (0.86-0.99)	**<0.001**

cont.

Artigo submetido à Revista Portuguesa de Cardiologia

Tabela 3: Factores preditores de 2ª aquisição

	2ª Aquisição		
	Sim (n=26)	**Não (n=244)**	**p**
Idade, anos	60 (53-67)	61 (51-67)	0.836
Sexo masculino	73% (n=19)	73% (n=178)	1.000
IMC, Kg/m^2	27.9 (24.1-30.1)	26.5 (24.4-29.1)	0.455
% ritmo sinusal	50% (n=13)	75% (n=183)	**0.011**
FC média, bpm	73 (65-89)	66 (58-77)	**0.039**
Protocolo			0.381
% Protocolo Retrospectivo	65.4% (n=17)	52.5% (n=128)	
% protocolo prospectivo	26.9% (n=7)	26.2% (n=64)	
% protocolo FLASH	7.7% (n=2)	21.3% (n=52)	
Volume de contraste, mL	95 (80-103)	90 (65-102)	0.397
Volume AE a 70% do ciclo cardíaco	93 (70-118)	82 (67-99)	0.087

IMC: Índice de massa corporal;
FLASH: protocolo de aquisição num só batimento cardíaco utilizando velocidade de mesa muito rápida; AE – aurícula esquerda

Tabela 4 – Comparação com outras publicações

	Marques et al. Protocolo actual - G3	**Lazoura et al**	**Teunissen et al**	**Iwayama et al**	**Annoni et al**
n do grupo referência (n total do estudo)	60 (270)	122	605	20 (60)	100 (200)
Sincronização electrocardiográfica	sim	sim	sim	não	não
Dupla administração de contraste	não	não	sim	não	não
Realizado para exclusão de trombo	sim	sim	sim	não	não
% de exames em que não foi possível excluir trombo	0%	0%	0%	NA	NA
% de 2ª aquisição	5%	100%	4,30%	NA	NA
necessidade de 2ª aquisição	5%	16%	4,30%	NA	NA
ETE prévio à ablação de FA	não necessária	não necessária	não necessária	necessária	necessária
Dose de radiação	0,6mSv	3,5mSv	3,1mSv	1,1mSv	0,4mSv
Dose de contraste	64ml	90ml	100ml	28,7ml	80ml

ETE: Ecocardiograma transesofagico; FA: Fibrilhação auricular; mSv: milisievert

cont.

Artigo submetido à Revista Portuguesa de Cardiologia

Responsabilidades éticas

Proteção de pessoas e animais. Os autores declaram que para esta investigação não se realizaram experiências em seres humanos e/ou animais.

Confidencialidade dos dados. Os autores declaram que não aparecem dados de pacientes neste artigo.

Direito à privacidade e consentimento escrito. Os autores declaram que não aparecem dados de pacientes neste artigo.

CAPÍTULO XI

Discussão Global

11.1. INTRODUÇÃO

A discussão pormenorizada dos resultados desta tese encontra-se nos **Capítulos VIII**, **IX** e **X**.
O presente capítulo pretende sumarizar e agregar, correlacionando, a informação disponível neles.

11.2. DISCUSSÃO GLOBAL

O trabalho que foi desenvolvido no âmbito desta tese reflete a importância clínica da aurícula esquerda (1-7) e o papel crescente da TC cardíaca no âmbito das doenças cardiovasculares (8-10).

Desde o início, na UNICA (Unidade de Imagem Cardiovascular por TC e RM), unidade que criámos com o colega Pedro Gonçalves que a TC cardíaca, na altura em fase emergente, se impôs com uma crescente expressão no arsenal diagnóstico. Decorrente do fato de estarmos inseridos num Hospital com uma unidade de Arritmologia de referência que se tinha proposto realizar técnicas ablativas percutâneas por radiofrequência com controlo magnético para tratamento de FA, foi, do acordo entre ambas as Unidades, que a TC cardíaca surgiu como o exame único a realizar em contexto pré-ablativo.
Foi com naturalidade também e pela ligação com a Faculdade de Ciências Médicas que foram sendo equacionados projetos de investigação que envolvessem as duas unidades.

Neste contexto e antecipando as evoluções tecnológicas dos aparelhos de TC, que julgávamos conduzir inexoravelmente para avaliações apenas em fase médio-diastólica, percebemos que o *gap* de conhecimento existente não iria permitir a avaliação dimensional das câmaras cardíacas nesses exames por falta de normogramas.
Assim surge o nosso primeiro objetivo — a criação de um normograma para a aurícula direita em fase médio-diastólica.

A primeira publicação sobre este tema surge apenas em 2016 por Walker (11). O trabalho desenvolvido nesta tese permite-nos dar um contributo para o conhecimento nesta área, nomeadamente por termos:

- desenvolvido um normograma com menor intervalo de confiança, provavelmente relacionável com um grupo de estudo maior e com uma melhor definição de "normal" (sem doença) dado termos incluído dados ecocardiográficos.
- avaliado a capacidade do uso do normograma de TC em doentes com FA paroxística, onde o valor dimensional da aurícula se reveste de uma importância particular (12), dado ser o fator que mais se correlaciona com a possibilidade de recidiva após a ablação. A identificação destes fatores levou à criação, pelo nosso grupo, de um *score* de risco de recidiva – ATLAS (13).
- criado uma regressão que permite calcular o volume auricular máximo com base em dados de fácil obtenção na fase medio-diastólica. Assim a AEsq pode ser avaliada eficientemente em qualquer exame de coronariografia por TC de forma quantitativa

Ao termos acesso à informação imagiológica de TC de um grande grupo de doentes com FA paroxística, interessámo-nos pelo seu estudo morfológico, dimensional e funcional. Num contexto de crescente utilização de aquisições de TC prospetivas, o grupo de doentes com informação funcional por TC tenderia a diminuir rapidamente. Direcionámos assim a nossa investigação para áreas sobretudo funcionais, associadas ao seguimento dos doentes que faziam a terapêutica ablativa. Estas informações poderiam contribuir para a melhor definição dos doentes que eram selecionados para a terapêutica ablativa, diminuindo um elevado número de recidivas que a caracterizam (14, 15).
Neste âmbito, apesar de dispormos de um grupo de 116 doentes com seguimento médio de 4,8 anos, com 34,5% de taxa de recidiva não foi possível estabelecer

nenhum valor prognóstico para valores funcionais da AEsq ou do AAEsq, ao contrario de outras séries (16, 17). Este aspeto, apesar de negativo, pode ser importante, por evidenciar (pelo menos no nosso grupo) a ausência de um marcador funcional precoce de recidiva após ablação. Na nossa série, apenas o volume máximo indexado da AEsq se revelou preditor independente de recidiva, na análise multivariada, quando ajustado para os fatores do *score* ATLAS (13).

No entanto, verificámos a existência de um marcador morfológico, de drenagem das veias pulmonares à direita que confere melhor prognóstico após a terapêutica ablativa. Este marcador (drenagem das veias pulmonares à direita, tipo R2a) poderá fazer equacionar a intensificação do procedimento de ablação nos doentes que tenham outra anatomia de drenagem, dado que a maior diferença na incidência de recidiva ocorre precocemente (sugerindo menor eficácia do tratamento). Quando efetuámos a avaliação deste preditor ajustando para os parâmetros do *score* ATLAS, ele manteve-se estatisticamente significativo de forma independente.

Explorámos a relação de características imagiológicas com *scores* de risco embólico, abrindo a possibilidade de associar ao *score* clínico marcadores imagiológicos.

Por ser Radiologista de formação, a relevância de otimização de cada exame de todo e qualquer doente e condição clínica faz parte da nossa génese. Assim surgiu o terceiro objetivo desta tese, avaliar o grau de otimização ao longo do tempo dos exames de TC cardíaca efetuados aos doentes em contexto prévio à ablação de FA. Foi-nos possível concluir que, ao longo do tempo e aproveitando a evolução tecnológica, realizamos hoje exames com dez vezes menor dose de radiação do que no início, sem qualquer compromisso na qualidade objetiva da imagem de TC obtida.

O nosso protocolo atual permite doses submilisiviert — 0,6mSv (0,39 — 0,7), com uma necessidade de 5% de segundas aquisições (tardias), num contexto de utilização da TC como exame único (dispensando a necessidade de ETE). Em contexto de TC cardíaca como exame único para avaliação de doentes em contexto prévio à ablação de FA, estes valores são, após consulta da literatura de referência, os valores mais baixos até agora descritos (18, 19) (ver **Tabela 1**).

Finalizamos com uma preocupação igualmente intrínseca ao Radiologista, a procura de toda a informação contida num exame:

Assim foi possível identificar a presença de apêndices acessórios da aurícula esquerda em 7% dos doentes avaliados. Este aspeto é relevante na escolha do tratamento e na equação do risco de evento tromboembólico, sendo a TC o melhor método não invasivo para o seu diagnóstico.

De realçar também que, nos exames realizados em contexto de pré-ablação de FA, cerca de 7% dos doentes apresentaram achados extra-cardíacos major (incluindo 3 neoplasias).

FIGURA 1

	Marques et al. Protocolo atual - G3	**Lazoura et al**	**Teunissen et al**
n do grupo referência (n total do estudo)	60 (270)	122	605
Sincronização eletrocardiográfica	sim	sim	sim
Dupla administração de contraste	não	não	sim
Realizado para exclusão de trombo	sim	sim	sim
% de exames em que não foi possível excluir trombo	0%	0%	0%
% de 2ª aquisição	5%	100%	4,30%
necessidade de 2ª aquisição	5%	16%	4,30%
ETE prévio à ablação de FA	não necessária	não necessária	não necessária
Dose de radiação	0,6mSv	3,5mSv	3,1mSv
Dose de contraste	65ml	90ml	100ml

BIBLIOGRAFIA

1. Benjamin EJ, D'Agostino RB, Belanger AJ, et al. Left atrial size and the risk of stroke and death. The Framingham Heart Study. Circulation. 1995;92(4):835-41.
2. Daccarett M, Badger TJ, Akoum N, et al. Association of left atrial fibrosis detected by delayed-enhancement magnetic resonance imaging and the risk of stroke in patients with atrial fibrillation. J Am Coll Cardiol. 2011;57(7):831-8.
3. Gottdiener JS, Kitzman DW, Aurigemma GP, et al. Left atrial volume, geometry, and function in systolic and diastolic heart failure of persons > or =65 years of age (the cardiovascular health study). Am J Cardiol. 2006;97(1):83-9.
4. Gupta S, Matulevicius SA, Ayers CR, et al. Left atrial structure and function and clinical outcomes in the general population. Eur Heart J. 2013;34(4):278-85.
5. Moller JE, Hillis GS, Oh JK, et al. Left atrial volume: a powerful predictor of survival after acute myocardial infarction. Circulation. 2003;107(17):2207-12.
6. Pritchett AM, Mahoney DW, Jacobsen SJ, et al. Diastolic dysfunction and left atrial volume: a population-based study. J Am Coll Cardiol. 2005;45(1):87-92.
7. Takemoto Y, Barnes ME, Seward JB, et al. Usefulness of left atrial volume in predicting first congestive heart failure in patients > or = 65 years of age with well-preserved left ventricular systolic function. Am J Cardiol. 2005;96(6):832-6.
8. ACCF/ACR/SCCT/SCMR/ASNC/NASCI/SCAI/SIR 2006 appropriateness criteria for cardiac computed tomography and cardiac magnetic resonance imaging. A report of the American College of Cardiology Foundation Quality Strategic Directions Committee Appropriateness Criteria Working Group. Journal of the American College of Radiology : JACR. 2006;3(10):751-71.
9. Moss AJ, Williams MC, Newby DE, et al. The Updated NICE Guidelines: Cardiac CT as the First-Line Test for Coronary Artery Disease. Current cardiovascular imaging reports. 2017;10(5):15.
10. Taylor AJ, Cerqueira M, Hodgson JM, et al. ACCF/SCCT/ACR/AHA/ASE/ASNC/NASCI/SCAI/SCMR 2010 Appropriate Use Criteria for Cardiac Computed Tomography. A Report of the American College of Cardiology Foundation Appropriate Use Criteria Task Force, the Society of Cardiovascular Computed Tomography, the American College of Radiology, the American Heart Association, the American Society of Echocardiography, the American Society of Nuclear Cardiology, the North American Society for Cardiovascular

Imaging, the Society for Cardiovascular Angiography and Interventions, and the Society for Cardiovascular Magnetic Resonance. Journal of cardiovascular computed tomography. 2010;4(6):407.e1-33.

11. Walker JR, Abadi S, Solomonica A, et al. Left-sided cardiac chamber evaluation using single-phase mid-diastolic coronary computed tomography angiography: derivation of normal values and comparison with conventional end-diastolic and end-systolic phases. European radiology. 2016;26(10):3626-34.
12. Costa C, Ferreira AM, Morais Sarmento P, et al. Complete recovery of myocardial inflammation imaged by T2 mapping. Rev Port Cardiol. 2016;35(9):503-4.
13. Mesquita JF, A.M.; Cavaco, D.; Costa, F.M.; Carmo, P.; Marques, H.; Morgado, F.; Mendes, Miguel; Adragão, P. Development and validation of a risk score for predicting atrial fibrillation recurrence after a first catheter ablation procedure – ATLAS score. Europace. 2017.
14. Darby AE. Recurrent Atrial Fibrillation After Catheter Ablation: Considerations For Repeat Ablation And Strategies To Optimize Success. Journal of Atrial Fibrillation. 2016;9(1):1427.
15. Wynn GJ, El-Kadri M, Haq I, et al. Long-term outcomes after ablation of persistent atrial fibrillation: an observational study over 6 years. Open Heart. 2016;3(2).
16. Kiuchi K, Yoshida A, Takei A, et al. Topographic variability of the left atrium and pulmonary veins assessed by 3D-CT predicts the recurrence of atrial fibrillation after catheter ablation. Journal of arrhythmia. 2015;31(5):286-92.
17. Im SI, Na JO, Kim SW, et al. Adjusted left atrial emptying fraction as a predictor of procedural outcome after catheter ablation for atrial fibrillation. Tex Heart Inst J. 2015;42(3):216-25.
18. Lazoura O, Ismail TF, Pavitt C, et al. A low-dose, dual-phase cardiovascular CT protocol to assess left atrial appendage anatomy and exclude thrombus prior to left atrial intervention. Int J Cardiovasc Imaging. 2016;32(2):347-54.
19. Teunissen C, Habets J, Velthuis BK, et al. Double-contrast, single-phase computed tomography angiography for ruling out left atrial appendage thrombus prior to atrial fibrillation ablation. Int J Cardiovasc Imaging. 2017;33(1):121-8.

CAPÍTULO XII

Conclusões e direções para futura investigação

12.1. CONCLUSÕES

Criámos um normograma para avaliação volumétrica e dimensional da AEsq em fase médio-diastólica. Determinámos que a maior área da aurícula esquerda em plano axial associado ao maior diâmetro crâneo-caudal em plano sagital se correlacionam muito bem com o volume máximo, permitindo eficiência na avaliação quotidiana da dimensão da aurícula esquerda em qualquer TC cardíaca , incluindo na angio-TC coronária.

> (artigo submetido — Capítulo VIII)

Determinámos a morfologia, a dimensão e a função da AEsq e do AAEsq, assim como o padrão de drenagem das veias pulmonares numa população com FA paroxística. Identificámos variáveis imagiológicas contidas no exame de TC como um menor volume mínimo indexado da AEsq e uma maior fracção de ejeção, que se associam a um *score* de risco de evento embólico (*score* CHA_2DS_2VASc) baixo.
Verificámos que o volume máximo indexado da AEsq, em análise multivariada, incluindo os fatores do *score* ATLAS, é um preditor independente de recidiva.
Em análise tipo "curvas de sobrevivência": em que se integram a presença de recidiva assim como o tempo a que essa recidiva ocorreu, verificámos que o padrão mais prevalente de drenagem das veias pulmonares à direita (R2a) confere benefício prognóstico estatisticamente significativo, inclusive em análise multivariável incluindo os elementos do *score* ATLAS. Este aspeto poderá levar à intensificação da ablação aos doentes portadores de outro padrão de drenagem.

A otimização dos exames de TC cardíaca prévia ao tratamento ablativo percutâneo de fibrilhação auricular permitiu ganhos na dose de radiação do exame, num fator

de ordem das dezenas (radiação do exame actual cerca de 10% do exame com protocolo inicial), com doses médias de 0,6mSv (0,39 – 0,7). O volume de contraste utilizado também diminuiu significativamente para os 65ml (60-65). No entanto, esta otimização do protocolo com menor dose de radiação e contraste, ficou igualmente associada a uma melhoria quantitativa da qualidade de imagem significativa, traduzida pelos rácios sinal/ruído; contraste/ruído e homogeneização da densidade AEsq/AAEsq.

> (artigo submetido — Capítulo X)

12.2. DIRECÇÕES PARA FUTURA INVESTIGAÇÃO

12.2.1. Relacionáveis com a área da otimização de protocolos de TC cardíaca, num contexto de exame único prévio a ablação de FA

1. A otimização de protocolos *per si* é constante, pelo que é uma área de investigação contínua.

2. Avaliação de fibrose

   Sabemos hoje da capacidade de estudos de RM, de avaliarem a fibrose da AEsq de forma não invasiva, com relevância prognóstica isolada (1), como no contexto pré-ablação, peri-ablação e pós-ablação (2-6).

   Não é, no entanto, uma técnica perfeita, com fraca resolução espacial (exacerbada num contexto de avaliação de uma parede fina) aliada a tempos de aquisição longos a traduzirem alguns exames não interpretáveis e outros com conclusões díspares (7-9).

   Existem duas formas de obter imagens de fibrose miocárdica na TC: por avaliação do realce tardio ou por utilização de técnicas de energia espetral. Ambas as técnicas apresentam já resultados interessantes no diagnóstico de fibrose miocárdica (10). As técnicas na TC de energia espetral têm vindo a ser desenvolvidas com evidentes melhorias nos últimos anos fruto da evolução tecnológica. Apesar da menor resolução de contraste em relação às técnicas de RM, a TC ao ter uma resolução espacial muito melhor e dado ao facto de ser hoje o exame

de eleição prévio à terapêutica ablativa poderá ter utilidade neste contexto. A avaliação de fibrose por TC, o desenvolvimento de um protocolo otimizado e a sua comparação com outros métodos não invasivos como a RM representam uma das áreas mais aliciantes de investigação atual neste contexto e podem ser integradas no protocolo de exame único prévio a ablação FA.

3. Avaliação de gordura e/ou inflamação
   Sabemos hoje que a inflamação está implicada na génese da fibrose/remodelagem da aurícula esquerda (11). A TC é um excelente método para quantificar gordura de forma não invasiva. Diferentes definições de densidade de gordura poderão ser utilizadas num mesmo doente, permitindo separar o volume de gordura mais densa (possivelmente inflamada) de gordura menos densa. Poderíamos então avaliar o volume de gordura epicárpica, o volume de gordura peri-auricular, as suas densidades, e a percentagem de um componente mais denso e estudar se permitem identificar um subgrupo de doentes que beneficiaria mais da terapêutica ablativa.

12.2.2. Relacionáveis com o trabalho desenvolvido nesta tese:

4. A correlação entre o *score* de risco de evento embólico CHA_2DS_2VASc e alguns dos parâmetros imagiológicos que se correlacionam com estase na AEsq ou no AAEsq poderá permitir a criação de um *score* com maior acuidade juntando parâmetros imagiológicos aos clínicos.

12.2.3. Relacionáveis com a TC no contexto de doença coronária

5. TC como exame pluripotencial no contexto de doença coronária

> Presentemente, integramos um grupo de investigação de três dos maiores registos de TC cardíaco coronário – CONFIRM (avaliação de prognóstico relacionável com a placa coronária); PARADIGM (avaliação das características de placa aterosclerótica e sua progressão documentada por TC); ICONIC (estudo da aterosclerose de doentes que tiveram um evento cardiovascular major). Se, a estes aspetos, juntarmos a avaliação de risco cardiovascular em doentes

assintomáticos pelo *score* de cálcio, a capacidade de avaliação de isquémia (técnicas de perfusão de primeira passagem *vs* técnicas espectrais *vs* FFR-virtual) e a avaliação de fibrose (por técnicas de realce tardio ou de energia espetral), verificamos o grau de globalidade de avaliação do doente e da doença coronária possível por TC. Enquanto se espera pelo desenvolvimento de novos contrastes marcadores de instabilidade de placa, é já possível por técnicas de inteligência artificial condensar toda esta informação (grande parte não perceptível ao olho humano treinado) para benefício do doente. A área da inteligência artificial irá revolucionar a medicina, começando pela imagem.

BIBLIOGRAFIA

1. King JB, Azadani PN, Suksaranjit P, et al. Left Atrial Fibrosis and Risk of Cerebrovascular and Cardiovascular Events in Patients With Atrial Fibrillation. J Am Coll Cardiol. 2017;70(11):1311-21.
2. Akoum N, Fernandez G, Wilson B, et al. Association of atrial fibrosis quantified using LGE-MRI with atrial appendage thrombus and spontaneous contrast on transesophageal echocardiography in patients with atrial fibrillation. J Cardiovasc Electrophysiol. 2013;24(10):1104-9.
3. Badger TJ, Daccarett M, Akoum NW, et al. Evaluation of left atrial lesions after initial and repeat atrial fibrillation ablation: lessons learned from delayed-enhancement MRI in repeat ablation procedures. Circulation Arrhythmia and electrophysiology. 2010;3(3):249-59.
4. Han FT, Akoum N, Marrouche N. Value of magnetic resonance imaging in guiding atrial fibrillation management. The Canadian journal of cardiology. 2013;29(10):1194-202.
5. Marrouche NF, Wilber D, Hindricks G, et al. Association of atrial tissue fibrosis identified by delayed enhancement MRI and atrial fibrillation catheter ablation: the DECAAF study. JAMA. 2014;311(5):498-506.
6. McGann CJ, Kholmovski EG, Oakes RS, et al. New magnetic resonance imaging-based method for defining the extent of left atrial wall injury after the ablation of atrial fibrillation. J Am Coll Cardiol. 2008;52(15):1263-71.
7. Chrispin J, Gucuk Ipek E, Zahid S, et al. Lack of regional association between atrial late gadolinium enhancement on cardiac magnetic resonance and atrial fibrillation rotors. Heart Rhythm. 2016;13(3):654-60.
8. Karim R, Housden RJ, Balasubramaniam M, et al. Evaluation of current algorithms for segmentation of scar tissue from late gadolinium enhancement cardiovascular magnetic resonance of the left atrium: an open-access grand challenge. J Cardiovasc Magn Reson. 2013;15:105.
9. Kiuchi K, Okajima K, Shimane A, et al. Visualizing radiofrequency lesions using delayed-enhancement magnetic resonance imaging in patients with atrial fibrillation: A modification of the method used by the University of Utah group. Journal of arrhythmia. 2015;31(2):71-5.
10. Lee HJ, Im DJ, Youn JC, et al. Assessment of myocardial delayed enhancement with cardiac computed tomography in cardiomyopathies: a prospective comparison with

delayed enhancement cardiac magnetic resonance imaging. Int J Cardiovasc Imaging. 2017;33(4):577-84.

11. Kume O, Teshima Y, Abe I, et al. Role of atrial endothelial cells in the development of atrial fibrosis and fibrillation in response to pressure overload. Cardiovasc Pathol. 2017;27:18-25.